Contributions négatives et positives de la galectine-9 au développement tumoral : étude dans des modèles tumoraux murins syngéniques

Valentin Baloche

Thèse de doctorat

NNT : 2020UPASS117

université PARIS-SACLAY

Contributions négatives et positives de la galectine-9 au développement tumoral : étude dans des modèles tumoraux murins syngéniques

Thèse de doctorat de l'université Paris-Saclay

École doctorale n°582 : cancérologie : biologie - médecine – santé (CBMS)
Spécialité de doctorat : aspects moléculaires et cellulaires de la biologie
Unité de recherche : UMR 9018 (ex UMR 8126)
Référent : faculté de médecine

Thèse présentée et soutenue à Villejuif, le 16 juillet 2020, par

Valentin BALOCHE

Composition du Jury

Dr Clara NAHMIAS Inserm U981, Gustave Roussy	Présidente
Dr Eliane PIAGGIO Inserm U932, Institut Curie	Rapporteuse
Pr Pascal REBOUL CNRS UMR 7365, IMoPA	Rapporteur
Dr François RADVANYI CNRS UMR 144, Institut Curie	Examinateur
Dr. Pierre BUSSON CNRS UMR 9018, Gustave Roussy	Directeur de thèse

REMERCIEMENTS

Je tiens tout d'abord à remercier l'ensemble des membres de mon jury qui me font l'honneur d'évaluer mon travail de thèse. Malgré les circonstances sanitaires actuelles, ceux-ci ont su se montrer disponibles et m'ont permis d'appréhender avec sérénité ces derniers mois de thèse. Je remercie plus particulièrement la docteure Eliane Piaggio et le professeur Pascal Reboul pour avoir accepté le rôle de rapporteur de ce manuscrit. Merci pour vos appréciations et vos critiques constructives.

J'aimerais également remercier toutes les personnes qui ont contribué à la réalisation de ce projet :

Je remercie donc mon directeur de thèse, le docteur Pierre Busson, pour m'avoir accepté dans son équipe. Je suis très satisfait du travail que nous avons pu réaliser ensemble, appuyé par un respect et une confiance mutuelle. Je te remercie d'avoir su te montrer toujours disponible et à l'écoute de mes suggestions. Je te suis également reconnaissant pour les opportunités scientifiques et professionnelles que tu m'as offertes.

Mon expérience de la recherche a été ponctuée de collaborations avec le monde de l'industrie, sans qui la fin de ma thèse aurait été plus difficile à appréhender. Ainsi, je tiens à remercier la société HiFiBio pour avoir participé au financement de ma 4ème année de thèse. Je remercie particulièrement la docteure Stéphanie Beq pour avoir cru et soutenu mon projet, ainsi que la docteure Muriel David qui a pris le temps d'analyser et de discuter des données avec moi. Je remercie également Luc Boblet et Laetitia Claër, qui ont permis à l'équipe de progresser dans l'évaluation pré-clinique des anticorps anti-gal-9.

Je remercie également les autres membres de mon équipe : Tram pour son aide indispensable dans les analyses bio-info et pour son amicalité. J'espère que nous aurons l'occasion de nous revoir au Viêt Nam ; Aurore pour son engagement dans la gestion du matériel, pièces, commandes, … et pour son dynamisme naturel (en tendant l'oreille, je crois bien que j'arrive à t'entendre depuis la pièce voisine finalement). Une pensée à ceux qui ont maintenant quitté le laboratoire mais qui ont également contribué à l'égayer au cours de ces

années : Nikiforos, Nayeli, Mathieu, Camille, … J'espère également que nous aurons l'occasion de nous recroiser.

J'ai commencé ma thèse au sein de l'unité « Signalisation, noyaux et innovations en cancérologie » (UMR 8126) et remercie la directrice Joëlle Wiels et le co-directeur Marc Lipinski de l'époque pour leur accueil. Je l'achève maintenant au sein de l'unité « METSY » (UMR 9018) et remercie les docteurs Catherine Brenner et Karim Benihoud qui dirigent ce nouveau groupe. Merci pour les efforts que vous investissez quotidiennement afin de renforcer la cohésion entre les membres et les thématiques de recherche. Je ne doute pas que vous conserverez cette dynamique dans les prochaines années.

Merci aux membres de ces différents laboratoires ainsi qu'aux personnes, nombreuses, qui m'ont apporté leur aide en partageant leurs connaissances, leur bonne humeur et leurs réactifs.

Je tiens à remercier particulièrement celles et ceux qui ont partagé la pièce 322 avec moi : Aude, merci pour tes conseils techniques et scientifiques. J'ai apprécié réparer les stores, machines à glace et autres ventilateurs avec toi. Ça nous sera sûrement très utile pour la suite. Je remercie également Florian pour son écoute, sa disponibilité et son aide dans la conversion de fichiers powerpoints en fichiers .tif 1200 dpi. J'aurai sûrement encore besoin de toi dans les mois qui viennent alors tâche de ne pas finir ta thèse trop vite. Avec un peu de chance, j'aurai peut-être des pitchs pour toi.

Une note particulière pour Amina, qui sera heureuse de trouver son nom dans un paragraphe. Merci pour les couscous, l'invitation en Tunisie et au Brésil (?). J'espère que nous aurons de nouveau l'occasion de t'accompagner nourrir les poissons de la Seine.

Un énorme merci aux amis qui m'ont permis de penser à autre chose qu'au rôle de la gal-9 dans la tumorigenèse. Merci à Céline pour les moments d'aventure, à Nico pour m'avoir appris comment voler un côlon, à Antoine pour ses histoires au coin du feu, à Marion et Cindy pour les bonnes balades à cheval, à Noémie pour m'avoir appris la chorégraphie de Pandi Panda, à Sylvain pour m'avoir présenté Noémie, …

Je remercie tout particulièrement mes parents, ma sœur, Giom et Jean-David pour les moments passés ensemble.

Enfin, je tiens à remercier Nimru d'avoir partagé son quotidien avec moi. Tu auras été très inspirant, un vrai mannequin chat …

SOMMAIRE

LISTE DES ABREVIATIONS

Actine-F : actine filamenteuse
AMP : adénosine monophosphate
ATP : adénosine triphosphate
BCG : bacille de Calmette et Guérin
bFGF : *basic fibroblast growth factor*
BLCA : *bladder carcinoma*
CAF : c*ancer-associated fibroblast*
Cas9 : *CRISPR associated protein 9*
CBS : *carbohydrate binding site*
CDR : *complementarity determining region*
CHC : carcinome hépatocellulaire
CRISPR : *clustered regular interspaced short palindromic repeats*
CRP : *C-reactive protein*
EBV : *Epstein-Barr virus*
EGF : *epidermal growth factor*
Fc : fragment constant
FGFR-3 : *fibroblast growth factor receptor-3*
FGL : *Forssman glycolipid*
Gal : galectine
Gp70 : *envelope glycoprotein* 70
GSL : glycosphingolipide
GTPase : *guanosine triphosphate hydrolysis enzyme*
HBV : *hepatitis B virus*
HCV : *hepatitis C virus*
HIF : *hypoxia inducible factor*
HMGB1 : *high mobility group box 1*
HSV : *herpes simplex virus*
IFN : interféron
Ig : immunoglobuline
Il : interleukine
KO : *knock-out*
LAM : leucémie aiguë myéloïde
LB : lymphocyte B
LEAD : lupus érythémateux aigu disséminé
LPS : lipopolysaccharide
LT : lymphocyte T
MDCK : *Madin-Darby canine kidney*
MDSC : *myeloid-derived suppressor cell*
MIBC : *muscle invasive bladder carcinoma*
MMP : *matrix metallopeptidase*
mTOR : *mechanistic target of rapamycin*
MuLV : *murine leukemia virus*

NAD : nicotinamide adénine dinucléotide
NK : *natural killer*
NMIBC : *non-muscle invasive bladder carcinoma*
NPC : *nasopharyngeal carcinoma*
PBMC : *peripheral blood mononuclear cell*
Pdgf : *platelet-derived growth factor*
PD-1 : *programmed cell death-1*
PDI : *protein disulfide-isomerase*
PD-L1 : *programmed death-ligand 1*
PI3-kinase : phosphoinositide 3-kinase
PPAR-γ : *peroxysome proliferator-activated receptor gamma*
S1PT : *detoxified S1 subunit pertussis toxin*
TAM : *tumor-associated macrophage*
TCR : *T cell receptor*
TGF : *transforming growth factor*
Th : *T helper*
TIL : *tumor-infiltrating lymphocyte*
Tim-3 : *T-cell immunoglobulin and mucin-domain containing-3*
TLR3 : *toll-like receptor 3*
TNF : *tumor necrosis factor*
TP53 : *tumor protein 53*
Treg : lymphocyte T régulateur
TWEAK : *TNF-related weak inducer of apoptosis*
UCB : *urothelial carcinoma of the bladder*
UTR : *untranslated region*
UVB : ultraviolet B
VEGF : *vascular endothelial growth factor*
VIH : virus de l'immunodéficience humaine

LISTE DES ILLUSTRATIONS

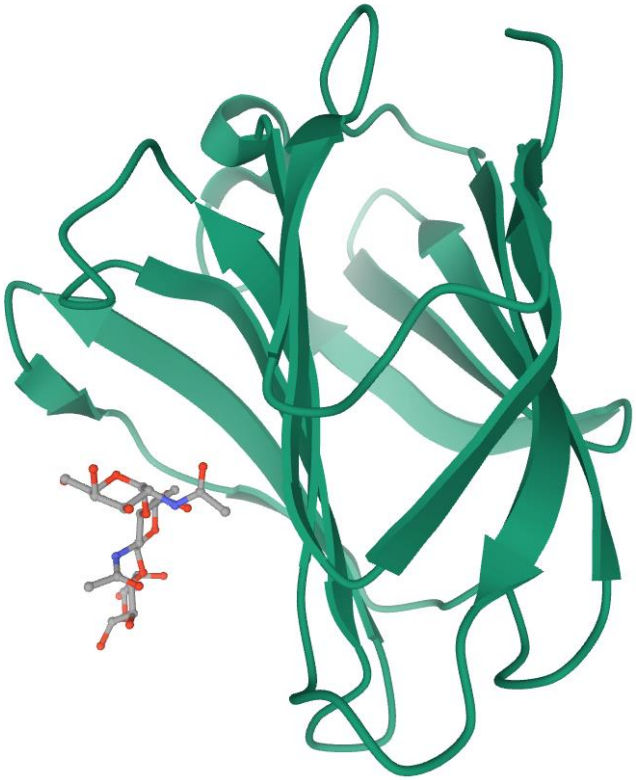

Figure 1. Organisation tridimensionnelle du CRD N-terminal de la galectine-9 humaine, en complexe avec l'antigène de Forssman (1).

Le feuillet F convexe et le feuillet S concave se font face pour former le domaine de reconnaissance des carbohydrates (CRD, carbohydrate recognition domain).

INTRODUCTION

I – Propriétés biologiques des galectines

a) Caractéristiques structurales

Les galectines, anciennement connues sous le nom de lectines de type S, regroupent un ensemble de protéines capables de se lier à des polysaccharides ou glycanes contenant des liaisons β-galactosides. Ces polysaccharides « reconnus » par les galectines sont généralement portés par des glycoprotéines ou des glycolipides. Les galectines ont été identifiées dans une large variété de métazoaires (17,18). Elles partagent une homologie au niveau de la structure primaire de leur « domaine de reconnaissance des carbohydrates » (CRD, *Carbodydrate recognition domain*). Ces domaines sont constitués d'environ 130 acides aminés, dont 8 sont invariants et une douzaine fortement conservée. L'identité de séquence entre les CRD des galectines varie de 20 à 50% en fonction de l'espèce. Les CRD ont des modalités de repliement communes qui aboutissent à une structure en sandwich incurvé avec deux feuillets β qui se font face : le feuillet F convexe et le feuillet S concave. Dans une incurvation du feuillet S du CRD se trouve la « poche à sucre » (CBS, *carbohydrate binding site*) (**Figure 1**). Le CBS interagit directement avec l'élément di-saccharidique contenant la liaison β1-4 ou β1-3 galactoside qui est reconnue au sein du polysaccharide cible. Le CBS contient les 8 acides aminés invariants mentionnés précédemment qui participent à sa structuration. Ce sont les suivants : His44, Asn46, Arg48, Val59, Asn61, Trp68, Glu71 et Arg73. La mutation du Trp68 en alanine ou en leucine abolit l'interaction avec le β-galactoside (19). Cependant, à elle seule, l'interaction entre le CBS et le β-galactoside aboutit à une liaison de faible affinité. Des interactions supplémentaires spécifiques de chaque galectine vont stabiliser ces liaisons et leur conférer une plus grande spécificité. Côté galectine, ces interactions mettent en jeu des acides aminés du CRD distincts du CBS. Du côté du ligand, elles mettent en jeu d'autres motifs moléculaires et atomiques, glucidiques ou non, distincts du β-galactoside reconnu par le CBS (20). Ainsi s'explique le fait que chacune des galectines, tout en utilisant le même mécanisme fondamental d'attachement, interagit avec un spectre de ligands polysaccharidiques spécifique. Au sein de ce spectre propre à chaque galectine, il existe une véritable gradation des affinités qui peut varier en fonction des conditions

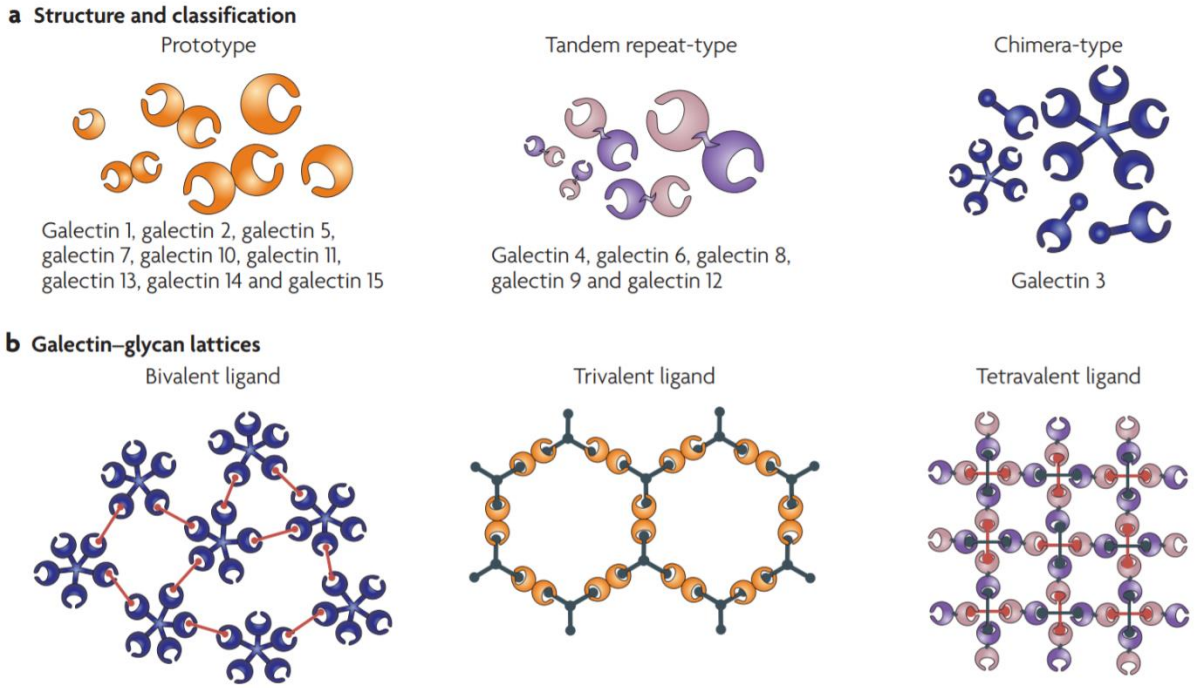

Figure 2. Interactions galectines-glycanes : caractéristiques structurales.

a) Représentation schématique des différentes catégories structurales des galectines (« prototypique », « avec répétition en tandem » et « de type chimérique »). b) Quelques exemples parmi les innombrables structures possibles de « lattices » ou de treillages résultant de l'interaction entre des galectines et des glycanes multivalents (2). De gauche à droite : galectine de type chimérique combinée à un glycane bivalent ; galectine prototypique combinée à un glycane trivalent ; galectine avec répétition en tandem combinée à un glycane quadrivalent. Dans la réalité, la complexité des « lattices » peut être beaucoup plus grande puisqu'elles peuvent englober différentes catégories de glycanes et probablement différentes galectines.

physico-chimiques, notamment en fonction de la concentration des galectines et de leur degré de polymérisation. Au maximum, on peut avoir une affinité comparable à celle d'un anticorps pour son antigène (21). En plus des interactions de type lectine avec des ligands polysaccharidiques qui mettent en jeu les CRD, les galectines peuvent se lier à d'autres types de ligands par des interactions protéine-protéine. Des études en cours tendent à prouver que ces interactions protéine-protéine peuvent modifier la conformation des galectines et par voie de conséquence le spectre de leurs interactions avec les ligands polysaccharidiques. Les interactions protéine-protéine des galectines ont été initialement rapportées pour des liaisons à des constituants cytosoliques et nucléaires (22) mais récemment elles ont été observées aussi pour les galectines extra-cellulaires. C'est par exemple le cas pour la galectine-1 qui interagit avec la région λ5 du pré-BCR au cours des étapes de prolifération et de différenciation des cellules B (23). Plus récemment, une interaction de la galectine-9 avec une autre lectine, la dectine-1, a été rapportée sur des macrophages dans un modèle de carcinome pancréatique murin (24).

Par soucis de normalisation de la nomenclature, la première galectine découverte (électrolectine) (25) fut finalement nommée galectine-1. Son homologue le plus proche fut nommé galectine-2, pour finalement rattacher à ce groupe les galectines 3 et 4 (26). Les autres membres de cette famille furent ensuite numérotés consécutivement par ordre de découverte jusqu'à un total actuel de 15 galectines, dont 11 retrouvées chez l'homme (27).

Sur la base de leur structure tertiaire, les galectines sont divisées en 3 groupes (28) : « prototype », « chimère » et « répétition en tandem ». Le premier groupe est constitué de galectines ne possédant qu'un seul CRD capable de s'homodimériser. Il comprend les galectines -1, -2, -5, -7, -10, -11, -13, -14 et -15. Le deuxième groupe n'est constitué que d'un seul membre, la galectine-3. Elle ne possède, elle aussi, qu'un seul CRD mais qui est associé à un domaine collagéneux N-terminal lui permettant de former des pentamères. Les membres du troisième groupe enfin, se caractérisent par la présence de deux CRDs reliés par une séquence polypeptidique (peptide de liaison). Il comprend les galectines -4, -6, -8, -9 et -12 (**Figure 2**). Dans certaines conditions, le fait de posséder deux CRDs pourrait renforcer les propriétés signalétiques de ces galectines (29). En effet, ces deux CRDs liés covalemment permettent, à des concentrations plus faibles que pour les galectines prototypes, la formation

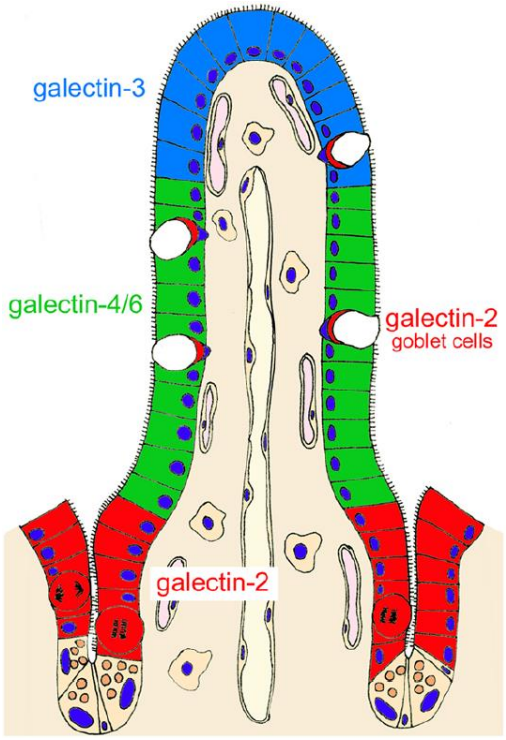

Figure 3. Profil d'expression de différentes galectines au sein d'une villosité du petit intestin, selon le stade de différenciation cellulaire (3).

de grands multimères. Ces grands multimères jouent un rôle important par exemple pour la formation de réseaux moléculaires structurés et étendus à la surface des membranes plasmiques que l'on appelle « *lattices* » (treillages en français).

b) Distribution tissulaire et fonctions

Les galectines peuvent être exprimées dans une grande variété de tissus. Leur profil d'expression, qui peut s'étendre d'un type tissulaire à plusieurs dizaines, peut évoluer au sein d'un même tissu selon son stade de développement (30), son degré de différenciation (3) (**Figure 3**) ou encore son état homéostasique (31).

Les galectines -1, -3, -8 et -9 sont les plus ubiquitaires. Chez l'homme, on les retrouve dans la moelle osseuse, les glandes endocrines, les organes lymphatiques, le placenta, et pour certaines d'entre elles également dans le tissu adipeux, le système nerveux central, les systèmes reproducteur et respiratoire (32). Au contraire, la galectine-13 présente un profil d'expression plus restreint et est principalement exprimée dans le placenta. Elle est d'ailleurs également connue sous le nom de *placental protein-13* (PP13) (33).

Dans la circulation enfin, les concentrations rapportées varient en fonction des galectines, des patients et des publications. Il est difficile d'estimer la concentration moyenne pour chacune d'entre elles tant la technique employée impacte la mesure (jusqu'à un facteur 50 d'écart) (34). Il est cependant possible pour une même technique de remarquer que certaines galectines, comme la galectine-1, sont abondantes dans la circulation alors que d'autres, comme la galectine-9, sont faiblement représentées (35).

Comme mentionné précédemment, l'expression des galectines est modulée au cours de différentes phases du développement, de la différenciation cellulaire ainsi que sous certaines conditions physiologiques, voire pathologiques, particulières. Plusieurs facteurs sont connus comme étant impliqué dans ces modifications d'expression. Le stress oxydant par exemple, mimé par la menadione, induit une augmentation de l'expression des galectines -1, -3 ,-8 et -10, ainsi que la diminution de l'expression de la gal-9 (36). Les régimes alimentaires hyper-caloriques entraînent des modifications d'expressions des galectines -1, -3, -9 et -12 dans la circulation, au niveau des adipocytes, ou de macrophages localisés dans les tissus adipeux

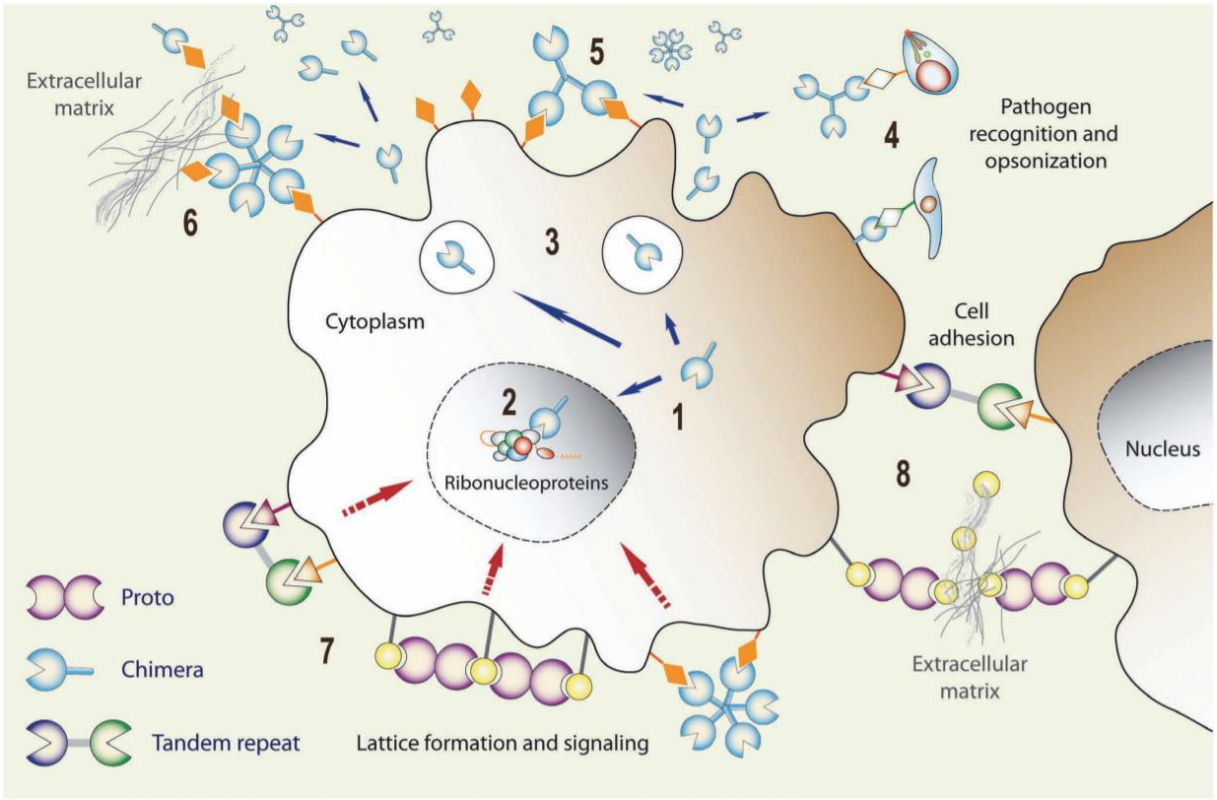

Figure 4. Expression, sécrétion, et diversité fonctionnelle des galectines.

1) Les transcrits des galectines sont traduits dans le cytoplasme, et les protéines peuvent transloquer dans le noyau 2) où elles peuvent s'associer avec des protéines ribonucléaires. 3) Les galectines néo-synthétisées peuvent être acheminées suivant des mécanismes non conventionnels et mal connus vers le milieu extra-cellulaire. Elles peuvent alors se lier à des glycanes présents à la surface de la membrane plasmique ou dans la matrice extra-cellulaire ou encore diffuser dans le milieu interstitiel. A la surface de la membrane plasmique les galectines favorisent la formation de treillages qui jouent un rôle dans l'organisation latérale de la membrane et dans des phénomènes d'internalisation et de signalisation. Les galectines de la surface cellulaire peuvent aussi favoriser les contacts entre cellules. Les interactions avec la matrice extra-cellulaire peuvent favoriser l'adhésion des cellules sur cette matrice et leur migration. Enfin, les galectines extra-cellulaire 4) peuvent se lier à des glycanes microbiens, 5) s'attacher à la surface de la cellule productrice ou des cellules voisines, 6) former des liaisons avec les glycanes de la matrice extra-cellulaire et ainsi promouvoir la migration cellulaire. 7) Elles peuvent également s'associer à la surface de la cellule pour former des lattices et induire des cascades signalétiques, 8) et peuvent promouvoir des interactions/adhésions cellules-cellules (4).

viscéraux et sous-cutanés (37). La modulation de l'expression des galectines intervient également dans la régulation de l'inflammation. L'interféron gamma est par exemple capable d'induire une augmentation de l'expression de la gal-9 (38). Dans le cas d'infections par le virus HTLV1, il a également été rapporté un impact direct de la protéine virale Tax sur l'augmentation de l'expression de gal-1 au niveau transcriptomique (39).

Plusieurs études ont été réalisées sur des modèles murins invalidés pour l'expression d'une des galectines. Ces travaux n'ont pas révélé de phénotype létal associé à l'absence de l'une d'entre elles. Il semblerait plutôt que leur absence soit associée à une difficulté de l'organisme à s'adapter à des situations de stress. Ainsi, on observe sur les souris KO gal-1 une diminution de la régénération des fibres musculaires (40). Sur les souris KO gal-7, on observe un défaut de réparation de l'épithélium qui se caractérise notamment par un ralentissement du processus de cicatrisation, ainsi qu'une hyper-kératinisation après exposition aux UVB (41). Les souris KO gal-3, elles, présentent des protrusions intestinales qui pourraient être associées à un défaut de différenciation des entérocytes. En effet, ceux-ci présentent, en l'absence de gal-3, un défaut au niveau du trafic protéique intra-cellulaire (42).

c) Localisation cellulaire et interactions moléculaires

L'abondance et la diversité des fonctions exercées par les galectines s'explique en partie par leur présence dans des compartiments cellulaires très diverses (**Figure 4**). Il est possible de distinguer trois grands types de localisations sub-cellulaires des galectines : 1) les localisations intra-cellulaires avec présence des galectines dans le cytoplasme ou dans le noyau ; 2) la localisation sur la surface externe de la membrane plasmique qui résulte généralement d'une interaction avec les polysaccharides de la surface cellulaire portés par des glycoprotéines ou des glycolipides (l'ensemble de ces polysaccharides formant le « glycocalix ») ; 3) enfin la présence possible de galectines dans le milieu extracellulaire.

L'exemple de la gal-3 donne une idée de la diversité des localisations et des fonctions que peuvent exercer les galectines à l'intérieur des cellules. Lorsque la gal-3 est présente dans le cytosol, elle est capable d'interagir avec la GTPase KRAS (43), et d'ainsi moduler l'intensité et la durée du signal (44). Elle peut également s'accumuler autour de vésicules endommagées

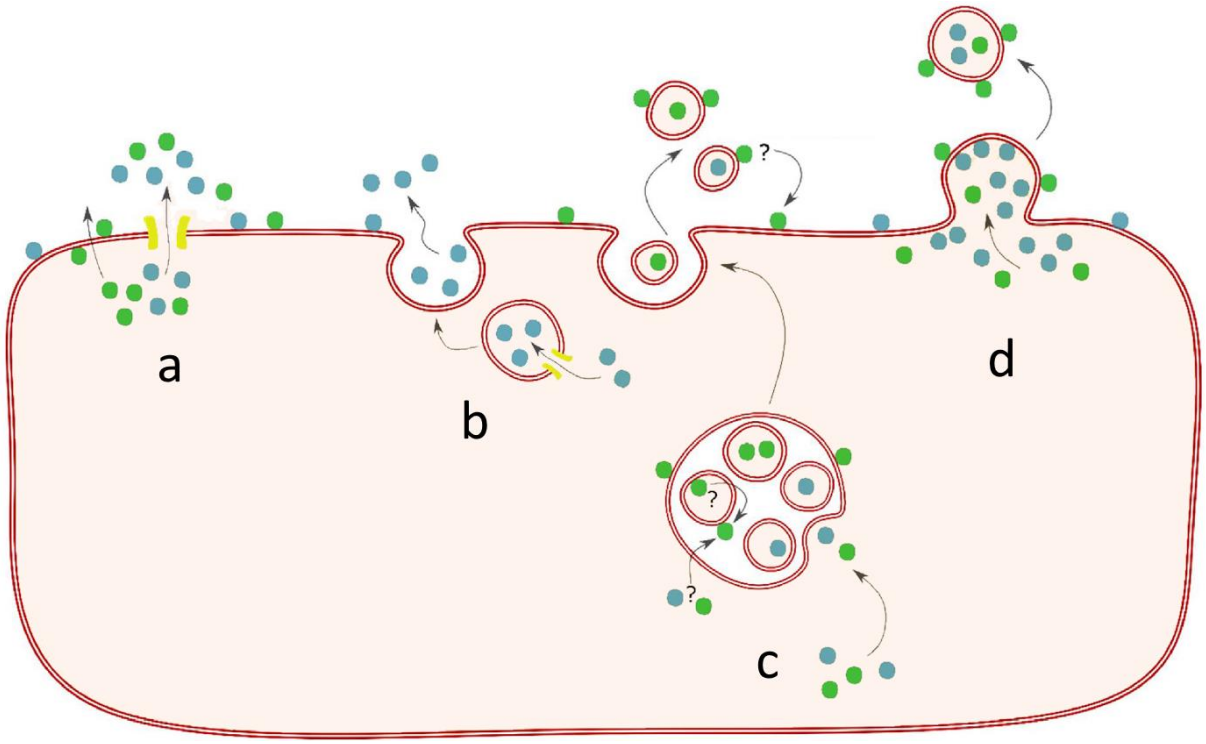

Figure 5. Mécanismes de sécrétion non-conventionnels des galectines.

a) Translocation directe facilitée ou non par un transporteur ; b) export en association à des endosomes, des lysosomes, ou c) des exosomes ; d) exocytose après accumulation des galectines sous la membrane plasmique (adaptée de S.J. Popa et al. (5)).

(45) et médier la réponse autophagique (46). Cette galectine est également capable d'interagir avec l'importine-α pour transiter à travers les pores nucléaires (47). Une fois dans le noyau, la gal-3 peut intervenir dans l'épissage des ARN pré-messagers (48). En règle générale, les galectines à l'intérieur des cellules vont exercer des fonctions relatives à la croissance, la différenciation, la survie, l'architecture et la polarisation cellulaires ou encore la migration cellulaire. La contribution des galectines au marquage, à la réparation et au recyclage des vésicules intra-cellulaires endommagées est un sujet d'étude qui s'est révélé particulièrement fécond au cours des dernières années. L'impulsion initiale a été donnée par l'équipe de Philippe Sansonetti à l'institut Pasteur. Leur étude portait sur la pénétration des bactéries de type Shigella dans les macrophages ou les cellules épithéliales. Ils ont montré que les phagosomes ou les vésicules porteuses de bactéries recrutaient la gal-3 cytosolique en modifiant le répertoire des polysaccharides exposés sur leur face externe. Il a été montré ensuite que ce marquage par les galectines des vésicules intra-cellulaires entraînait leur changement de destination vers des compartiments autophagiques (49). A la suite de ces travaux, les mêmes concepts ont été étendus à toute sorte de situations d'agression cellulaire impliquant des vésicules internes depuis l'utilisation d'agents de transfection pour la thérapie génique jusqu'aux effets toxiques d'agrégats protéiques dans les maladies nerveuses dégénératives (50).

Les galectines de la surface cellulaire y sont acheminées par divers types de cheminements (51). Soit elles s'associent aux polysaccharides en formation dans les vésicules post-golgiennes et se retrouvent exposées à la surface de la cellule lorsque ces véhicules s'incorporent la membrane plasmique, soit elles sont secrétées dans le milieu extracellulaire par des mécanismes encore mal connus (**Figure 5**) et s'attachent secondairement aux polysaccharides de la surface cellulaire. Chacune des galectines interagissant spécifiquement avec un sous-groupe de polysaccharides tend à créer des ponts intermoléculaires entre glycoprotéines et glycolipides à la surface de la cellule. Ces phénomènes sont amplifiés par la tendance des galectines à former des multimères et par la bivalence des galectines en tandem. Il en résulte des phénomènes de redistribution des biomolécules à la surface de la membrane plasmique. C'est pourquoi les galectines sont des acteurs clés dans ce qu'on appelle « l'organisation latérale de la membrane ». En particulier, elles peuvent induire une organisation en réseaux des glycoprotéines ou des glycolipides. On parle de la formation de

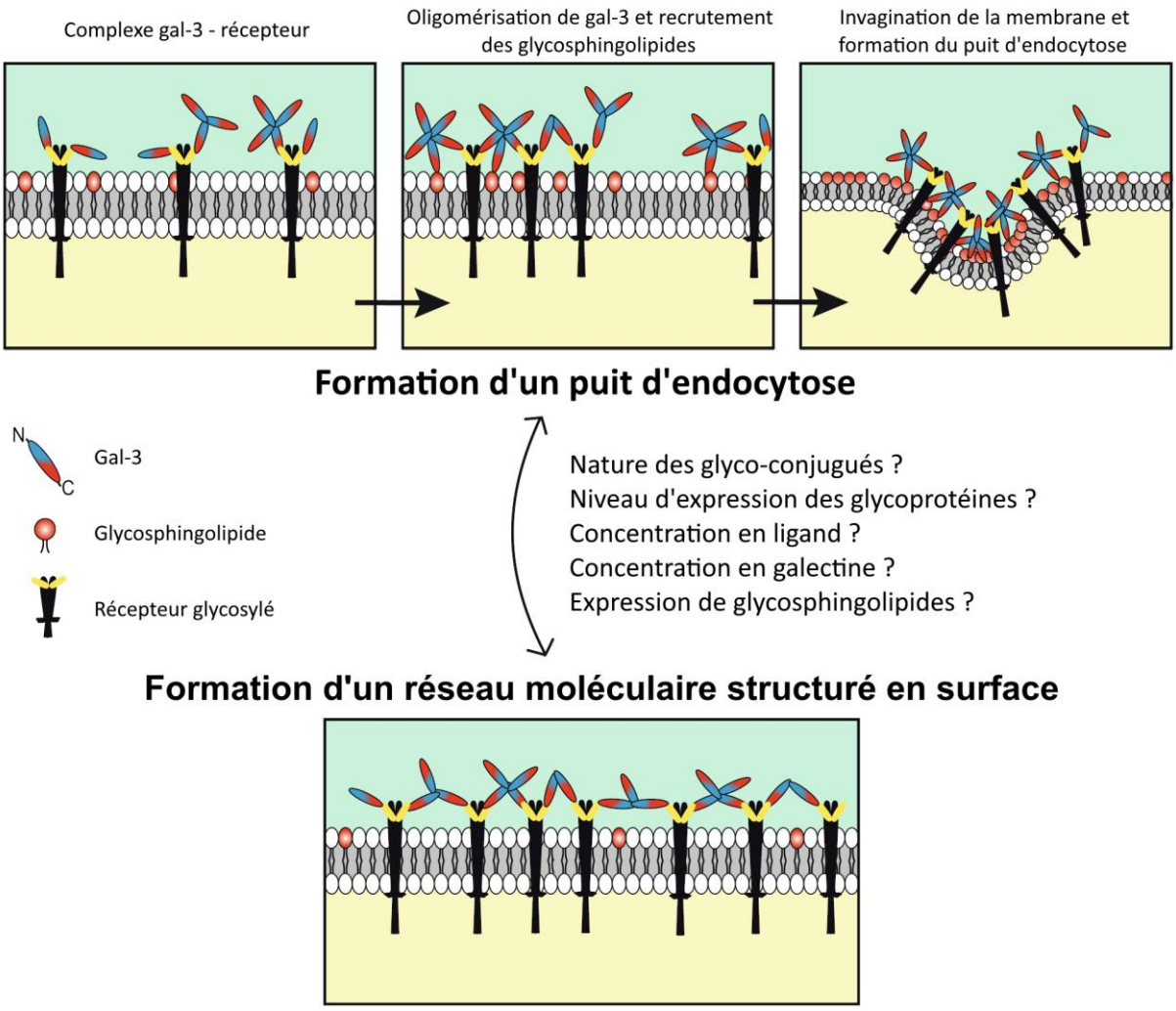

Figure 6. Exemples de complexes galectines-9/glycanes à la surface des cellules.

Représentation schématique de deux scénarios alternatifs. En haut : hypothèse de la formation d'un puit d'endocytose dépendante d'interactions entre la gal-3 et des glycosphingolipides. En bas : formation d'un réseau moléculaire structuré (treillage) à la surface des cellules par la gal-3, permettant la rétention et l'agglomération de récepteurs cellulaires. Différents éléments peuvent réguler la balance entre ces deux fonctions (adapté de L. Johannes et A. Billet (6), et R. Lakshminarayan et al. (7))

« *lattices* » (treillages en français). La formation de ces lattices enserrant des récepteurs de membrane retentit sur leur capacité de transmission des signaux vers l'intérieur de la cellule, soit pour les augmenter, soit pour les diminuer. Ces phénomènes de modulation par les galectines concernent notamment les récepteurs de facteurs de croissance et des cytokines, les récepteurs des antigènes des cellules T et des cellules B. En outre les galectines de la surface cellulaire peuvent entraîner une coalescence des microdomaines membranaires riches en glycolipides (encore appelés glycosphingolipides ou GSL). Des auteurs, et tout particulièrement l'équipe de L. Johannes à l'Institut Curie, ont montré que ce phénomène de coalescence des microdomaines riches en GSL pouvait déclencher des modifications mécaniques majeures impliquant le cytosquelette sous-jacent et aboutissant à un phénomène d'endocytose particulier appelé endocytose de type CLIC (*clathrin independent carriers*) (52). Ce phénomène est marqué morphologiquement par la formation de profondes invaginations membranaires ou puits d'endocytose et biochimiquement par la participation de la dynéine (**Figure 6**). Il jouerait un rôle physiologique dans l'internalisation de certaines protéines de la membrane plasmique. Par exemple, d'après les travaux de l'équipe de L. Johannes, la gal-3 jouerait un rôle majeur pour déclencher l'endocytose de type CLIC pour l'intégrine $\alpha 5\beta 1$ et pour le récepteur CD44 (7). Une des hypothèses majeures de cette équipe consiste à dire que les observations faites à propos de la gal-3 ne sont pas du tout accidentelles mais correspondent à un processus physiologique d'endocytose bien distinct de celui des vésicules mantelées par la clathrine ou des cavéoles. Leur idée est que d'autres galectines participent à des processus semblables. Cette idée est résumée dans le terme d'hypothèse « glycolipide et lectine » (GL-lect) (6,52).

En plus des fonctions exercées à l'intérieur ou à la surface des cellules, les galectines ont de nombreuses fonctions dans le milieu extra-cellulaire. Les mécanismes qui permettent aux galectines produites par une cellule de gagner l'espace extracellulaire restent encore très mal compris. En effet les galectines, dépourvues de peptide signal permettant leur adressage au réticulum endoplasmique, sont sécrétées via des mécanismes non conventionnels. Plusieurs études se sont penchées sur ces mécanismes. Ces derniers ne sont décrits que pour une poignée de galectines (gal-1 et -3 principalement) dans des contextes particuliers. Néanmoins, ces travaux nous permettent d'appréhender la diversité des voies de sécrétion exploitables par les membres de cette famille. Ainsi, il semblerait que la

translocation directe soit un moyen de sécrétion possible. Il a été montré que la gal-3 était capable d'interagir avec des lipides membranaires et de traverser spontanément la membrane plasmique dans des modèles de cellules vivantes, ainsi que dans des modèles de membrane dépourvus de protéines (53). Ce phénomène, également observé sur des modèles déficients pour les fonctions de glycosylation, semble donc indépendant d'interactions avec des glucides (54,55). Les autres moyens de sécrétion possibles sont axés sur la libération de vésicules porteuses de galectines. Il peut s'agir de microvésicules, dont la formation a par exemple été décrite pour la gal-1 après son accumulation sous la membrane plasmique (56). Il peut également s'agir d'une libération via des exosomes ou encore des lysosomes libérés dans le milieu extra-cellulaire (5). La manière dont les galectines intègrent le compartiment endosomal reste peu connue. Une voie possible pourrait être l'adsorption sur des vésicules endommagées. Mécanisme que nous avons mentionné précédemment et qui concerne les galectines (-1, -3, -8 et -9) (57). Ces dernières pourraient, après réparation de la vésicule, rester associées. Cette explication n'est toutefois pas satisfaisante pour la majorité des cellules qui sécrètent constitutivement des galectines. Elle représente néanmoins une piste intéressante dans le cadre de l'étude de signaux émis en réponse à un stress cellulaire. En ce qui concerne la libération via des exosomes, mon équipe d'accueil a été la première à la mettre en évidence pour le transport de la gal-9 extra-cellulaire (58,59). Toutefois, les indices du mécanisme de formation nous proviennent d'une étude récente menée sur la galectine-3. Celle-ci nous révèle une interaction directe de la protéine Tsg101 avec un motif très conservé de la gal-3 (P(S/T)AP). Tsg101 est une protéine faisant partie d'un complexe protéique impliqué dans la formation des vésicules intra-luminales au sein des corps multivésiculaires. Les auteurs ont démontré que l'interaction avec cette protéine permet le recrutement de la gal-3 dans ces vésicules intra-luminales (60).

Une fois dans le milieu extra-cellulaire, les galectines vont pouvoir interagir avec de nouveaux partenaires et intervenir dans la régulation d'autres processus. Elles sont notamment impliquées dans l'assemblage, l'organisation et la régulation de récepteurs membranaires (61). Certaines d'entre elles sont connues pour moduler l'adhésion cellulaire ou l'apoptose. Elles peuvent agir localement mais également à distance, après avoir transité dans la circulation et notamment dans la régulation du système immunitaire, les rendant comparables aux cytokines

II – Propriétés fonctionnelles de la galectine-9 intra-cellulaire

Comme d'autres galectines, lorsque la gal-9 s'exprime dans une cellule, elle est obligatoirement présente dans son cytoplasme, là-même où elle synthétisée. Elle peut également être transportée dans les divers compartiments cytoplasmiques, dans le noyau ainsi qu'à la surface de la membrane plasmique. Elle peut en outre être libérée dans le milieu extra-cellulaire. Nous envisagerons successivement les fonctions de la gal-9 lorsqu'elle est localisée dans le cytoplasme puis lorsqu'elle est localisée à la surface de la membrane plasmique. Ensuite, nous aborderons les fonctions de la gal-9 extra-cellulaire. A noter que l'on ignore encore les fonctions de la gal-9 nucléaire.

a) Fonctions dans la mise en place et le maintien de l'architecture cellulaire

Il y a déjà 10 ans, l'équipe de K. Simons a mis en évidence une contribution majeure de la gal-9 à l'entretien de la polarité apico-basale des cellules MDCK (*Madin-Darby canine kidney*) (62). La réduction d'expression de la gal-9 réduit fortement la polarisation de ces cellules qui semble dépendante d'un mécanisme de circulation de la gal-9 qui interagit à la surface de la membrane plasmique avec un glycosphingolipide appelé antigène de Forssman (FGL). Le complexe FGL-gal-9 est endocytosé et dirigé vers l'appareil de Golgi. De là, la gal-9 retourne à la membrane plasmique. Cette circulation de la gal-9 semble conditionner celle d'un ensemble de protéines de la surface cellulaire dont la distribution conditionne la polarité cellulaire.

b) Fonctions dans l'autophagie

La gal-9 exerce une influence sur 2 types de processus en relation avec l'autophagie :

1) Comme la gal-8, elle joue un rôle dans l'élimination des endovésicules endommagées. Elle est capable de venir se fixer sur la face cytoplasmique d'endomembranes endommagées. Ce phénomène, initialement décrit comme un mécanisme « d'étiquetage » du dommage a récemment été repris dans une étude publiée dans *Molecular Cell* (63). Celle-ci démontre l'implication de la gal-9 dans l'activation

d'AMPK (*AMP-activated protein kinase*), elle-même impliquée dans l'inhibition de mTOR (*mammalian target of rapamycin*). L'ensemble des interactions moléculaires décrites dans cette étude met à jour l'implication de la gal-9 dans la promotion d'une réponse autophagique en réponse à certains dommages des endomembranes.

2) D'autre part, la gal-9 est capable d'empêcher la fusion des lysosomes et des autophagosomes. Des auteurs ont ainsi décrit un effet toxique de la gal-9 sur des cellules tumorales dont la survie dépend d'un fort flux autophagique, nécessaire pour répondre à leurs besoins métaboliques et leur activité tumorigène (64). Dans cet article, la gal-9 agit sur les cellules tumorales après internalisation et accumulation dans les vésicules lysosomales, en empêchant la fusion de ces lysosomes avec les autophagosomes. Bien que le phénomène décrit soit différent, il représente un élément supplémentaire qui confirme la participation de la gal-9 à différents aspects du processus d'autophagie.

c) Organisation membranaire et signalisation

Comme mentionné dans la 1ère partie, les galectines extra-cellulaires participent à l'organisation de la membrane plasmique. Il semblerait que des fonctions similaires puissent également être attribuées à la gal-9 intra-cellulaire. En effet, une publication réalisée par une équipe spécialisée dans l'étude de l'organisation membranaire des cellules présentatrices d'antigènes, démontre l'implication de la gal-9 intra-cellulaire dans le processus de phagocytose des cellules dendritiques (65). Pour être plus précis, la perte d'expression de la gal-9 diminuerait la capacité des cellules dendritiques à phagocyter. Les auteurs montrent que la perte de gal-9, normalement présente dans le cortex cellulaire et étroitement associée au cytosquelette d'actine, entraîne une perte de rigidité de la membrane. Ce phénomène est plus globalement accompagné d'une perte d'activation de la protéine Rac1, une Rho GTPase impliquée dans la polymérisation de l'actine, ainsi qu'une diminution de la concentration d'actine filamenteuse (actine-F) dans la cellule. Cette dernière observation pourrait expliquer le déficit fonctionnel des cellules dendritiques invalidées pour la gal-9, puisque l'actine-F participe à la formation des protrusions membranaires à l'origine de la phagocytose.

Enfin, une autre étude récente a mis en évidence un recrutement de la gal-9 intra-cellulaire dans des lymphocytes T au niveau de la synapse immunologique après une stimulation avec des anti-CD3/CD28. Cette accumulation de gal-9 au niveau de la synapse semble être impliquée dans la signalisation induite au niveau du TCR. En effet, les cellules T *Lgals9*$^{-/-}$ prolifèrent moins et expriment moins d'IFN-γ, d'Il-17 and de TNF-α, en réponse à cette même stimulation (66).

Hormis ces quelques données, on ne dispose que de peu d'informations quant aux fonctions exercées par la gal-9 à l'intérieure de la cellule. La majorité des travaux de recherche qui touchent à la gal-9 sont davantage axées sur ses fonctions « *cytokine-like* », premières fonctions décrites pour cette galectine.

III – Propriétés fonctionnelles de la galectine-9 extra-cellulaire

La notion d'une activité biologique de la gal-9 extracellulaire a émergé en 2002 avec une publication du groupe d'Hirashima sur son activité comme facteur chimiotactique des éosinophiles (67). Cependant, c'est surtout la publication de Zhu et al. en 2005 qui a mis en exergue la gal-9 extra-cellulaire en l'identifiant comme l'un des principaux ligands du récepteur Tim-3 à la surface des lymphocytes T CD4^{+} Th1 (*T-helper 1*) chez la souris (68).

Dans les années qui ont suivi, mon équipe d'accueil a mis en évidence le transport de la gal-9 extracellulaire par les exosomes tumoraux de carcinome nasopharyngé (NPC, *Nasopharyngeal carcinoma*) (58), et a apporté des arguments expérimentaux en faveur de l'activité immunosuppressive de ces exosomes chez les patients porteurs de NPC (59).

Globalement, à l'échelle de l'organisme entier, la gal-9 a une activité immunosuppressive, démontrée dans des modèles murins variés : allogreffes, maladies auto-immunes expérimentales, modèles tumoraux syngéniques ; comme nous pourrons le constater dans les prochaines parties. Cette activité immunosuppressive globale résulte d'effets multiples sur de nombreux types cellulaires. En règle générale la gal-9 tend à inhiber l'activité des cellules effectrices des réponses immunitaires et à renforcer l'activité des cellules suppressives. Nous

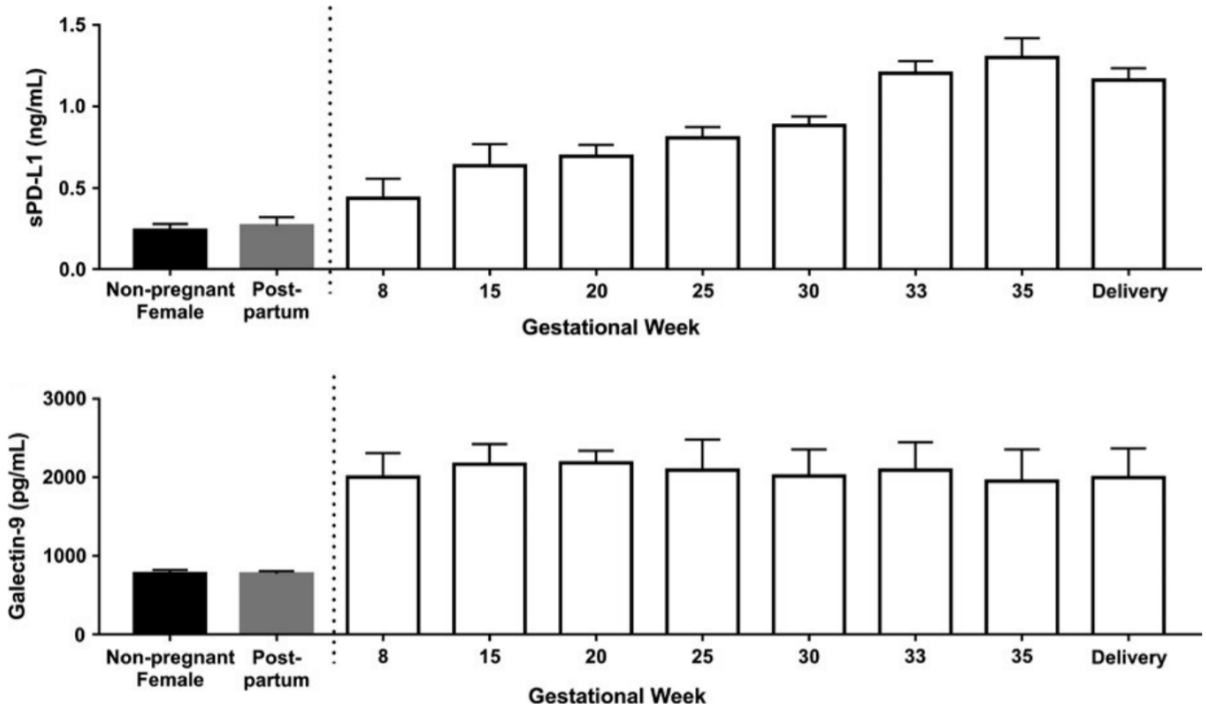

Figure 7. Augmentation des concentrations plasmatiques de PD-L1 (*Programmed death-ligand 1*) et de gal-9 chez les femmes enceintes.

Alors que la concentration de PD-L1 augmente régulièrement tout au long de la gestation et commence à baisser juste avant l'accouchement, la concentration de gal-9 reste, elle, très élevée tout au long de la gestation (8).

envisagerons successivement les effets de la gal-9 extracellulaire sur les cellules de l'immunité innée puis sur les cellules de l'immunité adaptative.

Enfin, même si les effets de la gal-9 sur le système immunitaire sont prépondérants, celle-ci peut aussi avoir d'autres effets, en particulier sur l'angiogenèse. Ceux-ci seront envisagés dans le dernier paragraphe de ce chapitre.

a) Régulation de la réponse immunitaire innée

Décrite en 1998, la capacité chimiotactique de la gal-9 fut la première fonction de cette protéine à être publiée (69). D'abord rapportée pour les granulocytes éosinophiles, elle n'a été que récemment décrite pour les cellules NK (*Natural Killer*) (70). Cette fonction, associée à l'induction de l'expression de la gal-9 en réponse à une stimulation du TLR3 (*Toll Like Receptor 3*) (71,72) ou en réponse à l'IFN-γ (Interféron-γ) (38), met en avant son rôle dans l'initiation de la réponse immunitaire innée. Elle exerce d'ailleurs, conjointement à ces effets chimiotactiques, plusieurs fonctions régulatrices sur les cellules de l'immunité innée qui sont détaillées ci-dessous.

- **Eosinophiles**. En plus de ses propriétés chimio-attractantes, la gal-9 induit la production de superoxydes et améliore la survie des éosinophiles *in vitro* de façon dépendant de Tim-3 (*T-cell immunoglobulin and mucin-domain containing-3*) (67). Cependant, ces effets de la gal-9 sur les éosinophiles n'ont pas été confirmés dans des publications ultérieures, ni par le groupe d'Hirashima lui-même, ni par d'autres groupes.

- **Neutrophiles**. La gal-9 induit la dégranulation et stimule l'activité NADPH oxydase des neutrophiles. On a également montré qu'elle était capable d'améliorer la phagocytose des bactéries du genre *Pseudomonas Aeruginosa* en facilitant leur opsonisation (73).

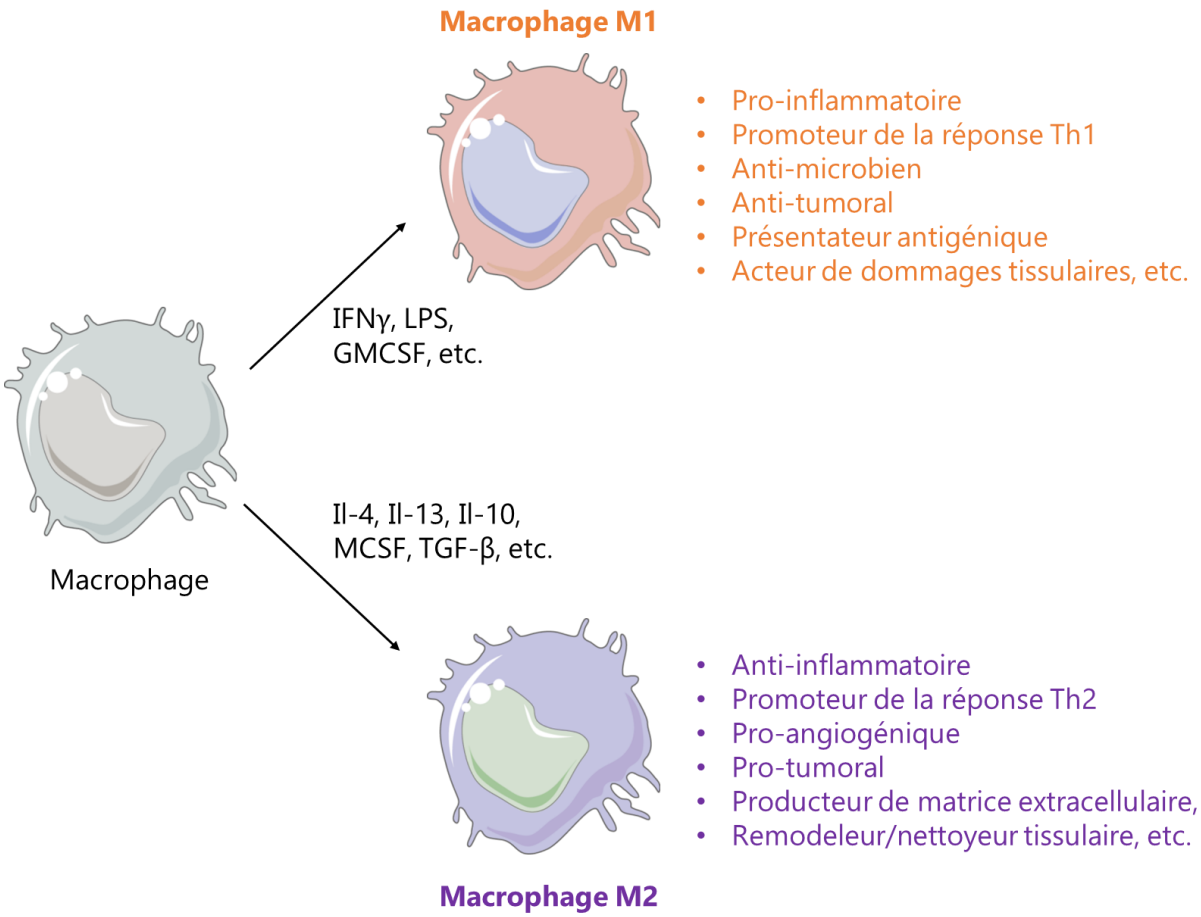

Figure 8. Polarisation des macrophages et fonctions spécifiques aux types 1 et 2.

Différents stimuli peuvent influencer la polarisation des macrophages vers un phénotype M1 ou M2. Alors que les macrophages M1 produisent des cytokines inflammatoires et exercent des fonctions cytotoxiques, les macrophages M2 sont associés à la diminution de la réponse immunitaire et la régénération du tissu (adaptée de U. Saqib et al. (9)).

- **Basophiles**. La gal-9 est capable de lier les immunoglobulines d'isotype IgD au CD44 présent à la surface des basophiles. Elle participe ainsi à l'activation de ces cellules, entraînant une production d'Il-4 et une augmentation de la réponse Th2 (74).

- **Cellules NK**. Plusieurs publications relatives à la physiologie et à l'immunologie de la grossesse, s'accordent pour dire que la gal-9 induit une diminution du potentiel cytotoxique des cellules NK. Dans les premières phases de la grossesse, l'expression du récepteur Tim-3 augmente sur les cellules NK du sang périphérique. Ce phénomène qui paraît dépendant de l'action de la progestérone (75), les rend sensibles à la gal-9 qui est abondamment exprimée au niveau du trophoblaste et de la membrane décidiuale. La gal-9, via le récepteur Tim-3, diminue la capacité de dégranulation des cellules NK (76), la production de perforine ou de TNF-α (*Tumor necrosis factor-α*), au profit d'une expression accrue de cytokines anti-inflammatoires (TGF-β1 (*Transforming growth factor-β1*), Il-10, Il-4) (75). Le rôle que la gal-9 joue dans l'établissement de cette immunosuppression (77,78) est fondamentale et ne va pas sans rappeler l'importance de PD-1 (79), un autre facteur immunosuppresseur fortement exprimé chez les femmes enceintes (8) (**Figure 7**).

  Nota bene : On remarque l'analogie qui existe entre l'établissement d'un environnement immunosuppresseur visant à préserver le fœtus et celui qui, dans un cadre pathologique, permet à la tumeur d'échapper à l'action du système immunitaire. Il est d'ailleurs intéressant de constater que certains chercheurs travaillent conjointement sur ces deux thématiques (8,80).

- **Monocytes/macrophages**. Plusieurs fois décrite dans un contexte tumoral, la capacité de la gal-9 d'induire une polarisation des macrophages vers un phénotype M2 au détriment d'un phénotype M1 (**Figure 8**) confirme le potentiel immunosuppresseur de cette protéine (80,81). Des essais *in vitro* visant à caractériser ce phénomène mettent en avant l'implication du récepteur Tim-3 (82). Un autre étude décrit, dans un modèle murin de carcinome pancréatique, une reprogrammation des macrophages vers un phénotype M2 dépendant de la dectine-1 (24). Dans ce modèle,

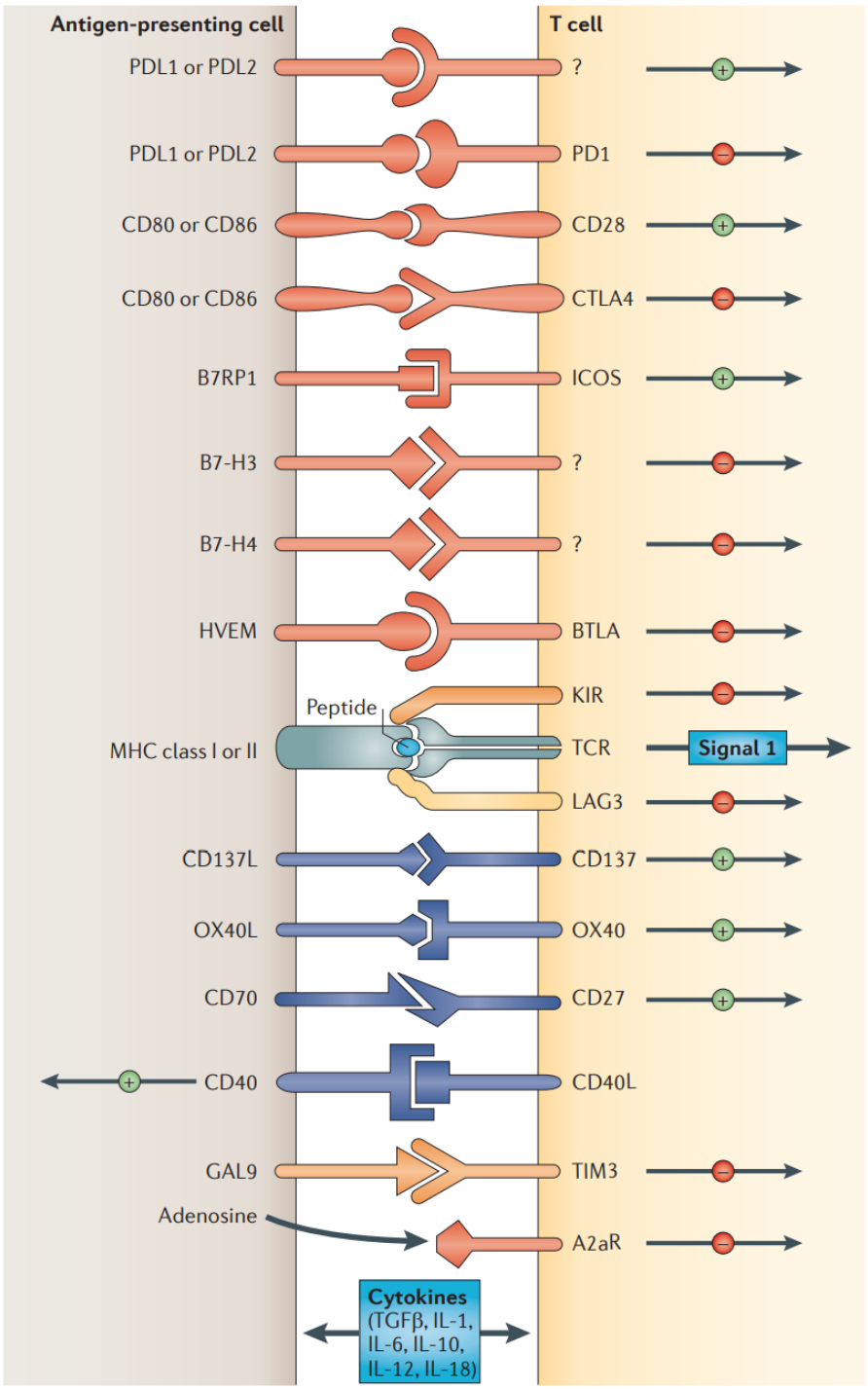

Figure 9. Molécules de co-stimulation et d'inhibition permettant de réguler la réponse T.

Différentes interactions ligand-récepteur entre la cellule T et la cellule présentatrice d'antigène sont représentées. Celles-ci permettent de réguler la réponse à l'antigène dans les ganglions, les tissus périphériques ou encore dans la tumeur. Généralement, les cellules T ne répondent à ces interactions qu'après avoir reconnu l'antigène, et les récepteurs inhibiteurs sont up-régulés après la phase d'activation. La communication entre les lymphocytes T et les cellules présentatrices d'antigènes est bidirectionnelle (10).

l'invalidation de la dectine-1 est associée à une diminution de l'infiltration par les macrophages $CD206^+$. Une étude complémentaire rapporte une redondance fonctionnelle entre la dectine-1 et CD206, dont l'interaction directe avec la gal-9 induit également une polarisation vers un phénotype M2 (83).

- **Cellules dendritiques**. Les cellules dendritiques présentes dans la muqueuse intestinale jouent un rôle crucial dans l'établissement d'une tolérance immunitaire en dépit des nombreux antigènes présents dans la lumière du tube digestif. Il semble que la gal-9 produite par les cellules intestinales joue un rôle dans ce phénomène. En effet, des chercheurs ont montré que la préexposition de cellules dendritiques à la gal-9 diminue l'expression de CD40 et de CD80 en réponse à une stimulation par du LPS (lipopolysaccharide) (84). La gal-9 permet également d'induire chez ces cellules une augmentation de l'activité ALDH (*Aldehydedehydrogenase*) (85). Paradoxalement, une autre étude a montré que l'ajout de gal-9 sur des cellules dendritiques immatures dérivées de monocytes en culture, participe à leur différenciation et leur maturation, notamment en induisant une augmentation du niveau d'expression des récepteurs CD80/86 (86).

- **MDSCs (*Myeloid-derived supressor cells*)**. L'interaction Tim-3/gal-9 participe à l'expansion des MDSC chez la souris ($CD11b^+Ly6G^+F4/80^{low}$) (87). Certaines données suggèrent même que l'augmentation d'expression de Tim-3 et de gal-9, notamment dans le compartiment des MDSC monocytiques, pourrait être associée avec la mise en place de résistances primaires et secondaires chez des patients traités avec des anti-PD-1 (88).

b) Régulation de la réponse immunitaire adaptative

Comme mentionné précédemment, plusieurs des fonctions associées à la gal-9 sont médiées par le récepteur Tim-3. Cette protéine, exprimée par plusieurs acteurs de l'immunité, est considérée comme une molécule de co-inhibition de la réponse T (10) (**Figure 9**). La première publication rapportant les fonctions immunosuppressives du couple Gal-9/Tim-3 a

été publiée en 2005. Elle représente le premier travail de recherche mettant en évidence le rôle immunosuppresseur de la gal-9. Cette publication a démontré comment la gal-9 est capable d'induire l'apoptose des lymphocytes $CD4^+$ Th1 (*T-helper1*) chez la souris (68). D'emblée, ces auteurs ont présenté la gal-9 comme un frein physiologique facilitant la terminaison de la réponse immunitaire : *« the IFN-γ that induces tissue inflammation also induces an inhibitory ligand (galectin-9) in the target tissue, which delete Th1 cells and thereby prevents protracted inflammation in target organs* ».

Plusieurs équipes et notamment mon équipe d'accueil ont mené des travaux pour déterminer si ces résultats pouvaient être étendus à l'homme. Mon équipe a observé que même des concentrations relativement faibles de gal-9 recombinante – de l'ordre de 30nM - entraînent l'apoptose des lymphocytes T, CD4 et CD8, indépendamment du phénotype Th1 et de l'expression de Tim-3 (89). Le mécanisme de cette entrée en apoptose reste mal compris. Mon équipe a montré que l'addition de gal-9 entraîne une mobilisation calcique presque immédiate qui nécessite l'intégrité du complexe TCR. L'invalidation de la chaîne TCRβ ou de la chaîne CD3ζ ou encore de la tyrosine kinase Lck abolit cette mobilisation calcique sans empêcher l'entrée en apoptose (89). On peut tirer de ces expériences une conclusion et une hypothèse. La conclusion est que l'induction de l'apoptose par la gal-9 recombinante est indépendante de la mobilisation calcique. L'hypothèse consiste à dire que la mobilisation calcique induite par la gal-9 résulte peut-être d'une interaction directe de celle-ci avec le TCR, ce qui reste à démontrer. Sachant qu'une stimulation continue et de faible intensité du TCR favorise l'émergence d'un phénotype suppresseur, des données sur ce point pourraient orienter vers une nouvelle fonction suppressive de la gal-9 (90).

Gooden et al. ont rapporté qu'en traitant *in vitro* des PBMC (*Peripheral blood mononuclear cells*) humains au repos avec de faibles concentrations de gal-9, on déclenche tout d'abord une vague d'apoptose parmi les cellules T. Vague qui est prédominante pendant 3 jours. Cependant, au-delà du $3^{ème}$ jour, on assiste à une expansion des lymphocytes T survivants (91). Ces lymphocytes T $CD4^+$ survivant et proliférant sont majoritairement de phénotype $CD4^+$ « *central memory* », c'est-à-dire $CCR7^+CD45RO^+$. Ils sont également fortement producteurs d'IFN-γ. Il pourrait donc s'agir de lymphocytes Th1 mais d'autres investigations seraient nécessaires pour le confirmer. Une étude en cours dans notre équipe portant sur les

lymphocytes T survivants après traitement par la gal-9 n'est pas en faveur de cette hypothèse (Tram Thi Bao Tran, thèse en cours).

Les cellules Th1 ne sont pas les seules cibles permettant à la gal-9 d'inhiber la réponse immunitaire à médiation cellulaire. Plusieurs équipes de recherche ont également mis en avant l'effet inhibiteur de la gal-9 sur les LT $CD8^+$. Cette régulation négative a d'abord été rapportée dans un modèle murin d'allogreffe dans lequel la gal-9 exogène induit l'apoptose des LT cytotoxiques alloréactifs (92), et a ensuite été vérifiée sur des LT $CD8^+$ isolés à partir d'un ganglion murin (93). Cet effet a également été étudié chez des patients atteints d'infections virales chroniques en révélant une dysfonction et un épuisement de ces cellules (94,95). Nous reviendrons plus en détail sur cet aspect dans la partie traitant des pathologies associées à la gal-9.

D'autres travaux réalisés *in vitro* sur des LT $CD4^+$ murins naïfs révèlent que la gal-9 induit la différenciation des cellules en Treg (lymphocytes T-régulateurs) et réprime leur différenciation en Th17 (96,97). Ces deux propriétés ont été décrites comme indépendantes d'interactions avec le récepteur Tim-3. Cette information s'est confirmée 2 ans plus tard dans le cadre d'une étude menée chez l'homme sur des Treg induits, mettant à jour un nouveau partenaire d'interaction de la gal-9. Dans cet article, les auteurs décrivent comment la gal-9, en permettant la formation d'un complexe CD44-TGFβRI, participe à la génération et la fonction des Treg induits (98). Récemment, le même type d'interaction faisant cette fois intervenir la gal-9, CD44 et des IgD, a été décrit comment étant à l'origine d'une amplification de la réponse Th2 (74). Ces résultats font échos à des observations rapportées chez des patients atteints d'un mélanome métastatique chez qui la gal-9 promeut une différenciation Th2, impactant la survie des patients (80).

Enfin, les principales informations concernant l'effet de la gal-9 sur les LB (lymphocytes B) proviennent de 2 études parues en 2018 (99,100). Cao et al. décrivent avec beaucoup de soin la manière dont la gal-9 régule la signalisation induite par le BCR. Elle agit à la surface des cellules en rapprochant des clusters d'IgM déjà existants, augmentant la taille et le nombre de molécules par cluster. Ceci a pour effet de diminuer la mobilité des IgM à la surface et, conjointement avec la limitation de la formation de plusieurs microclusters, impacte négativement l'activation des LB en présence de l'antigène spécifique. En outre Giovanonne

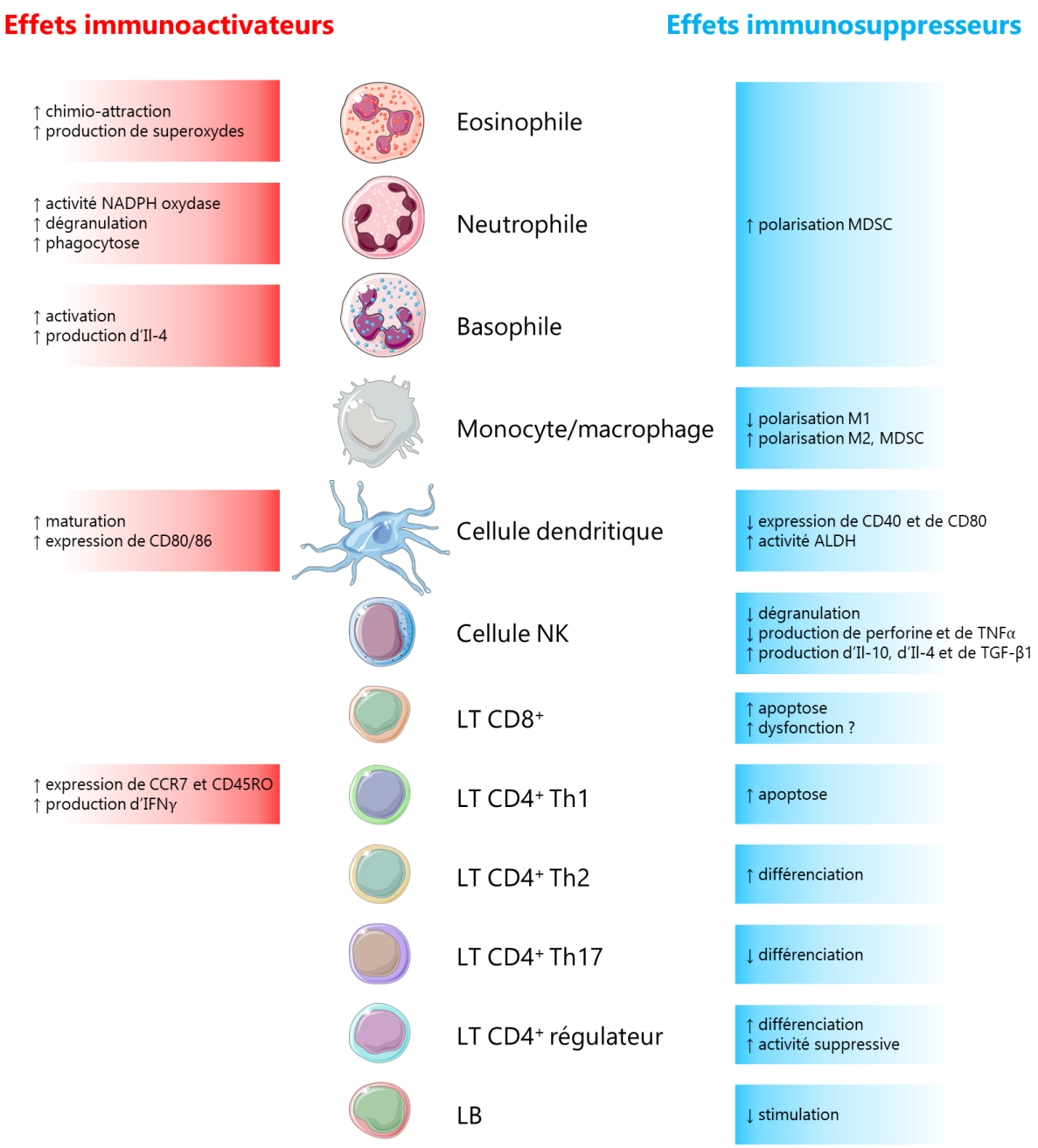

Figure 10. Effets de la gal-9 sur les cellules du système immunitaire.

Représentation synthétique des principaux effets immuno-modulateurs de la gal-9 sur les différentes populations de cellules immunitaires. La gal-9 exerce globalement des effets immunosuppresseurs. Les effets immunoactivateurs se concentrent principalement sur le lignage granulocytaire (adaptée des travaux de thèse de C. Lhuillier (11)).

et al. ont montré que la gal-9 se fixe également sur la protéine CD45 à la surface de la cellule B, ce qui bloque la signalisation calcique et l'activation des B en présence de l'antigène. Fait remarquable, les LB sont producteurs de la gal-9 qui agit sur eux comme un facteur inhibiteur. Cette inhibition s'exerce notamment sur les LB naïfs et mémoires. D'après Giovanonne et al., elle est levée au niveau des centres germinatifs en raison d'un changement du N-glycome, avec augmentation à la surface cellulaire, et notamment sur la protéine CD45, du taux de glycanes portant des branchements de type I. En effet, les glycanes de ce type ont peu d'affinité pour la gal-9. L'augmentation de leur synthèse résulte de l'expression accrue d'une enzyme appelée β1-6 N-acetylglucosaminyl transférase (100). De façon cohérente avec ces études mécanistiques, on sait que les souris KO gal-9 présentent une hyper-prolifération des cellules B conduisant à une production élevée d'anticorps, associé à une augmentation du nombre de cellules dans la rate, les ganglions, le thymus et les plaques de Peyer (101). Ce phénomène pourrait être impliqué dans l'augmentation de la susceptibilité de ces souris à développer des maladies auto-immunes, comme la polyarthrite rhumatoïde (96) (**Figure 10**).

c) Angiogenèse

En dehors de ses fonctions immunosuppressives, la gal-9 pourrait participer à la réparation tissulaire en modulant l'angiogenèse. Dans une première étude publiée en 2013, Heusschen et al. décrivent comment la gal-9 peut influencer la prolifération et la migration de cellules endothéliales isolées à partir de veines de cordons ombilicaux humains (102). Cette première étude, davantage accès sur les différents variants de la gal-9 exprimés par les cellules endothéliales, ne révèlent finalement que quelques modulations des fonctions des cellules endothéliales par la gal-9, sans pouvoir vraiment décrire un phénomène d'angiogenèse. Il faut attendre 2018 pour voir apparaître des travaux d'écrivant à la fois la migration et la formation de tubes de cellules endothéliales humaines après traitement par la gal-9 (103), suggérant un effet pro-angiogénique. Peu de temps après cependant, d'autres auteurs ont montré que le traitement de la membrane chorio-allantoïque d'un œuf de poule avec de la gal-9 entraînait une diminution de la longueur des vaisseaux générés sans pour autant en augmenter le nombre (104). Au total, on se trouve face à des résultats discordants en fonction du modèle expérimental qui ne permettent pas de tirer de conclusions.

IV – Galectine-9 et pathologies non tumorales

La grande majorité des études qui porte sur les fonctions de la galectine-9 au niveau des organismes entiers montre que ses effets immunosuppresseurs sont prédominants. Cela s'applique aux études menées chez la souris dans le domaine des maladies auto-immunes, des tumeurs expérimentales ou encore des allogreffes. De même chez l'homme le rôle immunosuppresseur prédominant de la galectine-9 ressort d'études aussi variées que celles qui concernent la physiologie de la grossesse, les mécanismes de l'auto-immunité ou de l'échappement immunitaire des tumeurs malignes.

a) Maladies inflammatoires

Plusieurs modèles murins permettent d'explorer les différentes contributions de la gal-9 dans le développement de maladies inflammatoires. On mesure par exemple assez bien sa valeur immunosuppressive dans les souris KO-gal-9 qui sont plus sensibles à l'induction de maladies auto-immunes comme la polyarthrite rhumatoïde (96). Il est également intéressant de constater que son administration par voie systémique (par exemple par voie intra-péritonéale) peut permettre de limiter la sévérité de la maladie, voire de prévenir son apparition (96,105,106). C'est le cas pour la polyarthrite rhumatoïde, mais c'est également le cas pour d'autres maladies auto-immunes. En effet, des chercheurs ont également mis en avant le potentiel thérapeutique de la gal-9 exogène dans un modèle de lupus érythémateux aigu disséminé (LEAD) murin. Chez l'homme, cette maladie se caractérise par une réponse immunitaire cellulaire et humorale dirigée contre différents tissus de l'organisme (peau, reins, cellules sanguines, poumons, …). Le modèle développé sur la souche murine MRL-lpr (*lupus-prone* ; mutée pour le gène *Fas*) présente cette auto-immunité systémique, et le traitement par de la gal-9 permet de diminuer la sévérité des signes cliniques. Pour expliquer ce phénomène, Les auteurs de ces travaux décrivent une diminution de la production d'auto-anticorps due à l'apoptose des plasmocytes (107).

Dans d'autres cas, les effets que joue la gal-9 dans l'apparition de la maladie sont plus difficiles à saisir. En effet, il a été démontré que le traitement par de la gal-9 pouvait être bénéfique, y compris dans des modèles de pathologie pourtant associés à une augmentation

de la concentration de gal-9. C'est par exemple le cas de modèles d'asthme murin (108–110) pour lesquels on rapporte une augmentation de la quantité de gal-9 dans les poumons (111,112). Il n'est pas impossible que dans ces cas de figure, les effets bénéfiques de la gal-9 administrée découlent d'un impact au niveau systémique tout en restant délétère au niveau pulmonaire. Il n'existe toutefois pas d'études à notre connaissance qui décrivent ce genre de mécanismes. Dans les maladies inflammatoires à composante auto-immune chez l'homme, on retrouve cette complexité puisque dans plusieurs cas on observe une augmentation de la gal-9 malgré une exacerbation de l'immunité contre certains auto-antigènes. Chez les patients atteins de polyarthrite rhumatoïde par exemple, la concentration de gal-9 tend à être augmentée dans le liquide synovial ainsi qu'au niveau des cellules dérivées du tissu synovial (fibroblastes, cellules endothéliales, macrophages, cellules T et B) (105). Chez les patients atteints de LEAD on retrouve également une augmentation de gal-9 dans les PBMC et le plasma (113,114). Dans certaines pathologies, le niveau de gal-9 est même corrélé à la gravité de la maladie. C'est le cas de la dermatite atopique, affection pour laquelle l'augmentation du niveau de gal-9 est visible dans le plasma des patients (115,116).

Dans cette dernière pathologie, comme dans d'autres associées à une composante auto-immune, on retrouve une accumulation de certains granulocytes, tels que les éosinophiles (117). Cette observation est d'autant plus intéressante que des travaux de recherche démontrent que la gal-9 favorise la citrullination (conversion de l'arginine en citrulline) des protéines intra-cellulaires dans les granulocytes (118). Or, ce phénomène a été plusieurs fois mentionné comme responsable de la production d'auto-anticorps en générant des protéines anormalement citrullinées reconnues comme des néo-(auto)antigènes.

b) Infections virales

La gal-9 joue également un rôle dans les réponses immunitaires qui accompagnent de nombreuses infections virales. Des augmentations de la concentration plasmatique de gal-9 ont par exemple été relevées chez des patients infectés par les virus HBV et HCV (*Hepatitis B/C virus*) (119,120). Cette augmentation de gal-9 est également corrélée à une expansion des Treg et une diminution de la réponse inflammatoire (95,121). A certains égards, ces effets sont bénéfiques puisqu'ils limitent les dégâts causés par l'inflammation durant l'infection

mais ils peuvent aussi faire courir le risque d'une réponse immunitaire insuffisante. Il semble aussi qu'une concentration élevée de gal-9 dans le plasma augmente le risque d'évoluer vers une infection chronique (122). Une étude rapporte même une concentration de gal-9 circulante encore plus élevée chez des patients infectés par HCV ayant développés un carcinome hépatocellulaire (94). De manière similaire, les cellules malignes de NPC associées au virus d'Epstein-Barr libèrent dans le milieu extra-cellulaire des exososomes chargés en gal-9 (58). Ces exosomes ont des propriétés immunosuppressives avérées (59,123).

Des auteurs rapportent que dans des modèles d'infections oculaires par le virus HSV (*Herpes Simplex Virus*) chez la souris, l'administration de gal-9 permet de réduire l'inflammation ainsi que les lésions associées à l'infection (124). Ceci s'explique probablement par le fait que dans le modèle utilisé, la formation des lésions résulte principalement d'une activité des T $CD4^+$ pro-inflammatoires. La diminution des lésions ne serait donc pas due à une inactivation du virus mais à une atténuation de la réponse immunitaire. D'ailleurs, des résultats complémentaires indiquent même que la gal-9 peut favoriser la réactivation du virus HSV1 dans les cellules nerveuses infectées de façon latente. En effet, le virus HSV-1 persiste dans le ganglion trigéminal et va se maintenir dans une phase de latence notamment grâce à la surveillance exercée par les T $CD8^+$. Le traitement par la gal-9 va donc induire, en même temps que l'apoptose de ces cellules, une réactivation du virus (93,125).

On observe également une forte augmentation de la concentration de gal-9 circulante lors de la primo-infection par le VIH (virus de l'immunodéficience humaine) (126). Cette concentration de gal-9 plasmatique est positivement corrélée à la virémie du patient. A la phase chronique, la concentration plasmatique de gal-9 quoique moins élevée qu'à la phase aigüe demeure plus forte que chez les sujets sains, y compris après restauration du taux de CD4 circulant sous tri-thérapie. Les spécialistes d'HIV s'intéressent à la gal-9 pour d'autres raisons. Plusieurs publications montrent que la gal-9 exogène peut déclencher *in vitro,* la réversion de la latence du virus (127). Cette réactivation serait due à une modulation de la transcription des gènes viraux, dépendante de l'activation du TCR, et impliquant les kinases ERK1/2 ainsi que le facteur de transcription CREB (128). Ce cas de figure est donc différent de ceux présentés précédemment puisque la réactivation ne passe à priori pas par une diminution de la réponse immunitaire, mais par un effet direct sur les cellules T infectées. La

persistance du HIV sous forme latente dans certains réservoirs cellulaires représente un obstacle majeur pour l'éradication complète du virus. Le traitement par de la gal-9 pourrait donc, conjointement avec une thérapie anti-rétrovirale, apporter un bénéfice dans la lutte contre l'infection. C'est du moins ce que proposent certains chercheurs, qui mettent également en avant l'effet inducteur de la gal-9 sur la protéine APOBEC3 (127). Cette protéine exerce un effet anti-rétroviral important en catalysant des réactions de déamination de la cytidine dans les simples brins (129), induisant des hypermutations qui diminuent l'infectivité du virus (127). Cependant, le fait que la gal-9 ait un effet positif direct sur la pénétration du virus dans les cellules encore indemnes d'infection, pourrait représenter un obstacle difficile à surmonter pour mettre en œuvre cette approche (130).

En conclusion, plusieurs infections virales s'accompagnent d'une augmentation de l'expression de gal-9 au niveau du tissu infecté ainsi qu'au niveau systémique, augmentation marquée notamment par une élévation de la concentration de gal-9 circulante. Ce phénomène qui contribue à une décroissance de la réponse immunitaire, peut favoriser la persistance de l'infection virale. En effet, la réponse inflammatoire doit être suffisamment intense pour permettre d'éliminer l'agent infectieux parfois au prix d'une aggravation des lésions du tissu infecté. Dans certaines situations, l'inhibition de la gal-9 pourrait donc améliorer la réponse anti-virale, voire le processus de vaccination comme le suggère une étude réalisée sur le virus influenza A (131). Cependant, les effets de la gal-9 sur les relations hôte/virus dépendent de la nature du virus. Comme nous l'avons vu, dans le cas du VIH, le traitement par de la gal-9 favorise une réactivation du virus dans les cellules infectées de façon latente. D'où l'idée d'utiliser la gal-9 en synergie avec un traitement antiviral, en vue d'éliminer totalement le VIH de l'organisme.

V – Notions générales sur les mécanismes d'oncogenèse, les propriétés des cellules malignes et leurs interactions avec le microenvironnement

Une tumeur maligne se présente comme une entité tissulaire qui échappe à l'homéostasie, c'est-à-dire qui se développe sans tenir compte des mécanismes régulateurs du volume et de

la morphologie des tissus et des organes. L'entité tumorale se développe sans tenir compte des barrières anatomiques, des cloisons entre tissus distincts ; c'est ce qu'on appelle le processus d'invasion qui se fait par contiguïté. En outre, on peut assister à des extensions à distance du processus tumoral qu'on appelle des métastases. Celles-ci s'opèrent le plus souvent de la manière suivante : des fragments microscopiques se détachent de la tumeur initiale (souvent appelée la tumeur primitive), sont entraînés par le flux sanguin ou le flux lymphatique et donnent naissance à distance à de nouvelles tumeurs, souvent localisées dans les ganglions lymphatiques, les os, le foie ou les poumons. D'un point de vue morphologique et fonctionnel, les tumeurs malignes se composent de 2 compartiments cellulaires distincts : 1) les cellules malignes qui sont généralement porteuses d'altérations du génome et qui ont le plus souvent un caractère clonal (c'est-à-dire qu'elles dérivent d'une seule cellule maligne initiale) et 2) les cellules du stroma qui présentent une grande diversité du point de vue du lignage et de la différenciation cellulaire. Ces cellules stromales, qui ne comportent généralement que peu voire pas d'altérations génétiques, sont très diverses : 1) cellules des vaisseaux intra- et péri-tumoraux, notamment des cellules endothéliales des parois vasculaires ; 2) cellules spécialisées de l'immunité innée et acquise : lymphocytes et cellules myéloïdes telles que les granulocytes, monocytes, macrophages, cellules dendritiques et MDSC ; 3) cellules du tissu conjonctif, dit de soutien, comme les fibroblastes ; 4) cellules nerveuses intra-tumorales.

Beaucoup d'auteurs distinguent les cellules stromales péri-tumorales, situées comme leur nom l'indique à la périphérie de la tumeur et souvent à une certaine distance des cellules malignes, et les cellules stromales intra-tumorales qui sont en contact étroit avec les cellules malignes.

Les cellules malignes ont longtemps étaient considérées comme les seules véritable actrices du processus tumoral. Il est vrai que les cellules malignes ont un rôle prépondérant dans l'émergence, la croissance et la dissémination tumorale mais le rôle des cellules stromales n'en est pas moins essentiel. Le phénotype particulier des cellules malignes résulte en premier lieu d'altérations génétiques, notamment de mutations activatrices de proto-oncogènes et de mutations invalidant les gènes suppresseurs de tumeur ou les systèmes de réparation de l'ADN. En deuxième lieu, le phénotype malin résulte aussi de modifications

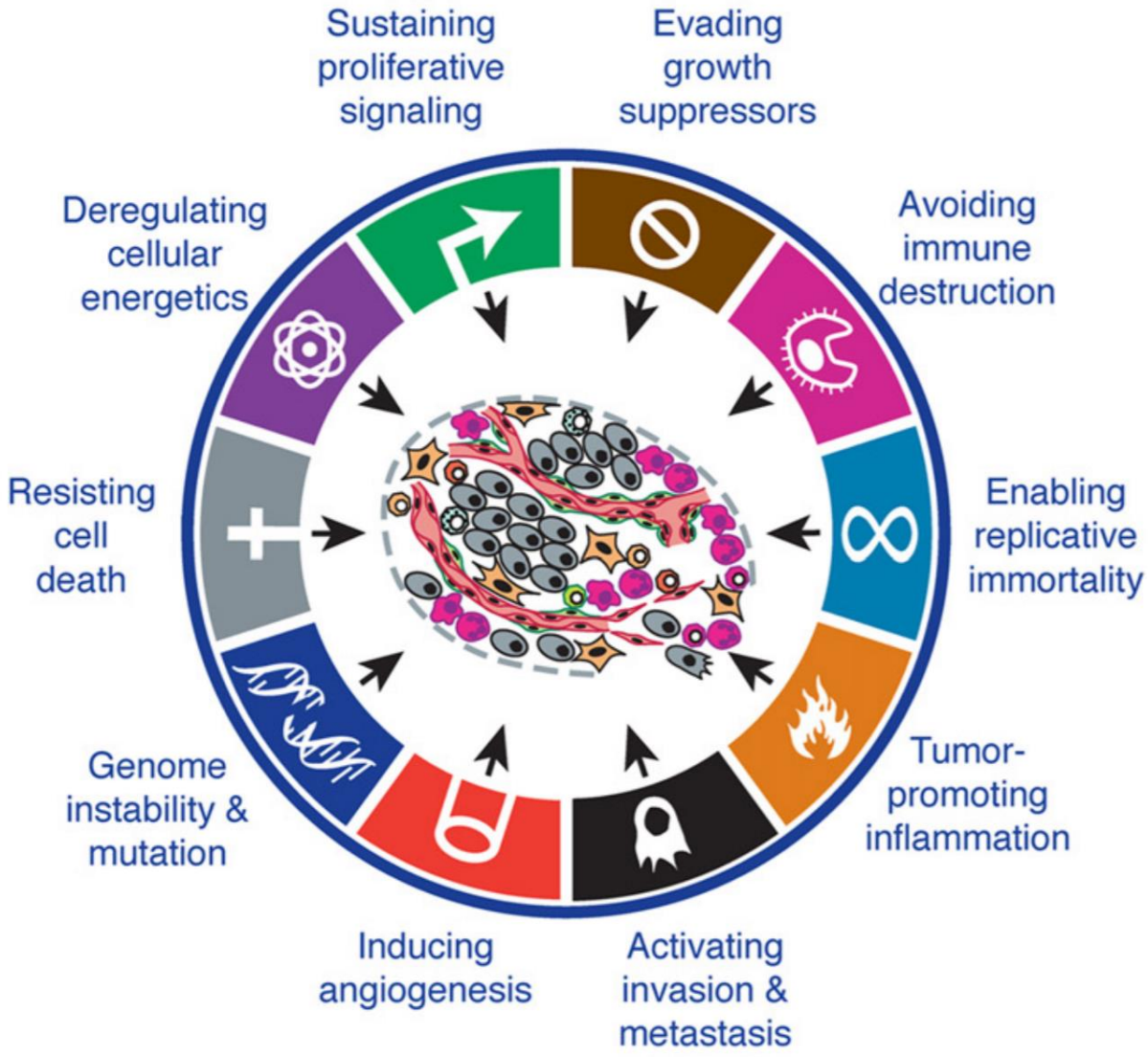

Figure 11. Les « *hallmarks* » du cancer d'après D.Hanahan et R.A Weinberg (12).

épigénétiques avec fréquemment une diminution globale de la méthylation de l'ADN et une augmentation de la méthylation au niveau des îlots CpG dans les régions régulatrices des gènes suppresseurs de tumeurs. A cela s'ajoute la mise en place progressive d'un réseau d'interactions entre cellules malignes et cellules stromales qui aboutit à un détournement des fonctions physiologiques des cellules stromales favorisant la survie et la multiplication des cellules malignes. Cependant la complémentarité entre cellules malignes et cellules stromales n'est généralement pas parfaite comme le montre en particulier le caractère défectueux de l'angiogenèse tumorale. En effet, pour qu'une tumeur maligne puisse grandir, l'édification du réseau vasculaire doit accompagner l'augmentation du volume tumoral permettant l'apport de nutriments et d'oxygène dans les secteurs tumoraux en expansion. La construction de nouveaux vaisseaux ou angiogenèse tumorale est souvent très défectueuse par rapport à ce qui s'observe dans un tissu non malin en développement ou en réparation. Il y a donc fréquemment une carence en oxygène dans de nombreux secteurs tumoraux et nous verrons que la capacité de s'adapter à l'hypoxie est l'une des caractéristiques les plus fréquentes des cellules malignes.

Ayant en tête, à la fois les caractéristiques structurales et physiologiques des tumeurs malignes *in situ* et de très nombreuses données biologiques obtenues *in vitro*, D. Hanahan et R.A. Weinberg ont proposé une synthèse et une classification rationnelle des propriétés des cellules malignes que nous allons présenter brièvement (**Figure 11**) (12) : 1) prolifération indéfinie, qui se traduit par une réactivation de la télomérase et une perte de réponse aux mécanismes de contrôle du cycle cellulaire, ce qui peut se décrire aussi comme un blocage des mécanismes de sénescence ; 2) résistance aux stimuli internes ou externes inducteurs de l'apoptose ; 3) instabilité génétique ; 4) induction de processus d'angiogenèse ; 5) résistance à l'hypoxie et réorientation métabolique favorisant notamment la glycolyse extra-mitochondriale (anaérobie), au détriment de la glycolyse couplée à la chaîne respiratoire et à la phosphorylation oxydative ; 6) capacité à participer à des interactions paracrines avec les cellules stromales comme les fibroblastes ou les macrophages intra-tumoraux ; 7) échappement aux réponses anti-tumorales du système immunitaire.

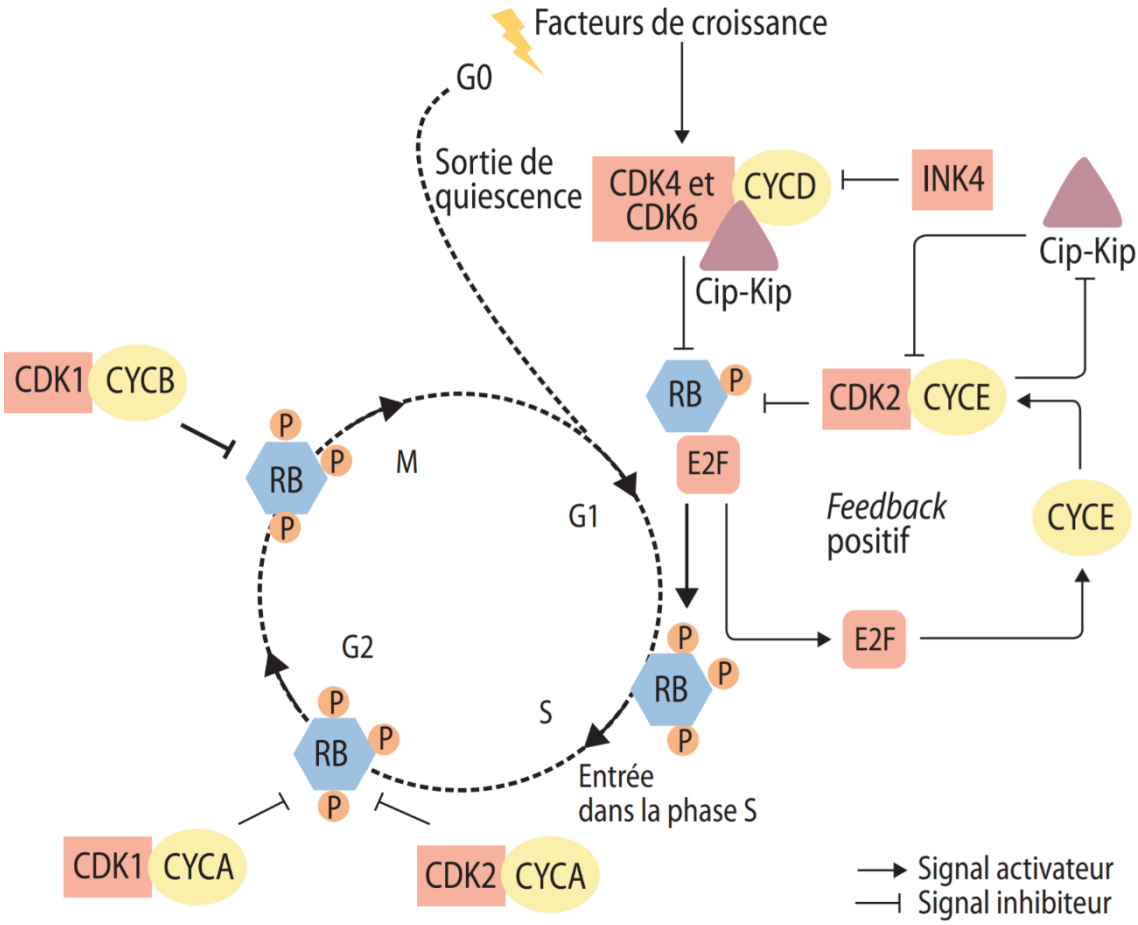

Figure 12. Initiation et progression dans le cycle cellulaire : rôle de Rb et des couples cycline/CDK (13).

Dans les lignes et les pages qui suivent, nous allons revenir plus en détail sur certaines de ces propriétés caractéristiques des cellules malignes. Dans un second temps, nous traiterons de l'impact que peut avoir la gal-9 sur le développement tumoral.

a) Capacité de prolifération indéfinie, résistance aux processus de sénescence et d'apoptose

Schématiquement, la prolifération indéfinie des cellules malignes, ainsi que la résistance à la sénescence et à l'apoptose résultent en proportions variables de deux grands types de mécanismes moléculaires : l'activation d'oncogènes et l'inactivation de gènes suppresseurs de tumeur, ou anti-oncogènes. Ces mécanismes sont extraordinairement divers et il n'est pas question de les décrire en détail dans le cadre de ce bref rappel bibliographique. Nous nous contenterons d'un court aperçu sur les voies de signalisation Rb et TP53 (132,133).

Il existe dans la physiologie cellulaire un certain nombre de dispositifs moléculaires qui servent de garde-fou pour empêcher une prolifération non contrôlée. Il s'agit en premier lieu des points de contrôle (« *checkpoints* ») du cycle cellulaire. Le plus important d'entre eux se situe à la transition GO/G1. Son franchissement nécessite l'inactivation de la protéine Rb (**Figure 12**). Dans les cellules malignes, cette inactivation peut s'effectuer de deux façons : soit par une mutation inactivatrice du gène correspondant, soit par le détournement d'un mécanisme physiologique qui est la phosphorylation de Rb. Cette phosphorylation est régulée de façon fine par des cyclines, notamment la cycline D1, par des kinases dépendantes des cyclines, notamment CDK4 et CDK6, et par des inhibiteurs de cyclines, notamment CDKN2A. L'expression anormalement élevée de la cycline D1 (oncoprotéine) ou l'absence de CDKN2A (suppresseur de tumeur) favorise l'inactivation permanente de Rb par phosphorylation et donc une prolifération incontrôlée. Cependant un autre mécanisme garde-fou peut intervenir à ce stade. En effet, l'inactivation de Rb déclenche une cascade de signalisation qui aboutit à la stabilisation de TP53 qui, suivant le contexte cellulaire, peut induire un arrêt du cycle cellulaire, soit réversible soit irréversible (sénescence), ou encore un phénomène d'apoptose. L'inactivation de TP53 résulte très souvent d'une mutation non-sens

ou faux-sens. Ce type de mutations s'observe dans environ 50% des cas de tumeurs malignes humaines.

Les cellules normales de l'organisme ont une capacité de prolifération limitée. Au terme de quelques dizaines de divisions cellulaires se produit un phénomène de sénescence physiologique qui rend les cellules incapables de se diviser. Le raccourcissement des télomères est l'un des principaux mécanismes responsables de ce processus. Les cellules peuvent le retarder ou l'empêcher de plusieurs manières, en particulier par une expression et une activité non régulée de la télomérase. Cela s'observe dans plus de 90% des tumeurs humaines (134). En dehors du gène de la cycline D2, d'autres oncogènes fréquemment activés dans les tumeurs humaines jouent un rôle dans la prolifération indéfinie, la résistance à la sénescence et l'apoptose. Nous nous contenterons de mentionner *RAS* (135), *WNT* (136) ou encore *MYC* (137).

b) Instabilité génomique et mutations

L'instabilité génétique est une autre caractéristique très commune des cellules malignes souvent installée à un stade précoce de la transformation tumorale. C'est à la fois un facteur favorisant les altérations des oncogènes et des gènes suppresseurs de tumeur, et une conséquence de leur dysfonctionnement. L'inactivation de TP53 en est une cause majeure. Cette instabilité s'installe en dépit d'une activation précoce des mécanismes de réponse aux dommages de l'ADN (138).

En permanence, le génome est affecté par des événements mutationnels qui surviennent de manière plus ou moins aléatoire, sous l'influence de facteurs internes et externes. Les cellules possèdent plusieurs mécanismes qui permettent de détecter et réparer les lésions génétiques à l'origine de ces mutations et c'est finalement un état d'équilibre entre dégâts et réparation qui régit le devenir cellulaire. Dans la biosphère, la relative vulnérabilité du génome aux mutations est considérée comme inhérente au processus évolutif. Au sein d'un organisme donné, cette même vulnérabilité conduit inévitablement à une accumulation de mutations et à l'apparition d'un mosaïcisme au cours du vieillissement (139).

Pour en revenir à la notion de lésion génétique, on qualifie de lésion une modification de la structure chimique de la double hélice d'ADN. Il peut s'agir d'une cassure de la chaîne nucléotidique ou encore de la modification chimique d'une ou plusieurs bases. Ces lésions, majoritairement prises en charge par les systèmes de réparation peuvent rester présentes durant la phase de réplication du génome. C'est durant cette phase que certaines lésions peuvent entraîner l'apparition de mutations sur le brin néo-synthétisé (140). Plusieurs évènements peuvent être à l'origine de l'introduction de lésions dans le génome, certains endogènes et d'autres exogènes. Alors que les premiers sont la résultante de processus métaboliques cellulaires, comme la production d'espèces réactives de l'oxygène (141), les autres proviennent de sources extérieures variées (rayonnements ultraviolet, X, gamma, agents intercalants, …). Les mutations apparaissant généralement durant le processus de réplication de l'ADN précédant la division cellulaire. Les cellules avec un taux de renouvellement élevé sont donc davantage sujettes à ces altérations. Physiologiquement, les cellules épithéliales et sanguines font partie de ces cellules plus vulnérables aux mutations somatiques (142). Plusieurs phénomènes stimulant la prolifération cellulaire peuvent donc, eux aussi, favoriser l'apparition de ces mutations. C'est notamment le cas dans des tissus endommagés par un processus inflammatoire, mais nous reviendrons plus en détail sur cet aspect dans la partie traitant des altérations du microenvironnement. Lors des états pré-tumoraux et au début du processus tumoral, on peut penser que les mutations apparaissent de façon aléatoire. Certaines sont létales. D'autres sont neutres par rapport au phénotype tumoral. Celles qui vont donner un avantage de survie ou de prolifération aux cellules malignes vont être sélectionnées.

c) Prolifération et altérations métaboliques

La prolifération dérégulée des cellules malignes s'accompagne généralement de besoins métaboliques importants. Fait majeur, les cellules malignes utilisent généralement le glucose d'une manière dispendieuse et « sale ».

Dans les cellules de mammifères, le glucose est un substrat privilégié du métabolisme énergétique. Dans des conditions normales, la glycolyse va fournir du pyruvate, de l'ATP

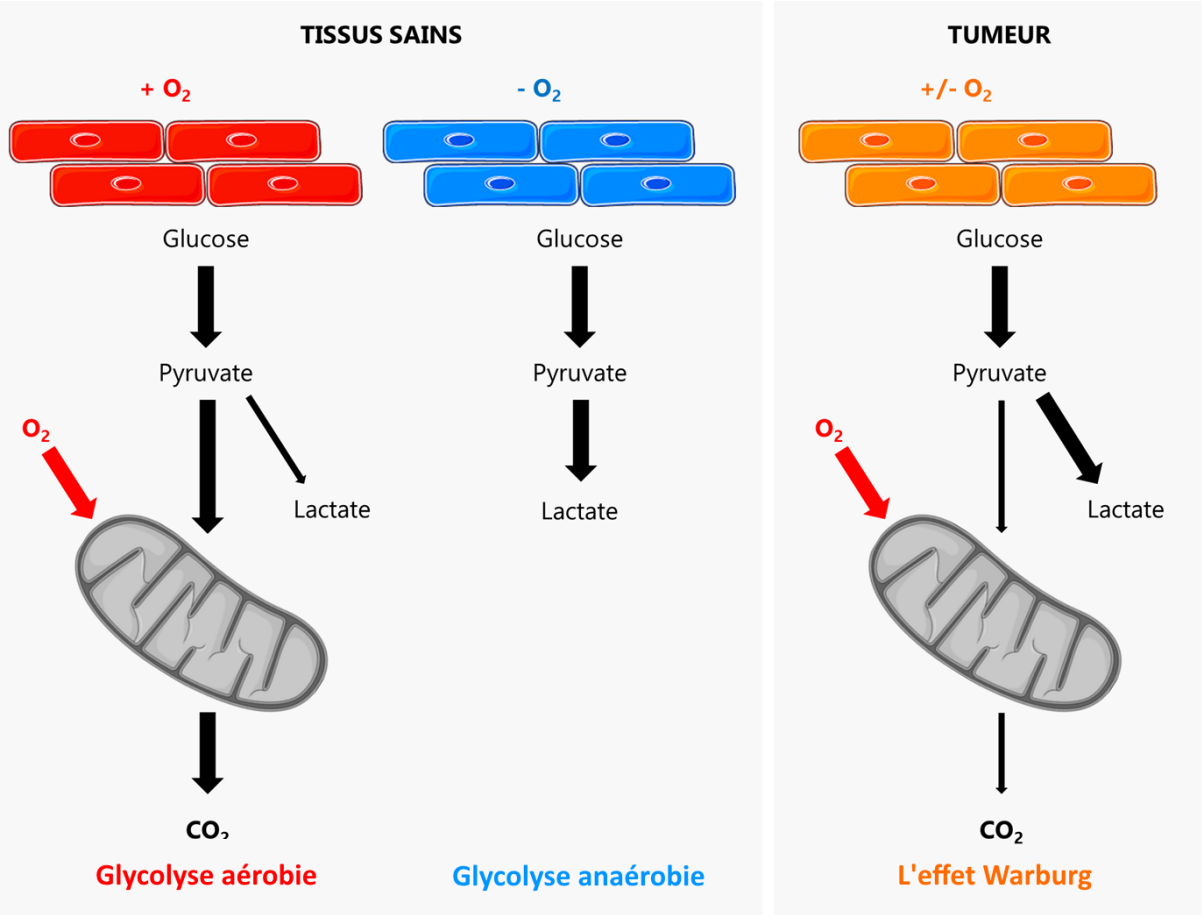

Figure 13. Le métabolisme de la cellule tumorale : l'effet Warburg.

La plupart des cellules cancéreuses puisent leur énergie essentiellement à partir du glucose, à travers la glycolyse. Dans les tissus sains, ce processus, qui participe également à la production de biomasse, passe majoritairement par une oxydation du pyruvate dans les mitochondries (glycolyse aérobie). En revanche, dans la plupart des cellules cancéreuses, la glycolyse se déroule préférentiellement de manière anaérobie dans le cytoplasme.

(adénosine triphosphate) et des coenzymes réduits notamment le NADH (nicotinamide adénine dinucléotide). Dans les mitochondries, le pyruvate va entrer dans le cycle de Krebs et ainsi aboutir à la génération de davantage de coenzymes réduits. Ces derniers vont pouvoir être réoxydés au niveau de la chaîne respiratoire et ainsi produire 36 molécules d'ATP, on parle alors de glycolyse aérobie. Dans une situation de déficit en oxygène, l'oxydation du glucose s'effectue entièrement en dehors des mitochondries. Elle aboutit à une molécule de lactate avec seulement 2 molécules d'ATP. Dans ces conditions, le rendement énergétique du catabolisme glucidique devient beaucoup plus faible. La production de lactate peut modifier les relations entre cellules stromales et cellules malignes. Dans ces dernières, la bascule du métabolisme du glucose vers la glycolyse anaérobie se produit fréquemment même dans un contexte riche en oxygène, comme l'a démontré pour la première fois Otto Warburg à partir d'ascites tumorales (143). Ce phénomène, appelé effet Warburg, est maintenant considéré comme une caractéristique distinctive de tumeurs agressives (**Figure 13**). L'implication de défaillances au niveau mitochondrial a été pendant un temps proposé pour expliquer ce phénomène. C'est effectivement le cas dans certains cancers, minoritaires. En réalité, plusieurs cancers qui présentent cet effet Warburg possèdent un système respiratoire mitochondrial intact (144). Il est clair que les mitochondries sont, du fait de leur implication dans la régulation de la mort cellulaire, de la production d'énergie ou encore de la synthèse de métabolites, des éléments clés dans le développement et la maintenance des cellules cancéreuses. Il n'est toutefois pas toujours évident d'identifier l'origine des modifications dans les mitochondries associées au développement tumoral.

d) Interactions des cellules tumorales avec leur microenvironnement

Parmi les changements observables dans le microenvironnement tumoral, nous pouvons déjà mentionner l'hypoxie et l'acidose. La réponse cellulaire à ce premier phénomène comprend un programme conservé par l'évolution, et piloté par les facteurs de transcription connus sous le nom de facteurs induits par l'hypoxie (HIF, *Hypoxia inducible factors*). La réponse à ces facteurs de transcription englobe divers processus qui aident à la réoxygénation du tissu, comme par exemple la stimulation de l'hématopoïèse (145), l'augmentation de la perméabilité épithéliale (146) ou l'induction de l'angiogenèse (147). Certains d'entre eux

apportent également leur contribution au développement tumoral en favorisant la motilité cellulaire, en impactant la composition de la matrice-extracellulaire et en participant au remodelage du tissu. Il a par exemple été démontré que HIF-1 régule directement le dépôt de collagène ce qui favorise l'invasion et les métastases des cellules cancéreuses hypoxiques du sein (148). D'autres mécanismes permettent de réduire la dépendance au métabolisme oxydatif en diminuant par exemple le nombre et la capacité de biogenèse des mitochondries (149) . Cette plurivalence participe sûrement à la difficulté de classer les facteurs induits par l'hypoxie en pro- ou anti-tumoraux. Les patients atteints de la maladie de Von Hippel-Lindau ne présentent d'ailleurs une prédisposition qu'à un type limité de cancers, suggérant une potentielle influence de l'origine tissulaire.

Les altérations du microenvironnement impliquent également les acteurs du système immunitaire. En effet, l'hypoxie, les dommages tissulaires comme les phénomènes de nécrose, ou encore les agents carcinogènes induisent l'expression de cytokines inflammatoires, de chimiokines et de facteurs de croissance qui conduisent au recrutement de différents sous-types cellulaires. L'inflammation vise normalement à détruire les corps reconnus comme étrangers et à remodeler le tissu lésé, afin de restaurer l'homéostasie tissulaire (150). Cette inflammation aiguë est un événement rapide puisque les signaux et les mécanismes qui déclenchent et maintiennent le processus disparaissent lorsque la guérison s'achève. Cependant, dans le cas du cancer, l'inflammation apparaît fréquemment comme un processus persistant et inefficace, constamment appuyé par l'émission soutenue de signaux pro-inflammatoires. Cette observation a d'ailleurs conduit le chercheur H.F. Dvorak à décrire la tumeur comme « une blessure qui ne guérit pas » (151). Au-delà de l'inefficacité de la réponse, l'inflammation chronique conduit à des changements de l'architecture du tissu et des constituants du stroma, qui favorisent la prolifération tumorale, l'angiogenèse et les métastases (152,153).

Indépendamment de la réponse inflammatoire, une sous-population de fibroblastes avec un phénotype myofibroblastique stimulée par les cellules tumorales, participe également à l'initiation et au développement tumoral (154,155). Plusieurs protéines – TGF-β, *platelet-derived growth factor* et *fibroblast growth factor* 2 – interviennent dans l'activation de ces CAF (*Cancer associated fibroblasts*) et de la fibrose du tissu. Ceux-ci ont un impact significatif

sur la progression tumorale en remodelant la matrice extracellulaire, en promouvant l'angiogenèse et le recrutement de cellules inflammatoires, voire en stimulant directement la prolifération des cellules cancéreuses via la sécrétion de facteurs solubles (156). Par exemple, la surexpression de la galectine-1 par les CAF a été décrite comme favorisant le développement des cellules tumorales adjacentes, et est corrélée à un mauvais pronostic dans le cancer du sein et gastrique (157,158). Dans un de ces articles, He et al. décrivent comment l'expression de la galectine-1 par les CAF induit la migration des cellules tumorales gastriques. Ces auteurs mettent en avant l'expression de l'intégrine-β1 dans les cellules cancéreuses corrélée à l'expression de galectine-1 dans les CAF. La conclusion de leur travail pointe l'induction de cette intégrine par les CAF, via la galectine-1, comme événement initiateur de la migration des cellules tumorales. En plus de sécréter des facteurs qui affectent la motilité cellulaire, les CAF représentent également une source de protéases, comme les métalloprotéases matricielles, qui permettent probablement aux cellules cancéreuses de traverser les frontières du tissu et de s'extirper du site de la tumeur primaire. Dans ce versant de recherche très actif, l'hypoxie apparaît encore une fois comme un facteur déterminant, pouvant influencer le devenir des fibroblastes (159). Cela illustre bien les communications intrinsèques qui existent entre les différentes caractéristiques des cellules tumorales.

e) Mécanismes d'échappement au système immunitaire

L'échec d'une réponse immunitaire anti-tumorale efficace trouve aujourd'hui plusieurs explications. Ce phénomène est fréquemment associé avec le concept « d'échappement au système immunitaire » qui caractérise assez bien le fait que le système immunitaire est mobilisé, mais que la tumeur réussit à le mettre en échec. Un des principes centraux de cet échappement repose sur l'idée d'une immunosurveillance constante du système immunitaire vis-à-vis des cellules transformées qui conduit à leur élimination, du moins à l'élimination de celles qui sont les plus vulnérables et corrélativement à l'émergence de cellules de plus en plus résistantes. Dans le contexte d'une réponse immunitaire, les cellules les plus vulnérables peuvent être, par exemple, celles qui expriment plusieurs néo-antigènes tumoraux qui en font des cibles facilement reconnaissables. Désigné sous le nom « d'immuno-édition du

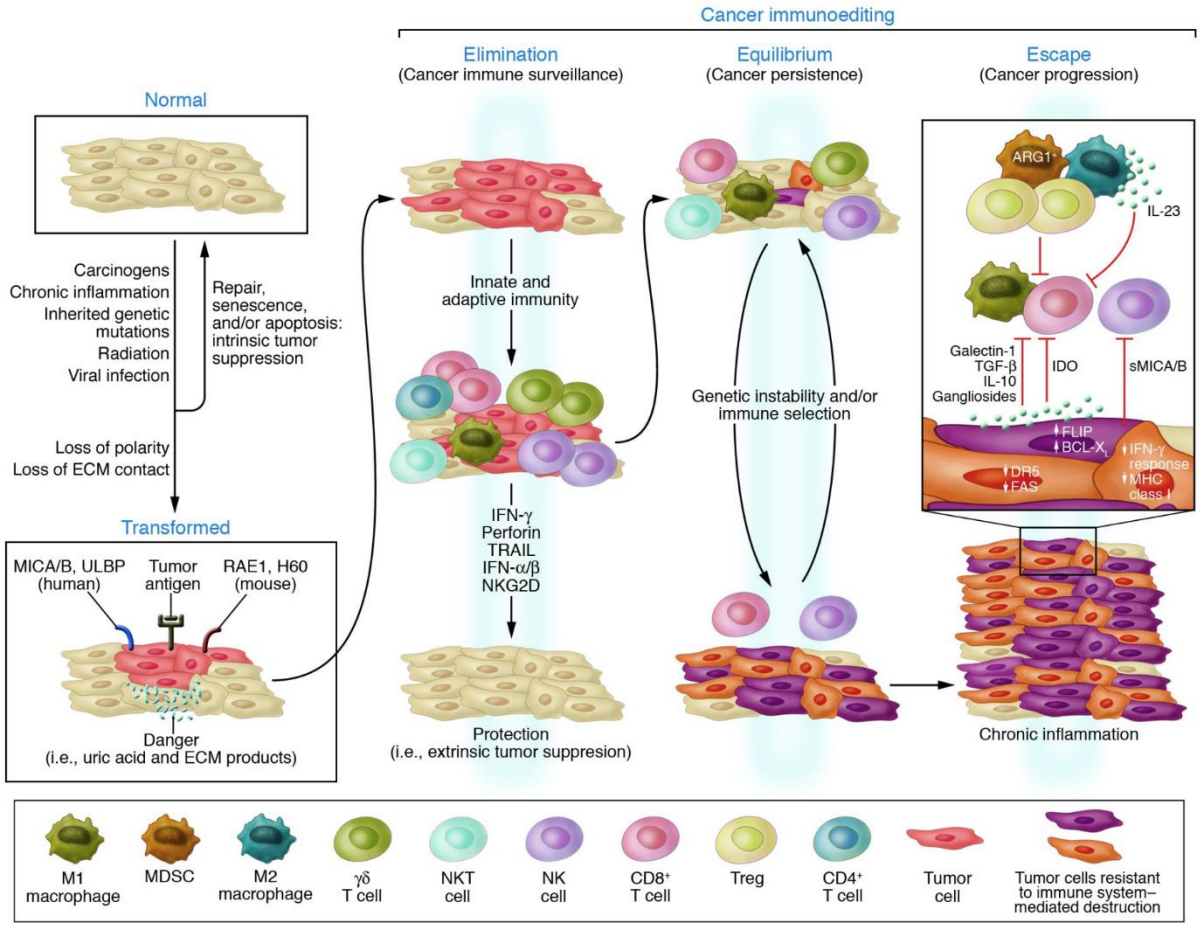

Figure 14. Concept « d'immuno-édition » du cancer (14).

Le processus « d'immuno-édition » du cancer est composé de trois phases : 1) l'élimination, qui correspond à l'immunosurveillance du cancer ; 2) l'équilibre, ou phase de dormance tumorale durant laquelle le système immunitaire sélectionne et « favorise » la génération de variants tumoraux résistants ; 3) l'échappement, qui reflète la progression non-contrôlée des cellules tumorales qui échappent au contrôle du système immunitaire. Ces trois phases font intervenir différents types cellulaires ainsi que de nombreux facteurs solubles.

cancer » (**Figure 14**), ce phénomène jouerait un rôle dans la sélection des clones tumoraux les plus résistants à la réponse (160).

La capacité du système immunitaire à distinguer les cellules normales des cellules malignes est fondamentale. Elle repose en partie sur le maintien d'une antigénicité suffisante des cellules malignes. En effet, la charge mutationnelle importante des tumeurs peut être associée à l'expression d'une grande variété d'antigènes mutés qui sont susceptibles de provoquer une réponse immunitaire (161). Un faible niveau de mutations peut donc diminuer l'efficacité de la réponse. Les analyses mutationnelles récentes nous ont toutefois révélé que certains cancers avec une charge mutationnelle relativement basse peuvent également répondre aux immunothérapies (162). La seule charge mutationnelle de la tumeur ne paraît donc pas être un critère suffisant pour attester de la potentielle sensibilité d'une tumeur à la réponse immunitaire. On peut également interpréter ces résultats comme étant dus à une inégalité du potentiel immunogène des différentes mutations. Actuellement, il semblerait surtout que l'antigénicité d'une tumeur soit principalement associée à la capacité de présentation antigénique par les biais du CMH (complexe majeur d'histocompatibilité) de classe I. On détecte ainsi une diminution de son expression ou des défauts dans le mécanisme de présentation des antigènes dans plusieurs types de cancers (163).

L'**antigénicité** d'une tumeur n'est pas le seul élément qui entre en ligne compte. En effet, une tumeur peut toujours échapper à la réponse immunitaire en diminuant son **immunogénicité** à d'autres niveaux. Par exemple, l'expression des « *immune-checkpoints* » (PD-L1, CTLA4, gal-9, …) (10) par les cellules tumorales et le tissu environnant influence également l'activation des lymphocytes mobilisés. Plusieurs acteurs de l'immunité, physiologiquement impliqués dans la terminaison de la réponse immunitaire, sont capables d'exprimer ces molécules inhibitrices. Leur étude représente un domaine de recherche très actif qui a conduit à décrire des sous-types cellulaires variés d'origine myéloïde et lymphoïde. Les plus décrites et les mieux caractérisées sont les TAM (*tumor-associated macrophages*), les MDSC et les Treg.

Les macrophages sont des cellules différenciées du lignage myéloïde dont les rôles sont d'éliminer les agents infectieux, promouvoir la régénération tissulaire et réguler l'immunité adaptative (164). Comme nous l'avons vu brièvement en figure 8 de la partie IIIa, les macrophages sont couramment classifiés en deux catégories : M1 et M2. Les macrophages

M1 sont activés par des cytokines dérivées de la réponse Th1 ou de produits bactériens comme le lipopolysaccharide et sécrètent des cytokines pro-inflammatoires comme l'Il-1β, l'Il-6 ou le TNF-α, des espèces réactives de l'oxygène et de l'oxyde nitrique, ainsi que des niveaux élevés de CMH de classe II. En revanche, les macrophages M2 sont activés par des cytokines dérivées de la réponse Th2 comme l'Il-4, l'Il-10 ou l'Il-13, ainsi que des hormones glucocorticoïdes. Ils se caractérisent par une activation de la voie de l'arginase, la production d'Il-10, de VEGF (*vascular endothelial growth factor*) et de métalloprotéinases matricielles. Alors que les premiers (M1) sont tumoricides, les deuxièmes (M2) facilitent la progression tumorale. Cette nomenclature, assez caricaturale, découlent en fait de phénotypes établis *in vitro* qui s'avèrent ne pas correspondre parfaitement aux macrophages retrouvés dans les tumeurs. Les études actuelles décrivent davantage un continuum de différenciation entre les macrophages M1 et M2 ainsi que des changements de polarité en réponse aux stimuli environnementaux qui complexifient l'établissement de marqueurs précis. Plusieurs auteurs préfèrent donc parler de TAM pro- ou anti-tumorigènes (165).

Les MDSC sont définies fonctionnellement comme des cellules myéloïdes (granulocytiques ou monocytiques) immatures immunosuppressives. Elles perturbent les mécanismes de surveillance immunitaire à plusieurs niveaux : activation des T, présentation antigénique des cellules dendritiques, polarisation des macrophages, cytotoxicité des cellules NK. Plusieurs des facteurs responsables de cette immunosuppression sont identiques à ceux décrits pour les macrophages M2. Ainsi, les MDSC sont eux aussi capables de produire de l'arginase-1, des espèces réactives de l'oxygène ou encore de l'Il-10 (166). D'autres fonctions des MDSC ont été décrites, comme la promotion de l'invasion tumorale ou la stimulation de l'angiogenèse (167). Ces fonctions sont indépendantes des capacités immunosuppressives des MDSC mais résultent de leur faculté à sécréter plusieurs médiateurs solubles (VEGF, bFGF (*basic fibroblast growth factor*), MMP9 (*matrix metallopeptidase 9*, …).

Comme les MDSC, les Treg facilitent la progression tumorale en interférant avec l'activité cytotoxique des lymphocytes T et la présentation antigénique. Ces cellules sécrètent également des cytokines immunosuppressives comme l'Il-10, l'Il-35 et le TFG-β, et bloquent l'activité des T par des interactions directes. De plus, les T reg expriment le CD39 et le CD73

qui induisent des altérations métaboliques sur les cellules NK et inhibent leur activité cytotoxique (168).

Enfin, un autre élément important de l'échappement de la tumeur à la réponse immunitaire concerne l'architecture de la tumeur et l'accessibilité des cellules tumorales. Les cellules épithéliales sont fortement liées entre elles par des jonctions serrées. Dans un contexte de prolifération intense et d'entassement des cellules, le front d'invasion de la tumeur peut former une réelle barrière physique qui limite le phénomène d'infiltration et dans certains cas même, qui diminue la pénétrance de molécules thérapeutiques (169).

f) Invasion tumorale et métastases

Comme nous l'avons expliqué au début de ce chapitre, le processus métastatique comporte plusieurs étapes consécutives : des phénomènes d'invasion locale au niveau de la tumeur primitive, le détachement de paquets cellulaires passant dans le flux sanguin ou lymphatique, puis l'extravasation dans un tissu distant et la formation d'une nouvelle tumeur (170). Ces nouvelles tumeurs diffèrent par plusieurs aspects de la tumeur primaire, et notamment dans la réponse au traitement pour lesquels elles sont souvent plus résistantes.

Plusieurs facteurs peuvent intervenir au sein de la tumeur pour augmenter la mobilité des cellules tumorales et conduire un contingent de cellules à quitter le site de la tumeur primaire, et aller former une nouvelle tumeur dans un autre tissu (hypoxie, modification de la composition de la matrice extracellulaire, contraintes physiques, …). Les mécanismes qui sous-tendent ce phénomène sont complexes et encore sujets à de nombreuses études qui représentent une des clés de la prise en charge thérapeutique du cancer. Les mieux caractérisées sont la perte de molécules d'adhésion cellules-cellules, et notamment de la E-cadhérine. Cette protéine permet normalement aux cellules de former des jonctions adhérentes entre elles et participe donc au maintien de la cohésion du tissu. Alors qu'une expression accrue de la E-cadhérine diminue le potentiel invasif des cellules tumorales, la réduction de son expression est au contraire connue pour favoriser ce phénomène (171). On sait maintenant que d'autres molécules d'adhésion cellules-cellules ou cellules-matrice sont impliquées. Globalement celles qui favorisent le cytostatisme sont régulées à la baisse alors

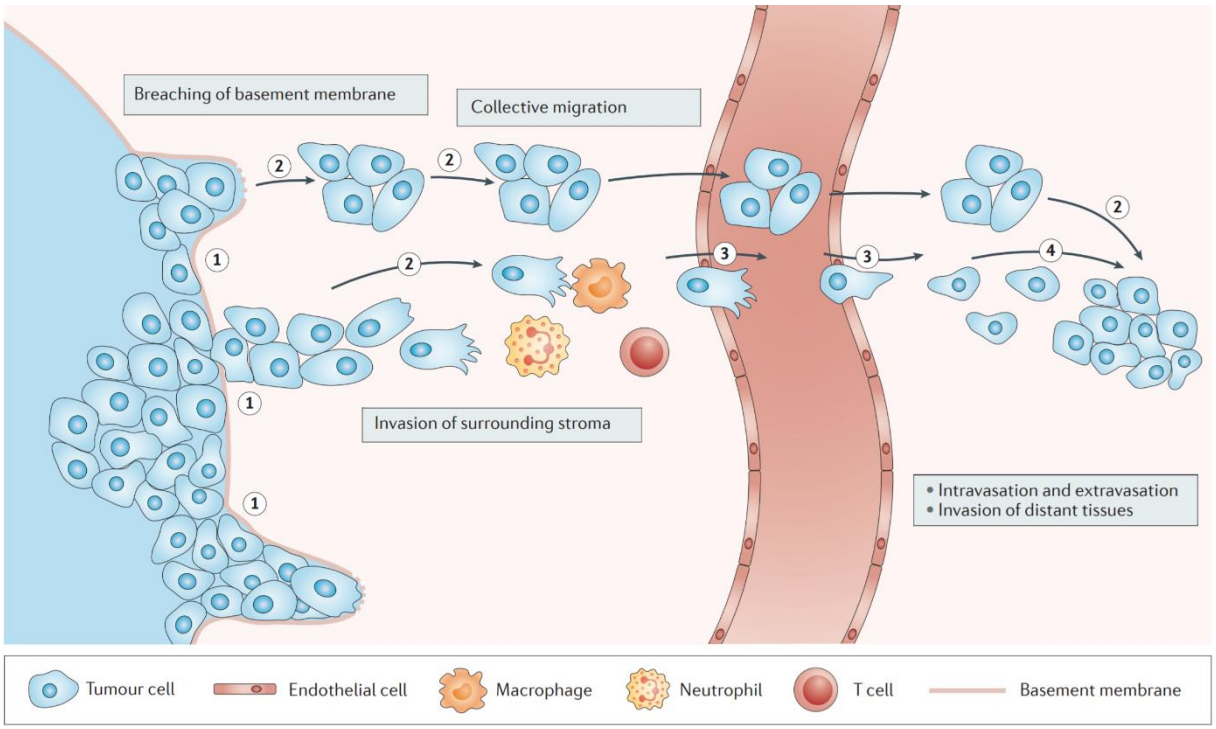

Figure 15. Etapes de l'invasion tumorale et du processus métastatique.

Le processus métastatique se déroule en plusieurs étapes au cours desquelles les cellules *tumorales (1) franchissent les frontières du tissu ; (2) migrent seules ou collectivement ; (3) entrent et sortent du système vasculaire ; (4) et forment des colonies sur des sites distants (adaptée de C.H. Stuelten et al. (15)).*

que celles qui sont normalement impliquées dans la migration cellulaire sont régulées à la hausse. Parmi ces dernières, on retrouve par exemple des molécules exprimées pendant l'embryogenèse. On se rend compte en effet, que plusieurs facteurs exprimés dans les cellules souches, sont réexprimés par les cellules tumorales lors de cette transition épithélio-mésenchymateuse (ex : SNAIL, SLUG, TWIST, …) (172). Le processus métastatique, initialement focalisé sur les mécanismes régissant la motilité au niveau d'une cellule unique, incorpore désormais les phénomènes coopératifs à l'échelle d'un groupe de cellules (173). La migration collective exploite les caractéristiques de tissus épithéliaux, qui sont conservés dans ce type de déplacement comme les jonctions cellule-cellule et la polarisation. Elle nécessite également des signaux qui permettent de guider le groupe de cellules. La vision actuelle de ce mécanisme se base sur la coordination de deux types de cellules : les « *leaders* » et les « *followers* ». Alors que les premières reçoivent et intègrent les signaux, les secondes migrent dans la direction qui leur est imposée (174) (**Figure 15**).

Enfin un autre aspect important du processus métastatique concerne l'adéquation entre les cellules constitutives du fragment métastatique et les caractéristiques du microenvironnement tissulaire au niveau du site d'implantation. On parle de « niche métastatique ». L'idée d'une adéquation entre cellules tumorales et niche métastatique est résumée par une allégorie ancienne de S. Paget qui parlait de la graine et du sol (« seed and soil theory ») (1889) (175). L'origine tissulaire de la tumeur primitive est l'un des facteurs déterminant dans la manière dont celle-ci va se propager à distance. Par exemple, les cancers du sein et de la prostate se disséminent le plus souvent aux os (176) alors que le cancer colorectal a plutôt tendance à se propager au foie. D'autres composantes du génotype et du phénotype tumoral vont déterminer les localisations préférentielles des lésions métastatiques. En outre, des éléments libérés par les cellules tumorales elles-mêmes – par exemple des microARN ou des exosomes – peuvent induire des transformations préparatoires à l'implantation du fragment métastatique au niveau de la niche métastatique (177).

VI – Galectine-9 et cancers

Nous l'avons vu précédemment, les effets immunosuppresseurs de la gal-9 peuvent influencer le développement d'affections malignes associées à une infection virale chronique : carcinomes hépatocellulaires (CHC) et nasopharyngés (NPC), associés respectivement aux virus HBV et HCV (CHC), et EBV (NPC). Des anomalies d'expression de la gal-9 s'observent dans d'autres cancers sans composantes étiologiques virales connues. Toutefois, concernant ces cancers, il n'y a pas d'unanimité au sujet d'un effet pro-tumoral de la gal-9. Au contraire, dans plusieurs cas, l'expression de la gal-9 dans les cellules malignes apparaît même comme un facteur de bon pronostic. Les études visant à étudier les effets de la gal-9 dans un contexte tumoral sont encore récentes et la plupart datent des 5 dernières années. Il est donc encore difficile de comprendre pourquoi l'expression de la gal-9 dans le tissu tumoral peut avoir une valeur pronostique très différente selon les cas. Cette partie a pour objectif de donner un aperçu des facteurs qui permettent de rendre compte des effets variables de la gal-9, tantôt pro- tantôt anti-tumoraux suivant les cas. Elle se conclura par un survol des mécanismes responsables des anomalies d'expression de la gal-9 dans les tumeurs.

a) Effets pro-tumoraux de la gal-9

Les effets pro-tumoraux de la gal-9 sont dus généralement à ses effets immunosuppresseurs. Dans le cas du gliome par exemple, on retrouve une augmentation de l'expression de la gal-9 au niveau tumoral accompagnée d'une augmentation de l'expression du récepteur Tim-3 sur les lymphocytes T infiltrants et périphériques (178). Ces caractéristiques qui sont associées à un état avancé de la pathologie (179), renvoient à l'immunosuppression locale et systémique qui lui est associée. La gal-9 est rarement décrite comme suffisante pour établir une immunosuppression et est généralement accompagnée de l'expression d'autres *immune-checkpoints* (180,181). Il est d'ailleurs intéressant de constater que l'augmentation de son expression a déjà été rapportée comme étant associée à un mécanisme de résistance aux anti-PD1 dans des carcinomes pulmonaires (88). Le carcinome à cellules claires du rein représente un autre type de cancer dans lequel les études actuelles mettent en évidence une corrélation entre l'augmentation d'expression de la gal-9 et une évolution défavorable de la

maladie (182,183). Cependant ces travaux n'expliquent pas comment l'expression augmentée de la gal-9 retentit sur le système immunitaire. En revanche, plusieurs publications portant sur le cancer du pancréas décrivent différents mécanismes d'immunosuppression mis en œuvre par la gal-9. Dans ces études, non seulement l'augmentation d'expression de la gal-9 est mesurée au niveau systémique dans la circulation sanguine (184), mais elle est également mesurée dans des cellules du système immunitaire. Dans les carcinomes du pancréas, la production de gal-9 provient majoritairement d'une variété particulière de cellules T $\gamma\delta$ ayant une activité suppressive. Elles expriment également PD-L1 et restreignent ainsi significativement l'activation des lymphocytes T $\alpha\beta$ (185). Les principaux mécanismes d'immunosuppression induits par cette gal-9 produite au sein des carcinomes pancréatiques semblent être la polarisation des macrophages vers un phénoytpe M2 (24). Chez les sujets porteurs de carcinomes pancréatiques, la concentration sérique de gal-9 est plus élevée en moyenne que chez les sujets sains ou les sujets porteurs de lésions bénignes du pancréas. En outre, un niveau élevé de concentration à une valeur pronostique péjorative chez les sujets porteurs de tumeurs de stade IV (184). Dans les mélanomes métastatiques, la gal-9 intra-tumorale provient principalement non pas de lymphocytes T $\gamma\delta$ mais d'une sous-population de cellules tumorales situées au niveau du front d'invasion. Son effet prédominant localement semble être la polarisation des lymphocytes T vers un phénotype Th2 (80). A chaque fois il s'agit, semble-t-il, de fonctions physiologiques de la gal-9 extra-cellulaire (décrites dans la partie III), qui sont mises en jeu de façon inappropriée dans le micro-environnement tumoral.

Alors que certaines études s'intéressent au parallèle entre gal-9 et résultats cliniques en mesurant le niveau de gal-9 circulante, une majorité d'entre elles se basent sur une quantification de la gal-9 réalisée au niveau tumoral à partir de marquages d'immunohistochimie, effectués sur des coupes de tumeurs de patients. Alors que la gal-9 plasmatique reflète la gal-9 extra-cellulaire, celle mesurée sur coupes histologiques reflètent plutôt la gal-9 intra-cellulaire. Dans un cas comme dans l'autre, il n'est pas toujours évident de mesurer la proportion de gal-9 provenant des cellules tumorales et celle provenant des cellules infiltrantes, surtout en l'absence de marquages complémentaires. Fait notable, on constate que la gal-9 n'est jamais décrite comme étant à la surface des cellules cancéreuses, mais plutôt dans le cytoplasme voire le noyau de celles-ci. La gal-9 membranaire n'est quant

à elle décrite que dans les cellules immunitaires. Il est difficile d'affirmer que la gal-9 peut être sécrétée par tous les types cellulaires dans la mesure où cette sécrétion ne dépend pas de mécanismes conventionnels. Une forte expression de gal-9 au niveau tumoral n'est donc pas forcément associée à une forte présence de gal-9 dans l'environnement de la tumeur et à distance de celle-ci. Cette subtilité représente un possible élément de réponse dans la compréhension de l'effet pro- ou anti-tumoral de la gal-9 d'un type de cancer à l'autre.

Au-delà de l'aspect sécrétoire, la nature du type cellulaire peut impacter par d'autres aspects la réponse à la gal-9. Il a par exemple été démontré que la gal-9 est capable d'induire l'auto-renouvellement des cellules souches leucémiques dans les LAM (leucémies aiguës myéloïdes). Ce phénomène, dépendant du récepteur Tim-3, s'entretient dans une boucle autocrine via la sécrétion de gal-9 par les cellules leucémiques elles-mêmes (186).

b) Effets anti-tumoraux de la gal-9

En dépit de ce qui a été dit dans les paragraphes précédents, il semble que dans un grand nombre de types tumoraux, l'abondance de la gal-9 intra-tumorale évaluée sur des coupes histologiques soit corrélée avec un bon pronostic. C'est ce qu'affirme Zhou et al. sur la base d'une méta-analyse compilant 14 études antérieures et portant au total sur 2326 patients (187). Afin de traiter la question en détail, prenons pour commencer le cas des cancers du col de l'utérus dans lesquels une diminution d'expression de la gal-9 au niveau tumoral est corrélée à un grade histologique plus sévère de la maladie d'après une publication de Liang et al. (188). A noter cependant un point surprenant dans cette étude, dans les carcinomes *in situ*, l'abondance de gal-9 serait plus faible que dans les carcinomes invasifs de bas grade. Contrairement à ce qui se passe pour les affections malignes où l'on suspecte un effet pro-tumoral de la gal-9, l'influence de la gal-9 extra-cellulaire sur le système immunitaire ne semble pas être en cause dans l'étude de Liang et al. Il s'agit plutôt d'effets intrinsèques au niveau des cellules malignes. En effet, cette étude révèle une diminution de l'expression de la E-cadhérine parallèle à la diminution de l'expression de la gal-9. D'autres études rapportent des observations similaires de diminutions d'expression concomitantes de la gal-9 et de la E-cadhérine, sans pour autant établir entre elles un lien de cause à effet. Ainsi, des chercheurs

ont décrit dans des cancers de la tête et du cou une absence totale de gal-9, alors que dans les tissus sains correspondants on peut habituellement observer une distribution très spécifique de la protéine au niveau de la membrane basale ; ce qui suggère un lien entre son expression et la différenciation du tissu (189). Une étude complémentaire rapporte dans ce même type de tumeurs une diminution de l'expression de la E-cadhérine, normalement exprimée au niveau des membranes basales et para-basales (190). La diminution d'expression de cette protéine, impliquée dans le maintien des liaisons cellule-cellule, est compatible avec l'idée d'un potentiel métastatique augmenté en rapport avec la diminution d'expression de la gal-9.

L'idée qu'une faible abondance de la gal-9 dans le tissu tumoral puisse favoriser le processus métastatique est étayée par plusieurs publications qui suggèrent que la diminution de son expression augmente le potentiel invasif des cellules tumorales. Les études les plus connues sur ce thème concernent les cancers du sein. Une étude souvent citée, publiée par Irie et al. en 2005 a évalué l'abondance de la gal-9 sur des coupes de tissu tumoral pour environ 84 patientes d'une série prospective. Les auteurs ont observé une corrélation inverse entre l'abondance de gal-9 et la fréquence des rechutes métastatiques (191). Dans le même article les auteurs ont comparé des cellules MCF7 ayant une expression forte ou faible de gal-9. Ils ont observé une tendance à l'agrégation plus forte pour les cellules avec une forte expression de gal-9 *in vitro* et dans des tumeurs sur souris nude. En effet, en l'absence de gal-9 dans ces tumeurs transplantées, les cellules malignes étaient dispersées en petits îlots au sein du stroma. Cependant les cancers du sein représentent un bon exemple d'une situation où les effets pléiomorphes et souvent divergents de la gal-9 rendent difficiles l'appréciation de son impact global sur le processus tumoral. *A fortiori* ils rendent difficile la prise en compte de l'abondance de la gal-9 dans le tissu tumoral comme facteur pronostic. En effet, une étude plus récente rapporte que dans les cancers du sein, la signalisation gal-9/Tim-3 à la surface des cellules dendritiques intra-tumorales inhibe leur production de CXCL9 ce qui entraîne une activité réduite des lymphocytes T $CD8^+$ intra-tumoraux (192).

D'autres types de cancers présentent cette complexité et cette divergence entre les effets anti-tumoraux intrinsèques dans les cellules tumorales (« *cell-autonomous* ») et les effets pro-tumoraux liés à l'inhibition des effecteurs du système immunitaire dans le

microenvironnement tumoral. Ainsi, en ce qui concerne les mélanomes, une étude souvent citée de Kageshita et al. (2002) tend à prouver que la gal-9 intra-cellulaire a un effet anti-métastatique, principalement sur la base d'expériences effectuées *in vitro* (193). Ces auteurs montrent que la gal-9 exogène induit l'agrégation et même l'apoptose dans des lignées de mélanome traitées *in vitro* (à noter que l'apoptose n'est significative que pour des concentrations élevées de gal-9 recombinante de l'ordre d'au moins 100 nM ce qui est au-delà des concentrations atteintes dans l'organisme) (même remarque au sujet d'une publication plus récente sur le même thème de Wiersma et al. 2012 (194)). Du point de vue clinique, l'étude de Kageshita montre une abondance de gal-9 plus faible dans les cellules malignes de mélanome que dans les mélanocytes des naevi bénins, et un meilleur pronostic pour une abondance élevée de gal-9 dans les cellules malignes sur les coupes de tissu tumoral. Un travail réalisé plus récemment sur des modèles murins – mélanome B16 et carcinome colique CT26 – donnaient des résultats qui allaient dans le même sens. Avec des effets supposés anti-métastatiques de la gal-9 extra-cellulaire *in vitro* – blocage de l'adhésion sur la matrice extra-cellulaire – et *in vivo* – diminution des métastases pulmonaires résultant de l'injection intra-veineuse de cellules malignes (195) . Là encore les concentrations de gal-9 recombinante utilisée in vitro étaient très élevées.

A l'opposé, des études effectuées sur des spécimens cliniques de mélanomes métastatiques mettent en évidence les faits suivants : une concentration de gal-9 plasmatique plus élevée chez les patients que chez les donneurs, un pronostic plus mauvais pour les patients avec la concentration plasmatique la plus élevée et une polarisation des lymphocytes circulants vers un phénotype Th2 plus marqué chez ces patients (80). D'après ces mêmes auteurs, chez ces patients ayant une concentration de gal-9 plasmatique élevée, la production de gal-9 s'observe dans les cellules malignes uniquement au niveau du front d'invasion tumoral. Ceci souligne le fait que la production de gal-9 n'a peut-être pas la même signification suivant la topographie de la production. A noter que dans les mélanomes métastatiques, la gal-9 extra-cellulaire pourrait provenir également des cellules myéloïdes infiltrantes comme le suggère une étude de Melief et al. portant sur le transfert adoptif de lymphocytes T pour des mélanomes de stade IV (196). En résumé, dans les mélanomes métastatiques, la production de gal-9 viendrait principalement des cellules malignes du front d'invasion et des cellules

myéloïdes infiltrantes. Ceci expliquerait, au moins en partie, l'apparente contradiction entre l'étude de Kageshita (193) et celle d'Enninga (80).

Dans le cancer du poumon, une étude de 2020 révèle qu'un concentration de gal-9 faible au niveau tumoral mais élevée au niveau des cellules infiltrantes est associée à un mauvais pronostique (197). Enfin, pour en revenir au carcinome pancréatique, il est également intéressant de constater que l'augmentation d'expression de gal-9 n'est pas constante au cours du développement tumoral. En effet, il semblerait qu'elle augmente au cours des stades II et III, avant de diminuer au stade IV de la maladie (184).

Un degré de complexité supplémentaire pourrait concerner l'expression des différentes isoformes de la gal-9. Pour rappel, la gal-9 s'exprime sous 3 isoformes principales : gal-9L, M et S (*long*, *medium*, *short*). Celles-ci diffèrent par leur longueur, leur stabilité et leur activité. On ignore encore s'il existe des différences fonctionnelles entre ces trois isoformes en dehors d'une stabilité plus grande pour la forme courte. Une connaissance plus développée de ces isoformes pourrait nous aider à mieux comprendre quelle contribution positive ou négative peut apporter la gal-9 dans le développement tumoral.

c) Dérégulations d'expression de la gal-9 dans un contexte tumoral

Les données de la littérature ne décrivent pas de mutations ou de polymorphismes du gène de la gal-9 associés au développement tumoral, comme ça peut être le cas dans la polyarthrite rhumatoïde (198). En revanche, plusieurs études se sont penchées sur la modification du profil de méthylation de ce gène et sur l'expression de micro-ARN régulateurs. Une étude assez complète s'est d'ailleurs penchée sur l'analyse du profil de méthylation du gène de la gal-9 dans les cellules de mélanome. Cette étude a l'avantage de permettre d'appréhender l'origine de la gal-9 exprimée en s'intéressant séparément aux mélanocytes et aux différentes cellules infiltrantes (monocytes, LT $CD4^+$ et $CD8^+$, LB et granulocytes). Les auteurs ont ainsi identifié un niveau de méthylation relativement bas dans les leucocytes contrairement aux mélanocytes qui présentent, eux, un niveau de méthylation important dans la région promotrice (199). Ce phénomène ne semble pas redondant d'un tissu à l'autre puisque les études menées sur les cancers colorectaux ne rapportent pas de

modifications au niveau de la méthylation de l'ADN ou des histones associés au gène *LGALS9* (200). Les informations relatives à une dérégulation d'expression de la protéine dans ce contexte décrivent davantage une régulation post-transcriptionnelle, par des micro-ARN. Un des candidats mis en avant est le miR-455-5p dont la production est significativement augmentée dans des tissus tumoraux, qui présentent dans le même temps une réduction significative de la gal-9. Ces données ne sont pour le moment appuyées que par des tests *in vitro* sur une lignée tumorale d'origine colique dans laquelle la reconnaissance de la région 3'UTR (*Untranslated transcribed region*) du transcrit par le miR a été vérifiée (201). Un autre miR potentiellement impliqué dans la régulation de l'expression de la gal-9 a été décrit dans le cadre d'études sur le carcinome hépatique. Il s'agit du miR-22 qui semble être régulé négativement dans ce type de cancer (202).

Bien entendu, plusieurs des fonctions exercées par la gal-9 dépendent de sa capacité à reconnaître des polysaccharides spécifiques. Des modifications même simples des glycanes, engendrées par des altérations épigénétiques, par exemple qui entraînent la modification d'expression de certaines glycosyltransférases ou encore de leur activité, peut directement impacter la sensibilité des cellules à la signalisation induite par la gal-9 (203). Il n'existe toutefois pas encore d'études rapportant des exemples concrets de ce type de modifications en lien avec la gal-9, dans un contexte tumoral.

d) La neutralisation des galectines comme nouvelle approche thérapeutique

L'implication de certaines galectines dans le développement tumoral a incité des équipes de recherche à développer des stratégies visant à inhiber leur action. Au-delà de l'aspect thérapeutique, ces inhibiteurs représentent des outils de choix dans l'investigation des fonctions biologiques des galectines. Parmi ces molécules inhibitrices on peut évidemment citer les saccharides pour lesquels les galectines présentent une affinité naturelle (galactose, lactose, N-acétyllactosamine, …). Bien que largement employés dans des expériences *in vitro*, ces ligands naturels souffrent cependant d'une stabilité chimique et métabolique limitée ainsi que d'une affinité relativement faible qui ne permet pas leur emploi dans un cadre

thérapeutique. Des molécules analogues ont donc été créées, avec une affinité pour leur galectine cible parfois 20 fois supérieure au galactose ou au lactose (204). L'effet anti-tumoral de certains de ces composés synthétiques a été observé sur des modèles animaux (205).

Des progrès ont également été réalisés en exploitant des formes tronquées des galectines. Par exemple, John *et al.* ont développé et breveté une forme tronquée de la gal-3 qui possède un CRD fonctionnel mais avec une queue polypeptidique qui empêche son oligomérisation. Là encore, l'effet anti-tumoral de cette molécule a été démontré (206). Plus largement, d'autres chercheurs ont développé de petits peptides synthétiques de forte affinité capables de bloquer les interactions galectines-galactosides (207).

Quelques travaux de recherche présentent également les aptamères comme un moyen possible pour neutraliser les galectines. Ces oligonucléotides synthétiques simples brins sont capables de se lier à des cibles spécifiques avec une grande affinité. A la manière des anticorps, certains aptamères sont capables d'antagoniser des protéines telles que le VEGF ou TLR2 (208,209). Une étude récente décrit l'action d'un aptamère inhibant la gal-1 dans un modèle tumoral murin. Celui-ci est capable de ralentir la progression tumorale en inhibant certaines des fonctions immunosuppressives de la gal-1 (210).

Enfin, il est également possible d'inhiber l'action des galectines à l'aide d'anticorps neutralisant. Dans ce contexte, notre équipe a produit des anticorps monoclonaux dirigés contre la gal-9 en vue de les employer comme outils d'investigation et afin d'évaluer leur potentiel thérapeutique. La caractérisation de ces anticorps a fait l'objet d'une publication parue en septembre 2018 qui est présenté dans la section résultats (211).

VII – Notions générales sur l'invalidation de gènes par la méthode CRISPR/Cas9

a) Historique

La technologie CRISPR/Cas9 (*Clustered Regularly Interspaced Short Palindromic Repeats/CRISPR associated protein 9*) représente sans aucun doute une des plus grandes révolutions technologiques de cette décennie. La promesse d'un outil capable de modifier

spécifiquement le génome a rapidement gagné les congrès ainsi que le grand public, ne manquant pas d'éveiller les idées et les craintes quant à son emploi. Cette technologie qui trouve son origine à la fin des années 1980, est née d'un mélange de hasard, de curiosité et de volonté d'innovation.

En 1987, sont publiés pour la première fois des travaux décrivant des répétitions palindromiques chez la bactérie *Escherichia coli*. Ces répétitions à la signification biologique encore inconnue, représente alors une organisation du génome inédite observée chez les procaryotes (212). Cette observation s'est par la suite généralisée chez plusieurs autres espèces bactériennes ainsi que chez les archées (213). Le recensement de ces différents micro-organismes a permis d'identifier une structure courante dans leur génome : des enchaînement palindromiques séparés par de courtes séquences nucléotidiques (*spacers*) (214). Au début des années 2000, au moment où plusieurs publications commençaient à paraître au sujet de ces répétitions, l'acronyme CRISPR fut choisi pour les définir. Dans le même temps, une famille de gènes étroitement associée aux gènes CRISPR fut identifiée : la famille de gènes Cas (*CRISPR associated*), constituée de plusieurs hélicases et nucléases (215).

En 2005, trois articles vont apporter un éclairage nouveau sur le rôle biologique du système CRISPR/Cas. Ceux-ci réunissent des éléments complémentaires sur les caractéristiques et les fonctions présumées du système :

1) Il existe une similarité entre les séquences des *spacers* et celle de virus connus pour avoir un tropisme bactérien. De plus, les bactéries qui possèdent ces séquences sont connues comme étant résistantes à ces bactériophages (216). Plus le nombre de spacers est important et plus la diversité des résistances est grande (217).

2) Les bactériophages « catalogués » dans le génome bactérien ont en commun une séquence conservée : le PAM (*Protospacer Adjacent Motif*) (216,217).

3) Les « *spacers* » sont sujets à une évolution dynamique qui se caractérise par l'ajout de nouvelles séquences de manière polarisée. L'acquisition de ces nouvelles séquences se fait dans des régions proches des gènes Cas, suggérant l'implication de ces derniers dans l'acquisition des nouveaux « *spacers* » (218).

Ensemble, ces découvertes ont ouvert la voie à la description d'un véritable système immunitaire adaptatif comparable à l'ARN interférent (219). Plusieurs autres travaux de recherche ont permis par la suite d'améliorer la compréhension du système.

b) Fonctionnement du système CRISPR/Cas

Le fonctionnement du système CRISPR/Cas se base sur un processus en 3 étapes : l'adaptation, l'expression et l'interférence. L'étape d'adaptation comprend la capture de nouveaux spacers, l'expansion ou la contraction des ensembles CRISPR, ou encore la maintenance des répétitions. Elle implique les protéines Cas1 et Cas2 qui sont très conservées au sein des différentes espèces. Les étapes d'expression et d'interférence correspondent à la partie exécutive du système, qui comprend la transcription des ARNs issus du locus CRISPR, le clivage de ce précurseur en un ARN maturés (crRNA) qui servira de guide, et le clivage de l'ADN double brin étranger. Contrairement à l'étape d'adaptation, les étapes d'expression et d'interférence font intervenir des acteurs qui diffèrent beaucoup d'un organisme à l'autre. On distingue d'ailleurs 3 types principaux de systèmes CRISPR/Cas qui se différencient par les protéines Cas impliquées, l'organisation des opérons *cas* et la structure des répétitions au sein des matrices CRISPR (220).

Les systèmes de type I et II utilisent tous les deux un module effecteur crRNA qui est soit multimérique pour le type I, soit monomérique pour le type II. Ainsi, on retrouve pour le type I, une endoribonucléase (Cas5d ou Cas6) chargée de la biogenèse du crRNA, et un complexe multimérique appelé Cascade (*CRISPR-associated complex for antiviral defense*) dans lequel va être incorporé le crARN et permettre le clivage de l'ADN invasif. Le système de type II est beaucoup plus simple puisqu'un petit ARN agissant en trans appelé tracrRNA (*trans-acting small RNA*) s'apparie avec chaque répétition du pre-crRNA pour former un ARN double brin clivé par la RNAse III en présence de l'endonucléase Cas9. Ces crRNA ainsi générés vont ensuite permettre, toujours en association avec une partie du tracrRNA et de la Cas9, de générer des cassures dans l'ADN double brin étranger. Les systèmes de type III sont les plus complexes. Comme dans les systèmes de type I, le clivage du pre-crRNA est réalisé par la Cas6 et la cassure nécessite un complexe multimoléculaire de ciblage (Cas10-Csm ou Cas10-

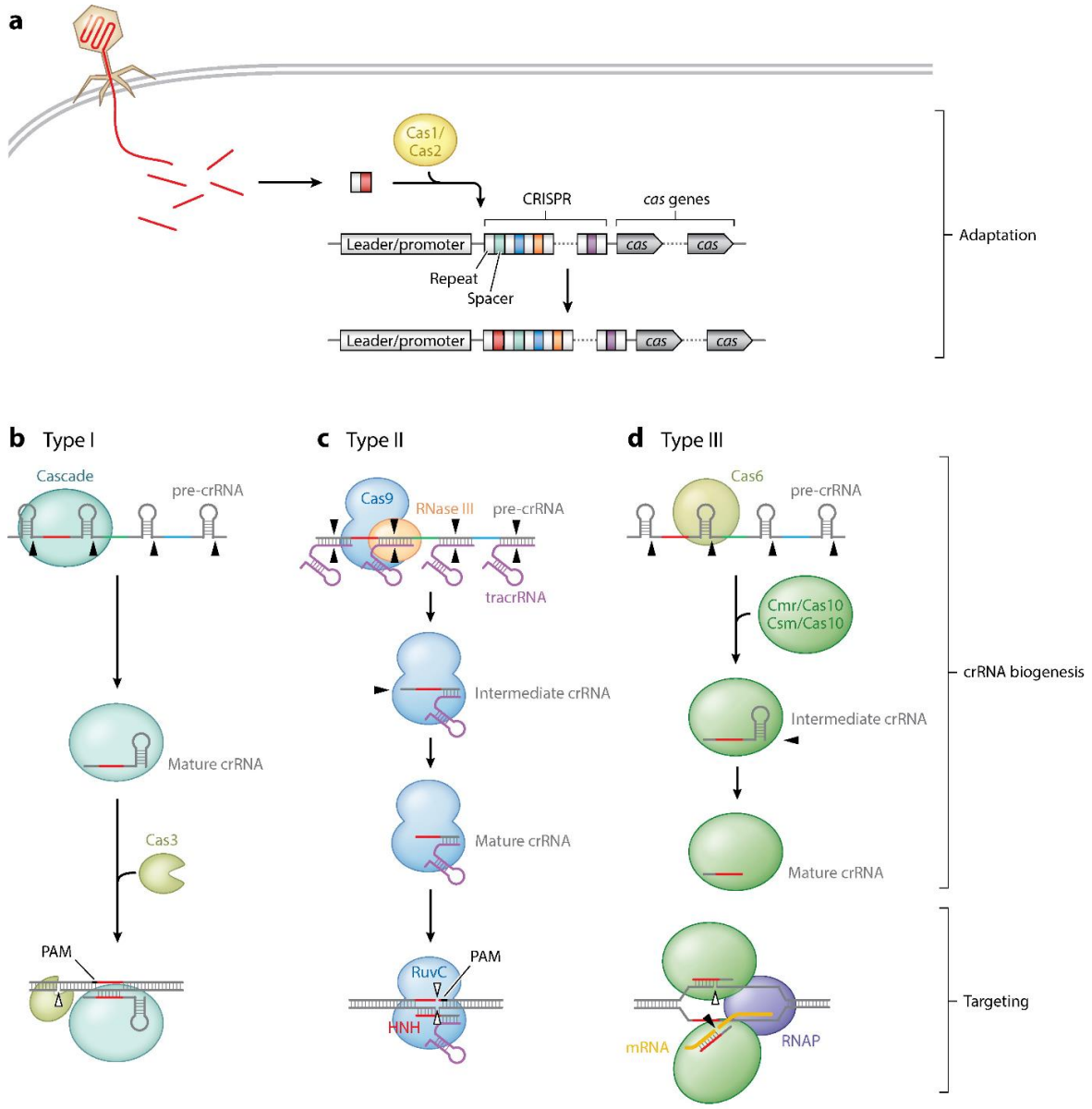

Figure 16. Mise en place de l'immunité CRISPR/Cas (17).

L'immunité CRISPR/Cas se compose de 3 phases distinctes. (a) Premièrement, durant la phase d'adaptation. Le système CRISPR intègre une courte séquence du virus ou du plasmide étranger dans le génome bactérien. Cette séquence « spacer » est intégrée au niveau du locus CRISPR par les Cas1 et 2. Les différentes séquences « spacers» ainsi collectées constituent la mémoire immunitaire de la bactérie. Elles sont séparées les unes des autres par des séquences répétées. La mise en place de cette immunité adaptative passe par la transcription de ces séquences « spacers » en partant de la région promotrice. Le transcrit qui en résulte est un précurseur crRNA (ou pre-crRNA). Celui-ci est ensuite maturé en un court crRNA (phase de biogenèse du crRNA). Ce crRNA est ensuite utilisé comme guide par les nucléases Cas (phase de ciblage). (b-d) On distingue 3 types de systèmes CRISPR/Cas qui se distinguent au niveau des phases de biogenèse du crRNA et de ciblage.

Cmr). Ces systèmes nécessitent en plus le transcrit de la cible qui sera clivé en même temps que l'ADN double (**Figure 16**) (16).

Un élément important de la régulation du système CRISPR/Cas concerne la séquence PAM. Celle-ci est indispensable au clivage du double brin d'ADN et n'est présente que dans le génome viral. Son absence dans le locus CRISPR bactérien évite ainsi à l'organisme de cliver son propre génome.

c) Applications

Du fait de sa simplicité, le système CRISPR/Cas9 a été détourné au profit de systèmes artificiels de modification du génome. Son emploi en tant que tel a nécessité la réalisation d'une modification majeure visant à améliorer sa mise en œuvre. Elle concerne la modification du couple crRNA/tracrRNA au profit d'une structure fusionnée : le sgRNA (*single guide RNA*). Cette séquence est plus facile à produire car elle ne nécessite plus de phase d'hybridation. En outre, elle est plus stable et, par la même, plus facile à cloner en grande quantité en laboratoire (221).

Sa plus simple utilisation est la génération d'une coupure double brin au niveau d'un site spécifique, de laquelle découle ensuite plusieurs applications en fonction du mécanisme de réparation endogène utilisé : le NHEJ (*non-homologous end-joining*), mécanisme de réparation peu fidèle et susceptible de générer des délétions voire des insertions provoquant un décalage du cadre de lecture ; et la recombinaison homologue qui utilise un brin donneur pour combler la coupure et permet donc de modifier finement une portion du génome.

Mis à part cette fonction de coupure, des modifications de la Cas9 elle-même permettent d'exploiter de nouvelles fonctionnalités du système. Il est par exemple possible de muter les régions nucléases HNH et/ou RUVc afin d'obtenir une variante de la Cas9 qui pourra ne cliver qu'un seul des deux brins d'ADN ou aucun des deux. Le clivage d'un seul des deux brins peut permettre d'augmenter la spécificité du clivage, mais nous reviendrons plus en détail sur cet aspect dans la partie traitant des *off-targets*. L'abolition complète de la fonction nucléase de la Cas9 (dCas9, *deadCas9*) cellulaire, tout en conservant la capacité du couple sgRNA/Cas9 de

reconnaître et de se lier à une séquence d'ADN (222), va permettre son utilisation dans diverses techniques :

- **CRISPR interférent (CRISPRi) :** la dCas9 peut être utilisée afin de bloquer la phase d'élongation pendant la transcription ou encore de bloquer la liaison de facteurs de transcriptions. Cette technique a l'avantage d'être réversible et elle évite de rentrer en compétition avec des processus endogènes, le système CRISPR étant absent des espèces eucaryotes (223).

- **Activation transcriptionnelle (CRISPRa) :** la fusion de protéines effectrices avec la dCas9 peut permettre de réguler l'expression des gènes soit via une fusion avec un régulateur transcriptionnel, soit avec une protéine permettant de réaliser des modifications épigénétiques du génome. Cette expérience a par exemple été réalisée avec l'histone déméthylase 1 (224).

- **Marquages :** la fusion de la dCas9 avec un fluorophore peut permettre de réaliser un marquage dynamique et *in vivo* de l'ADN (225). Les techniques les plus sophistiquées exploitent jusqu'à 6 fluorophores pour marquer différents *loci* (226).

- **Co-précipitation :** la dCas9 peut être utilisée pour purifier la portion d'ADN génomique reconnue par le guide et co-précipiter les protéines associées. Cette méthode repose sur l'emploi d'un anticorps reconnaissant un épitope fusionné à la dCas9 (227).

En cancérologie, outre les exploitations en laboratoire présentées ci-dessus, le système CRISPR/Cas9 est également exploité dans un cadre thérapeutique. Il fait notamment l'objet de plusieurs essais cliniques dans lesquels il permet d'abolir l'expression de PD1 (*Programmed cell death 1*) par invalidation de gènes dans des lymphocytes T autologues (228).

Cependant, même s'il se présente comme simple et efficace, l'outil CRISPR/Cas9 génère un taux significatif d'effets *off-target* qui limite donc son utilisation, notamment en clinique (229–231). La diminution de ces effets tout en conservant, voire en augmentant, l'activité de

ce système concentre plusieurs efforts de recherche. Ceux-ci visent actuellement à optimiser le *design* des sgRNA, améliorer la spécificité de la Cas9 ou encore à développer des systèmes d'acheminement aux tissus/cellules cibles.

VIII – Présentation des modèles CT26 et MB49

a) CT26

La lignée CT26 est dérivée d'un carcinome colique métastatique murin induit chez la souris par un traitement au N-nitroso-N-methylurethane (232). Cette lignée, établie en 1975 présente une mutation du gène *Kras*, qui est également la mutation la plus fréquemment retrouvée dans les cancers colorectaux chez l'homme. Des études plus approfondies permettent, à partir d'autres marqueurs, d'associer cette lignée à des sous-types établis à partir d'échantillons humains. Bien que les marqueurs employés changent d'un classement à l'autre, ceux-ci associent tous la lignée CT26 à un phénotype indifférencié (« *stem-like* »), agressif et peu répondeur aux thérapies (233–236). Ces similitudes avec certains cancers humains ont participé à son large emploi dans des études visant à évaluer l'efficacité ou les mécanismes de résistance à certains agents thérapeutiques, notamment ceux ciblant le récepteur à l'EGF (*Epidermal Growth Factor*) (237) ou la protéine MEK (Mitogen-activated protein kinase kinase) (238). La possibilité de réaliser des greffes syngéniques sur les souris BALB/c lui a également valu son emploi dans des essais d'immunothérapie. Plus encore, l'expression de la protéine gp70 (*envelope glycoprotein 70*), la protéine d'enveloppe d'un rétrovirus endogène (*Murine Leukemia Virus*, MuLV), a été et est encore exploitée pour étudier la réponse anti-tumorale T $CD8^+$ contre cette tumeur (239). Bien que cet antigène soit reconnu par les lymphocytes T, il ne peut pas être assimilé à un néo-antigène tumoral puisque son expression a également été rapportée dans les tissus sains de souris âgées de plus de 8 semaines (240). Il semble plutôt que son potentiel « immunogène » soit associé à sa surexpression dans les tumeurs. Il est également important de préciser que cette « immunogénicité » est relative, puisque la protéine gp70 est en réalité considérée comme un facteur de tolérance immunitaire (240). L'immunisation de souris avec la protéine seule n'est d'ailleurs pas capable d'améliorer la réponse immunitaire contre les tumeurs CT26 (241).

Si ce modèle est répondeur aux inhibiteurs de *checkpoints*, c'est donc peut-être davantage en raison de la forte charge mutationnelle de cette lignée. En effet, la lignée CT26 présente plusieurs aberrations chromosomiques, avec 45% de ses gènes situés dans des régions triploïdes et 39% dans des régions tétraploïdes. S'ajoute à cela une moyenne de 53 mutations par mégabase de gènes codants et entraînant une modification des séquences polypeptidiques, ce qui est du même ordre de grandeur que de ce que l'on peut observer chez l'homme (entre 1 et 100 mutations par mégabase) (233). Pour en revenir à la réponse aux inhibiteurs de checkpoints, les données publiées indiquent que la monothérapie anti-PD1 n'est pas efficace dans le traitement des tumeurs CT26 contrairement à la monothérapie par un anti-CTLA4. Néanmoins, le traitement par des anti-PD1 apporte une réelle amélioration en combinaison avec un anti-CTLA4. Cette amélioration s'accompagne d'une augmentation des cellules $CD8^+$ ainsi qu'une diminution des cellules $CD4^+FoxP3^+$ au niveau de la tumeur (242). Ces études, menées sur des tumeurs sous-cutanées ne sont pas transposables à des tumeurs orthotopiques. En effet, les tumeurs CT26 orthotopiques sont beaucoup plus immunosuppressives. Alors que l'infiltrat des tumeurs sous-cutanées expriment plusieurs gènes associés à une réponse Th1 (Il-12, IFN-γ et TNF), les tumeurs qui se développent dans le cæcum expriment davantage de gènes associés à une réponse Th2 ou à une immunosuppression (arginase-1, TGF-β, Il-6 et Il-3) (243).

En ce qui concerne le type de cellules infiltrantes retrouvé dans les tumeurs CT26, on retrouve une quantité relativement importante de cellules T mais qui diminue avec l'augmentation de la taille des tumeurs, suggérant une élimination des cellules infiltrantes et/ou l'inhibition de la mobilisation de nouveaux acteurs. Paradoxalement et dans le même temps, le nombre de cellules T $CD8^+$ augmente (244). Il n'est pas évident de comprendre comment les cellules T $CD8^+$ sont désactivées. On n'observe pas d'augmentation concomitante de cellules suppressives tels que les Treg ou les MDSC. Un mécanisme possible pourrait être l'épuisement des lymphocytes T, entraîné par une exposition prolongée de cellules à l'antigène, entraînant une perte progressive de leur fonction (245). Néanmoins, une caractéristique des cellules T CD8 épuisées est une régulation positive de plusieurs récepteurs inhibiteurs (PD1, KLRA7, KLRA3, LAG-3, CTLA4, …) (246), or aucune augmentation des transcrits de ces récepteurs n'a été détectée au cours de la croissance des tumeurs CT26 (244).

b) MB49

La lignée MB49 est dérivée d'une culture primaire de cellules vésicales murines (C57BL/Icrf-a') traitée pendant 24h avec du 7,12-dimethylbenz[a]anthracène, un puissant agent carcinogène (247). Ces cellules transformées sont capables de générer des tumeurs après inoculation sur des souris syngéniques. En particulier, l'inoculation orthotopique par instillation d'une suspension de ces cellules dans la vessie permet de développer un carcinome vésical qui mime plusieurs caractéristiques des carcinomes urothéliaux infiltrants humains, notamment l'invasion de la *lamina propria*. Les animaux présentent également une hématurie importante qui s'accompagne dans les cas les plus sévères d'une obstruction du conduit urinaire. La tumeur qui se développe ainsi à l'intérieure de la vessie est rouge, molle et extrêmement sanglante (248). Il est également possible de générer une tumeur en injectant les cellules sous la peau. Dans les deux cas, les tumeurs générées sont très agressives, ce qui implique un sacrifice des souris après quelques semaines. Des essais visant à évaluer le potentiel métastatique de cette lignée se sont d'ailleurs heurtés à cette contrainte temporelle, considérée comme trop courte pour permettre l'apparition de métastases. Un des arguments appuyant cette hypothèse nous vient d'une étude ayant révélé le potentiel métastatique d'une portion des cellules constituant les tumeurs MB49. En effet, la dissociation d'une tumeur MB49 sous-cutanée et la mise en culture des cellules *in vitro,* met en avant à la fois des cellules adhérentes semblables à la lignée parentale (majoritaires), mais également des cellules non adhérentes qui forment des sphéroïdes en culture. La réinjection de ces dernières sous la peau conduit à la génération d'une tumeur au point d'injection mais également au développement de métastases pulmonaires, ce qui n'est pas le cas pour les cellules adhérentes réinjectées (249). A notre connaissance, il n'y a pas eu de caractérisation moléculaire de ces 2 types cellulaires.

Le BCG (vaccin bilié de Calmette et Guérin) est un vaccin préparé à partir d'une souche atténuée de bacilles tuberculeux bovins (*Mycobacterium tuberculosis*) et qui est principalement connu comme moyen de prévenir la tuberculose humaine. Le BCG est également, et depuis longtemps, une immunothérapie employée pour traiter certains types de carcinomes vésicaux non invasifs par traitement intra-vésical (250). Les premières études cliniques ont mis en évidence un recrutement de T $CD4^+$ dans la vessie (251), ainsi que la

production d'Il-2 et de TNF mesurée dans les urines (252), en réponse à ce traitement. Ce vaccin ayant les mêmes effets sur la lignée MB49 (253), celle-ci s'est vu utilisée afin d'en clarifier le mécanisme d'action. Ces études ont ainsi mis en évidence un effet direct du BCG sur les cellules tumorales, comme l'induction de l'expression de PPAR-γ (P*eroxysome proliferator-activated receptor-γ*) (254) qui pourrait être impliqué dans une réduction de la croissance tumorale, un effet apoptotique direct dépendant de la cathepsine B (255), ou encore le relargage de la protéine HMGB1 (*High-mobility group box 1*) (256). Des effets sur les cellules stromales (257) et les cellules du système immunitaire (258) ont également été rapportés. Pour ces dernières, des essais de co-injection de la lignée MB49 et du BCG en sous-cutanée chez des souris, n'ont pas révélé la mise en place d'une réponse mémoire. En effet, les souris ayant survécu à la première injection ne répondaient pas mieux à une deuxième injection des cellules MB49 seules, mais nécessitaient encore l'ajout du BCG. Ces expériences, qui suggéraient un rôle prépondérant de la réponse innée, ont été complétées par des études menées *in vitro* et qui ont mis l'accent sur les cellules NK comme acteurs principaux de la réponse, avec cependant une contribution significative des LT $CD4^+$ et $CD8^+$.

La démonstration d'une certaine sensibilité des tumeurs MB49 vis-à-vis de la réponse immunitaire a ouvert la voie à d'autres approches thérapeutiques visant à renforcer cette réponse. Beaucoup d'entre elles reposent sur l'emploi d'un BCG recombinant surexprimant certaines cytokines ou antigènes : IFN-γ (259), IFN-α2b (260), antigène S1PT (*detoxified S1 subunit pertussis toxin*) (261). Dans des études plus récentes, des chercheurs ont également démontré la sensibilité des tumeurs MB49 aux inhibiteurs de *checkpoints* anti-PD-L1 (262) ou anti-CTLA4 (263) (*Cytotoxic T-lymphocyte-associated protein 4*). Ces données suggèrent que ces tumeurs présentent un terrain favorable au développement d'une réponse immunitaire adaptative en réponse à l'immunothérapie. Il n'existe toutefois pas de travaux visant à caractériser la composition en cellules infiltrantes de ces tumeurs en condition basale. Par rapport aux tumeurs CT26, portées par des souris BALB/c, on peut toutefois noter que les tumeurs MB49 sont portées par des souris (C57BL/6) avec une meilleure capacité de réponse anti-tumorale. En effet, les cellules T des souris C57BL/6 produisent davantage d'IFN-γ et leurs macrophages produisent plus de TNF-α et d'Il-12 après leur activation, alors que les cellules T et les macrophages activés des souris BALB/c produisent moins de ces mêmes cytokines (264–266).

Enfin, à l'instar de la protéine gp70 dans la lignée CT26, plusieurs études décrivent une réponse T anti tumorale spécifique dirigée contre des antigènes codés par le chromosome Y, lorsque les tumeurs sont greffées sur souris femelles (267,268). Suivant certains auteurs, ces antigènes, assimilables à des antigènes de tumeur, seraient les principales cibles moléculaires de la réponse immunitaire anti-MB49. Cette hypothèse est difficile à confirmer en raison notamment de l'absence de marqueurs moléculaires permettant d'authentifier la lignée dans les différents laboratoires. En effet, la présence du chromosome Y n'est pas constante dans les cellules MB49 suivant les différents laboratoires utilisateurs. Ainsi, une publication de l'institut Curie rapporte la présence du chromosome Y dans environ 60% des cellules MB49 (269), alors que pour d'autres auteurs, le chromosome Y est absent dans la totalité des cellules (270). En réalité l'instabilité et le caractère facultatif du chromosome Y est un phénomène connu dans les cellules malignes et même dans les cellules non-malignes vieillissantes (271). Ceci s'applique notamment au cancer de la vessie chez l'homme (272).

IX – Notes sur certaines caractéristiques biologiques des carcinomes de la vessie

Au point de départ de cette thèse, nous n'avions pas l'idée de nous intéresser plus particulièrement à la biologie des carcinomes de la vessie chez l'homme. En effet, contrairement à d'autres affections malignes humaines (carcinomes pancréatiques, rénaux, pulmonaires, mélanomes), les cancers de la vessie n'apparaissent pas dans la littérature comme des tumeurs dans lesquelles la gal-9 joue un rôle déterminant. A notre connaissance, il n'y a dans la littérature qu'un seul article mettant en relation gal-9 et cancers de la vessie, publié en 2017 par une équipe de Shangai (273). Il s'agit d'une série rétrospective de 202 patients qui ont fait l'objet d'une cystectomie radicale entre 2002 et 2014. D'après cet article, les cancers de la vessie qui présentent les plus fortes expressions de gal-9 sont les moins agressifs et ceux auxquels la chimiothérapie adjuvante bénéficie le plus. Cependant, cette publication présente au moins 3 faiblesses majeures : 1) l'anticorps et la méthode utilisés pour le marquage de la gal-9 en immunohistochimie ne sont pas mentionnés ; 2) l'hétérogénéité et la classification moléculaire des cancers de la vessie ne sont pas pris en

compte ; 3) aucune tentative n'est faite pour distinguer la gal-9 intra- et extra-cellulaire (la gal-9 plasmatique n'a pas été dosée). C'est pourquoi il m'a paru nécessaire d'inclure dans cette introduction à mon travail de thèse quelques éléments de mise à jour concernant les caractéristiques biologiques des carcinomes de la vessie chez l'homme. A l'avenir, cela devrait nous aider à rechercher des similitudes possibles avec les modèles MB49.

a) Caractères généraux

Les carcinomes de la vessie (BLCA, *bladder carcinomas*) représentent un problème important de santé publique. Par ordre de fréquence, au niveau mondial, ils représentent la septième cause de décès par cancer. Le tabagisme est un facteur de risque essentiel pour ces tumeurs. Plus de 90% sont des carcinomes urothéliaux (UCB, *urothelial caricnomas of the bladder*). Ils se développent aux dépens de l'épithélium de la muqueuse vésicale et en fonction de la profondeur d'envahissement, on distingue les UCB avec ou sans envahissement du muscle lisse sous-jacent : MIBC (*muscle invasive bladder carcinomas*) et NMIBC (*non-muscle invasive bladder carcinomas*). Parmi les carcinomes de vessie nouvellement diagnostiqués, les NMIBC sont environ 2 fois plus fréquents que les MIBC. Le diagnostic de MIBC est posé d'emblée dans la plupart des cas mais 10 à 20% des NMIBC peuvent évoluer vers des MIBC. Comme on peut s'y attendre, les MIBC ont un pronostic beaucoup plus sévère. La survie à 5 ans est de 60% en l'absence de métastases à distance lors de la prise en charge initiale, et de moins de 10% dans le cas contraire. Outre l'ablation chirurgicale, la chimiothérapie à base de cis-platine est un élément clé du traitement. Environ 20% des cas résistant d'emblée ou secondairement à la chimiothérapie sont sensibles à une immunothérapie basée le plus souvent sur l'administration d'anticorps anti-PD1 ou anti-PDL1 (274). Plusieurs approches de thérapies ciblées sont à l'étude pour le traitement des MIBC. Il s'agit notamment d'inhibiteurs du récepteur à activité tyrosine-kinase FGFR-3 (*fibroblast growth factor receptor 3*) et d'inhibiteurs de PI3-kinase (phosphoinositide 3-kinase) (275,276). Le bénéfice d'un anticorps monoclonal anti-VEGFR-2 (*vascular endothelial growth factor receptor-2*), le ramucirumab, a été démontré dans un essai de phase III (276).

Figure 17. Classification des MIBC (*muscle invasive bladder carcinomas*).

	Luminal Papillaire	Luminal Non-Specifique	Luminal Instable	Avec stroma riche	Basal/Epidermoïde	De type neuroendocrine
Principaux mécanismes oncogéniques	FGFR3+, PPARG+, CDKN2A ; Similitudes avec les cancers du sein luminaux (Gata3 - FoxA1)	PPARG+	PPARG+, ERBB2 + ; Instabilité génétique		EGFR + ; Similitudes avec les cancers épidermoïdes ORL	TP53-, RB1-
Mutations	*FGFR3* (40%) *KDM6A (*38%)	*ELF3* (35%)	*TP53* (76%) *ERCC2* (22%) Forte chage mutationnelle		*TP53* (61%) *RB1* (25%)	*TP53* (94%) *RB1* (94% mut or del)
Infiltrat stromal (cellules non-immunitaires)		Fibroblastes		Cellules musculaires lisses ; Fibroblastes ; Myofibroblastes	Fibroblastes ; Myofibroblastes	
Infiltrat immunitaire				Lymphos B	Lymphos T CD8 Cellules NK	
Histologie	Morphologie papillaire (59%)	Variant micropapillaire (36%)			Différenciation épidermoïde (42%)	Différenciation neuroendocrine
Caractéristiques cliniques	Stade T2 plus fréquent	Patients plus âgés (80 ans)			Plus fréquent chez la femme Stades T3/T4 plus fréquents	
Survie globale (médiane)	4 ans	1,8 ans	2,9 ans	3,8 ans	1,2 ans	1 an

En ce qui concerne les NMIBC, ils font l'objet, en fonction du risque de récidive, de traitements locaux basés sur la chimiothérapie intra-vésicale ou encore l'immunothérapie intra-vésicale par instillation de BCG. En cas d'échecs répétés, il faut parfois procéder à une cystectomie (277).

b) Classification moléculaire des MIBC

Comme pour d'autres tumeurs solides de diverses localisations, les MIBC forment un ensemble très hétérogène avec plusieurs dizaines de formes histologiques. Pour donner de façon concise une vision synthétique des caractéristiques biologiques et cliniques des MIBC, nous avons choisi de nous inspirer d'un article très récent d'A. Kamoun qui propose une classification des MIBC en 6 grandes catégories basées sur l'analyse de 1750 profils transcriptionnels. Ces 6 catégories qui ont fait l'objet d'un consensus entre une dizaine d'équipes de renom international sont présentées dans le tableau de la **Figure 17** (luminale papillaire, luminale non-spécifique, luminale instable, avec stroma riche, basale/épidermoïde, de type neuroendrocrine) (276).

c) Facteurs influençant la réponse aux immunothérapies par inhibiteurs de *checkpoints* dans les MIBC

Comme pour d'autres tumeurs solides, le développement des immunothérapies par les inhibiteurs de *checkpoint*s a représenté un progrès notable dans le traitement des MIBC avec des réponses tumorales objectives dans environ 20% des cas. Malheureusement, plus encore que pour d'autres localisations tumorales, on manque de biomarqueurs permettant de prédire avec une bonne assurance la réponse à ce type d'agents thérapeutiques. A l'heure actuelle, le niveau d'expression de PD-L1 par les cellules tumorales mesuré en immunohistochimie n'apparaît pas comme un bon marqueur prédictif (278). La valeur prédictive de la charge mutationnelle est encore débattue et fait toujours l'objet d'études sur des séries en cours. La valeur prédictive de l'abondance de l'infiltrat lymphoïde fait l'objet d'appréciations divergentes (275,279). A noter que la micro-topographie des cellules T est un

facteur important qui n'est peut-être pas encore suffisamment pris en compte. Une étude récente montre que l'expression de PD-1 s'accompagne d'un pronostic péjoratif lorsqu'il s'agit des TIL (*tumor-infiltrating lymphocytes*) présents au sein des nodules tumoraux mais non lorsqu'il s'agit des TIL du stroma périphérique (280). Cependant, l'abondance dans la tumeur de lymphocytes $CD8^+$ et de transcrits en rapport avec une stimulation par l'interféron-γ est associée à une bonne probabilité de réponse aux inhibiteurs de *checkpoints* (278). C'est l'opposé lorsqu'il s'agit de transcrits en rapport avec la réponse au TGF-β. Les biomarqueurs sériques ont également une valeur. Des concentrations plasmatiques élevées d'interleukines 6 et 8 et de CRP (*C-reactive protein*) sont associées à de faibles taux de réponse. C'est le contraire pour des concentrations élevées d'interféron-γ, de CXCL9, de CXCL10 et de TWEAK (*TNF-related weak inducer of apoptosis*) (280).

A noter qu'une approche actuellement en cours d'exploration pré-clinique consiste à combiner des inhibiteurs de *checkpoints* avec des petites molécules ciblées, par exemple des inhibiteurs de PI3-kinase (275).

A ma connaissance, il n'y a pas de données publiées sur le rôle de la galectine-9 dans la réponse aux inhibiteurs de *checkpoints* dans les MIBC. Cependant, un bref article de MF Chevalier publié en 2016 a mis en évidence une forte expression de Tim-3 par les cellules dendritiques circulantes et intra-tumorales chez les sujets porteurs de tumeurs urothéliales (281).

OBJECTIFS DES TRAVAUX DE THESE

Neutraliser les facteurs de tolérance qui bloquent la réponse immunitaire anti-tumorale est devenu un élément majeur des thérapeutiques anti-cancéreuses. Il y a de bonnes raisons de penser que la galectine-9 (gal-9) est l'un de ces facteurs et nous supposons, avec mon équipe d'accueil, que sa neutralisation pourrait apporter un bénéfice aux traitements de nombreuses affections malignes. Dans cette optique, et afin de produire de nouveaux outils d'étude, notre équipe s'est lancée dans la production d'anticorps monoclonaux.

Conjointement à ce développement, il nous a paru nécessaire de mettre en place un modèle syngénique murin avec des cellules produisant ou non de la gal-9, afin d'évaluer l'impact de la gal-9 tumorale sur le développement tumoral. En effet, ces dernières années, plusieurs équipes ont mis en évidence des fonctions de la gal-9 dans des tumeurs tel que les mélanomes, les carcinomes pulmonaires, pancréatiques ou ovariens. Cependant, il est difficile de faire la synthèse de ces données car, suivant les publications, les auteurs ont mis l'accent sur différents types de cellules productrices et différents types de cellules cibles. On ne dispose finalement que de peu de données sur la gal-9 produite par les cellules tumorales et sur le bénéfice à attendre en clinique de l'administration d'anticorps neutralisant la gal-9.

Ainsi, mes travaux de thèse ont été organisés autour de trois objectifs principaux :

1) Etudier le statut de la gal-9 dans différentes lignées tumorales murines *in vitro* afin de sélectionner celles l'exprimant abondamment. Produire, à partir de ces lignées, des outils visant à étudier les fonctions exercées par la gal-9 : 1) des clones invalidés pour le gène *LGALS9* ; 2) les « révertants » de ces clones exprimant, chacun, l'une des trois isoformes de la gal-9 (S, M et L).

2) Evaluer *in vitro* et *in vivo* les effets de la perte d'expression de gal-9 sur le phénotype des cellules tumorales (viabilité, prolifération, cinétique de croissance, nature de l'infiltrat immunitaire, …).

3) Poursuivre la caractérisation des anticorps neutralisant la gal-9, notamment en réalisant les premiers essais d'évaluation pré-cliniques.

La première partie de ce travail s'est focalisée sur la recherche de lignées tumorales murines exprimant un niveau élevé de gal-9. Nos investigations nous ont conduits à sélectionner les lignées CT26, dérivée d'un carcinome colique, et MB49, dérivée d'un carcinome vésical. L'invalidation du gène *LGALS9* a été réalisée sur ces deux lignées ainsi que la production de « révertants ». L'étude des effets de l'invalidation du gène *LGALS9* dans la lignée MB49 fait l'objet d'un article en préparation (article 2). En ce qui concerne la lignée CT26, les résultats seront développés dans la discussion, tout comme les résultats associés aux « révertants ».

La deuxième partie de mon projet de thèse s'est centrée sur la caractérisation et l'évaluation du potentiel neutralisant des anticorps monoclonaux anti-gal-9. Les travaux réalisés avant mon arrivée dans le laboratoire ont permis de sélectionner plusieurs anticorps capables de reconnaître spécifiquement la gal-9 et d'évaluer leur potentiel neutralisant *in vitro*. Les résultats obtenus dans le cadre de leur caractérisation ont fait l'objet d'une publication en 2018 (article 1). Parallèlement, nous avons initié l'évaluation du potentiel thérapeutique anti-tumoral de ces anticorps sur des modèles tumoraux murins syngéniques, à partir des lignées CT26 et MB49. Différentes modalités de croissance tumorale et de traitements ont été testées. Pour l'heure, les effets anti-tumoraux des anticorps ne se sont manifestés que discrètement voire pas du tout selon les conditions expérimentales. A la lumière des données présentées dans l'article 2, nous reviendrons plus en détail sur ces résultats au cours de la discussion.

RESULTATS

I- Article 1

Characterization of neutralizing antibodies reacting with the 213-224 amino-acid segment of human galectin-9

Claire Lhuillier, Clément Barjon, Valentin Baloche, Toshiro Niki, Aurore Gelin, Rami Mustapha, Laetitia Claër, Sylviane Hoos, Yoichi Chiba, Masaki Ueno, Mitsuomi Hirashima, Ming Wei, Olivier Morales, Bertrand Raynal, Nadira Delhem, Olivier Dellis, Pierre Busson.

Plos One, 2018, **DOI** : 10.1371/journal.pone.0202512.

a) Contexte et objectifs de l'étude

La gal-9 extra-cellulaire est une protéine immuno-modulatrice dont les fonctions s'apparentent à celles d'une cytokine. Elle exerce des fonctions majoritairement immunosuppressives qui sont associées au développement de plusieurs pathologies malignes chez l'homme dans lesquelles on décrit une expression dérégulée de cette protéine. Notre groupe a été le premier à mettre en évidence la contribution de la gal-9 à l'immunosuppression dans les NPC associés à EBV. Posant l'hypothèse que la neutralisation de la gal-9 et de ses effets immunosuppresseurs pourrait apporter un bénéfice thérapeutique substantiel, nous nous sommes engagés dans la production d'anticorps monoclonaux. Nous avons obtenu une série d'anticorps murins à la suite d'immunisations avec de la gal-9 recombinante humaine. Sur la base de leur capacité à neutraliser l'apoptose des lymphocytes T induite par la gal-9, deux anticorps ont été sélectionnés : Gal-Nab1 et Gal-Nab2. Le but de cette étude est de présenter le potentiel neutralisant de ces anticorps, d'identifier leurs épitopes respectifs et de tester leur capacité à reconnaître la gal-9 murine dans l'optique d'évaluer leur efficacité dans des modèles pré-cliniques.

b) Résultats

Les tests *in vitro* réalisés sur GalNab-1 et GalNab-2 révèlent plusieurs similitudes entre ces deux anticorps. Tout d'abord, ils sont capables de neutraliser l'apoptose induite par l'ajout de gal-9 exogène sur des lymphocytes T primaires. Les deux anticorps possèdent une chaîne lourde CDR3 (*complementarity determining region* 3) identique et reconnaissent des épitopes très semblables. Malgré ces similitudes, GalNab-1 et GalNab-2 présentent quelques différences fonctionnelles. En effet, les expériences menées sur la lignée cellulaire Jurkat montrent que l'anticorps GalNab-1 augmente la translocation des phosphatidylsérines et la mobilisation calcique induites par la gal-9, tout en réduisant le phénomène d'apoptose. Ces caractéristiques diffèrent de celles de GalNab-2 pour lequel on ne constate que la diminution de l'apoptose qui est de surcroît plus importante. Il est possible que ces divergences soient dues aux légères différences au niveau des épitopes linéraires mais éventuellement aussi à des différences dans les interactions avec d'autres régions de la protéine. Les analyses réalisées en collaboration avec la plateforme de biophysique moléculaire de l'Institut Pasteur ont révélé que, malgré leur affinité similaire pour la gal-9, les deux anticorps possèdent des constantes d'association et de dissociation différentes. En effet, GalNab-1 s'associe et se dissocie plus rapidement de la gal-9. Ces données pourraient aussi expliquer les propriétés distinctes observées.

Enfin, cette étude nous informe sur la spécificité de reconnaissance des anticorps. Ceux-ci ne reconnaissent pas les galectines -1, -4, -7, -8 ou -10. En revanche ils sont capables de reconnaître l'homologue murin de la gal-9. Pour rappel, ces anticorps ont été générés par immunisation avec de la gal-9 humaine chez des souris. Leur capacité à reconnaître également la gal-9 murine en fait donc des outils de choix pour évaluer leur potentiel thérapeutique dans des modèles pré-cliniques.

c) Conclusion

Ces résultats indiquent que les deux anticorps peuvent neutraliser efficacement certains des effets immunomodulateurs de la gal-9 *in vitro.* Les mécanismes qui sous-tendent ce phénomène d'inhibition ne sont pas encore connus et devront faire preuve d'investigations

supplémentaires. De plus, il serait intéressant de vérifier si les anticorps sont capables de neutraliser l'influence de la gal-9 sur d'autres acteurs de l'immunité comme les Treg, les macrophages ou les cellules NK.

Finalement, les résultats obtenus sont encourageants et appuient le développement d'études *in vivo* sur des modèles murins syngéniques ainsi que la production de variants humanisés.

PLOS ONE

RESEARCH ARTICLE

Characterization of neutralizing antibodies reacting with the 213-224 amino-acid segment of human galectin-9

Claire Lhuillier[1,2,3,4☯], Clément Barjon[1,2,3,4☯], Valentin Baloche[1,2,3], Toshiro Niki[5,6], Aurore Gelin[1,2,3], Rami Mustapha[7], Laetitia Claër[8], Sylviane Hoos[9], Yoichi Chiba[10], Masaki Ueno[10], Mitsuomi Hirashima[6,11], Ming Wei[4], Olivier Morales[7], Bertrand Raynal[9], Nadira Delhem[7], Olivier Dellis[12], Pierre Busson[1,2,3]*

1 CNRS, UMR 8126, Villejuif, France, **2** Gustave Roussy, Université Paris-Saclay, Villejuif, France, **3** Univ Paris Sud, Université Paris-Saclay, Le Kremlin-Bicêtre, France, **4** Cellvax , Romainville, France, **5** Department of Immunology, Faculty of Medicine, Kagawa University, Takamatsu, Kagawa, Japan, **6** GalPharma Co., Ltd., Takamatsu, Kagawa, Japan, **7** CNRS, UMR 8161, IRCV group, Institut de Biologie de Lille, Lille, France, **8** H-Immune Therapeutics, Paris, France, **9** Plate-forme de Biophysique Moléculaire, Institut Pasteur, Paris, France, **10** Department of Pathology and Host Defense, Faculty of Medicine, Kagawa University, Takamatsu, Kagawa, Japan, **11** Department of Gastroenterology & Neurology, Faculty of Medicine, Kagawa University, Takamatsu, Kagawa, Japan, **12** INSERM, UMR-S 1174, Univ Paris Sud, Université Paris-Saclay, Orsay, France

☯ These authors contributed equally to this work.
* pierre.busson@gustaveroussy.fr

OPEN ACCESS

Citation: Lhuillier C, Barjon C, Baloche V, Niki T, Gelin A, Mustapha R, et al. (2018) Characterization of neutralizing antibodies reacting with the 213-224 amino-acid segment of human galectin-9. PLoS ONE 13(9): e0202512. https://doi.org/10.1371/journal.pone.0202512

Editor: Ivan R. Nabi, University of British Columbia, CANADA

Received: February 15, 2018

Accepted: August 3, 2018

Published: September 11, 2018

Data Availability Statement: All data are within the paper and its Supporting Information files.

Funding: This work was supported by Idex Saclay - Satt Saclay, Prematuration Grant 2015, https://www.satt-paris-saclay.fr/; BMS Foundation for Immuno-Oncology- Grant 2016-2017, http://fondation-bms.fr/. Several authors were employed by commercial companies: Cellvax (CL, CB, MW), GalPharma Co, Ltd (TN), H-Immune Therapeutics (LC). These companies provided support in the form of salaries for authors [CL, CB, MW, TN, LC],

Abstract

Extra-cellular galectin-9 (gal-9) is an immuno-modulatory protein with predominant immuno-suppressive effects. Inappropriate production of gal-9 has been reported in several human malignancies and viral diseases like nasopharyngeal, pancreatic and renal carcinomas, metastatic melanomas and chronic active viral hepatitis. Therefore therapeutic antibodies neutralizing extra-cellular gal-9 are expected to contribute to immune restoration in these pathological conditions. Two novel monoclonal antibodies targeting gal-9 –Gal-Nab 1 and 2—have been produced and characterized in this study. We report a protective effect of Gal-Nab1 and Gal-Nab2 on the apoptotic cell death induced by gal-9 in primary T cells. In addition, they inhibit late phenotypic changes observed in peripheral T cells that survive gal-9-induced apoptosis. Gal-Nab1 and Gal-Nab2 bind nearly identical, overlapping linear epitopes contained in the 213–224 amino-acid segments of gal-9. Nevertheless, they have some distinct functional characteristics suggesting that their three-dimensional epitopes are distinct. These differences are best demonstrated when gal-9 is applied on Jurkat cells where Gal-Nab1 is less efficient than Gal-Nab2 in the prevention of apoptotic cell death. In addition, Gal-Nab1 stimulates non-lethal phosphatidylserine translocation at the plasma membrane and calcium mobilization triggered by gal-9 in these cells. Both Gal-Nab1 and 2 cross-react with murine gal-9. They bind its natural as well as its recombinant form. This cross-species recognition will be an advantage for their assessment in pre-clinical tumor models.

but did not have any additional role in the study design, data collection and analysis, decision to publish, or preparation of the manuscript. The specific roles of these authors are articulated in the 'author contributions' section.

Competing interests: Several authors were employed by commercial companies: Cellvax (CL, CB, MW), GalPharma Co, Ltd (TN), H-Immune Therapeutics (LC). This does not alter our adherence to PLOS ONE policies on sharing data and materials. Our antibodies are the subject of the following patent entitled "Antibody which is directed against galectin-9 and is an inhibitor of the suppressor activity of regulatory T lymphocytes", WO 2015/185875 A2. This does not alter our adherence to PLOS ONE policies on sharing data and materials.

Introduction

Galectins constitute a family of animal proteins defined by their binding specificity for glycans containing a β1–3 or β1–4 galactosyl bond carried either by glycoproteins or glycolipids. The domains of galectins that directly interact with carbohydrate ligands are called CRDs (for "carbohydrate recognition domains") [1, 2]. The CRDs are made of about 135 amino acids (aa) forming a groove in which the carbohydrate ligand can bind. Interaction with a galactosyl bond is crucial for binding of each CRD to its physiological ligands. However, the binding specificity of each type of galectin is further specified by the atoms and molecules located at the periphery of the galactosyl bond which also interact with the CRDs.

Galectin-9 (gal-9) belongs to the category of "tandem-repeat" galectins containing two CRDs with distinct specificity linked by a flexible peptide chain called "linker peptide" (three other human "tandem-repeat" galectins are galectin-4, -8 and -12). As a result of alternative splicing, gal-9 exists under three main isoforms characterized by the length of the linker peptide: long (49 aa), medium (27 aa) and short (15 aa,) abbreviated as gal-9L, gal-9M (also called Δ5) and gal-9S (also called Δ5/ Δ6)[3]. We do not yet know the functional differences between these isoforms although we know that the length of the linker peptide influences the relative mobility of the two CRDs [3].

In basal physiological conditions, gal-9 is weakly expressed in most tissues (with the greatest abundance in the thymus and kidney). Its expression increases in many cell types–including endothelial and epithelial cells—under the influence of the cytokines of the Th1 immune response especially interferon-γ (IFN-γ) [4, 5]. Gal-9 is trafficking in various cell compartments either as a soluble protein or bound to the cell membrane network. It is consistently found in the cytoplasm. Depending on the cell type, it is also detected in the nucleus and at the surface of the plasma membrane [6, 7]. Like other galectins, gal-9 has no signal sequence. However, it can be secreted by non-conventional pathways, either bound to nanovesicles called exosomes, or under a soluble form by mechanisms which are not yet fully understood [6, 8, 9]. Distinct functions have been assigned to intracellular, cell surface and extracellular gal-9 [3]. Both intracellular and cell surface gal-9 have an impact on cell signaling and contribute to the organization of cell polarity. Cell surface gal-9 plays a role in contacts with neighboring cells and adhesion with extracellular matrix. When released in the extracellular medium, gal-9 acts like a cytokine with multiple immune-modulatory—mainly immuno-suppressive—activities involving several target cells. It promotes the expansion of regulatory T cells (Tregs) and strengthens their immunosuppressive activity, while it reduces the development of Th17 cells [10–16]. Gal-9 has been shown to induce apoptosis of $CD4^+$ Th1 cells and $CD8^+$ cytotoxic cells [17, 18]. Interestingly, it has also been implicated in the expansion of granulocytic myeloid-derived suppressor cells (MDSCs; $CD11b^+Ly\text{-}6G^+F4/80^{low}Ly\text{-}6C^{low}$) and more recently, in the promotion of Th2 /M2 differentiation that favors tumor progression in melanoma patients [19]. Our group and others have shown that gal-9 has a bi-phasic impact on peripheral T cells with early apoptosis in a majority of target cells and late phenotypic changes in surviving cells [20, 21]. It is still unclear what cell surface receptors of extracellular gal-9 are involved in the various effects mentioned above. Tim-3 was initially identified as one receptor of gal-9 on T cells [17, 22]. This has been confirmed in later studies. However, gal-9 can also bind other receptors such as CD44, dectin 1 or the protein disulfide isomerase [10, 23, 24].

There is mounting evidence that massive and inappropriate production of gal-9 has deleterious immunosuppressive effects in a number of viral and/or malignant diseases. The contribution of gal-9 to tumor or viral immune evasion was first reported by our group in publications dealing with Epstein-Barr virus-related nasopharyngeal carcinomas [8, 25]. Later on, similar observations were reported in chronic active viral hepatitis with or without

hepatocellular carcinomas [26–28]. More recently, unwanted effects of gal-9 have been demonstrated or strongly suspected in a series of human malignancies without known viral etiology, including pancreatic and renal carcinomas, metastatic melanomas, a subgroup of lung carcinomas, glioblastomas and several types of acute myeloblastic leukemias [19, 22, 24, 29–31]. We believe that therapeutic antibodies neutralizing gal-9 are likely to become important therapeutic tools for the treatment of these diseases. Our general objective is to produce and characterize such antibodies. We have noticed that antibodies neutralizing extra-cellular gal-9 used in previous publications have not been precisely described in terms of affinities, sequences of variable segments, epitopes and cross-reactivity [22, 25]. Therefore, the aim of this report is to make these data publicly available for two novel neutralizing mAbs—Gal-Nab1 and Gal-Nab2—which are also well characterized in terms of functional activities. They were obtained following mouse immunization with the recombinant c-terminal part of gal-9. Their impact on the immuno-modulatory functions of extracellular gal-9 such as apoptosis induction, calcium mobilization or late phenotypic changes, was investigated *in vitro* using various functional assays based on Jurkat leukemic T cells or peripheral blood mononuclear cells (PBMCs). Intriguing functional differences were found between Gal-Nab1 and Gal-Nab2 although they bind to nearly identical linear epitopes (aa 213–224). These differences might be related to distinct contributions of other parts of the protein to the epitope/paratope interface. On the other hand, we found that both Gal-Nab1 and 2 react with murine recombinant and native gal-9 in two distinct types of binding assays. These characteristics might be helpful to use them in pre-clinical investigations.

Materials and methods

Reagents

The various forms of recombinant gal-9—human S and M isoforms and murine M isoform–were produced in Escherichia coli (E. coli) as GST fusion proteins. Tag-free proteins were purified by affinity chromatography on lactose-agarose column [32]. The c-terminus galectin-9 (residues 191 to 355 of the gal-9 long isoform) was produced in E. coli as a GST-fusion protein. The tag-free protein was purified by exclusion chromatography [7]. Only tag-free gal-9 proteins were used in our experiments. Lactose (β-lactose) was purchased from Sigma-Aldrich. In house anti-gal-9 mAbs (Gal-Nab1 and Gal-Nab2) were produced in mice as described in the next paragraphs and were both of the IgG1, κ isotype. The mouse control isotype antibody (control IgG) was from BioLegend. Commercial monoclonal anti-gal-9 antibodies were also used: 9M1-3 (BioLegend) and RG9-35 (BioLegend) directed against human and murine gal-9, respectively. A goat polyclonal antibody was used for detection of murine gal-9 by Western blotting (R&D System/Bio-Techne).

Animal care and immunizations

Procedures used for mouse handling and immunization were reviewed and approved by the following Ethics committee: "comEth Afssa/ENVA/UPEC" sponsored by "Ecole Nationale Vétérinaire d'Alfort" and "Université Paris-Est- Créteil -Val de Marne" (decision # 14/02/12-1, February 14, 2012). BALB/c female mice age 6–8 weeks were purchased from Charles Rivers Laboratories (Saint Germain–Nuelles, France) and housed in pathogen-free conditions in filter cap cages holding a maximum of 5 animals with irradiated aspen chip bedding and cotton fiber nesting material. They were maintained on a 12/12 light/dark cycle, with *ad libitum* UV-treated water and RM1 rodent diet. Immunogenic mixtures were injected intra-peritoneally. Intermediate blood collections were done by puncture of the orbital sinus (50 μl with intervals of at least 15 days). The animals were monitored every day for signs of pain, such as immobility

or restlessness, reduction of drinking and food intake. The persistence of abnormal behaviors for more than one day led to the euthanasia of animals with suffering presumption. Prior to spleen collection, mice were sacrificed by cervical elongation. Otherwise, mice were euthanatized by carbon dioxide asphyxiation.

Production of anti-galectin-9 monoclonal antibodies

Immunizations were conducted at PX'Therapeutics (Grenoble, France) [7]. Five BALB/c female mice (eight weeks old) were immunized with the recombinant c-terminus galectin-9. Immunizations (40 μg of protein) were administered intraperitoneally at days 0, 22, 37 and 54 with complete Freund's adjuvant for the first immunization, then with incomplete Freund's adjuvant for subsequent injections.

Anti-gal-9 antibodies were detected in mouse sera and hybridoma supermatants, by ELISA (enzyme-linked immunosorbent assay). Briefly, microtiter plates were coated with 0.05 M carbonate/bicarbonate buffer pH 9.6, containing 50 ng human c-terminus gal-9 per well, during 1h at room temperature. After washing with phosphate buffered saline (PBS) containing 0.1% Tween-20, the wells were saturated with 3% bovine serum albumine (BSA) in PBS at room temperature for 1h. They were then incubated with mouse sera or raw hybridoma supernatants in PBS with 1% BSA at room temperature for 2h. After a washing step with PBS 0.1% Tween-20, the anti-galectin-9 antibody level was determined using horseradish peroxidase-coupled (HRP) goat antibodies to mouse IgG (Sigma-Aldrich, St Quentin Fallavier, France).

An immune response against the c-terminal part of gal-9 was confirmed by ELISA in the five immunized mice. Splenocytes were collected from the two best responding mice which were sacrificed three days after the last boost. These splenocytes were used in liquid or semi-solid fusions with Sp2/0 cells at a ratio of 5:1 and 2:1, respectively. Hybridomas supernatants were assessed using gal-9 ELISA. The semi-solid fusion was successful and a collection of monoclonal hybridomas secreting anti-gal-9 antibodies was obtained. For subsequent experiments, antibodies were purified from hybridoma supernatants using protein A affinity chromatography. The concentrations of endotoxins in the final solutions were checked using the following kit: ToxinSensor^{TM} Chromogenic LAL Endotoxin Assay (GenScript). They were below 3 EU/ml.

Preparation and culture of galectin-9 target cells

The human T cell line Jurkat E6.1 (American Type Culture Collection) was grown in RPMI 1640 medium (Gibco-Life Technologies) supplemented with 10% fetal calf serum (FCS) at 37˚C in a 5% CO_2 humidified atmosphere. Human peripheral blood mononuclear cells (PBMCs) were obtained from anonymous healthy blood donors using standard density gradient centrifugation (Lymphocyte separation medium, Eurobio AbCys) and used for subsequent T cell purification or cultured at 37˚C with 5% CO_2 in RPMI 1640 medium supplemented with 10% FCS. $CD3^+$ T cells were purified using magnetic separation of untouched $CD3^+$ cells (pan T cell isolation kit; Miltenyi Biotec). For T cell activation, PBMCs or purified $CD3^+$ cells were cultured in anti-CD3-coated plates in the presence of soluble anti-CD28 antibodies (0.5 μg/mL; Miltenyi Biotec).

Apoptosis assessment

Jurkat cells were exposed in serum-free medium (Hybridoma-SFM, Gibco) to crude gal-9 or gal-9 previously pre-incubated for 30 min at 37˚C with lactose, a control isotype antibody or anti-gal-9 mAbs at 2X concentrations. During the subsequent incubation with target cells, reagents were at 1X concentration, as indicated in the figure legends. After 24h of incubation,

Jurkat cells were washed and stained with annexin-V (Thermo Fischer Scientific) and propidium iodide (PI; Sigma-Aldrich) before acquisition on the Accuri® C6 flow cytometer (BD Biosciences). For assessment of primary T cells apoptosis, purified $CD3^+$ cells were incubated in complete RPMI medium (10% FCS) and treated as indicated above. After 36h of incubation, $CD3^+$ cells were washed, stained with annexin-V and PI and analyzed by flow cytometry.

Measurement of cytosolic calcium concentration ($[Ca^{2+}]_{cyt}$)

$[Ca^{2+}]_{cyt}$ was recorded in Jurkat cells by a fluorimetric ratio technique [33]. The fluorescent indicator Indo-1 (4 μM; Invitrogen/Molecular Probes) was loaded by incubating the cells at room temperature under gentle agitation. Cells were then resuspended in Hepes Buffer Saline medium and treated with gal-9 (30 nM) preincubated or not with lactose (5 mM) or with anti-gal-9 mAbs (67 nM, i.e. 10 μg/mL). One million cells was put in a 1 cm width– 3 mL quartz cuvette, and inserted in a spectrofluorimeter (Varian Cary Eclipse), equipped with a thermostated cuvette holder. Excitation of Indo-1 was done at 360 nm, and emissions at 405 and 480 nm were recorded. Background and autofluorescence were subtracted from the values measured at 405 and 480 nm. Intracellular Ca^{2+} concentrations were calculated following the method already described by O. Dellis and collaborators [33]. Traces were given without SEM for clarity (SEM values were usually < 40 nM).

Phenotypic analysis and cell sorting

After one week of culture with indicated treatments, PBMCs were analyzed for their central memory, effector memory or naive T cell phenotype, by incubation with PE-conjugated anti-CD45RO, FITC-conjugated anti-CCR7, and APC-conjugated anti-CD3 antibodies (Biolegend). Isotype-matched non-specific antibodies were used as negative controls. Staining was analyzed on viable cells on forward scatter/sideward scatter plot, and on the $CD3^+$ population gate.

Intracellular cytokine staining

After one week of culture with indicated treatments, PBMCs were restimulated with 50 ng/mL phorbol 12-myristate 13-acetate (PMA) and 500 ng/mL ionomycin (Santa Cruz biotechnolgy) in the presence of 10 μg/mL brefeldin A (Sigma-Aldrich) for 4h. Cells were washed and stained with APC-conjugated anti-CD3 antibody. Then, cells were fixed, permeabilized and stained with FITC conjugated anti-IL-2 and PE-conjugated anti-IFN-γ antibodies (Biolegend).

Investigations of Gal-Nab1 and Gal-Nab2 binding to full length gal-9M by surface plasmon resonance (Biacore)

Assessment of antibody interactions with gal-9 was done by surface plasmon resonance using a T200 Biacore (GE Healthcare) device. In a first series of experiments, gal-9M was used as a ligand and covalently bound to the chip (Series S Sensor chip CM5, GE Healthcare) activated by NHS/EDC (mix of N-hydroxysuccinimide and 1-ethyl-3-(3-dimethyl-amino-propyl) carbodiimide**).** Covalent binding was done by injection of recombinant gal-9M in the microfluidic system at 10 μg/mL, at pH5, in acetate buffer. Purified Gal-Nab1 and Gal-Nab2 were used as the analytes. They were injected in the microfluidic system at various concentrations from 1.5 to 400 nM, with a flux of 40 μL/min, for 400s, in the presence of albumin (0.1 mg/mL) and tween 0.05%. The dissociation of the complex was followed for 500s. Regeneration of the chip was done with glycine (10 mM, pH 1.5).

Reciprocally, in the next series of experiments, Gal-Nab1 and Gal-Nab2 mAbs were used as ligands covalently bound to the CM5 chip activated by NHS/EDC. Covalent binding was done

by injection of the purified antibodies in the microfluidic system at 10 μg/mL in acetate buffer, at optimal pH (5 for Gal-Nab1 and 4.5 for Gal-Nab2). The injection lasted 400s and was followed by a 900 s washing step. Recombinant gal-9M was used as the analyte. It was injected at various concentrations from 0.39 to 100 nM, with a flux of 40 μL/min, for 400s, in PBS with albumin, 0.1 mg/mL, and tween 0.05%. The dissociation of the complex was followed for 600s. Regeneration of the chip was done with water containing SDS 0.1% for 1 min twice.

Binding parameters, especially the K_D (dissociation constant) were calculated using the Biacore T200 evaluation software. The on-rate constant (K_{on} in s^{-1} M^{-1}) was calculated from the ascending portion of the curve depicting the loading of the free Gal-Nab1 and 2 antibodies (analytes) on the immobilized gal-9-M (ligand) or the loading of the recombinant gal-9M (analyte) on the immobilized Gal-Nab1 and Gal-Nab-2 antibodies (ligands). The K_{on} characterizes how quickly the antibodies bind to their target. The off-rate constant (Koff in s^{-1} M^{-1}) was calculated from the down-side of the curve depicting the elution of the analytes from the immobilized ligands. It characterizes how quickly the antibodies dissociate from their target.

Investigations of Gal-Nab1 and Gal-Nab2 binding to a biotinylated peptide by surface plasmon resonance (Biacore)

In these experiments, the ligand was an oligopeptide called CTB containing the amino-acids 208 to 232 of gal-9L (176–200 and 164–188 of gal-9M and S, respectively), biotinylated at its c-terminus and bound to a streptavidin chip (Series S Sensor chip SA, GE Healthcare). In this 32-mer oligopeptide, the 25 gal-9 aa were flanked by stuffer aa not related to gal-9, designed to increase its solubility and accessibility (complete sequence with stuffer aa in italic: *KRE*FSTP AIPPMMYPHPAYPMPFITTIL*DRKK*(biotin)-OH). A biotinylated scramble oligopeptide was used as a control (complete sequence: biotin-PMTPYKPHTGK MYPIRQAPMAPFDSIERP MF-OH). To achieve streptavidin binding, the biotinylated oligopeptides were injected in the microfluidic system at a concentration of 500 ng/mL in PBS during at least 25s. Purified Gal-Nab1 and Gal-Nab2 mAbs were used as the analytes. They were injected at various concentrations from 0.05 to 3.2 nM, with a flux of 40 μL/min, for 700 s, in PBS with albumin 0.1 mg/mL and tween 0.05%. The dissociation of the complex was followed for 800s Regeneration of the chip was done with NaOH 500mM, SDS 0.1% and H_2O. Binding parameters were calculated as previously explained for Biacore experiments on full length gal-9-M.

The same CTB and control peptides were used in a functional assay based on apoptosis protection of $CD3^+$ T cells treated for 36h with gal-9 (gal-9S; 40 nM). Gal-Nab1, Gal-Nab2 and control IgG Abs (67 nM) were pre-incubated with the CTB or the scramble peptide (6.7 μM i.e. with a molar ratio of 100) for 30 min at 37˚C prior to their pre-incubation with gal-9.

Epitope mapping by oligopeptide competition

Epitope mapping for Gal-Nab1 and Gal-Nab2 mAbs was realized using 15 overlapping peptides of 15 aa (peptide 1 SAPGQMFSTPAIPPM to peptide 15 MMYPHPAYPMPFITT). These peptides were covering a segment of gal-9 mapping between aa 202 and 230 (using gal-9L coordinates; or 158 and 186 using gal-9S coordinates). This segment was chosen on the basis of prior experiments performed in our laboratory (data not shown). Gal-Nab1 and Gal-Nab2 were diluted at a concentration of 0.06 and 0.3 μg/mL, respectively (i.e. at the effective concentration 50 previously determined) and pre-incubated with increasing concentrations of each peptide (from 0.0001 to10 μg/mL). Then, mAbs/peptides mixtures were added to 96-wells plates coated with gal-9. Secondary HRP-conjugated anti-mouse antibodies were used to detect mAbs binding to gal-9. Experimental absorbance values (A_{exp}) or background values of absorbance ($A_{0;}$ measured in wells without mAbs/peptides) were subtracted from maximal

absorbance values (A_{max}; maximum binding of mAbs without peptides) and the percentages of inhibition were calculated as follows: $[(A_{max}—A_{exp}) / (A_{max}—A_0)] * 100$. Results are shown only for the peptides 7 to 14 because the percentage of inhibition was very low with the other peptides (1 to 6 and 15).

Determination of the hypervariable regions for Gal-Nab1 and Gal-Nab2

Total RNA was extracted from hybridoma cell pellets using a Trizol solution (Tri Reagent, Euromedex). It was then reverse-transcribed using the ImProm-II™ Reverse Transcription System from Promega. cDNA segments encoding the variable regions of the heavy and light chains of Gal-Nab1 and 2 were amplified using the Phusion "hot start" polymerase (Thermo Fisher Scientific) and flanking degenerated primers recommended by Srebe et al. [34]. Fragments amplified by efficient primers were excised from agarose gels and subjected to a second round of amplification using the same primers. The resulting fragments were ligated in the pJet1.2/blunt plasmid (Thermo Fisher Scientific), cloned in E. coli and subjected to Sanger sequencing. Hypervariable regions (CDR 1, 2 and 3 of heavy and light chains) were identified using the softwares provided by http://www.bioinf.org.uk/abs/.

Determination of monoclonal antibody cross-reactivity with murine gal-9 by ELISA and cold immuno-precipitation

A comparative assessment of mAbs binding to human gal-9M and S, murine gal-9M and several human galectins (1–4, 7, 8 and 10) was done by direct ELISA. Briefly, Gal-Nab1, Gal-Nab2 or IgG1 control mAbs were coated in a 96-well plate. Then, biotinylated galectins were incubated at 1 nM and detected by the classic streptavidin-HRP method. For cold immuno-precipitation, proteins were extracted from a BALB/c mouse thymus using a lysis buffer containing 10 mM Tris HCl pH 7.4, 150 mM NaCl, 1% Triton, 0,05%SDS and protease inhibitors (Complete, Roche). Primary antibodies (Gal-Nab1, Gal-Nab2, 9M1-3, RG9-35) and control mouse IgG1 were loaded on magnetic beads bearing covalently bound anti-mouse IgG sheep antibodies (10 μg purified antibodies for 1.6 X 10^6 beads) (M280 Dynabeads, Thermo Fischer Scientific). Immune complexes were formed by incubation of the thymic protein extract (120 μg proteins in 600 μl of lysis buffer) with antibody loaded beads (4 X 10^7) for a time interval of 3h to 18h at 4˚C with rotative agitation. Magnetic beads loaded with immune complexes were then washed 7 times with lysis buffer (without SDS and protease inhibitors). Finally, immune complexes were eluted by boiling the beads for 4min in Laemmli buffer and loaded on a PAGE gel for Western blot analysis.

Statistics

Statistical analyses were performed by one-way ANOVA followed by Dunnet post-test using GraphPad Prism 7 software. $p < 0.05$ was defined as a statistically significant difference. Where indicated * $p < 0.05$; ** $p < 0.01$; *** $p < 0.001$; ns: not significant.

Results

Impact of anti-gal-9 antibodies on gal-9-induced cell death and calcium mobilization in the Jurkat T cell line

A series of monoclonal antibodies reacting with gal-9 were obtained by mouse immunization with a recombinant protein representative of the c-terminal portion of gal-9L (long isoform) containing amino-acids 191 to 355 as previously described [7]. Two of them, named Gal-Nab1 and Gal-Nab2, were selected as potential neutralizing antibodies on the basis of preliminary

experiments (both are of the IgG1-κ isotype). Their reactivity with gal-9 was identical in the presence as well as in the absence of lactose (S1 Fig). To confirm their neutralizing activity, we first used the human leukemic T cell line Jurkat, which is known to be responsive to extracellular gal-9 [35, 36]. In a previous report, we have shown that in serum-free conditions, Jurkat cells are sensitive to nanomolar concentrations of gal-9 [20]. We first compared the ability of two isoforms of gal-9 (gal-9S and gal-9M) to induce apoptotic cell death in Jurkat cells by assessing the percentages of annexin-V-positive and propidium iodide-positive (annexin-V^+PI^+) cells after 24h of treatment (Fig 1A). Percentages of apoptosis reached a plateau at about 85–90% with 130 and 250 nM of gal-9S and gal-9M, respectively. The mean effective concentrations inducing apoptotic death in 50% of the cells (EC50) were 40 and 80 nM for gal-9S and gal-9M, respectively. Based on these data, 40nM was chosen as the common working concentration used for gal-9S and M in all subsequent experiments. Apoptosis induction was chosen as one initial end-point to assess the neutralizing capacity of our mAbs. For correct interpretation of our following results, one needs to keep in mind that extra-cellular galectins often induce both apoptotic death in a fraction of their target cells (rapid succession of annexin-V and PI staining) and a process of non-lethal phosphatidylserine (PS) translocation in another fraction (annexin-V positivity in the absence of subsequent PI staining) [37]. In this regard, distinct effects were obtained when using Gal-Nab1 and Gal-Nab2. As shown in Fig 1B, Gal-Nab2 completely abrogated gal-9-induced apoptosis (annexin-V^+PI^+) in Jurkat cells, but did not prevent the non-lethal PS translocation (annexin-V^+PI^-). In contrast, Gal-Nab1 was less efficient in reducing the percentage of apoptotic cell death, and rather increased the fraction of annexin-V^+/PI^- cells. As expected, both PS translocation and apoptotic cell death were not affected by the control IgG. This suggests that Gal-Nab1 favors the translocation of PS induced by gal-9 although it reduces its capacity to induce apoptosis. This functional difference between Gal-Nab1 and Gal-Nab2 was confirmed by the dose-response curves in Fig 1C and 1D where Gal-Nab2 decreased the percentage of apoptotic cells (to a level equivalent to the untreated condition) without modifying the unlethal PS translocation induced by gal-9. On the other hand, Gal-Nab1 reduced by about 50% the level of apoptosis cell death and even increased the percentage of annexinV^+/PI^- cells.

Another known effect of gal-9 on Jurkat cells is the induction of calcium mobilization [35, 38]. We previously demonstrated that the rapid calcium mobilization induced by gal-9 in Jurkat cells–which occurs in less than 1 minute—is not required for apoptosis induction [20]. Thus, we wondered whether our mAbs could neutralize this additional independent effect triggered by extracellular gal-9. Using the free calcium probe Indo-1, intracytosolic calcium release was assessed in Jurkat cells treated with recombinant gal-9. Like for apoptosis assays, experiments were performed in serum-free medium using nanomolar concentrations of gal-9. Calcium release was rapid, occurring within 30s after gal-9 addition (Fig 1E and 1F). It was inhibited by pre-treatment with 50 μM 2-APB, a Store-Operated Calcium Entry inhibitor (data not shown) [33]. Calcium mobilization was delayed of about 90s after gal-9 pre-incubation with Gal-Nab2 (Fig 1F). In contrast, calcium mobilization was not delayed and its amplitude was even increased when gal-9 was pre-incubated with Gal-Nab1 (Fig 1E). This observation strengthens the idea that Gal-Nab1 and 2 have distinct effects on the interactions of gal-9 with Jurkat cells.

Anti-gal-9 mAbs neutralize gal-9-induced apoptosis of primary T cells

Several studies have shown that gal-9 induces the apoptosis of peripheral primary T cells *in vitro* [17, 39]. Therefore, we investigated the capacity of our anti-gal-9 mAbs to protect primary T cells from apoptosis induced by exogenous gal-9. $CD3^+$ cells from human healthy

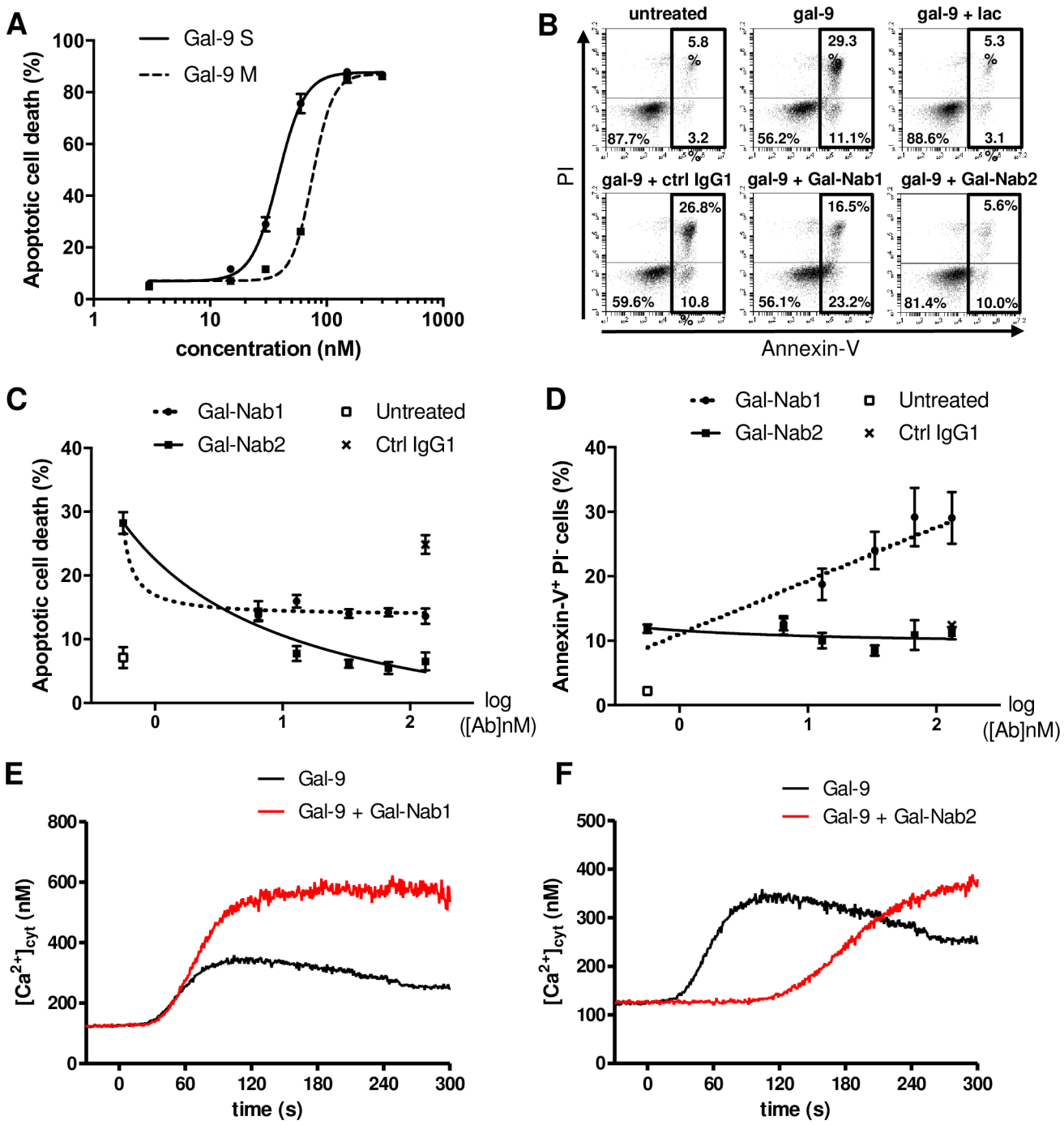

Fig 1. Jurkat cell responses to exogenous gal-9 in the presence of Gal-Nab1 and Gal-Nab2 antibodies. A. Jurkat cells were treated during 24h with increasing concentrations (3 to 300 nM) of human recombinant gal-9 (gal-9S or M) and percentages of apoptotic cell death were assessed by flow cytometry analysis of annexin-V^+ PI^+ cells (technical duplicates). **B.** Example of flow cytometry plots for Jurkat cells treated or not with gal-9 (gal-9S; 40 nM) alone or in combination with lactose (5 mM), control isotype mAbs (ctrl IgG1) or anti-gal-9 mAbs (Gal-Nab1 and Gal-Nab2) at 67 nM (i.e. 10 μg/mL) followed by annexin-V and PI staining after 24h. **C-D.** Dose-response curves for apoptotic cell death (annexin-V^+ PI^+) **(C)** or PS translocation (annexin-V^+ PI^-) **(D)** in Jurkat cells treated for 24h with increasing concentrations of Gal-Nab1 and Gal-Nab2 (6 to 130 nM). Empty squares indicate the percentages obtained in conditions without gal-9. Black crosses indicate the percentages obtained with isotype control IgG1 mAbs used at maximal concentration (130 nM). Data are presented as means ± SEM of four biological replicates. **E-F.** Variations of $[Ca^{2+}]_{cyt}$ in Jurkat cells treated with gal-9 (40 nM, added at t = 0 s) alone (black line) or with gal-9 combined with Gal-Nab1 **(E)** or Gal-Nab2 **(F)** (red line). $[Ca^{2+}]_{cyt}$ was assessed by Indo-1 fluorimetry as described under "Materials and Methods". Data presented here are representative of three similar independent experiments.

https://doi.org/10.1371/journal.pone.0202512.g001

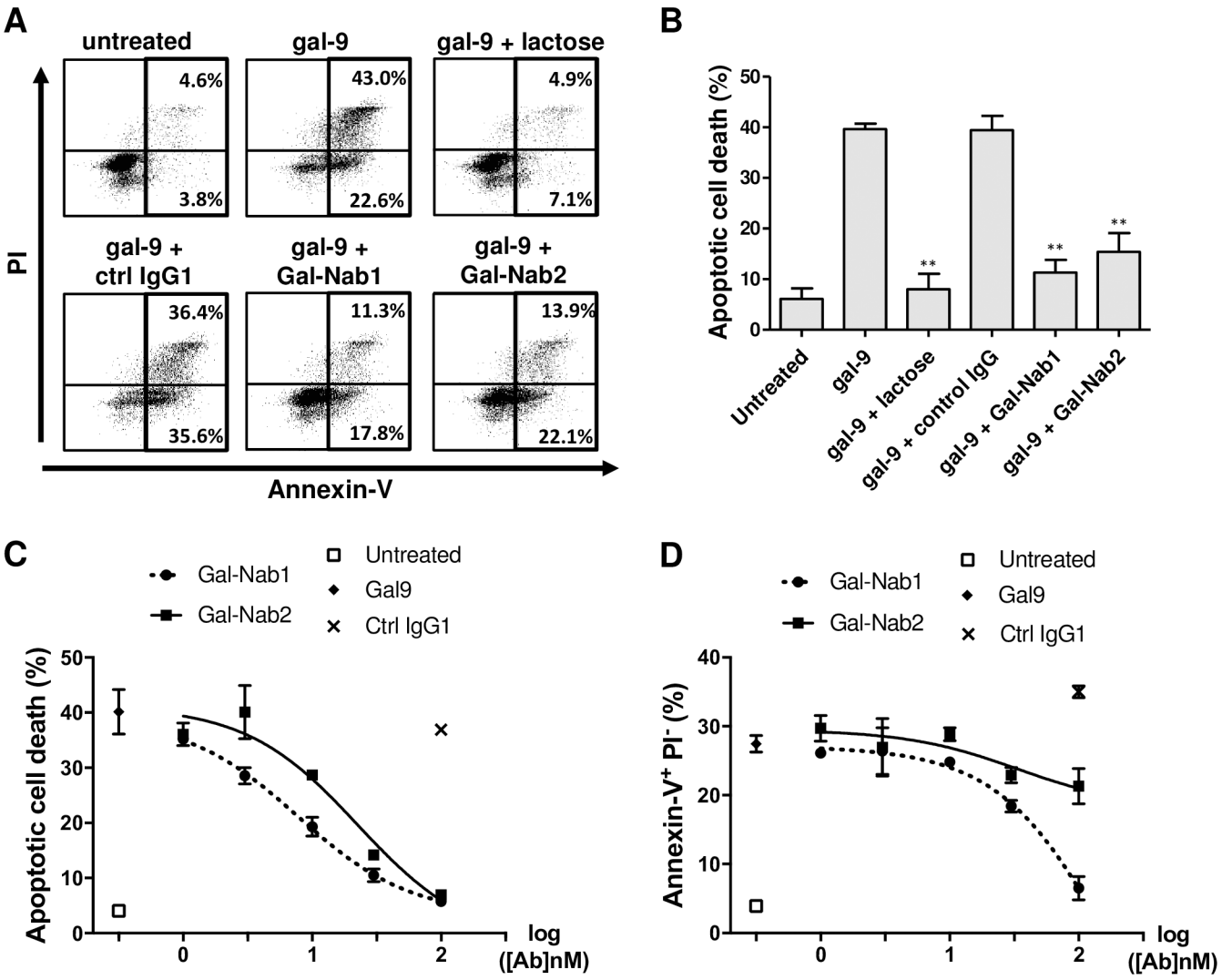

Fig 2. Anti-gal-9 mAbs efficiently neutralize gal-9-induced apoptosis in primary T cells. $CD3^+$ T-cells were isolated from healthy donors, activated by a combination of CD3/CD28 antibodies and treated or not with gal-9 (gal-9S; 40 nM) alone or in combination with lactose (5 mM), control isotype mAbs (ctrl IgG1) or anti-gal-9 mAbs (Gal-Nab1 and Gal-Nab2) at 67 nM (i.e. 10 μg/mL). After 36 h, they were subjected to annexin-V/PI staining and flow cytometry analysis. **A.** Examples of flow cytometry plots for purified $CD3^+$ cells from one donor. **B.** Synthesis of data from 3 similar experiments made with $CD3^+$ cells from 3 donors. **C and D.** Dose-response curves for apoptotic cell death (annexin-V^+ PI^+) **(C)** or PS translocation (annexin-V^+ PI^-) **(D)** in activated $CD3^+$ cells treated for 36h with gal-9 combined with increasing concentrations of Gal-Nab1 and Gal-Nab2 (0.3 to 100 nM). Empty squares indicate the percentages obtained in conditions without gal-9. Black crosses indicate the percentages obtained with isotype control IgG1 mAbs used at maximal concentration (100 nM). Data are presented as means ± SEM of three independent experiments made with three distinct donors.

https://doi.org/10.1371/journal.pone.0202512.g002

donors were activated by anti-CD3/CD28 Abs and treated with gal-9 for 36h in the presence or absence of Gal-Nab1, Gal-Nab2 or control antibodies. Gal-9 induced non-lethal PS translocation (annexin-V^+PI^-) and apoptotic cell death (annexin-V^+PI^+) in $CD3^+$ cells (Fig 2A and 2B). Both PS translocation and apoptotic cell death were almost entirely reversed by addition of lactose (5 mM) (Fig 2A and 2B). Apoptotic cell death was dramatically reduced (about 75–80% reduction) by both Gal-Nab1 and Gal-Nab2 (Fig 2A and 2B). The impact on PS translocation was much weaker; Gal-Nab2 had almost no effect (Fig 2A and 2B). These observations were confirmed when $CD3^+$ cells were treated with gal-9 in combination with increasing concentrations of the antibodies (dose/response curves; Fig 2C and 2D). Gal-Nab1 was slightly

more efficient than Gal-Nab2 to prevent apoptotic death of primary T cells (EC50 of 10 and 25 nM, respectively). Higher concentrations of Gal-Nab1 were required to reduce non-lethal PS translocation (EC50 of 50 nM) whereas Gal-Nab2 had almost no effect on this alteration.

Anti-gal-9 mAbs inhibit the late emergence of Th1-like and T_{CMs}-like T cells observed in PBMCs surviving apoptosis induced by gal-9

It has been shown that, when applied for several days on PBMCs, gal-9 induces the emergence of T cell subpopulations with a Th1-like or memory-like phenotype among the cells surviving gal-9-induced apoptosis [21]. We decided to evaluate the capacity of our mAbs to block these delayed effects of gal-9. Freshly isolated PBMCs (stimulated or not with anti-CD3/CD28 antibodies) were treated for seven days with gal-9 combined or not with lactose or mAbs. On day 7, cells were assessed for intracellular expression of IL-2 and IFN-γ (Fig 3A). We observed that gal-9 increased the proportion of $CD3^+IL\text{-}2^+$ and $CD3^+IFN\text{-}\gamma^+$ T cells in unstimulated or stimulated PBMCs, and that this effect was blocked in the presence of lactose. Gal-Nab1 and 2 significantly inhibited the apparent expansion of IFN-γ producing T cells, and to a lesser extent the apparent expansion of IL-2 producing cells (Fig 3B and 3C). At the next stage, we explored the impact of gal-9 and anti-gal-9 antibodies on the distribution of naïve ($CCR7^+$ $CD45RO^-$), effector memory (T_{EM}; $CCR7^-$ $CD45RO^+$), central memory (T_{CM}; $CCR7^+$ $CD45RO^+$) and effector ($CCR7^-$ $CD45RO^-$) phenotypes among T cells surviving gal-9 stimulation. Resting PBMCs were treated with gal-9 for one week resulting in a greater proportion of cells with a T_{CM} phenotype. Simultaneously, there was a consistent decrease of the $CCR7^-$ $CD45RO^-$ $CD3^+$ T cells corresponding to effector T cells (Fig 4A). These results confirmed that several days of gal-9 treatment resulted in a shift of T cells towards a T_{CM} phenotype. Moreover, our data indicated that Gal-Nab2 neutralized this shift almost entirely, in the same extent as lactose. Gal-Nab1 tended to inhibit the T_{CM} phenotype shift induced by gal-9, but to a lesser extent without reaching statistical significance (Fig 4B).

Gal-Nab1 and Gal-Nab2 capture gal-9 with distinct kinetics

We used surface plasmon resonance to analyse the binding characteristics of Gal-Nab1 and Gal-Nab2. In a first series of experiments, recombinant gal-9M was used as the ligand and subjected to the binding of soluble Gal-Nab1 and Gal-Nab2 (Table 1, left column). Reciprocally, in a second phase, Gal-Nab1 and Gal-Nab2 were covalently bound to the chip and soluble recombinant gal-9M was used as the analyte (Table 1, right column). In the first configuration, assessment of binding characteristics is likely to be biased by repetitive binding of the antibodies with a K_D reflecting avidity rather than affinity. In this setting, the K_D of Gal-Nab1 and Gal-Nab2 were of the same order of magnitude. In the opposite configuration, the K_D of Gal-Nab2 (8.79 nM) was almost 10 times smaller than the K_D of Gal-Nab1 (88.7 nM), reflecting a lower affinity of Gal-Nab1. The binding speed (k-on) was in the same order of magnitude for both antibodies. However, the speed of elution was much more rapid for Gal-Nab1 than for Gal-Nab2, as shown by the experimental determination of the dissociation and half-life parameters.

Gal-Nab1 and Gal-Nab2 react with nearly identical linear epitopes and share the same heavy chain CDR3 (complementary determining region 3)

In order to better understand the functional differences of these two anti-gal-9 mAbs, we sought to map their epitopes. Using a first set of overlapping peptides, we found that both antibodies were reacting with a segment of gal-9 covering the end of the linker peptide and the

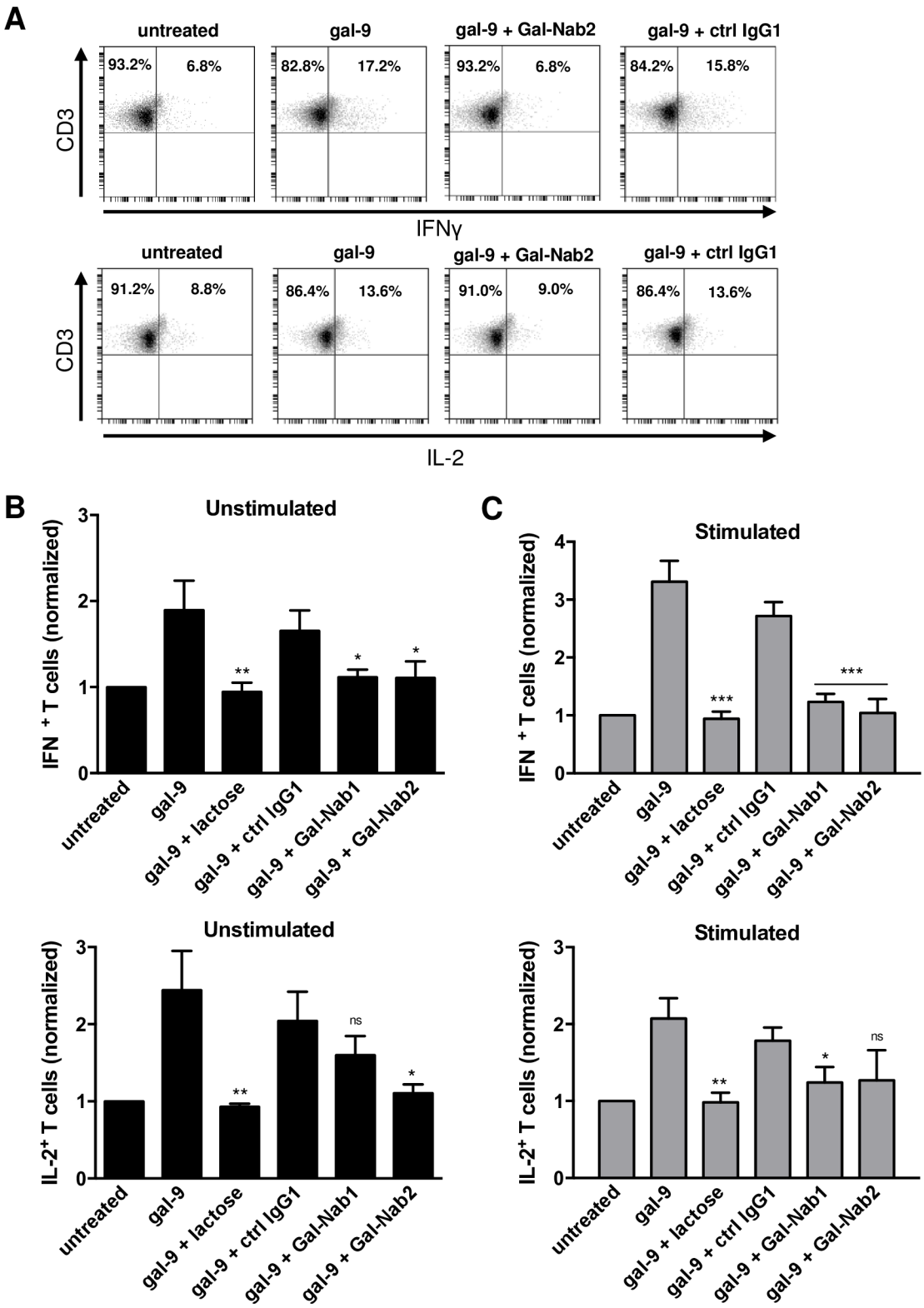

Fig 3. Anti-gal-9 mAbs inhibit the "Th1-like" phenotype shifting induced by gal-9 in resting or stimulated PBMCs. A-C. PBMCs from healthy donors were stimulated or not with anti-CD3/CD28 antibodies and treated for one week with human recombinant gal-9 (Gal-9S; 40 nM) with or without combination with lactose (5 mM), control isotype antibody (ctrl IgG1), Gal-Nab1 or Gal-Nab2 (67 nM i.e. 10 μg/mL). Intracellular cytokine expression was assessed by flow cytometry as explained under

"Materials and Methods". At least 50% of the cells were alive. Dead cells were gated out. **A.** Examples of flow cytometry plots obtained with stimulated PBMCs for one donor after gating on the $CD3^+$ T cell population: IFN-γ (upper plots) and IL-2 (lower plots) expression were analyzed. **B-C.** Percentages of $CD3^+$ $IFN\gamma^+$ (upper histogram) and $CD3^+$ $IL\text{-}2^+$ (lower histogram) cells were normalized with the basal percentages obtained in untreated cells using either unstimulated **(B)** or stimulated **(C)** PBMCs. Data are represented as means ± SEM of four independent experiments with different donors. All statistical differences displayed are compared with gal-9 treatment; $^{***}p<0.001$; $^{**}p<0.01$; $^{*}p<0.05$; ns: not significant (one-way ANOVA/Dunnet post-test).

https://doi.org/10.1371/journal.pone.0202512.g003

beginning of the gal-9 c-terminal CRD (segment spanning aa 202 to 232 in gal-9L; 158–188 in gal-9S). In order to confirm that both antibodies were targeting this segment of gal-9, we used surface plasmon resonance to investigate their binding to an oligopeptide containing aa 208 to 232. This peptide was biotinylated at its c-terminus (hereafter called CTB) and loaded on a streptavidin chip. A biotinylated scramble peptide was used as a control. As seen in Table 2, Gal-Nab1 and Gal-Nab2 were binding the CTB peptide with high avidity whereas no interaction was recorded with the scramble peptide. In addition, we noticed that the apparent affinities of Gal-Nab1 and Gal-Nab2 for the CTB peptide were much greater than their apparent affinities for the intact gal-9M (K_D of $1.0x10^{-11}$ M and $6.05x10^{-11}$ M, in contrast with $4.34x10^{-9}$ M and $1.48x10^{-9}$ M, respectively). Moreover, Gal-Nab1 exhibited a greater affinity than Gal-Nab2 for the CTB peptide whereas it was the opposite for the intact gal-9 (M isoform).

We also confirmed the specific binding of this peptide to our mAbs by performing a functional assay (Fig 5A). After pre-incubation with the scramble peptide, Gal-Nab1 and Gal-Nab2 inhibit gal-9-induced apoptosis of $CD3^+$ primary T cells. However, pre-incubation of the mAbs with the CTB-peptide completely abolishes their neutralizing capacity confirming their high affinity for an epitope carried by this peptide.

Finally, in a second round of epitope mapping, we used a set of 15 overlapping 15-mers spanning aa 202–230 with a shift of only one aa between consecutive oligo-peptides. We assessed the capacity of these peptides to block the interaction between Gal-Nab1/Gal-Nab2

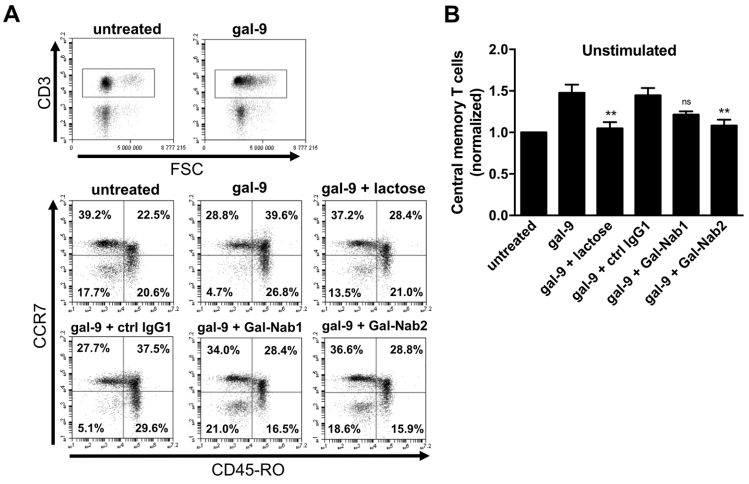

Fig 4. Effect of anti-gal-9 mAbs on the "T_{CM}-like" phenotype shifting induced by gal-9 in resting PBMCs. A-B. PBMCs freshly isolated from healthy donors were treated for one week with human recombinant gal-9 (Gal-9S; 40 nM) with or without combination with lactose (5 mM), control isotype antibody (ctrl IgG1), Gal-Nab1 or Gal-Nab2 (67 nM i.e. 10 μg/mL). **A.** Flow cytometry analysis was performed to determine the level of naive ($CCR7^+$ $CD45RO^-$), central memory ($CCR7^+$ $CD45RO^+$) effector memory ($CCR7^-$ $CD45RO^+$) and effector ($CCR7^-$ $CD45RO^-$) T cells within the $CD3^+$ population. At least 50% of the cells were alive. Dead cells were gated out. **B.** For each treatment condition, percentages of cells with an apparent central memory phenotype were normalized with the basal level of this subpopulation in untreated cells. Data are represented as means ± SEM of four independent experiments with different donors. $^{**}p<0.01$; ns: not significant; compared with gal-9 treatment (one-way ANOVA/Dunnet post-test).

https://doi.org/10.1371/journal.pone.0202512.g004

Table 1. Assessment of the interactions of Gal-Nab1 and Gal-Nab2 mAbs with gal-9M by surface plasmon resonance.

Immobilized ligand	Gal-9M		Gal-Nab1	Gal-Nab2
Analyte	Gal-Nab1	Gal-Nab2	Gal-9M	
K_D (M)	$(4.34 \pm 1.24) \times 10^{-9}$	$(1.48 \times 10^{-9} \pm 5.30 \times 10^{-10})$	$(8.87 \pm 1.64) \times 10^{-8}$	$(8.79 \pm 5.26) \times 10^{-9}$
K_{on} (s^{-1} M^{-1})	$(2.65 \times 10^{4} \pm 1.86 \times 10^{3})$	$(6.11 \pm 1.30) \times 10^{4}$	$(3.74 \pm 0.49) \times 10^{5}$	$(1.90 \pm 0.65) \times 10^{5}$
K_{off} (s^{-1})	$(1.15 \times 10^{-4} \pm 2.87 \times 10^{5})$	$(9.06 \pm 2.61) \times 10^{-5}$	$(3.32 \pm 0.44) \times 10^{-2}$	$(1.67 \pm 0.84) \times 10^{-3}$
$t_{1/2}$ (min)	124.2	127.2	0.35 s	7.32

K_D, K_{on} and K_{off} were calculated as described under "Material and Methods".

https://doi.org/10.1371/journal.pone.0202512.t001

and gal-9. As shown in Fig 5B, the peptide 12 induces the most potent inhibition for both antibodies. The peptide 13 had almost the same impact as the peptide 12 for Gal-Nab1 but not for Gal-Nab2, underlying the contribution of isoleucine 213 for Gal-Nab1 binding to gal-9 in contrast to Gal-Nab2. Taking in account the impact of the different peptides, we could determine the sequences of the linear epitopes recognized by our mAbs: "IPPMMYPHPAYP" (aa 213 to 224 in gal-9L; 169–180 in gal-9S) for Gal-Nab1 and "PPMMYPHPAYP" (aa 214 to 224 in gal-9L; 170–180 in gal-9S) for Gal-Nab2. These data mean that both mAbs react with the same linear epitope, at the exception of one residue (I; isoleucine) which is more critical for Gal-Nab1 binding to gal-9. In order to get some insights on structural similarities and differences between Gal-Nab1 and Gal-Nab2, we sequenced the variable portions of their heavy and light chain genes. As shown in Table 3, the CDR3 of their heavy chain were identical. Only minor differences were recorded for the CDR1 of the heavy chains and the CDR2 and 3 of the light chains. Greater variations were observed in the CDR2 of the heavy chains and CDR3 of the light chains.

Gal-Nab1 and Gal-Nab2 cross-react with murine gal-9

Because investigations in murine models are generally regarded as a pre-requisite for development of therapeutic antibodies, we investigated the capacity of Gal-Nab1 and 2 to cross-react with recombinant and native murine gal-9. First, the aa sequence containing the Gal-Nab1 and 2 overlapping epitopes (aa 213–224 of human gal-9) was compared to the homologous segment of murine gal-9 (aa 211–222 of murine gal-9) (Fig 6A). Out of 12 aa, four are divergent with only two non-conservative changes (aa 218 and 222 of murine gal-9). These observations were in favor of a cross-reactivity of Gal-Nab1 and 2 with murine gal-9. As shown in Fig 6B, Gal-Nab1 and Gal-Nab2 did cross-react with recombinant murine gal-9M as evaluated by ELISA. In contrast, there was no cross-reactivity with human galectins distinct from human gal-9 except a marginal reaction with human galectin-3. In order to explore the binding of

Table 2. Assessment of the interactions of Gal-Nab1 and Gal-Nab2 with the CTB oligo-peptide containing aa 208 to 232 of gal-9 by surface plasmon resonance.

Immobilized ligand	Scramble peptide	CTB-gal-9 peptide	Scramble peptide	CTB-gal-9 peptide
Analyte	Gal-Nab1		Gal-Nab2	
K_D (M)	No binding	$(1.0 \pm 0.48) \times 10^{-11}$	No binding	$(6.05 \pm 3.92) \times 10^{-11}$
K_{on} (s^{-1} M^{-1})		$(2.3 \pm 0.63) \times 10^{6}$		$(5.45 \pm 0.95) \times 10^{5}$
K_{off} (s^{-1})		$(2.3 \pm 0.28) \times 10^{-5}$		$(3.3 \pm 1.41) \times 10^{-5}$
$t_{1/2}$ (min)		8.37		6.23

K_D, K_{on} and K_{off} were calculated as described under "Material and Methods".

https://doi.org/10.1371/journal.pone.0202512.t002

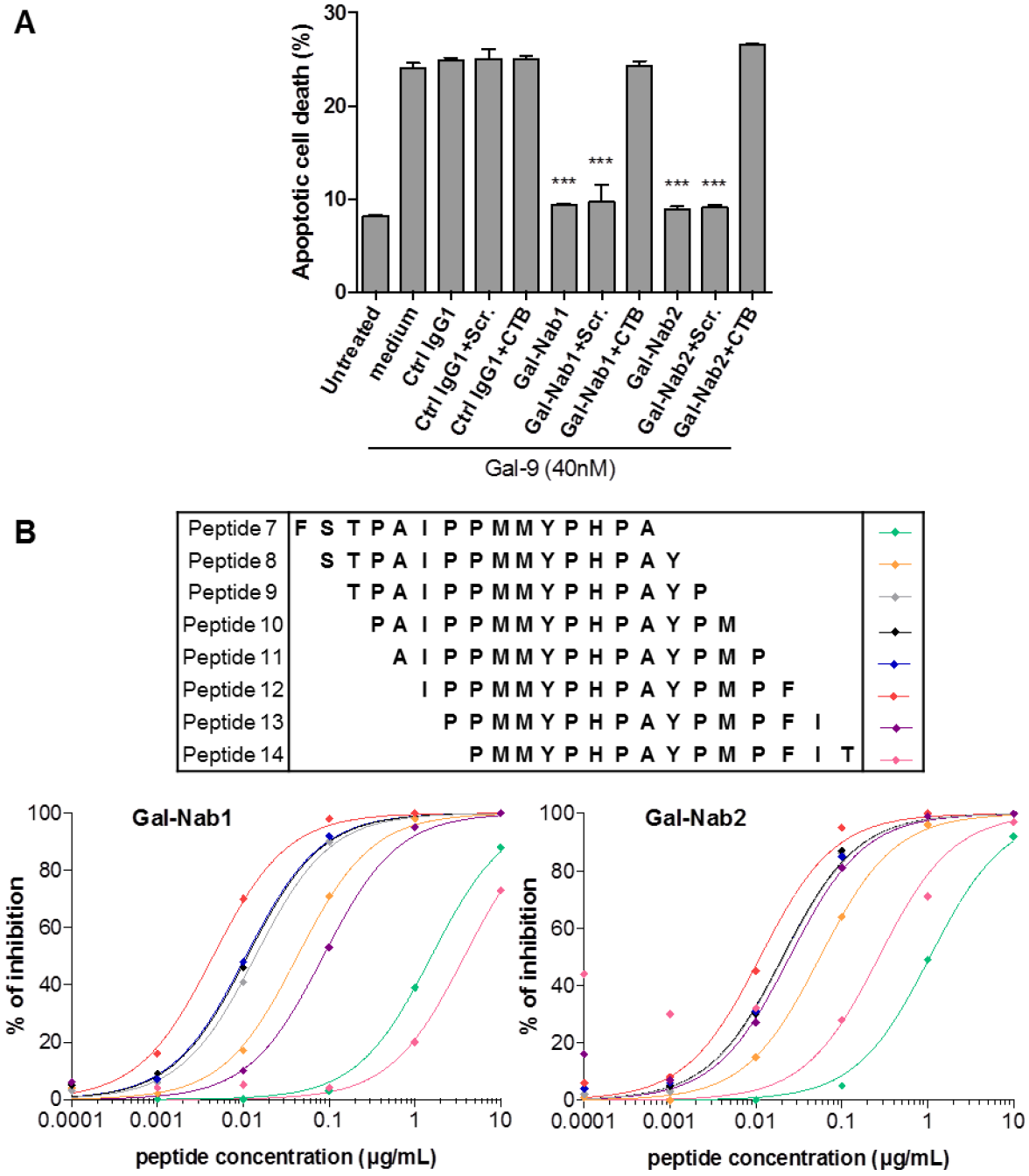

Fig 5. Gal-9 epitope recognition by Gal-Nab1 and Gal-Nab2. A. Apoptotic cell death assessed by flow cytometry in $CD3^+$ T cells treated for 36h with gal-9 (gal-9S; 40 nM) alone or in combination with mAbs (ctrl IgG1, Gal-Nab1, Gal-Nab2; 67 nM) pre-incubated or not with scramble peptide (Scr.) or gal-9 CTB-peptide (6.7 μM). **B.** Human recombinant gal-9 was immobilized in 96-wells plates and binding of Gal-Nab1 and Gal-Nab2 mAbs was measured after pre-incubation with overlapping peptides representative of human gal-9, as described under "Material and Methods". Gal-Nab1 **(left)** or Gal-Nab2 **(right)** were then detected using secondary HRP-conjugated anti-mouse antibodies. Percentages of inhibition induced by each peptide were calculated from the absorbance data as described under "Material and Methods".

https://doi.org/10.1371/journal.pone.0202512.g005

Gal-Nab1 and Gal-Nab2 to native murine gal-9, we performed a cold immunoprecipitation assay using a protein extract from murine thymus as the source of native gal-9. The precipitation output of Gal-Nab1 and 2 was compared to the output of two other monoclonal

Table 3. Sequences of heavy and light chains CDRs for Gal-Nab1 and Gal-Nab2.

	Heavy chain			Light chain (κ)		
	CDR1	CDR2	CDR3	CDR1	CDR2	CDR3
Gal-Nab1	GYTFT**D**YTIH	WFYPGS**H**S**IK**YNE**Q**F**K**D	HGGYDGFDY	KSSQSL**F**YS**T**NQKNYLA	WASTR**E**S	QQYY**YF**P**Y**T
Gal-Nab2	GYTFT**E**YTIH	WFYPGS**G**S**ME**YNE**K**FD	HGGYDGFDY	KSSQSL**L**YS**N**NQKNYLA	WASTR**G**S	QQYY**SY**P**F**T

Differences in amino acids between the antibodies sequences are marked in bold characters.

https://doi.org/10.1371/journal.pone.0202512.t003

antibodies, 9M1-3 and RG9-35, designed to react with human and murine gal-9, respectively. As shown in Fig 7, Gal-Nab2 and, to a lesser extent, Gal-Nab1, were able to precipitate a substantial amount of murine gal-9. As expected, the recovery of native murine gal-9 was maximal with RG9-35. It was very low with 9M1-3. Based on these data, one may consider a direct exploration of the therapeutic potential of Gal-Nab1 and 2 in murine syngeneic models.

Discussion

Hijacking physiological mechanisms involved in the down-regulation of the immune responses is one major component in the expansion strategy of malignant cells and pathogenic

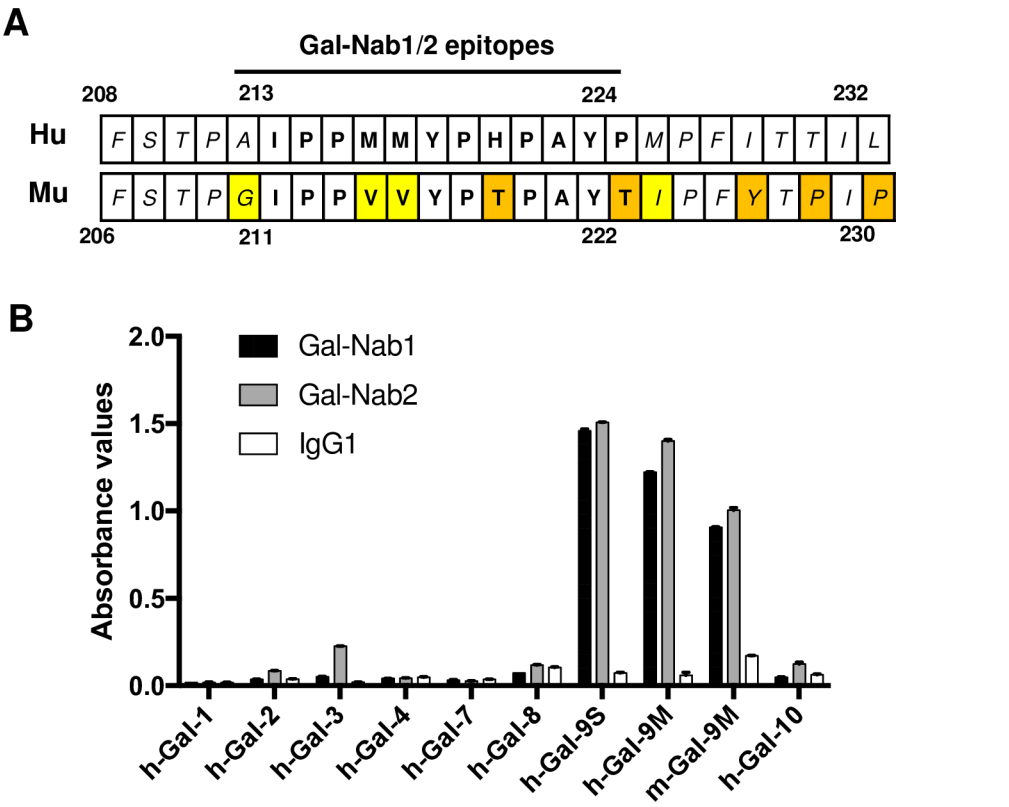

Fig 6. Partial cross-reaction of Gal-Nab1 and Gal-Nab2 with recombinant murine gal-9. A. Comparative display of the 208–232 aa sequence of human gal-9 (upper line) and its homologous aa sequence in murine gal-9 (lower line) (aa 206–230 for the long isoform, based on the UniProtKB database http://www.uniprot.org/uniprot/O00182 and O08573). Variant aa are highlighted in yellow (conservative changes) or in orange (non-conservative changes). Within the epitopes of Gal-Nab1 and Gal-Nab2, there are only 2 non-conservative changes. **B**. The binding of Gal-Nab1 and Gal-Nab2 to recombinant galectins was assessed by direct ELISA performed in triplicate. Target proteins were human galectins 1 to 4, 7, 8 and 10 (h-Gal); the S and M isoforms of human gal-9 (h-Gal-9S and M) and the M isoform of murine gal-9 (m-Gal-9M).

https://doi.org/10.1371/journal.pone.0202512.g006

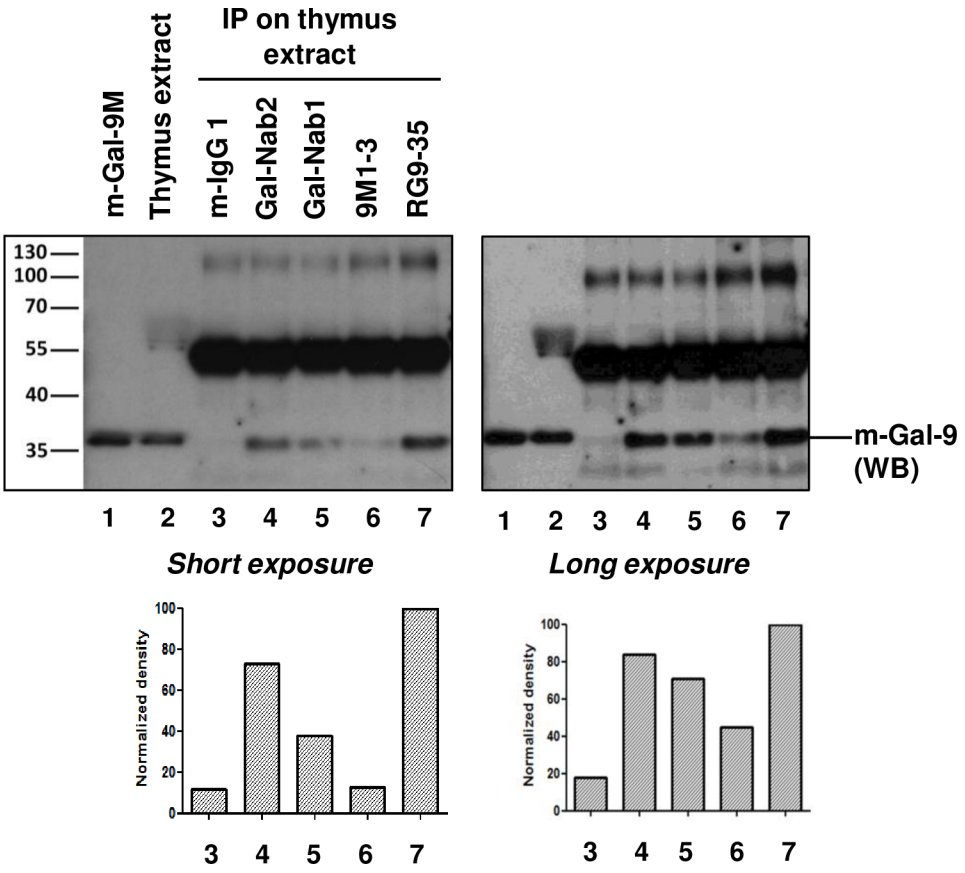

Fig 7. Partial cross-reaction of Gal-Nab1 and Gal-Nab2 with native murine gal-9. Western blot (WB) analysis of cold immuno-precipitation (IP) products obtained with various anti-gal-9 antibodies. The source of native gal-9 was a protein extract from a murine thymus. Concomitant IP were performed with non-specific mouse IgG1 (negative control), Gal-Nab1 and Gal-Nab2, 9M1 (a commercial antibody directed to human gal-9) and RG9-35 (a commercial antibody directed to murine gal-9). 15 ng of recombinant murine gal-9 M (lane 1) and 25 μg of crude murine thymus extract (lane 2) were used as WB controls. The primary antibody used for WB detection of murine gal-9 was a polyclonal goat serum. The secondary antibody reacted with this primary but also with the immunoglobulin heavy chains eluted from the beads giving strong bands at a molecular weight of about 55 Kd. These bands were of similar intensities for all five IP conditions, suggesting that bead capture of the immune complexes was in the same range of efficiency. The bands resulting from gal-9 staining (36 Kd) were assessed by densitometry (graphs for long and short exposure are presented at the bottom of the figure).

https://doi.org/10.1371/journal.pone.0202512.g007

viruses. Conversely, blocking mechanisms of immune tolerance towards tumor cells or viral pathogens increasingly appears as an essential–if not mandatory–component of the treatment of most malignancies and viral diseases [40, 41]. The benefit of this strategy is remarkably illustrated by the success of several checkpoint inhibitors like Ipilimumab or Nivolumab in various types of malignancies [42, 43]. So far gal-9 has been neglected as a potential therapeutic target although it is strongly suspected to impair the immune response in various pathological conditions, especially in nasopharyngeal, pancreatic, and renal carcinomas as well as chronic viral hepatitis [24, 26–28, 30, 44]. In addition, most authors seeking therapeutic inhibition of other galectins, for example galectin-1 or -3, have mainly resorted to small molecules especially glycomimetics [45, 46]. However, neutralizing antibodies are expected to carry several benefits over small molecules: 1) a greater specificity for each type of galectin species; 2) inhibitory effects restricted to extra-cellular galectins; 3) extensive knowledge already available on pharmacokinetics/pharmacodynamics and bio-distribution; 4) a known regulatory landscape.

Nevertheless, so far, to our knowledge, there was no report on antibodies neutralizing gal-9 or other galectins produced with a therapeutic intent [45]. In this context, our general objective was to pave the way for the development of humanized therapeutic antibodies neutralizing the unwanted immunosuppressive effects of gal-9.

We have obtained two lead monoclonal antibodies which neutralize gal-9 in various biological assays performed *in vitro*. They have many convergent effects. Their most promising common effect with regard of therapeutic development is their protection against the induction of the apoptosis of conventional primary T-cells by exogenous gal-9. Later on, additional investigations will be necessary to elucidate the mechanisms underlying this neutralizing activity. It is noteworthy that neither Gal-Nab1 nor Gal-Nab2 binds to T cells (S2 Fig). They might prevent the interaction of gal-9 with some of its receptors on the plasma membrane of the target cells by steric hindrance, modification of gal-9 3D conformation or impairment of its dimerization [47]. In other types of assays—cellular or a-cellular—Gal-Nab1 and Gal-Nab2 exhibit distinct functional properties, although they share the same heavy chain CDR3 and react with nearly the same linear epitope. The main differences are the rapid dissociation of Gal-Nab1 from gal-9 and its own stimulating effects on non-lethal PS translocation and calcium mobilization induced by extra-cellular gal-9 in Jurkat cells. One hypothesis is that the differences recorded in the CDR-1 and -2 of Gal-Nab1 and Gal-Nab2 determine distinct types of paratope/epitope interfaces. In addition to the 213–224 aa segment of gal-9 included in the CTB peptide, Gal-Nab1 and 2 are likely to react with other parts of the protein. Their apparent greater affinity for the CTB peptide than for the whole protein suggests that the other contact points of the three-dimensional epitopes have negative contributions to the stability of the antigen/antibody complexes. These negative contributions seem to be greater for Gal-Nab1 than for Gal-Nab2. More investigations will be required to address this hypothesis. Another intriguing observation is that Gal-Nab1 does not modulate in the same way the responses of Jurkat cells and primary T cells stimulated by extra-cellular gal-9. To address this question, one needs to remember that Jurkat cells are malignant cells and therefore have a glycan profile on their plasma membrane which is not identical to primary $CD3^+$ cells [48]. This might determine specific modalities of gal-9 interactions with Jurkat cells.

None of our two lead antibodies cross-react with human galectins 1 to 4, 7, 8 and 10 as shown in Fig 6B. In contrast, they show partial cross reaction with recombinant and native murine gal-9 which is consistent with the fact that the murine peptide sequence homologous to their target epitopes is highly conserved in rodents. Since it is even more conserved in primates, we can anticipate a possible use of these antibodies for preclinical evaluation in primates.

Further experiments are warranted to analyse more specifically the impact of gal-9 and our mAbs on various T-cell subpopulations. This is particularly important since gal-9 has been shown to be important for Tregs expansion and activity [6, 10, 49]. Thus, anti-gal-9 mAbs may limit the immunosuppressive activity of Tregs and therefore improve the overall anti-tumor immune response. Results presented in Figs 3 and 4 confirm previous data from Gooden *et al* who showed that following the initial wave of apoptosis, gal-9 treatment of PBMCs results in the emergence of T cells with a phenotype suggestive of Th1 cells ($CD3^+IFN\text{-}\gamma^+$) and central memory T cells ($CD45RO^+$ $CCR7^+$) [21]. We found that Gal-Nab1 and 2 prevent the late emergence of these T cell subpopulations. These observations raise the possibility that the expected benefits of anti-gal-9 antibodies might be balanced by some unwanted immunosuppressive effects. However, this possibility might not be true, and that for several reasons. First, we need further evidence that the increase in the percentages of $CD3^+IFN\text{-}\gamma^+$ and $CD45RO^+$ $CCR7^+$ cells following the apoptotic wave is real and not just a consequence of the depletion of other subpopulations. Proliferation assays will be required to address this point. Next, in light

of several recent publications that demonstrate dissociation between the function of some T cells and their membrane phenotype, one cannot exclude that these populations have in fact suppressive functions [50–52]. Sorting of these cells and direct evaluation of their potential suppressive activity will be required to answer this question. Finally, antigen-independent activation of conventional T cells by gal-9 might not be beneficial: it might favor permanent inflammation in the tumor microenvironment without enough focus of T cell cytotoxicity against malignant cells or virus-infected cells. For all these reasons, we believe that most effects of our mAbs are likely to contribute to an immune restoration in pathological conditions with excessive gal-9 production. These remarks underline the importance of future investigations in pre-clinical models, especially murine models. Our data demonstrate that Gal-Nab1 and 2 partially cross-react with murine gal-9. Therefore they will be probably well suited for use in syngeneic murine tumor models in order to assess their overall impact on host-tumor relationships.

Supporting information

S1 Fig. Capture of biotinylated galectins on surface-bound antibodies. The binding of Gal-Nab1, Gal-Nab2 and control mouse IgG1 antibodies to gal-9 was assessed by direct ELISA as described under "Materials & Methods" with the difference that biotinylated gal-9S (1 nM) was incubated during 1h at 37˚C in antibody-coated wells in the presence or absence of lactose (20mM) before washing and revelation.
(TIF)

S2 Fig. Gal-9 surface staining on primary T cells. $CD3^+$ purified T cells were stimulated (CD3/CD28 coated beads) or not and incubated with anti-MHC-I antibodies (as positive control), anti-gal-9 mAbs (9M1, Gal-Nab1 and Gal-Nab2; 5 μg/ml) or mouse irrelevant IgG1 for 30 min at 4˚C. Cells were then washed in ice-cold PBS and incubated 30 min at 4˚C with rat anti-mouse antibodies (Biolegend) coupled to fluorescein isothiocyanate (FITC). Grey histograms represent the background of fluorescence obtained with the irrelevant IgG1 as primary antibodies.
(TIF)

Acknowledgments

This work was supported by a pre-maturation contract from the Idex Saclay (2015-2016- PB coordinator) and by a grant from the Bristol-Myers-Squibb foundation (2016-2017-PB coordinator).

Author Contributions

Conceptualization: Claire Lhuillier, Clément Barjon, Olivier Morales, Bertrand Raynal, Nadira Delhem, Olivier Dellis, Pierre Busson.

Data curation: Valentin Baloche, Laetitia Claër, Sylviane Hoos.

Formal analysis: Sylviane Hoos, Olivier Dellis.

Funding acquisition: Ming Wei, Pierre Busson.

Investigation: Claire Lhuillier, Clément Barjon, Valentin Baloche, Toshiro Niki, Aurore Gelin, Rami Mustapha, Laetitia Claër, Sylviane Hoos, Olivier Dellis, Pierre Busson.

Methodology: Claire Lhuillier, Clément Barjon, Valentin Baloche, Toshiro Niki, Aurore Gelin, Laetitia Claër, Sylviane Hoos, Olivier Dellis, Pierre Busson.

Project administration: Claire Lhuillier, Pierre Busson.

Resources: Claire Lhuillier, Clément Barjon, Valentin Baloche, Toshiro Niki, Yoichi Chiba, Masaki Ueno, Mitsuomi Hirashima, Olivier Dellis, Pierre Busson.

Supervision: Bertrand Raynal, Olivier Dellis, Pierre Busson.

Validation: Claire Lhuillier, Clément Barjon, Valentin Baloche, Toshiro Niki, Aurore Gelin, Rami Mustapha, Sylviane Hoos, Olivier Dellis.

Visualization: Clément Barjon, Valentin Baloche, Aurore Gelin.

Writing – original draft: Pierre Busson.

Writing – review & editing: Toshiro Niki, Mitsuomi Hirashima, Olivier Morales, Nadira Delhem, Olivier Dellis, Pierre Busson.

References

1. Patnaik SK, Potvin B, Carlsson S, Sturm D, Leffler H, Stanley P. Complex N-glycans are the major ligands for galectin-1, -3, and -8 on Chinese hamster ovary cells. Glycobiology. 2006; 16(4):305–17. https://doi.org/10.1093/glycob/cwj063 PMID: 16319083.
2. Bacigalupo ML, Manzi M, Rabinovich GA, Troncoso MF. Hierarchical and selective roles of galectins in hepatocarcinogenesis, liver fibrosis and inflammation of hepatocellular carcinoma. World journal of gastroenterology : WJG. 2013; 19(47):8831–49. https://doi.org/10.3748/wjg.v19.i47.8831 PMID: 24379606; PubMed Central PMCID: PMC3870534.
3. Heusschen R, Griffioen AW, Thijssen VL. Galectin-9 in tumor biology: a jack of multiple trades. Biochimica et biophysica acta. 2013; 1836(1):177–85. https://doi.org/10.1016/j.bbcan.2013.04.006 PMID: 23648450.
4. Asakura H, Kashio Y, Nakamura K, Seki M, Dai S, Shirato Y, et al. Selective eosinophil adhesion to fibroblast via IFN-gamma-induced galectin-9. Journal of immunology. 2002; 169(10):5912–8. PMID: 12421975.
5. Imaizumi T, Kumagai M, Sasaki N, Kurotaki H, Mori F, Seki M, et al. Interferon-gamma stimulates the expression of galectin-9 in cultured human endothelial cells. Journal of leukocyte biology. 2002; 72 (3):486–91. PMID: 12223516.
6. Oomizu S, Arikawa T, Niki T, Kadowaki T, Ueno M, Nishi N, et al. Cell surface galectin-9 expressing th cells regulate th17 and foxp3(+) treg development by galectin-9 secretion. PloS one. 2012; 7(11): e48574. Epub 2012/11/13. https://doi.org/10.1371/journal.pone.0048574 PMID: 23144904; PubMed Central PMCID: PMC3492452.
7. Barjon C, Niki T, Verillaud B, Opolon P, Bedossa P, Hirashima M, et al. A novel monoclonal antibody for detection of galectin-9 in tissue sections: application to human tissues infected by oncogenic viruses. Infect Agent Cancer. 2012; 7(1):16. Epub 2012/07/19. https://doi.org/10.1186/1750-9378-7-16 1750-9378-7-16 [pii]. PMID: 22805533; PubMed Central PMCID: PMC3464730.
8. Keryer-Bibens C, Pioche-Durieu C, Villemant C, Souquere S, Nishi N, Hirashima M, et al. Exosomes released by EBV-infected nasopharyngeal carcinoma cells convey the viral latent membrane protein 1 and the immunomodulatory protein galectin 9. BMC cancer. 2006; 6:283. https://doi.org/10.1186/1471-2407-6-283 PMID: 17156439.
9. Mrizak D, Martin N, Barjon C, Jimenez-Pailhes AS, Mustapha R, Niki T, et al. Effect of nasopharyngeal carcinoma-derived exosomes on human regulatory T cells. J Natl Cancer Inst. 2015; 107(1):363. Epub 2014/12/17. https://doi.org/10.1093/jnci/dju363 [pii]. PMID: 25505237.
10. Wu C, Thalhamer T, Franca RF, Xiao S, Wang C, Hotta C, et al. Galectin-9-CD44 Interaction Enhances Stability and Function of Adaptive Regulatory T Cells. Immunity. 2014; 41(2):270–82. Epub 2014/07/30. https://doi.org/10.1016/j.immuni.2014.06.011 PMID: 25065622.
11. Oomizu S, Arikawa T, Niki T, Kadowaki T, Ueno M, Nishi N, et al. Cell surface galectin-9 expressing Th cells regulate Th17 and Foxp3+ Treg development by galectin-9 secretion. PloS one. 2012; 7(11): e48574. https://doi.org/10.1371/journal.pone.0048574 PMID: 23144904; PubMed Central PMCID: PMC3492452.
12. Oomizu S, Arikawa T, Niki T, Kadowaki T, Ueno M, Nishi N, et al. Galectin-9 suppresses Th17 cell development in an IL-2-dependent but Tim-3-independent manner. Clinical immunology. 2012; 143 (1):51–8. https://doi.org/10.1016/j.clim.2012.01.004 PMID: 22341088.

13. Lv K, Zhang Y, Zhang M, Zhong M, Suo Q. Galectin-9 ameliorates Con A-induced hepatitis by inducing CD4(+)CD25(low/int) effector T-Cell apoptosis and increasing regulatory T cell number. PloS one. 2012; 7(10):e48379. https://doi.org/10.1371/journal.pone.0048379 PMID: 23118999; PubMed Central PMCID: PMC3485226.

14. Seki M, Oomizu S, Sakata KM, Sakata A, Arikawa T, Watanabe K, et al. Galectin-9 suppresses the generation of Th17, promotes the induction of regulatory T cells, and regulates experimental autoimmune arthritis. Clin Immunol. 2008; 127(1):78–88. https://doi.org/10.1016/j.clim.2008.01.006 PMID: 18282810.

15. Kared H, Fabre T, Bedard N, Bruneau J, Shoukry NH. Galectin-9 and IL-21 mediate cross-regulation between Th17 and Treg cells during acute hepatitis C. PLoS pathogens. 2013; 9(6):e1003422. https://doi.org/10.1371/journal.ppat.1003422 PMID: 23818845; PubMed Central PMCID: PMC3688567.

16. Madireddi S, Eun SY, Mehta AK, Birta A, Zajonc DM, Niki T, et al. Regulatory T Cell-Mediated Suppression of Inflammation Induced by DR3 Signaling Is Dependent on Galectin-9. Journal of immunology. 2017; 199(8):2721–8. Epub 2017/09/08. https://doi.org/10.4049/jimmunol.1700575 PMID: 28877989; PubMed Central PMCID: PMC5659314.

17. Zhu C, Anderson AC, Schubart A, Xiong H, Imitola J, Khoury SJ, et al. The Tim-3 ligand galectin-9 negatively regulates T helper type 1 immunity. Nat Immunol. 2005; 6(12):1245–52. https://doi.org/10.1038/ni1271 PMID: 16286920.

18. Wang F, He W, Zhou H, Yuan J, Wu K, Xu L, et al. The Tim-3 ligand galectin-9 negatively regulates CD8+ alloreactive T cell and prolongs survival of skin graft. Cellular immunology. 2007; 250(1–2):68–74. https://doi.org/10.1016/j.cellimm.2008.01.006 PMID: 18353298.

19. Enninga EA, Nevala WK, Holtan SG, Leontovich AA, Markovic SN. Galectin-9 modulates immunity by promoting Th2/M2 differentiation and impacts survival in patients with metastatic melanoma. Melanoma Res. 2016; 26(5):429–41. Epub 2016/07/28. https://doi.org/10.1097/CMR.0000000000000281 PMID: 27455380.

20. Lhuillier C, Barjon C, Niki T, Gelin A, Praz F, Morales O, et al. Impact of Exogenous Galectin-9 on Human T Cells: CONTRIBUTION OF THE T CELL RECEPTOR COMPLEX TO ANTIGEN-INDEPENDENT ACTIVATION BUT NOT TO APOPTOSIS INDUCTION. J Biol Chem. 2015; 290(27):16797–811. Epub 2015/05/08. https://doi.org/10.1074/jbc.M115.661272 PMID: 25947381; PubMed Central PMCID: PMC4505427.

21. Gooden MJ, Wiersma VR, Samplonius DF, Gerssen J, van Ginkel RJ, Nijman HW, et al. Galectin-9 activates and expands human T-helper 1 cells. PloS one. 2013; 8(5):e65616. Epub 2013/06/07. https://doi.org/10.1371/journal.pone.0065616 PMID: 23741502; PubMed Central PMCID: PMC3669208.

22. Kikushige Y, Miyamoto T, Yuda J, Jabbarzadeh-Tabrizi S, Shima T, Takayanagi S, et al. A TIM-3/Gal-9 Autocrine Stimulatory Loop Drives Self-Renewal of Human Myeloid Leukemia Stem Cells and Leukemic Progression. Cell stem cell. 2015; 17(3):341–52. https://doi.org/10.1016/j.stem.2015.07.011 PMID: 26279267.

23. Bi S, Hong PW, Lee B, Baum LG. Galectin-9 binding to cell surface protein disulfide isomerase regulates the redox environment to enhance T-cell migration and HIV entry. Proceedings of the National Academy of Sciences of the United States of America. 2011; 108(26):10650–5. https://doi.org/10.1073/pnas.1017954108 PMID: 21670307; PubMed Central PMCID: PMC3127870.

24. Daley D, Mani VR, Mohan N, Akkad N, Ochi A, Heindel DW, et al. Dectin 1 activation on macrophages by galectin 9 promotes pancreatic carcinoma and peritumoral immune tolerance. Nat Med. 2017; 23(5):556–67. Epub 2017/04/11. https://doi.org/10.1038/nm.4314 nm.4314 [pii]. PMID: 28394331; PubMed Central PMCID: PMC5419876.

25. Klibi J, Niki T, Riedel A, Pioche-Durieu C, Souquere S, Rubinstein E, et al. Blood diffusion and Th1-suppressive effects of galectin-9-containing exosomes released by Epstein-Barr virus-infected nasopharyngeal carcinoma cells. Blood. 2009; 113(9):1957–66. https://doi.org/10.1182/blood-2008-02-142596 PMID: 19005181.

26. Mengshol JA, Golden-Mason L, Arikawa T, Smith M, Niki T, McWilliams R, et al. A crucial role for Kupffer cell-derived galectin-9 in regulation of T cell immunity in hepatitis C infection. PloS one. 2010; 5(3):e9504. https://doi.org/10.1371/journal.pone.0009504 PMID: 20209097.

27. Nebbia G, Peppa D, Schurich A, Khanna P, Singh HD, Cheng Y, et al. Upregulation of the Tim-3/galectin-9 pathway of T cell exhaustion in chronic hepatitis B virus infection. PloS one. 2012; 7(10):e47648. https://doi.org/10.1371/journal.pone.0047648 PMID: 23112829; PubMed Central PMCID: PMC3480425.

28. Golden-Mason L, Rosen HR. Galectin-9: Diverse Roles in Hepatic Immune Homeostasis and Inflammation. Hepatology. 2017. Epub 2017/02/15. https://doi.org/10.1002/hep.29106 PMID: 28195343.

29. Liu Z, Han H, He X, Li S, Wu C, Yu C, et al. Expression of the galectin-9-Tim-3 pathway in glioma tissues is associated with the clinical manifestations of glioma. Oncol Lett. 2016; 11(3):1829–34. Epub 2016/

03/22. https://doi.org/10.3892/ol.2016.4142 OL-0-0-4142 [pii]. PMID: 26998085; PubMed Central PMCID: PMC4774531.

30. Fu H, Liu Y, Xu L, Liu W, Fu Q, Liu H, et al. Galectin-9 predicts postoperative recurrence and survival of patients with clear-cell renal cell carcinoma. Tumour Biol. 2015; 36(8):5791–9. Epub 2015/02/27. https://doi.org/10.1007/s13277-015-3248-y PMID: 25716202.

31. Ohue Y, Kurose K, Nozawa R, Isobe M, Nishio Y, Tanaka T, et al. Survival of Lung Adenocarcinoma Patients Predicted from Expression of PD-L1, Galectin-9, and XAGE1 (GAGED2a) on Tumor Cells and Tumor-Infiltrating T Cells. Cancer Immunol Res. 2016; 4(12):1049–60. Epub 2016/11/02. doi: 2326-6066.CIR-15-0266 [pii] https://doi.org/10.1158/2326-6066.CIR-15-0266 PMID: 27799141.

32. Nishi N, Itoh A, Fujiyama A, Yoshida N, Araya S, Hirashima M, et al. Development of highly stable galectins: truncation of the linker peptide confers protease-resistance on tandem-repeat type galectins. FEBS Lett. 2005; 579(10):2058–64. https://doi.org/10.1016/j.febslet.2005.02.054 PMID: 15811318.

33. Djillani A, Nusse O, Dellis O. Characterization of novel store-operated calcium entry effectors. Biochim Biophys Acta. 2014; 1843(10):2341–7. Epub 2014/03/25. https://doi.org/10.1016/j.bbamcr.2014.03.012 PMID: 24657813.

34. Strebe FB N., Moosmayer D., Brocks B., Dübel S. Cloning of Variable Domains from Mouse Hybridoma by PCR. In: Kontermann SD R., editor. Antibody Engineering. Springer Protocols. 1. Heildelberg: Springer; 2010. p. 3–14.

35. Kashio Y, Nakamura K, Abedin MJ, Seki M, Nishi N, Yoshida N, et al. Galectin-9 induces apoptosis through the calcium-calpain-caspase-1 pathway. J Immunol. 2003; 170(7):3631–6. PMID: 12646627.

36. Lu LH, Nakagawa R, Kashio Y, Ito A, Shoji H, Nishi N, et al. Characterization of galectin-9-induced death of Jurkat T cells. J Biochem. 2007; 141(2):157–72. Epub 2006/12/15. https://doi.org/10.1093/jb/mvm019 PMID: 17167046.

37. Stowell SR, Karmakar S, Arthur CM, Ju T, Rodrigues LC, Riul TB, et al. Galectin-1 induces reversible phosphatidylserine exposure at the plasma membrane. Mol Biol Cell. 2009; 20(5):1408–18. Epub 2009/01/01. https://doi.org/10.1091/mbc.E08-07-0786 PMID: 19116313; PubMed Central PMCID: PMC2649277.

38. Lu LH, Nakagawa R, Kashio Y, Ito A, Shoji H, Nishi N, et al. Characterization of galectin-9-induced death of Jurkat T cells. Journal of biochemistry. 2007; 141(2):157–72. https://doi.org/10.1093/jb/mvm019 PMID: 17167046.

39. Steelman AJ, Smith R 3rd, Welsh CJ, Li J. Galectin-9 protein is up-regulated in astrocytes by tumor necrosis factor and promotes encephalitogenic T-cell apoptosis. The Journal of biological chemistry. 2013; 288(33):23776–87. https://doi.org/10.1074/jbc.M113.451658 PMID: 23836896; PubMed Central PMCID: PMC3745324.

40. Rouse BT, Sehrawat S. Immunity and immunopathology to viruses: what decides the outcome? Nature reviews Immunology. 2010; 10(7):514–26. https://doi.org/10.1038/nri2802 PMID: 20577268; PubMed Central PMCID: PMC3899649.

41. Butt AQ, Mills KH. Immunosuppressive networks and checkpoints controlling antitumor immunity and their blockade in the development of cancer immunotherapeutics and vaccines. Oncogene. 2014; 33(38):4623–31. https://doi.org/10.1038/onc.2013.432 PMID: 24141774.

42. Borghaei H, Paz-Ares L, Horn L, Spigel DR, Steins M, Ready NE, et al. Nivolumab versus Docetaxel in Advanced Nonsquamous Non-Small-Cell Lung Cancer. The New England journal of medicine. 2015; 373(17):1627–39. https://doi.org/10.1056/NEJMoa1507643 PMID: 26412456.

43. Vanpouille-Box C, Lhuillier C, Bezu L, Aranda F, Yamazaki T, Kepp O, et al. Trial watch: Immune checkpoint blockers for cancer therapy. Oncoimmunology. 2017; 6(11):e1373237. https://doi.org/10.1080/2162402X.2017.1373237 PMID: 29147629; PubMed Central PMCID: PMCPMC5674958.

44. Klibi J, Niki T, Riedel A, Pioche-Durieu C, Souquere S, Rubinstein E, et al. Blood diffusion and Th1-suppressive effects of galectin-9–containing exosomes released by Epstein-Barr virus–infected nasopharyngeal carcinoma cells. Blood. 2009; 113(9):1957–66. https://doi.org/10.1182/blood-2008-02-142596 PMID: 19005181

45. Wdowiak K, Francuz T, Gallego-Colon E, Ruiz-Agamez N, Kubeczko M, Grochola I, et al. Galectin Targeted Therapy in Oncology: Current Knowledge and Perspectives. Int J Mol Sci. 2018; 19(1). Epub 2018/01/11. https://doi.org/10.3390/ijms19010210 PMID: 29320431; PubMed Central PMCID: PMC5796159.

46. Denavit V, Lainé D, Tremblay T, St-Gelais J, Giquère D. Synthetic Inhibitors of Galectins : Structures and Syntheses. Trends in Glycoscience and Glycotechnology. 2018; 30(172):SE21–SE40. https://doi.org/10.4052/tigg.1729.1SE

47. Nonaka Y, Ogawa T, Oomizu S, Nakakita S, Nishi N, Kamitori S, et al. Self-association of the galectin-9 C-terminal domain via the opposite surface of the sugar-binding site. J Biochem. 2013; 153(5):463–71. Epub 2013/02/08. https://doi.org/10.1093/jb/mvt009 PMID: 23389308.

48. Hoja-Lukowicz D, Przybylo M, Duda M, Pochec E, Bubka M. On the trail of the glycan codes stored in cancer-related cell adhesion proteins. Biochim Biophys Acta. 2017; 1861(1 Pt A):3237–57. Epub 2016/08/28. https://doi.org/10.1016/j.bbagen.2016.08.007 PMID: 27565356.

49. Madireddi S, Eun SY, Mehta AK, Birta A, Zajonc DM, Niki T, et al. Regulatory T Cell-Mediated Suppression of Inflammation Induced by DR3 Signaling Is Dependent on Galectin-9. Journal of immunology. 2017. Epub 2017/09/08. https://doi.org/10.4236/oji.2017.71001 PubMed PMID: 28944101.

50. Stock P, Akbari O, Berry G, Freeman GJ, Dekruyff RH, Umetsu DT. Induction of T helper type 1-like regulatory cells that express Foxp3 and protect against airway hyper-reactivity. Nat Immunol. 2004; 5 (11):1149–56. Epub 2004/09/28. https://doi.org/10.1038/ni1122 PMID: 15448689.

51. Dominguez-Villar M, Baecher-Allan CM, Hafler DA. Identification of T helper type 1-like, Foxp3+ regulatory T cells in human autoimmune disease. Nat Med. 2011; 17(6):673–5. Epub 2011/05/05. https://doi.org/10.1038/nm.2389 PMID: 21540856; PubMed Central PMCID: PMC3675886.

52. Koenecke C, Lee CW, Thamm K, Fohse L, Schafferus M, Mittrucker HW, et al. IFN-gamma production by allogeneic Foxp3+ regulatory T cells is essential for preventing experimental graft-versus-host disease. Journal of immunology. 2012; 189(6):2890–6. Epub 2012/08/08. https://doi.org/10.4049/jimmunol.1200413 PMID: 22869903.

II- Article 2

In the MB49 murine model, genetic ablation of galectin-9 enhances anti-tumor immune response: possible role of a greater CXCL9/Il-6 production.

Valentin Baloche, Julie Rivière, Thi Bao Tram Tran, Aurore Gelin, Olivia Bawa, Muriel David, Pierre Busson

a) Contexte et objectifs de l'étude

La gal-9 est une protéine qui intervient dans la régulation du système immunitaire. Lorsqu'elle est sécrétée dans le milieu extra-cellulaire, elle se comporte comme une cytokine en exerçant des fonctions principalement immunosuppressives. Ces effets sont médiés par des interactions avec plusieurs récepteurs membranaires glycosylés. Son expression peut être dérégulée dans le cadre de développements tumoraux. Chez l'homme ainsi que dans les modèles animaux, la gal-9 tumorale est souvent produite par les cellules malignes et les cellules infiltrantes. Cependant, à notre connaissance, il n'existe pas de modèle d'étude permettant d'étudier spécifiquement le rôle que joue la gal-9 exprimée par les cellules tumorales séparément de celle exprimée par les cellules infiltrantes. Afin de répondre à ce manque, nous avons généré des clones isogéniques, dérivés de la lignée tumorale murine MB49, invalidés ou non pour la gal-9. L'objectif de cette étude est de présenter l'impact de cette invalidation sur le développement tumoral dans un contexte syngénique.

b) Résultats

Les expériences réalisées *in vivo* démontrent une diminution progressive de la croissance des tumeurs KO-gal-9 sur souris immunocompétentes syngéniques, après quelques cycles de croissance. Ces cycles correspondent aux transplantations itératives de fragments tumoraux d'une souris donneuse vers une souris receveuse, réalisées tous les 10 jours. Ce phénomène de réduction tumorale n'est pas observé sur les souris immunodéficientes nudes, ce qui met en avant l'implication de la réponse immunitaire anti-tumorale dans l'établissement de ce phénotype. Des investigations complémentaires, basées sur de l'IHC, une analyse RNAseq,

ainsi qu'un profilage cytokinique des tumeurs confirment cette hypothèse. En effet, on observe une augmentation de l'infiltration par des cellules T dans les nodules tumoraux des cellules invalidées après 3 voire 4 cycles de croissance. Ces cycles correspondent également au maximum de passages qui peuvent être réalisés avec les tumeurs KO-gal-9. Au-delà, la décroissance tumorale ne permet plus de réaliser davantage de transplantations à partir des tumeurs KO-gal-9. Cette augmentation de l'infiltration des cellules T est précédée par un enrichissement du répertoire des chaînes β du TCR par les lymphocytes T présents dans la tumeur. On relève également des changements transcriptionnels précoces qui évoquent l'émergence de la réponse immunitaire avec notamment un impact de la perte d'expression de gal-9 sur la réponse induite par l'IFN-γ. De manière cohérente, le profilage des cytokines montre une augmentation substantielle de l'expression de plusieurs cytokines dans les tumeurs KO à un stade « pré-terminale ». Le niveau d'expression de ces cytokines au niveau transcriptomique est positivement corrélé au niveau d'expression d'IFN-γ.

D'autre part, des essais de stimulation *in vitro* des cellules tumorales WT et KO-gal-9 avec de l'IFN-γ ont permis d'observer une réponse plus faible dans les cellules WT. Celle-ci se traduit par une expression de CXCL10 plus faible par ces cellules.

c) Conclusion

Ces résultats indiquent que la gal-9 exprimée par les cellules tumorales favorise son échappement à la réponse immunitaire. Ils mettent également en évidence une nouvelle fonction immunosuppressive exercée par la gal-9, à savoir sa capacité à réduire la signalétique induite par l'IFN-γ, qui est probablement impliqué dans le phénomène d'échappement au système immunitaire dans les tumeurs WT. Une question majeure à laquelle il faudra répondre maintenant est de savoir si c'est la gal-9 extra-cellulaire et/ou intra-cellulaire qui participe à la mise en place de cette résistance. Il sera également important de vérifier si cette observation peut s'étendre à d'autres types cellulaires.

Genetic ablation of galectin-9 enhances cell responses to interferon-γ and strengthens anti-tumor immune response in the MB49 murine model

Valentin Baloche[1], Julie Rivière[2], Thi Bao Tram Tran[1], Aurore Gelin[1], Olivia Bawa[3], Nicolas Signolle[3], M'boyba Khadija Diop[4], Philippe Dessen[4], Stéphanie Beq[5], Muriel David[5], Pierre Busson[1]

[1] CNRS, UMR 9018, Gustave Roussy and Université Paris-Saclay, 39 rue Camille Desmoulins, F-94805 Villejuif, France.

[2] Inserm, U1170, Gustave Roussy, 39 rue Camille Desmoulins, F-94805 Villejuif, France.

[3] Plateforme d'évaluation préclinique, Gustave Roussy, 39 rue Camille Desmoulins, F-94805 Villejuif, France.

[4] Plateforme de Bioinformatique, UMS AMMICA, Gustave Roussy, 39 rue Camille Desmoulins, F-94805 Villejuif, France.

[5] HiFiBiO Therapeutics, Pépinière Paris Santé Cochin, 29 rue du Faubourg Saint-Jacques, 75014 Paris, France.

Contact

Pierre Busson
CNRS, UMR 9018, Gustave Roussy and Université Paris-Saclay
39, rue Camille Desmoulins
94 805 Villejuif, France
Pierre.busson@gustaveroussy.fr
+33 1 42 11 45 48

Abstract

A number of studies have reported evidence of positive or negative contributions of galectin-9 (gal-9) to human and experimental malignancies. Some clinical observations and *in vitro* experiments suggest that cell-associated gal-9 has anti-metastatic effects. On the other hand, extra-cellular gal-9 consistently enhances tumor immune escape. So far, all animal studies on this subject have been focused on gal-9 released by infiltrating cells – for example γ/δ suppressive cells – without paying attention to gal-9 specifically produced by malignant cells. To address this issue, we derived by gene editing, isogenic clones - either positive or negative for gal-9 - from the MB49 murine bladder carcinoma cell line. A progressive and dramatic reduction of tumor growth was observed when gal-9-KO cells were subjected to serial transplantations into syngenic mice. In contrast, this phenomenon was completely absent during parallel serial transplantations into nude mice, thus accounting the tumor growth reduction in syngenic mice to a better immune response. At an early stage, the deployment of the anti-tumor response was marked with transcriptional modifications suggestive of a better response of tumor cells to interferon-γ and the widening of the stromal T-cell repertoire. The inverse relationship between gal-9 expression and the magnitude of interferon-γ response was confirmed *in vitro* by investigations on CXCL10 production. Gal-9 expression is known to be enhanced by interferon-γ in multiple cell types. Therefore gal-9 appears as the agent of a cell-autonomous negative feed-back on interferon-γ response and a factor of tumor resistance to the immune response.

Key words

Galectin-9, interferon-γ, tumor immunology, murine tumor models, serial transplantation, CXCL10, bladder carcinoma, MB49.

Introduction

Galectins are a family of mammalian lectins sharing the capacity to bind β-galactoside bonds contained in glycans carried by glycolipids or glycoproteins (Johannes et al., 2018)). Each galectin selectively binds a specific range of glycans which can be located inside the cells, at the cell surface or in the extra-cellular matrix. Several galectins can be released in the extra-cellular medium by non-classical pathways and behave like intercellular messengers. Galectin-9 (gal-9) plays a major role in the physiology of the immune system (John and Mishra, 2016). When secreted in the extra-cellular medium, it behaves like a cytokine with mainly immunosuppressive effects. These effects are mediated by multiple glycoprotein or glycolipid membrane receptors containing β-galactoside bonds including Tim-3 (on T-cells) and Dectin-1 (on macrophages)(Daley et al., 2017; Zhu et al., 2005). In physiological conditions, gal-9 is expressed at a low level in most tissues and organs. Its production is enhanced under inflammatory conditions. This occurs in epithelial and endothelial cells, under stimulation by interferon-γ (Zhu et al., 2005).

Several years ago, our group was the first to show the contribution of gal-9 to immune suppression in the micro- and macro-environment of a human malignancy, namely nasopharyngeal carcinomas, a tumor which is almost constantly associated with the Epstein-Barr virus (EBV) (Klibi et al., 2009). Since this publication, the contribution of gal-9 to immune evasion has been reported in a number of other malignancies as diverse as lung, breast and pancreatic carcinomas, melanomas and acute myeloid leukemias (Daley et al., 2017; Enninga et al., 2016, 2018; Gonçalves Silva et al., 2017). *In vitro* and in animal models, the immunosuppressive effects of gal-9 result from the inhibition of both the innate and adaptative immune responses. Regarding innate immunity, gal-9 inhibits NK cell cytotoxicity while enhancing the activity of MDSCs (Golden-Mason et al., 2013; Dardalhon et al., 2010). Regarding adaptive immunity, it is known to induce cell death of $CD4^+$ Th1 and Th17 cells and exhaustion of $CD8^+$ cells while enhancing the expansion and activity of suppressive cells like iTregs (Zhu et al., 2005; Zhou et al., 2011; Oomizu et al., 2012b; Wu et al., 2014; Oomizu et al., 2012a). Despite multiple observations supporting the contribution of extracellular gal-9 to tumor immune escape, there are still many unknowns and controversies about the relevance of gal-9 as a therapeutic target. Difficulties and sometimes confusion in this research area are, in our view, due to two main causes: 1) cells producing gal-9 in the tumor microenvironment are quite diverse depending on the type of malignancies; 2) there is a suspicion that cell-associated gal-9 - inside malignant cells or at their surface - can have anti-metastatic effects. This hypothesis is mainly supported by observations from a prospective cohort of breast carcinoma patients where the abundance of gal-9 in tumor tissue sections is inversely correlated to the risk of metastatic relapse (Irie et al., Clinical Cancer Res 2013). On the other hand, elevated concentrations of plasma or serum gal-9 are consistently associated with a more severe prognosis in various types of malignancies, including pancreatic carcinomas, metastatic melanomas and renal carcinomas (Enninga et al., 2016; Fu et al., 2015; Tavares et al., 2018).

In humans as well as in animal models, tumor gal-9 is often produced both by malignant cells and by infiltrating cells of lymphoid or myeloid origin (Daley et al., 2017, 2016). So far, to our knowledge, there is no murine tumor model designed to assess the immunosuppressive effect of gal-9 produced by the malignant cells themselves separately from gal-9 released by the infiltrating cells. To address this need, we used gene editing to create isogenic gal-9-positive and gal-9-negative clones derived from the murine bladder carcinoma cell line MB49. The MB49 line was chosen for 2 reasons: 1) it has a substantial baseline expression of gal-9; 2) it is known to trigger a robust although ineffective immune response in C57BL/6 syngenic mice (El Behi et al., 2013; Melchionda et al., 2005; Perez-Diez et al., 2007). Using this approach, we could demonstrate that gal-9 gene ablation makes

MB 49 cells much more sensitive to the anti-tumor immune response. The emergence of this immune response is progressive requiring at least 3 serial passages and growth cycles on syngenic mice to reach full efficiency and blockade of tumor growth. To elucidate the mechanisms of the immune response unmasked by gal-9 gene ablation, we combined assessment of the diversity of the stromal T-cell repertoire, differential RNAseq of gal-9-KO and WT tumors, characterization of infiltrating leucocytes by IHC and intra-tumoral cytokine detection at successive cycles of tumor growth. One of the main changes occurring prior to the blockade of tumor growth was a broad increase in transcription of genes encoding proteins involved in tumor cell response to interferon-γ. Consistently, *in vitro*, the production of CXCL10 induced by exogenous interferon-γ was much more abundant in gal-9-KO cells than in control clones. Gal-9 expression is known to be enhanced in various cell types with interferon-γ (Zhu et al., 2005). Therefore gal-9 appears as the agent of a cell-autonomous feed-back on interferon-γ response with possible repercussions for the resistance of malignant cells to anti-tumor immune responses.

Material and methods

Cell lines. MB49 is a murine bladder carcinoma cell line derived from the C57BL/6 mouse strain which was purchased from Merck Inc (Cat. #: SCC148). Cells were grown in DMEM medium (Gibco, Life Technologies) supplemented with 5% fetal calf serum, 2 mM glutamine and 5 µg/mL gentamycin.

Plasmid constructs, transfection and clones screening. Our strategy to invalidate the gal-9 gene was to make a deletion framing the start codon by concomitant transfection of 2 guide RNAs. The sequences of these guide RNAs were designed *in silico* using the CRISPOR tools (Haeussler et al., 2016). They were matching a sequence in the first exon and first intron of the gal-9 gene, respectively. The DNA inserts encoding the upstream and downstream guide RNAs were generated from two pairs of single strand oligonucleotides, respectively (F: 5'-CACCGCTGTCGTCCACCATCGAGTG-3'; R: 5'-AAACCACTCGATGGTGGACGACAGC-3') and (F: 5'-CACCGAGTCGCCGTGTGTGCAGGT-3'; R: 5'-AAACACCTGCACACACGGCGACTC-3'). These two pairs of oligonucleotides were annealed by denaturation and slow renaturation prior to vector insertion. These inserts were ligated to a backbone Lenti-CRISPR-V2puro plasmid (Addgene, #52961) to co-express the guide RNA sequences with *Streptococcus pyogenes* Cas9 linked either to the GFP or mCherry sequence by a P2A sequence encoding a self-cleaving peptide. These plasmids were digested by *BsmBI* and ligated with the annealed guide RNA sequences. Cell lines were transfected with both GFP and mCherry plasmids, using the TurboFect™ (Thermo Scientific) reagent according to the manufacturer's instructions. They were harvested, 48h after transfection, sorted according to their double GFP/mCherry positive expression and automatically seeded at one cell/well in a 96 well cloning plate (BD Influx™). After 2 weeks, emerging clones were tested for their gal-9 expression by intracellular staining using rat anti-mouse gal-9 antibody clone 108A2 conjugated with allophycocyanin (APC) (#137911, Biolegend); they were analysed with an Accuri™ C6 flow cytometer (BD Biosciences). After sequencing analysis confirming their knock-out status, 3 of them were selected for the study (KO #175, #345 and #377). In addition, we selected 2 clones having undergone the same transfection treatment, sorting and clonal selection, but having preserved an intact gene sequence at the sites targeted by the guides and still strongly expressing gal-9 (Ctrl #116 and #376). Furthermore, we generated a list of the most probable off-targets by *in silico* analysis (**Supplementary table 1 and Supplementary figure 1**) and compared the FPKM values of these transcripts in KO clones with the controls and parental lines. No differences went outside this analysis.

Genomic DNA extraction, PCR and sequencing analysis. Cells were lysed in TRI reagent (MRC) and genomic DNA isolated according to the manufacturer's instructions, using chloroform for the phase separation. DNA quality was assessed by spectrophotometry (NanoDrop™ 2000c, Thermo Scientific). PCR were performed (F: 5'-CCGTGCTAGATCAGGCTCTG-3'; R: 5'-TGGCCATGTGACTGGTTCTC-3') to amplify the guides targeted region, with a high-fidelity DNA polymerase Q5® (New England BioLabs) (amplicon size = 1360 bp for the WT). After migration on a 1.5% agarose gel, PCR products were extracted with DNA/RNA extraction/purification kit (SmartPure Gel kit, Eurogentec). After quality assessment, samples were sequenced by Sanger sequencing (Eurofins) using both forward and reverse primers. Sequencing results were analysed using FinchTV software.

Western Blotting. Cells were lysed with RIPA buffer (150 mM NaCl, 50 mM Tris-HCl pH 7.4, 5 mM EDTA, 0.5% sodium deoxycholate, 0.5% Nonidet P-40, 0.1% SDS) supplemented with the cOmplete™ Protease Inhibitor Cocktail (Roche Applied Science) and sonicated on ice. The extracts were then clarified and the protein concentration determined by the Bradford method using protein assay (Bio-Rad) and a microplate reader (Tecan Infinity F200 Pro). Proteins were separated by SDS-PAGE on a 12% gel and transferred on an Immobilon®-P PVDF membrane (Millipore). The following primary antibodies were used: polyclonal goat anti-mouse gal-1 (#AF1245, R&D Systems), mouse anti-human gal-3 clone B2C10 (#sc-32790, Santa Cruz Biotechnology), polyclonal rabbit anti-human gal-8 (#MBS828618, MyBioSource), rat anti-mouse galectin-9 clone 108A2 (#137901, Biolegend); mouse anti-β-actin clone AC-74 (Sigma). Detection was performed using peroxidase-conjugated secondary antibodies and Immobilon® Western Chemoluminescent HRP substrate (Millipore).

Cell proliferation assay. MB49 cells (WT and KO) were seeded in a 96-well plate at the rate of 2000 cells/well. The proliferation rate in 24h was determined by measuring the ATP concentration in the wells at 24 and 48h (ATPlite Luminescence Assay System, PerkinElmer®).

RNAseq analyses. RNAseq analyses were performed in 2 distinct sequences for *in vitro* cultured cells and tumor cells transplanted on syngenic mice.

In *vitro* cultured cells were lysed in TRI reagent (MRC) and total RNA isolated according to the manufacturer's instructions, using chloroform for the phase separation. RNA quality was assessed by spectrophotometry (NanoDrop™ 2000c, Thermo Scientific). RNA sequencing and analysis were performed by IntegraGen (Evry, France). The quality of reads was assessed for each sample using FastQC. Fastq files were aligned to the reference Mouse genome mm10 with STAR1 (--twopassMode Basic --outReadsUnmapped None --chimSegmentMin 12 --chimJunctionOverhangMin 12 --alignSJDBoverhangMin 10 --alignMatesGapMax 200000 --alignIntronMax 200000 --chimSegmentReadGapMax parameter 3 --alignSJstitchMismatchNmax 5 -1 5 5 --quantMode GeneCounts --outWigType wiggle --sjdbGTFtagExonParentGene gene_name). Reads mapping to multiple locations were removed. Gene expression was quantified using the full Gencode vM18 annotation. STAR was also used to obtain the number of reads associated to each gene in the Gencode vM18 database (restricted to protein-coding genes, antisense and lincRNAs). Bioconductor DESeq package2 was used to import raw HTSeq counts for each sample into R statistical software and the count matrix was extracted. After normalizing for library size, the count matrix was normalized by the coding length of genes to compute FPKM scores (number of fragments per kilobase of exon model and millions of mapped reads).

When dealing with tumors carried by syngenic mice, RNA was extracted from frozen tumor fragments (30 mg) using the RNAeasy kit (Qiagen) according to the manufacturer's instructions. During the cell lysis step, tumor fragments were crushed with TissueRuptor (Qiagen) in RLT buffer supplemented with 40 mM dithiothreitol (DTT). RNA concentration and quality were assessed with a

Bioanalyzer instrument (Agilent). RNA sequencing and analysis were performed by Novogene (Cambridge, UK). Sequencing libraries were generated using NEBNext® Ultra™ RNA Library Prep Kit for Illumina® (NEB, USA), following manufacturer's recommendations, and index codes were added to attribute sequences to each sample. Clustering of the index-coded samples was performed on a cBot Cluster Generation System using PE Cluster Kit cBot-HS (Illumina) according to manufacturer's instructions. After cluster generation, libraries were sequenced on an Illumina platform and paired-end reads were generated. Raw data (raw reads) of FASTQ format were firstly processed through in-house scripts. In this step, clean data (clean reads) were obtained by removing reads containing adapter and poly-N sequences and reads with low quality from raw data. At the same time, Q20, Q30 and GC content of the clean data were calculated. All the downstream analyses were based on the paired-end clean reads which were aligned to the reference genome (*Mus musculus* GRCm38) using the Spliced Transcripts Alignment tool of the software. HTSeq was used to count the read numbers mapped of each gene. Then FPKM for each gene was calculated based on gene lengths and mapped reads counts.

Differential expression was performed on raw counts of RNAseq, by applying DESeq2 (Love et al., 2014) package, version 1.26.0, combined with the RUVseq package (Risso et al., 2014), version 1.20.0 (both in R language). We identified genes with absolute value of fold change > 2 and FDR adjusted p value of F test < 0.05 as differentially expressed (DE). Heatmaps of DE genes were generated with Pheatmap R package, version 1.0.12, after a transformation of raw counts using the function of variance stabilizing transformation of DESeq2.

Gene ontology was explored using ClusterProfiler package (Yu et al., 2012) version 3.14.3, with DE genes identified from DESeq2 analysis. Over-representation and gene set enrichment analysis were done against MSigDb gene sets, which were loaded through the MSigDbr package version 7.1.1 (Broad Institute Molecular Signatures Database), and genome wide annotation for Mouse, sourced from org.Mm.eg.db package version 3.10.0 (available at www.bioconductor.org). Enrichment analyses were later visualized by enrichplot (R package, version 1.6.1) (www.bioconductor.org).

Raw data (.bam) are available on ArrayExpress under the id: E-MTAB-9220.

Animal care and tumor models. Animal procedures were performed according to protocols approved by the Ethics Committee CEEA26 (project number n°20171108124492). Female C57BL/6N were purchased from Janvier Labs (France) and housed in the Gustave Roussy animal facility. Mice were used between 8 and 12 weeks of age. They were housed in pathogen-free conditions in filter cap cages holding a maximum of 5 animals with irradiated aspen chip bedding and cotton fiber nesting material. They were maintained on a 12/12 light/dark cycle, with *ad libitum* UV-treated water and RM1 rodent diet. The animals were monitored every day for signs of pain, such as immobility or restlessness, reduction of drinking and food intake. The persistence of abnormal behaviors for more than one day led to the euthanasia of animals with suffering presumption. Prior to tumor collection, mice were sacrificed by cervical elongation. Otherwise, mice were euthanatized by carbon dioxide asphyxiation. For initial tumor inoculation, *in vitro* expanded cells were injected subcutaneously (5.10^5 cells suspended in 100µl of PBS). After 10 to 20 days of sub-cutaneous growth, tumors were collected, cut in small fragments (70 or 100 mg) which were then subcutaneously engrafted on recipient mice. Tumor dimensions were measured every day using a digital caliper, starting from day 5-post-graft, and volumes were calculated based on the formula: $width^2$ x length / 2. In addition, tumors collected at the time of sacrifice were weighed. A part of them was fixed in 4% paraformaldehyde in order to carry out IHC and/or RNAscope analysis, and the rest was frozen for RNA/protein extractions.

RNAscope® (ACD™). Fixed (4% PFA) and paraffin-embedded tumors were cut into 5 +/- 1 µm sections using a microtome. The paraffin ribbons were mounted on SUPERFROST® PLUS SLIDES and deparaffinized before starting the RNAscope® workflow. This was performed following the manufacturer's instructions. Anti-gal-9 mRNA probe was specifically designed by BioTechne's team and we validated it on our samples making parallel staining with a positive (Mm-Ppib) and negative control (DapB) probe. After the signal detection step, slides were counterstained with 50% hematoxylin staining solution and dehydrated with 70% ethanol. After mounting slides, images were acquired with a Virtual Slide microscope VS120-SL (Olympus, Tokyo, Japan), 20X air objective (0.75 NA, 345 nm/pixel).

Histology and immunohistochemistry. After fixation of tumors in 4% PFA, paraffin-embedded tumors were cut into 4µm thick sections. At least one section per tumor was stained with hematoxylin-eosin-saffranin (HES) for quality control. For Ki-67 and CD8 detection, slides were incubated with rabbit monoclonal antibodies specific of Ki-67 (#12202, 1:500, Cell Signaling Technology®) and CD8 (#98941, 1:200, Cell Signaling Technology®). Primary antibody binding was revealed with the Rabbit PowerVision Kit (UltraVision Technologies) and the DAB PowerVision kit (ImmunoVisionTechnologies Co.). For detection of CD45 and CD4, slides were incubated with rat monoclonal antibodies specific of CD45 (#10051.05, 1:100, Histopathology) and CD4 (#MA1-146, 1:100, Thermo Scientific). Primary antibody binding was revealed with Polink 2 plus rat HRP kit (GBI Labs). All antibody applications were performed with a Bond RX automated Leica Slide Stainer. Image acquisition was performed with a Virtual Slide microscope VS120-SL (Olympus, Tokyo, Japan), 20X air objective (0.75 NA, 345 nm/pixel). Quantification of immunostaining was done using the Definiens Tissue Studio software (Definiens AG, Munich, Germany). For Ki-67 which is concentrated in the nuclei, we used an algorithm performing automatic detection of nuclei stained with DAB according to their spectral properties. Positive and negative nuclei were counted in a manually selected Region of Interest (ROI) (excluding areas of necrosis, preparation artifacts, etc.). Results were expressed as a number of stained cells – equivalent to stained nuclei - per mm^2 of analyzed tissue. $CD45^+$, $CD4^+$ and $CD8^+$ cells were detected using another algorithm performing detection of stained "objects" with a high probability of being single cells. This analysis resulted in numbers of positively stained cells per surface unit.

Cytokines profile. Protein extraction was performed from 30 mg of frozen tumor fragments by crushing them with TissueRuptor (Qiagen) in low detergent lysis buffer (20 mM Tric-HCl pH 7.5, 0.5% tween20, 150 mM NaCl) supplemented with the cOmplete™ Protease Inhibitor Cocktail (Roche Applied Science). Extracts were then clarified and protein concentrations were determined by the Bradford method using protein assay (Bio-Rad) and a microplate reader (Tecan Infinity F200 Pro). Undiluted samples from 1.23 to 5.38 mg/mL were used to perform the mouse cytokine array / chemokine array 31-Plex (MD31, Evetechnologies) (Eotaxin, G-CSF, GM-CSF, IFN-γ, IL-1α, IL-1β, IL-2, IL-3, IL-4, IL-5, IL-6, IL-7, IL-9, IL-10, IL-12 (p40), IL-12 (p70), IL-13, IL-15, IL-17A, IP-10, KC, LIF, LIX, MCP-1, M-CSF, MIG, MIP-1α, MIP-1β, MIP-2, RANTES, TNFα, VEGF (LIX results are included but not validated)). The cytokine concentrations were then normalized to protein concentration.

Deep profiling of the expressed TCR beta repertoire. RNAs extracted from tumor fragments (as explained above) were used to profile the TCR beta repertoire of tumor lymphocytes. Wet lab and bioinformatics analyses were performed by iRepertoire Inc. (Alabama, USA). Sequencing libraries were generated using their proprietary dimer avoiding multiplex(dam)-PCR technology which uses iterative rounds of amplification and amplicon recovery to selectively amplify the TCR beta chains (all possible murine VDJ combinations in one single reaction). Libraries were then sequenced on an

Illumina MiSeq® platform and paired-end reads were generated. Data analysis and tree map illustration were performed by iRepertoire Inc.

CXCL10 ELISA assay. WT (MB49, Ctrl #116 and #376) and KO (KO #175, #345 and #377) cells were cultured in normal media supplemented or not with recombinant murine IFN-γ (#315-05-100UG, PeproTech®): 0, 2, 5, 10 and 25 ng/mL. After 72h of IFN-γ treatment, supernatants were collected and secreted CXCL10 was assayed with mouse CXCL10 ELISA kit (#DY466-05, #DY008, R&S Systems®) according to the manufacturer's instructions.

Statistical analysis. Except for RNAseq data, statistical tests were performed using GraphPad Prism version 7.00 (GraphPad Software, San Diego, CA). Kaplan-Meier survival curves were generated and analyzed using the log-rank, Mantel-cox test. Significant differences when comparing two groups were determined by two-tails Mann-Whitney test. P-value < 0.05 was considered as significant.

Results

Lgals9 gene invalidation in the murine cell line MB49: impact on its *in vitro* phenotype and gene expression profile

In order to explore the contribution of gal-9 produced by malignant cells to tumor immune escape, we selected the MB49 murine tumor model. MB49 cells originated from a bladder carcinoma and are compatible with C57BL/6 mice. They are known for generating hot tumors in syngenic mice and to trigger relatively strong although inefficient primarily CD8 cytolytic adaptive immune response (El Behi et al., 2013; Melchionda et al., 2005; Perez-Diez et al., 2007). They are also known to be responsive to immune-checkpoint inhibitors. MB49 cells were shown to have constitutive, permanent expression of gal-9. The *LGALS9* gene was invalidated in clones derived from MB49 cells using the CRISPR/Cas9 strategy. Two guides were designed, inserted in plasmids expressing GFP or mCherry respectively and transfected simultaneously together with a Cas9 expressing construct in order to delete a sequence containing the gal-9 ATG start codon (**Figure 1A**). Two days after transfection, single cells with concomitant high GFP and m-Cherry expression were sorted, seeded at one cell per well and grown in 96-well plates. After an average of 2 weeks of expansion, replicas of these clones were subjected to detection of intra-cellular gal-9 by flow cytometry. Using this procedure, we selected three gal-9-KO clones (KO #175, #345 and #377) and two WT-control clones (Ctrl #116 and #376). Control clones were derived from cells subjected to the same transfection and clonal selection processes, but which had retained gal-9 expression with an intact gene sequence (**Figure 1B**). As the single cell growth step resulted in clonal growth of no more than 45% of the cells, the WT-Ctrl clones were essential to take into account the clonal selection process. In addition, they made it possible to take into account potential off-target effects and therefore represented essential controls in addition to the parental line (**Supplementary Table 1 and Figure 1**). As shown in **Figure 1C**, both the parental MB49 cell line and the WT-Ctrls expressed gal-9. Two isoforms of the protein were observed, the gal-9L and the gal-9M, the latter being predominant. This experiment also confirmed the absence of gal-9 protein in the gal-9-KO clones. Next experiments intended to find functional repercussions of gal-9 silencing in the context of *in vitro* culture. However *in vitro* proliferation assays did not record any difference between WT and KO cells (**Supplementary figure 2**). In addition, RNAseq analysis fail to identify any subset of transcripts with a pattern of expression distinctive of gal-9-KO by comparison with WT-Ctrl clones (**Supplementary figure 3**). Finally, we found no influence of gal-9 gene silencing on gal-1, -3 and -8 expressions (**Supplementary figure 4**).

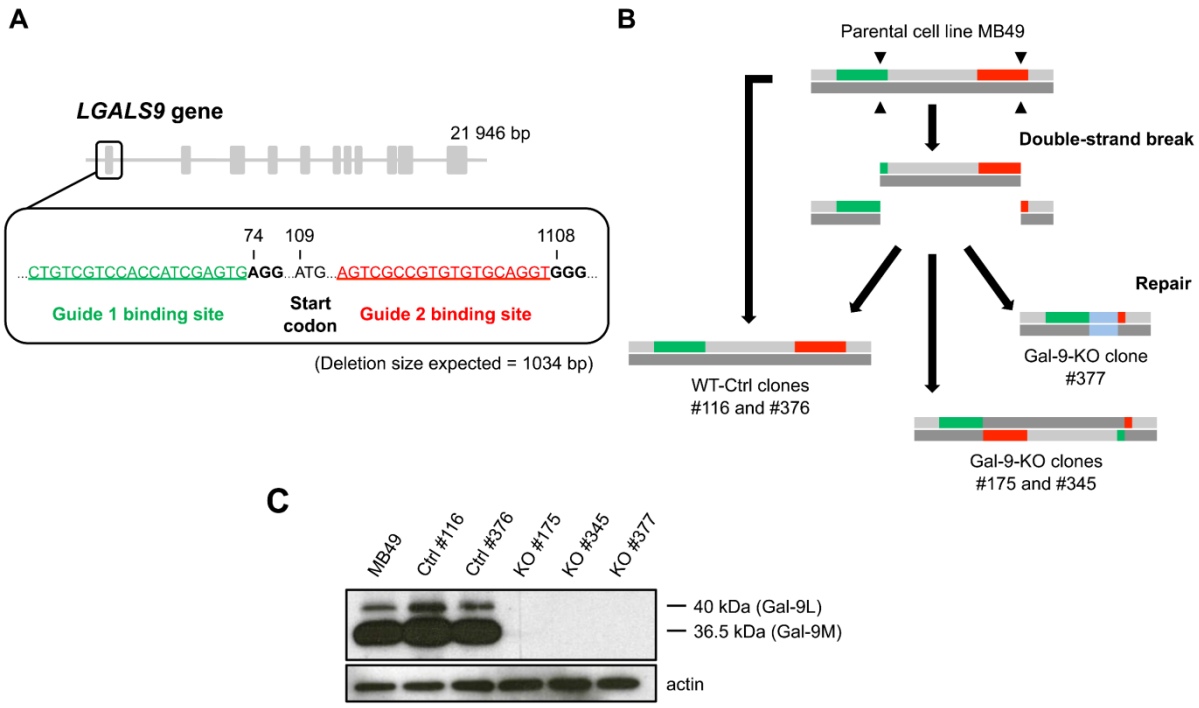

Figure 1. Invalidation of the gal-9 gene in the MB49 cell line. (A) Schematic representation of the gal-9 gene and the target sites of the CRISPR guides 1 and 2 located respectively in the first exon and the first intron. (B) Sequence analysis of the WT-Ctrl clones #116 and #376 indicated that the *LGALS9* locus were unaffected in both alleles (possible explanations might be absence of Cas9-mediated double-strand DNA break or efficient repair of the breaks). For the three-selected gal-9-KO clones, the deleted fragments were either replaced by a new DNA sequence (#377) or by the deleted fragments oriented in the reverse direction (#175 and #345). (C) Western-Blot analysis of the gal9 protein in the selected clones: the parental line and the WT-Ctrl clones expressed two isoforms: gal-9L and gal-9M; the latter being predominant. Absence of Gal9 expression was confirmed in the gal-9-KO clones.

Elaboration of a serial tumor transplantation assay for a more sensitive assessment of *in vivo* tumor growth of the MB49 cells

In order to assess the influence of gal-9 invalidation on host-tumor relationships, we investigated the 3 gal-9-KO clones, the 2 WT-Ctrl clones and the parental MB49 cells in the context of subcutaneous tumors resulting from cell grafts in syngenic female mice (C57BL/6N). At the beginning of these experiments, we faced technical concerns regarding the mode of cell injections: either early skin ulcerations resulting from superficial injections or unwanted infiltration of underlying organs when making deeper injections. Therefore, we decided to set up tumor growth assays based on subcutaneous implantation of small tumor fragments (70 or 100 mg depending on the experiments). Cell injection was the method retained for the first passage allowing collection of tumor fragments for subsequent passages (**Figure 2A**). Implantation of small tumor fragments was successful in reducing the incidence of tumor ulcerations or tumor infiltrations in underlying organs. Tumor volumes were roughly identical for gal-9-KO and WT-Ctrl clones at the first cycle of tumor growth following subcutaneous cell injections. However, at the next cycles based on grafts of tumor fragments, we started to observe a trend towards a slower growth for gal-9-KO compared to WT-Ctrl tumors. This was hardly visible at the 2nd cycle but became obvious at subsequent passages. Multiple experiments were done in order to ensure the consistency of this phenomenon. For example, in one pilot experiment, we compared tumor growth of two gal-9-KO clones (#345 and #377), one WT-Ctrl clone (#116) and the parental line, through 4 successive passages in syngenic female mice. As shown on **Figures 2B and 2C**, at the 4th cycle, the growth of the gal-9-KO clones was drastically reduced. Only small necrotic tumors were recovered. This experimental sequence was thereafter designated as "serial tumor transplantation assay". In order to assess the expression level of gal-9 in these tumors, some of them were fixed and paraffin-embedded to carry out *in situ* hybridization of gal-9 mRNA (RNAscope). The staining results are shown in **Figure 2D**. At the end of the 4th cycle, we observed a strong staining of gal-9 transcripts in all the WT tumor tissue. The gal-9-KO tumors also presented some gal-9 transcripts but they were much less abundant. Indeed, the gal-9 expression was limited to infiltrating cells and the vascular endothelium, both originating from host mice.

Gal-9 invalidation impairs *in vivo* tumor growth of MB49 cells in syngenic mice suggesting its contribution to immune escape

To get stronger evidence of the progressive decline of gal-9-KO tumor growth in syngenic mice, we designed a serial transplantation assay involving all 3 gal-9-KO clones along with two WT-Ctrl clones and the parental MB49. The experimental scheme presented in Fig.2 was slightly modified in order to facilitate its parallel application to immunodeficient mice without risking excessive tumor growth. The amount of transplanted tumor fragments as well as the delay between successive passages were thus reduced (tumor growth cycle reduced to 10 days; amounts of transplanted tumor fragments reduced to 70 mg). As shown in **Figure 3A**, a progressive reduction of tumor growth was observed for gal-9-KO clones through successive passages. This reduction was hardly visible at the 2nd cycle, but stronger at the 3rd although not statistically significant. At the 4th cycle, it was even more marked and statistically significant (individual growth curves are visible in **Supplementary figures 5A and 5B**). Data based on tumor growth curves were confirmed by weight measurements of tumors excised following mouse euthanasia at the completion of each cycle, every 10 days. As shown in **panel B of Figure 3**, the relative decline of tumor growth for gal-9-KO clones transplanted on syngenic mice was statistically significant at cycle 3 and even more dramatic at cycle 4. Beyond cycle 4, we made one additional graft cycle involving all control tumors along with remaining gal-9-KO tumors (those which were above 90mg at the completion of the 4th cycle). At this next step, additional gal-9-KO clones

stopped growing whereas all control clones still grew at a rapid path (**Supplementary figure 5C**). Since gal-9-KO and WT MB49 cells had the same growth properties *in vitro*, our observations suggested that the progressive growth reduction of gal-9-KO tumors was related to a more efficient immune response in syngenic mice.

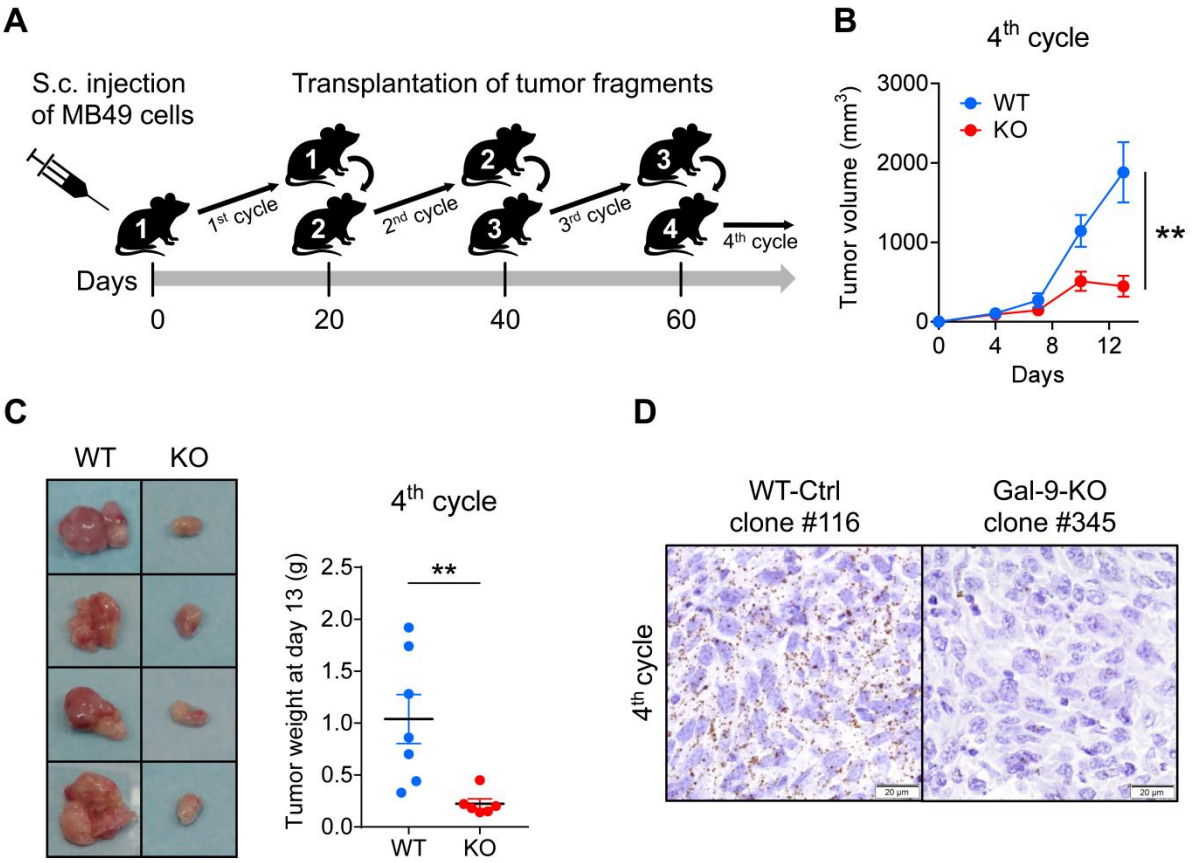

Figure 2. Pilot serial tumor transplantation assay using MB49-derived cells and syngenic mice. (A) Cartoon depicting the main steps of the assay. The MB49 parental cell line (n=3), the WT-Ctrl clone #116 (n=4), the gal-9-KO clone #345 (n=2) and the gal-9-KO clone #377 (n=4), were subcutaneously injected into C57BL/6 female mice (opening the 1st cycle of tumor growth involving mice n°1). Twenty days later, tumors were collected and cut into small fragments. For each mouse donor, a small aggregate of tumor fragments (100 mg) was then subcutaneously transplanted into a single recipient mouse (2nd cycle involving mice n°2). This operation was repeated twice (opening the 3rd and 4th cycles of tumor growth involving mice n°3 and mice n°4 respectively). (B) Comparison of tumor growth curves for WT and KO tumors during the 4th cycle (mean volumes +/- SEM). WT tumors include tumors derived from the parental cells (MB49) and the 2 WT-Ctrl clones #116 and # 376. Significant differences in tumor volumes were recorded at day 13 (Mann-Whitney test). (C) Tumor collection and comparison of tumor weights between the WT and KO groups at the completion of the 4th cycle of tumor growth (with significant differences between the 2 groups)(Mann-Whitney test). D) RNAscope detection of gal-9 transcripts in WT and KO tumor sections at the completion of the 4th cycle of tumor growth. In tumors derived from parental and WT-Ctrl cells numerous dots corresponding to gal-9 transcripts were detected in the vast majority of the cells. On the contrary, in gal-9-KO tumors, gal-9 RNA dots were much less abundant and restricted to some isolated cells (likely infiltrating immune cells or endothelial cells from the recipient mice).

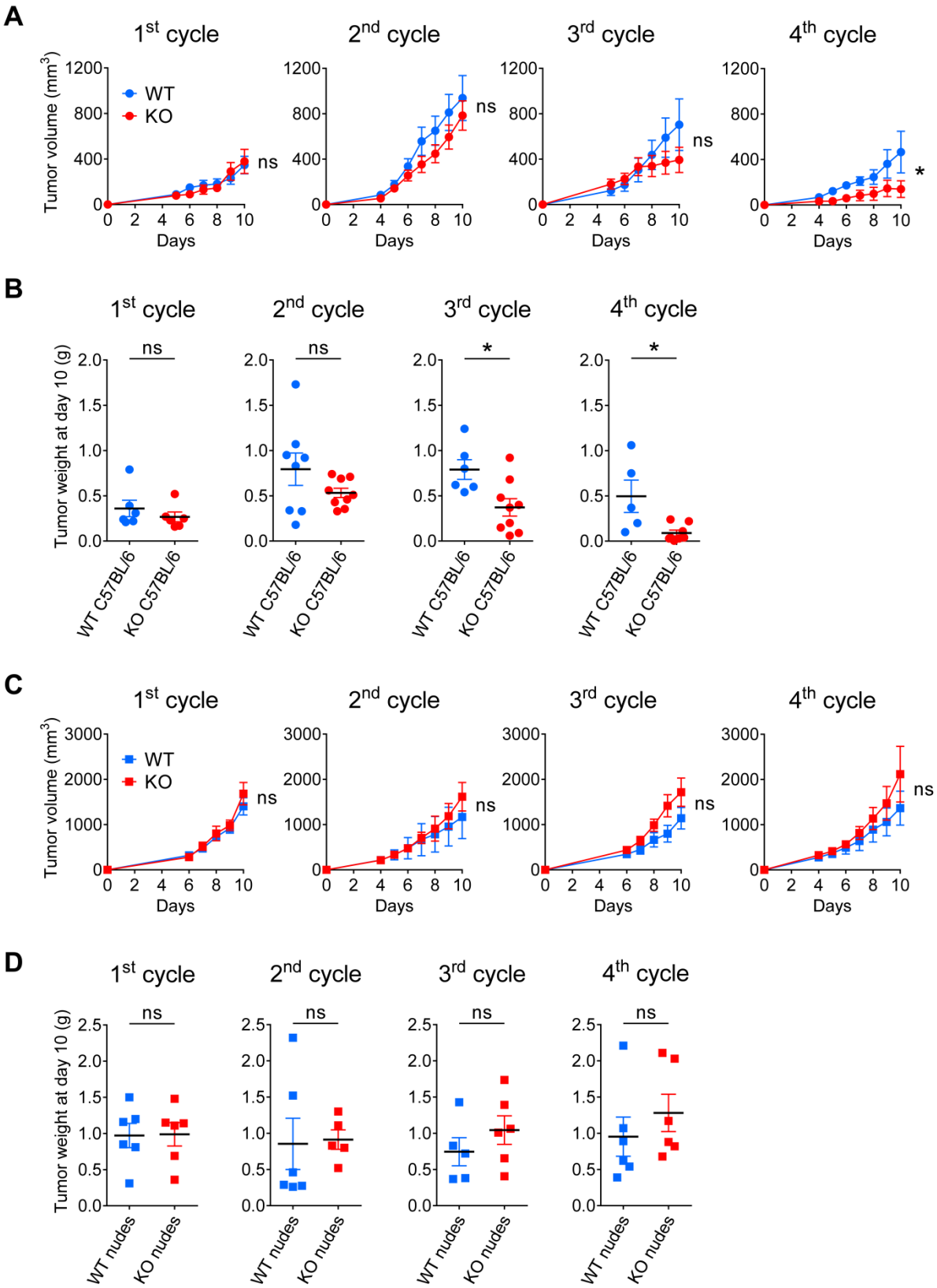
A
1st cycle
2nd cycle
3rd cycle
4th cycle
Tumor volume (mm3)
WT
KO
ns
*
Days
B
Tumor weight at day 10 (g)
WT C57BL/6
KO C57BL/6
C
D
WT nudes
KO nudes

Figure 3. Serial tumor transplantation assays using immunocompetent or immunodeficient mice. (A) Comparison of tumor growth curves for WT and KO tumors at each cycle (mean volumes ± SEM). WT tumors include tumors derived from the parental cells (MB49) and the 2 WT –Ctrl clones #116 and # 376. For the 1st cycle of tumor growth, cells from the MB49 parental cell line (n=3), WT-Ctrl clones #116 (n=3), #376 (n=3) and gal-9-KO clones #175 (n=3), #345 (n=3) and #377 (n=3), were subcutaneously injected into C57BL/6 female mice. Subsequent passages were done using subcutaneous inoculation of aggregated tumor fragments (70mg). Comparison of WT and KO groups were performed at the last point of each cycle and subjected to Mann-Whitney tests. As in the pilot experiment, the serial transplantations on syngenic mice led to a progressive decrease in tumor volume for gal-9-KO tumors compared to WT-Ctrl and parental MB49-derived tumors. (B) Comparison of the tumor weights when mice were sacrificed at the completion of each cycle. The differences between the two groups were significant from the 3rd cycle (Mann-Whitney test). (C and D) The same experimental scheme was carried out in parallel on nude mice. In the context of these immunodeficient mice, there was no growth reduction during serial transplantation for gal-9-KO-derived tumors, as compared to WT-derived tumors (a slight, though non-significant, increase was actually observed). These observations highlight the contribution of the adaptative immune response to the reduction of gal-9 KO tumor growth.

T-cells are involved in the improved immune response resulting from gal-9 invalidation in MB49 cells

We suspected that the progressive reduction of tumor growth for gal-9-KO clones was related to some improvement in the anti-tumor immune response. To confirm this hypothesis, in parallel with the previously presented experiments, we performed serial tumor growth assays on athymic (nudes) mice comparing the 3 gal-9-KO clones, the 2 WT-Ctrl clones and the parental MB49. As shown in **Figures 3C and 3D**, in the context of athymic mice, there was no more tumor growth reduction for the gal-9-KO clones. Moreover, they grew even faster than the WT cells at cycles 3 and 4 (individual growth curves are visible in **Supplementary figures 5D and 5E**). Because athymic mice are characterized by a complete absence of T-cell ontogenesis, these results suggested that the tumor growth reduction of the gal-9-KO clones was dependent on T-cells. To strengthen this hypothesis, we used immunohistochemistry to investigate T-cell infiltration of WT and gal-9-KO tumors grown on syngenic mice. Tumor sections made at cycle 2, 3 and 4 were processed using antibodies reacting with Ki-67, CD45, CD4 and CD8. For each marker, density staining was quantified by digital imaging. Upon visual examination, we made two main observations. First, we noted that the bulk of leucocytes ($CD45^+$), including T-cells ($CD4^+$ and $CD8^+$), were concentrated in peri-tumoral margins. Their abundance in these areas was identical for KO and WT tumors at all cycles of tumor growth (**Figure 4A**). In contrast, leucocytes were quite rare inside the tumor nodules of almost all tumors. However, we found that a specific feature of KO tumors at cycle 4 was the presence of a substantial number of $CD45^+$, $CD4^+$ and $CD8^+$ T-cells inside the tumor nodules (**Figure 4B**). This was confirmed by digital assessment of the 4 markers (Ki-67, $CD45^+$, $CD4^+$ and $CD8^+$) inside the tumor nodules as shown by the histograms of **Figure 4C**. At cycles 2 and 3, densities of the 4 markers were almost identical for KO and WT tumors. We decided to use the density of Ki-67 staining to normalize the density of the other markers. At cycle 4, the density of CD45 staining inside the tumor nodules was much higher for KO than for WT tumors. CD4 and CD8 densities were also at higher levels in KO compared to WT tumors, although the differences did not reach statistical significance. Overall, our conclusion was that T-cell infiltration of tumor nodules was specific for gal-9-KO tumors. However, it was detectable only at cycle 4, therefore at a late stage of the anti-tumor immune response, when tumor growth was already strongly impaired (5/8 KO tumors were of minimal size, weighing less than 70 mg). These observations suggested that, upstream of T-cells infiltration, some immune-related events were occurring in a different manner in gal-9-KO and WT tumors, at an earlier stage of the serial transplantation assay, possibly during cycles 3 or 2. A glimpse of these early events was given by quantitative assessment of the diversity of the stromal T-cell repertoire. Using total tumor c-DNA, the diversity of the TCR complementary determining region 3 (CDR3) was assessed by PCR amplification and high throughput sequencing (**Figure 5**). This analysis resulted in clonotypes characterized by a unique sequence and a frequency of reads matching this sequence. Clonotypes with a minimal frequency of reads are represented by rounded rectangles of sufficient size to be visible in the tree maps shown in figure 5. The table at the bottom of the figure shows a greater number of unique sequences in KO than WT tumors and an increasing trend in cycle 3 by comparison with cycle 2. Interestingly the tree maps shows that these gains in unique sequences are associated with the emergence of novel clonotypes -represented by small rounded rectangles - rather than further accumulation in large, pre-existing clonotypes represented by big rectangles. This is what was expected in a context of diversification of the T-cell response. Overall these observations suggested a structure of the T-cell repertoire which tends to increase in diversity from cycle 2 to cycle 3 and which is more diverse in KO than WT tumors at cycle 3 as well as cycle 2. In other words, they suggested that long before intra-nodular T-cell infiltration, as early as the second cycle of tumor growth, changes in T-cell distribution and behavior were taking place preferentially in gal-KO tumors.

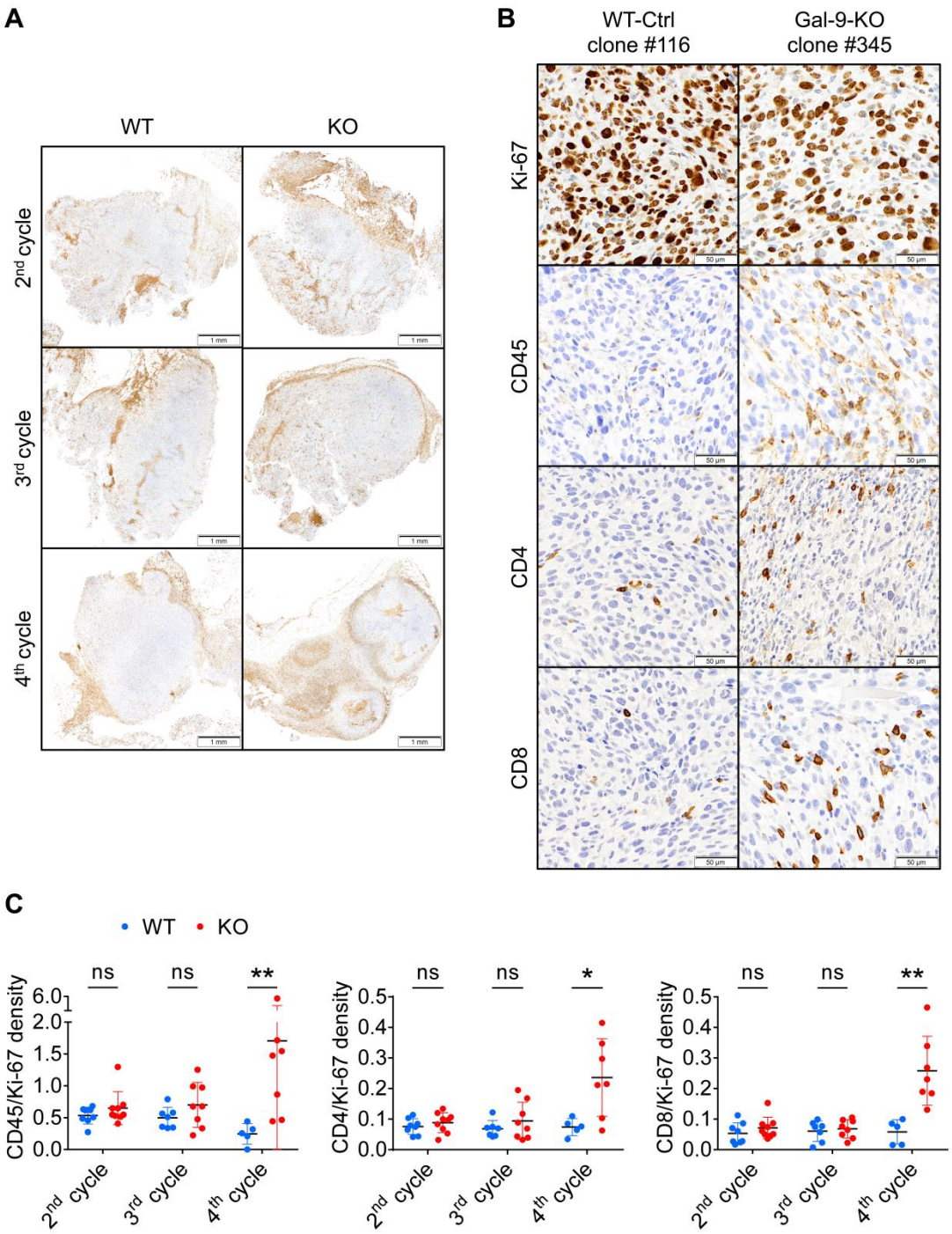

Figure 4. In gal-9-KO tumors, late stages of tumor growth reduction are associated with an increase in T-cells infiltrating tumor nodules. (A) Low magnification of CD45 staining on sections of WT and gal-9-KO tumors at cycles 2, 3 and 4 (tumors derived from clones #116 and #345, respectively). (B) High magnification of CD45, Ki-67, CD4 and CD8 staining on serial sections of a WT-Ctrl tumor (#116) and a gal-9-KO tumor (#345) at cycle 4. (C) Quantitative assessment of CD45, CD4 and CD8 staining on serial setions of tumors collected at cycles 2, 3 and 4 of tumor growth. Digitalization was performed in large Regions of Interest (ROIs) covering in as much as possible the whole tumor sections and excluding areas with absence or very low levels of Ki-67 staining. Therefore these ROIs were covering mainly the internal parts of the tumor nodules and excluding peri-nodular margins. Ratios of CD45, CD4 or CD8 to Ki-67 staining intensities were acquired in these ROIs and plotted for each tumor growth cycles.

A

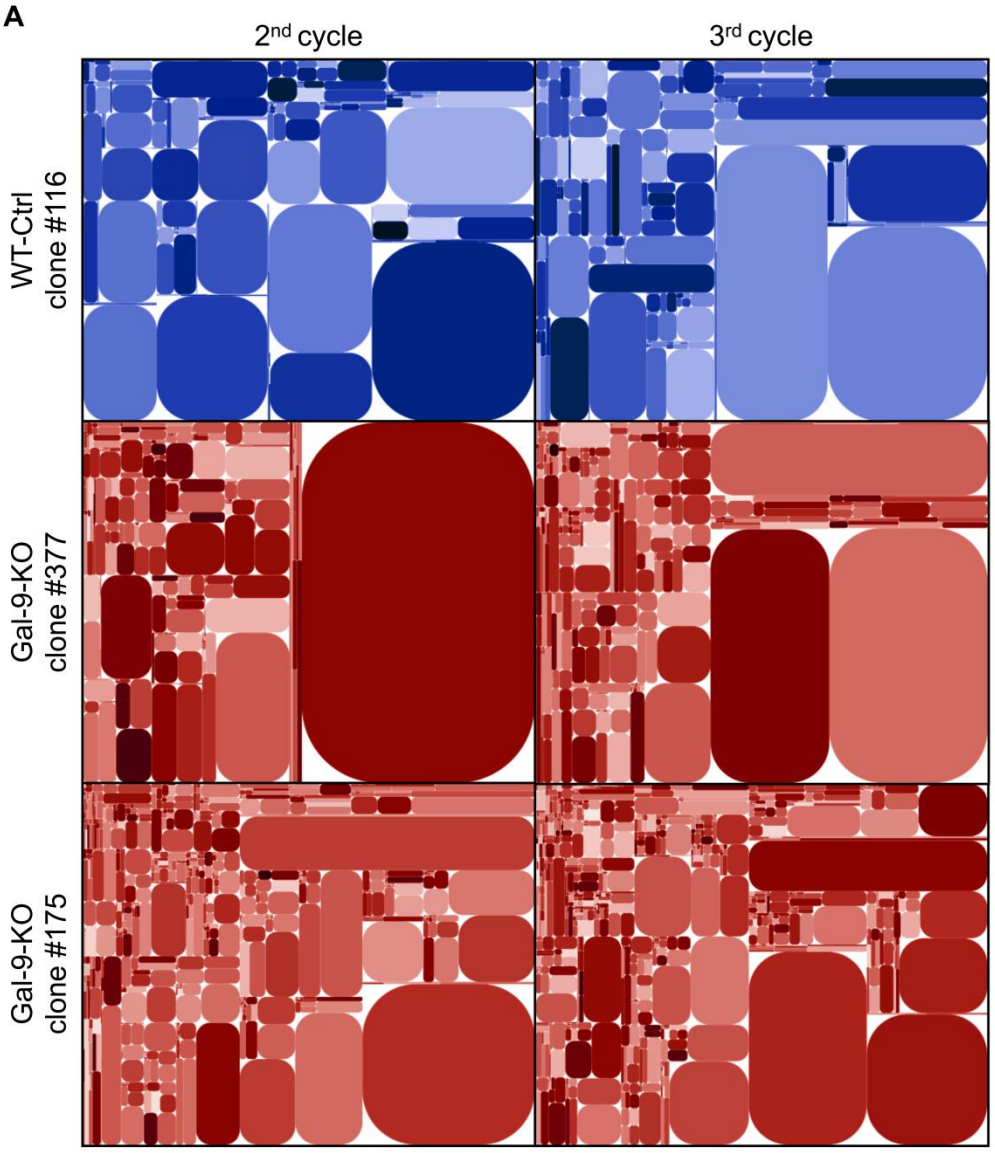

B

Sample	Reads	Unique reads	
		Frequency > 1	Frequency > 100
WT-Ctrl clone #116 (2nd cycle)	669,565	517	107
WT-Ctrl clone #116 (3rd cycle)	567,525	641	130
Gal-9-KO clone #377 (2nd cycle)	536,629	660	139
Gal-9-KO clone #377 (3rd cycle)	439,445	927	212
Gal-9-KO clone #175 (2nd cycle)	501,260	1,337	305
Gal-9-KO clone #175 (3rd cycle)	554,846	1,552	400

Figure 5. Modifications of T-cell clonotype profile at an early stage of tumor growth reduction in Gal-9-KO tumor. The diversity of the CDR3 segment of the TCR β-chain was investigated using total tumor RNA subjected to reverse transcription, selective PCR amplification of the CDR3 coding region and deep sequencing. (A) Tree maps of the clonotypes identified in 1 WT-Ctrl and 2 gal-9-KO tumors at the 2^{nd} and 3^{rd} cycles of tumor growth. These tree maps were generated as follows: he entire plot area was divided into sub-areas according to V-usage, then subdivided according to J-usage and again according to unique CDR3 sequence resulting from somatic hypermutations. Each clonotype is characterized by its unique sequence and the frequency of the reads matching this sequence. Those with a sufficient frequency of reads are represented by a rounded rectangle whose size is proportional to this frequency. The table of the lower panel shows that the total number of unique reads is greater in cycle 3 than in cycle 2 and in KO than in WT tumors. The same applies to the number of clonotypes as shown in the upper panel.

Gal-9 ablation enhances transcription of genes related to interferon-γ response

To further investigate biological events occurring prior to T-cell infiltration and blockade of tumor growth, we performed a comparative transcriptome analysis of gal-9-KO and WT tumors through the successive cycles of the serial tumor transplantation assay **(Figure 6A)**. Our aim was to find correlations between the dynamics of transcriptional changes and the progressive inhibition of KO-tumor growth. RNAseq data from 30 samples were subjected to various types of comparative bioinformatics analyses. Unsupervised clustering as well as supervised comparisons did not achieved separation of gal-9-KO from WT tumors or early from late passages while there was a robust clusterization of tumors derived from the same clones (**Supplementary figure 6**). It seems that biological characteristics related to the progressive immune response were, to a large extent, relegated to the background by other clonal private characteristics. We reasoned that it was not sufficient to compare the whole set of WT tumors with the whole set of KO tumors. We thought that it was possible to gain sensitivity by focusing the comparison on the subset of KO-tumors taken at the late stages of the serial transplantations, especially at the last cycles preceding the collapse or quasi-collapse of tumor growth, hereafter named pre-terminal cycles (**Figure 6A**). Our bet was that it would be easier to find transcriptional characteristics consistent with the enhancement of the immune response in this subset of "pre-terminal" tumors. Reciprocally these characteristics were expected to be absent or less visible in the rest of the KO tumors, non-pre-terminal tumors thereafter called aggressive KO tumors **(Figure 6A).** Combining the RUVseq package with the DESeq2 software we generated a list of differentially expressed (DE) genes resulting from the comparison of "pre-terminal" KO vs all WT tumors (Love et al., 2014). This list of 344 genes resulted in effective separation of "pre-terminal" gal-9-KO from WT tumors as shown by the heat map in **Figure 6B**. This same list was subjected to enrichment analysis using the package ClusterProfiler (Yu et al., 2012). The greater enrichment scores were for the following general functions: cell response to interferon-γ, allograft rejection and inflammatory response (**Figure 6C**). One gene related to these 3 general functions – *CCL5* (also called *Rantes*) – appeared to be strongly express in "pre-terminal" KO tumors.

Progressive increase in the concentrations of CXCL10 in gal-9-KO tumors

In order to better understand the immune mechanisms of the progressive growth inhibition of gal-9-KO tumors we used a multiplex ELISA assay to investigate the expression of a panel of 31 cytokines in the tumor cells and their microenvironment. This assay was carried on whole proteins extracted from WT and KO tumor fragments collected at cycle 2 and 3 of tumor growth. Cytokine concentrations were compared between these 3 sets of tumors: WT, aggressive gal-9-KO and "pre-terminal" KO tumors **(Figure 7A**). Significant differences between "pre-terminal" KO tumors and WT tumors were found for 4 cytokines - IL-1 α and β, IL-2, IL-9 and TNF-α - which were more abundant in "pre-terminal" KO tumors than in WT tumors and even than aggressive KO tumors for IL-1α and IL-2. The concentrations of CXCL9 and CXCL10 were also increased in "pre-terminal" KO tumors, although the differences with WT tumor did not reach statistical significance. However, we paid attention to this observation to design subsequent experiments because we were struck by the fact that even at baseline (WT tumors) the concentrations of CXCL9 and CXCL10 in tumor extracts were greater than those of other cytokines by 2 orders of magnitude. In an attempt to connect these results with the data resulting from transcriptome profiling, we investigated a potential correlation between the abundance of the transcripts encoding the seven cytokines overexpressed in "pre-terminal" KO tumors and the mRNAs encoding interferon-γ. As shown in **Figure 7B**, for all these cytokines except IL-9, there was a strong positive linear correlation of their expression with interferon-γ expression in

all KO and WT tumors. This was one additional observation suggesting a critical role of interferon-γ in the progressive deployment of the anti-tumor immune response.

Gal-9 gene ablation in MB49 cells enhances CXCL10 induction in response to recombinant interferon-γ

In order to confirm the hypothesis of a greater sensitivity of MB49 cells to their stimulation by interferon-γ in the absence of gal-9, we performed the following experiment *in vitro*. Gal-9-KO and WT cells were subjected to a 72h treatment with increasing concentrations of recombinant interferon-γ (from 2 to 25 ng/ml). Then the concentration of CXCL10 was assayed in the conditioned medium. As shown in **Figure 8**, CXCL10 production was completely absent at baseline, it was induced in a dose-dependent manner by interferon-γ. This induction was much stronger for gal-9-KO clones than for WT clones or MB49 parental cells. This was a confirmation of the greater sensitivity of MB49 cells to their stimulation by interferon-γ in the absence of gal-9.

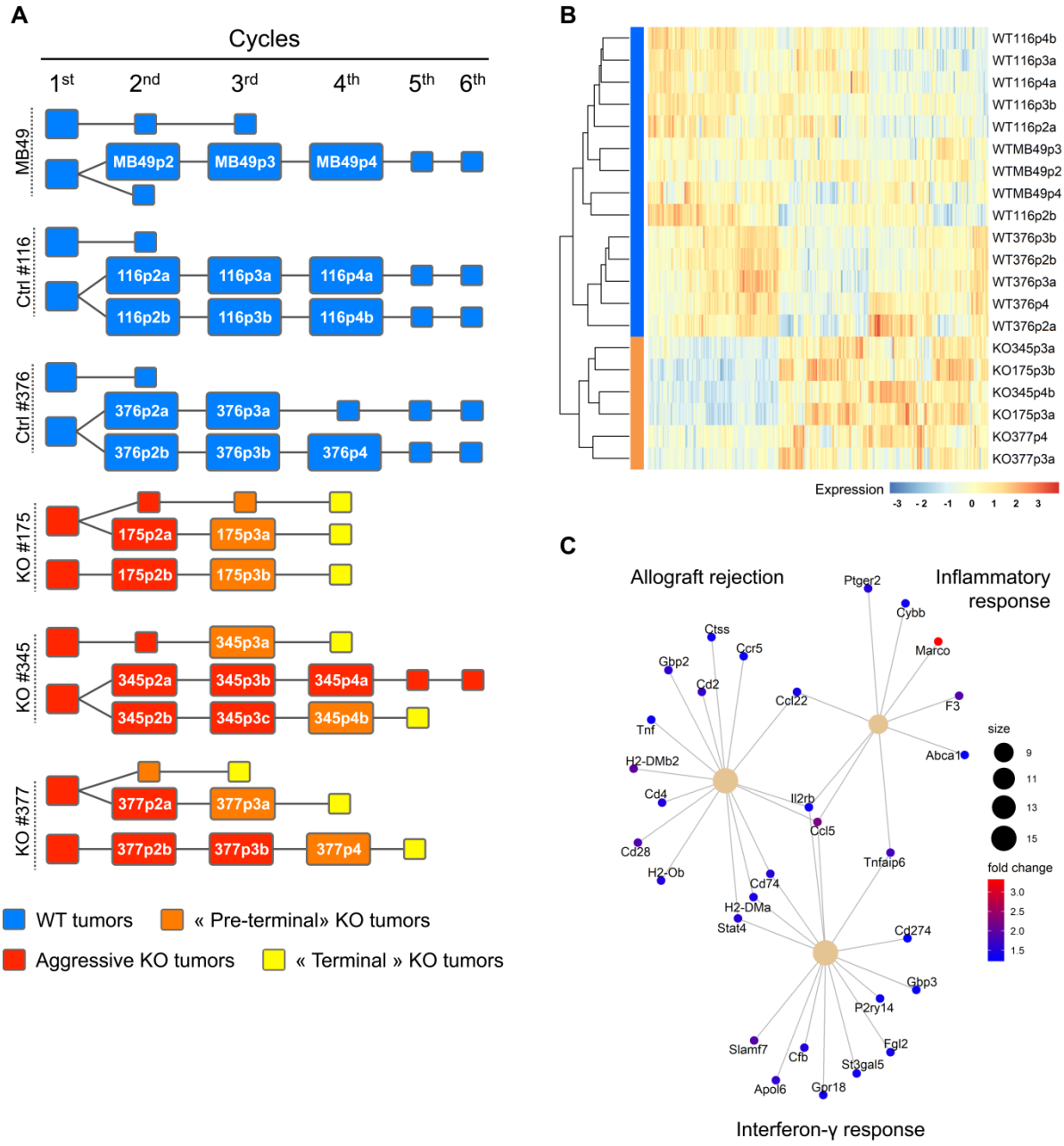

Figure 6. RNAseq analysis of WT and KO tumors at different cycles of *in vivo* tumor growth. A) Cartoon depicting the serial tumor transplanatation assay with emphasis on the tumor "lineages" and their changes in growth and aggressiveness : WT tumors are represented in blue, aggressive (WT-like) KO tumors in red, "terminal" (infiltrated by T-cells and exhausted) KO tumors in yellow and the "pre-terminal" KO tumors in orange. B) Heatmap representing the expression profile of the 344 most differentially expressed genes between WT and "pre-terminal" KO tumors, based on RUVseq (k=3) and DEseq2 analysis (fold change > 2, adjusted p-value < 0.05). C) Enrichment analysis of the differentially expressed genes within the "hallmark" gene sets with the clusterProfiler package: 15 up-regulated gene in the "pre-terminal" KO tumors are associated with the "allograft rejection", 9 with the "inflammatory response" and 15 with the "interferon-γ response".

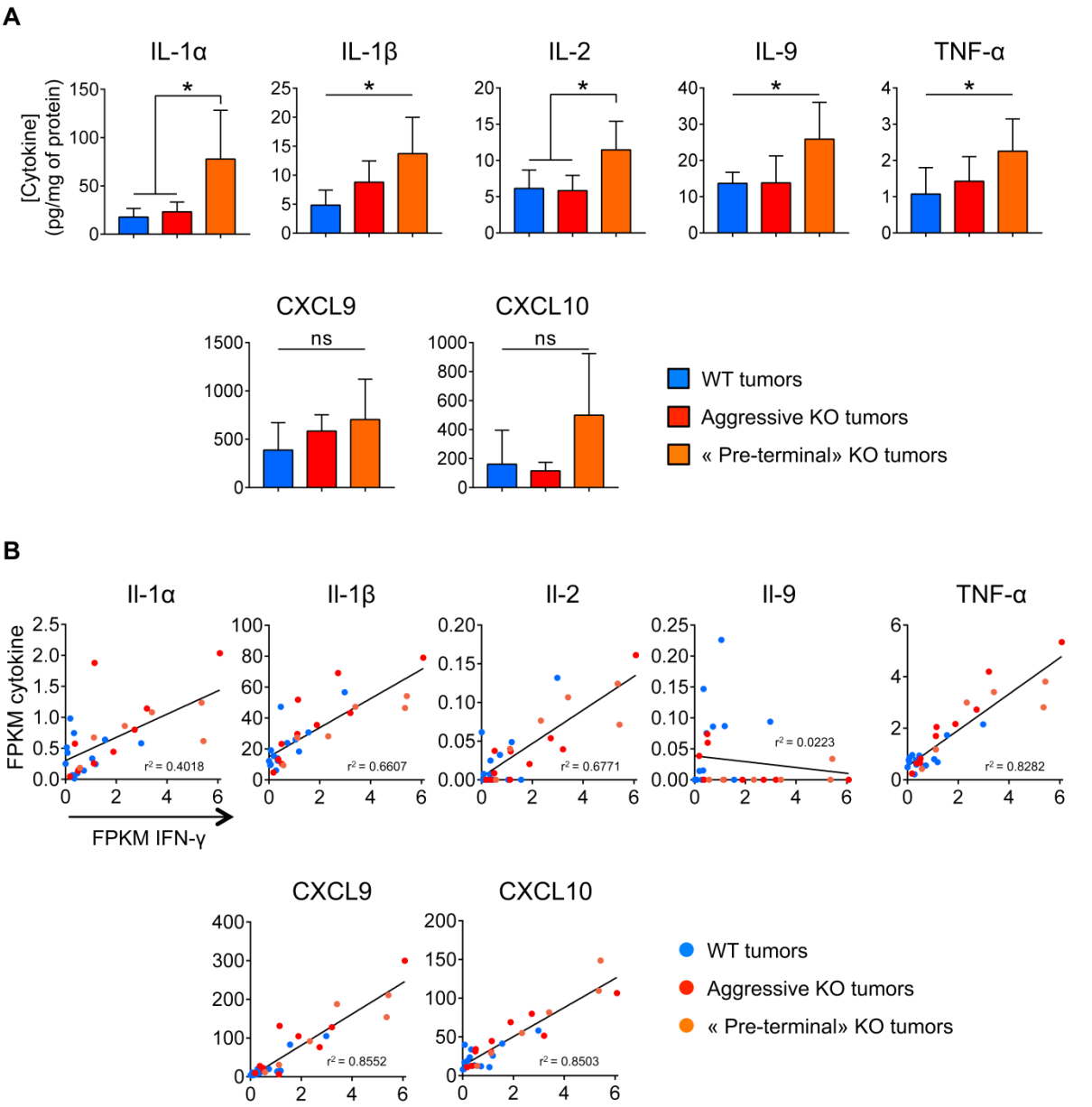

Figure 7. Cytokine status in gal-9-KO and WT tumors. A) Concentration of seven cytokines measured in tumor protein extracts at various cycles of tumor growth. For Il-1 α and β, IL-2, IL-9 and TNF-α there is a significant increase in their concentrations in the extract of "pre-terminal" KO tumors compared to the WT tumors or even to the aggressive KO tumors (Il-1α and Il-2). There is evidence that the production of CXCL9 and CXCL10 is enhanced in KO tumors, although the figures are not statistically significant. However, it is worth to mention these observations because the concentrations of CXCL9 and CXCL10 in tumor extracts are greater than those of other cytokines by 2 orders of magnitude even at baseline. B) Abundance of the messenger RNAs of the above-mentioned cytokines (FPKM values in RNAseq data) as a function of the amount of IFN-γ transcripts. For most cytokines overexpressed in "pre-terminal" KO tumors, there is a strong positive linear correlation between their level of expression and that of IFN-γ in all KO as well as WT tumors.

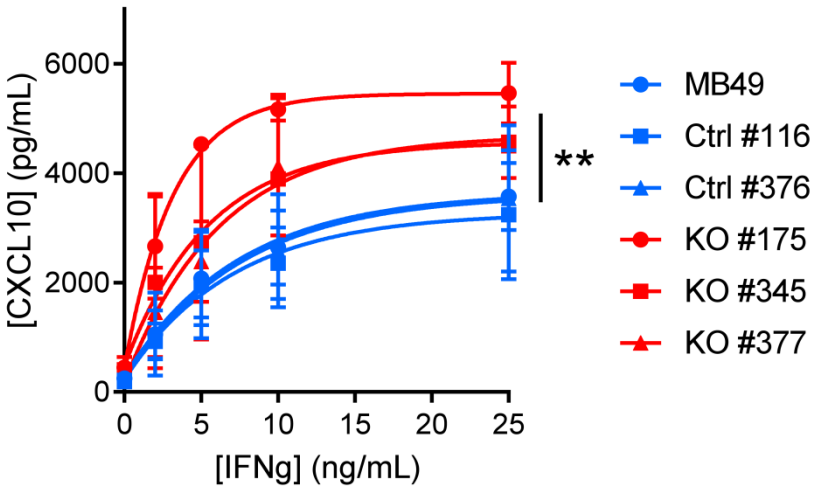

Figure 8. Dose-dependent induction of CXCL10 production by gal-9-KO and WT MB49 cells stimulated *in vitro* by recombinant interferon-γ. Conditioned media were collected after 72h of stimulation with increasing concentrations of interferon-γ and subjected to CXCL10 ELISA assay. At 25ng/mL of interferon-γ there was a significant difference of CXCL10 concentration in the medium between KO (KO#175 (n=2); KO#345 (n=2); KO#377 (n=2)) and WT cells (MB49 (n=2); Ctrl#116 (n=2); Ctrl#376 (n=2))(Mann-Whitney test).

Discussion

The aim of this study was to build a murine tumor model allowing to assess the role of gal-9 in host-tumor relationships in the context of immunocompetent syngenic animals. Our approach was based on the production of MB49 isogenic clones with or without gal-9 expression. These clones were generated by the CRISP-Cas9 method of gene editing. One major advantage of this approach was to guaranty that the silencing of the gal-9 gene would be irreversible. One disadvantage was the possibility of off-target genetic lesions that could randomly affect the phenotype of edited clones in a way which had nothing to do with gal-9 biology. Another source of heterogeneity was the cloning step taking place after transfection of the editing material. In order to minimize the influence of unwanted heterogeneity we have compared the gal-9-KO clones with control clones subjected to the same editing process but having retained gal-9 expression. They were used in addition to the parental MB49 cells through the whole study. No differences in terms of tumor growth were apparent when gal-9-KO or WT-Ctrl cells were injected subcutaneously. However serial transplantations of tumor fragments unmasked a completely different pattern of growth for gal-9-KO and Ctrl-cells. Gal-9-KO tumors were affected by a progressive inhibition of tumor growth resulting in minute, “exhausted” tumors at passage 3 or 4. This reduction of tumor growth was dependent on the immune response and involved T-cells since it was not observed when the serial transplantation was made in nude mice.

Our investigations based on IHC, RNAseq and cytokine profiling have confirmed the progressive enhancement of the immune response through 2 or 3 cycles of tumor growth. T-cell infiltration in the tumor nodules was only detected in terminal “exhausted” tumors. However, this change of histological pattern concomitant of growth termination was preceded by transcriptional changes in the micro-environment of “pre-terminal” tumors i.e. tumors taken at the last cycle of growth prior to the exhaustion. A fraction of these changes was highly suggestive of the emergence of an immune response. Enrichment analysis of genes differentially expressed between pre-terminal KO and WT tumors have highlighted three main processes related to the immune response: cell response to γ-interferon, allograft rejection and inflammatory response. In this context, the CCL5 gene presents two remarkable characteristics: 1) it is much more abundant in pre-terminal KO than WT tumors (fold-change); 2) it stands at the intersection of the three sets of genes highlighted by the enrichment analysis. Profiling of the T-cell repertoire by deep sequencing unveils specific events in host-tumor interactions which take place in KO-tumors upstream of pre-terminal tumors as early as the second cycle of tumor growth. Indeed, already at this stage, the repertoire of T-cell clonotypes is more diverse for gal-9-KO tumors. Thanks to our data obtained by IHC; we know that at this stage, the overwhelming majority of T-cells are contained in perinodular margins. Therefore our observations on the T-cell repertoire suggest a mobilization of T-cells in these margins taking place before nodular invasion.

Overall our data show that for tumors derived from KO-gal-9 clones, the deployment of the immune response leading to tumor growth arrest requires 2 simultaneous conditions: 1) serial transplantation for 2 or 3 cycles of tumor growth and 2) absence of gal-9 produced by tumor cells. We now have to discuss by which mechanisms these two conditions are suspected to contribute to the anti-tumor immune response.

Serial transplantations are common in experimental hematology and onco-hematology, especially in studies dealing with stem cells. In contrast, to our knowledge, this method has not been previously reported for solid tumors. It was introduced in our protocol partly by chance while we were seeking better conditions of tumor growth which were achieved by transplantation of tumor fragments instead of cells expanded *in vitro*. Then, we realized that serial transplantation was the

only assay available so far to unmask the greater vulnerability of gal-9-KO tumors to the immune response. On the side of malignant cells, it is difficult to consider a type of immuno-editing that would result in the selection of cells with greater sensitivity to the immune response. In fact, it would be the contradiction of the concept of immuno-editing. On the other hand, tumor fragments used for serial transplantation are the only possible "vectors" going from one mouse to another with the capacity to increase the efficiency of the immune response. Since transplanted tumor fragments contain infiltrating leucocytes, their implantation in the recipient mice may result in the adoptive transfer of immune cells which may facilitate and accelerate the onset of the recipient immune response. This effect might be enhanced by the preparation of the transplanted tumor fragments which are minced and therefore subjected to mechanical aggressions which may enhance their immunogenicity. Investigating the role of immune cells contained in tumor fragments and passively transferred from one mouse to another is conceivable but obviously it would be another project.

Regarding the contribution of gal-9 ablation to the enhancement of the immune response, as mentioned previously, transcriptional studies have drawn our attention to a better tumor response to γ-interferon. This was confirmed by additional investigations focused on cytokines. Cytokine profiling on tumor protein extracts showed a substantial increase in the expression of IL-1 α and β, IL-2, TNFα, CXCL9 and CXCL10 in pre-terminal gal-9-KO tumors by comparison with WT and aggressive gal-9-KO tumors. In addition, going back to the transcriptional level, we found remarkable correlations between the abundance of interferon-γ transcripts and those of the above-mentioned cytokines including CXCL9 and CXL10. Finally we obtained direct evidence of the influence of gal-9 expression on tumor cell response to γ-interferon by *in vitro* comparative stimulation of gal-9-KO and WT MB49 clones. All these cell types respond to recombinant γ-interferon by a *de novo*, dose-dependent release of CXCL10. However, this release is much more abundant for gal-9-clones than for WT-Ctrl clones or parental cells. As of today we do not know how the presence of gal-9 alters the response of malignant epithelial cells their stimulation by γ-interferon. In human B-cells, gal-9 has been shown to inhibit BCR signaling by nanoclustering of these receptors at the surface of the plasma membrane and their close association with CD22 which contribute to this inhibition (Cao et al., 2018). The impact of galectin-9 produced by MB49 cells on the status of the γ-interferon receptors at the surface of their plasma membrane is currently under investigation. Even without precise knowledge about the mechanism of gal-9 inhibition of γ-interferon signaling, it is worth to place this observation in the broader context of the relationships between gal-9 and γ-interferon. Indeed γ-interferon has long been known to be a major inducer of gal-9 expression in epithelial and endothelial cells(Zhu et al., 2005). If we combine these published data with our current results we end up with the model summaried in the cartoon of Figure 9. In the absence of gal-9, we have an amplification loop where CD4+Th1+ Y-cell release γ-interferon which in turns stimulates CXCL10 release by target epithelial cells leading to greater attraction of T-cells. In contrast, if gal-9 is produced it will restrain the sensitivity of epithelial cells to γ-interferon and exert a negative feed–back on the amplification loop. One implication of this model is that we have in fact 2 types of negative feed-backs exerted by gal-9 on the CD4+Th1+ response. One which has long been described and which is cell-dependent resulting from the contact of extra-cellular gal-9 with CD4+Th1+ cells triggering their apoptosis and one which is cell-autonomous resulting from changes occurring directly in non-immune cells producing gal-9 (Zhu et al., 2005). One point that will need to be elucidated in our model is whether or not gal-9 has to be released in the extra-cellular medium to inhibit γ-interferon signaling in non-immune cells.

Finally our data showing that gal-9 from malignant cells impairs the anti-tumor immune response seems to contradict reports of a better prognosis for human malignancies – especially

breast carcinomas – with abundant expression of gal-9; an effect possibly related to a lower metastatic potential (Irie, 2005). To solve this paradox, one has to keep in mind that some biomolecules can have both pro- and anti-tumoral effects. For example they may limit the metastatic potential but at the cost of some immunosuppressive effects.

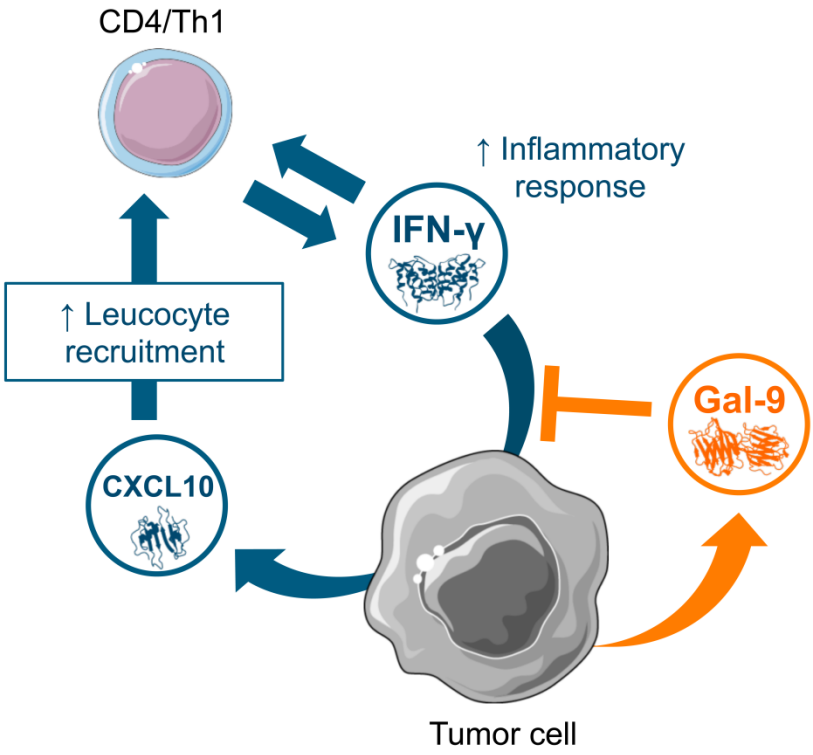

Figure 9. A proposed model of a negative feed-back of endogenous gal-9 on the amplification loop involving interferon-γ and CXCL10. interferon-γ released by activated T-cells stimulates the production of CXCL10 by malignant cells and simultaneously their expression of gal-9. In turn, CXCL10 stimulates T-cell infiltration, therefore boosting the anti-tumor immune response. However, the expression of gal-9 by malignant cells reduces their sensitivity to interferon-γ therefore blocking the amplification loop and compromising the anti-tumor immune response.

References

Cao, A., Alluqmani, N., Buhari, F.H.M., Wasim, L., Smith, L.K., Quaile, A.T., Shannon, M., Hakim, Z., Furmli, H., Owen, D.M., Savchenko, A., Treanor, B., 2018. Galectin-9 binds IgM-BCR to regulate B cell signaling. Nat Commun 9, 3288. https://doi.org/10.1038/s41467-018-05771-8

Daley, D., Mani, V.R., Mohan, N., Akkad, N., Ochi, A., Heindel, D.W., Lee, K.B., Zambirinis, C.P., Pandian, G.S.B., Savadkar, S., Torres-Hernandez, A., Nayak, S., Wang, D., Hundeyin, M., Diskin, B., Aykut, B., Werba, G., Barilla, R.M., Rodriguez, R., Chang, S., Gardner, L., Mahal, L.K., Ueberheide, B., Miller, G., 2017. Dectin 1 activation on macrophages by galectin 9 promotes pancreatic carcinoma and peritumoral immune tolerance. Nat Med 23, 556–567. https://doi.org/10.1038/nm.4314

Daley, D., Zambirinis, C.P., Seifert, L., Akkad, N., Mohan, N., Werba, G., Barilla, R., Torres-Hernandez, A., Hundeyin, M., Mani, V.R.K., Avanzi, A., Tippens, D., Narayanan, R., Jang, J.-E., Newman, E., Pillarisetty, V.G., Dustin, M.L., Bar-Sagi, D., Hajdu, C., Miller, G., 2016. γδ T Cells Support Pancreatic Oncogenesis by Restraining αβ T Cell Activation. Cell 166, 1485-1499.e15. https://doi.org/10.1016/j.cell.2016.07.046

Dardalhon, V., Anderson, A.C., Karman, J., Apetoh, L., Chandwaskar, R., Lee, D.H., Cornejo, M., Nishi, N., Yamauchi, A., Quintana, F.J., Sobel, R.A., Hirashima, M., Kuchroo, V.K., 2010. Tim-3/Galectin-9 Pathway: Regulation of Th1 Immunity through Promotion of CD11b $^{+}$ Ly-6G $^{+}$ Myeloid Cells. J.I. 185, 1383–1392. https://doi.org/10.4049/jimmunol.0903275

El Behi, M., Krumeich, S., Lodillinsky, C., Kamoun, A., Tibaldi, L., Sugano, G., De Reynies, A., Chapeaublanc, E., Laplanche, A., Lebret, T., Allory, Y., Radvanyi, F., Lantz, O., Eiján, A.M., Bernard-Pierrot, I., Théry, C., 2013. An essential role for decorin in bladder cancer invasiveness. EMBO Mol Med 5, 1835–1851. https://doi.org/10.1002/emmm.201302655

Enninga, E.A.L., Chatzopoulos, K., Butterfield, J.T., Sutor, S.L., Leontovich, A.A., Nevala, W.K., Flotte, T.J., Markovic, S.N., 2018. CD206-positive myeloid cells bind galectin-9 and promote a tumor-supportive microenvironment: Galectin-9/CD206 binding. J. Pathol. 245, 468–477. https://doi.org/10.1002/path.5093

Enninga, E.A.L., Nevala, W.K., Holtan, S.G., Leontovich, A.A., Markovic, S.N., 2016. Galectin-9 modulates immunity by promoting Th2/M2 differentiation and impacts survival in patients with metastatic melanoma: Melanoma Research 26, 429–441. https://doi.org/10.1097/CMR.0000000000000281

Fu, H., Liu, Y., Xu, L., Liu, W., Fu, Q., Liu, H., Zhang, W., Xu, J., 2015. Galectin-9 predicts postoperative recurrence and survival of patients with clear-cell renal cell carcinoma. Tumor Biol. 36, 5791–5799. https://doi.org/10.1007/s13277-015-3248-y

Golden-Mason, L., McMahan, R.H., Strong, M., Reisdorph, R., Mahaffey, S., Palmer, B.E., Cheng, L., Kulesza, C., Hirashima, M., Niki, T., Rosen, H.R., 2013. Galectin-9 Functionally Impairs Natural Killer Cells in Humans and Mice. Journal of Virology 87, 4835–4845. https://doi.org/10.1128/JVI.01085-12

Gonçalves Silva, I., Yasinska, I.M., Sakhnevych, S.S., Fiedler, W., Wellbrock, J., Bardelli, M., Varani, L., Hussain, R., Siligardi, G., Ceccone, G., Berger, S.M., Ushkaryov, Y.A., Gibbs, B.F., Fasler-Kan, E., Sumbayev, V.V., 2017. The Tim-3-galectin-9 Secretory Pathway is Involved in the Immune Escape of Human Acute Myeloid Leukemia Cells. EBioMedicine 22, 44–57. https://doi.org/10.1016/j.ebiom.2017.07.018

Haeussler, M., Schönig, K., Eckert, H., Eschstruth, A., Mianné, J., Renaud, J.-B., Schneider-Maunoury, S., Shkumatava, A., Teboul, L., Kent, J., Joly, J.-S., Concordet, J.-P., 2016. Evaluation of off-target and on-target scoring algorithms and integration into the guide RNA selection tool CRISPOR. Genome Biol 17, 148. https://doi.org/10.1186/s13059-016-1012-2

Irie, A., 2005. Galectin-9 as a Prognostic Factor with Antimetastatic Potential in Breast Cancer. Clinical Cancer Research 11, 2962–2968. https://doi.org/10.1158/1078-0432.CCR-04-0861

Johannes, L., Jacob, R., Leffler, H., 2018. Galectins at a glance. J. Cell. Sci. 131. https://doi.org/10.1242/jcs.208884

John, S., Mishra, R., 2016. Galectin-9: From cell biology to complex disease dynamics. J. Biosci. 41, 507–534. https://doi.org/10.1007/s12038-016-9616-y

Klibi, J., Niki, T., Riedel, A., Pioche-Durieu, C., Souquere, S., Rubinstein, E., Le Moulec, S., Guigay, J., Hirashima, M., Guemira, F., Adhikary, D., Mautner, J., Busson, P., 2009. Blood diffusion and Th1-suppressive effects of galectin-9–containing exosomes released by Epstein-Barr virus–infected nasopharyngeal carcinoma cells. Blood 113, 1957–1966. https://doi.org/10.1182/blood-2008-02-142596

Love, M.I., Huber, W., Anders, S., 2014. Moderated estimation of fold change and dispersion for RNA-seq data with DESeq2. Genome Biol 15, 550. https://doi.org/10.1186/s13059-014-0550-8

Melchionda, F., Fry, T.J., Milliron, M.J., McKirdy, M.A., Tagaya, Y., Mackall, C.L., 2005. Adjuvant IL-7 or IL-15 overcomes immunodominance and improves survival of the CD8+ memory cell pool. J. Clin. Invest. 115, 1177–1187. https://doi.org/10.1172/JCI23134

Oomizu, S., Arikawa, T., Niki, T., Kadowaki, T., Ueno, M., Nishi, N., Yamauchi, A., Hattori, T., Masaki, T., Hirashima, M., 2012a. Cell Surface Galectin-9 Expressing Th Cells Regulate Th17 and Foxp3+ Treg Development by Galectin-9 Secretion. PLoS ONE 7, e48574. https://doi.org/10.1371/journal.pone.0048574

Oomizu, S., Arikawa, T., Niki, T., Kadowaki, T., Ueno, M., Nishi, N., Yamauchi, A., Hirashima, M., 2012b. Galectin-9 suppresses Th17 cell development in an IL-2-dependent but Tim-3-independent manner. Clin. Immunol. 143, 51–58. https://doi.org/10.1016/j.clim.2012.01.004

Perez-Diez, A., Joncker, N.T., Choi, K., Chan, W.F.N., Anderson, C.C., Lantz, O., Matzinger, P., 2007. CD4 cells can be more efficient at tumor rejection than CD8 cells. Blood 109, 5346–5354. https://doi.org/10.1182/blood-2006-10-051318

Risso, D., Ngai, J., Speed, T.P., Dudoit, S., 2014. Normalization of RNA-seq data using factor analysis of control genes or samples. Nat Biotechnol 32, 896–902. https://doi.org/10.1038/nbt.2931

Tavares, L.B., Silva-Filho, A.F., Martins, M.R., Vilar, K.M., Pitta, M.G.R., Rêgo, M.J.B.M., 2018. Patients With Pancreatic Ductal Adenocarcinoma Have High Serum Galectin-9 Levels: A Sweet Molecule to Keep an Eye On. Pancreas 47, e59–e60. https://doi.org/10.1097/MPA.0000000000001126

Wu, C., Thalhamer, T., Franca, R.F., Xiao, S., Wang, C., Hotta, C., Zhu, C., Hirashima, M., Anderson, A.C., Kuchroo, V.K., 2014. Galectin-9-CD44 Interaction Enhances Stability and Function of Adaptive Regulatory T Cells. Immunity 41, 270–282. https://doi.org/10.1016/j.immuni.2014.06.011

Yu, G., Wang, L.-G., Han, Y., He, Q.-Y., 2012. clusterProfiler: an R Package for Comparing Biological Themes Among Gene Clusters. OMICS: A Journal of Integrative Biology 16, 284–287. https://doi.org/10.1089/omi.2011.0118

Zhou, Q., Munger, M.E., Veenstra, R.G., Weigel, B.J., Hirashima, M., Munn, D.H., Murphy, W.J., Azuma, M., Anderson, A.C., Kuchroo, V.K., Blazar, B.R., 2011. Coexpression of Tim-3 and PD-1 identifies a CD8+ T-cell exhaustion phenotype in mice with disseminated acute myelogenous leukemia. Blood 117, 4501–4510. https://doi.org/10.1182/blood-2010-10-310425

Zhu, C., Anderson, A.C., Schubart, A., Xiong, H., Imitola, J., Khoury, S.J., Zheng, X.X., Strom, T.B., Kuchroo, V.K., 2005. The Tim-3 ligand galectin-9 negatively regulates T helper type 1 immunity. Nat Immunol 6, 1245–1252. https://doi.org/10.1038/ni1271

Guide 1	Guide 2
3:intergenic:Rnf168-Ubxn7	2:exon:Slc38a10
4:intron:Ahcyl2	4:intergenic:Fam173b-Tas2r119
3:exon:Timm17b	4:intergenic:Sec16b-Brinp2
3:intergenic:Ly96-Gm5828	4:intergenic:Gm10398-Gm26660
4:intergenic:Gm23274-Gm26901	3:intergenic:Cdh10-Gm25976
4:intergenic:Gm3867-Gm7257	4:intergenic:Gm7361-4930584F24Rik
4:intron:Dach1	4:intergenic:Mthfsd-Foxc2
4:intergenic:Gm22544-Gm22509	4:intergenic:Trpc6-Pgr
4:exon:Tmem67	4:intron:Kazn
4:intron:Banf2	4:intergenic:4933428C19Rik-Gm12391
4:intron:Zfp457	4:intergenic:Gm23905-Zfp36l2
4:intergenic:Gm10247-Grin2a	4:intergenic:S100z-F2rl1
4:intergenic:ZFP953	4:intergenic:Gm23406-Mis18a
4:intergenic:A330102I10Rik-Gm11363	4:intergenic:Gm25608-Pgm1
4:intergenic:Gm20918-Gm21820	4:intron:Cacna2d2
4:exon:Mavs	4:intergenic:Gm22016-Cdc73
4:intergenic:Gm23558-Galc	4:intron:Gm5155
4:intron:Mast4	4:intron:Gsg1l
4:intergenic:Rgs17-Gm10945	4:intergenic:Gm7452-1700111E14Rik
4:intron:Dst	4:intergenic:Nptx2-Gm6272
4:intergenic:Tmem108-Nphp3	4:exon:Snai3
4:intron:Dock8	4:intergenic:Kif26a-A730018C14Rik
4:intron:Col22a1	4:intergenic:Gm26674/Sash1-Gm9930
4:intergenic:Six2-Srbd1	4:intron:Car5a
4:intergenic:Dusp10-Gm23349	4:intron:Lpcat1
4:intergenic:Pkp1-Igfn1	4:exon:Nsd1
4:intergenic:Gm11468-Gm14268	4:exon:Arhgdia
4:intergenic:Prkaa2-Ppap2b	4:intron:Susd1
4:intron:Plekha7	4:intergenic:Gm13605-Gsn
4:intron:Mad1l1	4:intergenic:Fopnl-Abcc1
4:intergenic:Maf/Gm15655-Dynlrb2	4:intergenic:Gm5415-Gm24732
4:intron:Tspan32	4:intergenic:Gm20711-Pbx1
4:intergenic:1810011O10Rik/Gm26714-Ido2	4:intergenic:Carns1-Tbc1d10c
4:intergenic:Impg1-RP24-325L16.1	3:intergenic:2610028E06Rik-Csf3r
4:intron:Fam172a	3:intergenic:Gm26216-Trerf1
4:exon:Pard3	4:intron:Ccbl2
	4:intron:9030624J02Rik
	4:intergenic:Tex14-Gm11492
	4:intergenic:4931417E11Rik-Gm26179
	4:intergenic:A930003A15Rik/AC164558.1-Klhl6
	4:intergenic:Gm16202-Ube2cbp
	4:intergenic:Mitf-Gm765
	4:intron:Pex14
	4:exon:Colgalt2
	4:intergenic:Gm22132-Nr5a2
	4:intron:Filip1l
	3:intergenic:Rbfox1-Gm23476
	4:intron:Dpp10
	4:intron:Tns3
	4:intron:Ppard
	4:intergenic:Ntm-Gm26435
	3:intergenic:Gm25830-4930555F03Rik
	4:intergenic:Top1mt-Rhpn1
	4:intergenic:Hcfc1-Gm8545
	4:intron:Dcdc2a
	4:intron:Tenm3
	3:intron:Orc6
	4:intron:Sh3pxd2a
	4:intron:Wdtc1
	4:intron:Ift122
	4:intergenic:Gm12718-Gm23064
	4:intergenic:Gm9855-Foxo3

Supplementary Table 1. Potential off-targets of each guide used in our genome editing procedure were predicted using the CRISPOR web tool applied on the mm10 mouse genome. The number preceding the name of each genome locus indicates the number of missmatches required for complete alignment of the guide sequence. For both guides, none of the predicted target sites shows a perfect match.

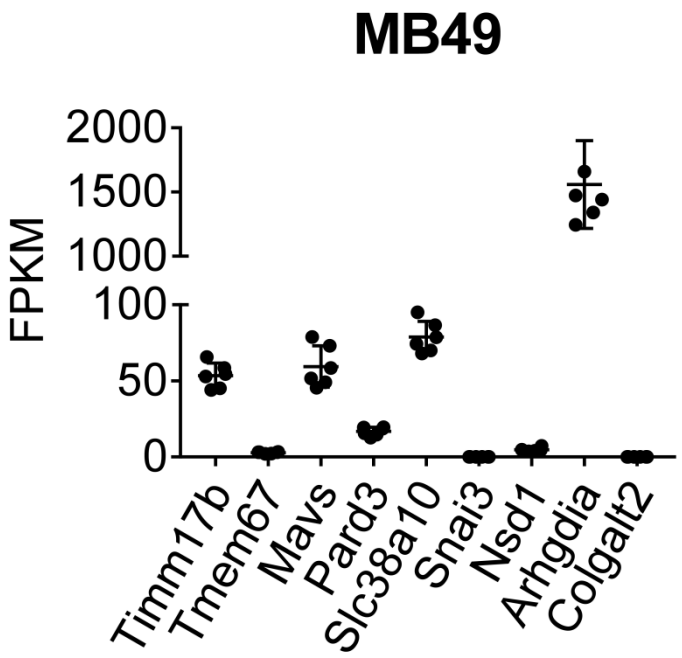

Supplementary figure 1. A total of 9 exons (4 for the guide 1 and 5 for the guide 2) were identified as potential off-targets. The abundance of the corresponding transcripts reflected by FPKM (fragments per kilobase of exon per million reads mapped) values were checked in the RNAseq data obtained from MB49 and its derived clones (either gal-9-KO or WT-Ctrl) grown *in vitro.* No difference was detected for any of these transcripts between parental cells and clones subjected to the CRISPR procedure.

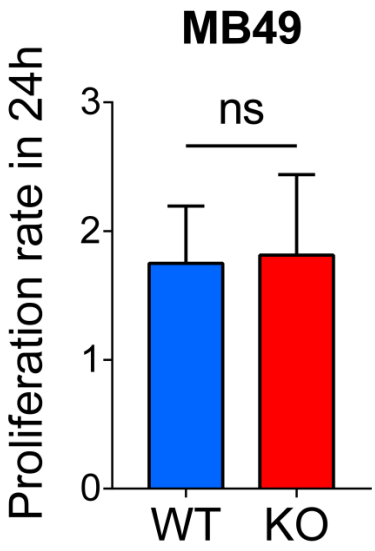

Supplementary figure 2. *In vitro* growth assays were carried out on parental MB49 and its derived clones (either gal-9-KO or WT-Ctrl). The assays were performed using an ATP luminescence assay (ATPlite, Perkin Elmer). No differences in growth rate were recorded *in vitro* between WT and KO cells. MB49 cells had doubling time of about 24h.

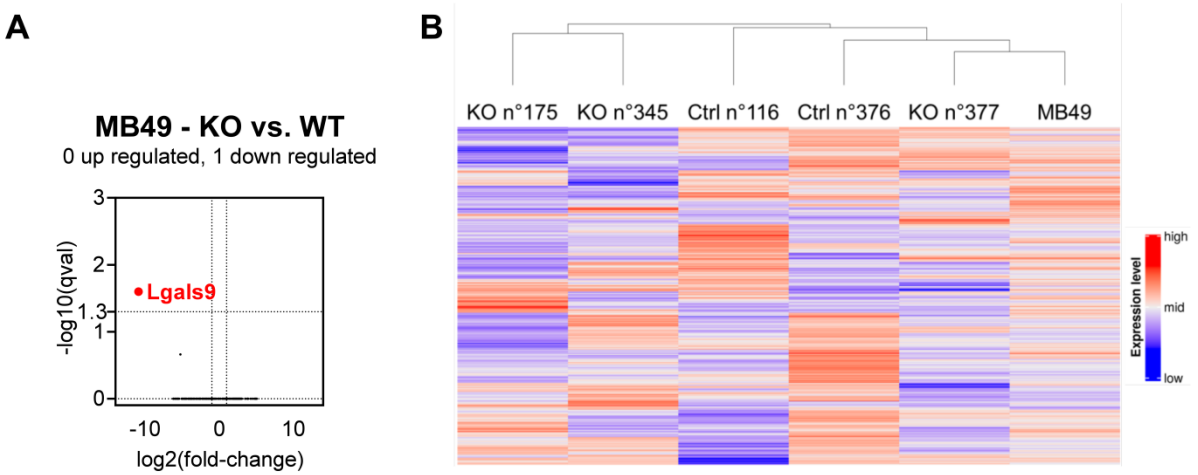

Supplementary figure 3. *In vitro* transcriptional profiles of isogenic cells derived the MB49 cell line (parental, WT-Ctrl and gal-9-KO). For each cell line, the RNAseq analysis was performed on RNAs extracted from cells propagated *in vitro* including the parental cells, 2 WT-Ctrl clones and 3 gal-9-KO clones. (A) The volcano plots intend to represent genes differentially expressed when comparing gal-9-KO cells on the one hand with parental and WT-Ctrl cells on the other hand. They are virtually absent, except *lgals9.* (B) Results of the non-supervised hierarchical clustering are consistent with data from the volcano plots since there is no separation of the transcription profiles of the gal-9-KO cells. Potential weak differences related to gal-9 invalidation seem to be outweighed by random clonal differences.

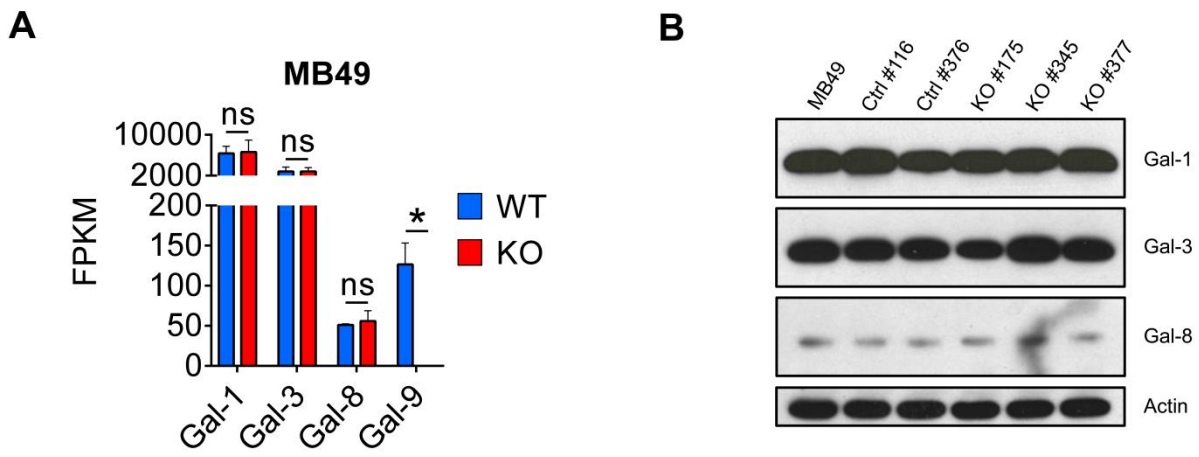

Supplementary figure 4. Comparative assessment of galectin-1, -3 and -8 transcription and protein expression in WT and gal-9-KO cells. (A) Abundance of galectin transcripts recorded by RNA-seq in parental MB49 and its derived clones. In blue, WT, parental or control clones. In red, gal-9-KO clones. (B) WB analysis were performed on the same cellular materials. All cells express galectins -1, -3, and -8 with the first two being the most abundant. The gal-9 invalidation has no impact on the expression of other galectins at both the transcriptional and the protein level.

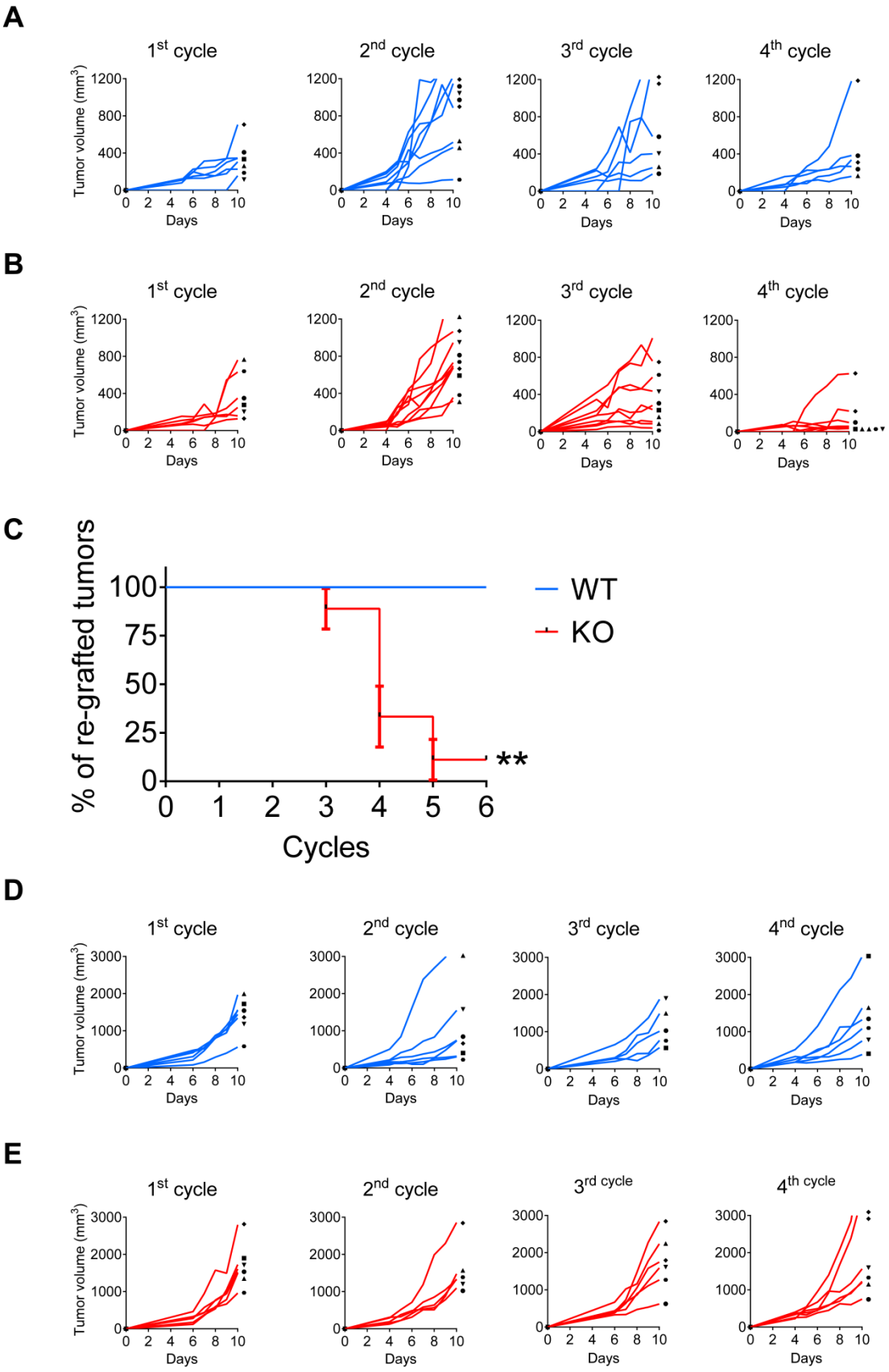
A
1st cycle
2nd cycle
3rd cycle
4th cycle
Tumor volume (mm3)
Days
B
C
% of re-grafted tumors
Cycles
WT
KO
**
D
4nd cycle
E

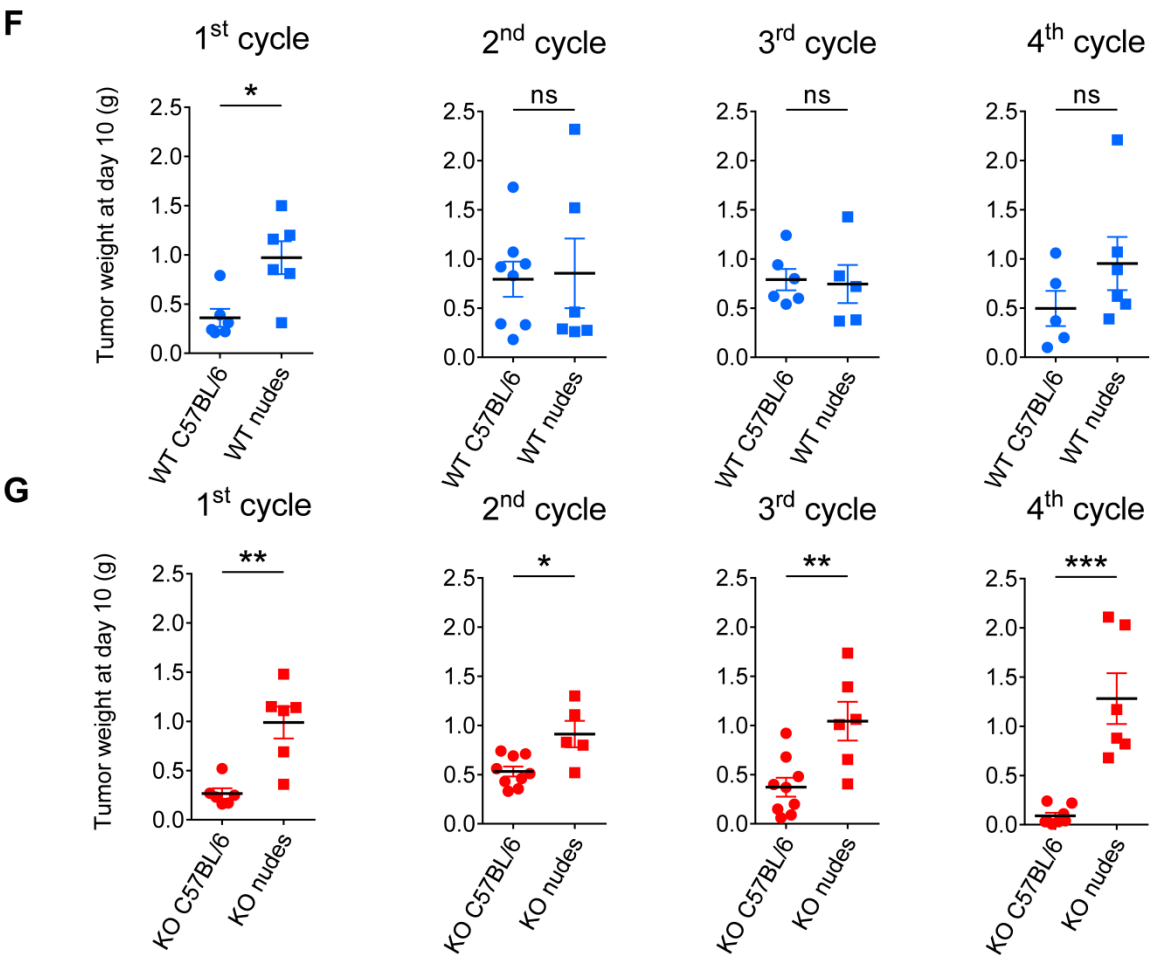

Supplementary figure 5. (A) Growth curves for single WT tumors grafted on C57BL/6 mice are shown in blue. At the beginning of the experiment, each cell type - MB49 cells and WT-Ctrl clones - was injected subcutaneously into two mice (MB49: ▲,▼; WT-Ctrl #116: ■, ◆; #376: ●, ⬣). For the subsequent cycles of tumor growth, each tumor was passaged on a single mouse. For a given tumor « lineage », the same symbol is used through the 4 cycles of tumor growth (B) Growth curves for KO tumors on C57BL/6 mice are shown in red (gal-9-KO clone #175: ▲,▼; #345: ■, ◆; #377: ●, ⬣). Again, for a given tumor « lineage », the same symbol is used through the 4 cycles. (C) From cycle 3, the growth of some KO tumors was not sufficient in the interval of 10 days to allow their subsequent passage on another mouse for an additional cycle of tumor growth (< 70mg). The consequence was the termination of this tumor « lineage ». To give a quantitative assessment of this aspect of tumor growth reduction, the survival of WT and KO tumor « lineages » are represented on a Kaplan-Meier plot (with blue and red color respectively). We observe that after 5 cycles of tumor growth, all WT tumor « lineages » are still active in contrast with only one for the KO tumors. (D and E) Growth curves for single WT (blue) and KO (red) tumors grafted into nude mice with the same mode of representation as for C57BL/6. (F) and (G) Comparative assessment of tumor weights at the termination of each cycle of tumor growth for WT (F) or KO (G) tumors grafted either into syngenic or nude mice. In the case of WT tumors, there were no significant differences at cycle 2, 3 and 4. Regarding gal-9-KO tumors, the average tumor mass is consistently greater on the nude mice.

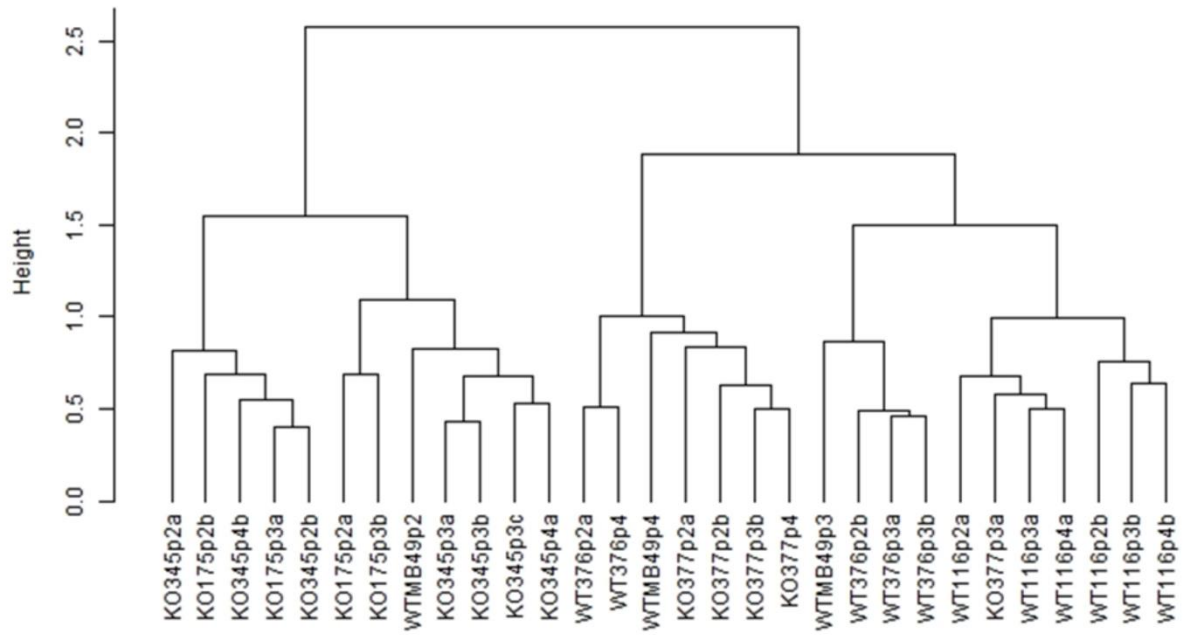

Supplementary figure 6. Unsupervised RNAseq analysis of WT and KO tumors at different cycles of tumor growth. Dendrogram using centered correlation and ward linkage.

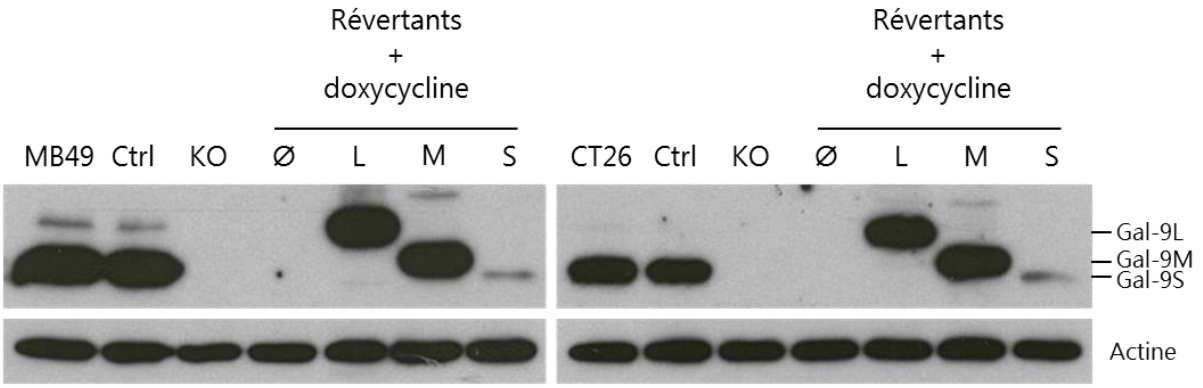

Figure 18. Essais d'expression des différentes isoformes de la gal-9 dans les « révertants », *in vitro*.

Après vérification de l'absence d'expression des isoformes par les « révertants » dans les cellules non traitées, nous avons cultivé ces cellules en présence de doxycyline à 400 ng/mL pendant 48h. L'analyse en western-blot confirme l'absence d'expression de gal-9 dans les clones ayant été transfectés avec le vecteur vide. Elle confirme également l'expression des différentes isoformes en réponse au traitement par la doxycycline. Quelle que soit la lignée, on remarque cependant que la quantité de gal-9S dans les extraits cellulaires est toujours moins élevée que celle des 2 autres isoformes. La séquence du transgène ne diffère pourtant qu'au niveau de la séquence qui code pour le peptide de liaison, et qui est plus courte pour la gal-9S. Ces résultats soulèvent l'hypothèse d'une sécrétion beaucoup plus intense de la gal-9S.

DISCUSSION GENERALE ET PERSPECTIVES

Au cours de ma thèse, je me suis intéressé à la contribution de la gal-9 dans la tumorigenèse, et notamment à l'impact d'une diminution de son expression et/ou présence au niveau tumoral. Mes travaux de recherche se sont axés autour de deux approches : l'invalidation du gène codant pour la gal-9 dans des lignées tumorales et l'utilisation d'anticorps neutralisant.

I- Discussion en rapport avec les objectifs 1 et 2

Mon premier objectif était de sélectionner des lignées tumorales murines sur la base de leur niveau d'expression de gal-9 afin de réaliser d'une part une invalidation du gène *LGALS9* sur celles-ci, et d'autre part afin d'employer ces lignées pour la réalisation de l'objectif 3.

Par une approche d'analyse en *western-blot,* nous avons sélectionné les lignées CT26 et MB49 qui présentaient une expression de gal-9 plus importante que les autres lignées cellulaires testées. Nous avons ensuite élaboré et réalisé l'invalidation du gène *LGALS9* dans ces deux lignées. Nous avons sélectionné pour chacune d'entre-elles 3 clones KO ainsi que 2 clones Ctrl, ces derniers permettant d'apprécier l'influence de la sélection clonale et de prendre en compte d'éventuels effets *off-targets*. Dans le but d'identifier d'éventuelles différences fonctionnelles entre les isoformes L, M et S de la gal-9, nous avons également réalisé, à partir des différents clones KO générés, des « révertants » exprimant une seule des 3 isoformes (**Figure 18**).

Nous avons ensuite exploité ces outils afin de réaliser les tâches programmées dans l'objectif 2. Celui-ci comportait deux parties. La première avait pour but 1) d'évaluer *in vitro* les effets de la perte d'expression de gal-9 sur le phénotype des cellules tumorales : viabilité, prolifération, sensibilité à l'apoptose, clonogénicité, etc., et explorer les mécanismes sous-jacents à ces changements de phénotype, au niveau cellulaire et moléculaire. La deuxième partie portait sur 2) l'évaluation *in vivo*, sur souris syngéniques, des effets de la perte d'expression de la gal-9 sur le phénotype tumoral, notamment sur la cinétique de croissance et sur la nature de l'infiltrat lymphoïde et myéloïde.

A l'aide des outils générés, nous avons mis en évidence un effet pro-tumoral de la gal-9 dans la lignée MB49. En effet, bien que l'invalidation du gène *LGALS9* n'entraîne pas de modifications transcriptionnelles ou phénotypiques notables *in vitro*, elle entraîne en revanche une diminution progressive de la croissance tumorale après plusieurs transplantations itératives sur des souris syngéniques immunocompétentes. Cette observation ne se vérifie toutefois pas sur des souris nudes immunodéficientes, ce qui met en évidence l'implication d'une réponse immunitaire efficace dans ce phénomène de réduction de croissance tumorale. Les investigations que nous avons menées par IHC, RNAseq et profilage cytokinique suggèrent que l'amélioration de la réponse immunitaire, qui se manifeste après 2 ou 3 cycles de croissance tumorale, est multifactorielle. Tout d'abord l'analyse du répertoire des chaînes β du TCR met en évidence un enrichissement plus important de la diversité des chaînes des lymphocytes présents dans les tumeurs KO. Ensuite, le profilage des cytokines montre une augmentation substantielle de l'expression d'IL-1α, IL-1β, IL-2, IL-9 et TNF-α dans les tumeurs KO « pré-terminales ». Conjointement à ce phénomène, on observe en IHC une augmentation de l'infiltration des leucocytes dans le compartiment épithélial des tumeurs KO. L'analyse RNAseq révèle un impact de la perte d'expression de gal-9 sur la réponse à l'IFN-γ. De manière cohérente avec les résultats obtenus, nous avons pu vérifier *in vitro* que les cellules WT expriment moins de CXCL10 en réponse à l'IFN-γ que les cellules KO-gal-9. Ces différences pourraient expliquer le plus grand recrutement leucocytaire dans les tumeurs KO-gal-9 ainsi que l'amplification de la réponse immunitaire anti-tumorale.

Les résultats de notre étude (cf. article 2) soulèvent plusieurs interrogations qui vont maintenant être discutées. Certaines sont en lien direct avec les résultats obtenus, et d'autres en lien avec l'exploitation des autres outils que nous avons générés, notamment les clones dérivés de la lignée CT26.

Les expériences en cours actuellement ont deux objectifs principaux :

Le premier objectif consiste à vérifier que l'action inhibitrice de la gal-9 sur la signalétique induite par l'IFN-γ peut se vérifier vis-à-vis d'autres molécules exprimées en réponse à l'IFN-γ (ex : PD-L1, CMH II, …). Nous aimerions également vérifier si l'IFN-γ est capable d'induire

l'expression de gal-9 par les cellules tumorales MB49, comme cela a déjà été démontré pour d'autres types cellulaires, ce qui permettrait d'amplifier le phénomène d'inhibition. L'analyse porte sur l'ARN des cellules WT et KO-gal-9 traitées par l'IFN-γ *in vitro*.

Le deuxième objectif consiste à identifier l'implication de la gal-9 extra-cellulaire dans l'inhibition de la signalisation induite par l'IFN-γ. Les expériences en cours visent à étudier l'effet de l'ajout de gal-9 exogène de manière concomitante au traitement par l'IFN-γ.

Le troisième objectif porte sur la réalisation d'une étude corrélative *in silico* chez l'homme afin de savoir s'il existe un lien entre une forte expression de gal-9 et un faible niveau de réponse à l'IFN-γ chez les patients.

Enfin, le quatrième objectif vise à vérifier la transposition du phénomène à d'autres types cellulaires. Pour ce faire nous allons réaliser le même type d'expérience sur une autre lignée tumorale murine invalidée pour la gal-9, la lignée CT26. Nous avons également initié l'élevage de souris KO-gal-9 afin de pouvoir étendre l'étude à d'autres types cellulaires (fibroblastes, macrophages, …).

Réalisation de transplantations itératives et suivi de la croissance tumorale

La réalisation de transplantations itératives est fréquemment rencontrée dans le domaine de l'hématologie et notamment dans les études qui touchent aux cellules souches. Ce procédé est basé, comme son nom l'indique, sur la transplantation de cellules d'un organisme à un autre. Dans les études qui portent sur les cellules souches hématopoïétiques, ces transplantations présentent plusieurs avantages puisqu'elles peuvent permettre d'amplifier ces cellules tout en maintenant leur état indifférencié.

En revanche, dans le domaine d'étude des tumeurs solides, ce procédé n'est pas répandu. On génère généralement une tumeur à partir de cellules tumorales injectées ou de fragments greffés, et le suivi de la croissance tumorale est réalisé à partir du jour de l'inoculation jusqu'à l'arrêt de l'expérience sur l'animal. Dans le cas de notre expérience, la mise en place d'un protocole de transplantations itératives d'une tumeur solide découle en réalité de plusieurs difficultés expérimentales relatives aux modalités d'injection. En effet, l'injection des cellules MB49 de manière très superficielle entraîne assez rapidement une ulcération de la peau. D'un

autre côté, l'injection plus profonde entraîne, elle, un envahissement rapide des organes sous-jacents. Assez rapidement, la réalisation de greffes de fragments tumoraux sous la peau – au lieu de suspensions cellulaires – nous est apparue comme une bonne alternative pour réaliser facilement le suivi de la croissance des tumeurs. Etant sous la peau, on évite les ulcérations précoces et utilisant des fragments on évite la diffusion vers les organes sous-jacents. Ensuite, ayant adopté cette modalité de transplantation, c'est de manière en partie fortuite, en essayant de perfectionner nos protocoles, que nous avons constaté la diminution progressive de croissance des tumeurs KO par rapport aux tumeurs WT lors des cycles de transplantation successifs.

Avec le recul, cette modalité de suivi de la croissance tumorale présente, malgré sa singularité, un certain intérêt. En effet, contrairement à une approche conventionnelle, le fait de réaliser plusieurs cycles de croissance augmente artificiellement la durée du développement tumoral. Celui-ci devrait normalement s'arrêter précocement en raison du caractère très agressif de la tumeur qui atteint rapidement son seuil de volume éthique. A l'instar d'expériences réalisées sur les cellules souches hématopoïétiques qui visent, au travers de transplantations itératives, à simuler l'évolution de cette population cellulaire sur le long terme, la transplantation itérative des tumeurs MB49 offre peut-être un aperçu de ce que deviendrait la tumeur si son caractère agressif n'obligeait pas à sacrifier prématurément l'animal porteur.

En ce qui concerne maintenant la question de la nécessité de devoir attendre 2 voire 3 cycles de croissance en série pour mettre en avant la vulnérabilité des cellules KO-gal-9 à la réponse immunitaire, il est très difficile avec nos données actuelles d'aller au-delà des spéculations. Les fragments de tumeurs utilisés pour la transplantation en série sont les seuls « vecteurs » possibles pour expliquer la vulnérabilité croissante des tumeurs KO-gal-9. Les modifications qui se produisent d'un cycle de croissance à l'autre pourraient concerner soit les cellules malignes, soit l'infiltrat. Concernant les cellules malignes, il faut envisager des processus d'adaptation à leur nouvel environnement *in vivo* relativement lents et héritables, ce qui fait penser à des modifications épigénétiques. Concernant les leucocytes infiltrant contenus dans les fragments de tumeur transplantés, l'implantation de ces fragments chez la souris receveuse pourrait réaliser un transfert adoptif de cellules immunitaires, ce qui d'un cycle à l'autre pourrait faciliter et accélérer le démarrage de la réponse immunitaire du receveur. Cet

effet pourrait être renforcé par la préparation des fragments de tumeur transplantés qui sont découpés et donc soumis à des agressions mécaniques susceptibles de renforcer leur immunogénicité. On peut également envisager des modifications concernant d'autres cellules du micro-environnement tumoral, par exemple les fibroblastes.

Impact de la localisation de la gal-9 sur son caractère pro- vs. anti-tumoral

La gal-9 exerce des fonctions distinctes selon qu'elle se trouve dans le milieu intra- ou extra-cellulaire. Les données de la littérature s'accordent pour dire que les fonctions immunosuppressives que la gal-9 exerce dans le milieu extra-cellulaire sont associées au développement tumoral de plusieurs pathologies. Au contraire, les fonctions, encore peu connues, que la gal-9 exerce à l'intérieur de la cellule semblent prévenir l'évolution du cancer vers un développement métastatique. Il n'est pas impossible non plus que certaines caractéristiques des cellules ayant effectué une transition épithélio-mésenchymateuse, avec notamment une perte de jonctions cellulaires, puissent voir leur perméabilité augmentée vis-à-vis des cellules infiltrantes. De ce point de vue-là, il est donc important d'avoir en tête que la gal-9 intra-cellulaire pourrait avoir des effets à la fois pro- et anti- tumoraux.

Les données de l'article 2 ne permettent pas d'identifier si c'est la gal-9 sécrétée par les cellules tumorales et/ou celle qui est contenue à l'intérieur de celles-ci qui favorise la tumorigenèse des tumeurs MB49. Une manière simple de le savoir serait de démontrer l'absence de sécrétion de gal-9 par les cellules tumorales. En l'occurrence, des expériences réalisées *in vitro* nous ont montré que les cellules MB49 sécrètent de la gal-9. Même si aucun des outils de détection que nous avons utilisé ne nous permet d'affirmer que c'est également le cas *in vivo*, on peut légitimement le penser. C'est un point que nous espérons pouvoir vérifier.

Un élément de réflexion nouveau relatif à l'emploi des anticorps neutralisant sera présenté et discuté dans la partie relative à l'objectif 3.

Différences fonctionnelles des isoformes de la gal-9

Il existe plusieurs isoformes de la gal-9. Les plus connues sont au nombre de trois : gal-9L, gal-9M et gal-9S. Elles ne diffèrent d'un point de vue structurale que par la taille de leur peptide de liaison. En ce qui concerne leurs différences fonctionnelles, il semblerait que plus l'isoforme est petite et plus elle est active et stable. Des chercheurs ont d'ailleurs créé une isoforme artificielle totalement dépourvue de peptide de liaison afin d'exploiter ces propriétés. La recherche de possibles différences fonctionnelles entre ces isoformes représente un sujet d'étude encore largement inexploré pour lequel nous avons essayé d'apporter de nouveaux éléments de réflexion. Dans ce but, nous avons produit des « révertants » exprimant une seule des trois isoformes de la gal-9 sous le contrôle d'un promoteur inductible, à partir des clones KO que nous avions généré, et à l'aide de lentivirus.

La lignée MB49 exprime normalement les isoformes L et M. La surexpression de ces isoformes, ainsi que de l'isoforme S dans les « révertants », n'est pas associée à des différences phénotypiques notables *in vitro*. Nous avons tenté de réaliser des expériences in vivo à partir de ces « révertants » en suivant le même schéma expérimental que celui présenté dans l'article 2, mais en ajoutant ou non la doxycycline à l'alimentation des souris. Nous avons pu confirmer que cette dernière permet d'induire l'expression de nos transgènes dans les tumeurs. Malheureusement, nous n'avons pas pu poursuivre l'étude au-delà de 2 cycles de croissance. En effet, les souris traitées à la doxycycline présentent une décroissance tumorale même en présence du transgène codant pour la gal-9. Cela pourrait être dû à des effets non mesurés de la doxycycline. Nous pensons aussi que l'expression de la mCherry, également induite par la doxycycline, a pu impacter l'immunogénicité des cellules transduites.

Même si ces « révertants » ne semblent pas adaptés pour la poursuite d'analyses *in vivo*, ils pourront toutefois être employés dans plusieurs expériences *in vitro*. Il serait par exemple intéressant vérifier si une des isoformes altère préférentiellement le phénomène d'inhibition de la signalisation induite par l'IFN-γ. Nous nous intéressons également à de potentielles différences de localisation, dans la cellule, dépendantes de l'isoforme.

Transposition de l'étude au modèle CT26

Comme mentionné précédemment, l'invalidation du gène de la gal-9 a été réalisée sur deux lignées cellulaires : MB49 et CT26. Des études *in vitro* et *in vivo* ont également été réalisées sur cette deuxième lignée. Les résultats, différents de ceux obtenus pour MB49, ne font pas partie de l'article 2.

L'invalidation du gène *LGALS9* induit un changement notable des propriétés d'adhésion des cellules CT26 en culture. Celles-ci, normalement bien adhérentes et d'aspect fibroblastiques, prennent un aspect sphérique en l'absence de gal-9. Nous avons réalisé une analyse RNAseq sur ces cellules *in vitro*. Contrairement à l'étude portant sur MB49 et ses différents clones, ici les clones CT26 KO-gal-9 présentaient plusieurs gènes différentiellement exprimés par rapport à la lignée parentale et aux clones Ctrl. Plusieurs d'entre eux étaient associés à une transition épithélio-mésenchymateuse d'après une analyse Msig. Les expériences complémentaires que nous avons réalisées n'ont toutefois pas permis de mettre en évidence une augmentation des protéines SNAIL, SLUG, TWIST2 ou ZEB, qui aurait pu confirmer cette hypothèse. Il n'en reste pas moins que la perte de la gal-9 induit dans la lignée CT26 une perte d'adhésion au support de culture et augmente peut-être ainsi significativement leur mobilité. Ce dernier point sera à investiguer. Malgré ce phénotype, les cellules KO-gal-9 ne présentent pas de baisse de viabilité ou de potentiel prolifératif par rapport aux cellules WT.

Nous avons également réalisé des expériences de croissance *in vivo*, sur des souris syngéniques. Ni les expériences de suivi sur individu unique, ni les expériences de transplantations itératives n'ont permis d'observer de différences de vitesse de croissance entre les tumeurs CT26 WT et KO-gal-9. Cette différence avec la lignée MB49 est probablement liée à leur origine cellulaire distincte. Ainsi, on observe, dès l'étape de culture in vitro, des différences importantes en réponse à l'invalidation du gène entre ces deux lignées. On peut imaginer que ces différences se manifestent encore davantage au cours de la formation de la tumeur. On sait par exemple que les tumeurs CT26 se développent en formant une masse tumorale dense alors que les tumeurs MB49 ont tendance à former des structures polarisées avec des cellules de plus petite taille à la périphérie des nodules. Cela va parfois jusqu'à la formation de kystes liquidiens au centre des tumeurs. Etant conscient du rôle que peut jouer la gal-9 dans le maintien des interactions cellule-cellule et

potentiellement cellule-matrice, il est possible que ces différences d'architectures influencent la réponse à la perte d'expression de cette protéine. Enfin, il est également possible que la balance entre effets pro- et anti-tumoraux soient nulles dans les cellules CT26, et que l'invalidation de la gal-9 ne permette donc pas de mesurer de différences avec les cellules WT. Enfin, comme mentionné dans l'introduction, les souris C57BL/6, desquelles dérive la lignée MB49, et les souris BALB/c, desquelles dérive la lignée CT26, ne présentent pas le même profil immunologique. Ces différences pourraient également justifier l'absence d'effets observés.

II- Discussion en rapport avec l'objectif 3

La 3^{e} partie des résultats de ma thèse, se rattache au domaine de la recherche translationnelle. L'objectif de ces travaux consistait à caractériser deux anticorps monoclonaux anti-gal-9, GalNab-1 et GalNab-2, produits par l'équipe. Cette caractérisation comprenait un volet *in vitro* dans lequel je me suis investi. Il s'agissait pour moi d'effectuer des expériences de neutralisation des effets de la gal-9 sur des cellules en culture. En complément d'autres analyses, comme la caractérisation des épitopes cibles et le séquençage des régions variables, ces résultats ont fait l'objet d'une publication en 2018 (article 1). Le deuxième volet de ces travaux sur les anticorps anti-gal-9 avait pour but la mise en place d'un modèle murin permettant d'évaluer le potentiel thérapeutique anti-tumoral de ces anticorps *in vivo*. Ces études *in vivo* ne sont pas encore achevées. Les résultats obtenus jusqu'ici n'ont pas été rapportés dans la section résultats. Cependant, ils feront l'objet de quelques commentaires à la fin de ce chapitre.

Caractérisation des anticorps monoclonaux anti-gal-9 in vitro

Les résultats publiés dans notre article (Lhuillier et al., 2018 ; PlosOne) démontrent, entre autres, la capacité de ces anticorps à neutraliser efficacement l'apoptose des LT CD4^{+} humains déclenchée par l'addition de gal-9 exogène. Ils démontrent également leur capacité à neutraliser, au moins partiellement, l'effet de la gal-9 sur l'expansion de sous-populations productrices d'IFN-γ et d'Il-2. Bien qu'il reste encore à vérifier si leur action neutralisante

s'observe sur d'autres types cellulaires sensibles à la gal-9, comme les cellules NK ou les macrophages, ces anticorps semblent déjà apparaître comme candidats pour un possible développement thérapeutique.

Cette étude met également en exergue des différences fonctionnelles entre les deux anticorps. Ces différences se manifestent dans les expériences réalisées sur la lignée cellulaire Jurkat, une lignée de leucémie T humaine. GalNab-2 neutralise l'apoptose et la mobilisation calcique induite par la gal-9 dans les cellules Jurkat alors que GalNab-1 neutralise moins bien l'apoptose et augmente l'exposition des phosphatidylsérines et la mobilisation calcique induites par la gal-9. Les différences entre ces 2 anticorps se manifestent également dans les tests d'interactions. Dans ces expériences, bien que l'affinité de GalNab-1 et GalNab-2 pour la gal-9 soit similaire, le premier s'associe et se dissocie plus rapidement de la gal-9 que le second. Ces différences nous ont incités à privilégier l'emploi de l'anticorps GalNab-2 dans les études menées *in vivo*. Enfin, cet article met en évidence la capacité de ces anticorps, produits chez la souris à partir de gal-9 recombinante humaine, à reconnaître également la gal-9 murine. Cette caractéristique a rendu possible leur emploi dans des modèles d'études pré-cliniques dont nous allons maintenant discuter.

Quelques commentaires sur la caractérisation *in vivo* des anticorps anti-gal-9

Le choix des lignées tumorales murines testées pour l'évaluation pré-clinique des anticorps s'est porté sur des lignées exprimant un niveau important de gal-9. Nous nous sommes donc arrêtés sur les lignées CT26 (carcinome colique murin de fonds génétique BALB/c) et MB49 (carcinome vésical murin de fond génétique C57BL/6). Ces expériences ont été menées en collaboration étroite avec des compagnies de biotechnologie qui avaient pris en charge l'humanisation de ces anticorps, notamment Gal-Nab2. Ces compagnies ont souhaité que l'évaluation des anticorps sur les lignées tumorales murines soit réalisée avec la version humanisée de Gal-Nab2. Ce choix s'explique par le souhait d'une transition aussi rapide que possible vers l'application chez l'homme. Du point de vue de la qualité des expériences, il faut reconnaître que le choix d'utiliser des anticorps humanisés et non des anticorps murins chez la souris complique l'interprétation des résultats. En effet, on peut considérer qu'un anticorps humanisé agira moins efficacement chez la souris, notamment parce que les anticorps

humains n'interagissent pas efficacement avec les récepteurs Fc (fragments constants) murins. Nous devrons garder ces réserves à l'esprit en évoquant les résultats ci-dessous.

J'ai participé comme investigateur principal ou en collaboration à plusieurs essais de traitement systémique par des anticorps anti-Gal-9 pour des souris immunocompétentes greffées soit avec des tumeurs MB49 (C57BL/6) soit avec des tumeurs CT26 (BALB/c). Jusqu'à présent aucun effet anti-tumoral n'a été observé lors du traitement par ces anticorps, excepté un effet discret de ralentissement de la croissance tumorale pour CT26 lors du traitement par Gal-Nab2. Paradoxalement nous n'avons obtenu aucun effet sur les tumeurs MB49 même avec des traitements appliqués lors des passages en série alors que les tumeurs MB49 KO-gal-9 montrent un déficit de croissance au fil des passages. Réciproquement, nous avons obtenu un petit effet anti-tumoral avec des anticorps anti-gal-9 dans le modèle CT26 alors que l'invalidation de la gal-9 ne change pas la croissance de CT26 même lors des passages en série. Ces observations tendent à confirmer le fait que la gal-9 peut avoir des contributions différentes à la croissance tumorale suivant qu'elle est extra-cellulaire ou intra-cellulaire. Les anticorps injectés par voie systémique ne sont sensés agir que sur la gal-9 extracellulaire. Celle-ci joue peut-être un rôle plus important dans le modèle CT26 que dans le modèle MB49. Gardons cependant présent à l'esprit le fait que les conclusions sur les résultats obtenus dans MB49 sont hypothéquées par le fait que nous avons employé des anticorps humanisés et non des anticorps murins dans ce modèle.

Production de nouveaux anticorps monoclonaux reconnaissant de nouveaux épitopes de la gal-9

GalNab-1 et GalNab-2 ont été générés chez la souris en utilisant la partie C-terminale de la gal-9 recombinante humaine. Ces deux anticorps reconnaissent des épitopes très proches. Nous nous sommes lancés dans la production de nouveaux anticorps neutralisant en utilisant la gal-9S entière chez le rat. Cette approche nous permettra peut-être de produire des anticorps qui reconnaissent des épitopes différents. Un avantage supplémentaire concerne les anticorps de rats qui possèdent des régions charpentes relativement proches de celles des immunoglobulines humaines en termes de séquences peptidiques, ce qui facilitera le processus d'humanisation.

ANNEXES

Kapetanakis NI, **Baloche V**, Busson P. *Tumor exosomal microRNAs thwarting anti-tumor immune responses in nasopharyngeal carcinomas*. Annals of Translational Medicine. Avr 2015;5(7):164-164.
DOI : 10.21037/atm.2017.03.57

Makowska A, Braunschweig T, Denecke B, Shen L, **Baloche V**, Busson P, Kontny U. *Interferon β and Anti-PD1/PD-L1 Checkpoint Blockade Cooperate in NK Cell-Mediated Killing of Nasopharyngeal Carcinoma Cells*. Translational Oncology. Sept 2019;12(9):1237-56.
DOI : 10.1016/j.tranon.2019.04.017

Makowska A, Franzen S, Braunschweig T, Denecke B, Shen L, **Baloche V**, Busson P, Kontny U. *Interferon beta increases NK cell cytotoxicity against tumor cells in patients with nasopharyngeal carcinoma via tumor necrosis factor apoptosis-inducing ligand*. Cancer Immunol Immunother. Août 2019;68(8):1317-29.
DOI : 10.1007/s00262-019-02368-y

Baloche V, Ferrand FR, Makowska A, Even C, Kontny U, Busson P. *Emerging therapeutic targets for nasopharyngeal carcinoma: opportunities and challenges*. Expert Opinion on Therapeutic Target. Juin 2020;24(6):545-58.
DOI : 10.1080/14728222.2020.1751820

Zhang C, Huang D, **Baloche V**, Zhang L, Xu J, Li B, Zhao X, He J, Mai H, Chen Q, Zhang X, Busson P, Cui J, Li J. *Galectin-9 promotes a suppressive microenvironment in human cancer by enchancing STING degradation*. Oncogenesis. Juillet 2020;9(7):65.
DOI : 10.1038/s41389-020-00248-0

Tumor exosomal microRNAs thwarting anti-tumor immune responses in nasopharyngeal carcinomas

Nikiforos-Ioannis Kapetanakis, Valentin Baloche, Pierre Busson

CNRS UMR8126, Gustave Roussy and Université Paris-Sud/Paris-Saclay, 39 rue Camille Desmoulins, Villejuif, France

Correspondence to: Dr. Pierre Busson. CNRS UMR8126, Gustave Roussy PR1, 39 rue Camille Desmoulins, 94805 Villejuif, France. Email: pierre.busson@gustaveroussy.fr.

Provenance: This is a Guest Editorial commissioned by Section Editor Mingzhu Gao (Department of Laboratory Medicine, Wuxi Second Hospital, Nanjing Medical University, Wuxi, China).

Comment on: Ye SB, Zhang H, Cai TT, *et al.* Exosomal miR-24-3p impedes T-cell function by targeting FGF11 and serves as a potential prognostic biomarker for nasopharyngeal carcinoma. J Pathol 2016;240:329-40.

Submitted Jan 13, 2017. Accepted for publication Jan 21, 2017.

doi: 10.21037/atm.2017.03.57

View this article at: http://dx.doi.org/10.21037/atm.2017.03.57

The considerable progress achieved in the past 10 years in the field of tumor biology and therapeutics has strengthened the idea that cancer is not only a cellular but also a tissue disease. This concept is likely to apply to nasopharyngeal carcinoma (NPC), characterized by the consistent expression of oncogenic viral proteins in a context of inflammation and immune escape (1). In its typical undifferentiated form, NPC is constantly associated with the Epstein-Barr virus, whose genome is contained in the nuclei of all malignant cells, but not in the surrounding tissue. Latency is the predominant mode of virus-cell interactions, meaning that most viral genes are silent in the vast majority of malignant cells. However, a small fraction of them are consistently expressed coding a handful of viral products, both viral proteins and untranslated RNAs, most of them with proven oncogenic properties. The inflammatory context of NPC is obvious for pathologists: almost all NPC primary tumors are heavily infiltrated by non-malignant leucocytes, mainly T-lymphocytes but also B lymphocytes, macrophages, dendritic cells and neutrophils. This inflammatory infiltration often disappears in metastatic lesions. The immune escape is also obvious because of the rapid proliferation of malignant cells despite the consistent expression of EBNA1, LMP1 and LMP2 which are known to be the targets of CD4+ and CD8+ cytotoxic T-cells in EBV-carriers. One interpretation of the paradox of tumor inflammation combined with tumor immune escape is that malignant cells in the primary tumor benefit to some extent from the proximity of leucocytes while developing mechanisms of immune escape.

High-scale genomic studies have brought evidence that the immune escape mechanisms in NPC can be cellular intrinsic alterations, for example defects in the expression of HLA class I molecules (Lo KW, 17th International Symposium on Epstein-Barr virus and associated diseases, Zurich, August 2016, abstract EBV2016-1040). These alterations are probably the most difficult to deal with for the oncologist. However, there is also evidence of a major contribution of extra-cellular "micro-environmental" immunosuppressive factors. Data from previous studies support the role of immunosuppressive proteins either secreted in a soluble form or carried by tumor exosomes, for example CCL20, galectin-9 or IDO (indoleamine 2, 3-dioxygenase) (2-4). One recent elegant publication from Jiang Li's group in Guangzhou provides new insight on the role of tumor exosomes carrying immunosuppressive microRNAs (5) (*Figure 1*). For the sake of brevity, one can distinguish two types of results in this study. Most data are based on *in vitro* experiments. They demonstrate that malignant cells mixed with T-cells from healthy donors can deliver miR-24-3p to these T-cells using exosomes as intercellular carriers. Then it is shown that miR-24-3p decreases the proliferation of target T-cells by down-regulation of FGF11 and subsequent modifications of ERK and STAT protein phosphorylation. Simultaneously, there is a decrease in the expression of interferon-γ and

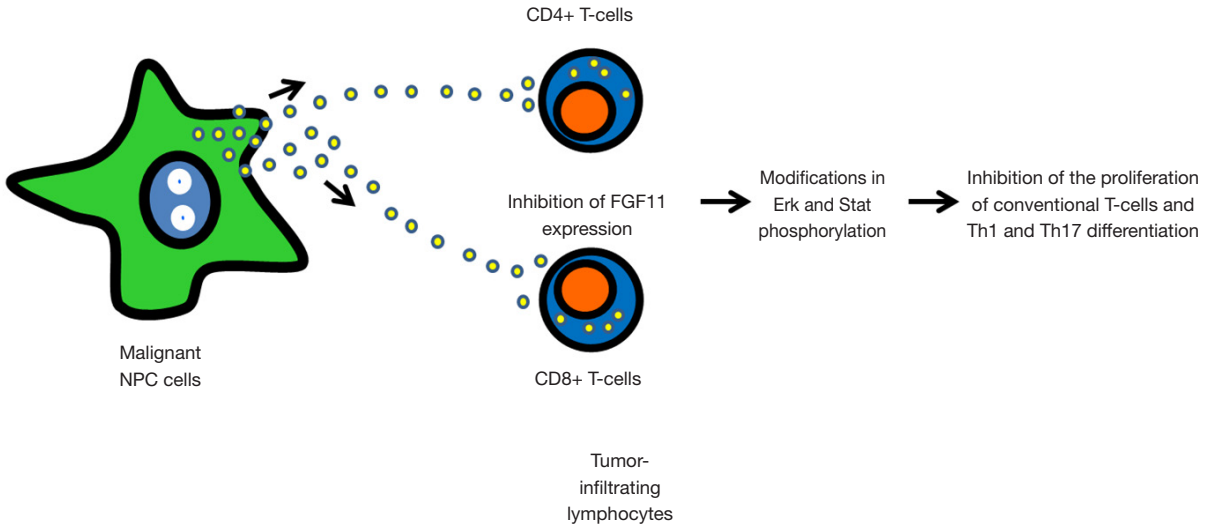

Figure 1 Main steps of the scenario linking the inhibition of the proliferation and differentiation of tumor-infiltrating T-lymphocytes to the release of tumor exosomes carrying miR-24-3p in the microenvironment of nasopharyngeal carcinomas. Exosomes carrying miR-24-3p are released by malignant NPC cells and up-taken by tumor-infiltrating lymphocytes. The internalization of miR-24-3p in target cells results in the downregulation of FGF11 with subsequent modifications in the phosphorylation of Erk and Stat proteins. These signaling events result in the inhibition of the proliferation of conventional T-cells (CD4+ and CD8+) and probably impair Th1 and Th17 differentiation. This scenario is based on *in vitro* and *in vivo* investigations reported by Ye *et al.* (5).

IL-17 expression in CD4 T-cells suggesting the impairment of Th1 and Th17 differentiation. From these data, the authors infer that similar interactions are likely to occur in the tumor microenvironment where malignant cells are in close contact with tumor infiltrating lymphocytes (TILs). Other data, based on investigations of serum samples or tumor tissue sections, support this inference. First, the authors show that the abundance of FGF11 in TILs is inversely correlated with the serum concentration of miR-24-3p. Later, they show on tumor sections that a low abundance of CD4+ and CD8+ TILs correlates with a low abundance of FGF11 in TILS (and in malignant cells as well). Moreover, a high concentration of exosomal miR-24-3p in the serum and a low amount of FGF11 in TILs and malignant cells were associated with a shorter disease-free survival. A few more experiments demonstrated that, at least *in vitro*, hypoxia enhances the concentration of miR-24-3p in tumor exosomes. The data are less consistent with regard to regulatory T-cells (T-regs). Indeed, *in vitro* T-regs' expansion and Fox-P3 expression were enhanced by the uptake of miR-24-3p and FGF11 down-regulation. However, *in vivo*, there was no significant correlation between the abundance of Fox-P3-positive cells among stromal cells and the depletion of FGF11 in TILs and malignant cells. This reminds us that the role of T-regs in NPC remains controversial (3,6).

In terms of methodology, it is important to note that almost all *in vitro* investigations were done using an EBV-negative malignant epithelial cell line, TW03. This approach is likely to have both positive and negative consequences. TW03 cells are easier to handle *in vitro* that genuine NPC cells carrying an endogenous EBV genome. The authors have largely taken advantage of the ease of DNA transfection into these cells to make an intense use of microRNA mimics, microRNA sponges and reporter assays. However, in many respects, TW03 cells lack several major characteristics of NPC cells. For example, NPC cells carry on their surface an array of inflammatory molecules like HLA class II molecules, CD54 and CD70 which are not found on TW03 (1). Moreover, a huge fraction of the total microRNAs produced by NPC cells—often as much as one sixth or even one third of them—are EBV—encoded microRNAs of which some might have an impact on T-cell functions (7). On the other hand, to a large extent, TW03 cells have a phenotype which is reminiscent of the phenotype of malignant cells from squamous cell carcinomas of the upper aero-digestive tract. Therefore, the findings reported by Ye *et al.* may have applications for

non-NPC epithelial malignancies, for example squamous carcinomas of the upper aero-digestive tract where hypoxia is often highly prevalent.

Tumor immunosuppression is usually a multifactorial process. As mentioned previously, other immunosuppressive factors, especially proteins are known to be released by NPC cells either in a soluble form or conveyed by exosomes. Therefore an integrated approach will be required to assess the respective contributions to the immune evasion of NPCs of the various immunosuppressive agents, regardless of their chemical nature, proteins, nucleic acids and probably lipids like prostaglandins. It is noteworthy that in virtually all experiments reported by Ye *et al.*, the reduction of the T-cell proliferation induced by exosomes carrying the miR-24-3p did not exceed 20%. Thus, there is ample room for potential synchronic or non-synchronic cooperation of miR-24-3p with other immunosuppressive factors. In future research, one major challenge will be to identify the predominant mechanisms of immune suppression for each clinical and molecular subtype of NPC or even for a given patient, at each stage of his treatment and surveillance. NPC clearly is a heterogeneous disease, in terms of growth pattern (with either early metastases or predominantly local growth), in terms of malignant cell phenotypes (with more or less epithelio-mesenchymal transition) or in terms of immune "contexture" (variable relative abundance of various types of T-lymphocytes, macrophages, NK cells and dendritic cells) (1,6,8). Although currently there is no consensus on molecular subcategories, it is obvious that the NPC malignant phenotypes can be supported by different genetic and epigenetic alterations as well as different modes of virus-cell interactions, for example a high, low or very low level of LMP1 expression (Lo KW, 17th International Symposium on Epstein-Barr virus and associated diseases, Zurich, august 2016, abstract EBV2016-1040). The work published by Ye *et al.* is also quite exemplary insofar as it shows the importance of combining the investigations on the tumor tissue with investigations on serum or plasma samples (5). One can presume that, in the future, the diagnosis of the immune "contexture" and immune suppressive mechanisms will rely on tumor tissue analysis combined with assays performed on serum or plasma factors including microRNAs and proteins like CCL20 and galectin-9 (8).

What are the consequences of the findings reported by Ye *et al.*, in terms of therapeutics? One option seems to be the use of miR antagonists (antagomiRs or anti-miRs) to neutralize plasma miR-24-3p. Vectorization of these antagonists to the malignant cells or the tumor-infiltrating leucocytes remains a major challenge. Another option is to attempt a capture and depletion of tumor exosomes using systemic injections of therapeutic antibodies. Because exosomes released by endothelial cells or leukocytes are very abundant in plasma and many interstitial fluids, it will be necessary to use antibodies reacting with molecules expressed selectively on the surface of NPC exosomes. Some years ago, we made the empirical and surprising observation that selective capture of tumor exosomes from plasma samples from NPC patients was facilitated by the use of anti-HLA class II antibodies (2). Galectin-9 is another protein present on the surface of NPC tumor exosomes (ibid.). Thus, the use of anti-galectin-9 or anti-HLA II antibodies might play a role in a future strategy of NPC exosome capture and depletion.

Acknowledgements

The authors would like to thank Bristol-Myers Squibb Foundation (2016-2017) for research funding.

Footnote

Conflicts of Interest: The authors have no conflicts of interest to declare.

References

1. Gourzones C, Barjon C, Busson P. Host-tumor interactions in nasopharyngeal carcinomas. Semin Cancer Biol 2012;22:127-36.
2. Klibi J, Niki T, Riedel A, et al. Blood diffusion and Th1-suppressive effects of galectin-9-containing exosomes released by Epstein-Barr virus-infected nasopharyngeal carcinoma cells. Blood 2009;113:1957-66.
3. Mrizak D, Martin N, Barjon C, et al. Effect of nasopharyngeal carcinoma-derived exosomes on human regulatory T cells. J Natl Cancer Inst 2014;107:363.
4. Ben-Haj-Ayed A, Moussa A, Ghedira R, et al. Prognostic value of indoleamine 2,3-dioxygenase activity and expression in nasopharyngeal carcinoma. Immunol Lett 2016;169:23-32.
5. Ye SB, Zhang H, Cai TT, et al. Exosomal miR-24-3p impedes T-cell function by targeting FGF11 and serves as a potential prognostic biomarker for nasopharyngeal carcinoma. J Pathol 2016;240:329-40.

6. Zhang YL, Li J, Mo HY, et al. Different subsets of tumor infiltrating lymphocytes correlate with NPC progression in different ways. Mol Cancer 2010;9:4.
7. Lee KT, Tan JK, Lam AK, et al. MicroRNAs serving as potential biomarkers and therapeutic targets in nasopharyngeal carcinoma: A critical review. Crit Rev Oncol Hematol 2016;103:1-9.
8. Becht E, Giraldo NA, Germain C, et al. Immune Contexture, Immunoscore, and Malignant Cell Molecular Subgroups for Prognostic and Theranostic Classifications of Cancers. Adv Immunol 2016;130:95-190.

Cite this article as: Kapetanakis NI, Baloche V, Busson P. Tumor exosomal microRNAs thwarting anti-tumor immune responses in nasopharyngeal carcinomas. Ann Transl Med 2017;5(7):164. doi: 10.21037/atm.2017.03.57

Translational Oncology
www.transonc.com

Volume 12 Number 9 September 2019 pp. 1237–1256 1237

Interferon β and Anti-PD-1/PD-L1 Checkpoint Blockade Cooperate in NK Cell-Mediated Killing of Nasopharyngeal Carcinoma Cells

Anna Makowska[*], Till Braunschweig[†], Bernd Denecke[‡], Lian Shen[*], Valentin Baloche[§], Pierre Busson[§] and Udo Kontny[*]

[*]Division of Pediatric Hematology, Oncology and Stem Cell Transplantation, Medical Faculty, RWTH Aachen University, Aachen, Germany; [†]Institute of Pathology, Medical Faculty, RWTH Aachen University, Aachen, Germany; [‡]IZKF, Medical Faculty, RWTH Aachen University, Aachen, Germany; [§]CNRS UMR 8126, Gustave Roussy and Université Paris-Sud/Paris-Saclay, Villejuif, France

Abstract

Nasopharyngeal carcinoma (NPC) is a highly malignant epithelial cancer linked to EBV infection. Addition of interferon-β (IFNβ) to chemo- and radiochemotherapy has led to survival rates >90% in children and adolescents. As NPC cells are sensitive to apoptosis via tumor necrosis factor-related apoptosis inducing ligand (TRAIL), we explored the role of TRAIL and IFNβ in the killing of NPC cells by natural killer (NK) cells. NPC cells, including cells of a patient-derived xenograft were exposed to NK cells in the presence or absence of IFNβ. NK cells killed NPC- but not nasoepithelial cells and killing was predominately mediated via TRAIL. Incubation of NK cells with IFNβ increased cytotoxicity against NPC cells. Concomitant incubation of NK- and NPC cells with IFNβ before coculture reduced cytotoxicity and could be overcome by blocking the PD-1/PD-L1 axis leading to the release of intracellular TRAIL from NK cells. In conclusion, combination of IFNβ and anti-PD-1, augmenting cytotoxicity of NK cells against NPC cells, could be a strategy to improve NPC-directed therapy and warrants further evaluation *in vivo*.

Translational Oncology (2019) 12, 1237–1256

Introduction

Nasopharyngeal carcinoma (NPC) is a malignant tumor arising from the surface epithelium of the posterior nasopharynx. Infection by Epstein–Barr-Virus (EBV), ethnic background and environmental carcinogens play a major role in its pathogenesis [1,2]. Survival rates in patients with localized disease range between 80% and 90%, and are usually less than 20% in patients with metastatic disease or relapse [3]. State of the art treatment in adults consists of radiochemotherapy, usually with doses around 70 Gy to the primary tumor [4]. In children and adolescents radiochemotherapy is usually preceded by several blocks of cisplatin-containing chemotherapy allowing lower dosing of radiotherapy [5–8]. In the studies NPC-93 and -2001 of the German Society of Pediatric Oncology and Hematology (GPOH) overall and event-free survival rates >90% have been achieved, applying radiation doses less than 60 Gy [6,7]. Both protocols are unique by the fact that neoadjuvant chemotherapy and radiochemotherapy were followed by a 6 months lasting maintenance period with interferon beta (IFNβ). The introduction of IFNβ in these protocols was based on a previous response rate of 26% in patients refractory to conventional therapy [9,10]. Type 1 interferons, such as IFNα and β have been reported to display direct and indirect anti-tumor activities [11,12]. Recently, we were able to demonstrate that IFNβ, at concentrations achievable in patients, induces apoptosis in NPC cells, including cells of a patient-derived xenograft [13]. IFNβ induced apoptosis by expressing the death ligand TRAIL on the surface of NPC cells and the subsequent induction of apoptosis via an intact TRAIL-receptor signaling pathway. TRAIL is also expressed on lymphocytic effector cells such as T lymphocytes and NK cells, and NPC tumors have been shown to be sensitive to cytotoxicity of EBV-specific T lymphocytes [14,15]. In addition, IFNβ has been shown to

Address all correspondence to: Udo Kontny, MD, Division of Pediatric Hematology, Oncology and Stem Cell Transplantation, Medical Faculty, RWTH Aachen University, Pauwelsstraße 30, 52074 Aachen, Germany. E-mail: ukontny@ukaachen.deReceived 21 March 2019; Accepted 22 April 2019

1936-5233/19
https://doi.org/10.1016/j.tranon.2019.04.017

increase the expression of TRAIL on lymphocytic effector cells [16,17]. On the other hand, it was recently demonstrated, that IFNβ may upregulate expression of the negative checkpoint regulator PD-L1 on tumor cells, thereby possibly downregulating an anti-tumor response [11,12]. Inhibition of the PD-1/PD-L1 interaction has been demonstrated to be of clinical benefit in the treatment of various tumors, such as Hodgkin lymphoma and malignant melanoma [18,19]. Both tumors like NPC are characterized by marked lymphocytic infiltration and expression of PD-L1. In this paper, we have analyzed the killing of NPC cells by NK cells and its possible modulation by IFNβ and PD-1/PD-L1 checkpoint-inhibition.

Materials and Methods

Cell Lines and Culture

Two NPC cell lines and one nasopharyngeal epithelial cell line as a control were used in this study. The EBV-negative cell line CNE-2 was kindly provided by Prof. Pierre Busson (Gustave Roussy Institute, Paris, France) [20]. The EBV-positive cell line C666–1 was a gift from Prof. Fei-Fei Liu, University of Toronto, Canada [21]. The SV40T-antigen immortalized nasopharyngeal epithelial cell line NP69 [22] was obtained from Prof. George Tsao (The Chinese University of Hong Kong, Hong Kong, China). All cell lines were cultured as described before [13]. The authenticity of NPC cell lines (C666–1, CNE-2) and the immortalized nasopharyngeal epithelial cell line (NP69) was investigated by DNA fingerprinting analysis using the AmpF/STR Identifiler PCR Amplification Kit (Applied Biosystem, Foster City, CA, USA) and detected on an ABI Prism 3100 Genetic Analyzer (Applied Biosystems) according to the manufacturer's protocol. Data were analyzed and allele(s) of each locus were determined by GeneScan and Gene-Mapper TM ID Software (Applied Biosystems). STR profiles of NPC cell lines and the nasopharyngeal epithelial cell line NP69 are as previously described [13].

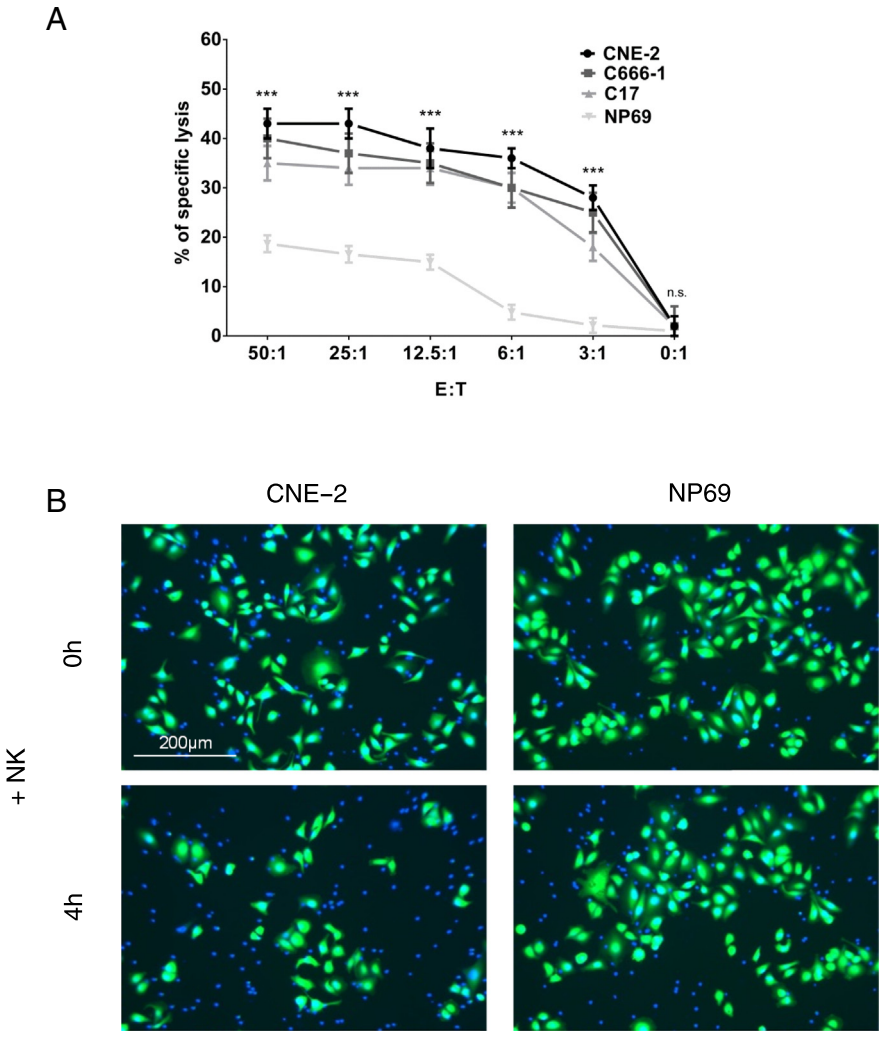

Figure 1. Killing of NPC cells by NK cells. (A) NK cells kill NPC cells starting at an effector:target (E:T) ratio of 3:1. Minor killing of nasoepithelial cells (NP69) at low E:T ratios. Cytotoxicity assays were performed in quintuplicates coculturing NK cells isolated from healthy donors and target cells labeled with calcein for 4 h. Lysis of target cells was determined by measurement of calcein in collected supernatants by an ELISA reader. (B) Bright-field and fluorescence overlay images of NPC cells cocultured with NK cells. NPC cells were stained with Calcein AM, NK cells with Hoechst 33258. (C) Preincubation of NK cells with 100 ng/ml anti-TRAIL antibody or preincubation of NPC cells with anti-FAS antibody, clone ZB4, inhibits killing of NPC cells by NK cells to 71,42% and 54,29%, respectively. Blocking of both pathways with the respective antibodies reduces killing of NPC cells by NK cells up to 90%. Data are presented as means ± S.E.M. Asterisks indicate statistically significant differences between all cell lines in one ratio-group (two-way ANOVA; $*P < .05$; $**P < .01$; $***P < .001$).

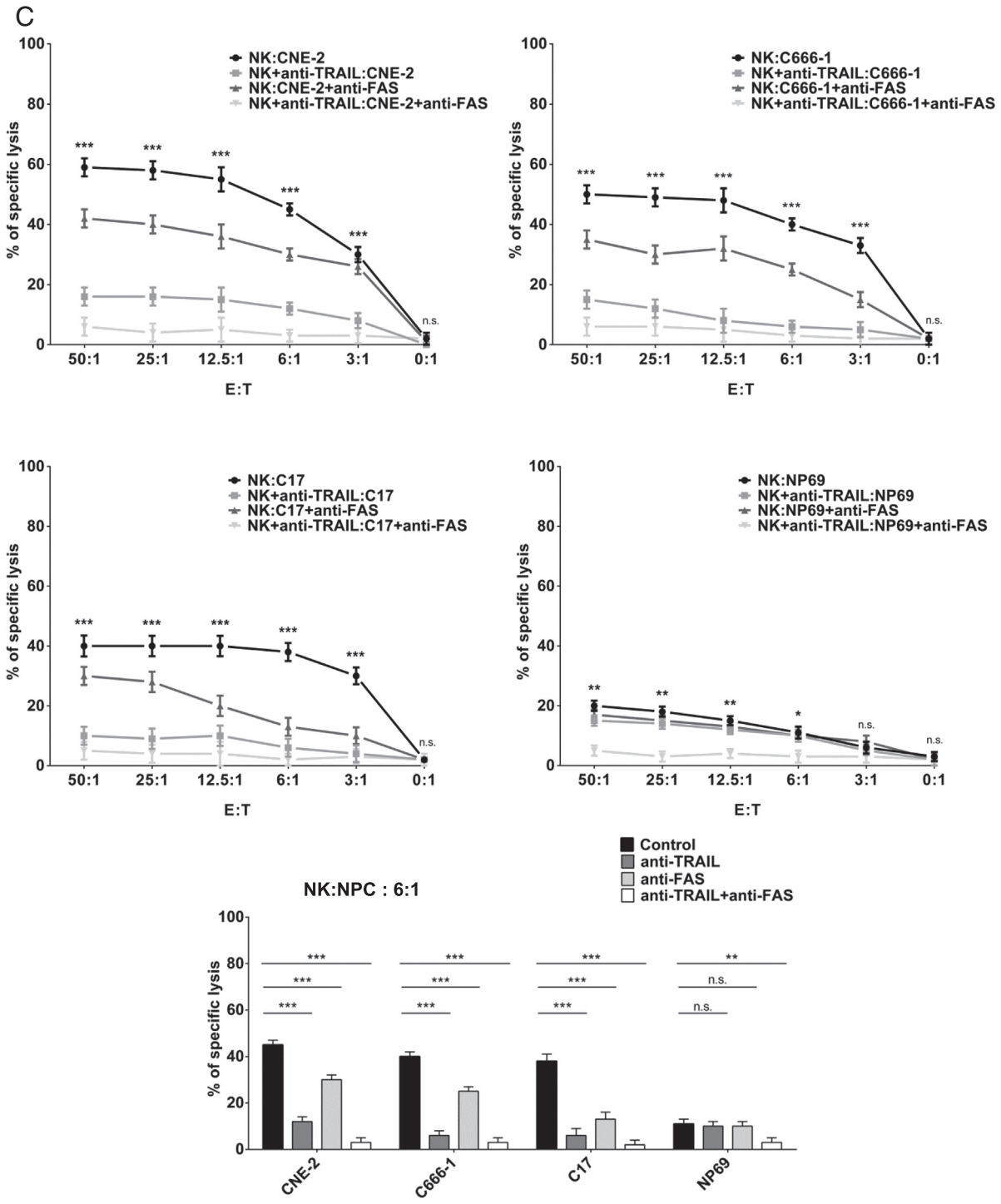

Figure 1. (*continued.*)

Patient-Derived Xenograft

The xenograft C17 was established from a patient with an EBV-positive metastatic NPC by Prof. Pierre Busson, Paris in nude mice [23]. For the experiments described below, single cells suspensions were derived from freshly isolated C17 tumor fragments by collagenase cell dispersion. C17 cells were kept in culture using RPMI1640 Medium (Gibco) supplemented with 25 mM HEPES, 7,5% fetal bovine serum (Gibco) and 100 U/ml penicillin and 100 mg/ml streptomycin (Gibco).

Isolation of Primary Human NK Cells

Human peripheral blood mononuclear cells (PBMC) were purified from buffy coats of 20 healthy donors using Ficoll–Hypaque (Biochrom, Berlin, Germany) density gradient centrifugation. Informed consent was obtained from all donors for the use of buffy coat cells for research. Positive magnetic selection of $CD56^+$ cells from PBMCs was performed according to the manufacturer's instructions (Miltenyi; Bergisch Gladbach, Germany). Purified NK cells were cultivated in RPMI1640 medium supplemented with 10% FCS and 100 U/ml penicillin and 100 mg/ml streptomycin (Gibco).

Reagents

Human recombinant interferon beta (IFNβ) was obtained from R&D System (NY, USA). The primary mouse monoclonal antibody against TRAIL, clone 2E5 was purchased from Enzo Life Science (Paris, France). The caspase inhibitors: Z-VAD-fmk, Z-IETD-fmk and Z-DEVD-fmk and primary mouse monoclonal antibody against PD-1, clone 913,429 were obtained from R&D System (Wiesbaden, Germany). The primary mouse monoclonal antibody against FAS Ligand, clone NOK-1, was purchased from Abcam (Cambridge, UK). Anti-FAS antibody, clone ZB4, was obtained from Millipore (California, USA), anti-human B7-H1/PD-L1 monoclonal antibody, clone 130,021, and anti-human B7-DC/PD-L2 antibody, clone 176,611, were obtained from R&D System (Minneapolis, USA). To assess TRAIL- and FAS Ligand-mediated cytotoxicity, we used freshly eluted GST-TRAIL fusion protein, produced as described before [24] and FAS Ligand obtained from Enzo Life Science (Paris, France).

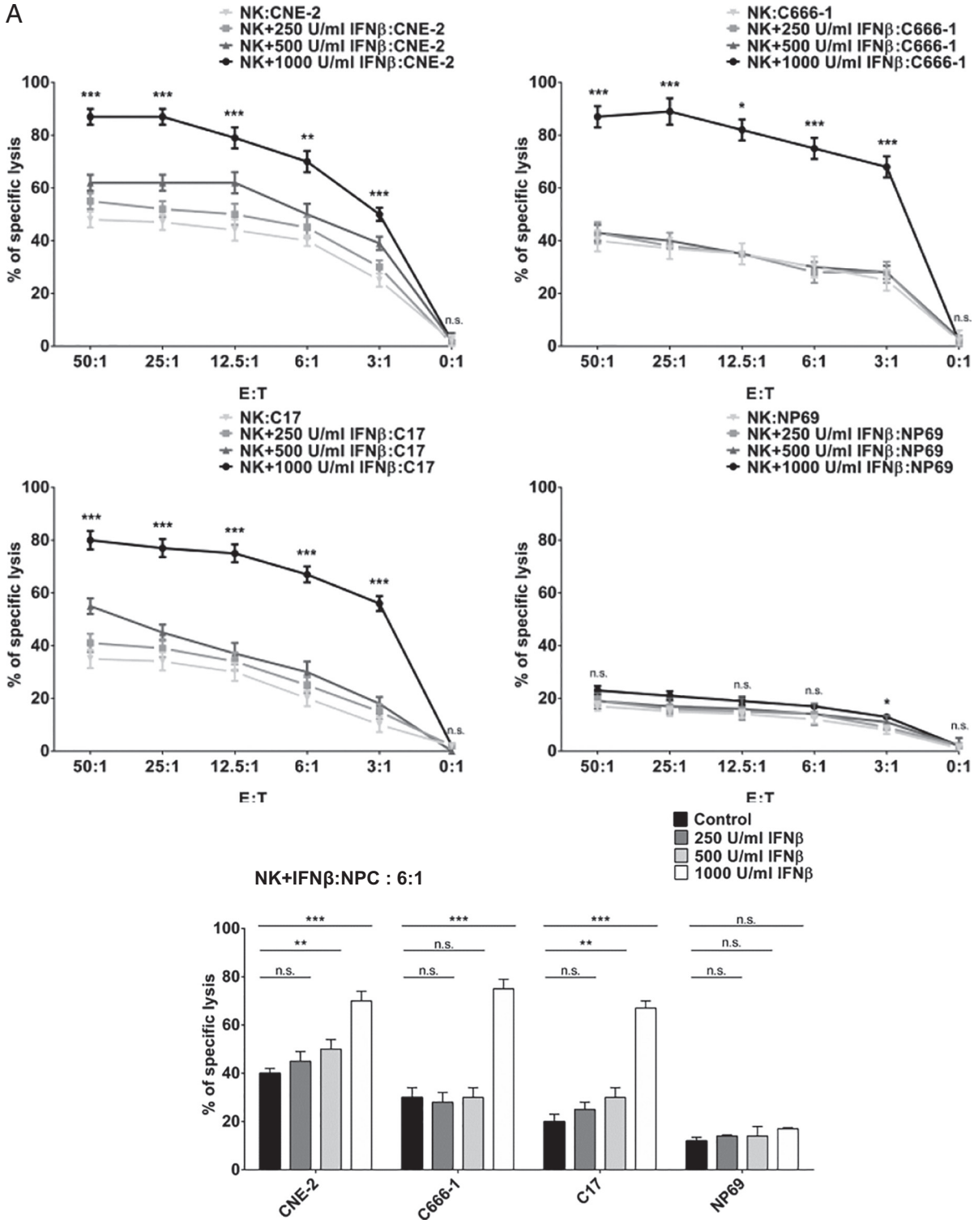

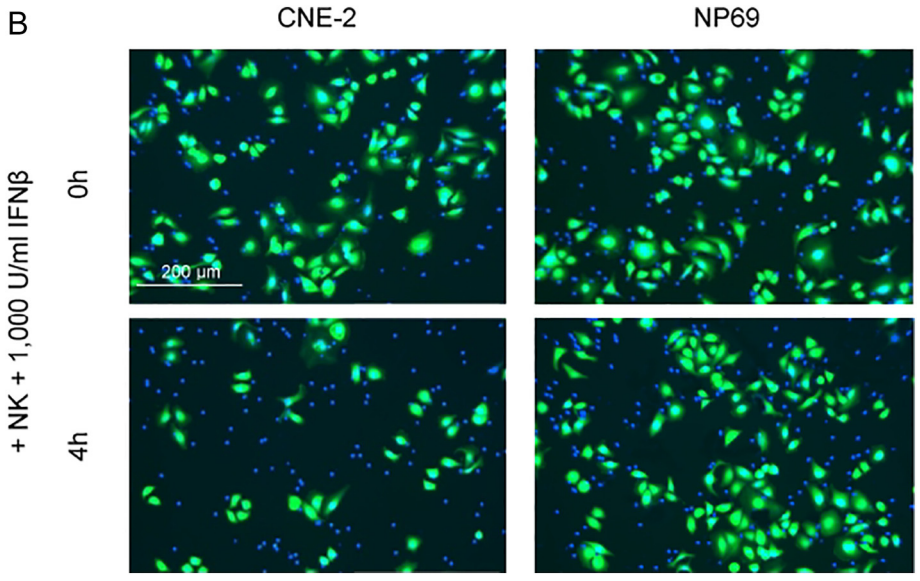

Figure 2. (*continued.*)

Interferon-β Treatment

To analyze the effect of IFNβ on the killing of NPC cells by NK cells, effector cells, target cells or both were incubated with IFNβ as indicated. NK cells, growing in suspension, were seeded at 1 x 10^6 cells/ml and treated with various concentration of IFNβ (0–1,000 U/ml) for 24 h. NPC cells were cultured to 70–80% confluence and treated in the presence or absence of 1,000 U/ml IFNβ for 24 h. Treated and untreated cells were evaluated for surface expression of NK cell ligands as well as PD-1, PD-L1 and PD-L2 by flow cytometry. Sensitivity of NPC cells to NK-cell mediated lysis was measured by calcein release assay.

Calcein Release Assay

Calcein-acetoxymethyl (Calcein-AM) is proved to be specific and sensitive for the detection and tracking of apoptosis in living cells [25,26]. The acetoxymethyl ester of calcein is a lipid-soluble fluorogenic diester that passively crosses the cell membrane in an electrically neutral form, then being converted by intracellular esterases, which are active only in living cells, into the negatively charged, green fluorescent calcein. The fluorescence based calcein-AM release assay was used here to assess NK cell-induced cytotoxicity. NPC cells were washed and resuspended in 15 µM calcein-AM (Thermo Fisher; Eugene, USA) for 30 min at 37 °C, before co-incubation with NK cells at different effector to target (E:T) ratios (50:1, 25:1, 12,5:1, 6:1, 3:1, 0:1) for 4 h at 37 °C. 4% Triton (Merck; Darmstadt, Germany) was added to ensure maximum calcein release in controls. After centrifugation, cell free supernatant was transferred to a Cellcarrier Plate (Sarstedt; Nümbrecht, Germany) to measure relative fluorescence units (RFU) using the spectrophotometer (TECAN Infinite 200 Pro, Tecan, Männedorf, Switzerland). The percentage of specific lysis was calculated as follows: ((RFU value in respective treatment – RFU value in control (spontaneous release))/(RFU value Triton (maximum release) – RFU value in control (spontaneous release)) × 100).

Analysis of NK Cell Cytotoxicity

NPC cells were incubated with the following caspase inhibitors for 1 h prior to adding NK cells: Pan-caspase-inhibitor Z-VAD-fmk (10 µM), caspase-8-inhibitor Z-IETD-fmk (10 µM) and caspase-3-inhibitor Z-DEVD-fmk (10 µM). To analyze the contribution of death ligands in NK cell-mediated killing, NK cells were incubated with the blocking anti-TRAIL mAb, clone 2E5 (100 ng/ml) and NPC cells were incubated with the anti-FAS antibody, clone ZB4 mAb (100 ng/ml); cells were pretreated for 1 h with the respective

Figure 2. IFNβ augments killing of NPC cells by NK cells predominately via TRAIL. (A) Killing of NPC cells by NK cells starts at an E:T ratio of 3:1 and is markedly enhanced by preincubation of NK cells with IFNβ (1,000 U/ml) for 24 h. Minor killing of nasoepithelial cells (NP69) at low E:T ratios. Target cells were labeled with calcein, plated in a 96-well plate and incubated with NK cells for 4 h at the indicated E:T ratios. Lysis of target cells was determined by measurement of calcein in collected supernatants by an ELISA reader. (B) Bright-field and fluorescence overlay images of NPC cells cocultured with NK cells treated with or without 1,000 U/ml IFNβ for 24 h. NPC cells were stained with Calcein AM, NK cells with Hoechst 33258. (C) Increase in the cytotoxicity of NK cells after treatment with IFNβ against NPC cells is predominately mediated by the TRAIL signaling pathway. NK cells pretreated with IFNβ were incubated with a blocking anti-TRAIL antibody before coculture with NPC cells, and/or NPC cells and nasopepithelial cells NP69 were treated with the FAS-blocking mAb for 1 h before coculture. NPC lysis was then measured as before via calcein release assay. Data are presented as means ± S.E.M. Asterisks indicate statistically significant differences between all cell lines in one ratio-group (two-way ANOVA; $*P < .05$; $**P < .01$; $***P < .001$). D) IFNβ increases surface expression of TRAIL on NK cells. Only minor upregulation of FASL was observed. TRAIL and FASL surface expression were measured by flow cytometry 24 h after incubation of NK cells with 1000 U/ml IFNβ. (E) Addition of recombinant TRAIL to cocultures of unstimulated NK cells and NPC cells augments killing of NPC cells to a similar extent as by NK cells pretreated with IFNβ. Cytotoxicity assays were performed in quintuplicates using the calcein release assay. (F) Transfection of NPC cells with TRAIL-receptor 1 and− 2 siRNA blocks killing of NPC cells by IFNβ-stimulated NK cells. Data are presented as means ± S.E.M. Asterisks indicate statistically significant differences between all cell lines in one ratio-group (two-way ANOVA; $*P < .05$; $**P < .01$; $***P < .001$).

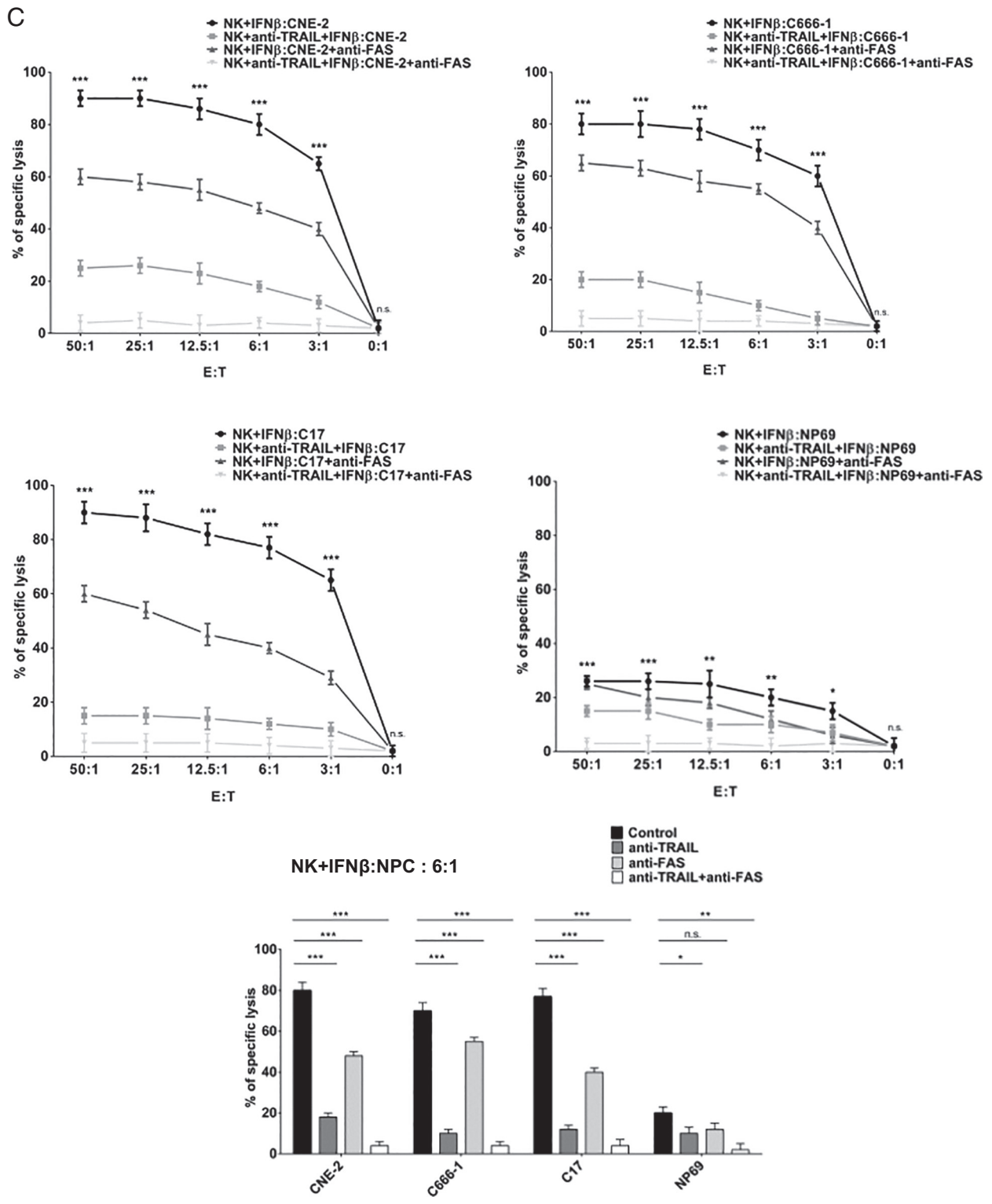

Figure 2. (*continued.*)

antibodies before coculture. In some experiments, NK cells were pretreated with 2.5 μg/ml conconavalin A (ConA; Sigma, St. Louis/USA) for 2 h to inactivate the perforin/granzyme B pathway. For inhibition of the PD-1/PD-L1/2 checkpoint NK cells were incubated with the PD-1 inhibitor nivolumab (Bristol-Myers; Anagni, Italien) for 1 h prior to coculture with NPC cells. Cytotoxicity was determined via calcein release assay as described above.

Flow Cytometry

NPC and NK cells were suspended at a density of 1 x 10^6 cells in 500 μl of medium. Where indicated cells had been pretreated with IFNβ at 1,000 U/ml for 24 h. For analysis of surface expression of death effectors NPC cells were incubated with the following anti-human monoclonal antibodies: anti-TRAIL (5 μl), anti-TRAIL receptor 1 (5 μl), anti-Trail receptor 2 (5 μl), anti-FASL (5 μl). For

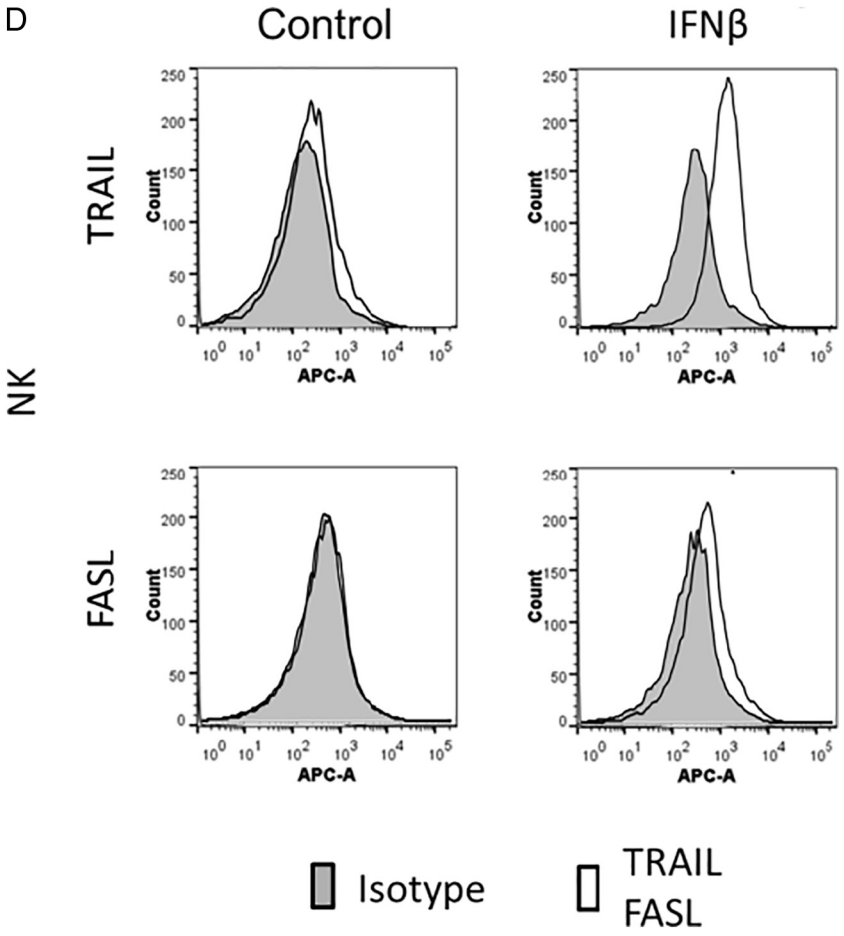

Figure 2. (*continued.*)

analysis of surface expression of checkpoint modulators, NPC and NK cells were incubated with anti-PD-1 (10 µl), anti-PD-L1 (10 µl) and anti-PD-L2 (10 µl) antibody. Incubation with primary antibodies was 1 h on ice. All cells were also stained with their corresponding isotype-matched control monoclonal antibodies. After washing in PBS three times (5 min each), APC-conjugated goat-anti-mouse antibody (1:200) was added to the cell suspensions and incubated for 1 h on ice. Subsequent to rinsing in PBS, samples were analyzed by flow cytometry. Data were analyzed by the FlowJo software (FlowJo LLC, Ashland, USA). Three independent experiments were performed for each assay.

RNA Extraction

Total RNA was isolated from C666–1, CNE-2, C17, NP69 and NK cells treated with 1,000 U/ml IFNβ for 0 h (control), 6 h or 24 h using the Maxwell RSC Simply RNA Tissue kit (Promega, Mannheim, Germany) according to the manufacturer's instructions. RNA quality was evaluated using the Agilent 4200 Tape Station (RNA screen tape assay) (Agilent, Santa Clara, USA) and quantification was performed using the Quantus Fluorometer (Promega).

RNA Library Construction and Sequencing

Libraries were generated from 1 µg of total RNA with the TrueSeq Stranded Total RNA Library Prep Kit (Illumina, San Diego, USA) and Ribo-Zero Gold Kit (Illumina) as described by the manufacturer. Quality and quantity of the RNA libraries were assessed using the 4200 Tape Station (D1000 screen tape assay) and the Quantus Fluorometer, respectively. The libraries were run on an Illumina NextSeq500 platform using the High Output 150 cycles Kit (2 x 76 cycles, paired-end reads, single index) (Illumina) resulting in 101.5 M reads per sample in average. Data were analyzed with an inhouse pipeline embedded in the workflow management system of the Quick NGS-environment [27].

Confocal Microscopy

NK cells were allowed to settle onto poly-L-lysine (Sigma) -coated coverslips for 15 min. Cells were then fixed with 4% paraformaldehyde (Sigma) and incubated with monoclonal antibody recognizing TRAIL (Alexis Biochemicals, San Diego, CA, USA; 1:200) for 60 min in PBS containing 0.1% Tween 20 and 5 mg/ml BSA (PBST/BSA) followed by 30 min incubation with Alexa Fluor™ 488-conjugated anti-mouse IgG (Invitrogen, Carlsbad, CA, USA; 1:200 in PBST/BSA). The nuclear marker Hoechst 33258 was added for 10 min. Samples were mounted between slide and coverslip in gel mounting medium (Sigma) and analyzed on a confocal microscope LSM 510 laser scanning confocal/Confocor 2 microscope (Zeiss, Jena, Germany) using a 40 x DIC oil immersion objective and LSM 510 software; acquired images were imported into ImageJ (National Institute of Health; http://rsbweb.nih.gov/ij/).

Determination of sTRAIL Serum Levels

Supernatants from NK cells after stimulation with 1,000 U/ml IFNβ for 24 h, incubated with or without the anti-PD-1 inhibitor

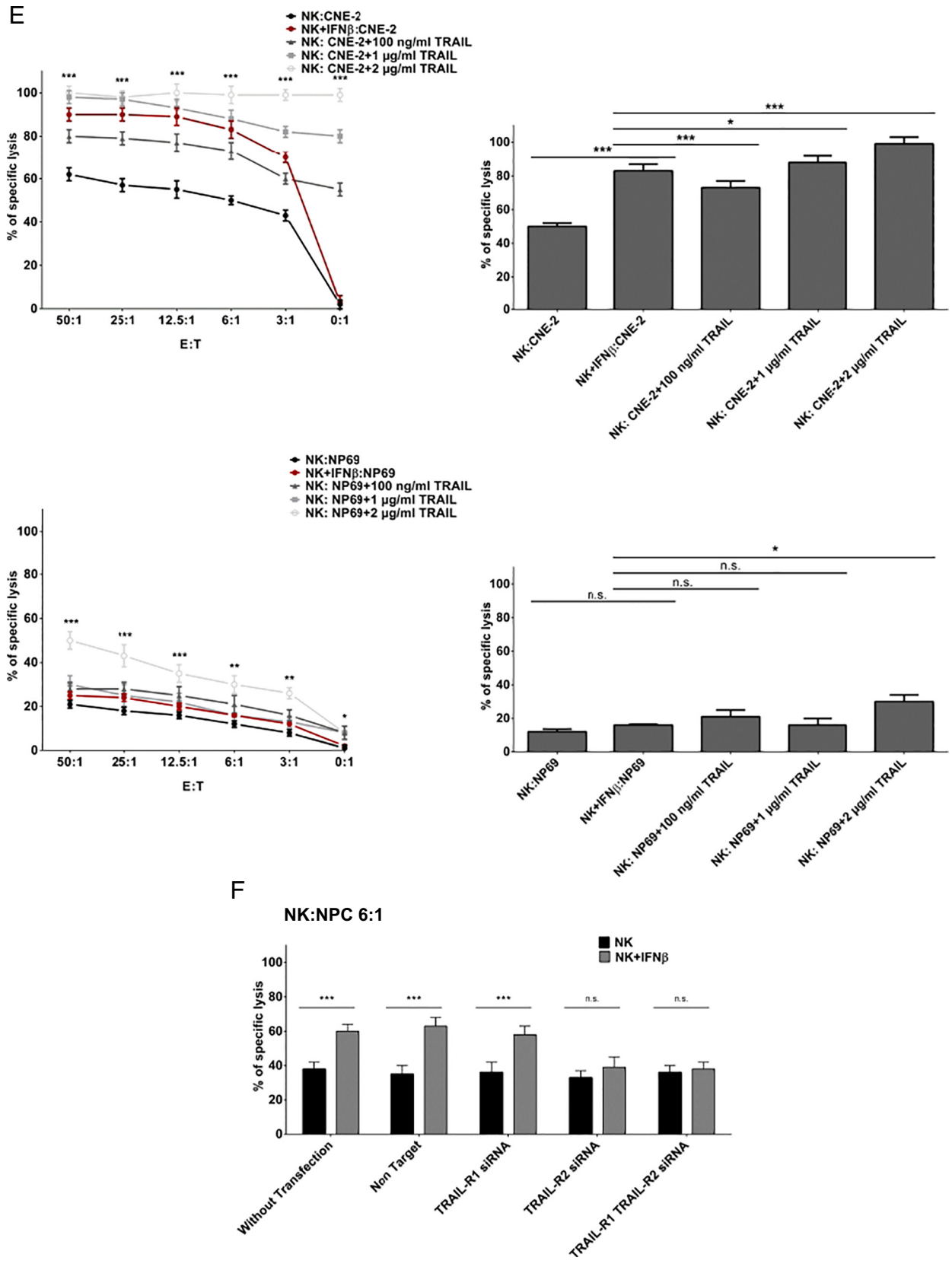

Figure 2. (*continued.*)

nivolumab at 10 μg/ml for 1 h, and then cocultured or not for 4 h with C666–1 cells either pretreated or not with 1,000 U/ml IFNβ for 24 h, were measured using a commercial ELISA kit (R&D Systems, Minneapolis, USA) according to the manufacturer's instructions. Briefly, 100 μl of each sample and standards were tested in triplicates. After 1 h incubation and plate washing, 100 μl of HRP substrate was

added to each well. After further incubation for 1 h and washing the plate, 100 µl TMP substrate solution was added to each well followed by stop solution. Absorbance was read in a microplate reader at 450 nm. Samples were diluted, as necessary, for the absorbance (450 nm) to fall within the range of the standard curve. Final results were given as pg/ml.

Transfection of siRNA

Cells were seeded at 10^5 cells/well in 24 well plates. When the cells reached about 75%–85% confluency, culture medium was aspirated, cells washed with PBS, followed by transfection with Lipofectamine (Invitrogen, Carlsbad, CA, USA) of siRNA against TRAIL, TRAIL-receptor-1, TRAIL-receptor-2 or scrambled siRNA. After 16 h the transfection mix was replaced with normal growth medium and the cells were incubated with NK cells, 1,000 U/ml IFNβ, or 100 ng/ml recombinant TRAIL for the indicated time periods. Transfection efficiency was monitored by measuring surface expression of TRAIL or TRAIL-receptor 1 and – 2 by flow cytometry. Three independent experiments were performed for each assay.

Cell Cycle Analysis

Propidium-iodide staining of nuclei was used for cell cycle analysis as described before [13].

Statistical Analysis

Data are represented as a mean ± S.E. Each set of data represents the mean from at least three independent experiments conducted in quintuplicates for calcein release assays and triplicates for flow cytometric analyses. Differences between groups were examined for significant differences by two-way ANOVA. The level of statistical significances was set at $P < .05$.

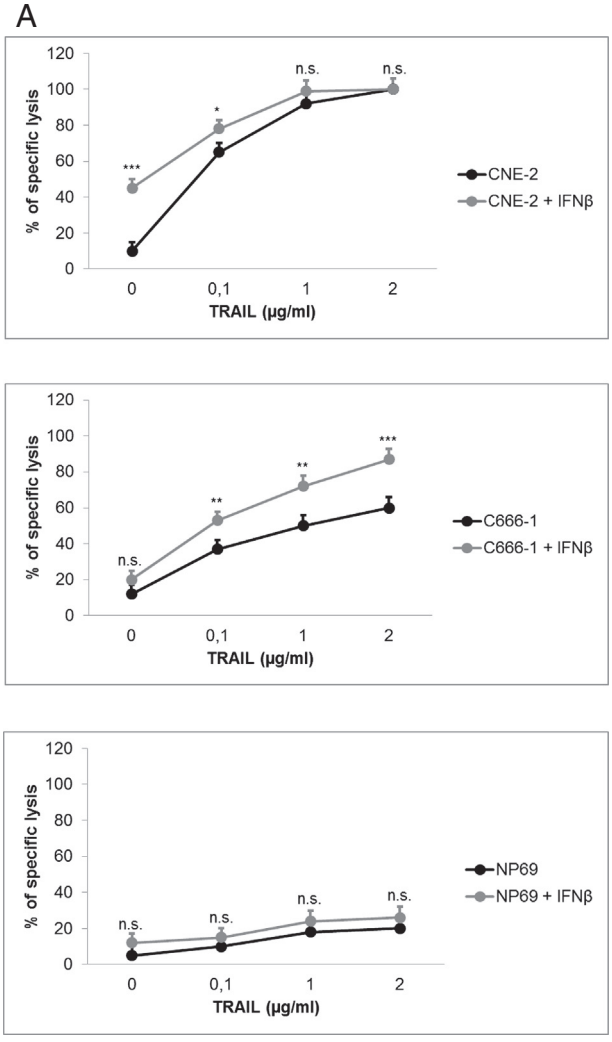

Figure 3. Preincubation of NPC cells with IFNβ decreases the cytotoxicity of IFNβ-pretreated NK cells. (A) Preincubation of NPC cells with IFNβ increases their sensitivity to cytotoxicity by recombinant TRAIL. NPC cells were incubated with 1,000 U/ml IFNβ for 24 h and then treated with recombinant TRAIL at 0, 0.1, 1 or 2 µg/ml for 4 h. Cytotoxicity was measured by the calcein release assay as described before. (B) Pretreatment of NPC cells with IFNβ reduced their sensitivity against lysis by NK cells activated with IFNβ. NK and NPC cells were incubated in the presence or absence of IFNβ (1,000 U/ml) for 24 h. Cells were then washed and cocultured at the indicated E:T ratios for 4 h. Cytotoxicity assays were performed in quintuplicates using the calcein release assay. Data are presented as means ± S.E.M. Asterisks indicate statistically significant differences between all cell lines in one ratio-group (two-way ANOVA; *$P < .05$; **$P < .01$; ***$P < .001$).

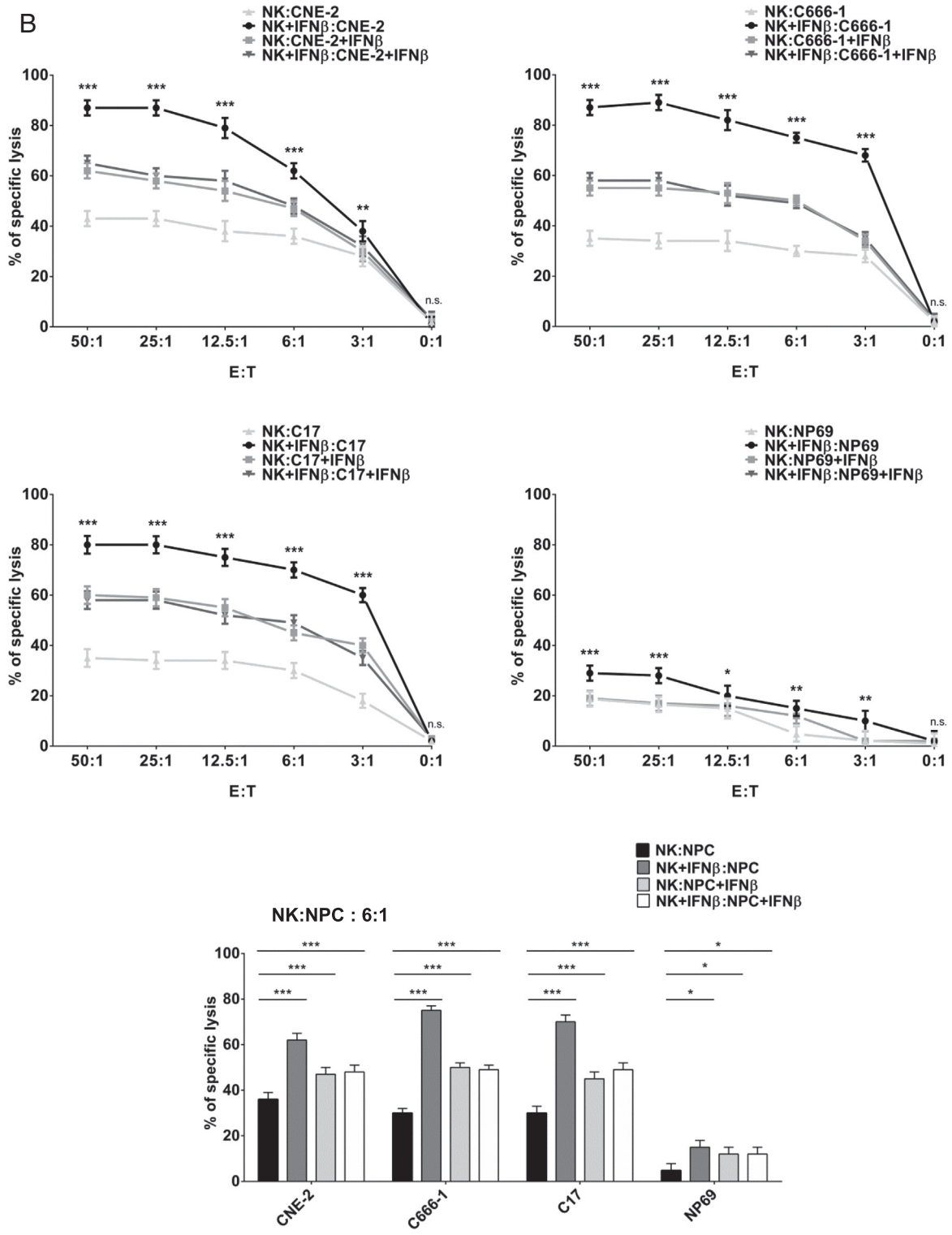

Figure 3. (*continued.*)

Results

NK Cells Kill NPC Cells

In a first experiment, we tested whether NK cells showed cytotoxic activity against NPC cells. NPC cells, labeled with calcein, were incubated with NK cells at increasing effector/target (E:T) ratios (0:1–50:1) for 4 h. The concentration of calcein in the supernatant was then measured as a marker for NPC cytotoxicity. NK cells induced high level of calcein release in an E:T ratio-dependent manner in both NPC cell lines and PDX cells C17. In contrast, only low calcein release was observed in the nasopharyngeal epithelial cell line NP69. Even at a low effector/target ratio of 6:1, 35.78 ± 2.13%

Table 1. IFNβ upregulates PD-L1 mRNA expression in NPC cell lines and PDX cells

Molecule	C666-1			CNE-2			C17			NP69		
	Control	6h IFNβ	24h IFNβ	Control	6h IFNβ	24h IFNβ	Control	6h IFNβ	24h IFNβ	Control	6h IFNβ	24h IFNβ
PD-1	0	0	0.010	0	0.019	0	0	0	0	0.031	0	0
PD-L1	0.040	0.220	0.240	0.060	0.630	0.450	0.160	O.267	0.102	1.250	3.620	0.700
PD-L2	0.030	0.080	0.030	0.110	0.210	0.330	0.308	0.420	0.210	0.450	1.050	0.740
CTLA-4	0	0	0	0	0	0	0.097	0.064	0.073	0	0	0
CD80	3.900	3.730	3.040	0.040	0.037	0.030	0.238	0.269	0.217	0.050	0.080	0.180
CD86	0.007	0.011	0.013	0.006	0.005	0.003	0.098	0.096	0.152	0.001	0.001	0.002

Values are given as TPM (transcripts per kilobase million). mRNA expression was analyzed by RNAseq before, 6 h and 24 h after incubation with 1,000 U/ml IFNβ.

of cells of NPC cell line CNE-2, 30.21 ± 3.80% of cell line C666–1 and 30.69 ± 2.95% of PDX cells C17 were lysed by NK cells, whereas cytotoxicity in nasoepithelial cells NP69 was 5.33 ± 3.01% (Figure 1, *A* and *B*). The same pattern of cytotoxicity was observed using NK cells from different healthy donors (n = 20). In summary, these results suggest that human primary NK cells can effectively kill NPC cells.

NK cells use two different pathways to eliminate target cells, a granule-dependent (perforin/granzyme-mediated) and a granule-independent (death ligand-mediated) mechanism [28]. The latter is executed by the death ligands TRAIL and FAS Ligand (FASL) expressed on the surface of NK cells which upon binding to their respective receptors on target cells can induce apoptosis [29]. As we have previously shown that NPC cells bear receptors for TRAIL and exogenous TRAIL is able to induce apoptosis in NPC cells [13], we asked whether and to what extent the induction of cytotoxicity in NPC cells by NK cells was mediated by TRAIL. Therefore, NK cells were incubated with an inhibiting anti-TRAIL antibody for 1 h prior to coculture with NPC cells; similarly, to study involvement of the FASL/FAS pathway in the cytotoxicity of NK cells, NPC cells were incubated with a FAS blocking antibody 1 h prior to coincubation with NK cells. As shown in Figure 1*C*, killing of NPC cells by NK cells was inhibited by 57.5% to 71.42% with anti-TRAIL- and 42.2% to 54.29% with anti-FAS antibody. Blocking of both pathways with the respective antibodies reduced killing of NPC cells by NK cells up to 90%. Killing of NPC cells by granule-dependent cytotoxicity therefore appears to occur only to a minor extent which was supported by the observation that pretreatment of NK cells with the granzyme B inhibitor ConA only weakly inhibited NK cytotoxicity against NPC cells (Supplemental Figure 1). In addition, incubation of NPC cells with different caspase-inhibitors prior to coincubation with NK cells shows that blockade of caspase-8 which plays as major role in the induction of apoptosis after activation of death receptors but not granzyme B, reduces calcein-release of NPC cells (Supplemental Figure 2). The effect was observed in all NPC cell lines as well as PDX cells but not in nasoepithelial cells. This data suggests that NK cell-induced cytotoxicity against NPC cells is predominately mediated by death ligands TRAIL and FASL, and only to a small extent by the perforin/granzyme system.

Treatment of NK Cells With IFNβ Augments Killing of NPC Cells Predominately via TRAIL

As type-I interferons are known to upregulate expression of TRAIL on lymphocytes [16], we wondered whether preincubation of NK cells with IFNβ would increase their killing activity against NPC cells. Therefore, NK cells were treated with various concentrations of IFNβ (0–1,000 U/ml) for 24 h and then coincubated with NPC cells at different E:T ratios. The upper concentration of 1,000 U/ml was chosen, as this was the highest concentration measured in patients treated with IFNβ for multiple sclerosis [30,31]. The experiment shows that preincubation of NK cells with IFNβ significantly increased NK killing of all NPC cells in a dose-dependent manner. At an IFNβ concentration of 1,000 U/ml, calcein release increased from about 40% to approximately 90% and from 40% to 80% in the two NPC cell lines and PDX cells, respectively, whereas no significant change was observed in nasoepithelial cells NP69 (Figure 2, *A* and *B*).

We then investigated whether the augmentation of NK cell cytotoxicity depended on the death ligand pathways (TRAIL and/or FASL) or the perforin/granzyme B system. NK cells pretreated with IFNβ were incubated with a blocking anti-TRAIL antibody before coculture with NPC cells, and/or NPC cells and nasoepithelial cells NP69 were treated with the FAS-blocking mAb for 1 h before coculture. Additionally, NK cells pretreated with IFNβ were either incubated for 1 h with ConA or fixed with paraformaldehyde to block granzyme B activity. NPC lysis was then measured via the calcein release assay as before. The results demonstrate that the increase in the cytotoxicity of NK cells after treatment with IFNβ against NPC cells is predominately mediated by the TRAIL signaling pathway and to a smaller extent by the FASL/FAS signaling pathway (Figure 2*C*). IFNβ did not augment killing via granzyme B/perforin. (Supplemental Figure 3, *A* and *B*).

We next asked the question whether the increased killing of NPC cells by NK cells pretreated with IFNβ is due to an increased expression of TRAIL and FASL by IFNβ. As shown in Figure 2*D* and Supplemental Figure 4, IFNβ upregulated expression of TRAIL and to a minor extent of FASL on NK cells after an incubation of 24 h. Addition of recombinant TRAIL to cocultures of unstimulated NK cells and NPC cells increased cytotoxicity against NPC cells to a similar extent as pretreatment of NK cells with IFNβ indicating that on engagement of unstimulated NK cells with NPC cells only a part of TRAIL receptors on NPC cells were saturated and that adding TRAIL either externally as recombinant molecule or by IFNβ-stimulated NK cells leads to a dose-dependent increase in NPC killing (Figure 2*E*). Recombinant FASL added to cocultures of unstimulated NK cells and NPC cells increased cytotoxicity of NK cells against NPC cells only to a small amount (Supplemental Figure 5).

In order to confirm that TRAIL signaling plays a key role in the cytotoxicity of NK cells toward NPC cells, especially in the setting of IFNβ-pretreated NK cells, TRAIL-receptor 1 and– 2 expression in target cells was silenced by specific siRNA before coincubation with NK cells. The efficiency of siRNA-knock down was monitored by measuring apoptosis after treatment with recombinant TRAIL via

flow cytometry (Supplementary Figure 6). As shown in Figure 2*F*, transfection of NPC cells with TRAIL-receptor siRNA against TRAIL-receptors but not scr-RNA (nontarget) reduced killing by IFNβ-stimulated NK cells. These results indicate that the cytotoxicity of IFNβ-stimulated NK cells against NPC cells predominately depends on the activation of the TRAIL-signaling pathway.

Pretreatment of NPC Cells with IFNβDecreases Their Sensitivity to Lysis by IFNβ-Activated NK Cells

We next asked the question whether preincubation of NPC cells with IFNβ would further increase the cytotoxicity of IFNβ-pretreated NK cells. In a first experiment NPC cells were incubated IFNβ (1,000 U/ml) for 24 h and then exposed to different concentrations of recombinant TRAIL. As shown in Figure 3*A* pretreatment of NPC but not nasoepithelial cells with IFNβ increased their sensitivity to TRAIL-mediated killing. Also, NPC cells pretreated with IFNβ were more sensitive to killing by non-stimulated NK cells than untreated cells (Figure 3*B*). In contrast, pretreatment of NPC cells with IFNβ reduced their sensitivity against lysis by NK cells activated with IFNβ (Figure 3*B*).

IFNβ Leads to Activation of Inhibitory Checkpoints

As pretreatment with IFNβ of either NK cells or NPC cells increased the sensitivity of NPC cells to NK cell cytotoxicity, but incubation of both cell populations with IFNβ had a smaller effect on NPC lysis than exclusive pretreatment of NK cells with IFNβ, we asked whether IFNβ would impair killing by upregulation of inhibitory checkpoint molecules on both NK and NPC cells. As the PD-1/PD-L1/2 and CTLA-4/B7 checkpoints are amenable to pharmaceutical intervention [32], we focused on the expression of these molecules on NK and NPC cells and their possible modulation by IFNβ. Table 1 shows RNA expression by RNAseq of the checkpoint members above in NPC cell lines before, 6 h and 24 h after incubation with IFNβ. Whereas IFNβ did not modulate mRNA expression of the CTLA-4 members, it upregulated mRNA expression of PD-L1, and to a smaller extent of PD-L2 in all NPC cell lines and PDX cells. Increased expression of PD-L1 but not PD-L2 after incubation of NPC cells with IFNβ was also seen on the cell surface using flow cytometry (Figure 4*A*). No surface expression of PD-1 was observed in NPC cells, either untreated or treated with IFNβ. In addition, unstimulated NK cells weakly expressed PD-1

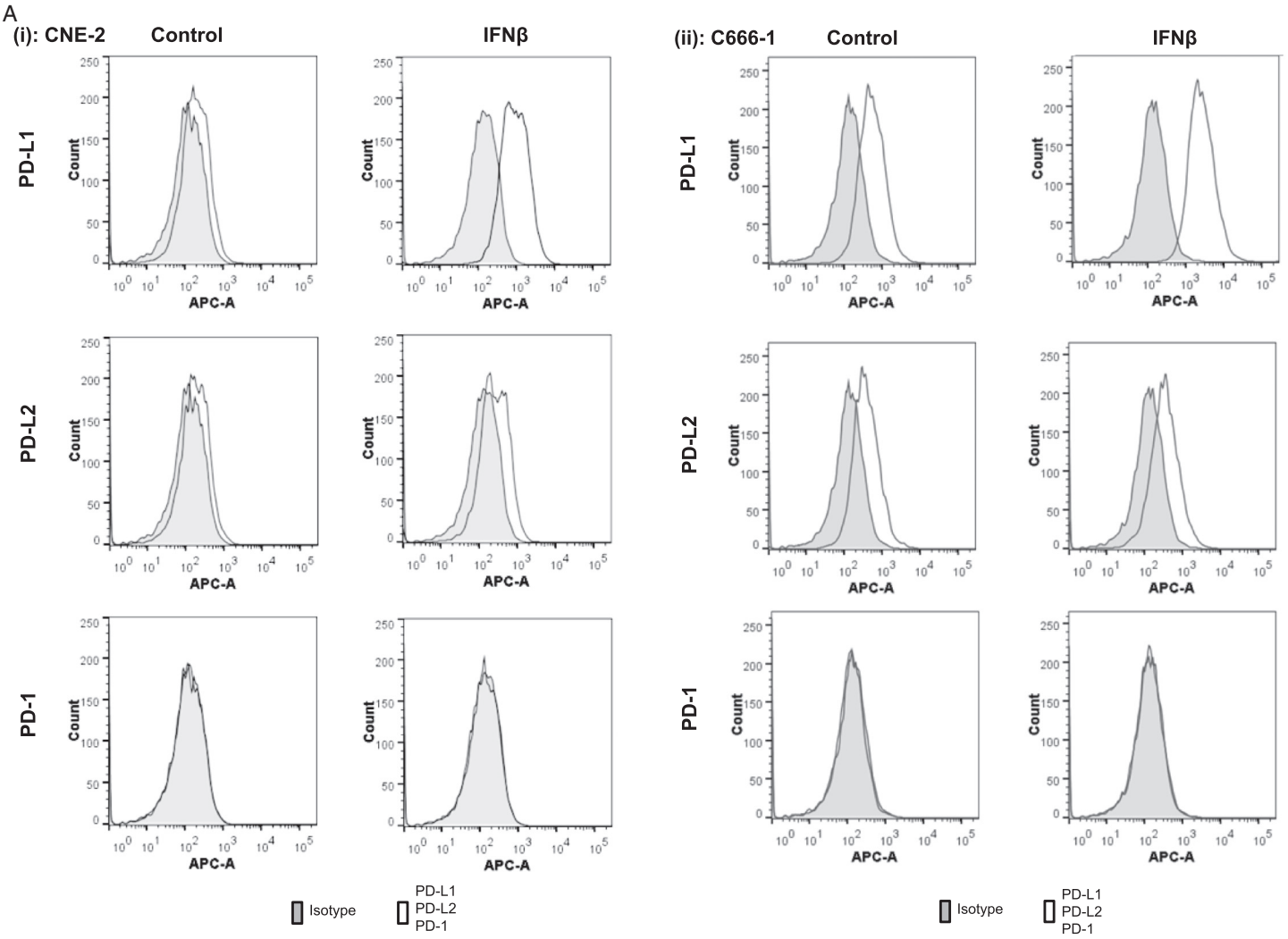

Figure 4. IFNβ activates the PD-L1/PD-1 checkpoint. (A) IFNβ induces surface expression of PD-L1 but not PD-L2 and PD-1 in NPC cells. PD-L1, PD-L2 and PD-1-expression was measured 24 h after incubation with 1,000 U/ml IFNβ. (B) IFNβ upregulates surface expression of PD-1 on NK cells. Cells were incubated with 1,000 U/ml IFNβ for 24 h and PD-1, PD-L1, PD-L2 expression was analyzed by flow cytometry.

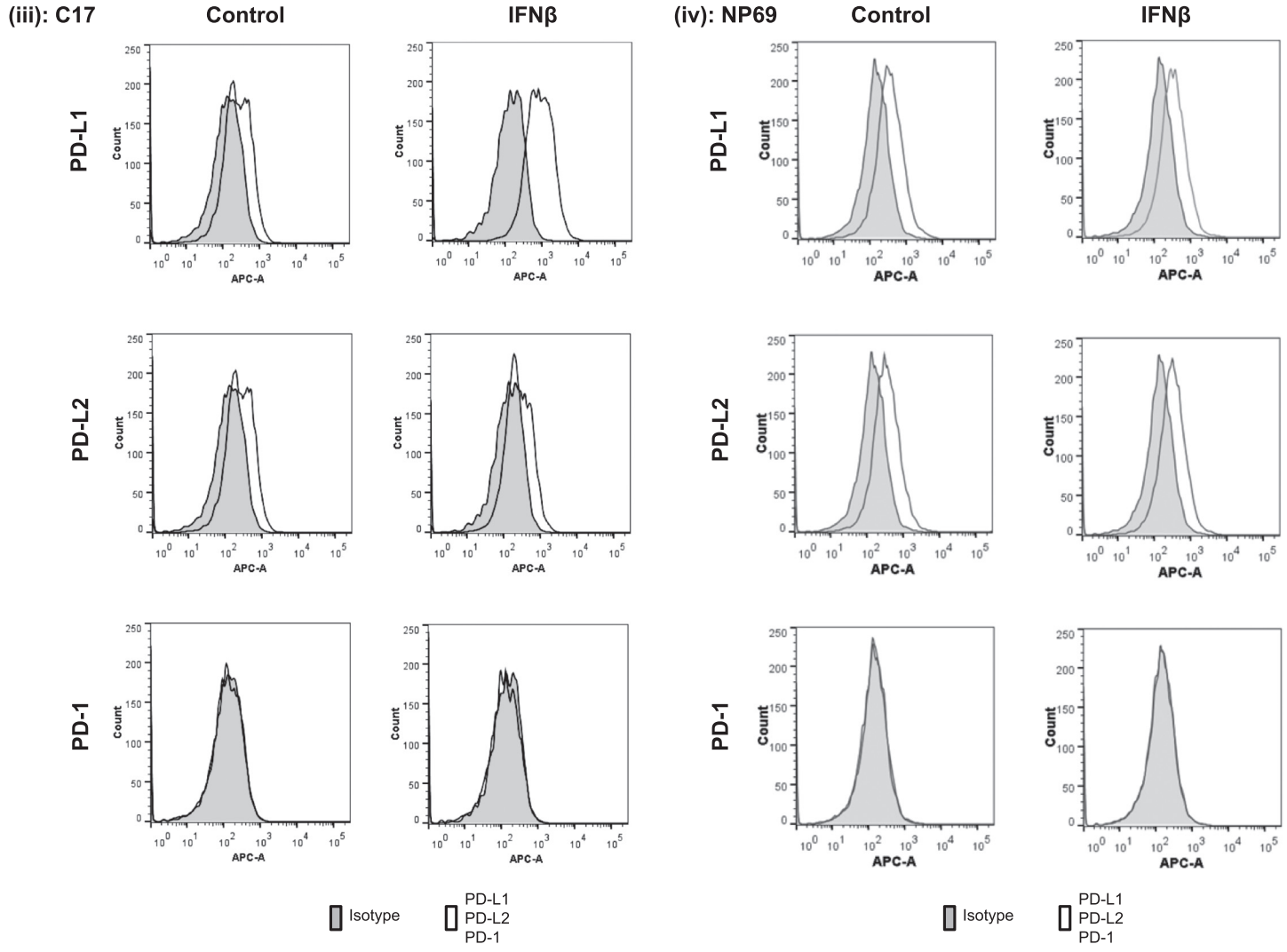

Figure 4. (*continued.*)

which in contrast to CTLA-4 increased after incubation of cells with IFNβ as shown by RNAseq and flow cytometry (Table 2, Figure 4*B*).

Incubation of IFNβ-Pretreated NK Cells With an Anti-PD1 Antibody Increases Their Toxicity Against NPC Cells Pretreated With IFNβ

Having shown that IFNβ increases expression of PD-1 on NK cells and PD-L1 on NPC cells, we asked the question whether activation of the PD-1/PD-L1 checkpoint by IFNβ could explain that pretreatment of NPC cells with IFNβ decreased their sensitivity against IFNβ-pretreated NK cells and whether blockade of this checkpoint with an anti-PD-1 antibody could increase killing. To study this, IFNβ-pretreated NK cells were incubated with the anti-PD-1 antibody nivolumab for 1 h before coculturing them with IFNβ-pretreated NPC cells. Figure 5*A* demonstrates that addition of nivolumab markedly increased sensitivity of IFNβ-pretreated NPC cells to NK cell lysis, making them more sensitive to lysis by IFNβ-pretreated NK cells than NPC cells without IFNβ pretreatment. Nivolumab only slightly increased killing of IFNβ-pretreated NK cells against untreated NPC cells, of unstimulated NK cells against IFNβ-pretreated NPC cells and of unstimulated NK cells against unstimulated NPC cells indicating that marked checkpoint activation only occurred when both effector and targets were stimulated with IFNβ (Figure 5*A* and Supplemental Figure 7). When the experiment above was repeated in the presence of an anti-TRAIL-, or anti-Fas-antibody, or in the presence of concanvalin A to block the respective NK effector pathways, it could be shown that the increased killing after PD-1 blockade was predominately mediated through TRAIL (Figure 5*B*).

PD-1 Blockade Increases the Cytotoxicity of IFNβ-Activated NK Cells Against IFNβ-Treated NPC Cells by Releasing Intracellular TRAIL From NK Cells

We then wondered whether the increase of cytotoxicity of IFNβ-activated NK cells by anti-PD-1 blockade was due to upregulation of TRAIL. Therefore, TRAIL-surface expression was measured by flow cytometry in IFNβ-activated NK cells treated with or without nivolumab. TRAIL surface expression was slightly increased after nivolumab exposure (Figure 6*A*). Interestingly, when IFNβ-pretreated NK cells got cocultured with IFNβ-treated NPC cells, TRAIL expression was lost in NK cells treated with nivolumab but not in cells without nivolumab. Similarly, TRAIL expression was markedly reduced in IFNβ-treated NK cells when cocultured with untreated NPC cells, suggesting that killing of NPC cells by NK cells

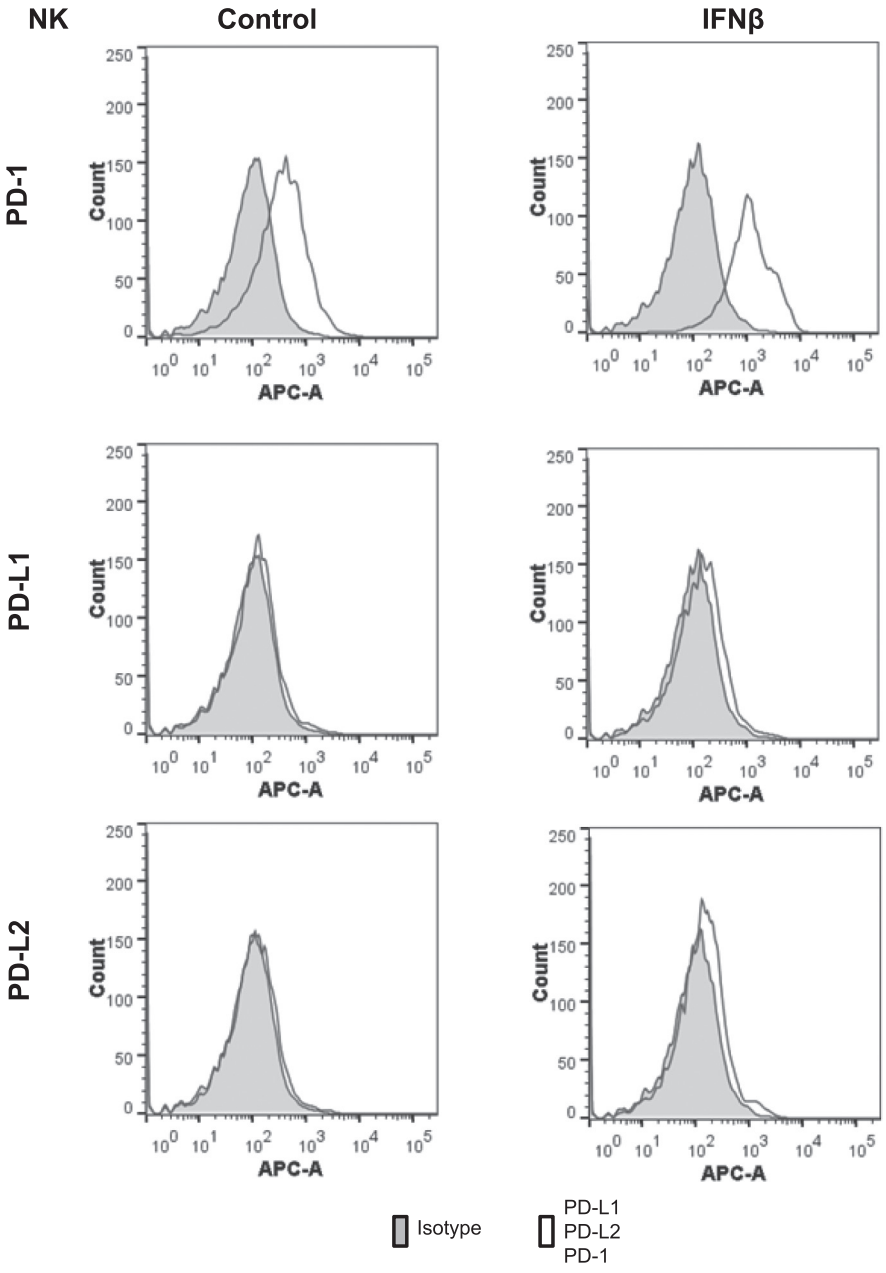

Figure 4. (*continued.*)

was associated with decreased surface expression of TRAIL on NK cells. This was confirmed by confocal microcopy depicting that TRAIL expression of IFNβ-activated NK cells cocultured with IFNβ-activated NPC cells got lost when cells were incubated with nivolumab (Figure 6*B*). As staining of IFNβ-activated NK cells for TRAIL was predominately intracytoplasmic, we examined the concentration of soluble TRAIL (sTRAIL) in the supernatant of cocultures. As shown in Figure 6*C*, treatment of IFNβ-activated NK cells with the anti-PD-1 antibody nivolumab led to a marked increase of sTRAIL after coculture with IFNβ-activated NPC cells compared to cells treated without nivolumab. To investigate whether the increase in sTRAIL was from NK cells or NPC cells, the experiment was repeated with NPC cells treated or not with siRNA against TRAIL. No difference was observed in the amount of sTRAIL measured in the supernatant of cocultures indicating that sTRAIL in cocultures stemmed from NK cells (Supplemental Figure 8). Therefore, it can be assumed that the PD-1/PD-L1 interaction between IFNβ-treated NK- and NPC cells inhibits the release of

Table 2. IFNβ upregulates PD-1 and PD-L1 mRNA expression in NK cells

Molecule	NK		
	Control	6h IFNβ	24h IFNβ
PD-1	0.049	0.244	0.260
PD-L1	0.202	0.963	1.173
PD-L2	0.197	0.220	0.246
CTLA-4	0.093	0.129	0.133
CD80	0.211	0.697	0.591
CD86	0.331	0.207	0.797

Values are given as TPM (transcripts per kilobase million). mRNA expression was analyzed by RNAseq before, 6 h and 24 h after incubation with 1,000 U/ml IFNβ.

cytoplasmic TRAIL from NK cells thereby limiting their cytotoxicity. Upon checkpoint-blockade with anti-PD1 antibody, intracellularly stored TRAIL gets released from IFNβ-activated NK cells increasing their cytotoxicity.

Discussion

In this paper we have demonstrated that (**1**) NK cells effectively kill NPC cells and that killing occurs predominately via the TRAIL signaling pathway, that (**2**) IFNβ increases the cytotoxic activity of

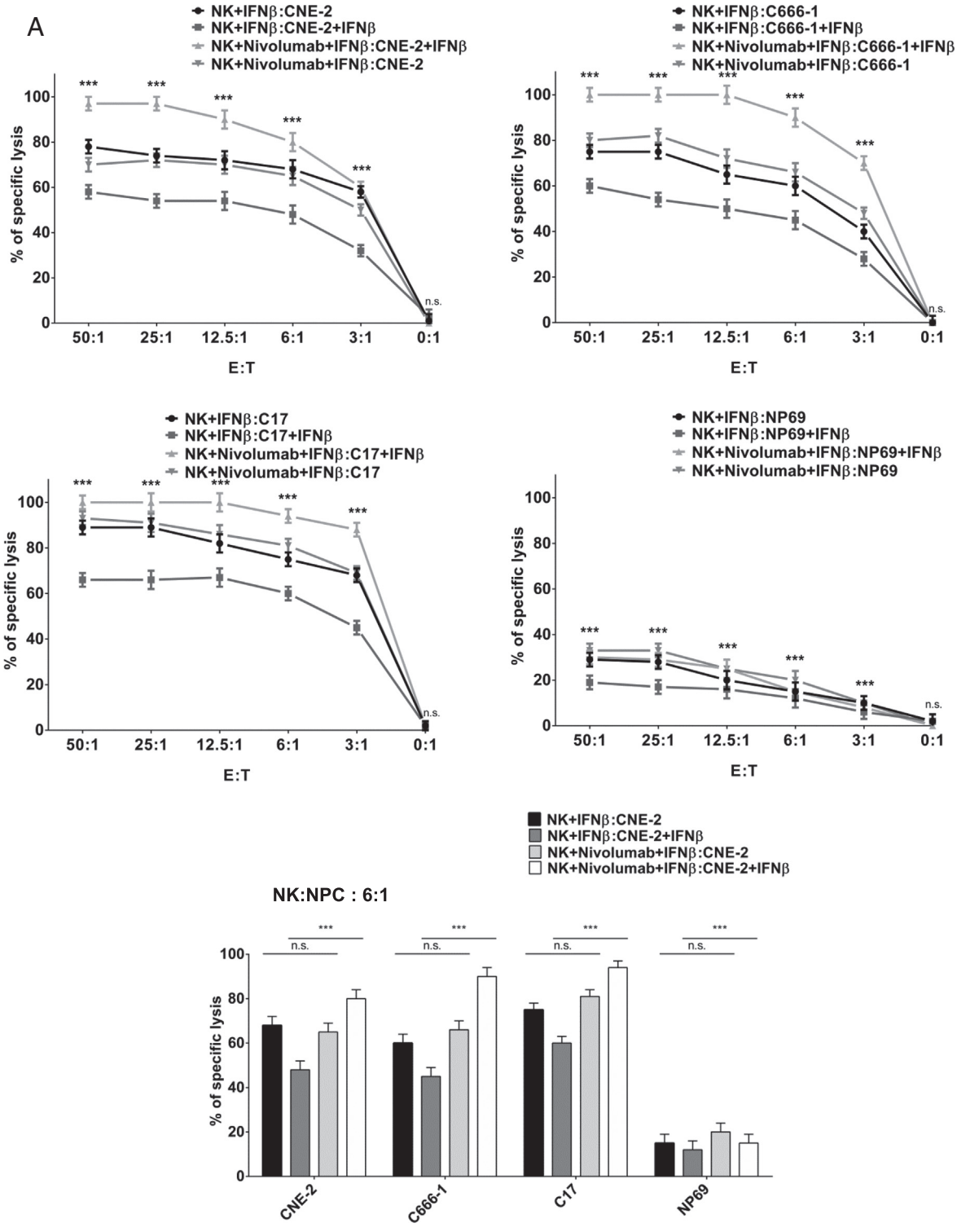

Figure 5. Inhibition of PD-1 increases killing of NPC cells by NK cells in the presence of IFNβ. (A) Pretreatment of NK cells with the PD-1 inhibitor nivolumab leads to a marked increase in killing of NPC cells when effector and targets are both pretreated with IFNβ (1,000 U/ml), as compared when only NK cells are exposed to IFNβ (B) Preincubation of IFNβ-activated and anti-PD1-treated NK cells with anti-TRAIL antibody (100 ng/ml) inhibits the killing of IFNβ-pretreated NPC cells by 80%. Treatment of IFNβ-activated and anti-PD1-treated NK cells with Con A or treatment of IFNβ-pretreated NPC cells with an anti-FAS-antibody reduces killing by 15% and 20%, respectively. Cytotoxicity assays were performed in quintuplicates using the calcein release assay. Data are presented as means ± S.E.M.Asterisks indicate statistically significant differences between all cell lines in one ratio-group (two-way ANOVA; **P* < .05; ***P* < .01; ****P* < .001).

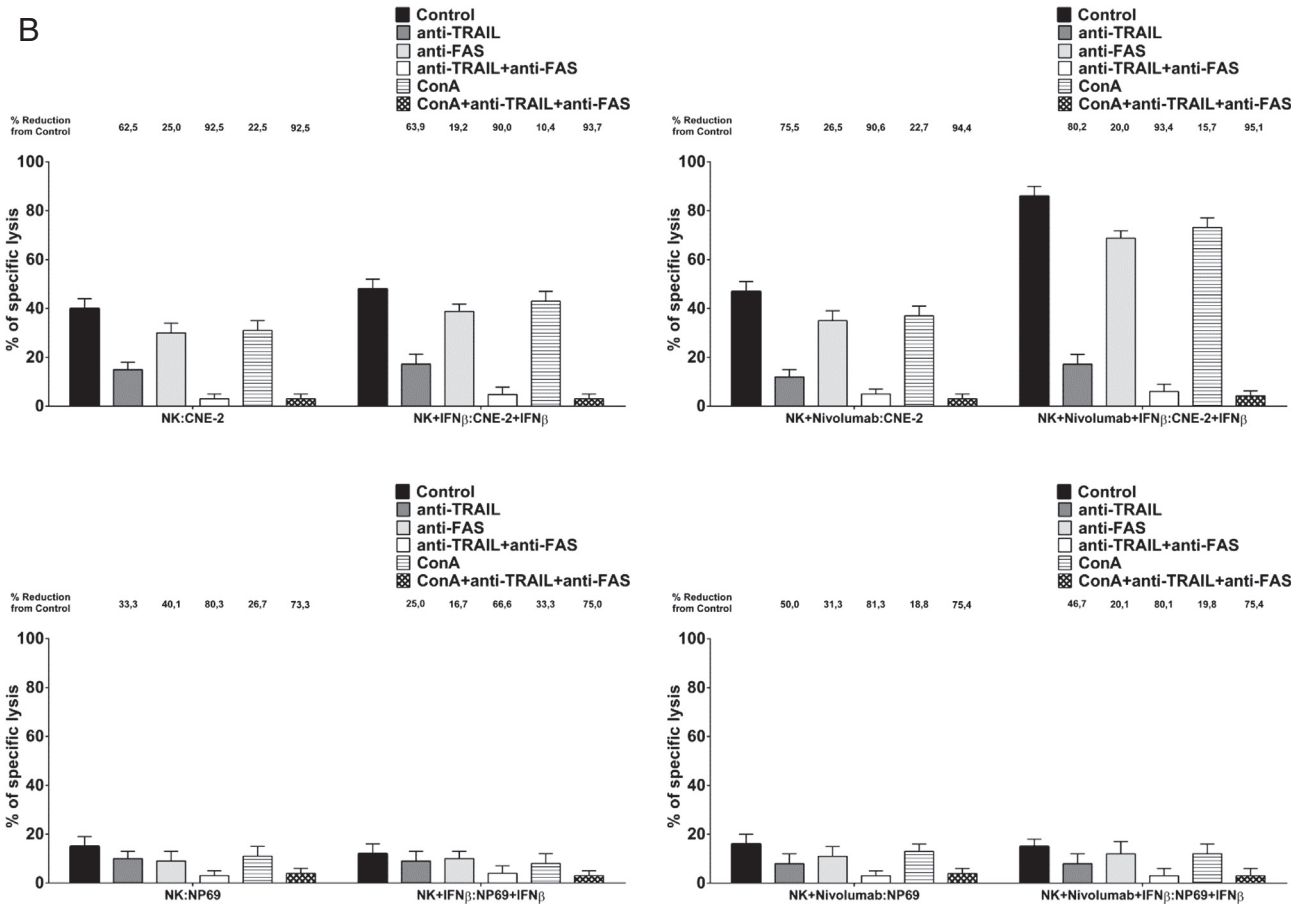

Figure 5. (*continued.*)

NK cells against NPC cells, that (**3**) blocking of the PD-1/PD-L1 checkpoint further increases the killing activity of NK cells against NPC cells in the presence of IFNβ and that **(4)** the increased killing after PD-1/PD-L1 checkpoint blockade is linked to the release of soluble TRAIL from IFNβ-activated NK cells (Figure 7). Our results point to a potential clinical benefit of a combination therapy of IFNβ and PD-1/PD-L1 checkpoint blockade in patients with NPC.

NPC is an immunogenic tumor as the majority of NPC tumors are characterized by a marked lymphomononuclear infiltrate and immune effector mechanisms such as the transfer of EBV-specific T lymphocytes, cytokine-induced killer cells or blockade of the anti-PD-1/PD-L1 checkpoint can lead to tumor control in patients [33–36]. We have previously shown that NPC cells in contrast to nasoepithelial cells have an intact TRAIL signaling pathway and that exposure of NPC cells to IFNβ induced expression of TRAIL in the majority of NPC cell lines studied, leading to subsequent activation of the TRAIL-receptor signaling pathway and apoptosis [13]. TRAIL is also used by lymphocytic effector cells such as T lymphocytes and NK cells to induce apoptosis in susceptible target cells [16,37,38]. Using NK cells from healthy donors, we were able to show that these cells induce cell death in different NPC cells, including cells of a patient-derived xenograft. Cell death was predominately induced by TRAIL, whereas the granzyme B/perforin system played only a minor role in cytotoxicity.

Incubation of NK cells with IFNβ at concentrations achievable in patients increased cytotoxicity of NK cells and was mainly mediated by upregulation of TRAIL expression on NPC cells. Upregulation of TRAIL expression by type-I-interferons has been shown previously and the TRAIL promoter has been demonstrated to contain an interferon-responsive element [16,17,39]. Incubation of NPC cells with IFNβ also increased their susceptibility to NK cell-mediated cytotoxicity or exogenous TRAIL. However, preincubation with IFNβ decreased the sensitivity of NPC cells against IFNβ-activated NK cells which could be overcome by incubating NK cells with the anti-PD-1 inhibitor nivolumab. Here, we could demonstrate that IFNβ increased PD-L1 expression on NPC cells and induced PD-1 expression on NK cells. As in our NPC model, IFNβ has been shown to upregulate PD-L1 expression in different tissues such as human macrophages [40], hepatocytes [41], endothelial cells [42] and in monocytes and dendritic cells of patients with multiple sclerosis [43]. Similar to our observation, induction of PD-1 expression on NK cells has been described when cells were activated and expanded *in vitro* using anti-CD16 antibody and IL-2 [44]. When such activated NK cells were either cocultured *in vitro* with PD-L1 expressing myeloma cells or injected into mice with myeloma xenografts, their cytotoxicity was enhanced by blockade of the PD-1/PD-L1 checkpoint. Upregulation of PD-1 and PD-L1 by type I interferons has also been shown in a melanoma mouse model [45]. Here, targeted activation of the type I IFN system by poly (I:C) in the microenvironment of immune cell-poor melanoma in mice, resulted in cytotoxic immune cell recruitment, upregulation of PD-L1 expression in tumor tissue and increased expression of PD-1 on peripheral blood CD8 + T-cells. The addition of an anti-PD-1 antibody together with but not without poly (I:C), prolonged survival

of mice, indicating that activation of the type I IFN system as in our NPC system leads to subsequent functional activation of the PD-L1/PD-1 immune-inhibitory signaling axis. So far, there has been not much knowledge how blockade of PD-1 leads to increased cytotoxicity of NK cells. In T lymphocytes binding of PD-1 by its ligand PD-L1 or PD-L2 leads to phosphorylation of the PD-1

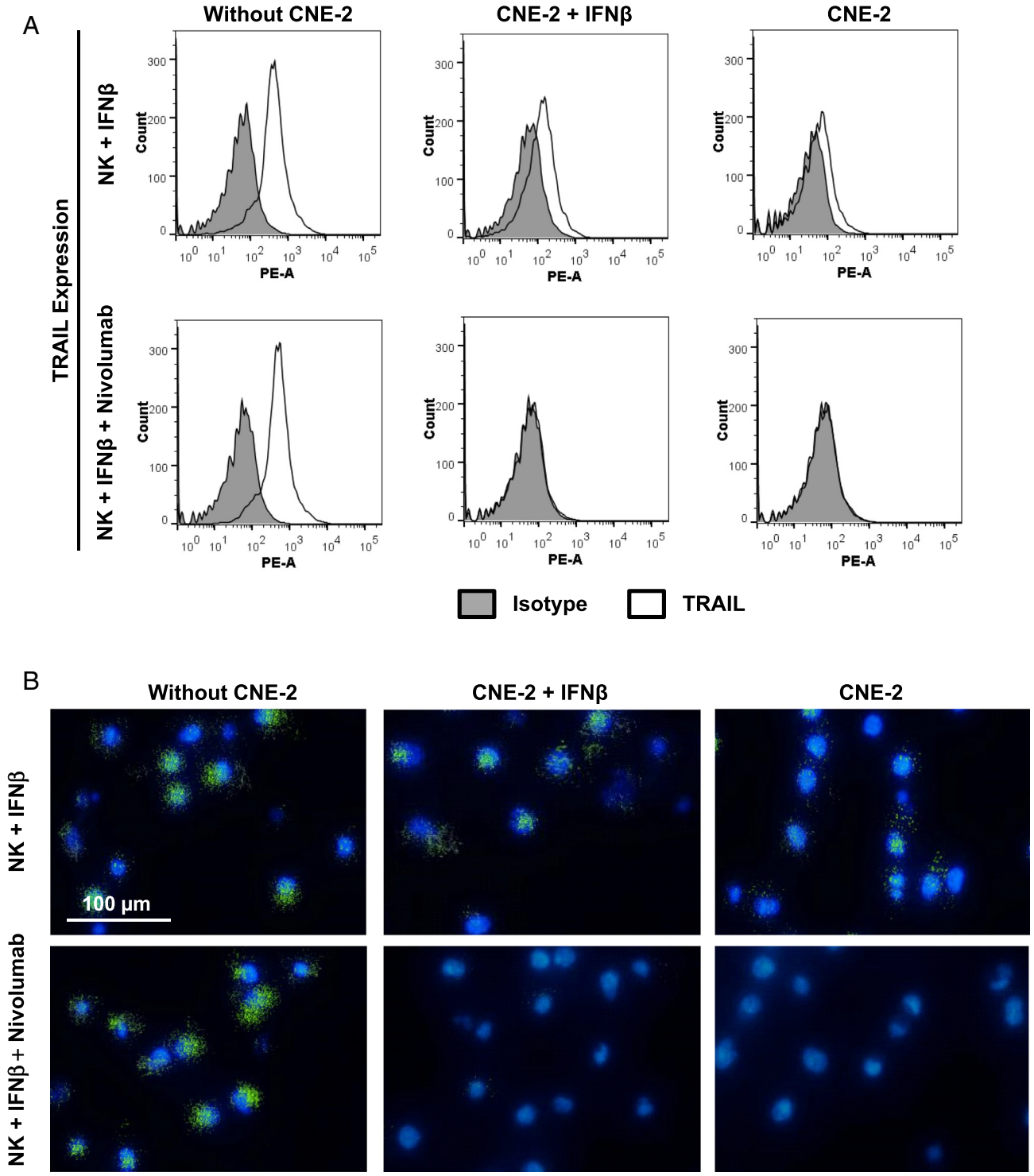

Figure 6. PD-1 blockade increases the cytotoxicity of IFNβ-activated NK cells against IFNβ-treated NPC cells by releasing intracellular TRAIL from NK cells. (A) Surface expression of TRAIL by FACS in IFNβ-activated NK cells treated or not with anti-PD-1 antibody, before or after 4 h coculture with IFNβ-pretreated or untreated NPC cells. Anti-PD-1 treatment leads to loss of TRAIL expression of IFNβ-activated NK cells when cocultured with IFNβ-pretreated NPC cells. (B) Confocal microscopy depicting predominately intracytoplasmic staining for TRAIL in IFNβ-activated NK cells. Loss of TRAIL in anti-PD-1-treated and IFNβ-activated NK cells after coculture with IFNβ-pretreated NPC cells. (C) Soluble TRAIL concentration measured by ELISA. Anti-PD-1 treatment leads to a marked increase in the concentration of sTRAIL in the supernatant of cocultures of IFNβ-activated NK cells with IFNβ-pretreated NPC cells. Data are presented as means ± S.E.M. Asterisks indicate statistically significant differences between all cell lines in one ratio-group (two-way ANOVA; $*P < .05$; $**P < .01$; $***P < .001$).

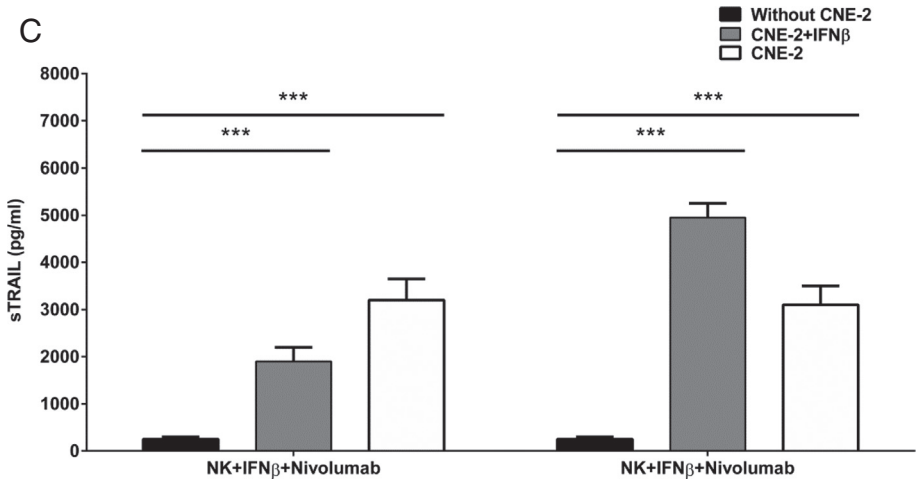

Figure 6. (*continued.*)

cytoplasmic domain and recruitment of the tyrosine phosphatase SHP-2, resulting in reduced phosphorylation of TCR signaling molecules leading to decreased T cell activation and cytokine production and cytokine release [46]. γδ-T lymphocytes have been shown to produce and release soluble TRAIL upon activation leading to apoptosis of lung cancer cells in one model [47]. Based on our experiments we can postulate that blockade of PD-1 in IFNβ-activated NK cells leads to the secretion of soluble TRAIL which then contributes to the killing of TRAIL-susceptible NPC cells.

Our results also suggest that the clinical application of NK cells, together with IFNβ and PD-1/PD-L1 checkpoint blockade could be of therapeutic potential in patients with NPC. Over the last years several clinical trials either with autologous or allogeneic NK cells have been performed in patients with cancer [48]. Infusion of large doses of NK cells have been generally shown to be safe [49]. In a clinical trial involving 10 patients with renal cell carcinoma, the infusion of autologous NK cells expanded and activated *ex vivo* with feeder cells and IL-2, led to a complete and partial remission in 4 and 2 patients, respectively [50]. Tumor responses after the transfer of autologous NK cells have also been observed in patients with glioma and breast cancer [51,52]. In the haploidentical setting the transfer of allogeneic NK cells has been shown to induce complete remissions in

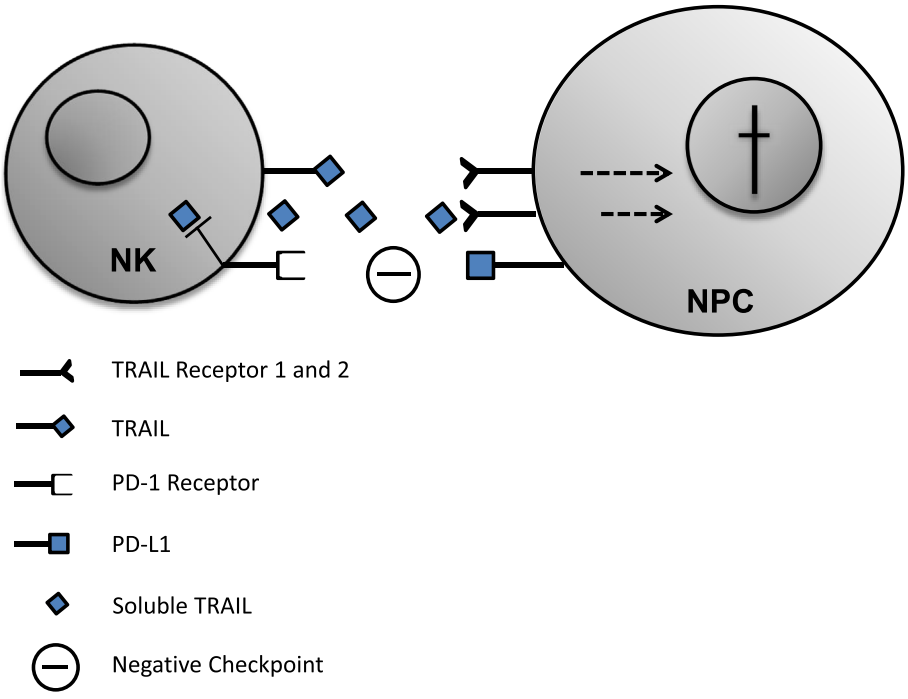

Figure 7. Mechanism of NK killing against NPC. Activation of NK cells by IFNβ induces cytotoxicity against NPC cells through upregulation of expression of surface and soluble TRAIL by NK cells and subsequent activation of the TRAIL-signaling pathway in NPC cells. This cytotoxicity is enhanced by blockade of the PD-1/PD-L1 checkpoint. Blockade of PD-1 in IFNβ-activated NK cells increases the secretion of soluble TRAIL contributing to the killing of TRAIL-susceptible NPC cells.

patients with acute lymphatic and myeloid leukemia, and neuroblastoma [53–55]. Transferred NK cells have been shown to persist and expand *in vivo* [56,57].

Conclusion

In conclusion, IFNβ augments NK-induced cytotoxicity against NPC cells through upregulation of TRAIL expression in NK cells and subsequent activation of the TRAIL-signaling pathway. PD-1 blockade further enhances cytotoxicity of natural killer cells in the presence of IFNβ toward NPC cells. The presented findings suggest that the combination of IFNβ with PD-L1/PD-1 blockade could be of clinical potential in NPC therapy and warrants further studies *in vivo*.

Acknowledgments

We thank Ute Stahlberg for writing assistance.

Funding

The study has been funded internally by the Medical Faculty, RWTH University Aachen.

Appendix A. Supplementary Data

Supplementary data to this article can be found online at https://doi.org/10.1016/j.tranon.2019.04.017.

References

[1] Chua M, Wee J, Hui E, and Chan A (2016). Nasopharyngeal carcinoma. *Lancet* **387**, 1012–1024. doi:10.1016/S0140-6736(15)00055-0.

[2] Huang S, Tsao S, and Tsang C (2018). Interplay of Viral Infection, Host Cell Factors and Tumor Microenvironment in the Pathogenesis of Nasopharyngeal Carcinoma. *Cancers (Basel)* **10**E106. doi:10.3390/cancers10040106.

[3] Kontny U, Franzen S, Behrends U, Buehrlen M, Christiansen H, Delecluse H, Eble M, Feuchtinger T, Gademann G, and Granzen B, et al (2016). Diagnosis and Treatment of Nasopharyngeal Carcinoma in Children and Adolescents - Recommendations of the GPOH-NPC Study Group. *Klin Padiatr* **228**, 105–112. doi:10.1055/s-0041-111180.

[4] Baujat B, Audry H, Bourhis J, Chan A, Onat H, Chua D, Kwong D, Al-Sarraf M, Chi K, and Hareyama M, et al (2006). Chemotherapy as an adjunct to radiotherapy in locally advanced nasopharyngeal carcinoma. *Cochrane Database Syst Rev* **4**, 13–21. doi:10.1002/14651858.

[5] Rodriguez-Galindo C, Wofford M, Castleberry R, Swanson G, London W, Fontanesi J, Pappo A, and Douglass E (2005). Preradiation chemotherapy with methotrexate, cisplatin, 5-fluorouracil, and leucovorin for pediatric nasopharyngeal carcinoma. *Cancer* **103**, 850–857. doi:10.1002/cncr.20823.

[6] Mertens R, Granzen B, Lassay L, Bucsky P, Hundgen M, Stetter G, Heimann G, Weiss C, Hess C, and Gademann G (2005). Treatment of nasopharyngeal carcinoma in children and adolescents: definitive results of a multicenter study (NPC-91-GPOH). *Cancer* **104**, 1083–1089. doi:10.1002/cncr.21258.

[7] Buehrlen M, Zwaan C, Granzen B, Lassay L, Deutz P, Vorwerk P, Staatz G, Gademann G, Christiansen H, and Oldenburger F, et al (2012). Multimodal treatment, including interferon beta, of nasopharyngeal carcinoma in children and young adults: preliminary results from the prospective, multicenter study NPC-2003-GPOH/DCOG. *Cancer* **118**, 4892–4900. doi:10.1002/cncr.27395.

[8] Casanova M, Bisogno G, Gandola L, Cecchetto G, Di Cataldo A, Basso E, Indolfi P, D'Angelo P, Favini F, and Collini P, et al (2012). A prospective protocol for nasopharyngeal carcinoma in children and adolescents: the Italian Rare Tumors in Pediatric Age (TREP) project. *Cancer* **118**, 2718–2725. doi:10.1002/cncr.26528.

[9] Mertens R, Lassay L, and Heimann G (1993). Combined treatment of nasopharyngeal cancer in children and adolescents-concept of a study. *Klin Padiatr* **205**, 241–248. doi:10.1055/s-2007-1025233.

[10] Treuner J., Niethammer D., Dannecker G., Hagmann R., Neef V., Hofschneider P. (1980). Successful treatment of nasopharyngeal carcinoma with interferon. Lancet, 1, pp. 817–818, , https://doi.org/10.1016/S0140-6736(80)91308-2.

[11] Swann J, Hayakawa Y, Zerafa N, Sheehan K, Scott B, Schreiber R, Hertzog P, and Smyth M (2007). Type I IFN contributes to NK cell homeostasis, activation, and antitumor function. *J Immunol* **178**, 7540–7549. doi:10.4049/jimmunol.178.12.7540.

[12] Müller L, Aigner P, and Stoibner D (2017). Type I Interferons and Natural Killer Cell Regulation in Cancer. *Front Immunol* **8**, 304. doi:10.4049/jimmunol.178.12.7540 pp.

[13] Makowska A, Wahab L, Braunschweig T, Kapetanakis N, Vokuhl C, Denecke B, Shen L, Busson P, and Kontny U (2018). Interferon beta induces apoptosis in nasopharyngeal carcinoma cells via the TRAIL-signaling pathway. *Oncotarget* **9**, 14228–14250. doi:10.18632/oncotarget.24479.

[14] Mirandola P, Ponti C, Gobbi G, Sponzilli I, Vaccarezza M, Cocco L, Zauli G, Secchiero P, Manzoli F, and Vitale M (2004). Activated human NK and CD8+ T cells express both TNF-related apoptosis-inducing ligand (TRAIL) and TRAIL receptors but are resistant to TRAIL-mediated cytotoxicity. *Blood* **104**, 2418–2424, https://doi.org/10.1182/blood-2004-04-1294.

[15] Louis C, Straathof K, Bollard C, Ennamuri S, Gerken C, Lopez T, Huls M, Sheehan A, Wu M, and Liu H, et al (2010). Adoptive transfer of EBV-specific T cells results in sustained clinical responses in patients with locoregional nasopharyngeal carcinoma. *J Immunother* **33**, 983–990. doi:10.1097/CJI.0b013e3181f3cbf4.

[16] Kayagaki N, Yamaguchi N, Nakayama M, Eto H, Okumura K, and Yagita H (1999). Type I interferons (IFNs) regulate tumor necrosis factor-related apoptosis-inducing ligand (TRAIL) expression on human T cells: A novel mechanism for the antitumor effects of type I IFNs. *J Exp Med* **189**, 1451–1460. doi:10.1084/jem.189.9.1451.

[17] Sato K, Hida S, Takayanagi H, Yokochi T, Kayagaki N, Takeda K, Yagita H, Okumura K, Tanaka N, and Taniguchi T, et al (2001). Antiviral response by natural killer cells through TRAIL gene induction by IFN-alpha/beta. *Eur J Immunol* **31**, 3138–3146, https://doi.org/10.1002/1521-4141(200111)31.

[18] Yun S, Vincelette N, Green M, Wahner Hendrickson A, and Abraham I (2016). Targeting immune checkpoints in unresectable metastatic cutaneous melanoma: a systematic review and meta-analysis of anti-CTLA-4 and anti-PD-1 agents trials. *Cancer Med* **5**, 1481–1491, https://doi.org/10.1002/cam4.732.

[19] Hude I, Sasse S, Engert A, and Bröckelmann P (2017). The emerging role of immune checkpoint inhibition in malignant lymphoma. *Haematologica* **102**, 30–42, https://doi.org/10.3324/haematol.2016.150656.

[20] Sizhong Z, Xiukung G, and Yi Z (1983). Cytogenetic studies on an epithelial cell line derived from poorly differentiated nasopharyngeal carcinoma. *Int J Cancer* **31**, 587–590. doi:10.1002/ijc.2910310509|.

[21] Cheung S., Huang D., Hui A., Lo K., Ko C., Tsang Y., Wong N., Whitney B., Lee J. (1999). Nasopharyngeal carcinoma cell line (C666-1) consistently harbouring Epstein-Barr virus. Int J Cancer, 83, pp. 121–126, , https://doi.org/10.1002/(SICI)1097-0215(19990924)83:1%3C121::AID-IJC21%3E3.0.CO;2-F%A6.

[22] Tsao S., Wang X., Liu Y., Cheung Y., Feng H., Zheng Z., Wong N., Yuen P., Lo A., Wong Y., et al. (2002). Establishment of two immortalized nasopharyngeal epithelial cell lines using SV40 large T and HPV16E6/E7 viral oncogenes. Biochim Biophys Acta, 1590, pp. 150–158, , https://doi.org/10.1016/S0167-4889(02)00208-2.

[23] Gressette M, Vérillaud B, Jimenez-Pailhès A, Lelièvre H, Lo K, Ferrand F, Gattolliat C, Jacquet-Bescond A, Kraus-Berthier L, and Depil S, et al (2014). Treatment of nasopharyngeal carcinoma cells with the histone-deacetylase inhibitor abexinostat: cooperative effects with cisplatin and radiotherapy on patient-derived xenografts. *PLoS One* **9**E91325. doi:10.1371/journal.pone.0091325.

[24] Keane M, Ettenberg S, Nau M, Russell E, and Lipkowitz S (February 1999). (1999). Chemotherapy augments TRAIL-induced apoptosis in breast cell lines. Cancer Res., 59, pp. 734–741. DOI: Published; February 1999 .

[25] Gatti R, Belletti S, Orlandini G, Bussolati O, Dall'Asta V, and Gazzola G (1998). Comparison of annexin V and calcein-AM as early vital markers of apoptosis in adherent cells by confocal laser microscopy. *J Histochem Cytochem* **46**, 895–900. doi:10.1177/002215549804600804.

[26] Bevers E, Comfurius P, and Zwaal R (1996). Regulatory mechanisms in maintenance and modulation of transmembrane lipid asymmetry: pathophysiological implications. *Lupus* **5**, 480–487. doi:10.1177/096120339600500531.

[27] Wagle P, Nikolić M, and Frommolt P (2015). QuickNGS elevates Next-Generation Sequencing data analysis to a new level of automation. *BMC Genomics* **16**E487, https://doi.org/10.1186/s12864-015-1695-x.

[28] Martínez-Lostao L, Anel A, and Pardo J (2015). How Do Cytotoxic Lymphocytes Kill Cancer Cells? *Clin Cancer Res* **21**, 5047–5056. doi:10.1158/1078-0432.CCR-15-0685.

[29] Guicciardi M., Gores G. (2009). Life and death by death receptors. FASEB J, 23, pp. 1625–1637, http:// doi: , https://doi.org/10.1096/fj.08-111005.

[30] Oliver B, Kohli E, and Kasper L (2011). Interferon therapy in relapsing-remitting multiple sclerosis: a systematic review and meta-analysis of the comparative trials. *J Neurol Sci* **302**, 96–105. doi:10.1016/j.jns.2010.11.003.

[31] Buchwalder P, Buclin T, Trinchard I, Munafo A, and Biollaz J (2000). Pharmacokinetics and pharmacodynamics of IFN-beta 1a in healthy volunteers. *J Interferon Cytokine Res* **20**, 857–866. doi:10.1089/10799900050163226.

[32] Hao C, Tian J, Liu H, Li F, Niu H, and Zhu B (2017). Efficacy and safety of anti-PD-1 and anti-PD-1 combined with anti-CTLA-4 immunotherapy to advanced melanoma: A systematic review and meta-analysis of randomized controlled trials. *Medicine (Baltimore)* **96**E7325. doi:10.1097/MD.0000000000007325.

[33] Huang J, Fogg M, Wirth L, Daley H, Ritz J, Posner M, Wang F, and Lorch J (2017). Epstein-Barr virus-specific adoptive immunotherapy for recurrent, metastatic nasopharyngeal carcinoma. *Cancer* **123**, 2642–2650. doi:10.1002/cncr.30541.

[34] Smith C, Lee V, Schuessler A, Beagley L, Rehan S, Tsang J, Li V, Tiu R, Smith D, and Neller M, et al (2017). Pre-emptive and therapeutic adoptive immunotherapy for nasopharyngeal carcinoma: Phenotype and effector function of T cells impact on clinical response. *Oncoimmunology* **6**E1273311. doi:10.1080/2162402X.2016.1273311.

[35] Li Y, Pan K, Liu L, Li Y, Gu M, Zhang H, Shen W, Xia J, and Li J (2015). Sequential Cytokine-Induced Killer Cell Immunotherapy Enhances the Efficacy of the Gemcitabine Plus Cisplatin Chemotherapy Regimen for Metastatic Nasopharyngeal Carcinoma. *PLoS One* **10**E0130620. doi:10.1371/journal.pone.0130620.

[36] Hsu C, Lee S, Ejadi S, Even C, Cohen R, Le Tourneau R, Mehnert J, Algazi A, Brummelen E, and Saraf S, et al (2017). Safety and Antitumor Activity of Pembrolizumab in Patients With Programmed Death-Ligand 1-Positive Nasopharyngeal Carcinoma: Results of the KEYNOTE-028 Study. *J Clin Oncol* **35**, 4050–4056. doi:10.1200/JCO.2017.73.3675.

[37] Lelaidier M, Dìaz-Rodriguez Y, Cordeau M, Cordeiro P, Haddad E, Herblot S, and Duval M (2015). TRAIL-mediated killing of acute lymphoblastic leukemia by plasmacytoid dendritic cell-activated natural killer cells. *Oncotarget* **30**, E29440-29455. doi:10.18632/oncotarget.4984.

[38] Wennerberg E, Sarhan D, Carlsten M, Kaminsky V, D'Arcy P, Zhivotovsky B, Childs R, and Lundqvist A (2013). Doxorubicin sensitizes human tumor cells to NK cell- and T-cell-mediated killing by augmented TRAIL receptor signaling. *Int J Cancer* **133**, 1643–1652. doi:10.1002/ijc.28163.

[39] Allen J., El-Deiry W. (2012). Regulation of the human TRAIL gene. Cancer Biol Ther, 13, pp. 1143–51, http:// doi: , https://doi.org/10.4161/cbt.21354.

[40] Staples K., Nicholas B., McKendry R., Spalluto C., Wallington J., BraggC., Robinson E., Martin K., Djukanović R., Wilkinson T. (2015). Viral infection of human lung macrophages increases PDL1 expression via IFNβ. PLoS One, 10, E0121527, http:// doi: , https://doi.org/10.1371/journal.pone.0121527.

[41] Mühlbauer M, Fleck M, Schütz C, Weiss T, Froh M, Blank C, Schölmerich J, and Hellerbrand C (2006). PD-L1 is induced in hepatocytes by viral infection and by interferon-alpha and -gamma and mediates T cell apoptosis. *J Hepatol* **45**, 520–528. doi:10.1016/j.jhep.2006.05.007.

[42] Eppihimer M, Gunn J, Freeman G, Greenfield E, Chernova T, Erickson J, and Leonard J (2002). Expression and regulation of the PD-L1 immunoinhibitory molecule on microvascular endothelial cells. *Microcirculation* **9**, 133–145. doi:10.1038/sj/mn/7800123.

[43] Schreiner B, Mitsdoerffer M, Kieseier B, Chen L, Hartung H, Weller M, and Wiendl H (2004). Interferon-beta enhances monocyte and dendritic cell expression of B7-H1 (PD-L1), a strong inhibitor of autologous T-cell activation: relevance for the immune modulatory effect in multiple sclerosis. *J Neuroimmunol* **155**, 172–182. doi:10.1016/j.jneuroim.2004.06.013.

[44] Guo Y, Feng X, Jiang Y, Shi X, Xing X, Liu X, Li N, Fadeel B, and Zheng C (2016). PD1 blockade enhances cytotoxicity of in vitro expanded natural killer cells towards myeloma cells. *Oncotarget* **7**, E48360-48374. doi:10.18632/oncotarget.10235.

[45] Bald T., Landsberg J., Lopez-Ramos D., Renn M., Glodde N., Jansen P., Gaffal E., Steitz J., Tolba R., Kalinke U., et al. (2014), Immune cell-poor melanomas benefit from PD-1 blockade after targeted type I IFN activation. Cancer Discov, 4, pp. 674–687, http:// doi: , https://doi.org/10.1158/2159-8290.CD-13-0458.

[46] Baumeister S., Freeman G., Dranoff G., Sharpe A. (2016). Coinhibitory Pathways in Immunotherapy for Cancer. Ann Rev Immunol, 34, pp. 539–573, http:// doi: , https://doi.org/10.1146/annurev-immunol-032414-112049.

[47] Dokouhaki P., Schuh N., Joe B., Allen C., Der S., Tsao M., Zhang L. (2013). NKG2D regulates production of soluble TRAIL by ex vivo expanded human γδ T cells. Eur J Immunol, 43, pp. 3175–3182, http:// doi: , https://doi.org/10.1002/eji.201243150.

[48] Dahlberg C, Sarhan D, Chrobok M, Duru A, and Alici E (2015). Natural Killer Cell-Based Therapies Targeting Cancer: Possible Strategies to Gain and Sustain Anti-Tumor Activity. *Front Immunol* **6**E00605. doi:10.3389/fimmu.2015.00605.

[49] Sakamoto N., Ishikawa T., Kokura S., Okayama T., Oka K., Ideno M., Sakai F., Kato A., Tanabe M., Enoki T., et al. (2015), Phase I clinical trial of autologous NK cell therapy using novel expansion method in patients with advanced digestive cancer. J Transl Med, 13, pp. 277, http:// doi: , https://doi.org/10.1186/s12967-015-0632-8.

[50] Escudier B., Farace F., Angevin E., Charpentier F., Nitenberg G., Triebel F., Hercend T. (1994). Immunotherapy with interleukin-2 (IL2) and lymphokine-activated natural killer cells: improvement of clinical responses in metastatic renal cell carcinoma patients previously treated with IL2. Eur J Cancer, 30A, pp. 1078–1083, , https://doi.org/10.1016/0959-8049(94)90460-X.

[51] Ishikawa E, Tsuboi K, Saijo K, Harada H, Takano S, Nose T, and Ohno T (2004). Autologous natural killer cell therapy for human recurrent malignant glioma. *Anticancer Res* **24**, 1861–1871. doi:10.1159/000492509.

[52] deMagalhaes-Silverman M, Donnenberg A, Lembersky B, Elder E, Lister J, Rybka W, Whiteside T, and Ball E (2000). Posttransplant adoptive immunotherapy with activated natural killer cells in patients with metastatic breast cancer. *J Immunother* **23**, 154–160. doi:10.1097/00002371-200001000-00018.

[53] Brehm C, Huenecke S, Quaiser A, Esser R, Bremm M, Kloess S, Soerensen J, Kreyenberg H, Seidl C, and Becker P, et al (2011). IL-2 stimulated but not unstimulated NK cells induce selective disappearance of peripheral blood cells: concomitant results to a phase I/II study. *PLoS One* **6**E27351. doi:10.1371/journal.pone.0027351.

[54] Passweg J, Tichelli A, Meyer-Monard S, Heim M, Stern D, Kühne T, Favre G, and Gratwohl A (2004). Purified donor NK-lymphocyte infusion to consolidate engraftment after haploidentical stem cell transplantation. *Leukemia* **18**, 1835–1838, https://doi.org/10.1038/sj.leu.2403524.

[55] Miller J, Soignier Y, Panoskaltsis-Mortari A, McNearney S, Yun G, Fautsch S, McKenna D, Le C, Defor D, and Burns L, et al (2005). Successful adoptive transfer and in vivo expansion of human haploidentical NK cells in patients with cancer. *Blood* **105**, 3051–3057. doi:10.1182/blood-2004-07-2974.

[56] Rubnitz J, Inaba H, Ribeiro R, Pounds S, Rooney B, Bell T, Pui C, and Leung W (2010). NKAML: a pilot study to determine the safety and feasibility of haploidentical natural killer cell transplantation in childhood acute myeloid leukemia. *J Clin Oncol* **28**, 955–959, https://doi.org/10.1200/JCO.2009.24.4590.

[57] Szmania S, Lapteva N, Garg T, Greenway A, Lingo J, Nair B, Stone K, Woods E, Khan J, and Stivers J, et al (2015). Ex vivo-expanded natural killer cells demonstrate robust proliferation in vivo in high-risk relapsed multiple myeloma patients. *J Immunother* **38**, 24–36. doi:10.1097/CJI.0000000000000059.

Cancer Immunology, Immunotherapy
https://doi.org/10.1007/s00262-019-02368-y

ORIGINAL ARTICLE

Interferon beta increases NK cell cytotoxicity against tumor cells in patients with nasopharyngeal carcinoma via tumor necrosis factor apoptosis-inducing ligand

Anna Makowska[1] · Sabrina Franzen[1] · Till Braunschweig[2] · Bernd Denecke[3] · Lian Shen[1] · Valentin Baloche[4] · Pierre Busson[4] · Udo Kontny[1]

Received: 2 February 2019 / Accepted: 5 July 2019

Abstract

Background Nasopharyngeal carcinoma (NPC) is an EBV-associated neoplasm occurring endemically in Southeast Asia and sporadically all over the world. In children and adolescents, high cure rates have been obtained using chemotherapy, radiochemotherapy and maintenance therapy with interferon beta (IFNβ). The mechanism by which IFNβ contributes to a low systemic relapse rate has not yet been fully revealed.

Patients and methods NK cells and serum samples from two patients with NPC were analyzed before and at different time points during IFNβ therapy, for assessment of TRAIL expression and NK cell cytotoxicity. Cytotoxicity was measured using the calcein release assay and the contribution of different death effector pathways was analyzed using specific inhibitors.

Results Treatment with IFNβ induced TRAIL expression on patients' NK cells and increased their cytotoxicity against NPC targets in vitro. NK cell-mediated cytotoxicity was predominately mediated via TRAIL. IFNβ also induced the production of soluble TRAIL (sTRAIL) by NK cells and its release upon contact with NPC cells. IFNβ treatment increased serum levels of sTRAIL in patients. Moreover, sTRAIL concentrated from patients' serum samples induced apoptosis ex vivo in NPC cells from a patient-derived xenograft.

Conclusion Increased cytotoxicity of NK cells against NPC cells and increased serum levels of biologically active TRAIL in patients treated with IFNβ could be a means to eliminate micrometastatic disease and explain the low systemic relapse rate in this patient group.

Keywords Nasopharyngeal carcinoma · Interferon beta · Natural killer cells · Tumor necrosis factor apoptosis-inducing ligand · Adolescents · Children

Abbreviations

Calcein-AM	Calcein-acetyoxymethyl
EBV	Epstein–Barr virus
FAS	First apoptosis signal
FASL	FAS ligand
GPOH	German Society of Pediatric Oncology and Hematology
IFNα, -β	Interferon alpha, -beta
IFNAR1, -2	Interferon alpha and beta receptor subunit 1, -2
NGS	Next-generation sequencing
NPC	Nasopharyngeal carcinoma
PDX	Patient-derived xenograft
RFU	Relative fluorescence units
sTRAIL	Soluble TRAIL
TRAIL-R1, -R2	TRAIL receptor 1, -2

Electronic supplementary material The online version of this article (https://doi.org/10.1007/s00262-019-02368-y) contains supplementary material, which is available to authorized users.

✉ Udo Kontny
ukontny@ukaachen.de

[1] Division of Pediatric Hematology, Oncology and Stem Cell Transplantation, Medical Faculty, Rhenish-Westphalian Technical University, Pauwelsstraße 30, 52074 Aachen, Germany

[2] Institute of Pathology, Medical Faculty, Rhenish-Westphalian Technical University, Aachen, Germany

[3] Interdisciplinary Center for Clinical Research, Medical Faculty, Rhenish-Westphalian Technical University, Aachen, Germany

[4] CNRS, UMR 8126, Gustave Roussy, Université Paris-Saclay, 94805 Villejuif, France

Published online: 16 July 2019

Introduction

Nasopharyngeal carcinoma (NPC) is an EBV-associated neoplasm mainly occurring in adolescents/young adults and in people above 60 years of age [1, 2]. It is endemic in Southeast Asia, occurs less frequently in Northern Africa, and is rarely seen in Europe and the Americas. Tumors in the endemic region and the young age group are usually undifferentiated and characterized by a marked lymphomononuclear infiltrate [3, 4]. State-of-the-art treatment in adolescents and young adults consists of the combination of neoadjuvant chemotherapy and radiochemotherapy resulting in 5-year event-free survival rates of around 80% in patients with localized disease [5–8]. Relapse occurs in about 20% of patients and is almost exclusively metastatic. The addition of interferon beta (IFNβ) as maintenance therapy has led to event-free survival rates above 90% as demonstrated by two prospective multicenter studies, NPC-GPOH-91 and NPC-GPOH-2003 [6, 7]. Though there is sufficient clinical evidence about the effectiveness of IFNβ in the treatment of NPC [6, 7, 9–12], studies exploring the mechanisms of the anti-tumor effects of IFNβ against NPC have only started recently. In a first study, we could show that IFNβ induces apoptosis in NPC cell lines and cells of a patient-derived xenograft at concentrations achievable in humans [13]. Apoptosis was dependent on the induction of surface expression of the death ligand TRAIL on NPC cells and subsequent activation of the TRAIL signaling pathway. However, the anti-tumor effect of IFNβ, in general, is not only mediated by its direct action on tumor cells but also indirectly by activating an anti-tumor immune response [14, 15]. IFNβ has been shown to induce TRAIL expression on NK cells [16, 17]. NK cells play a major role in protecting against tumor initiation and metastasis [18–21]. Recently, a higher extent of tumor infiltration by NK cells was shown to be associated with a better overall and progression-free survival in NPC patients [22]. There is evidence that the anti-metastatic effect of NK cells is mediated by TRAIL and that this effect can be augmented by type I interferons [23, 24]. In a mouse model of hepatic metastasis, injection of IFNα into mice led to activation of liver NK cells and metastasis rejection [25].

In this study, we have analyzed the effects of IFNβ treatment on two NPC patients with regard to the expression of TRAIL and its influence on NK cell cytotoxicity.

Materials and methods

Patients

Blood samples from two patients with EBV-positive nasopharyngeal carcinoma were used in this study. Patients were two 18-year-old females who were coincidentally diagnosed with EBV-positive NPC at the same time, which was classified by histology as nonkeratinizing squamous cell carcinoma of undifferentiated subtype in both cases. Both patients had locoregional NPC with stage II (T2N1M0) in one patient and stage III (T3N1M0) in the other one. Patients were treated according to the recommendations of the Nasopharyngeal Carcinoma Study Section of the German Society of Pediatric Oncology and Hematology (GPOH) which propose three cycles of chemotherapy with 5-fluorouracil and cisplatin, followed by radiochemotherapy and then maintenance therapy with IFNβ over 6 months [26]. Therapy with IFNβ was started with 3 Mio U of human recombinant IFNβ s.c. three times a week for the 1st week, and was afterwards increased to 6 Mio U s.c. three times a week. Blood samples were drawn at 0 h, 6 h and 24 h on day 1 of weeks 1, 2 and 4 of maintenance treatment with IFNβ. Both patients received recombinant human interferon beta 1a (Rebif®, Merck, Darmstadt, Germany). For comparison, peripheral blood mononuclear cells (PBMC) from healthy volunteers were obtained.

Purification of NK cells

PBMC were obtained from EDTA blood samples by Ficoll density gradient centrifugation. NK cells were isolated from PBMC by positive magnetic selection of CD56+ cells according to the manufacturer's instructions (Miltenyi, Bergisch Gladbach, Germany). Purified NK cells were used immediately for flow cytometric analysis, cytotoxicity assays and RNA sequencing. NK cells were held in RPMI1640 medium (Gibco, Paisley, UK) supplemented with 10% FCS and 100 U/ml penicillin and 100 mg/ml streptomycin (Gibco).

Cell lines

The NPC cell line C666-1 and the nasopharyngeal epithelial cell line NP69 were used. C666-1 cells were maintained in RPMI1640 medium (Gibco) supplemented with 10% fetal bovine serum (Gibco), 100 U/ml penicillin, 100 mg/ml streptomycin (Gibco), and NP69 cells in keratinocyte serum-free medium (Gibco). Cells were cultured in a humidified incubator with 95% air and 5% CO_2 at 37 °C. Cell line C666-1 expresses FAS and TRAIL-R2, cell line NP-69 FAS and TRAIL-R1 as previously shown [13].

Patient-derived xenograft

The xenograft C17 was established from a patient with an EBV-positive metastatic NPC in nude mice [27]. For the

experiment described, single cells suspensions were derived from freshly isolated C17 tumor fragments as described before [13]. C17 cells express FAS and TRAIL-R2 as reported previously [13].

Animal studies

Swiss nude mice were bred in the animal facility at Gustave Roussy and housed in pathogen-free conditions in filter cap cages holding a maximum of five animals with irradiated aspen chip bedding and cotton fiber nesting material. They were maintained on a 12/12 light/dark cycle, with ad libitum UV-treated water and RM1 rodent diet. Typically, xenografts were performed on 6–8 female mice by subcutaneous introduction of tumor fragments (about 200 mg) under general anesthesia. They were sacrificed when the total tumor volume reached 1700 mm^3. The animals were monitored for signs of pain, such as immobility or restlessness, reduction of drinking and food intake. The persistence of abnormal behaviors led to the euthanasia of animals with suffering presumption. Prior to tumor collection, mice were sacrificed by cervical dislocation. Otherwise, mice were euthanatized by carbon dioxide asphyxiation.

Reagents

For cell culture studies, human recombinant interferon beta (IFNβ) was obtained from R&D System, the primary mouse monoclonal antibody against TRAIL, clone 2E5, from Enzo Life Science (Paris, France), anti-FAS antibody, clone ZB4, from Millipore (Temecula, USA) and concanavalin A from Sigma (St. Louis, USA). For immunohistochemistry, the following antibodies were used: mouse anti-human TRAIL-R1 monoclonal antibody (Enzo Life Science, Clone TR1.02), mouse anti-human TRAIL-R2 monoclonal antibody (Enzo Life Science, Clone DJR2-2), mouse anti-human TRAIL monoclonal antibody (Enzo Life Science, Clone III6F) as well as mouse anti-pan Keratin-, anti-CD3- and anti-CD56 antibodies (DAKO-Agilent).

Immunohistochemistry

Immunohistochemistry was performed on 3 µm sections of formalin-fixed, paraffin-embedded tissue samples as previously described [13].

Calcein release assay

A standard fluorescence-based calcein-AM release assay was used to determine the cytotoxic activity, using patients' and healthy donors' NK cells as effector cells and C666-1, C17 and NP69 cells lines as a source of target cells. Target cells were washed and resuspended in 15 µM calcein-AM (Thermo Fisher, Eugene, USA) for 30 min at 37 °C, before co-incubation with NK cells at different effector to target (E:T) ratios as indicated for 4 h at 37 °C. 4% Triton (Merck, Darmstadt, Germany) was added to ensure maximum calcein release in controls. After centrifugation, cell-free supernatant was transferred to a Cell Carrier Plate (Sarstedt, Nümbrecht, Germany) to measure relative fluorescence units (RFU) using a spectrophotometer (TECAN Infinite 200 Pro, Tecan, Männedorf, Switzerland). The percentage of specific lysis was calculated as follows: [(RFU value in respective treatment − RFU value in control (spontaneous release))/(RFU value Triton (maximum release) − RFU value in control (spontaneous release)) × 100].

Analysis of NK cell cytotoxicity

To analyze the contribution of death ligands in NK cell-mediated killing, NK cells were incubated with the blocking anti-TRAIL mAb, clone 2E5 (100 ng/ml) and NPC cells were incubated with the anti-FAS antibody, clone ZB4 (100 ng/ml); cells were pretreated for 1 h with the respective antibodies before co-culture. In some experiments, NK cells were pretreated with 2.5 µg/ml concanavalin A (ConA; Sigma) for 2 h to inactivate the perforin/granzyme B pathway. Cytotoxicity was determined via calcein release assay as described above.

Flow cytometric analysis

NK cells from patients were suspended at a density of 1×10^5 cells in 500 µl of medium. Additionally, NK cells from healthy donors had been pretreated with or without IFNβ at 1000 U/ml for 24 h. Analysis of surface expression of TRAIL was done as previously described [13].

RNA extraction, library construction and sequencing

Total RNA was isolated from patients' NK cells and NK cells of healthy donors treated with 1000 U/ml IFNβ for 0 h (control), 6 h or 24 h using the Maxwell RSC Simply RNA Tissue kit (Promega, Mannheim, Germany) according to the manufacturer´s instructions. RNA quality was evaluated using the Agilent 4200 Tape Station (RNA screen tape assay) (Agilent, Santa Clara, USA) and quantification was done using the Quantus Fluorometer (Promega). Libraries were generated from 1 µg of total RNA with the TrueSeq Stranded Total RNA Library Prep Kit (Illumina, San Diego, USA) and Ribo-Zero Gold Kit (Illumina) as described by the manufacturer. Quality and quantity of the RNA libraries were assessed using the 4200 Tape Station (D1000 screen tape assay) and the Quantus Fluorometer, respectively. The libraries were run on an Illumina NextSeq 500 platform using the High Output 150 cycles Kit (2 × 76 cycles,

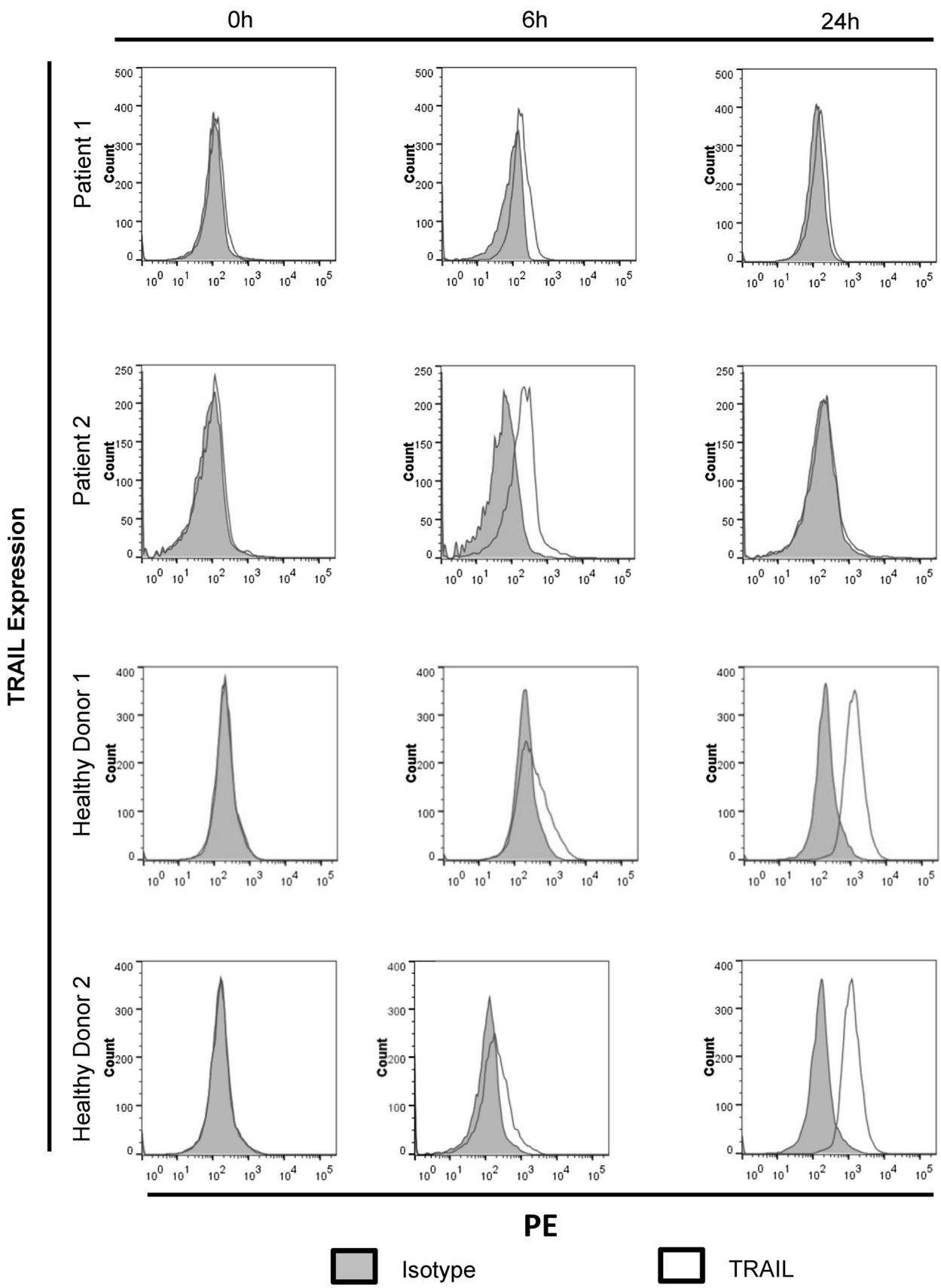
0h
6h
24h
TRAIL Expression
Patient 1
Patient 2
Healthy Donor 1
Healthy Donor 2
Count
PE
Isotype
TRAIL

◂**Fig. 1** Induction of TRAIL expression on NK cells of NPC patients after subcutaneous administration of IFNβ. Two patients with NPC received 3 Mio U IFNβ s.c. at day 1 of week 1 of IFNβ maintenance therapy. NK cells were isolated before, 6 h and 24 h after IFNβ administration. TRAIL expression was measured by flow cytometry. As controls, NK cells from two healthy volunteers were incubated in vitro with 1000 U/ml IFNβ. Representative histograms of triplicates are shown

paired-end reads, single index) (Illumina), resulting in 101.5 M reads per sample in average. Data were analyzed with an inhouse pipeline embedded in the workflow management system of the Quick NGS environment.

Determination of sTRAIL serum levels

Serum samples from patients were obtained at the time points described above and were stored at − 80° C until analysis. Supernatants from 4 h co-cultures of NK cells, either stimulated or not with 1000 U/ml IFNβ, with C666-1 cells, were collected and stored in − 80° C until analysis. In all samples, levels of soluble TRAIL (sTRAIL) were measured using a commercial ELISA kit (R&D Systems, Minneapolis, USA) according to the manufacturer's instructions.

Concentration of sTRAIL and cytotoxicity assay

Serum from both patients obtained at 24 h after IFNβ injection on day 1 of week 2 was concentrated for protein by centrifugation using Vivaspin columns (Sartorius, Göttingen, Germany). Total protein concentration was then determined by the NanoDrop method [28] (Peqlab, Erlangen, Germany) and sTRAIL concentration was calculated by the initial TRAIL concentration multiplied by the total protein concentration factor. Supernatants or PBS as a control were then added to C17 cells labeled with calcein as above. Where indicated, C17 cells were preincubated with a blocking anti-TRAIL mAb. After incubation for 24 h, cells were centrifuged and cell-free supernatant was analyzed as described before for the calcein assay. As a control, supernatant from PBMC and NK cells of healthy controls incubated for 24 h with 1000 U/ml IFNβ was used.

Confocal microscopy

NK cells were allowed to settle onto poly-L-lysine (Sigma)-coated coverslips for 15 min and were then fixed with 4% paraformaldehyde (Sigma). Staining for TRAIL was done as previously described with a monoclonal antibody recognizing TRAIL (Alexis Biochemicals, San Diego, CA, USA; 1:200) [13].

Statistical analysis

Data are represented as a mean ± SE. Each set of data represents the mean from at least three independent experiments conducted in quintuplicates for calcein release assays and triplicates for flow cytometric analyses. Differences between groups were examined for significant differences by unpaired *t* test. The level of statistical significances was set at $p < 0.05$.

Results

Expression of TRAIL receptors on patients' tumor cells and detection of NK cells in tumor infiltrates

Tumors of both patients were analyzed by immunohistochemistry. Staining for both TRAIL-R1 and -R2 revealed a low to moderate membranous expression pattern in carcinoma cells and histiocytic cells. Inflammatory infiltrates contained mainly CD3-positive T lymphocytes and few NK cells, both expressing TRAIL. The staining patterns were similar for both patients and results are shown for patient 1 (Supplementary figure 1).

IFNβ administered to patients with nasopharyngeal carcinoma induces expression of TRAIL in NK cells

As IFNβ induces the expression of TRAIL on lymphomononuclear cells [16, 17] and nasopharyngeal carcinoma cells have been shown to be susceptible to TRAIL-mediated apoptosis [13], we investigated whether the dosage of IFNβ administered to NPC patients was able to induce TRAIL expression on patients' NK cells. At the beginning of maintenance therapy, PBMCs from two NPC patients were obtained before, 6 h and 24 h after the subcutaneous injection of the first dose of 3 Mio U human recombinant IFNβ. NK cells were isolated and TRAIL surface expression was analyzed by flow cytometry. NK cells isolated from two healthy donors treated in vitro with 1000 U/ml IFNβ served as controls.

As shown in Fig. 1, TRAIL surface expression was not detectable at baseline in NK cells from patients and controls. 6 h after IFNβ administration, TRAIL could be detected on NK cells of both patients, decreasing again at 24 h. Similarly, in NK cells of healthy controls, in vitro incubation with IFNβ led to the appearance of TRAIL after 6 h, further increasing after 24 h. Upregulation of TRAIL by NK cells after in vivo exposure to IFNβ in patients or in vitro exposure in controls was also noted at the mRNA level through RNAseq analysis (Supplementary table 1). Interestingly, the surface expression of TRAIL in patients' NK cells almost disappeared 24 h after administration of IFNβ, but the TRAIL mRNA expression at 24 h was higher than at 6 h.

Increased TRAIL expression of NK cells during IFNβ maintenance therapy

In the GPOH treatment recommendations for NPC, maintenance therapy with IFNβ started with 50% of the IFNβ dose in the 1st week, for optimal monitoring of side effects [6, 7, 26]. If IFNβ is well tolerated, as it was the case for these two patients, the dosage is increased to 100%, equaling 6 Mio U s.c. three times a week, for a total of 6 months. To investigate whether a dose-dependent increase in TRAIL expression of NK cells was seen under the full dose of IFNβ and whether this effect prevailed in the course of maintenance therapy, TRAIL expression on NK cells was also studied on day 1 of weeks 2 and 4 after the start of IFNβ therapy. As shown in Table 1, at week 2, NK cells of both patients already expressed TRAIL at baseline, prior to the next injection of IFNβ, and baseline levels were further increased at week 4. Though the baseline expression of TRAIL at day 1 of weeks 2 and 4 was higher in NK cells of patient 1, TRAIL expression levels on NK cells 6 h after IFNβ administration were in a similar range for both patients, with 88.1% for patient 1 and 87.0% for patient 2 at week 4.

IFNβ administered to patients with nasopharyngeal carcinoma increases NK cell killing of NPC cells in vitro

Since NK cells can be induced to express TRAIL and NPC cells are susceptible to TRAIL-mediated apoptosis, we investigated whether NK cells from NPC patients were able to kill NPC cells, and whether killing could be augmented by IFNβ. Therefore, NK cells isolated from the two patients were incubated with calcein-labeled cells of NPC cell line C666-1 at an effector target (E:T) ratio of 6:1. Cells of the non-malignant nasoepithelial cell line NP69 served as controls. After 4 h of incubation, calcein release of NPC cells was measured as a means of cell death. In addition, NK cells isolated from two healthy donors were stimulated with IFNβ in vitro as above and used as controls.

Figure 2a shows that NK cells from both patients were able to kill NPC cells. Specific killing by NK cells of patient 1 was 30.2 ± 2.4% and of patient 2 34.9 ± 3.2% and was similar to killing by NK cells isolated from two healthy volunteers (32.4 ± 2.9% and 33.9 ± 3.3%). Killing significantly increased when NK cells were isolated from patient 1 after 6 h and patient 2 after 24 h of the first subcutaneous injection of IFNβ. Interestingly, similar to the increase of TRAIL expression on NK cells at weeks 2 and 4, baseline cytotoxicity of NK cells from both patients against C666-1 cells rose 2 and 4 weeks after the start of maintenance therapy and cytotoxicity was even further increased 6 h and 24 h after application of IFNβ, reaching levels of 78.8 ± 3.5% in patient 1 and 75.5 ± 4.9% in patient 2 24 h after IFNß application on day 1 of week 4. Addition of IFNβ in vitro to NK cells isolated from healthy volunteers increased their cytotoxicity to NPC cells after 6 h and 24 h. In contrast, NK cells from patients and controls, either unexposed or exposed to IFNβ were unable to kill nasoepithelial cells NP69. Taken together, these results show that NK cells isolated from patients with NPC are able to kill NPC cells in vitro and that killing is increased when NK cells have been exposed to IFNβ in vivo.

In the next step, we analyzed the contribution of the different death effector pathways in NK cell killing against NPC cells. NK cells kill target cells via two major pathways, the granzyme/perforin pathway and the death ligand pathway with FasL and TRAIL as main effectors in the latter one [29, 30]. To block the granzyme/perforin and TRAIL pathway, NK cells from both patients isolated at day 1 of week 4 and from two healthy volunteers were incubated with concanavalin A and an anti-TRAIL antibody, respectively, before coculturing them with NPC cells; for blockage of the FasL/Fas pathway, NPC cells were incubated with a FAS blocking antibody before coculture with NK cells. Cytotoxicity was measured as shown above using the calcein assay. Figure 2b demonstrates that blocking of TRAIL reduced cytotoxicity of NK cells the most, followed by blockade of FAS; no major effect of concanavalin A was observed. When patients' NK cells were isolated 6 and 24 h after injection of IFNβ, the contribution of TRAIL to NK cell-mediated cytotoxicity was even higher. This suggests that the increase in NK cell cytotoxicity induced by IFNβ results to a large extent from the increase in TRAIL expression on NK cells as shown in Fig. 1. A similar pattern was observed in NK cells isolated from two healthy volunteers stimulated with IFNβ in vitro

Table 1 Induction of TRAIL on the surface of NK cells from NPC patients treated with IFNβ

	Patient 1			Patient 2		
	0 h	6 h	24 h	0 h	6 h	24 h
Week 1	0.05 ± 2.4	9.9 ± 3.0	2.3 ± 2.9	0.04 ± 2.7	18.8 ± 3.1	0.04 ± 3.3
Week 2	22.0 ± 3.3	28.9 ± 2.9	20.1 ± 2.7	11.0 ± 2.5	21.2 ± 3.1	9.1 ± 3.0
Week 4	79.1 ± 3.0	88.1 ± 3.6	83.4 ± 3.0	61.1 ± 3.3	87.0 ± 3.7	84.4 ± 3.1

Values are net fluorescent intensities between mean fluorescent intensity of anti-TRAIL antibody and mean fluorescent intensity of the respective isotype

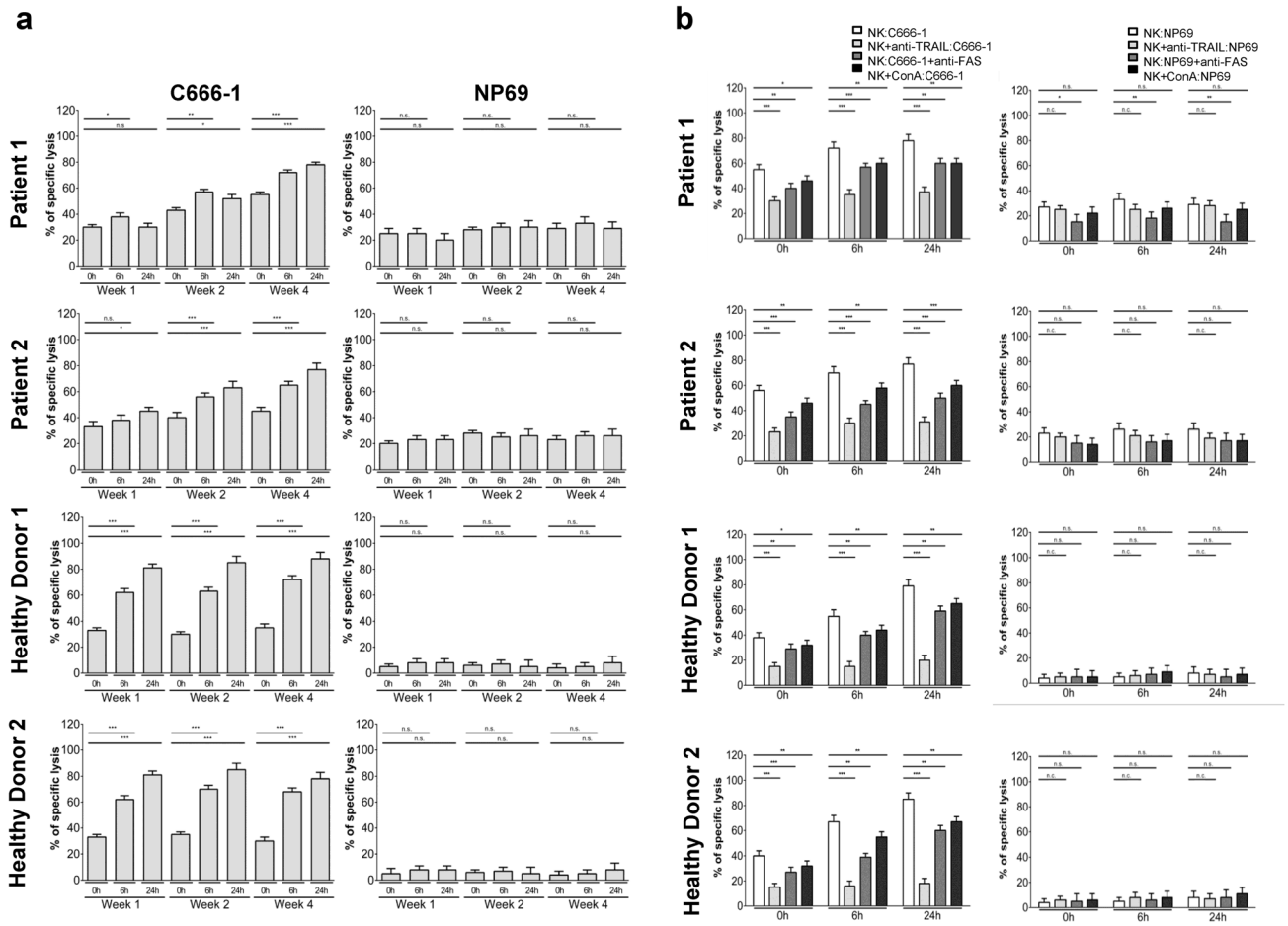

Fig. 2 Increased NK cell cytotoxicity against NPC cells after administration of IFNβ to patients. Patients received 3 Mio U IFNβ at day 1 of week 1 and 6 Mio U IFNβ at day 1 of weeks 2 and 4. NK cells were isolated before, 6 h and 24 h after IFNβ administration and co-cultured at an E:T ratio of 6:1 with calcein-labeled C666-1 cells. NK cells from healthy volunteers, incubated in vitro with IFNβ were used as positive controls for effectors and nasoepithelial cells NP69 for targets. **a** Data are presented as means ± SEM (Student's *t* test; $*P<0.05$; $**P<0.01$; $***P<0.001$). **b** Killing of NPC cells by NK cells is predominately mediated via TRAIL. NK cells from patients isolated before, 6 h and 24 h after IFNβ administration on day 1 of week 4 of IFNβ maintenance therapy were incubated as above with calcein-labeled NPC cells with or without an anti-TRAIL antibody, anti-FAS antibody or concanavalin A. NK cells from healthy donors, incubated in vitro with 1000 U/ml IFNβ were used as controls for effectors and nasoepithelial cells NP69 for targets. Data are presented as means ± SEM (Student's *t* test; $*P<0.05$; $**P<0.01$; $***P<0.001$)

or when NPC cells were exposed to IFNβ before co-culture with NK cells (data not shown).

Increased serum levels of soluble TRAIL during IFNβ maintenance therapy

TRAIL also exists in a soluble form (sTRAIL) which is able to induce apoptosis in susceptible cells [31]. As IFNβ has been previously shown to promote the release of sTRAIL from cell populations such as neutrophils, monocytes, T and B lymphocytes [32], we investigated whether sTRAIL could be detected in the serum of the two patients treated with IFNβ. As shown in Fig. 3, serum sTRAIL levels were in a similar low range for the two NPC patients before the start of IFNβ treatment and the two healthy controls. sTRAIL levels slightly rose 6 h after injection of IFNβ in both patients and doubled after 24 h. Baseline levels of sTRAIL before injection of IFNβ were higher in the 2nd week of maintenance therapy compared to the 1st week, and increased further in the 4th week. These results go along with the previous observations underlining that the effect of IFNβ on expression of membrane-bound TRAIL on NK cells and the release of sTRAIL increases during the 1st month of maintenance therapy.

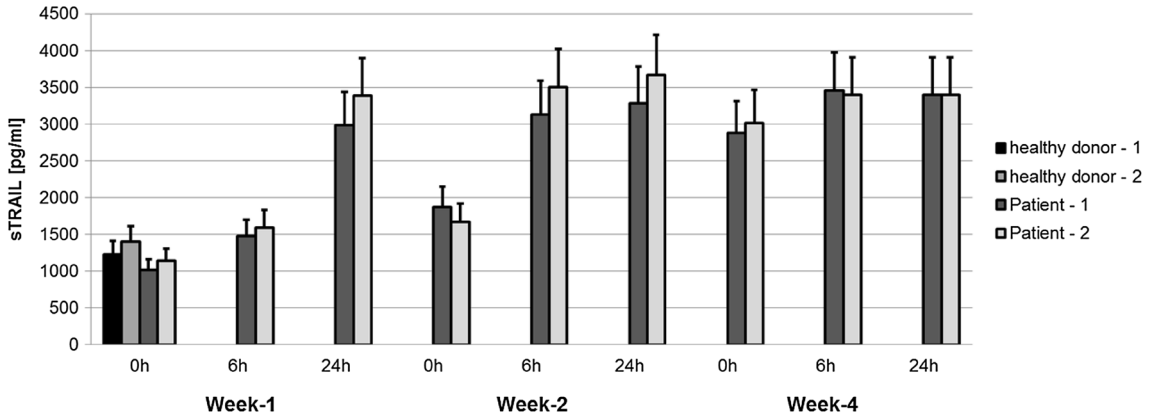

Fig. 3 Increased detection of soluble TRAIL in the serum of NPC patients treated with IFNβ. Serum from two patients with NPC, treated with IFNβ was obtained at the indicated time points; sTRAIL was measured by ELISA. Serum from two healthy volunteers was used as a control. Data are presented as means ± SEM

IFNβ induces the production of soluble TRAIL in NK cells which gets released upon interaction with NPC cells

We were then interested in knowing whether NK cells also produced sTRAIL. For this, NK cells of a healthy volunteer were cultured in the presence or absence of IFNβ for 24 h and then co-cultured with NPC cells C666-1 at an E:T ratio of 6:1. After 4 h of co-culture, supernatant was analyzed for the presence of sTRAIL. sTRAIL was already detectable in the supernatant of unstimulated NK cells and was about four times higher in NK cells incubated with IFNβ (Fig. 4a). When NK cells treated as above were stained for TRAIL and analyzed by confocal microscopy, a predominately cytoplasmatic staining pattern was detected in cells incubated for 24 h with IFNβ but not in unstimulated NK cells. Interestingly, when staining of NK cells was done after 4 h of co-culture with NPC cells, TRAIL could not be detected in IFNβ-stimulated NK cells anymore, indicating that the contact with NPC cells lead to the release of intracellularly stored TRAIL and the loss of surface expression of TRAIL (Fig. 4b). This loss of surface expression of TRAIL could be confirmed by flow cytometry of NK cells treated as above (Fig. 4c), as treatment of NK cells with IFNβ for 24 h lead to marked upregulation of surface TRAIL which then markedly diminished after 4 h of co-culture with NPC cells. Interestingly, downregulation of TRAIL on NK cells was also observed in patients' NK cells obtained 24 h after application of IFNβ compared to 6 h (Fig. 1), suggesting that during the time period of 24 h NK cells had encountered TRAIL receptor-positive target cells inducing the release of sTRAIL as well as leading to the loss of TRAIL surface expression.

Induction of apoptosis by sTRAIL from serum of NPC patients treated with IFNβ

As sTRAIL levels increased in the serum of NPC patients after application of IFNβ, we questioned, whether such sTRAIL was able to induce apoptosis in NPC cells. Therefore, serum from both patients obtained 24 h after IFNβ injection on day 1 in week 4 was concentrated for protein using Vivaspin columns. C17 cells isolated from a patient-derived NPC xenograft and labeled with calcein were then incubated with protein-concentrated serum at 30 ng/ml sTRAIL. As shown in Fig. 5, sTRAIL-containing serum specifically killed NPC cells as killing could be greatly impaired by a TRAIL-blocking antibody. Supernatant of PBMC and NK cells stimulated in vitro with IFNβ also killed C17 cells in a TRAIL-specific manner, indicating that IFNβ induces expression functional sTRAIL by NK cells.

Discussion

In this manuscript, we have shown that IFNβ applied to two patients with NPC (1) induced TRAIL expression on patients' NK cells, (2) increased their cytotoxicity against NPC cells, and (3) that this killing effect was largely mediated by TRAIL. Furthermore, treatment of patients with IFNβ increased serum levels of biologically functional soluble TRAIL (sTRAIL) indicating an additional way to induce apoptosis in NPC cells.

Malignant NPC cells are known to express TRAIL receptors in situ. Examining 174 tumor biopsy specimens from patients with NPC by immunohistochemistry, Wang et al. detected TRAIL-R1 in 29.9% and TRAIL-R2 in 36.6% of tumors [33]; the percentage of biopsy specimens which expressed at least one TRAIL receptors was not given, but

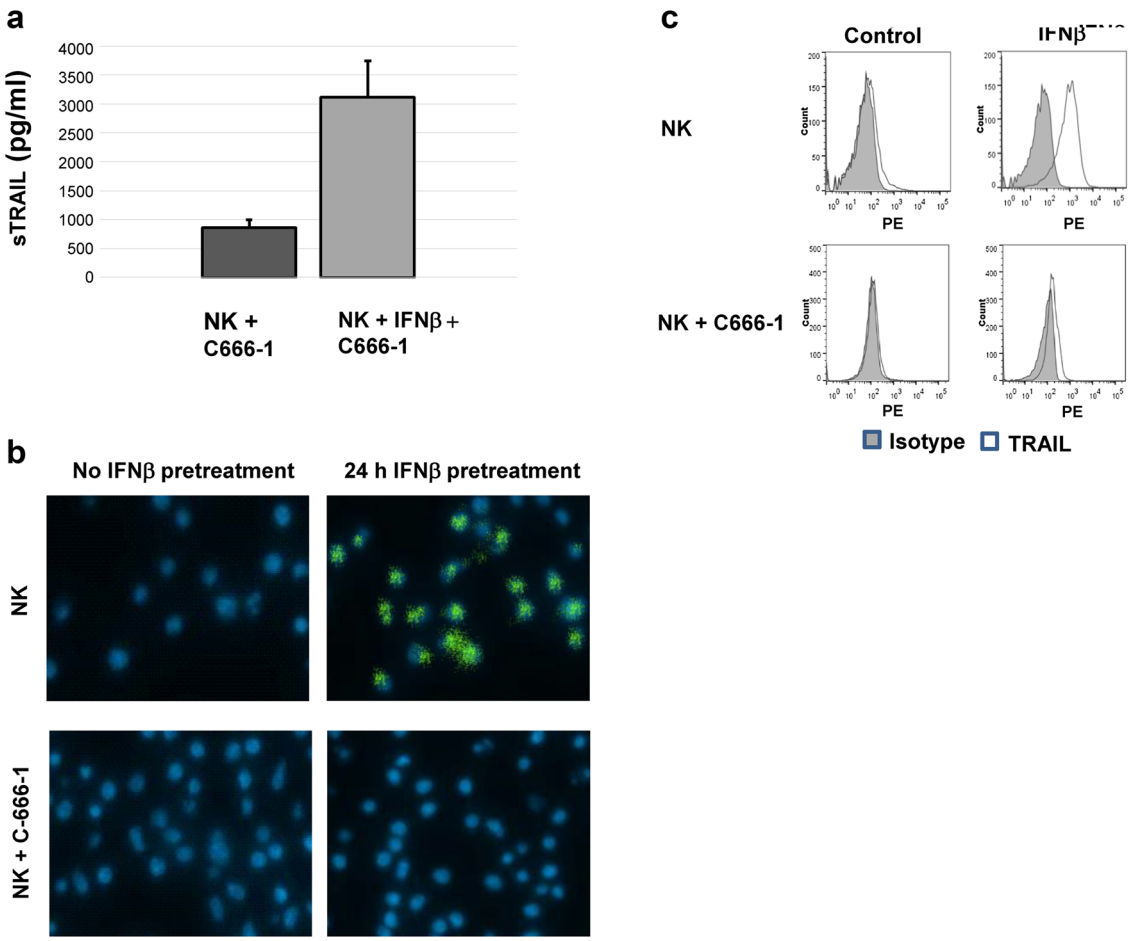

Fig. 4 IFNβ-stimulated NK cells produce soluble TRAIL which gets released upon co-culture with NPC cells. **a** Supernatant from NK cells stimulated or not for 24 h with IFNβ at 1000 U/ml and then co-cultured for 4 h with NPC cells C666-1, and then was analyzed for sTRAIL by ELISA. NK cells treated as above and co-cultured or not for 4 h with NPC cells C666-1 were stained with anti-TRAIL antibody and analyzed by **b** confocal microscopy or **c** flow cytometry

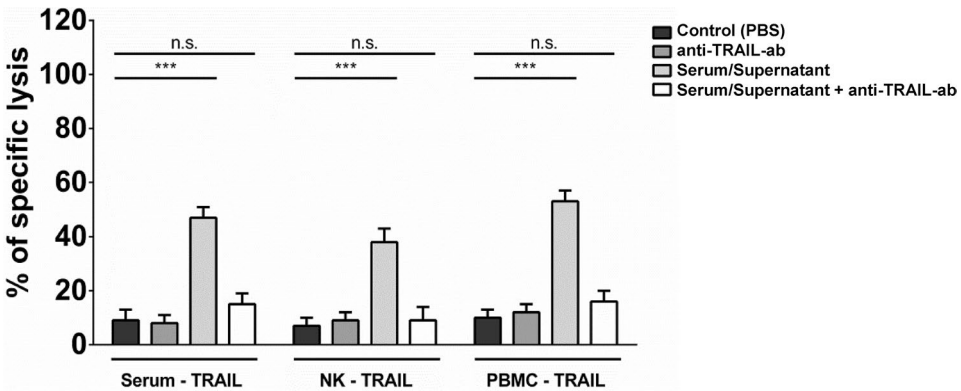

Fig. 5 Soluble TRAIL from the serum of NPC patients kills cells of a patient-derived NPC xenograft. Serum obtained 24 h after injection of IFNβ at d1 of week 4 of IFNβ maintenance therapy was concentrated about tenfold via Vivaspin centrifugation and added to calcein-labeled C17 PDX cells for 24 h. Lysis of target cells was determined by measurement of calcein in collected supernatants by an ELISA reader. Killing could be inhibited by anti-TRAIL antibody. As a control supernatant from PBMC or NK cells incubated in vitro with 1000 U/ml IFNβ was used

one can assume that it ranged between 36.6% and 66.5%. As the activation of either TRAIL-R1 or -R2 is sufficient for eliciting apoptosis, this suggests that a large number of NPC patients bear tumors which are sensitive to apoptosis induction by TRAIL. The authors also found that the expression of TRAIL-R2 was associated with a better survival rate, indicating that the TRAIL signaling pathway is of importance in the elimination of NPC tumor cells [33]. Using a panel of six different NPC cell lines and cells of one patient-derived xenograft (PDX) we have previously shown that all NPC cell lines studied and PDX cells expressed TRAIL receptors and that they were susceptible to TRAIL-mediated apoptosis [13]. In addition, IFNβ-induced expression of TRAIL in all cell lines except for cell line C666-1 and led to the induction of apoptosis in an autocrine way. We were also able to show that IFNβ markedly increased the expression of TRAIL-R2 in NPC cells including PDX cells, suggesting that the clinical use of IFNβ in patients could sensitize tumors to the induction of apoptosis by TRAIL. As IFNβ has been shown to induce TRAIL expression in lymphomononuclear cells in vitro [16, 17], such cells could be an additional means to induce apoptosis in TRAIL-sensitive NPC cells, especially in NPC cells which are refractory to induction of endogenous TRAIL expression like C666-1 cells.

Investigating the expression of TRAIL on NK cells of two patients who started maintenance therapy with IFNβ, we demonstrate that the dosages applied were able to induce TRAIL expression. Upregulation of TRAIL expression on NK cells was already seen when patients received 3 Mio U IFNβ s.c., which was given as a 50% starting dose in the 1st week of maintenance treatment. TRAIL expression on NK cells of both patients was higher when patients got 6 Mio U at week 2 and week 4. Induction of TRAIL in NK cells has also been shown on the mRNA level in patients with chronic HepC infection receiving IFNα which like IFNβ belongs to the type I IFNs [34]; IFNα and IFNβ both signal mainly through IFNAR1 and -AR2 [35].

NK cells have been previously shown to kill NPC cells in vitro [36]. However, killing was only studied after culture of cells for 4 weeks. Killing of NPC cell lines CNE2 and 915 used as targets in that study was at E:T ratios of 3:1 and 10:1 around 20% and 30%, respectively, and in a similar range as for NK cells of the two patients in this study before start of IFNβ maintenance therapy. In our experiments, NK cells isolated from both patients before start of IFNβ treatment killed cells of the NPC cell line C666-1 to a similar extent as did NK cells isolated from two healthy volunteers. When NK cells were isolated from patients after injection of IFNβ, killing of NPC cells by patients' NK cells increased with respect to NK cells from healthy controls. Similarly to the increase in TRAIL expression during the course of maintenance therapy, an increase in the killing ability of patients' NK cells was observed at week 2, when the IFNβ dose was doubled and at week 4 of maintenance therapy. Increased killing of NK cells isolated from cancer patients when treated with IFNβ has been described before by Fujimiya et al., using the CML cell line K562 as a target [37]. In that study, NK cell cytotoxicity increased 24 h after injection of IFNβ; in contrast to our observations, NK cytotoxic activity fell below the original baseline levels after 2 weeks of alternate daily injections of IFNβ in the Fujimiya study.

To kill their targets, NK cells use diverse effectors which belong to two main categories: the granzyme B/perforin and the death ligand pathway with FASL and TRAIL as its major constituents for killing [38]. We investigated the contribution of these different pathways in the killing of NPC cells by NK cells. Our results show that TRAIL is the main effector of apoptosis induction in NPC cells. The contribution of the TRAIL pathway to NPC killing increased when NK cells were isolated after injection of IFNβ or NK cells from healthy volunteers were incubated in vitro with IFNβ. This is in contrast to the killing of other targets by NK cells. The killing of K562 cells by NK cells has been shown to be completely dependent on the granzyme B/perforin pathway [38]. Also, in the killing of neuroblastoma cell lines by NK cells, the granzyme B/perforin pathway represents the major pathway of killing and is supplemented by the TRAIL signaling pathway in TRAIL-sensitive cell lines [39]. In contrast, killing of FAS-positive Jurkat cells by NK cells is only partly dependent on the granzyme B/perforin system and mainly mediated by FASL [40]. The contribution of different death effector pathways probably reflects the sensitivity of target cells to the corresponding death mechanism.

TRAIL is expressed as a membrane-bound protein on the cell surface. It also exists in a soluble form (sTRAIL), generated through enzymatic shedding of surface-anchored TRAIL or by cellular secretion [32]. Type I interferons have been shown to increase the intracellular production of TRAIL in neutrophils, monocytes and T cells [41, 42]. Though only a minor part of TRAIL is secreted after exposure to type I interferons, additional stimuli like TNFα or lipopolysaccharides in neutrophiles or PHA in T cells lead to a rapid release of intracellularly stored TRAIL [42, 43]. The role of sTRAIL derived from NK cells has not been studied so far. Here, we show that IFNβ induces production of TRAIL in NK cells, and that TRAIL is being stored intracellularly and is expressed on the cell membrane, similarly to neutrophils, monocytes and T cells. Contact with NPC cells as targets then leads to the release of intracellularly stored TRAIL and its detection in the supernatant. Interestingly, co-culture with NPC cells also leads to the loss of membranous expression of TRAIL in NK cells, a phenomenon which has not been previously described in other cell systems, especially T cells. The loss of surface expression of TRAIL from NK cells when co-cultured with NPC cells in vitro is consistent with the observation made in vivo that

circulating NK cells lose their TRAIL expression 24 h after the application of IFNβ. One possible explanation could be that in vivo as in vitro NK cells lose their surface TRAIL molecules after the interaction with TRAIL receptor-bearing target cells. As surface-anchored TRAIL has been shown to be cleaved by cathepsin E [44], one can speculate that either NPC cells do express cathepsin on their cell surface or that cathepsin is secreted by NK cells or NPC cells upon cell to cell interaction.

Increased levels of sTRAIL have been measured in patients treated with type I interferons [45, 46]. Treatment of melanoma patients with IFNα resulted in TRAIL plasma levels around 3000 pg/ml [46] which were in a similar range as the levels in our two NPC patients. sTRAIL isolated from PBMC stimulated in vitro with IFNα has been shown to be biologically active and to induce apoptosis in leukemic cells [46]. In our experiments, we directly demonstrate that sTRAIL from serum of NPC patients was able to kill NPC cells of a patient-derived xenograft. We can therefore speculate that the clinical efficacy of IFNβ in patients with NPC might also rely on the induction of apoptosis by circulating sTRAIL in NPC cells.

In summary, IFNβ could mediate an anti-tumor effect in patients with nasopharyngeal carcinoma through induction of TRAIL via three distinct pathways: (1) induction of TRAIL expression on NPC cells and subsequent activation of the TRAIL pathway in an autocrine and paracrine manner [13], (2) induction of TRAIL on NK cells and elimination of NPC cells by activated NK cells, and (3) direct induction of apoptosis in NPC cells via soluble TRAIL. As relapse in the treatment of NPC is nowadays mainly systemic, the activation of these pathways by IFNβ could explain the clinical observation that NPC patients participating in the GPOH studies have an increased disease-free survival and lower risk of distant failure compared to patients on other pediatric studies without adjuvant IFNβ [5–8]. Distant failure rates are even higher in treatment protocols for adult NPC patients which mainly rely on radiochemotherapy [47]. Therefore, the extension of maintenance therapy with IFNβ to adults with NPC is expected to decrease the risk for metastatic relapse and should ideally be tested in a randomized clinical trial. In addition, our study suggests a potential therapeutic benefit of IFNβ-activated NK cells in patients with NPC. The adoptive transfer of NK cells has been shown to be safe and efficacious in various malignancies refractory to standard treatment [48]. A clinical trial using high levels of NK cells in patients with small NPC metastases is currently ongoing in patients with relapsed disease in Guangzhou, China [NCT03007836].

Acknowledgements We thank Anshu Babbar who carefully proofread the manuscript.

Author contribution Conception and design: AM, UK; development of methodology: AM, BD, VB, PB; acquisition of data: AM, SF, TB, LS, BD; analysis and interpretation of data: AM, TB, BD, PB, UK; writing and review of the manuscript: AM, PB, UK; material support: BD, PB; study supervision: UK.

Funding The study has been funded internally by the Medical Faculty, Rhenish-Westphalian Technical University Aachen, Germany.

Compliance with ethical standards

Conflict of interest The authors declare that they have no conflicts of interest.

Ethical standards The final protocol was approved by the ethics committee of the Rhenish-Westphalian Technical University, Aachen, Germany [EK 005/18]. The study was conducted in accordance with the Declaration of Helsinki (2013 revision).

Ethical approval Procedures for mouse handling and xenografts were reviewed and approved by the Ethics Committee for animal experimentation n°26 (Gustave Roussy, Villejuif, France), in accordance with the European directive 2010/63/EU and the decrees of the French ministry of Agriculture R. 214-87 to R. 214-126. The approval was given in November 26, 2015, under the Number Apafis #1605—2015090216498538-v2.

Informed consent Written informed consent was obtained from all individual participants included in the study. Patients were treated at the Uniklinik RWTH Aachen. Informed consent including use of biological specimen (tumor, peripheral blood, urine) and data acquisition and processing was obtained from patients prior to the initiation of the study. Informed consent including the use of peripheral blood and anonymous processing of data was obtained from healthy volunteers who were part of the laboratory staff.

Animal source Swiss nude mice were bred in the animal facility at Gustave Roussy.

Cell line authentication C666-1 was a gift from Prof. Fei–Fei Liu, University of Toronto, Canada [49] and the SV40T-antigen immortalized nasopharyngeal epithelial cell line NP69 [50] was obtained from Prof. George Tsao (The Chinese University of Hong Kong, Hong Kong, China). Cell authentication was done using short tandem repeated profiles as described previously [13], and cell lines were tested at regular intervals by PCR to rule out mycoplasma contamination. Authentication of C17 cell was done by checking of HLA class I alleles by PCR (A02.01/A26.01–B44.02/B51.01).

References

1. Chang ET, Adami HO (2006) The enigmatic epidemiology of nasopharyngeal carcinoma. Cancer Epidemiol Biomarkers Prev 15:1765–1777
2. Chua M, Wee J, Hui E, Chan A (2016) Nasopharyngeal carcinoma. Lancet 387(10022):1012–1024
3. Jayasurya A, Bay BH, Yap WM, Tan NG (2000) Lymphocytic infiltration in undifferentiated nasopharyngeal cancer. Arch Otolaryngol Head Neck Surg 126(11):1329–1332
4. Huang S, Tsao S, Tsang C (2018) Interplay of viral infection, host cell factors and tumor microenvironment in the

pathogenesis of nasopharyngeal carcinoma. Cancers (Basel) 10(4):106
5. Rodriguez-Galindo C, Wofford M, Castleberry RP et al (2005) Preradiation chemotherapy with methotrexate, cisplatin, 5-fluorouracil, and leucovorin for pediatric nasopharyngeal carcinoma. Cancer 103:850–857
6. Mertens R, Granzen B, Lassay L et al (2005) Treatment of nasopharyngeal carcinoma in children and adolescents. Definitive results of a multicenter study (NPC-91-GPOH). Cancer 104:1083–1089
7. Buehrlen M, Zwaan CM, Granzen B et al (2012) Multimodal treatment, including interferon beta, of nasopharyngeal carcinoma in children and young adults. Cancer 118:4892–4900
8. Casanova M, Bisogno G, Gandola L et al (2012) A prospective protocol for nasopharyngeal carcinoma in children and adolescents. Cancer 118:2718–2725
9. Treuner J, Niethammer D, Dannecker G, Hagmann R, Neef V, Hofschneider P (1980) Successful treatment of nasopharyngeal carcinoma with interferon. Lancet 1(8172):817–818
10. Connors JM, Andiman WA, Howarth CB, Liu E, Merigan TC, Savage ME, Jacobs C (1985) Treatment of nasopharyngeal carcinoma with human leukocyte interferon. J Clin Oncol 3(6):813–817
11. Mertens R, Lassay L, Heimann G (1993) Combined treatment of nasopharyngeal cancer in children and adolescents-concept of a study. Klin Padiatr 205(4):241–248
12. Wolff HA, Rödel RM, Gunawan B et al (2010) Nasopharyngeal carcinoma in adults: treatment results after long-term follow-up with special reference to adjuvant interferon-beta in undifferentiated carcinomas. J Cancer Res Clin Oncol 136:89–97
13. Makowska A, Wahab L, Braunschweig T, Kapetanakis N, Vokuhl C, Denecke B, Shen L, Busson P, Kontny U (2018) Interferon beta induces apoptosis in nasopharyngeal carcinoma cells via the TRAIL-signaling pathway. Oncotarget. 9(18):14228–14250
14. Parker BS, Rautela J, Hertzog PJ (2016) Antitumour actions of interferons: implications for cancer therapy. Nat Rev Cancer 16:131–144
15. Bekisz J, Sato Y, Johnson C, Husain SR, Puri RK, Zoon KC (2013) Immunomodulatory effects of interferons in malignancies. J Interf Cytokine Res 33:154–161
16. Kayagaki N, Yamaguchi N, Nakayama M, Eto H, Okumura K, Yagita H (1999) Type I interferons (IFNs) regulate tumor necrosis factor-related apoptosis-inducing ligand (TRAIL) expression on human T cells: a novel mechanism for the antitumor effects of type I IFNs. J Exp Med 189(9):1451–1460
17. Sato K, Hida S, Takayanagi H, Yokochi T, Kayagaki N, Takeda K, Yagita H, Okumura K, Tanaka N, Taniguchi T, Ogasawara K (2001) Antiviral response by natural killer cells through TRAIL gene induction by IFN-alpha/beta. Eur J Immunol 31:3138–3146
18. Morvan MG, Lanier LL (2016) NK cells and cancer: you can teach innate cells new tricks. Nat Rev Cancer 16(1):7–19
19. Smyth MJ, Crowe NY, Godfrey DI (2001) NK cells and NKT cells collaborate in host protection from methylcholanthrene-induced fibrosarcoma. Int Immunol 13(4):459–463
20. Street SE, Hayakawa Y, Zhan Y, Lew AM, MacGregor D, Jamieson AM, Diefenbach A, Yagita H, Godfrey DI, Smyth MJ (2004) Innate immune surveillance of spontaneous B cell lymphomas by natural killer cells and gammadelta T cells. J Exp Med 199(6):879–884
21. Gorelik E, Wiltrout RH, Okumura K, Habu S, Herberman RB (1982) Role of NK cells in the control of metastatic spread and growth of tumor cells in mice. Int J Cancer 30(1):107–112
22. Lu J, Chen XM, Huang HR, Zhao FP, Wang F, Liu X, Li XP (2018) Detailed analysis of inflammatory cell infiltration and the prognostic impact on nasopharyngeal carcinoma. Head Neck 40(6):1245–1253
23. Takeda K, Hayakawa Y, Smyth MJ, Kayagaki N, Yamaguchi N, Kakuta S, Iwakura Y, Yagita H, Okumura K (2001) Involvement of tumor necrosis factor-related apoptosis-inducing ligand in surveillance of tumor metastasis by liver natural killer cells. Nat Med 7(1):94–100
24. Müller L, Aigner P, Stoiber D (2017) Type I interferons and natural killer cell regulation in cancer. Front Immunol 8:304
25. Takehara T, Uemura A, Tatsumi T, Suzuki T, Kimura R, Shiotani A, Ohkawa K, Kanto T, Hiramatsu N, Hayashi N (2007) Natural killer cell-mediated ablation of metastatic liver tumors by hydrodynamic injection of IFNalpha gene to mice. Int J Cancer 120(6):1252–1260
26. Kontny U, Franzen S, Behrends U, Bührlen M, Christiansen H, Delecluse H, Eble M, Feuchtinger T, Gademann G, Granzen B et al (2016) Diagnosis and treatment of nasopharyngeal carcinoma in children and adolescents—recommendations of the GPOH-NPC study group. Klin Padiatr 228(3):105–112
27. Gressette M, Vérillaud B, Jimenez-Pailhès A, Lelièvre H, Lo K, Ferrand F, Gattolliat C, Jacquet-Bescond A, Kraus-Berthier L, Depil S et al (2014) Treatment of nasopharyngeal carcinoma cells with the histone-deacetylase inhibitor abexinostat: cooperative effects with cisplatin and radiotherapy on patient-derived xenografts. PLoS One 9(3):e91325
28. Desjardins P, Hansen JB, Allen M (2009) Microvolume protein concentration determination using the NanoDrop 2000c spectrophotometer. J Vis Exp 33:1610
29. Martínez-Lostao L, Anel A, Pardo J (2015) How do cytotoxic lymphocytes kill cancer cells? Clin Cancer Res 21(22):5047–5056
30. Guicciardi M, Gores GJ (2009) Life and death by death receptors. FASEB J 23(6):1625–1637
31. Shi J, Zheng D, Liu Y, Sham MH, Tam P, Farzaneh F, Xu R (2005) Overexpression of soluble TRAIL induces apoptosis in human lung adenocarcinoma and inhibits growth of tumor xenografts in nude mice. Cancer Res 65(5):1687–1692
32. Ehrlich S, Infante-Duarte C, Seeger B, Zipp F (2003) Regulation of soluble and surface-bound TRAIL in human T cells, B cells, and monocytes. Cytokine 24(6):244–253
33. Wang W, Li J, Wen Q, Luo J, Chu S, Chen L, Qing Z, Xie G, Xu L, Alnemah MM, Li M, Fan S, Zhang H (2016) 4EGI-1 induces apoptosis and enhances radiotherapy sensitivity in nasopharyngeal carcinoma cells via DR5 induction on 4E-BP1 dephosphorylation. Oncotarget 7:21728–21741
34. Stegmann KA, Björkström NK, Veber H, Ciesek S, Riese P, Wiegand J, Hadem J, Suneetha PV, Jaroszewicz J, Wang C et al (2010) Interferon-alpha-induced TRAIL on natural killer cells is associated with control of hepatitis C virus infection. Gastroenterology 138(5):1885–1897
35. Medrano RFV, Hunger A, Mendonça SA, Barbuto JAM, Strauss BE (2017) Immunomodulatory and antitumor effects of type I interferons and their application in cancer therapy. Oncotarget 8(41):71249–71284
36. Zheng Y, Cao KY, Ng SP, Chua DT, Sham JS, Kwong DL, Ng MH, Lu L, Zheng BJ (2006) Complementary activation of peripheral natural killer cell immunity in nasopharyngeal carcinoma. Cancer Sci 97(9):912–919
37. Fujimiya Y, Wagner RJ, Groveman S, Sielaff K, Kohsaka T, Nakayama M (1995) In vivo priming effects of interferon-beta ser on NK activity of peripheral blood mononuclear cells in cancer patients. Ther Immunol 2(1):15–22
38. Vrazo AC, Hontz AE, Figueira SK, Butler BL, Ferrell JM, Binkowski BF, Li J, Risma KA (2015) Live cell evaluation of granzyme delivery and death receptor signaling in tumor cells targeted by human natural killer cells. Blood 126(8):e1–e10

39. Sheard MA, Asgharzadeh S, Liu Y, Lin TY, Wu HW, Ji L, Groshen S, Lee DA, Seeger RC (2013) Membrane-bound TRAIL supplements natural killer cell cytotoxicity against neuroblastoma cells. J Immunother 36(5):319–329
40. Zamai L, Ahmad M, Bennett IM, Azzoni L, Alnemri ES, Perussia B (1998) Natural killer (NK) cell-mediated cytotoxicity: differential use of TRAIL and Fas ligand by immature and mature primary human NK cells. J Exp Med 188(12):2375–2380
41. Halaas Ø, Liabakk NB, Vik R, Beninati C, Henneke P, Sundan A et al (2004) Monocytes stimulated with group B streptococci or interferons release tumour necrosis factor-related apoptosis-inducing ligand. Scand J Immunol 60:74–81
42. Cassatella MA, Huber V, Calzetti F, Margotto D, Tamassia N, Peri G et al (2006) Interferon-activated neutrophils store a TNF-related apoptosis-inducing ligand (TRAIL/Apo-2 ligand) intracellular pool that is readily mobilizable following exposure to proinflammatory mediators. J Leukoc Biol 79:123–132
43. Monleón I, Martínez-Lorenzo MJ, Monteagudo L, Lasierra P, Taulés M, Iturralde M et al (2001) Differential secretion of Fas ligand- or APO2 ligand/TNF related apoptosis-inducing ligand-carrying microvesicles during activation-induced death of human T cells. J Immunol 167:6736–6744
44. Kawakubo T, Okamoto K, Iwata J, Shin M, Okamoto Y, Yasukochi A et al (2007) Cathepsin E prevents tumor growth and metastasis by catalyzing the proteolytic release of soluble TRAIL from tumor cell surface. Cancer Res 67:10869–10878
45. Buttmann M, Merzyn C, Hofstetter HH, Rieckmann P (2007) TRAIL, CXCL10 and CCL2 plasma levels during long-term Interferon-beta treatment of patients with multiple sclerosis correlate with flu-like adverse effects but do not predict therapeutic response. J Neuroimmunol 190(1–2):170–176
46. Tecchio C, Huber V, Scapini P, Calzetti F, Margotto D, Todeschini G, Pilla L, Martinelli G, Pizzolo G, Rivoltini L, Cassatella MA (2004) IFNalpha-stimulated neutrophils and monocytes release a soluble form of TNF-related apoptosis-inducing ligand (TRAIL/Apo-2 ligand) displaying apoptotic activity on leukemic cells. Blood 103:3837–3844
47. Blanchard P, Lee A, Marguet S, Leclercq J, Ng WT, Ma J, Chan AT, Huang PY, Benhamou E, Zhu G, Chua DT, Chen Y, Mai HQ, Kwong DL, Cheah SL, Moon J, Tung Y, Chi KH, Fountzilas G, Zhang L, Hui EP, Lu TX, Bourhis J, Pignon JP, MAC-NPC Collaborative Group (2015) Chemotherapy and radiotherapy in nasopharyngeal carcinoma: an update of the MAC-NPC meta-analysis. Lancet Oncol 16(6):645–655
48. Dahlberg C, Sarhan D, Chrobok M, Duru A, Alici E (2015) Natural killer cell-based therapies targeting cancer: possible strategies to gain and sustain anti-tumor activity. Front Immunol 6:605
49. Cheung S, Huang D, Hui A, Lo K, Ko C, Tsang Y, Wong N, Whitney B, Lee J (1999) Nasopharyngeal carcinoma cell line (C666-1) consistently harbouring Epstein–Barr virus. Int J Cancer 83(1):121–126
50. Tsao S, Wang X, Liu Y, Cheung Y, Feng H, Zheng Z, Wong N, Yuen P, Lo A, Wong Y et al (2002) Establishment of two immortalized nasopharyngeal epithelial cell lines using SV40 large T and HPV16E6/E7 viral oncogenes. Biochim Biophys Acta 1590(1–3):150–158

EXPERT OPINION ON THERAPEUTIC TARGETS
2020, VOL. 24, NO. 6, 545–558
https://doi.org/10.1080/14728222.2020.1751820

Taylor & Francis
Taylor & Francis Group

REVIEW

Emerging therapeutic targets for nasopharyngeal carcinoma: opportunities and challenges

Valentin Baloche[a], François-Régis Ferrand[b], Anna Makowska[c], Caroline Even[d], Udo Kontny[c] and Pierre Busson [a]

[a]CNRS, UMR 9018, Gustave Roussy and Uuniversité Paris-Saclay, 39, rue Camille Desmoulins, Villejuif, France; [b]Service d'oncologie, hôpital d'instruction des armées Bégin, F-94160, St Mandé, France; [c]Division of Pediatric Hematology, Oncology and Stem Cell Transplantation, Medical Faculty, RWTH Aachen University, Aachen, Germany; [d]Département de cancérologie cervico-faciale, Gustave Roussy and université Paris-Saclay, 39, rue Camille Desmoulins, F-94805, Villejuif, France

ABSTRACT

Introduction: Nasopharyngeal carcinoma (NPC) is a major public health problem in several countries, especially those in Southeast Asia and North Africa. In its typical poorly differentiated form, the Epstein-Barr virus (EBV) genome is present in the nuclei of all malignant cells with restricted expression of a few viral genes. The malignant phenotype of NPC cells results from the influence of these viral products in combination with cellular genetic, epigenetic and functional alterations. With regard to host/tumor interactions, NPC is a remarkable example of immune escape in the context of a hot tumor.

Areas covered: This article has an emphasis on emerging therapeutic targets that are considered upstream or at an early stage of clinical application. It examines targets related to cellular oncogenic alterations, latent EBV infection and tumor interactions with the immune system.

Expert opinion: There is a remarkable emergence of new agents that target EBV products. The clinical application of these agents would benefit from a systematic and comprehensive molecular classification of NPCs and from easy access to pre-clinical models in public repositories. There is a strong rationale for more investigations on the potential of immune modulators, especially those related to NK cells.

ARTICLE HISTORY
Received 30 January 2020
Accepted 1 April 2020

KEYWORDS
Nasopharyngeal carcinomas; cdk4/6 inhibitors; latent EBV-infection; EBNA1; LMP1/LMP2; immune checkpoint inhibitors; galectin-9; interferon-β; NK cells; Head and Neck carcinomas

1. Introduction: a reminder on the epidemiological and etiological aspects of NPCs

1.1. Geographic distribution and nosology

Nasopharyngeal carcinomas (NPC) are a special entity among human Head and Neck carcinomas (HNCs) due to their peculiar geographic distribution, their histological characteristics and their consistent association to the Epstein-Barr virus (EBV). Our literature search in PubMed was focused on the words "NPC", EBV and Head and Neck carcinomas as the main key words. Most references were from the last 10 years with a few older publications including one from 1964. The incidence of NPCs is low in most countries but it is high in some specific geographic areas like Southern China, especially the Guangdong province and the Northern part of Borneo Island (about 25 cases/100 000 inhabitants/year). Intermediate incidence areas encompass a number of countries, mainly in Southeast Asia (Philippines, Taïwan, Vietnam, Thailand, Indonesia) and Northern Africa (Tunisia, Algeria, Morocco)(about 5 cases/100 000/year). In several places in South East Asia, especially in Singapore and Hong-Kong, there is a trend toward a decreasing incidence of NPCs [1]. It is probably related to major changes in living habits, especially food habits in early childhood. However, even in Hong-Kong and Singapore, NPC remains one of the first cause of cancer for individuals of less than 60 years old [2]. In addition, some regions of intermediate incidence might be overlooked, for example in sub-Saharan Africa [3,4]. A better awareness of NPCs in these regions might arise with the decline of other pathologies and acquisition of appropriate diagnostic tools.

The overwhelming majority of NPCs belongs to the group of squamous cell carcinomas but in contrast with other Head and Neck carcinomas, their squamous differentiation remains minimal according to morphological criteria. One consistent and striking characteristics of NPCs is their heavy infiltration by non-malignant nonmalignant leukocytes, especially T-lymphocytes. These infiltrating lymphocytes may account for more than 50% of the tumor mass in the primary tumor. It is not well known to what extent this infiltrate persists in metastatic lesions [5]. The implication of the Epstein-Barr virus (EBV) is mainly attested by the presence of the EBV genome inside the nuclei of all malignant cells. EBV infection in NPC cells is mainly latent. In other words, there is no production of viral particles *in situ* and most viral genes are transcriptionally silent. However, some of them are consistently active inside NPC cells encoding a few proteins called 'latent' viral proteins and a number of untranslated 'latent' viral transcripts whose contribution to NPC oncogenesis is increasingly recognized.

1.2. Etiological aspects and pre-tumoral conditions

NPC is a multifactorial disease with a viral etiological component. The magnitude of EBV contribution has long been debated. EBV is indeed a ubiquitous virus in the humankind. More than 95% individuals are healthy carriers. Nevertheless,

CONTACT Pierre Busson Pierre.Busson@gustaveroussy.fr CNRS, UMR 9018, Gustave Roussy and Université Paris-Saclay 39 Rue Camille Desmoulins, Villejuif, France

Article Highlights

- Several Epstein-Barr virus-products are oncogenic drivers for malignant NPC cells.
- Most emerging non-immune anti-viral strategies are focused on the EBNA1 protein in order to block its interactions with cellular partners or selectively disturb its translation from its messenger RNA.
- Regarding target cellular proteins, most advanced strategies intend to lift the functional inactivation of the Rb and TP53 proteins.
- Like in other Head and Neck carcinomas, there is probably room for the development of SMAC mimetics.
- Because NPCs are characterized by a process of immune escape in the context of a hot tumor, there is probably a wide margin of progression for the use of immune modulators. The potential of targets like HLA-G/ILT4, B7H4/B7-H4-R and galectin-9/Tim-3 is worth to be investigated.
- New modalities of administration and combination will probably emerge for immune modulators which are already in use in the clinics (for example interferon-β and anti-PD1/PD-L1 antibodies). Reactivation of NK cells increasingly appears as a promising approach.

the etiological contribution of EBV to NPC is now undisputable. It is supported by clinical observations: 1) the consistency of EBV infection in typical undifferentiated NPCs regardless of the geographic origin of the patients and 2) the precession of alterations in circulating EBV-markers. In addition, thanks to the recent elaboration of anti-EBNA1 compounds, there is now pharmacological evidence that EBV products contained in malignant NPC cells are required not only for the initiation but also for the maintenance of the malignant phenotype [6]. Recent publications have shown that some EBV strains prevalent in endemic regions bear a higher risk of NPC in otherwise healthy carriers, may be because they undergo more frequent bursts of viral replication in the tonsils [7–9]. Indeed, epithelial cells of the nasopharyngeal mucosa are located at close proximity to the pharyngeal tonsils. When these cells are affected by preexisting genetic or epigenetic alterations, for example silencing of *CDKN2A*, they are more prone to enter a state of latent infection upon EBV penetration and simultaneously to switch from a premalignant to a fully malignant phenotype [10].

The striking geographical distribution of NPC is not yet entirely explained but it should be considered in the light of its multifactorial etiology, involving genetic predisposition, environmental risk factors, especially dietary factors and prevalence of more aggressive EBV strains in some geographic areas [7,8,11]. NPC risk in a given country or region is probably related to a combination of these 3 categories of factors. One important characteristic of NPC is the occurrence of alterations in circulating EBV markers which precede the onset of invasive tumors. Current serological markers are sensitive but they lack specificity. Until recently the standard tool for population screening was the combined assessment of anti-EBNA1 IgGs and anti-VCA-p16 IgAs [12]. Several investigators intend to achieve better specificities mainly using two approaches based either on detection and sizing of circulating EBV DNA or on system serology (multiplex assessment of antibodies directed to diverse proteins of EBV) [13,14].

2. Biological characteristics of NPCs

2.1. Biological models of NPC

Malignant NPC cells are notoriously difficult to grow in culture and even to permanently transplant on immunosuppressed mice. For a long time, many investigators who attempted derivation of NPC cell lines from fresh tumor fragments failed to get anything or ended-up with EBV-negative malignant epithelial cells, therefore not truly representative of the vast majority of NPCs. For decades, the C666-1 cell line has been the unique NPC cell line propagated *in vitro* with stable retention of the viral genome [15]. Until now, most investigations on novel therapeutic targets for NPC have used C666-1 cells *in vitro* as well as in murine systems as their unique 'natural' NPC model (see for example Table 1). Fortunately, things are changing, thanks to progress made in the past decade. First, we and others have found that using chemical inhibitors of the Rho kinase (Rhock) greatly improves the *in vitro* survival and proliferation of malignant NPC cells as well as their retention of the EBV genome [16,17]. In addition, several institutions, mainly in South-East Asia, have made substantial investments to obtained NPC PDXs (patient-derived xenografts) which are propagated on immunosuppressed mice and retain the EBV genome [18–20].

2.2. Viral oncogenesis

As previously mentioned, the presence of EBV products in malignant NPC cells is critical not only for the initiation but also the maintenance of the malignant phenotype. The EBV genome is contained in the nuclei of malignant cells as extrachromosomal circular copies called 'episomes'. The number of

Table 1. Artficial ligands and blockers of viral proteins as candidate drugs for NPC treatment.

Mechanism of action	Lead compound	Current stage of development	Reference
Blocker of EBNA1 interaction with the OriP DNA sequence	VK-2019	Phase I/II clinical trials in several institutions (NCT03682055)	Messick et al., Sci. Transl. Med. (2019)
Blocker of EBNA1 dimerization	ZRL_5P_4	Active on C666-1 xenografted tumors (growth delay and induction of the lytic cycle)	Jiang et al., PNAS (2019)
Blockers of the interactions of the LMP1 C-terminus with TRAF2 and TRAF6	Z370	Peptides and small molecules delaying growth of EBV-positive cells *in vitro* *Not yet published in pair-review journals*	2018 Int Conf on EBV and KHSV – talk #15 and poster #128
Affibody targeting the C-terminus of LMP2	Z142	Active on C666-1 xenografted tumors (retention in tumor cells and growth delay when combined to a toxin) *Confirmation needed on other NPC models*	Zhu et al., Plos Pathogens (2020)
Monoclonal antibody targeting the BARF1 protein	3D4 mAb	Active on C666-1 tumors xenografted into nude but not into [RAG-/-, γ chain-/-] mice (contribution of ADCC?) *Confirmation needed on other NPC models*	Turrini et al., Oncoimmunology (2017)

episomes per cell can vary from one to more than 50 copies. The EBV episomes can coexist with one or a few integrated copies [21]. We do not know whether there are specific sites of integration in the cellular genome and what the functional consequences of these integrations are.

As previously mentioned, a minority of EBV genes are consistently expressed in NPC cells. By their diversity and abundance, the non-coding RNAs represent the strongest component of viral expression in malignant NPC cells. They belong to two categories, the EBERs (Epstein-Barr encoded RNAs) and the viral microRNAs. The EBERs 1 and 2 are single stranded RNAs of 170 base pairs folded in a complex secondary structure allowing specific interactions with several cellular proteins, especially PKR (protein-kinase R) and TLR3 (Toll-like receptor 3) [22]. EBERs which are extremely abundant in NPC cells (about one million per cell) have proven oncogenic roles. Overall, they tend to trigger and corrupt intracellular innate immune responses favoring proliferative signals over cytostatic effects [22,23]. The other category of untranslated viral RNAs is the BART family of microRNAs named according to the viral genome segment where they are encoded (BamH1 A segment Rightward Transcripts). They are both diverse – over 45 species – and extremely abundant. On average, the BARTs account for one third of the total microRNAs contained in NPC cells [24]. Their target mRNAs and their functions are diverse and not entirely elucidated. They are known to contribute to the malignant phenotype in several ways: repression of anti-oncogenic or pro-apoptotic proteins like PTEN, E-cadherin and PUMA, maintenance of the viral latency by repression of proteins involved in viral replication, tuning of the expression of oncogenic viral proteins which have cell toxicity when expressed in excess [24,25].

In contrast to non-coding RNAs, viral proteins are usually expressed at a low level in NPC cells. Only one of them – EBNA1 (Epstein-Barr nuclear Antigen 1) – is constantly expressed. EBNA1 interacts with the viral genome, the cell genome and various cellular proteins [26,27]. It is a transactivator required for the replication of the viral episomes at each cell division by the cell DNA replicating machinery. It is also required for the balanced segregation of the newly replicated episomes at each cell division. In this regard, it has a crucial role for the maintenance of the EBV episomes in malignant cells undergoing proliferation. This is its main indirect contribution to the malignant phenotype of NPC cells. EBNA1 has also direct oncogenic effects for example by disturbing the assembly of the PML nuclear bodies. There is now experimental evidence that blocking EBNA1 functions impairs the malignant phenotype (see the section on viral inhibitors). Three other EBV proteins are frequently, although not constantly, expressed in NPC cells: LMP1, LMP2 and BARF1 [28]. There are multiple indirect evidences of their contribution to the malignant phenotype of NPC cells (although no direct demonstration like for EBNA1). LMP1 and LMP2 are integral membrane proteins with multiple transmembrane segments. They are associated to lipid rafts, circulate in the internal cellular membrane network with transient exposure at the plasma membrane. LMP1 and LMP2 constitutively induce multiple non-physiological signaling activities resulting from inappropriate recruitment and redistribution of cellular signaling adaptors. For example LMP1 interacts with TRAF2, TRAF3 and TRAF6. It activates canonical and non-canonical NF-κB pathways as well as the Pi3-kinase and MEK pathways. There are 2 isoforms of LMP2, generated by alternative splicing. LMP2A has the capacity to recruit signaling adaptors like ubiquitin ligases of the NEDD4 family or the syk tyrosine kinase [29,30]. It activates the nuclear translocation of β-catenin and the epithelial-mesenchymal transition [29,31]. Our knowledge of BARF1 is much more limited. According to a recent report, this viral protein is detectable at the surface of NPC cells. There are reports indicating that a large portion of the protein is cleaved and released in the extra-cellular medium with growth promoting and immune suppressive activity [32].

2.3. Cellular oncogenesis

Beside latent EBV-infection, multiple genetic, epigenetic and functional alterations contribute to the malignant phenotype of NPC cells. On the one hand, we have a set of alterations which are consistent in the vast majority of NPCs and will be presented in the next paragraphs, mainly alterations of the Rb and TP53 pathways, permanent activation of the NF-KB and Stat3 pathways and overexpression of various genes like Notch3, c-IAP2 and CCL20. On the other hand, there are cellular alterations which are suspected to support the malignant phenotype but only for a fraction of NPCs. Some of them will be briefly mentioned.

Regarding Rb and TP53, it is useful to remind that the active Rb protein maintains a physiological barrier at the entry of the cell cycle (G0/G1 transition) whereas TP53 has the power to induce cell cycle arrest or apoptosis, especially in a context of Rb deregulation. Therefore, structural or functional inactivation of both proteins is a common feature of most human malignancies. Inactivating mutations of *Rb* rarely occur in NPCs. However, in most cases, Rb is functionally inactivated by its phosphorylation resulting from inappropriate activity of the cyclin-dependent kinases CDK4 and CDK6. Indeed, in most NPCs, *CDKN2A* silencing and/or *CCND1* overexpression result in the deregulation of CDK4/6. The *CDKN2A* gene maps to chromosome 9p21. By alternate reading of the same frame, it encodes 2 proteins named INK4 (p16) and ARF (p14). INK4 is a negative regulator of the CDK4/6-cyclin-D1 complex whereas ARF is an inhibitor of MDM2 (an E3-ubiquitin ligase involved in the degradation of TP53). *CDKN2A* is the most frequently altered tumor suppressor gene in NPCs (about 80% of the cases). It is silenced through loss of the 2 alleles or loss of one allele and methylation of the promoter of the remaining allele [33,34]. Like in other Head and Neck carcinomas, the *CCND1* gene is frequently amplified resulting in overexpression of cyclin D1 (15% of NPC cases) [35].

Oncogenic mutations of the *TP53* gene can be detected in a fraction of NPCs but at a much lower frequency than in other Head and Neck carcinomas [33,36,37]. According to Li et al., *TP53* mutations are found in about 6% of primary tumors and 15% of metastatic lesions [33]. A functional inactivation of wild-type TP53 is suspected for the majority of NPCs but its mechanisms are not yet fully understood. The silencing of the ARF protein and the subsequent enhancement of the MDM2 activity are expected to result in enhanced TP53 degradation. Recently, data supporting this hypothesis has come from a genome-wide CRISPR-based gene knockout screen performed on the C666-1 and C17 cell lines (EBV-positive NPC cells propagated *in vitro)*(Wang et al., J. Biol. Chem. 2019).

Another potential mechanism of TP53 degradation involves EBNA1 which has been shown to sequester USP7 (ubiquitin specific protease 7). USP7 normally deubiquitinates TP53 and protects it from MDM2-mediated degradation [38]. However in these scenarios of enhanced degradation, one would expect a low abundance of TP53 in malignant NPC cells. This is not the case. On the contrary, wild type TP53 is often very abundant in these cells despite the absence of mutations stabilizing the protein [37]. Overall, more investigations are needed to understand the mechanisms of TP53 inactivation in NPC cells.

Constitutive activations of NF-κB pathways are more frequent in NPCs than in other HNCs [33,39]. Moreover, these activations are supported by peculiar complexes of NF-κB transcription factors that are rarely found outside NPC cells like p50/RelB and p50/p50/Bcl3[39] [40] . The expression of the EBV protein LMP1 by itself is sufficient to induce activation of these unusual NF-kB pathways. However, a substantial expression of LMP1 is detected in less than 50% of NPCs. Other viral factors are suspected to contribute to NF-kB activation, especially the EBERs when they interact with the Toll-Like Receptor 3 (TLR3) [23]. Cellular factors also contribute to the activation of NF-kB pathways, especially mutations crippling genes encoding negative regulators of NF-kB like TRAF3 and CYLD [33] . Overexpression of the lymphotoxin-β receptor resulting from the amplification of the *LTBR* gene is found in about 50% NPCs. It is one additional factor contributing to the activation of NF-kB pathways [41]. Strikingly, two types of NF-kB-related oncogenic mechanisms, LMP1 expression on the one hand and alterations of cellular NF-kB regulators on the other hand, are mutually exclusive in NPC tumors [33].

Constitutive activation of the STAT3 pathway is suspected to consistently support the malignant phenotype in NPCs as well as in a number of non-NPC Head and Neck carcinomas. NF-kB, IL-6/IL6-R and EGFR signaling are potential upstream activators of the STAT3 pathway [42,43]. However, more investigations on laboratory NPC models would be useful to assess the role of STAT3 activation in the specific context of NPC cells. A recent publication has reported frequent mutations impairing the Smad-dependent TGF-β pathway. They involve genes like *TGFBR2* and *SMAD4* [44]. Overexpression of c-IAP2 and Notch3 proteins are mentioned in the section on cellular targets.

Numerous other dysregulated or vulnerable cellular pathways have been reported in various studies dealing with NPC models or specimens. They are related to chromatin remodeling, DNA repair, Ras-dependent pathways, purine synthesis etc … However, these alterations or vulnerabilities are generally restricted to small percentages of patients and will not be considered as priority targets in this review [33,42,45,46].

2.4. Tumor microenvironment and immune evasion

As previously mentioned, heavy leucocytic infiltration in primary NPC tumors is one major characteristics of this disease. Most infiltrating leucocytes are EBV-negative CD3 + T-lymphocytes. Other infiltrating leucocytes are NK cells, B-cells and various types of myeloid cells including macrophages, dendritic cells, myeloid-derived suppressor cells and polynuclear leucocytes. The formation and the expansion of this infiltrate probably results from several causes like the constitutive production of inflammatory cytokines (IL-1, IL-18) by malignant cells and the proximity of the pharyngeal tonsil which may facilitate leucocyte extravasation [47]. The rapid growth of most NPC tumors – taking place despite the abundance of the leucocyte infiltrate and the consistent presence of EBV antigens – makes manifest the absence of effective immune response. NPC is a striking example of immune escape occurring in the context of a hot tumor.

Various cell types with immune suppressive activity are present in the leucocyte infiltrate, like regulatory T-cells (T-regs), M2 macrophages and myeloid-derived suppressor cells (MDSCs) [48–50]. Various types of biomolecules produced by malignant cells are suspected to contribute to the immunosuppressive context, including cytokines, lectins, agonists of inhibitory immune checkpoints and enzymes. Leukemia inhibitory factor (LIF) and CCL20 are abundantly and consistently released by NPC cells. Both molecules are detected in the plasma of NPC patients with high concentrations associated to a pejorative outcome [51–53]. LIF enhances NPC cell growth while CCL20 stimulates their migration. In addition to these autocrine effects, both LIF and CCL20 have paracrine immunosuppressive effects including promotion of T-regs (expansion and suppressive activity) [54,55]. Galectin-9 is another type of immunosuppressive biomolecule consistently expressed by NPC cells [56]. Galectin-9 is a lectin (or glycan-binding protein) whose role in human malignancies is increasingly recognized [57,58]. When released in the extra-cellular medium, galectin-9 acts on numerous target cells with predominant immuno-suppressive effects. It induces apoptosis of Th1 + CD4 + T-cells, impairs NK cell functions, favors M2 polarization of macrophages and enhances suppression by induced T-regs [59–61]. Galectin-9 is extremely abundant in NPC cells [62]. It is released in the extra-cellular medium probably in two fractions, one conveyed by exosomes and one soluble fraction [63]. It is also detected in the plasma of NPC patients [64]. Surface ligands of inhibitory immune checkpoints are also abundantly and consistently expressed by NPC cells, especially HLA-class II molecules, agonists of Lag3 [65]. Other agonists like PD-L1, HLA-G and B7-H4 are expressed by malignant cells in at least a fraction of NPCs [66,67]. IDO (indoleamine 2,3-dioxygenase) is an enzyme involved in tryptophan degradation which has negative effects on T-cell proliferation and function and is suspected to contribute to immune suppression in NPCs [67,68].

Despite the strong suppressive context, cells with a molecular phenotype of immune effector cells are consistently detected inside NPC tumors. CD56 + NK cells are present and their abundance is indicative of a better prognosis [69]. Regarding effector T-cells, the CD8+ to CD4+ ratio is variable [50]. A substantial fraction of CD4 + T-cells bears Th1+ or Th17+ markers [50,70]. However, they are probably functionally impaired. For example, a study comparing TILs and PBMCs from NPC patients has shown that LMP1 and LMP2 tetramer positive cells are detected in both populations. However, cytotoxicity and IFN-γ production were recovered only from PBMCs [71]. A number of questions remain to be addressed regarding NPC TILs, for example the significance of their spatial distribution inside the tumor nests or at their periphery, the diversity of TCR rearrangement and its relationship with EBV-protein expression and the mutational burden.

2.5. Tumor macro-environment: the systemic aspects of NPCs

As most solid tumors, NPC is increasingly recognized not only as a loco-regional disease but also as a systemic disease, even in the absence of distant metastases. The systemic impact of the disease can be observable clinically, for example because of altered general condition or cachexia and sometimes because of paraneoplastic syndromes. There are also biological evidence of the systemic impact detected by routine biology like a decrease in the total count of lymphocytes more marked on CD4+ cells with an increase in the fraction of T-regs (CD4+, CD25 +, Foxp3+) [72]. However there is no overt systemic immune deficiency in NPC patients who retain for example a number of circulating precursors for anti-EBV CD4 and CD8 T-cells [71]. Several tumor products are consistently detected in the plasma of NPC patients, especially EBV DNA and BART microRNAs [73,74]. The kinetics of the concentration of plasma EBV DNA has proven to be a remarkable biomarker to monitor treatment response [12,75]. When plasma EBV-DNA is detectable at the diagnosis prior to the treatment, its complete disappearance at the completion of the primary treatment – most often concurrent chemo-radiotherapy – is of good prognosis. On the contrary, persistence of detectable plasma EBV DNA is associated with a high risk of local or metastatic relapse. Moreover the kinetics of plasma EBV-DNA clearance during induction chemotherapy and concurrent chemo-radiotherapy has prognostic value and can be used for risk-adapted de-intensification/intensification of the treatment [75]. In addition, tumor exosomes are abundant in the plasma of most NPC patients. They have an immunosuppressive activity supported by surface proteins like PD-L1, galectin-9, CCL20 and by microRNAs (probably intraluminal) [54,64,76]. Circulating tumor cells are detectable in NPC patients. Their abundance has prognostic value [77].

3. Current therapeutic landscape and possible transitions to innovative therapeutic approaches

3.1. Overview of current cytotoxic and targeted therapies

Because of their anatomical situation, surgical ablation is not indicated for NPCs, except some rare cases of local relapses treated by expert surgical teams. Radiotherapy is the cornerstone of the treatment for the primary tumor and regional lymph nodes [1,78]. Exclusive radiotherapy is restricted to small tumors (T1 or T2N0). Concurrent chemo-radiotherapy is the standard of care for larger tumors or tumors associated with cervical lymph node involvement [79]. Remarkable progress has been achieved in radiotherapy of NPC with the advent of IMRT (Intensity-Modulated Radiotherapy). However local relapses still occur in about 10% of the cases and a large fraction of patients who are cured still suffer late undesirable effects strongly undermining their quality of life (xerostomia, muscular atrophy and, sometimes, temporal lobe necrosis). Conventional chemotherapy is also a major arm for the treatment of NPCs. Among the most efficient drugs are platin-derivatives (especially cis-platinum), 5-fluoro-uracil, taxanes and gemcitabin. Chemotherapy is used for the treatment of synchronous or metachronous metastases but it has also a major role for the treatment of primary tumors [80]. As explained previously, concurrent chemo-radiotherapy is the standard of care for large primary tumors. Overall, there is no obvious benefit of adjuvant chemotherapy, even after selection of high-risk patients [81]. This is due to a large extent to its toxicity in the aftermath of concurrent chemo-radiotherapy. In contrast, there is a growing consensus that induction or neo-adjuvant chemotherapy increases disease-free and overall survival. For example, in a recent phase III trial, Zhang et al. have demonstrated the benefit of 3 cycles combining gemcitabine and cisplatinum prior to chemoradiotherapy in patients with advanced local disease [82]. While NPCs are known to be more sensitive to radiotherapy and chemotherapy than HNCs, current targeted therapies have not brought superior benefits by comparison with other Head and Neck malignancies. For example, Cetuximab has not proven to be useful for nasopharyngeal carcinomas [83]. So far, multitargeted tyrosine kinase inhibitors (TKI) and TKI targeting VEGFR have not been successful in NPC patients. Among anti-angiogenic compounds, Endostatin seems to be the most efficient [84].

3.2. Immunotherapeutic approaches

Regarding immune checkpoint inhibitors, so far, anti-PD1/PD-L1 antibodies (Pembrolizumab, Nivolumab and Spartalizumab) have resulted in ORR of about 20% in several phase II studies dealing with relapsed or metastatic NPCs [85,86](Lim et al., AACR annual meeting 2019, abstract # CT150). This is not bad but not better than for other HNCs despite the presence of viral antigens in malignant NPC cells. However, studies on this topic are far from over. Phase III studies are ongoing [87]. Novel antibodies targeting PD1 (Camrelizumab) are under evaluation with seemingly better results [88]. The combination of an anti-PD1 with an anti-CTLA4 is also tested in one study (NCT03097939).

Because of the presence of EBV antigens in malignant NPC cells, multiple approaches of adoptive transfer of immune cells have been attempted since the early millennium years [87]. Most of these trials were based on *in vitro* expansion of autologous lymphocytes targeting EBV proteins, EBNA1, LMP1 and LMP1. Overall, the results have been somehow disappointing, especially by comparison with the excellent results obtained in the treatment and prevention of EBV-related post-transplant lympho-proliferative disorders (PTLD) [87]. However, in most studies, long term remissions have been observed for a few cases of patients bearing advanced and/or resistant tumors, thus stimulating investigators to undertake novel studies. One reason of the overall low success rate of immune adoptive transfer is presumably the poor representation of EBV antigenic proteins in NPC cells. EBNA1, LMP1 and LMP2 are less immunogenic than other latent EBV proteins. The abundance of LMP1 and LMP2 is often very low and they are completely absent in a large fraction of the cases [89]. Even more important in our opinion is the prevalence of active immunosuppressive effectors inside the tumor environment and, to a lesser extent, at the systemic level (see the previous sections

on tumor micro- and macro-environment). At the time when the invasive tumors are taken in consideration for treatment, these cellular and molecular effectors of immune evasion have been selected, educated and expanded for many years in the face of normal anti-EBV CD4+ and CD8+ conventional T-cells [71].

The development of therapeutic vaccination may face the same obstacles. Currently, one of the most advanced studies in this field is based on a modified vaccinia Ankara virus (MVA-EL) encoding a recombinant protein fusing a truncated half of EBNA1 to the full-length of LMP2A. This vaccine is currently tested in a phase II study [90](NCT01094405).

3.3. Challenges of the transition to innovative approaches

Beside the early detection of small tumors and adequate management of pre-tumoral conditions, advanced therapeutic research in NPCs has three main goals: 1) to design new instruments to cure synchronous or metachronous metastatic diseases; 2) to prevent recurrence in high risk patients with apparent remission, especially those with persistent detection of plasma EBV DNA after the completion of concurrent chemo-radiotherapy; 3) and last but not least, to reduce long term sequelae of radiotherapy, especially for small size tumors. For its long term contribution to these aims, the clinical research on novel therapeutic targets has to comply with 2 requirements. First, introduction of novel agents should avoid competition with proven therapeutic modalities. Because conventional radiotherapy and chemotherapy, often achieve cures for localized diseases and long-term remissions for metastatic forms, clinical oncologists might be reluctant to replace standard drugs by innovative agents. Next, investigators favor situations where short term clinical and biological endpoints are available as surrogates of the long term survival; for example, reduction of tumor mass, evolution of the tumor immune contexture on secondary biopsies and kinetics of plasma EBV DNA load. One gateway entry to assess new therapeutic agents is to deal with metastatic diseases at the second or third line of treatment. This approach has proven to be successful to make the proof of principle for Cytolytic Viral Activation in NPC [91]. With the growing consensus on the effectiveness of induction chemotherapy, there are new possibilities. This segment of the treatment (often called 'window of opportunity') allows evaluation of novel therapeutic agents, especially immune-modulators which are not expected to result in cumulative toxicity when combined with chemotherapy. In this context, endpoints related to primary tumor response are available in addition to the kinetics of plasma EBV DNA load. This strategy might even be applied to low income countries where there are long queues to access adequate facilities for radiotherapy.

4. Innovative therapies targeting cellular signaling pathways

In this section, our review will be focused on a small group of pathways which are consistently altered or critically involved in a majority of NPCs as explained in our previous section on NPC cellular oncogenesis.

4.1. Targeting the Rb pathway

As previously explained, the functional inactivation of Rb in NPC cells often results from the inappropriate activity of the cyclin-dependent kinases CDK4/6 in a context of *CDKN2A* inactivation or *CCND1* overexpression. Therefore, there is a strong rationale to use pharmacological inhibitors of the CDK4/6 kinases (provided that these compounds have sufficient selectivity for malignant cells). One of this inhibitor, Palbociclib has proven to have anti-tumor effects on NPC-PDX models and there are a few observations of objective responses in patients with advanced diseases ([19] and ASCO 2019 (DOI: 10.1200/PO.18.00340)). Another CDK4/6 inhibitor, ribociclib, was also reported to be efficient in NPC-PDX models with additional synergistic effect when it was combined with an alpha-specific PI3 K-inhibitor, alpelisib [92].

4.2. Targeting TP 53

As previously mentioned, the vast majority of primary NPCs retain a wild-type *TP53* gene, including more than 80% metastatic NPC lesions. A functional inactivation of TP53 is strongly suspected although its precise mechanisms are not fully understood. Nevertheless, compounds which inhibit TP53 interaction with MDM2 – like Nutlin 3 and its derivative Idasanutlin or RG7388 – antagonize NPC cell growth *in vitro* [93,94]. Such compounds are under clinical trials mainly in hematological malignancies. In most cases, they are poorly active by themselves. Combinations with other drugs are often required to induce a transition of the TP53 protein from its 'arrester' to 'killer' status, involving distinct phosphorylation events [95]. This transition will have to be investigated in the context of NPC cells.

4.3. Targeting NF-kB pathways

The major contributions of NF-KB factors to the malignant phenotype of NPC cells argue in favor of using NF-KB inhibitors as therapeutic agents. Unfortunately, most pharmacological NF-KB inhibitors which are currently available have poor selectivity. They often impact normal tissues especially immune effector cells [96]. However, in the specific case of NPCs there is room for future innovative approaches that would target the previously mentioned unusual NF-KB complexes (especially p50/RelB and p50/p50/Bcl3) [39][40].

4.4. Miscellaneous cellular targets

Regarding STAT3, the most promising inhibitors are small molecules blocking its homodimerization domain like OBP-31,121 and OBP-51,602. These molecules are currently in early clinical trials for various malignancies but not NPCs to our knowledge. As for current NF-kB inhibitors, the most prevalent difficulty with STAT3 inhibitors is their lack of selectivity for malignant cells. Regarding c-IAP2, we have previously reported the consistent overexpression of this anti-apoptotic protein in NPC cells [97]. Treatment of these cells with a small molecule acting as a SMAC mimetic induced the degradation of c-IAP2 and subsequent cell death. The addiction of NPC

cells to high expression of c-IAP2 is probably related to permanent endogenous stimulation of the TLR3 receptor by the EBERs [16,98]. Interestingly, Debio 1143, an orally available SMAC mimetic has given promising results in a phase II trial in combination with chemoradiation for patients with non-NPC locally advanced Head and Neck carcinomas (ESMO 2019, abstract LBA65). Its evaluation in NPC patients would be warranted. NOTCH3 and its ligand Hey1 are overexpressed in virtually all EBV-positive NPC tumor lines and primary tumors [99]. Knocking-down Notch3 in NPC cells *in vitro* inhibit their proliferation in 2D and 3D cultures and make them more vulnerable to cis-platinum. However, so far, there has been no breakthrough of Notch pharmacological inhibitors in oncology.

5. Emerging non-immune anti-viral strategies

5.1. Artificial ligands and blockers of viral proteins

EBNA1 is usually seen as the most relevant viral target in NPCs because of its consistent expression and obligatory role in EBV genome maintenance. VK-2019 is currently the most advanced compound directly targeting EBNA1 [6] (Table 1). This drug inhibits EBNA1 interaction with the OriP sequence of the EBV genome. It was designed using the 3D structure of the complex formed by the EBNA1 DNA-binding domain (DBD) with the Ori-P sequence. The formation of this complex requires EBNA1 dimerization [100]. Candidate inhibitors were derived from a chemical fragment library, using *in silico* methods and X-ray diffraction. Following validation in EBNA1/DNA binding assays and cell-based assays, they were tested *in vivo* using NPC PDX. Remarkably, lead compounds were able to delay tumor growth but also to synergize with radiotherapy. Simultaneously the EBV-genome was lost from these rapidly growing tumors in less than 6 days [6]. In addition to open the way to a novel therapeutic approach, this study was an elegant confirmation of the continuous contribution of EBV to the malignant phenotype of NPC cells. VK-2019, one of these compounds, is currently tested on NPC patients in phase I/IIa clinical trials in several institutions (NCT03682055).

Another strategy for direct targeting of EBNA1 is based on oligopeptides homologous to EBNA1 dimeric interface, designed to block the dimerization process (and consequently the DNA binding). Recently, one of these peptides has been incorporated in a complex compound bearing a Zn++ chelator and a fluorophore with enhanced emission in response to EBNA1 and Zn++ binding. This compound, called ZRL_5P_4, prevents EBNA1 dimerization and oligomerization, reduces the viability of NPC cells *in vitro* and delays the growth of NPC xenografts. It also induces the viral lytic cycle in treated cells [101].

Although EBNA1 is currently at the front-stage, it is not the unique viral protein which can be targeted in NPCs. Other potential targets are LMP1, LMP2 and BARF1 (Table 1). Studies in this field are very exciting but one should keep in mind that they are still at an early stage, either not published in pair-review journals or supported by only one publication. Some investigators work to apply to the oncoprotein LMP1 a strategy of inhibition similar to the strategy implemented for EBNA1 with VK 1019, in other words, they intend to block its interaction with cellular partner biomolecules. The group led by A. Kieser (Helmholtz center, Munich) investigates peptides or small molecules blocking the interactions of the C-terminal part of LMP1 with cellular signaling adaptors like TRAF2 and TRAF6 (2018 International Conference on EBV & KSHV, oral talk #15 and poster #128). Very recently, promising data have been reported by Zhu et al. (2020) for artificial protein ligands of LMP2 [102]. They were obtained by screening a phage display library of affibodies. Affibodies are recombinant small proteins (7kd, 58 aa) with the capacity to bear highly diverse motifs on a scaffold derived from the B-domain of the Staphylococcal Protein A. They can achieve specific binding of target proteins with high affinity (sometimes reaching the pM range) [103]. The LMP2 specific affibodies reported by Zhu et al. bind the C-terminus of LMP2 which, according to the current LMP2 topological model, is intracytoplasmic. However, these antibodies are readily internalized by EBV-positive latently infected cells including the C666-1 NPC cells *in vitro*. Moreover, they accumulate in C666-1 xenografts under systemic treatment of tumor-bearing mice. Tumor growth inhibition is observed when the affibodies are coupled to a toxin [102]. If these data are confirmed with other NPC models, they might quickly lead to clinical applications. Understanding the mechanisms of affibody internalization by LMP2-positive cells will be of major interest. Finally, there is a report of a murine monoclonal antibody targeting a segment of the BARF1 protein (aa 28–38) which induces a growth delay for C666-1 tumors xenografted in nude mice but not in RAG-/-, γ-/- mice suggesting a contribution of ADCC against malignant cells [32]. It will be interesting to see whether this observation is confirmed in future studies.

5.2. Modulation of EBNA1 protein translation

The EBNA1 protein contains a long series of Glycine/Alanine repeats mapping between its amino-acids 89 and 325. R. Fåhraeus et al. have shown that the portion of the EBNA1 messenger RNA encoding this repeat tends to slow down the path of its own translation. Moreover, in collaboration with the group led by M. Blondel, they have shown that this RNA sequence retains the same function when inserted in recombinant genes and transcripts expressed in yeast. This has resulted in a powerful tool to screen small molecule library for compounds with the capacity to further inhibit or increase the translation of EBNA1. Currently, one perspective is to enhance EBNA1 expression in order to increase the immunogenicity of malignant cells [26].

5.3. Possible targeting of untranslated viral RNAs

As mentioned in the section on viral oncogenesis, untranslated RNAs – EBERs and BART microRNAs – are the most abundant viral products in NPC cells and increasingly appear as critical determinants of the malignant phenotype. One strategy to antagonize the functions of viral microRNAs is to bring to malignant cells complementary RNAs with blocking properties [104,105]. One limiting factor for these approaches, like for all RNA-based therapies, is the capacity to vectorize therapeutic RNAs to malignant cells. This is even more critical for NPCs due to the extreme abundance of the viral

microRNAs in malignant cells. To our knowledge, no specific strategy has been proposed for direct targeting of the EBERs.

5.4. Cytolytic viral activation (CLVA)

Like for all *herpesviridae*, production of EBV viral particles results *ipso facto* in the death of the infected cell, hence the name of lytic cycle to characterize a state of infection oriented toward production of viral particles. The idea of disrupting viral latency in EBV-positive malignant cells has been in the air for decades (for a review see Oker et al., Intechopen.com, DOI: 10.5772/64738). Initially the idea was to use EBV as a kind of endogenous oncolytic virus but this was not realistic for at least 2 reasons. First, the mechanisms blocking the lytic cycle operate at multiple levels and it is much easier to obtain partial activation of several lytic genes than to achieve viral production in all cells. Next, activation of the lytic cycle is known to favor the release of soluble factors, especially cytokines, with potential oncogenic activity on bystander cells. Therefore, most investigators in the field aim to partial activation of lytic genes in order to induce expression of viral enzymes with the capacity to transform prodrugs in cytotoxic drugs, specifically in malignant cells. The two main candidate enzymes for this function are EBV thymidine kinase (EBV-TK) and EBV protein-kinase (EBV-PK). Another aim of partial lytic induction could be to increase the immunogenicity of malignant cells.

The proof of concept of the potential benefits of combining drugs inducing the lytic cycle with prodrugs has been made in clinical studies dealing with EBV-associated lymphomas and more recently with NPCs [106]. In a landmark study published by Wildeman et al., the lytic induction was achieved by a combination of valproic acid – used as a histone deacetylase inhibitor (HDACi) – and gemcitabin which like some other compounds of conventional chemo has proven to favor the disruption of latency in various types of EBV-infected cells. The prodrug was ganciclovir [91]. There is currently intense research in the academia and in the industry to investigate and optimize chemical inducers of the lytic cycle. A number of epigenetic modifiers are under investigation – especially HDACi – but also miscellaneous agents like tetrahydrocarboline derivatives, intra-cellular iron chelators or compounds inducing 'unfolded protein response' [107–109]. It seems that much less efforts are devoted to the development of adequate prodrugs. Most pre-clinical studies rely on ganciclovir or related oral compounds. Ganciclovir is activated by EBV-PK – not EBV TK – but it was initially designed as a substrate of HSV1-TK [110]. From the development of compounds specially designed for EBV enzymes, including EBV-PK and – TK, one may expect a better therapeutic index that would benefit the development of CLVA. There is also a margin of progression with regards to the biomarkers useful to monitor CLVA. Habib et al. have reported extra-cellular release of the BZLF1 protein and its detection in the plasma of AIDS patients bearing EBV-related lymphomas [111]. BZLF1 is an immediate early viral protein whose expression occurs at a very early stage of lytic activation. Its detection in the plasma of NPC patients might become a surrogate marker of lytic activation in tumor cells. However, its detection might be hampered by the concomitant presence of anti-BZLF1 antibodies which have been reported in NPC patients.

6. Immune modulators for immune restoration against malignant cells

As explained in the last sections of this review (Expert Opinon), there is a strong rationale to develop therapeutic approaches based on immuno-modulators for NPC treatment. These approaches aim to neutralize immune suppressive cells and to boost immune effector cells (Table 2).

6.1. Neutralization of immune checkpoints and related systems

Typical immune checkpoint systems are made of an inhibitory or stimulatory co-receptor at the surface of T-cells and their ligands at the surface of tumor cells or infiltrating cells like macrophages. In this setting, the aim of immunotherapy is usually to block the inhibitory co-receptors (for example PD1) or their ligands (for example PD-L1). Two ligands of T-cell inhibitory co-receptors are abundantly and consistently expressed by malignant NPC cells: HLA class II molecules and galectin-9 (Gal-9) whose receptors are Lag-3 and Tim-3, respectively. However, according to a recent study, Lag-3 and Tim-3 are usually expressed at a low level by tumor infiltrating lymphocytes of NPCs [67]. These observations that will need confirmation do not rule out a potential interest of antibodies blocking Lag-3 or Tim-3. Indeed, the efficiency of neutralizing antibodies is not always proportional to the expression of the inhibitory co-receptor. The HLA-G/ILT4 system might also be a potential target for immunotherapy [66,112]. So far, there is no data about the expression of ILT4 by stromal or malignant cells of NPCs, although therapeutic antibodies are currently developed against this molecule. B7-H4 is another inhibitory ligand (acting on the B7-H4-R co-receptor) which seems to be strongly expressed by NPC cells [67]. It is also a target for therapeutic antibodies under development. Because there is mounting evidence that mobilization of NK cells could benefit the treatment of NPCs, it will be useful to explore the potential of immune checkpoint inhibitors designed for this purpose, for example antibodies against NKG2A [113]. In addition to their positive impact on NK cells, these antibodies have been reported to concomitantly promote CD8 T-cell immunity [114].

6.2. Neutralization of immunosuppressive extra-cellular biomolecules

In the section about NPC tumor microenvironment, we have mentioned several biomolecules released by malignant cells which are suspected to contribute to the local immunosuppression, including LIF, CCL20 and galectin-9. Antibodies neutralizing LIF are currently in clinical development for human malignancies but, to our knowledge, have not been specifically tested in NPC patients [115](NCT03490669). The development of antibodies neutralizing CCL20 is much less advanced [116]. Therapeutic antibodies neutralizing extra-cellular galectin-9 are currently under pre-clinical development [117]. CCR4 is a chemokine receptor expressed at the surface of T-regs which mediates the chemotactic effect of CCL17 and CCL22. Both cytokines are abundant in some EBV-related malignancies like NK/T cell

Table 2. Examples of immune modulators potentially useful for NPC treatment.

Categories of therapeutic agents	Examples of targets	Current stage of development	References suggesting relevance to NPC
Therapeutic antibodies blocking immune checkpoint agonists or their receptors	HLA II/Lag3 (lymphocyte activation gene 3) Immune suppr. signal delivered to T- cells	Anti-Lag3 antibodies have already shown benefit in melanoma patients	Wang et al., J. Immunother. Cancer (2019)
	HLA G/ILT4 Immune suppr. signal delivered to myeloid cells	Anti-ILT4 antibodies currently in pre-clinical development (for example, AACR Annual Meeting 2019, abstract # 5007)	Cai et al., Int. J. Biol. Sci. (2012)
	B7H4/B7H4-R Immune suppr. signal delivered to Th1+ and Th17+ cells. Activation of Tregs.	One anti-B7H4 antibody currently in phase I trial for patients with advanced solid tumors (NCT0351421)	Wang et al., J. Immunother. Cancer (2019)
	HLA-E/NKG2A Immune suppr. signal delivered to NK-cells and CD8 + T-cells	Phase III trial in Head and Neck carcinomas to come soon	To our knowledge, the expression of HLA-E and NKG2A has not yet been investigated in NPCs
Therapeutic antibodies neutralizing immunosuppressive products released by tumor cells	Leukemia inhibitory factor (LIF)	One anti-LIF antibody currently in phase I trial for patients with advanced solid tumors (NCT03490669)	Liu and Chang, Mol Cell Oncol (2014)
	CCL20	In SCID mice xenotransplanted with C666-1 tumors, systemic administration of anti-CCL20 decreases T-reg accumulation in the tumor (Mrizak et al., JNCI, 2015)	Chang et al., Clin. Cancer Res. (2008) - Mrizak et al., JNCI (2015)
	Galectin-9	Anti-gal-9 antibodies currently in pre-clinical developpment (Lhuillier et al., Plos One, 2019)	Klibi et al., Blood (2009) - Chen et al., Scientific reports (2017)
Interferon β (IFN β)	Increases TRAIL and TRAIL-receptor expression by NK and NPC cells, respectively	Suggestion of a better outcome for pediatric NPCs treated with adjuvant IFN beta (Buehrlen et al., Cancer, 2012).	Makowska et al., Cancer Immunol. Immunother. (2019)

lymphomas [118]. It would be interesting to know their status in NPCs. Small molecules blocking CCR4 are currently in pre-clinical development (American Association for Cancer Research meeting, 2018, abstract #4752).

6.3. Interferon-β: new perspectives for an old immunotherapeutic agent

Several clinical trials, performed mainly in Germany, suggest that adjuvant immunotherapy based on systemic administration of interferon-β during 6 months following radiotherapy or concomitant chemo-radiotherapy results in better disease-free and overall survival [119]. More recently, laboratory investigations have been performed to assess the contribution of NK cells in these positive effects of IFN-β. Using xenografted EBV-positive NPC cells and clinical materials, we have shown that IFN-β enhances the action of NK cells by two synergistic modifications: induction of TRAIL-receptor expression on NPC cells and TRAIL expression by NK cells with release of extra-cellular soluble TRAIL (sTRAIL). Consistently, sTRAIL concentration is increased in the serum of NPC patients treated with IFN-β [120,121]. However, in the same time, IFN-β enhances PD-L1 and PD1 expression by NPC cells and NK cells, respectively. As expected, NK cell cytotoxic effect is maximal, at least *in vitro*, when combining activation of NK-cells by IFN-β and PD1 blockade with Nivolumab [122].

7. Conclusion

In spite of remarkable progress made in the treatment of NPCs by radiotherapy and chemotherapy, there is a deep need for more effective and more selective treatments. The aim is to achieve a higher rate of cure for advanced forms and a reduction in long-term side effects for all patients. The increasingly detailed study of the viral and cellular mechanisms of oncogenesis has unmasked elements of vulnerability that are ultimately very diverse. In the field of host-tumor interactions, there are also a number of possible tumor vulnerabilities. Some of the next challenges will be to assess the relative effectiveness of these potential targets and to design combinations adapted to the distinct clinico-biological forms of NPCs.

8. Expert Opinion

8.1. A novel context

The recent openings of clinical studies based on cell cycle inhibitors (§ 4.1) or those based on direct blockers of viral proteins (§ 5.1 and Table 1) open a new era in the therapy of NPCs. It gives factual proof that it is now possible to progress from the elucidation of viral and cellular NPC oncogenesis to molecular pharmacology and clinical research.

8.2. These advances highlight the need for a better histo-molecular classification of NPCs

To some extent, NPC appears as a unified pathological entity with biological and clinical characteristics shared by virtually all tumors like EBNA1 expression, constitutive NF-kB activation and

sensitivity to radiotherapy. However, beyond this frame, there are multiple factors of heterogeneity in NPC models as well as in clinical specimens. For example, the morphology of the malignant cells, the spatial distribution of the lymphoid infiltrate, the spectrum of EBV transcripts, the stringency of the latent infection, the mechanisms underlying constitutive NF-KB activation and many cellular genetic and epigenetic alterations are diverse. A more systematic and comprehensive molecular classification that would take in account all these characteristics would facilitate the development of novel therapeutic tools.

8.3. Sustained development of pre-clinical NPC models will remain critical for rapid evaluation of emerging therapeutic targets

As mentioned in section 2.1, after a long period of stagnation, a numbers of NPC PDX and a few EBV-positive NPC cell lines propagated *in vitro* have been obtained in the last five years in several laboratories. This is a major breakthrough which has long been awaited. However, two types of additional progress are desirable for rapid development of novel therapeutic tools. One aim is to secure and make available wide panels of EBV-positive NPC models in public repositories. Indeed, investigators interested in novel therapeutic approaches will need to access a pool of EBV-positive preclinical models of sufficient size, reflecting the heterogeneity of the disease in real life. Another aim is to obtain NPC cell lines or PDX with matched autologous immune cells. This would greatly help investigations on immune modulators, especially their possible combination with radiotherapy [123].

8.4. There is a strong rationale for more investigations on the potential of immune modulators

This assumption is based on 3 observations. 1) NPC is a hot tumor with consistent expression of viral antigens (at least EBNA1). 2) In contrast with PTLDs (post-transplant lymphoproliferative diseases) tumor immune escape is due to local production of immunosuppressive factors rather than to a primary deficit of the immune system [71]. 3) Immunomodulators are expected to be compatible with induction chemotherapy and may benefit from clinical and biological evaluation during the window of opportunity prior to the start of concurrent radiochemotherapy. In this field, it is important to keep in mind two potential pitfalls. The expression of immune checkpoints and their ligands might change under treatment by radiotherapy or chemotherapy, with either induction or suppression [65]. Circulating tumor exosomes often express checkpoint ligands at their surface entailing a risk of titration of therapeutic antibodies and reduced access to the tumor [124].

8.5. Strengthening NK cell responses seems to be a promising strategy

This assumption is based on the following observations. The abundance of NK cells in the tumor seems to have positive prognostic value [69]. HLA class I expression is deficient in about 30% NPC tumors which presumably makes them more vulnerable to NK cytotoxicity [33]. Paradoxically, this subset of tumors seems to be more sensitive to anti-PD1/PD-L1 antibodies suggesting enhancement of NK-cell functions [85]. This hypothesis would be consistent with our recent *in vitro* observations on the synergy of interferon-β and anti-PD1 antibodies in the activation of NK cell cytotoxicity against NPC cells [122].

8.6. It will be important to optimize the sequential use of new therapeutic agents

For example, if acquired resistances to EBNA1 inhibitors results from the emergence of EBV-negative malignant cells, CLVA therapy will not be useful for rescue of these patients. In contrast, if resistance results from EBNA1 mutations with persistence of the EBV genome in malignant cells, CLVA will be a rational approach. In the field of immune checkpoint inhibitors, there are also evidence that one antibody given first can make the tumor more sensitive to another antibody given at the next stage of the treatment [88,125].

8.7. On the long term, adoptive immunotherapy and EBV-vaccination may find their best indications in prophylactic settings

For example, adoptive immunotherapy is expected to be useful for intensification treatment and prevention of relapses in patients who retain circulating EBV-DNA at the completion of concurrent radio-chemotherapy. Anti-EBV vaccination might be useful for subjects in NPC endemic areas who exhibit pre-tumoral systemic alterations of EBV markers, i.e. repeated detection of circulating EBV-DNA and/or alterations in the profile and abundance of circulating anti-EBV antibodies.

Funding

The work of the authors is supported by the Bristol-Myers-Squibb Foundation for Research on Immuno-Oncology (grant number: 1709-04-040).

Declaration of interest

The team of P Busson has contracts of collaboration with HiFiBiO Therapeutics, a company developing therapeutic antibodies, including antibodies neutralizing human galectin-9, and Viracta Therapeutics, a company developing HDAC inhibitors for EBV-related malignancies. Furthermore, C Even is a partner of Cullivan Apollo Corporation for a clinical trial of VK2019. The authors have no other relevant affiliations or financial involvement with any organization or entity with a financial interest in or financial conflict with the subject matter or materials discussed in the manuscript. This includes employment, consultancies, honoraria, stock ownership or options, expert testimony, grants or patents received or pending, or royalties.

Reviewer disclosures

Peer reviewers on this manuscript have no relevant financial or other relationships to disclose

ORCID

Pierre Busson http://orcid.org/0000-0003-1027-3400

References

Papers of special note have been highlighted as either of interest (•) or of considerable interest (••) to readers.

1. Limkin EJ, Blanchard P. Does east meet west? Towards a unified vision of the management of nasopharyngeal carcinoma [comparative study review]. Br J Radiol. 2019 Oct; 92(1102):20190068.
2. Xie SH, Yu IT, Tse LA, et al. Sex difference in the incidence of nasopharyngeal carcinoma in Hong Kong 1983-2008: suggestion of a potential protective role of oestrogen. Eur J Cancer. 2013 Jan; 49(1):150–155.
3. Linsell CA. Nasopharyngeal cancer in Kenya: Pathology. Br J Cancer. 1964 Mar; 18:49–57.
4. Gaye AM, Mouamba FG, Dieme MJ, et al. [Undifferentiated carcinoma of the nasopharynx in Dakar, an area supposed to be non-endemic: About 13 cases]. Bull Soc Pathol Exot. 2018; 111 (2):84–89.
5. Viguer JM, Jimenez-Heffernan JA, Lopez-Ferrer P, et al. Fine-needle aspiration cytology of metastatic nasopharyngeal carcinoma. Diagn Cytopathol. 2005 Apr; 32(4):233–237.
6. Messick TE, Smith GR, Soldan SS, et al. Structure-based design of small-molecule inhibitors of EBNA1 DNA binding blocks Epstein-Barr virus latent infection and tumor growth.. Sci Transl Med. 2019 Mar 6; 11:482.

•• ***Description of one of the most innovative agents targeting EBV in NPC and currently investigated in clinical trials***

7. Hui KF, Chan TF, Yang W, et al. High risk Epstein-Barr virus variants characterized by distinct polymorphisms in the EBER locus are strongly associated with nasopharyngeal carcinoma. Int J Cancer. 2019 Jun 15; 144(12):3031–3042.
8. Zhang JB, Huang SY, Wang TM, et al. Natural variations in BRLF1 promoter contribute to the elevated reactivation level of Epstein-Barr virus in endemic areas of nasopharyngeal carcinoma [clinical trial]. EBioMedicine. 2018 Nov; 37:101–109.
9. Xu M, Yao Y, Chen H, et al. Genome sequencing analysis identifies Epstein-Barr virus subtypes associated with high risk of nasopharyngeal carcinoma. Nat Genet. 2019 Jul; 51(7):1131–1136.
10. Tsang CM, Yip YL, Lo KW, et al. Cyclin D1 overexpression supports stable EBV infection in nasopharyngeal epithelial cells. Proc Natl Acad Sci USA. 2012 Dec 11; 109(50):E3473–82.
11. Feng BJ. Descriptive, environmental and genetic epidemiology of nasopharyngeal carcinoma. In: Bussson P, *Editor*. Nasopharyngeal carcinoma: Keys for translational medicine and biology. Austin/New-York: Landes/Springer; 2013. p. 23–41.
12. Gourzones C, Ferrand F-R, Vérillaud B, et al. Biological tools for NPC population screening and disease monitoring. In: Busson P, *Editor*. Nasopharyngeal carcinoma: Keys for translational medicine and biology. Austin/New-York: Landes/Springer; 2013. p. 101–117.
13. Lam WKJ, Jiang P, Chan KCA, et al. Sequencing-based counting and size profiling of plasma Epstein-Barr virus DNA enhance population screening of nasopharyngeal carcinoma. Proc Natl Acad Sci USA. 2018 May 29; 115(22):E5115–E5124.
14. Yu KJ, Hsu WL, Pfeiffer RM, et al. Prognostic utility of anti-EBV antibody testing for defining NPC risk among individuals from high-risk NPC families. Clin Cancer Res. 2011 Apr 1; 17 (7):1906–1914.
15. Cheung ST, Huang DP, Hui AB, et al. Nasopharyngeal carcinoma cell line (C666-1) consistently harbouring Epstein-Barr virus. Int J Cancer. 1999 Sep 24; 83(1):121–126.
16. Verillaud B, Gressette M, Morel Y, et al. Toll-like receptor 3 in Epstein-Barr virus-associated nasopharyngeal carcinomas: consistent expression and cytotoxic effects of its synthetic ligand poly(A:U) combined to a Smac-mimetic. Infect Agent Cancer. 2012 Dec 3; 7(1):36.

• **The first publication recording NPC vulnerability to SMAC mimetics**

17. Yip YL, Lin W, Deng W, et al. Establishment of a nasopharyngeal carcinoma cell line capable of undergoing lytic Epstein-Barr virus reactivation. Lab Invest. 2018 Aug; 98(8):1093–1104.
18. Lin W, Yip YL, Jia L, et al. Establishment and characterization of new tumor xenografts and cancer cell lines from EBV-positive nasopharyngeal carcinoma. Nat Commun. 2018 Nov 7; 9(1):4663.

•• ***Description of a new generation of long-awaited laboratory NPC models***

19. Hsu CL, Lui KW, Chi LM, et al. Integrated genomic analyses in PDX model reveal a cyclin-dependent kinase inhibitor Palbociclib as a novel candidate drug for nasopharyngeal carcinoma. J Exp Clin Cancer Res. 2018 Sep 20; 37(1):233.
20. Hoe SL, Tan LP, Jamal J, et al. Evaluation of stem-like side population cells in a recurrent nasopharyngeal carcinoma cell line. Cancer Cell Int. 2014; 14(1):101.
21. Kripalani-Joshi S, Law HY. Identification of integrated Epstein-Barr virus in nasopharyngeal carcinoma using pulse field gel electrophoresis. Int J Cancer. 1994 Jan 15; 56(2):187–192.
22. Iwakiri D, Zhou L, Samanta M, et al. Epstein-Barr virus (EBV)-encoded small RNA is released from EBV-infected cells and activates signaling from Toll-like receptor 3. J Exp Med. 2009 Sep 28; 206(10):2091–2099.
23. Li Z, Duan Y, Cheng S, et al. EBV-encoded RNA via TLR3 induces inflammation in nasopharyngeal carcinoma. Oncotarget. 2015 Sep 15; 6(27): 24291–24303.
24. Raab-Traub N. Nasopharyngeal Carcinoma:An Evolving Role for the Epstein-Barr Virus. Curr Top Microbiol Immunol. 2015; 390:339–363.
25. Hsu CY, Yi YH, Chang KP, et al. The Epstein-Barr virus-encoded microRNA MiR-BART9 promotes tumor metastasis by targeting E-cadherin in nasopharyngeal carcinoma. PLoS Pathog. 2014 Feb; 10(2):e1003974.
26. Wilson JB, Manet E, Gruffat H, et al. EBNA1: Oncogenic activity, immune evasion and biochemical functions provide targets for novel therapeutic strategies against Epstein-Barr virus- associated cancers [review]. Cancers (Basel). Apr 2018 6; 10(4). 10.3390/cancers10040109.
27. Frappier L. EBNA1 [Review]. Curr Top Microbiol Immunol. 2015; 391:3–34.
28. Gourzones C, Busson P,, Raab-Traub N. Epstein-Barr virus and the pathogenesis of nasopharyngeal carcinomas. In: Busson P, *Editor*. Nasopharyngeal carcinoma: Keys for translational medicine and biology. Austin/New-York: Landes/Springer; 2013. p. 42–60.
29. Morrison JA, Raab-Traub N. Roles of the ITAM and PY motifs of Epstein-Barr virus latent membrane protein 2A in the inhibition of epithelial cell differentiation and activation of {beta}-catenin signaling. J Virol. 2005 Feb; 79(4):2375–2382.
30. Zhou X, Matskova L, Rathje LS, et al. SYK interaction with ITGbeta4 suppressed by Epstein-Barr virus LMP2A modulates migration and invasion of nasopharyngeal carcinoma cells. Oncogene. 2015 Aug 20; 34(34):4491–4499.
31. Kong QL, Hu LJ, Cao JY, et al. Epstein-Barr virus-encoded LMP2A induces an epithelial-mesenchymal transition and increases the number of side population stem-like cancer cells in nasopharyngeal carcinoma. PLoS Pathog. 2010; 6(6):e1000940.
32. Turrini R, Merlo A, Martorelli D, et al. A BARF1-specific mAb as a new immunotherapeutic tool for the management of EBV-related tumors. Oncoimmunology. 2017; 6(4):e1304338.
33. Li YY, Chung GT, Lui VW, et al. Exome and genome sequencing of nasopharynx cancer identifies NF-kappaB pathway activating mutations. Nat Commun. 2017 Jan; 18(8):14121.

•• **A landmark study giving an overview of NPC genetic alterations and highlighting the key role of NF-kB pathways in the oncogenesis of NPCs**

34. Lo KW, Cheung ST, Leung SF, et al. Hypermethylation of the p16 gene in nasopharyngeal carcinoma. Cancer Res. 1996 Jun 15; 56 (12): 2721–2725.
35. Hui AB, Or YY, Takano H, et al. Array-based comparative genomic hybridization analysis identified cyclin D1 as a target oncogene at 11q13.3 in nasopharyngeal carcinoma. Cancer Res. 2005 Sep 15; 65 (18): 8125–8133.
36. Effert P, McCoy R, Abdel-Hamid M, et al. Alterations of the p53 gene in nasopharyngeal carcinoma. J Virol. 1992 Jun; 66 (6):3768–3775.
37. Niedobitek G, Agathanggelou A, Barber P, et al. P53 overexpression and Epstein-Barr virus infection in undifferentiated and squamous cell nasopharyngeal carcinomas. J Pathol. 1993 Aug; 170 (4):457–461.

38. Saridakis V, Sheng Y, Sarkari F, et al. Structure of the p53 binding domain of HAUSP/USP7 bound to Epstein-Barr nuclear antigen 1 implications for EBV-mediated immortalization. Mol Cell. 2005 Apr 1; 18(1):25–36.
39. Chung GT, Lou WP, Chow C, et al. Constitutive activation of distinct NF-kappaB signals in EBV-associated nasopharyngeal carcinoma. J Pathol. 2013 Nov; 231(3):311–322.
40. Thornburg NJ, Raab-Traub N. Induction of epidermal growth factor receptor expression by Epstein-Barr virus latent membrane protein 1 C-terminal-activating region 1 is mediated by NF-kappaB p50 homodimer/Bcl-3 complexes. J Virol. 2007 Dec; 81(23):12954–12961.
41. Or YY, Chung GT, To KF, et al. Identification of a novel 12p13.3 amplicon in nasopharyngeal carcinoma. J Pathol. 2010 Jan; 220 (1):97–107.
42. Tsang CM, Lui VWY, Bruce JP, et al. Translational genomics of nasopharyngeal cancer [review]. Semin Cancer Biol. 2020 Apr; 61:84–100. doi: 10.1016/j.semcancer.2019.09.006
43. Pan Y, Wang S, Su B, et al. Stat3 contributes to cancer progression by regulating Jab1/Csn5 expression. Oncogene. 2017 Feb 23; 36 (8):1069–1079.
44. Chung AK, OuYang CN, Liu H, et al. Targeted sequencing of cancer-related genes in nasopharyngeal carcinoma identifies mutations in the TGF-beta pathway. Cancer Med. 2019 Sep; 8 (11):5116–5127.
45. Chow YP, Tan LP, Chai SJ, et al. Exome sequencing identifies potentially druggable mutations in nasopharyngeal carcinoma. Scii Rep. 2017 Mar 3; 7:42980.
46. Wang C, Jiang S, Ke L, et al. Genome-wide CRISPR-based gene knockout screens reveal cellular factors and pathways essential for nasopharyngeal carcinoma. J Biol Chem. 2019 Jun 21; 294 (25):9734–9745.
47. Gourzones C, Klibi-Benlagha J, Friboulet L, et al. Cellular interactions in nasopharyngeal carcinomas. In: Busson P, *Editor*. Nasopharyngeal carcinoma: Keys for translational medicine and biology. Austin/New York: Landes/Springer; 2013. p. 82–100.
48. Li ZL, Ye SB, OuYang LY, et al. COX-2 promotes metastasis in nasopharyngeal carcinoma by mediating interactions between cancer cells and myeloid-derived suppressor cells. Oncoimmunology. 2015 Nov; 4(11):e1044712.
49. Ooft ML, van Ipenburg JA, Sanders ME, et al. Prognostic role of tumour-associated macrophages and regulatory T cells in EBV-positive and EBV-negative nasopharyngeal carcinoma. J Clin Pathol. 2018 Mar; 71(3):267–274.
50. Gourzones C, Barjon C, Busson P. Host-tumor interactions in nasopharyngeal carcinomas. Semin Cancer Biol. 2012 Apr; 22(2):127–136.
51. Liu SC, Chang YS. Role of leukemia inhibitory factor in nasopharyngeal carcinogenesis [review]. Mol Cell Oncol. 2014; 1(1):e29900.
52. Liu SC, Hsu T, Chang YS, et al. Cytoplasmic LIF reprograms invasive mode to enhance NPC dissemination through modulating YAP1-FAK/PXN signaling. Nat Commun. 2018 Nov 30; 9(1):5105.
53. Chang KP, Hao SP, Chang JH, et al. Macrophage inflammatory protein-3alpha is a novel serum marker for nasopharyngeal carcinoma detection and prediction of treatment outcomes. Clin Cancer Res. 2008 Nov 1; 14(21):6979–6987.
54. Mrizak D, Martin N, Barjon C, et al. Effect of nasopharyngeal carcinoma-derived exosomes on human regulatory T cells. J Natl Cancer Inst. 2015 Jan; 107(1):363.
55. Metcalfe SM. LIF in the regulation of T-cell fate and as a potential therapeutic [review]. Genes Immun. 2011 Apr; 12(3):157–168.
56. Pioche-Durieu C, Keryer C, Souquere S, et al. In nasopharyngeal carcinoma cells, Epstein-Barr virus LMP1 interacts with galectin 9 in membrane raft elements resistant to simvastatin. J Virol. 2005 Nov; 79(21):13326–13337.
57. Daley D, Zambirinis CP, Seifert L, et al. Cell. Gamma-delta T cells support pancreatic oncogenesis by restraining alpha-beta T cell activation. Cell. 2016 Sep 8; 166(6):1485–1499. doi: 10.1016/j.cell.2016.07.046.
58. Daley D, Mani VR, Mohan N, et al. Dectin 1 activation on macrophages by galectin 9 promotes pancreatic carcinoma and peritumoral immune tolerance. Nat Med. 2017 May; 23(5):556–567.
59. Golden-Mason L, McMahan RH, Strong M, et al. Galectin-9 functionally impairs natural killer cells in humans and mice. J Virol. 2013 May; 87(9):4835–4845.
60. Wu C, Thalhamer T, Franca RF, et al..Galectin-9-CD44 interaction enhances stability and function of adaptive regulatory T cells. Immunity. 2014 Aug 21;41(2):270–82. doi: 10.1016/j.immuni.2014.06.011
61. Enninga EAL, Chatzopoulos K, Butterfield JT, et al. CD206-positive myeloid cells bind galectin-9 and promote a tumor-supportive microenvironment. J Pathol. 2018 Aug; 245(4):468–477.
62. Chen TC, Chen CH, Wang CP, et al. The immunologic advantage of recurrent nasopharyngeal carcinoma from the viewpoint of Galectin-9/Tim-3-related changes in the tumour microenvironment. Sci Rep. 2017 Sep 4; 7(1):10349.
63. Keryer-Bibens C, Pioche-Durieu C, Villemant C, et al. Exosomes released by EBV-infected nasopharyngeal carcinoma cells convey the viral latent membrane protein 1 and the immunomodulatory protein galectin 9. BMC Cancer. 2006; 6:283.
64. Klibi J, Niki T, Riedel A, et al. Blood diffusion and Th1-suppressive effects of galectin-9–containing exosomes released by Epstein-Barr virus–infected nasopharyngeal carcinoma cells. Blood. 2009; 113 (9):1957–1966.
65. Ruan Y, Hu W, Li W, et al. Analysis of plasma EBV-DNA and soluble checkpoint proteins in nasopharyngeal carcinoma patients after definitive intensity-modulated radiotherapy. Biomed Res Int. 2019 May 5; 2019:3939720.
66. Cai MB, Han HQ, Bei JX, et al. Expression of human leukocyte antigen G is associated with prognosis in nasopharyngeal carcinoma. Int J Biol Sci. 2012; 8(6):891–900.
67. Wang YQ, Zhang Y, Jiang W, et al. Development and validation of an immune checkpoint-based signature to predict prognosis in nasopharyngeal carcinoma using computational pathology analysis. J Immunother Cancer. 2019 Nov 13; 7(1):298.
68. Ben-Haj-Ayed A, Moussa A, Ghedira R, et al. Prognostic value of indoleamine 2,3-dioxygenase activity and expression in nasopharyngeal carcinoma. Immunol Lett. 2016 Jan; 169:23–32.
69. Lu J, Chen XM, Huang HR, et al. Detailed analysis of inflammatory cell infiltration and the prognostic impact on nasopharyngeal carcinoma. Head Neck. 2018 Jun; 40(6):1245–1253.
70. Li J, Mo HY, Xiong G, et al. Tumor microenvironment macrophage inhibitory factor directs the accumulation of interleukin-17-producing tumor-infiltrating lymphocytes and predicts favorable survival in nasopharyngeal carcinoma patients. J Biol Chem. 2012 Oct 12; 287(42):35484–35495.
71. Li J, Zeng XH, Mo HY, et al. Functional inactivation of EBV-specific T-lymphocytes in nasopharyngeal carcinoma: implications for tumor immunotherapy. PloS One. 2007 Nov 7; 2(11):e1122.

•• **The best study showing that in NPC patients, the functional deficit of anti-EBV immunity is much more accentuated in the tumor microenvironment than at the systemic level.**

72. Lau KM, Cheng SH, Lo KW, et al. Increase in circulating Foxp3+CD4 +CD25(high) regulatory T cells in nasopharyngeal carcinoma patients. Br J Cancer. 2007 Feb 26; 96(4):617–622.
73. Gourzones C, Ferrand FR, Amiel C, et al. Consistent high concentration of the viral microRNA BART17 in plasma samples from nasopharyngeal carcinoma patients - evidence of non-exosomal transport. Virol J. 2013 Apr 16; 10(1):119.
74. Gao W, Wong TS, Lv KX, et al. Detection of Epstein-Barr virus (EBV)-encoded microRNAs in plasma of patients with nasopharyngeal carcinoma. Head Neck. 2019 Mar; 41(3):780–792.
75. Lv J, Chen Y, Zhou G, et al. Liquid biopsy tracking during sequential chemo-radiotherapy identifies distinct prognostic phenotypes in nasopharyngeal carcinoma. Nat Commun. 2019 Sep 2; 10(1):3941.
76. Ye SB, Zhang H, Cai TT, et al. Exosomal miR-24-3p impedes T-cell function by targeting FGF11 and serves as a potential prognostic biomarker for nasopharyngeal carcinoma. J Pathol. 2016 Nov; 240 (3):329–340.
77. Ou G, Xing S, Li J, et al. Circulating tumor cells: a valuable marker of poor prognosis for advanced nasopharyngeal carcinoma. Mol Med. 2019 Nov 15; 25(1):50.

78. Chen YP, Chan ATC, Le QT, et al. Nasopharyngeal carcinoma [Review]. Lancet. 2019 Jul 6; 394(10192):64–80.
79. Blanchard P, Lee A, Marguet S, et al. Chemotherapy and radiotherapy in nasopharyngeal carcinoma: an update of the MAC-NPC meta-analysis. Lancet Oncol. 2015 Jun; 16(6):645–655.
80. Frikha M, Auperin A, Tao Y, et al. A randomized trial of induction docetaxel-cisplatin-5FU followed by concomitant cisplatin-RT versus concomitant cisplatin-RT in nasopharyngeal carcinoma (GORTEC 2006-02) [clinical trial]. Ann Oncol. 2018 Mar 1; 29(3): 731–736.
81. Chan ATC, Hui EP, Ngan RKC, et al. Analysis of plasma Epstein-Barr virus DNA in nasopharyngeal cancer after chemoradiation to identify high-risk patients for adjuvant chemotherapy: A randomized controlled trial. J Clin Oncol. 2018 Jul 10; abstract JCO 2018777847. doi: 10.1200/JCO.2018.77.78475f
82. Zhang Y, Chen L, Hu GQ, et al. Gemcitabine and cisplatin induction chemotherapy in nasopharyngeal carcinoma [clinical trial]. N Engl J Med. 2019 Sep 19; 381(12):1124–1135.
83. Iqbal MS, Wilkinson D, Tin A, et al. Cetuximab in the management of nasopharyngeal carcinoma - a narrative review. J Laryngol Otol. 2019; 11:1–13.
84. Almobarak AA, Jebreel AB, Abu-Zaid A. Molecular targeted therapy in the management of recurrent and metastatic nasopharyngeal carcinoma: A comprehensive literature review [review]. Cureus. 2019 Mar 9; 11(3):e4210.
85. Ma BBY, Lim WT, Goh BC, et al. Antitumor activity of nivolumab in recurrent and metastatic nasopharyngeal carcinoma: An international, multicenter study of the mayo clinic phase 2 consortium (NCI-9742) [clinical trial]. J Clin Oncol. 2018 May 10; 36 (14):1412–1418.
86. Hsu C, Lee SH, Ejadi S, et al. Safety and antitumor activity of pembrolizumab in patients with programmed death-ligand 1-positive nasopharyngeal carcinoma: Results of the KEYNOTE-028 study [clinical trial, phase i multicenter study]. J Clin Oncol. 2017 Dec 20; 35(36):4050–4056.
87. Chow JC, Ngan RK, Cheung KM, et al. Immunotherapeutic approaches in nasopharyngeal carcinoma. Expert Opin Biol Ther. 2019 Nov; 19(11):1165–1172.
88. Fang W, Yang Y, Ma Y, et al. Camrelizumab (SHR-1210) alone or in combination with gemcitabine plus cisplatin for nasopharyngeal carcinoma: results from two single-arm, phase 1 trials [clinical trial, phase i comparative study multicenter study research support]. Lancet Oncol. 2018 Oct; 19(10):1338–1350.
89. Gourzones C, Busson P, Raab-Traub N. Epstein-Barr virus and the pathogenesis of nasopharyngeal carcinomas. In: Busson P, *Editor*. Nasopharyngeal carcinoma: Keys for translational medicine and biology. Austin/New York: Landes/Springer; 2013. p. 42–60.
90. Taylor GS, Jia H, Harrington K, et al. A recombinant modified vaccinia Ankara vaccine encoding Epstein-Barr Virus (EBV) target antigens: a phase I trial in UK patients with EBV-positive cancer [clinical trial, phase i multicenter study]. Clin Cancer Res. 2014 Oct 1; 20(19):5009–5022.
91. Wildeman MA, Novalic Z, Verkuijlen SA, et al. Cytolytic virus activation therapy for Epstein-Barr virus-driven tumors. Clin Cancer Res. 2012 Sep 15; 18(18):5061–5070.
•• **So far the most authoritative study on a pilot trial of cytolytic virus activation (CLVA) therapy that has brought a clinical benefit for a few NPC patients**
92. Wong CH, Ma BBY, Hui CWC, et al. Preclinical evaluation of ribociclib and its synergistic effect in combination with alpelisib in non-keratinizing nasopharyngeal carcinoma. Sci Rep. 2018 May 22; 8 (1):8010.
93. Voon YL, Ahmad M, Wong PF, et al. Nutlin-3 sensitizes nasopharyngeal carcinoma cells to cisplatin-induced cytotoxicity. Oncol Rep. 2015 Oct; 34(4):1692–1700.
94. Fan X, Wang Y, Song J, et al. MDM2 inhibitor RG7388 potently inhibits tumors by activating p53 pathway in nasopharyngeal carcinoma. Cancer Biol Ther. 2019; 20(10):1328–1336.
95. Kocik J, Machula M, Wisniewska A, et al. Helping the released guardian: drug combinations for supporting the anticancer activity of HDM2 (MDM2) antagonists [review]. Cancers (Basel). Jul 2019 19; 11(7). 10.3390/cancers11071014.
96. Zeligs KP, Neuman MK, Annunziata CM. Molecular pathways: the balance between cancer and the immune system challenges the therapeutic specificity of targeting nuclear factor-kappaB signaling for cancer treatment [review]. Clin Cancer Res 2016 Sep 1; 22 (17):4302–4308.
97. Friboulet L, Pioche-Durieu C, Rodriguez S, et al. Recurrent overexpression of c-IAP2 in EBV-associated nasopharyngeal carcinomas: critical role in resistance to Toll-like receptor 3-mediated apoptosis. Neoplasia. 2008 Nov; 10(11):1183–1194..
98. Friboulet L, Gourzones C, Tsao SW, et al. Poly(I:C) induces intense expression of c-IAP2 and cooperates with an IAP inhibitor in induction of apoptosis in cancer cells. BMC Cancer. 2010; 10:327.
99. Man CH, Wei-Man Lun S, Wai-Ying Hui J, et al. Inhibition of NOTCH3 signalling significantly enhances sensitivity to cisplatin in EBV-associated nasopharyngeal carcinoma. J Pathol. 2012 Feb; 226 (3):471–481.
100. Bochkarev A, Barwell JA, Pfuetzner RA, et al. Crystal structure of the DNA-binding domain of the Epstein-Barr virus origin-binding protein EBNA 1. Cell. 1995; 83(1):39–46.
101. Jiang L, Lung HL, Huang T, et al. Reactivation of Epstein-Barr virus by a dual-responsive fluorescent EBNA1-targeting agent with Zn(2+)--chelating function. Proc Natl Acad Sci USA. 2019 Dec 10; 117(10):5542
102. Zhu S, Chen J, Xiong Y, et al. Novel EBV LMP-2-affibody and affitoxin in molecular imaging and targeted therapy of nasopharyngeal carcinoma. PLoS Pathog. 2020 Jan; 16(1):e1008223.
103. Stahl S, Graslund T, Eriksson Karlstrom A, et al. Affibody molecules in biotechnological and medical applications [review]. Trends Biotechnol. 2017 Aug; 35(8):691–712.
104. Cai L, Li J, Zhang X, et al. Gold nano-particles (AuNPs) carrying anti-EBV-miR-BART7-3p inhibit growth of EBV-positive nasopharyngeal carcinoma. Oncotarget. 2015 Apr 10; 6(10):7838–7850.
105. Hooykaas MJG, Soppe JA, De Buhr HM, et al. RNA accessibility impacts potency of tough decoy microRNA inhibitors. RNA Biol. 2018; 15(11):1410–1419.
106. SP P, Hermine O, Small T, et al. A phase 1/2 trial of arginine butyrate and ganciclovir in patients with Epstein-Barr virus-associated lymphoid malignancies [clinical trial, phase i clinical trial, phase ii]. Blood. 2007 Mar 15; 109(6):2571–2578.
107. Tikhmyanova N, Schultz DC, Lee T, et al. Identification of a new class of small molecules that efficiently reactivate latent Epstein-Barr Virus. ACS Chem Biol. 2014 Mar 21; 9(3):785–795.
108. Yiu SPT, Hui KF, Choi CK, et al. Intracellular Iron chelation by a novel compound, C7, reactivates Epstein-Barr Virus (EBV) lytic cycle via the Erk-autophagy axis in EBV-positive epithelial cancers. Cancers (Basel). 2018 Dec 11; 10(12). 10.3390/cancers10120505.
109. Lee J, Kosowicz JG, Hayward SD, et al. Pharmacologic activation of lytic Epstein-Barr virus gene expression without virion production. J Virol. 2019 Oct 15; 93:20.
110. Meng Q, Hagemeier SR, Fingeroth JD, et al. The Epstein-Barr virus (EBV)-encoded protein kinase, EBV-PK, but not the thymidine kinase (EBV-TK), is required for ganciclovir and acyclovir inhibition of lytic viral production. J Virol. 2010 May; 84(9):4534–4542.
111. Habib M, Buisson M, Lupo J, et al. Lytic EBV infection investigated by detection of soluble Epstein-Barr virus ZEBRA in the serum of patients with PTLD [clinical trial]. Sci Rep. 2017 Sep 5; 7(1):10479.
112. Gao A, Sun Y, Peng G. ILT4 functions as a potential checkpoint molecule for tumor immunotherapy. Biochim Biophys Acta Rev Cancer. 2018 Apr; 1869(2):278–285.
113. Andre P, Denis C, Soulas C, et al. Anti-NKG2A mAb Is a checkpoint inhibitor that promotes anti-tumor immunity by unleashing both T and NK cells. Cell. 2018 Dec 13; 175(7):1731–1743.
114. van Montfoort N, Borst L, Korrer MJ, et al. NKG2A blockade potentiates CD8 T cell immunity induced by cancer vaccines. Cell. 2018 Dec 13; 175(7):1744–1755.
115. Pascual-Garcia M, Bonfill-Teixidor E, Planas-Rigol E, et al. LIF regulates CXCL9 in tumor-associated macrophages and prevents CD8 (+) T cell tumor-infiltration impairing anti-PD1 therapy. Nat Commun. 2019 Jun 11; 10(1):2416.

116. Ranasinghe R, Eri R. Modulation of the CCR6-CCL20 Axis: A potential therapeutic target in inflammation and cancer [review]. Medicina (Kaunas). 2018 Nov 16; 54:5.
117. Lhuillier C, Barjon C, Baloche V, et al. Characterization of neutralizing antibodies reacting with the 213-224 amino-acid segment of human galectin-9. PloS One. 2018; 13(9):e0202512.
118. Kumai T, Nagato T, Kobayashi H, et al. CCL17 and CCL22/CCR4 signaling is a strong candidate for novel targeted therapy against nasal Natural Killer/T-cell lymphoma. Cancer Immunol Immunother. 2015 Jun; 64(6):697–705.
119. Buehrlen M, Zwaan CM, Granzen B, et al. Multimodal treatment, including interferon beta, of nasopharyngeal carcinoma in children and young adults: preliminary results from the prospective, multicenter study NPC-2003-GPOH/DCOG [clinical trial multicenter study]. Cancer. 2012 Oct 1; 118(19):4892–4900.
120. Makowska A, Wahab L, Braunschweig T, et al. Interferon beta induces apoptosis in nasopharyngeal carcinoma cells via the TRAIL-signaling pathway. Oncotarget. 2018 Mar 6; 9(18):14228–14250.
121. Makowska A, Franzen S, Braunschweig T, et al. Interferon beta increases NK cell cytotoxicity against tumor cells in patients with nasopharyngeal carcinoma via tumor necrosis factor apoptosis-inducing ligand. Cancer Immunol Immunother. 2019 Aug; 68(8):1317–1329.
122. Makowska A, Braunschweig T, Denecke B, et al. Interferon beta and anti-PD-1/PD-L1 checkpoint blockade cooperate in NK cell-mediated killing of nasopharyngeal carcinoma cells. Transl Oncol. 2019 Sep; 12(9):1237–1256.
123. Yeo ELL, Li YQ, Soo KC, et al. Combinatorial strategies of radiotherapy and immunotherapy in nasopharyngeal carcinoma [review]. Chin Clin Oncol. 2018 Apr; 7(2):15.
124. Poggio M, Hu T, Pai CC, et al. Suppression of exosomal PD-L1 induces systemic anti-tumor immunity and memory. Cell. 2019 Apr 4; 177(2):414–427.
125. Roh W, Chen PL, Reuben A, et al. Integrated molecular analysis of tumor biopsies on sequential CTLA-4 and PD-1 blockade reveals markers of response and resistance. Sci Transl Med. 2017 Mar 1; 9:379.

Zhang et al. *Oncogenesis* (2020)9:65
https://doi.org/10.1038/s41389-020-00248-0

Oncogenesis

ARTICLE Open Access

Galectin-9 promotes a suppressive microenvironment in human cancer by enhancing STING degradation

Chuan-xia Zhang[1,2], Dai-jia Huang[1,3], Valentin Baloche[4], Lin Zhang[1], Jing-xiao Xu[1], Bo-wen Li[5], Xin-rui Zhao[2], Jia He[1,2], Hai-qiang Mai[1,3], Qiu-yan Chen[1,3], Xiao-shi Zhang[1,3], Pierre Busson[4], Jun Cui[1,2,6] and Jiang Li[1]

Abstract

Galectin-9 (Gal-9) is known to enhance the expansion of myeloid-derived suppressor cells (MDSCs) in murine models. Its contribution to the expansion of MDSCs in human malignancies remain to be investigated. We here report that Gal-9 expression in nasopharyngeal carcinoma (NPC) cells enhances the generation of MDSCs ($CD33^+CD11b^+HLA\text{-}DR^-$) from $CD33^+$ bystander cells. The underlying mechanisms involve both the intracellular and secreted Gal-9. Inside carcinoma cells, Gal-9 up-regulates the expression of a variety of pro-inflammatory cytokines which are critical for MDSC differentiation, including IL-1β and IL-6. This effect is mediated by accelerated STING protein degradation resulting from direct interaction of the Gal-9 carbohydrate recognition domain 1 with the STING C-terminus and subsequent enhancement of the E3 ubiquitin ligase TRIM29-mediated K48-linked ubiquitination of STING. Moreover, we showed that extracellular Gal-9 secreted by carcinoma cells can enter the myeloid cells and trigger the same signaling cascade. Consistently, high concentrations of tumor and plasma Gal-9 are associated with shortened survival of NPC patients. Our findings unearth that Gal-9 induces myeloid lineage-mediated immunosuppression in tumor microenvironments by suppressing STING signaling.

Introduction

Galectins are an intriguing family of β-galactoside-binding animal lectins, which have multiple functions inside the cells but can also be secreted by unconventional pathways independently of the classical endoplasmic reticulum/Golgi trafficking machinery[1]. Extra-cellular galectin-9 (Gal-9) was originally described as an eosinophil chemoattractant[2]. More recently it has been identified as a versatile immune-modulator acting on a wide range of target cells. It is known to induce the apoptosis of effector T-cells through binding with T-cell immunoglobulin and mucin domain-containing molecule 3 (Tim-3)[3]. In contrast, extra-cellular Gal-9 enhances the differentiation and suppressive activity of regulatory T cells, and is involved in dendritic cell (DC) maturation[1]. Intracellular Gal-9 also has multiple functions. It is involved in intracellular trafficking, cell adhesion and migration, proliferation and apoptosis[4–6].

In the past 5 years, various immunosuppressive effects of Gal-9 have been reported for several types of human malignancies, for example its induction of M2 polarization of macrophages in melanoma[7,8]. However, the contribution of Gal-9 to the generation and expansion of MDSCs in human malignancies is barely known. Dardalhon et al. have reported an excess of $CD11b^+Ly6G^+$ MDSCs in transgenic mice overexpressing Gal-9 or Tim-3. A role for extra-cellular Gal-9 binding the Tim-3

Correspondence: Pierre Busson (pierre.busson@gustaveroussy.fr) or Jun Cui (cuij5@mail.sysu.edu.cn) or Jiang Li (lijiang2@mail.sysu.edu.cn)
[1]Department of Biotherapy, State Key Laboratory of Oncology in South China, Collaborative Innovation Center for Cancer Medicine, Guangdong Key Laboratory of Nasopharyngeal Carcinoma Diagnosis and Therapy, Sun Yat-sen University Cancer Center, and School of Life Sciences, Sun Yat-sen University, 510060 Guangzhou, P. R. China
[2]MOE Key Laboratory of Gene Function and Regulation, State Key Laboratory of Biocontrol, Sun Yat-sen University, 510275 Guangzhou, China
Full list of author information is available at the end of the article
These authors contributed equally: Chuan-xia Zhang, Dai-jia Huang

receptor was supported by the abrogation of Gal-9 effect on MDSC expansion in Tim-3 knockout (KO) mice. However, this report provides no clue on whether or not intra-cellular Gal-9 is also involved in the promotion of MDSCs[9]. Moreover, to our knowledge, no similar investigations have been made on human MDSCs, especially in the context of malignant tumors. To address these questions, we returned to the model of nasopharyngeal carcinoma (NPC) for two main reasons. Firstly, our previous studies showed that the expansion of the MDSC population in peripheral blood and tumor tissues from NPC patients was associated with a more aggressive tumor behavior[10,11]. Secondly, we and others have shown that Gal-9 concentrations are at a high level in malignant NPC cells in situ, especially in recurrent tumors, in NPC-derived PDX (patient-derived xenograft model) as well as in plasma exosomes from NPC patients[12–14], suggesting a role of Gal-9 in tumor progression. In addition, NPC is a major public health problem in various countries especially Southern China. While malignant NPC cells consistently express Epstein–Barr virus latent antigens, the NPC microenvironment is heavily infiltrated by various kinds of inflammatory cells[15]. Until now, the cellular and viral mechanisms of tumor immune escape have not been fully understood.

Myeloid-derived suppressor cells (MDSCs), neutrophils, and DCs have been implicated in T-cell suppression in a wide range of malignancies. They are recruited in the tumor microenvironment and educated by tumor cells to create a localized immunosuppressive niche for tumor survival[16,17]. Generally, the tumor-promoting myeloid response is linked to the environmental cytokine and chemokine release. For instance, the high levels of IL-1β, IL-6, and CXCL2 in the tumor microenvironment favor MDSC expansion[18,19]. Recent studies showed that innate immune regulators including stimulator of interferon genes (STING) and toll-like receptors (TLR) are involved in the regulation of myeloid cell generation and differentiation in cancers[20,21]. However, the molecular mechanisms that contribute to the rise of tumor-promoting myeloid responses in the cancer microenvironment is complex and still enigmatic.

To explore the biological functions of intra- and extracellular Gal-9 in regulating myeloid cell differentiation in human cancer, we used in vitro experimental systems based on the co-cultivation of $CD33^+$ peripheral leucocytes with NPC cells engineered to express and release various amounts of Gal-9. Using these models, we demonstrated that both intra-cellular and extra-cellular Gal-9 are key players for the promotion of immunosuppressive myeloid cells in the tumor microenvironment. To a large extent, this effect is supported by down-regulation of the STING protein inside Gal-9-producing carcinoma cells. Furthermore, we have confirmed that high amounts of Gal-9 in the tumor tissue and the serum from tumor-bearing patients is associated with a pejorative outcome.

Results

Forced Gal-9 expression in malignant NPC cells promotes a cytokine profile conducive to myeloid cell differentiation

To understand the molecular characteristics of malignant cell with endogenous overexpression of Gal-9, we set up an experimental system based on transfected NPC cells allowing in vitro modulation of Gal-9 expression. Firstly, we assessed the baseline protein expression of Gal-9 in different NPC cell lines TW03 (EBV negative, low Gal-9 expression) and C666-1 (EBV-positive, high Gal-9 expression) (Supplementary Fig. S1a). From parental NPC cells, we generated Gal-9 stably overexpressed or knockdown NPC cells including TW03-Gal-9 and C666-1-sh-Gal-9 and their corresponding control cells including TW03-EV (empty vector) and C666-1-sh-control cells for further studies (Supplementary Fig. S1b, c). We employed a full transcriptome analysis to identify differentially regulated genes and pathways in the TW03-Gal-9 and TW03-EV cells. A total of 728 genes were differentially regulated between control (EV) and Gal-9 overexpression cells (523 genes up-regulated vs. 205 genes down-regulated). Pathway analysis revealed that many of these altered genes are involved in cytokine-cytokine receptor interactions (Supplementary Fig. S1d). Further analyses of the gene transcription profiles showed that a series of genes encoding cytokines and chemokines such as CXCL8, IL-1α, CX3CL1, IL-6, CCL5, CCL22, and IL-1β, were significantly up-regulated ($p < 0.0001$; Fig. 1a). We further verified that the mRNA levels of *CXCL8*, *IL-1α*, *CX3CL1*, *IL-6*, *CCL5*, *CCL22*, and *IL-1β* were increased in TW03-Gal-9 cells, while decreased in C666-1-shGal-9-01 and C666-1-shGal-9-02 cells compared with the corresponding control cells (Fig. 1b, c). Overall, these data suggested that Gal-9 mainly up-regulated the production of a subset of cytokines involved in myeloid cell differentiation, especially IL-1β and IL-6.

Intracellular and extracellular Gal-9 expressed by malignant cells promotes tumor-associated MDSC differentiation in a cytokine-induced manner

Considering that Gal-9 is a secreting protein, here we further assess the repercussions of Gal-9 expression in malignant cells on the regulation of bystander $CD33^+$ cells belonging to the human myeloid lineage and the effect of extracellular Gal-9 on $CD33^+$ cell function and differentiation using RhGal-9 protein or tumor-derived exosomes (T-EXO) with substantial Gal-9 abundance. Firstly, we found that the production of IL-1β and IL-6 were increased in TW03 and $CD33^+$ cells with forced up-regulation of Gal-9 compared with that of corresponding control cells, while decreased in C666-1-shGal-9-01 and

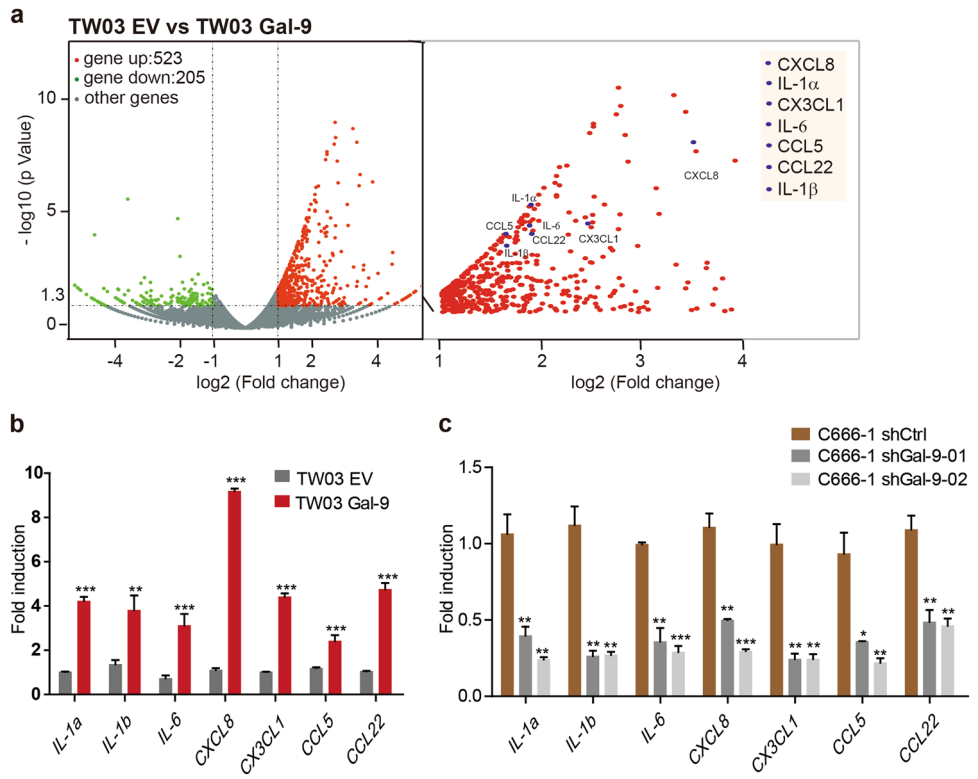

Fig. 1 Gal-9 expression in NPC cells modulates the expression of genes related to innate immune cell differentiation. a RNA sequencing was performed on stably transfected TW03 cells with or without Gal-9 overexpression, TW03-Gal-9 (Gal-9 vector) and TW03-EV (empty vector) respectively. The differentially expressed genes were selected according to the criteria of p value < 0.05 and fold change >2. Differentially expressed genes are visualized on a Volcano plot. The mRNA levels of indicated genes were determined, using quantitative real time PCR (qRT-PCR), in four distinct cell types: TW03-Gal-9 and TW03-EV cells (**b**) and Gal-9 knockdown (shGal9-01 and shGal9-02) or control C666-1 cells (shCtrl) (**c**). The experiments in (**b**, **c**) were performed at least three times, and the data were plotted as the mean ± SEM. Statistics were conducted with an unpaired Student's t test, *p < 0.05 vs. the corresponding control. NS not significant, EV Empty vector.

C666-1-shGal-9-02 cells compared with the corresponding control cells (Fig. 2a, b). In a previous work, we have shown that IL-1β and IL-6 promote myeloid cell generation and differentiation in vitro[10]. Therefore, for in vitro mimicking of the tumor microenvironment, we used a Transwell co-culture system in vitro, connecting carcinoma cells and $CD33^+$ myeloid cells. We found that forced Gal-9 expression in TW03 cells significantly enhanced the induction of $CD33^+CD11b^+HLA\text{-}DR^-$ MDSCs from $CD33^+$ myeloid lineage cells in the neighborhood of TW03 cells (Fig. 2c). Reciprocally, depletion of Gal-9 in C666-1 cells lowered the induction of $CD33^+CD11b^+HLA\text{-}DR^-$ MDSCs derived from $CD33^+$ cells, however forced Gal-9 expression in C666-1-shGal-9 cells was able to restore the same capacity of MDSCs induction as the parental cells (Fig. 2d). Consistently, the treatment of $CD33^+$ cells with RhGal-9 resulted in their enhanced differentiation in $CD33^+CD11b^+HLA\text{-}DR^-$MDSC (Fig. 2e). Interestingly, the same effect was achieved when treating $CD33^+$ cells with exosomes derived from NPC cells having high Gal-9 production (Supplementary Fig. S2). Simultaneously, the proliferation of IFNγ−producing T cells, including $CD4^+$ and $CD8^+$ T cells, was strongly suppressed by TW03-Gal-9- induced MDSCs, while the C666-1-shGal-9-induced MDSCs displayed weaker suppression on the proliferation of IFNγ −producing $CD4^+$ and $CD8^+$ T cells (Fig. 2f). Our data suggest that up-regulation of Gal-9 expression in NPC cells promotes MDSC expansion depending on IL-1β and IL-6 induction from tumor cell and myeloid cell itself.

Endogenous Gal-9 downregulates STING expression leading to tumor-derived MDSC expansion in a cytokine-dependent manner

Our next goal was to elucidate how endogenous Gal-9 was able to induce a change in the cytokine profile in NPC cell lines TW03 and C666-1, or $CD33^+$ myeloid cells. We investigated the status of several proteins involved in cytokine regulation, including the type I IFN (p-TBK1 and TBK1) and MAPK (p38, JNK, and ERK) signaling pathways. We found that overexpression of Gal-9 specifically inhibited the type I interferon (IFN) signaling pathway,

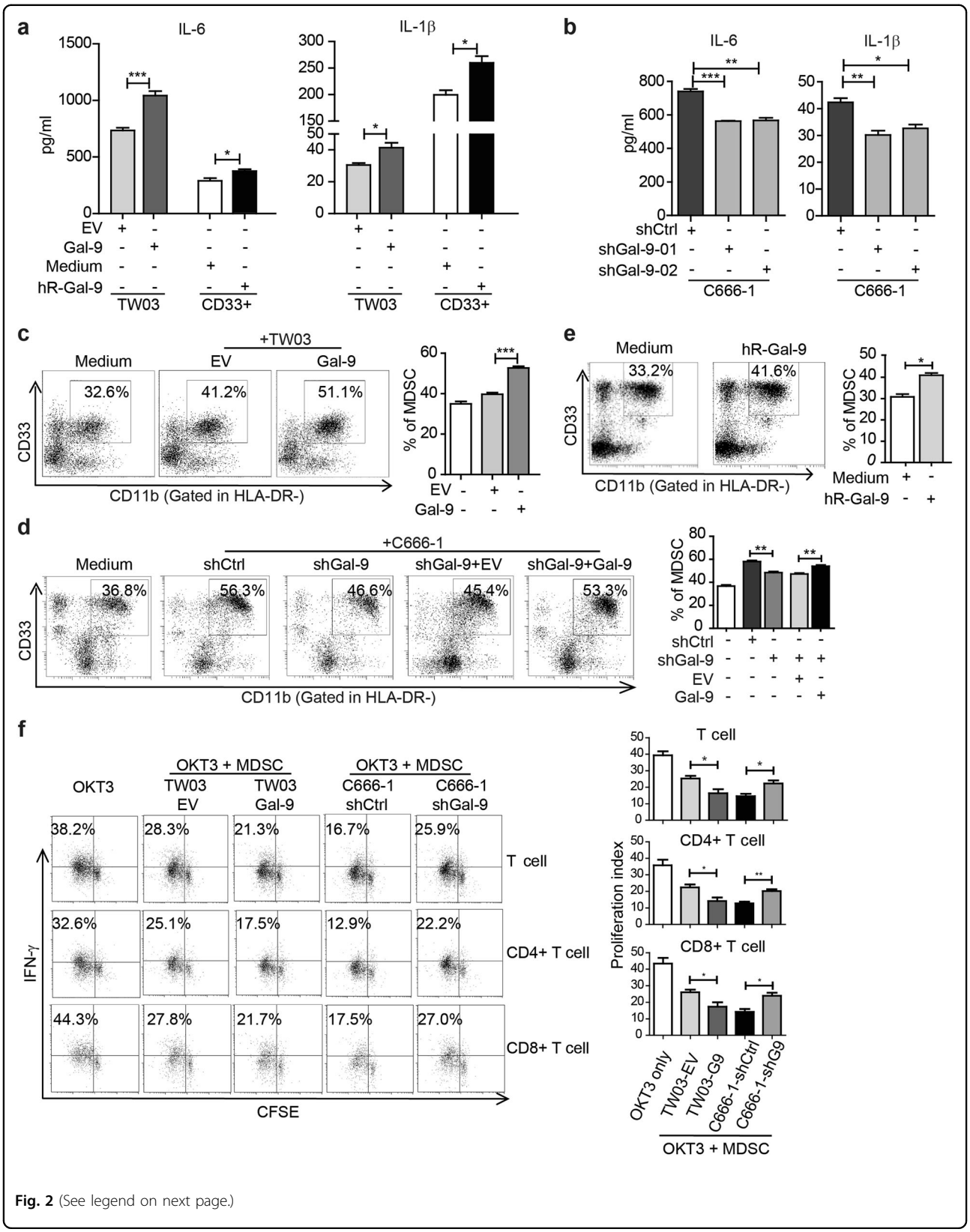

Fig. 2 (See legend on next page.)

(see figure on previous page)
Fig. 2 The effect of intra- and extra-cellular Gal-9 on MDSC differentiation and expansion in vitro. ELISA assay of IL-6 and IL-1β concentrations in the conditioned media of TW03-EV and TW03-Gal-9 cells or $CD33^+$ cells (**a**) or Gal-9 knockdown (shGal9-01 and shGal9-02) and control C666-1 cells (**b**) with or without addition of human recombinant Gal-9 (hR-Gal-9). **c** Differentiation of $CD33^+$ cells isolated from healthy PBMCs investigated after treatment with control medium, co-cultivation with TW03-EV or TW03-Gal-9. Representative flow cytometry plots (**left**) and histogram (**right**) of MDSC differentiation assays showing the percentage of $CD33^+CD11b^+$ cells in the $HLA\text{-}DR^-$ gate arising from $CD33^+$ cells. **d** Similar experiment based on co-cultivation with C666-1 cells using four experimental conditions: C666-1-shCtrl cells (shCtrl), unmodified C666-1-shGal9-01 (shGal-9), C666-1-shGal9-01 co-transfected with a control lentiviral vector (shGal9 + EV) or a Gal-9 lentiviral vector (ShGal-9+Gal-9). **e** Representative flow cytometry plots (**left**) and histogram (**right**) of MDSC differentiation assays showing the percentage of $CD33^+CD11b^+$ cells in the $HLA\text{-}DR^-$ gate arising from $CD33^+$ cells with or without addition of human recombinant Gal-9 (hR-Gal-9). **f** Representative flow cytometry plots (**left**) and histogram (**right**) of the IFN-γ-positive, proliferating T cells (CSFE assay) to test the immune-suppressive activity of MDSC cells induced by TW03-EV and TW03-Gal-9 or C666-1-shCtrl and C666-1-shGal9 (shGal9-01) cells. All experiments were performed at least three times, and the quantification data were plotted as the mean ± SEM. Statistics were conducted with an unpaired Student's *t* test, $*p < 0.05$, $**p < 0.01$, $***p < 0.001$ vs. the corresponding control. NS not significant, EV Empty vector.

but not the MAPK signaling pathways (Fig. 3a). We further found that STING, the key adapter protein in type I IFN signaling, was down-regulated at the protein level in TW03 and $CD33^+$ cells undergoing forced expression of Gal-9 (Fig. 3b). Reciprocally, the STING signaling was up-regulated in C666-1 cells following Gal-9 silencing (Fig. 3c). In addition, the mRNA levels of downstream genes of the STING signaling pathway including *ISG15*, *ISG54*, and *ISG56* were down-regulated in TW03-Gal-9 cells (Fig. 3d), but up-regulated in C666-1-shGal-9-01 and C666-1-shGal-9-02 cells (Fig. 3e). Previously, we have shown that inactivation of STING signaling in NPC cells leads to the tumor-derived MDSC expansion in a cytokine-dependent manner via the STING/SOCS1/STAT3 axis[22]. Thus, these results led us to hypothesize a connection between the biological function of Gal-9 and the STING signaling pathway. We then employed STING knockout NPC cells in additional coculture experiments. Interestingly, we found that the forced expression of Gal-9 in TW03-vector control cells resulted in a consistent increase in their secretion of IL-1β and IL-6, however the Gal-9-mediated increase of IL-1β and IL-6 secretion was disrupted in TW03-STING-KO cells. (Fig. 3f and Supplementary Fig. S3). Consistently, an effect of Gal-9 to promote the generation of MDSCs in the vicinity of TW03 cells was observed in cells retaining STING expression but not in STING-KO cells whose capacity to enhance MDSC differentiation was already close to its maximum (Fig. 3g). These data suggested that Gal-9 promotes tumor-associated MDSC differentiation in a STING-dependent manner.

Gal-9 interacts with STING

Based on the above data (Fig. 3b, c), we wondered whether Gal-9 could suppress the STING protein through a network of protein interactions. We determined that Gal-9 interacted with STING by co-immunoprecipitation of Gal-9 with STING using anti-Myc on HEK293T cell extracts (Fig. 4a). Reciprocally the endogenous STING was co-immunoprecipiatated with Flag-Gal-9 from TW03 extract (Fig. 4b). Finally the endogenous Gal-9 was co-immunoprecipitated with the endogenous STING from wild type C666-1 extracts (Fig. 4c). In addition, we observed that Gal-9 colocalized with STING in the cytoplasm of C666-1 and $CD33^+$ cells using immunofluorescent staining (Fig. 4d).

To explore the domain of the Gal-9 protein interacting with STING, we generated two domain-deletion mutants of Gal-9 (Gal-9-CBD1 and Gal-9-CBD2, containing only one carbohydrate-binding domain, respectively). Co-immunoprecipitation analyses showed that STING strongly interacted with Gal-9-CBD1, but not Gal-9-CBD2 (Fig. 4e). Importantly, the CBD1 domain of Gal-9 was also responsible for STING degradation (Supplementary Fig. S4). We next generated two domain-deletion mutants of STING and found that STING interacted with Gal-9 only at its C-terminal domain (Fig. 4f). These data suggested that Gal-9 promoted STING degradation via direct protein-protein interactions.

Gal-9 enhances the TRIM29-mediated K48-linked ubiquitination of STING by protein-to-protein binding

We further explored the molecular mechanisms of Gal-9-dependent the decrease of STING expression, and found that the half-life of STING was shorter in TW03-Gal-9 cells or lenti-Gal-9-treated $CD33^+$ cells than in TW03-EV cells or lenti-Control-treated $CD33^+$ cells using cycloheximide (CHX) 'chase' assays (Fig. 5a), suggesting that Gal-9 enhance STING protein degradation. Importantly, it is the proteasomal inhibitor MG132 but not 3MA or CQ (lysosomal or autophagic inhibitors) that inhibited the STING protein degradation in TW03-Gal-9 cells or lenti-Gal-9-treated $CD33^+$ cells (Fig. 5b). Our observations suggested that the degradation of the STING protein mediated by Gal-9 is dependent on the ubiquitin-proteasome pathway.

We further found that Gal-9 promotes the ubiquitination of STING in TW03 cells (Fig. 5c). It has been

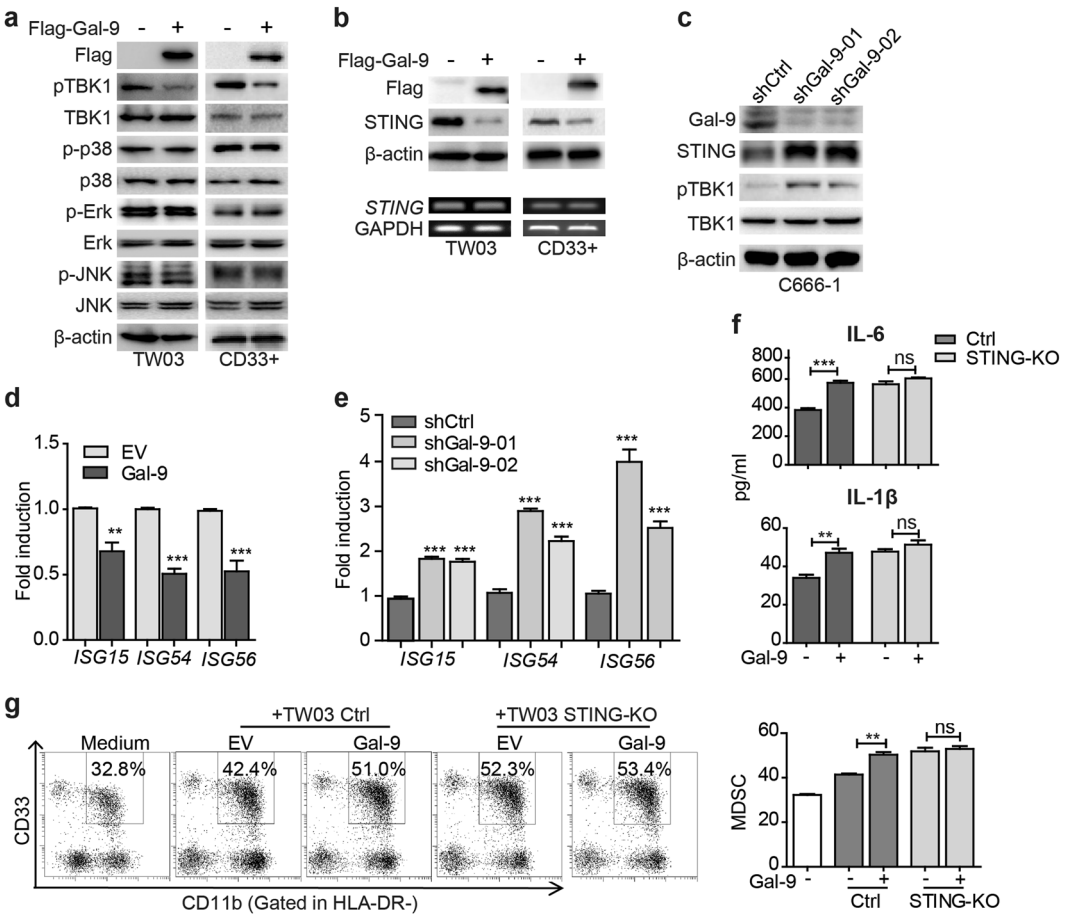

Fig. 3 Endogenous Gal-9 downregulates STING leading to tumor-associated MDSC expansion depending on cytokine-induction. a The extracts of TW03 cells stably expressing Flag-tagged-EV or Gal-9 (left) and $CD33^+$ cells transfected with lenti-flag-tagged-EV or lenti-flagged-Gal-9 vector (right) were subjected to immunoblot with the indicated antibodies. **b** Upper panel: the lysates of TW03 cells and $CD33^+$ cells expressing Flag-tagged EV or Gal-9 were subjected to immunoblot with the indicated antibodies. Lower panel: RT-PCR analysis of *STING* mRNA; *GAPDH* mRNA served as a transcript of reference. **c** The lysates of C666-1 cells transfected with Gal-9-specific shRNAs were subjected to immunoblot with the indicated antibodies. The mRNA expression levels of ISG genes were determined in TW03 cells transfected with the Gal-9-expressing vector or EV (**d**) C666-1 cells transfected with shRNA targeting Gal-9 (**e**) or corresponding control vectors using quantitative real time PCR (qRT-PCR). **f** ELISA assay of IL-6 and IL-1β concentrations in the supernatants from control or STING-KO TW03 cells, transfected with Flag-EV and Flag-Gal-9 for 48 h. **g** Representative flow cytometry plots (**left**) and histogram (**right**) of MDSC differentiation assay for $CD33^+$ cells co-cultured with Control (Ctrl) or STING-KO TW03 cells, transfected with Flag- EV or Flag-Gal-9 for 48 h. All experiments were performed at least three times, and the quantification data were plotted as the mean ± SEM. Statistics were conducted with an unpaired Student's *t* test, $^*p < 0.05$, $^{**}p < 0.01$, $^{***}p < 0.001$ vs. the corresponding control. NS not significant, EV empty vector, Ctrl control, KO knock out.

reported that K48-linked ubiquitination is typically associated with protein degradation via ubiquitin-proteasome pathway. Here, we demonstrated that Gal-9 specifically promoted K48-linked poly-ubiquitination of STING, but not other ubiquitination linkages (Fig. 5d). Our data indicated that Gal-9 mediates the proteasomal degradation of STING protein by enhancing its K48-linked ubiquitination.

Since Gal-9 is not an E3 ubiquitin ligase, we hypothesize that Gal-9 might recruit certain E3 ligase to mediate the ubiquitination of STING. The E3 ubiquitin ligase tripartite motif containing 29 (TRIM29) has been reported to mediate the K48-linked ubiquitination of STING[23]. Hence, we generated TW03-TRIM29-KO cells (Supplementary Fig. S5a), and found that Gal-9 failed to degrade STING in TW03-TRIM29-KO cells anymore (Fig. 5e). In addition, forced expression of both Gal-9 and TRIM29 resulted in more rapid STING degradation (Supplementary Fig. S5b). Of note, TRIM29 deficiency completely impaired the ability of Gal-9 to induce K48-linked ubiquitination of STING (Fig. 5f). Furthermore, we found that Gal-9 interacted with TRIM29 in $CD33^+$ and TW03 cells (Fig. 5g and Supplementary Fig. S5c), and we found that Gal-9 enhanced the interaction between TRIM29 and

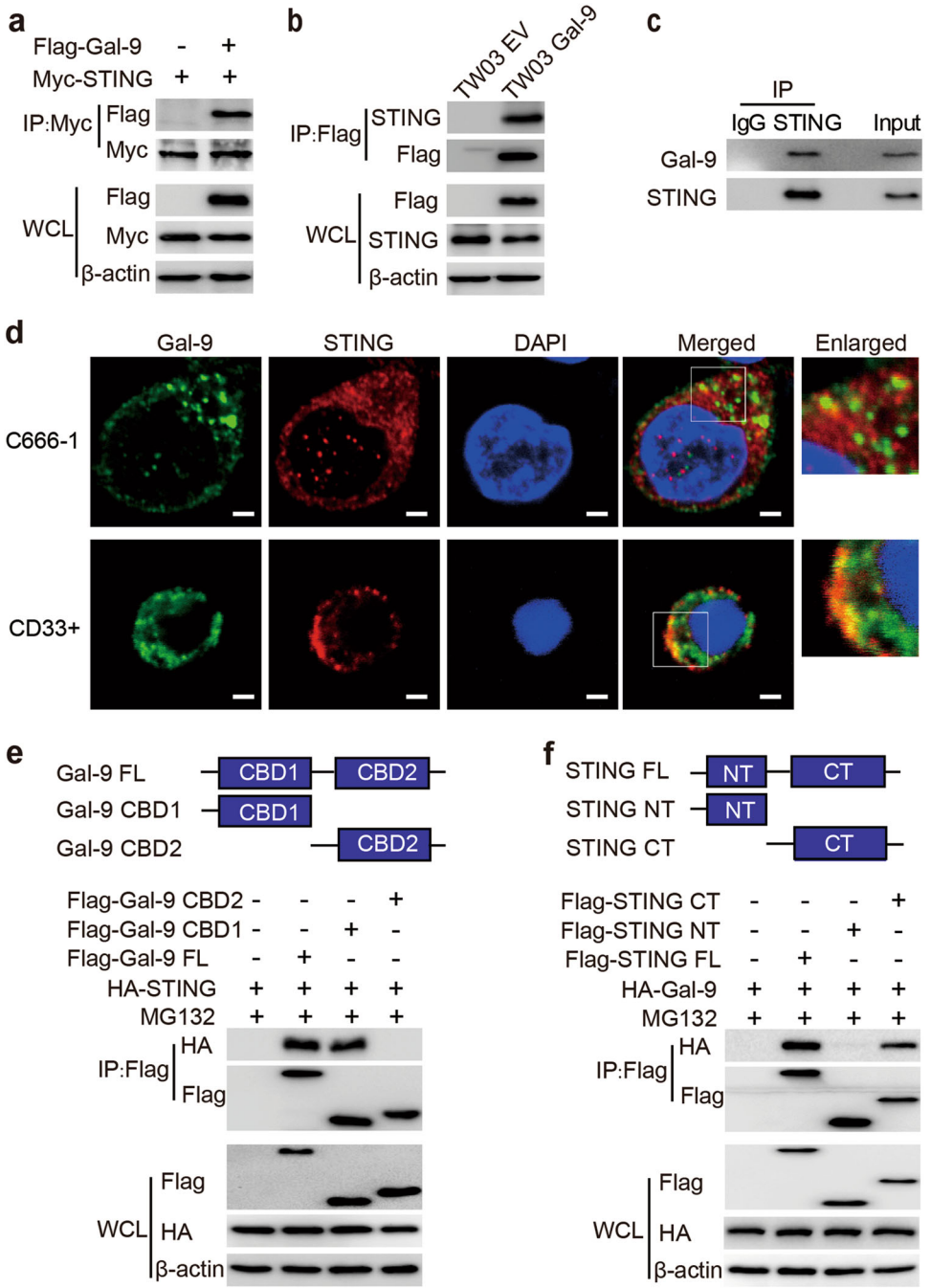

Fig. 4 Gal-9 interacts with STING. a HEK293T cells were transfected with Flag-Gal-9 or Flag-EV vector together with a Myc-STING expression vector for 24 h. The cell extracts were subjected to immunoprecipitation with anti-Myc-beads and immunoblot analysis with anti-Flag antibody. **b** The lysates of TW03 cells stably expressing Flag- EV or Flag-Gal-9 were subjected to immunoprecipitation with anti-Flag-beads and immunoblot analysis with anti-STING antibody. **c** Extracts of C666-1 cells were subjected to immunoprecipitation with an anti-STING antibody and immunoblot analysis with the anti-Gal-9 antibody. **d** Immunofluorescence assay to detect the colocalization of Gal-9 (green) and STING (red) in C666-1 and $CD33^{+}$ cells. Cell nuclei were stained with DAPI (blue). Scale bar: 2 μm. **e** Top: Schematic diagram of Gal-9 and its domain mutants. Bottom: HEK293T cells transfected with Flag-EV, Flag-Gal-9-FL, Flag-Gal-9-CBD1 and Flag-Gal-9-CBD2 mutants, together with HA-STING for 24 h, then treated with MG132 (10 μM) for 6 h. The extracts from HEK293T cells subjected to immunoprecipitation with anti-Flag-beads and immunoblot analysis with anti-HA antibody. **f** Top: Schematic diagram of STING and its domain mutants. Bottom: HEK293T cells transfected with Flag-EV, Flag-STING-FL, Flag-STING-NT and Flag-STING-CT, together with HA-Gal-9 for 24 h, then treated with MG132 (10 μM) for 6 h. The extracts from HEK293T cells were subjected to immunoprecipitation with anti-Flag-beads and immunoblot analysis with anti-HA antibody. All experiments were performed at least three times. EV empty vector, FL full length, CBD carbohydrate-binding domain, NT N terminal, CT C terminal, WCL whole cell lysis.

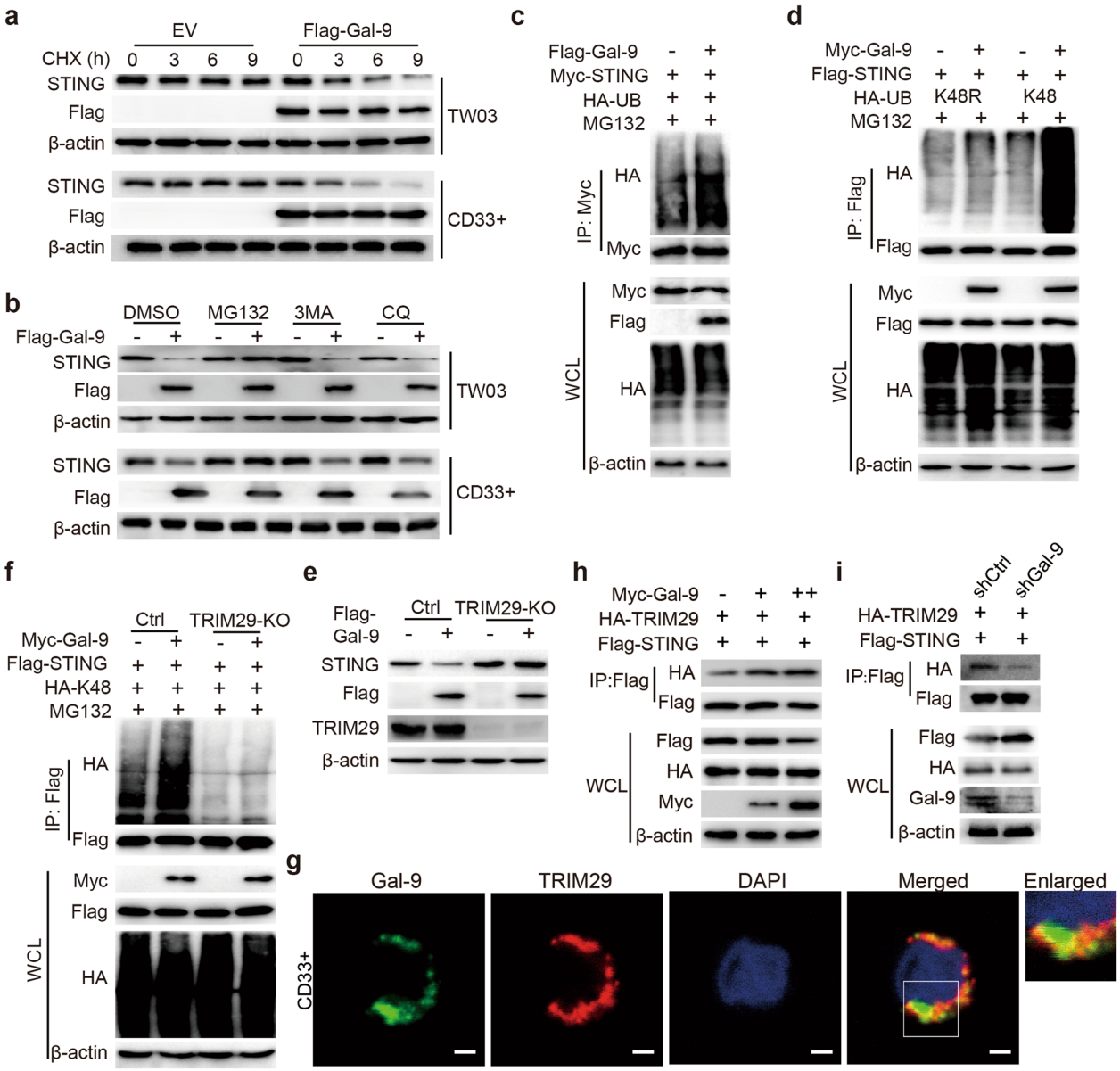

Fig. 5 Gal-9 enhances STING interaction with and ubiquitination by TRIM29. a Upper panel: TW03 cells stably expressing Flag-Gal-9 or EV were treated with cycloheximide (CHX, 20 μg/ml) for indicated time points (in hours) and then harvested for immunoblot. Lower panel: $CD33^+$ cells transfected with lenti-flag-tagged-EV or lenti-flagged-Gal-9 vector for 36 h, then treated with CHX (20 μg/ml) for indicated time points (in hours) and harvested for immunoblot. **b** Upper panel: Immunoblot analysis of protein extracts of TW03 cells stably expressing Flag-Gal-9 or EV, and treated with DMSO, MG132 (10 μM), 3-Methyladenine (3-MA, 2.5 mM) or Chloroquine phosphate (CQ, 20 mM) for 6 h. Lower panel: $CD33^+$ cells transfected with lenti-flag-tagged-EV or lenti-flagged-Gal-9 vector for 36 h, then treated with DMSO, MG132 (10 μM), 3-Methyladenine (3-MA, 2.5 mM) or Chloroquine phosphate (CQ, 20 mM) for 6 h and harvested for immunoblot. **c** Protein extracts of HEK293T cells transfected with a combination of plasmids coding for Myc-STING and HA-UB, in the presence or absence of Flag-Gal-9 and subjected to immunoprecipitation with anti-Myc-beads and immunoblot analysis with anti-HA antibody. **d** Protein extracts of HEK293T cells transfected with various combinations of plasmids coding for Flag-STING, Myc-Gal-9, HA-UB-K48, or HA-UB-K48R (arginine instead of lysine 48) and subjected to immunoprecipitation with anti-Flag-beads and immunoblot analysis with indicated antibodies. **e** Control (Ctrl) and TRIM29-KO TW03 cells were transfected with Flag-Gal-9 or EV for 24 h. The cell protein extracts were immunoblotted with the indicated antibodies. **f** Control (Ctrl) and TRIM29-KO TW03 cells were transfected with a combination of plasmids coding for Flag-STING, HA-K48, Myc-Gal-9 for 36 h, and treated with MG132 (10 μM) for 6 h. The extracts from TW03 cells were subjected to IP with an anti-Flag-beads and immunoblot analysis with anti-HA antibody. **g** Immunofluorescence assay demonstrating the partial colocalization of endogenous Gal-9 (green) and TRIM29 (red) in $CD33^+$ cells. Cell nuclei were stained with DAPI (blue). Scar bar: 2 μm. **h** HEK293T cells were transfected with Flag-STING and HA-TRIM29 followed by transfection with increasing amounts of Myc-Gal-9 for 24 h. The protein extracts were subjected to IP with anti-Flag-beads and immunoblot analysis with an anti-HA antibody. **i** C666-1 cells were transfected with shRNA targeting Gal-9 (C666-1-shGal-9) or corresponding control vectors (C666-1-shCtrl) for 24 h, then transfected with HA-TRIM29 and Flag-STING for 24 h, finally subjected to IP with anti-Flag-beads and immunoblot with indicated antibodies. All experiments were performed at least three times. Ctrl Control, KO knock out, WCL whole cell lysis, IP Immunoprecipitation.

STING (Fig. 5h, i). Altogether, these observations suggested that Gal-9 recruits TRIM29 to mediate the K48-linked ubiquitination and degradation of STING.

High abundance of Gal-9 in tumor tissue and serum is associated with a more aggressive phenotype of NPC tumors

Whether Gal-9 expressed by malignant cells enhances or attenuates the malignant phenotype remains a subject of controversy[12,24]. To address this issue in the case of NPCs, we performed concomitant assessment of Gal-9 abundance in the primary tumors by IHC on tissue sections and in the peripheral blood by ELISA on plasma samples. Gal-9 staining on tumor sections was followed by semi-quantitative scoring for 92 patients (IHC score). We found that for almost all patients for whom adjacent nonmalignant tissue was available, Gal-9 was consistently more abundant in tumor tissues including tumor cells and tumor-infiltrated cells than in surrounding non-tumor tissues ($p < 0.001$, $n = 14$, Fig. 6a). By ELISA, we also made a comparative assessment of the Gal-9 concentration in 93 serum samples from NPC patients and samples from 20 healthy donors. Gal-9 serum concentrations were much greater for NPC patients ($p < 0.001$, Fig. 6b). The abundance of Gal-9 in the tumor and, even more, in the serum was associated with a less favorable outcome (shorter DFS and OS for patients with high IHC score in the tumor sections and high concentrations of Gal-9 in the serum, Fig. 6c, d). As shown in Table S1, there were no significant correlations between the IHC score and clinical parameters. On the other hand, serum Gal-9 concentrations were correlated with the clinical extension stage and consistently with the stage of lymph nodes (Table S1). Importantly, consistent with the aforementioned in vitro observations, we found that IL-6 concentrations were positively correlated to Gal-9 concentrations in serum samples from NPC patients ($p < 0.05$, Fig. 6e). Overall, these observations were compatible with the idea that the production of intracellular and extracellular Gal-9 by carcinoma cells promotes tumor development.

Discussion

Immunotherapies targeting immune checkpoint molecules, including PD1, CTLA-4, and Tim-3 have been a major breakthrough in cancer therapy and have changed our understanding of host-tumor interactions[25,26]. However, in most types of human malignancies, only a fraction of the patients, generally about 20–30%, achieved a good response to the current immune checkpoint inhibitors[27,28]. Therefore, there is a need to characterize factors of immune suppression distinct from the classical checkpoints PD1 and CTLA4. There is strong evidence that extra-cellular Gal-9 is one of them. Indeed, extra-cellular Gal-9 has an almost constant immunosuppressive function in vitro and in murine models. It has been shown that extracellular Gal-9 contributes to tumor growth in several syngeneic murine tumor models[29]. In several human malignancies, high concentrations of Gal-9 in plasma are associated with a more aggressive tumor phenotype[30,31]. However, a distinct picture emerges when dealing with Gal-9 detected in tumor tissue sections. There is evidence that high abundance of Gal-9 in tumor sections is associated with a better prognosis for a number of human malignancies for example gastric and mammary carcinomas[8,32]. To address this paradox, it is important to keep in mind that most Gal-9 detected in tissue sections is probably intra-cellular and that intra-cellular Gal-9 is expected to decrease cell motility and tumor invasion[32]. However, in the case of NPC, high abundance of Gal-9 in tissue sections has been reported to be associated with more aggressive diseases[12]. This is compatible with the hypothesis that in some cellular backgrounds, even intracellular Gal-9 can have oncogenic activity or favor an immunosuppressive activity[30]. To address this last hypothesis, we have compared the cytokine profiles of NPC cells with various abundances of intra-cellular Gal-9. This set of experiments has shown that intra-cellular Gal-9 as well as extra-cellular Gal-9 induces production of cytokines, which enhance MDSC expansion. For memory, MDSCs have multiple deleterious effects in tumor progression. In addition to their immunosuppressive effects, they can contribute to angiogenesis and even have a direct impact on the proliferation of malignant cells through their secretion of growth factors[33].

The present study reveals that in NPC cells, Gal-9 significantly up-regulates the genes encoding cytokines and chemokines related to myeloid cell differentiation and expansion, including IL-1β, IL-1α, IL-6, CXCL8, CX3CL1, CCL22, and CCL-5. While IL-1β and IL-6 have been linked to the generation of MDSC inside tumor tissues, CX3CL1 and CCL22 have been found to induce the recruitment of MDSCs into the tumor microenvironment in tumor-bearing hosts[34–36]. The data from previous reports on the effects of Gal-9 on the differentiation and function of innate immune cells are not entirely consistent. In a small number of cases, Gal-9 has been shown to stimulate innate immunity and play a protective role against microbial infection or tumor progression[37–39]. However, other studies have highlighted mechanisms of immune suppression involving cells of the innate immune system. Golden-Mason et al. have reported functional impairment of human NK cells by extra-cellular Gal-9[40]. Using transgenic mice Dardhalon et al. have shown that systemic overexpression of Gal-9 results in the expansion of splenic $CD11b^{+}Ly\text{-}6G^{+}$ MDSCs[9]. More recently, Zhang et al. have reported a similar effect obtained by IP or IV injections of recombinant Gal-9 in a murine model

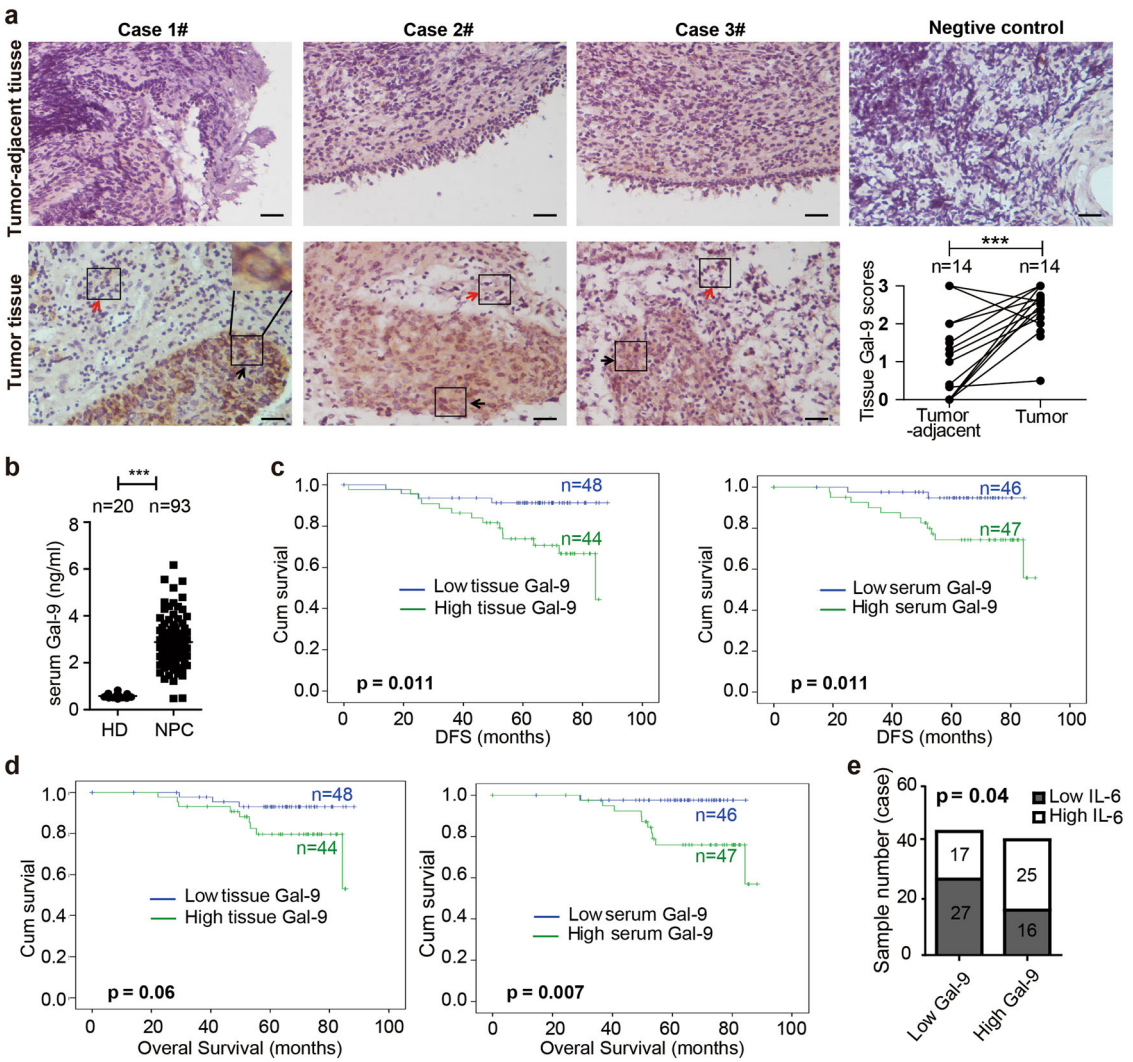

Fig. 6 Overexpression of Gal-9 in NPC is associated with an unfavorable outcome. a Images of the three left most columns: comparative IHC assessment of in situ Gal-9 expression on tissue sections of NPC tumors (lower panels) and matched tumor-adjacent tissues from the same patients (upper panels). Black arrows and red arrows point to the Gal-9-positive tumor cells and tumor-infiltrated cells, respectively. Upper panel of the right most column: one example of a tumor section stained with an irrelevant primary antibody of the same isotype as the anti-Gal-9. Lower panel of the right most column: results of the semi-quantitative scoring of Gal-9 staining on pairs of tumor/tumor-adjacent tissues from 14 NPC patients, Scale bar: 50 µm. **b** Serum concentrations of Gal-9 in NPC patients and healthy donors assessed by ELISA ($n = 93$ and 20, respectively). **c** Disease-free survival (DFS) rates showing that the intracellular tumor ($n = 92$, $p = 0.011$) and the extracellular serum Gal-9 ($n = 93$, $p = 0.011$) levels were significantly associated with a pejorative outcome of NPC patients (for both tumor and serum Gal-9, the threshold between patients with low and high abundance were the median values of the IHC score and serum concentration respectively). **d** Overall survival (OS) rates showing that the intracellular tumor ($n = 92$, $p = 0.06$) and the extracellular serum Gal-9 ($n = 93$, $p = 0.007$) levels were associated with a poor outcome of NPC patients. **e** Existence of a positive correlation between the serum concentrations of Gal-9 and IL-6 in NPC patients ($n = 85$, $p = 0.04$). Statistical significance of (**a**, **b**) was determined by an unpaired Student's *t* test, (**c**, **d**) was determined by Kaplan–Meier and log-rank test and (**e**) was determined by a χ^2 test, $^*p < 0.05$, $^{**}p < 0.01$, $^{***}p < 0.001$ and $p < 0.05$ was considered significant.

of myocarditis[41]. Here, for the first time, we report a stimulating effect of Gal-9 on human MDSCs. We demonstrate that Gal-9 expressed inside malignant cells maximizes the induction of MDSCs in their microenvironment, leading to myeloid cell-mediated T cell inhibition. In addition, our findings support the concept that extracellular soluble or exosomal Gal-9 induces differentiation of $CD33^+CD11b^+HLA\text{-}DR^-$MDSCs from $CD33^+$ cells through their production of cytokines IL-1β and IL-6, which have been linked to MDSC differentiation[42]. Moreover, we have shown in our previous studies that IL-1β and IL-6 are up-regulated in NPC cells by LMP1-induced glycolysis or suppression of STING signals, leading to tumor-associated MDSC expansion[10,22].

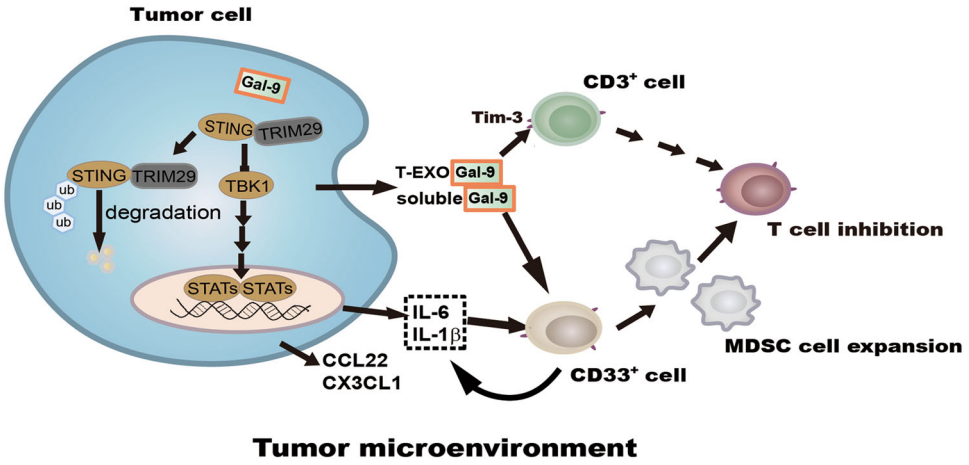

Fig. 7 A cartoon recapitulating the contribution of intracellular and extracellular tumor Gal-9 to the differentiation and expansion of MDSCs and the subsequent inhibition of T-cells. Acceleration of STING degradation by Gal-9 inside tumor cells is one key step of this process.

Therefore, here our results suggest that intracellular and extracellular Gal-9 promotes MDSC differentiation and expansion through enhanced production of suppressive cytokines and chemokines such as IL-1β and IL-6 from both tumor cells and $CD33^+$ cells (see our tentative synthesis in Fig. 7).

The STING signaling pathway has emerged as a central TLR-independent mediator of host innate defense stimulated by cytosolic nucleic acids from foreign microbial infection[43]. Emerging evidence suggests that the STING pathway represents a central node in bridging innate immunity and subsequent adaptive immunity in virus infection and cancers[44]. Our and others' recent studies demonstrated that inactivation of the STING pathway is linked to MDSC expansion in both human and murine tumor model[21,22]. We have previously reported that STING restrains MDSC differentiation by decreasing IL1β and IL-6 production from NPC or $CD33^+$ cells through suppressing the SOCS1/STAT3 signaling pathway[22]. Here we have been a step further by showing that Gal-9 could suppress STING expression in NPC cells and myeloid cells, and that deactivation of STING signaling is required for Gal-9-mediated MDSC expansion.

In virus-associated tumors like EBV- and HPV-positive carcinomas, the virus products, including viral DNA molecules, usually trigger antivirus signals especially TLR and STING signaling pathways. Accordingly, the tumor cells have to restrain these antivirus pathways to escape the host immune surveillance[23]. Here, our data show that Gal-9 negatively regulates STING stability through protein-protein binding in both tumor cells and $CD33^+$ cells. In addition, we found that the interaction of Gal-9 and STING enhance the TRIM29-mediated K48-linked ubiquitination of STING. It has been reported that human airways epithelial cells selectively express TRIM29 and that its expression can be further induced by EBV infection. In turn, TRIM29 induced K48-linked ubiquitination of STING for protein degradation, which enhances EBV-positive tumor cell survival[23]. Here, our data further suggest that Gal-9 enhances the interaction of STING and TRIM29 to accelerate the degradation of the STING protein. The mobilization of the Gal-9/TRIM29/STING axis results in myeloid-cell-mediated T-cell suppression, which is beneficial for EBV-positive tumor cell survival. Importantly, our observations highlight a novel molecular mechanism explaining STING down-regulation in tumors with abundant Gal-9 production. The role of Gal-9 in auto-immune diseases is probably variable depending on the tissue and pathological context. For example, depending on the publications, Gal-9 has been reported either to increase or, on the contrary, to decrease the severity of SLE (systemic lupus erythematosus) in patients and in murine models[45–47].

In NPC patients, we observed that Gal-9 was abundant in the tumor cells by comparison with the surrounding non-tumor tissue and in the serum by comparison with serum samples from healthy individuals (Fig. 6a, b). Moreover, the abundance of Gal-9 in tumor cells and serum samples was indicative of a pejorative outcome in terms of DFS and OS. High expression of Gal-9 in tumor cells was correlated with the risk of relapse but not with the tumor stage whereas serum concentration of Gal-9 was correlated with both parameters. To explain these differences, we speculated that Gal-9 serum concentration is probably more dependent on the total number of producing cells than on the average cellular amount of Gal-9. In other words, it might be more dependent on the total tumor volume which can vary by at least one order of magnitude from one patient to another. One major aim of our future studies on NPC specimens will be to seek

correlations between Gal-9 abundance in tumor cells and/or in serum samples and the abundance of MDSCs in the tumor leucocyte infiltrate as well as in the PBMCs. This will help us to determine the potential of circulating Gal-9 as a tumor biomarker.

Our findings highlight a novel mechanism involving Gal-9 and supporting cytokine-induced expansion of MDSCs to create a tumor suppressive microenvironment, which favor tumor progression (Fig. 7). They point to Gal-9 as a possible physiological partner of STING in the regulation of innate immunity.

Materials and methods

Patient samples and cell lines

Paraffin-embedded tumor tissues ($n = 92$) and serum samples ($n = 93$) were collected from 117 NPC patients at the Sun Yat-Sen University Cancer Center, Guangzhou, China from 2011 to 2015 (Supplementary Tables S1 and S2). Tumor-adjacent tissues were collected from 14 of 92 NPC patients with tumor tissue samples and both tumor specimens and serum samples were obtained from 68 of 117 NPC patients. Twenty healthy donors were included as controls. All patients and healthy donors signed a consent form approved by the Research Ethics Committee of the Sun Yat-sen University Cancer Center (GZR2013-040). This study was performed in accordance with the Helsinki Declaration.

HEK293T, TW03, and C666-1 cells were cultured in DMEM (Life Technologies) or RPMI-1640 medium (Life Technologies) supplemented with 10% fetal bovine serum (Gibco) and 1% L-glutamine (Gibco). All cell lines were tested Mycoplasma-free as determined by PCR-based method (16s rDNA-F: 5′-ACTCCTACGGGAGGCAG CAGTA-3′, 16s rDNA-R: 5′-TGCACCATCTGTCACTC TGTTAACCTC-3′). Mycoplasma testing was carried out every 2 weeks, and the cells were not cultured for more than 2 months.

RNA extraction, RNA-seq and quantitative RT-PCR (qRT-PCR) analysis

Total RNA was isolated with Trizol reagent (Invitrogen) according to the manufacturer's protocol. The concentration and quality control of total RNA were determined in triplicate with a NanoDrop2000 spectrophotometer (Thermo Scientific). RNA sequencing was performed with poly(A)-enriched mRNAs at Guangzhou RiboBio Company. Biological pathway analysis was performed using the Kyoto Encyclopedia of Genes and Genomes (KEGG, http://www.genome.jp/kegg/pathway.html), and the selective pathway program for the significantly different gene expression profiles was drawn using KOBAS 2.0 software (http://kobas.cbi.pku.edu.cn/index.php). Raw read counts per loci were normalized across samples, and differential gene expression was analyzed using DESeq. The RNA-seq data were deposited in the NCBI Gene Expression Omnibus under accession code GSE125942. Quantitative RT-PCR was performed with the SYBR Green qPCR Mix (GenStar), the detailed methods have been previously described[22]. Specific primers for qPCR are listed in Supplementary Table S3.

Fluorescence-activated cell sorting (FACS) analysis

For FACS analysis, single-cell suspensions were stained with fluorescent antibodies according to the manufacturer's instructions. Fluorescent antibodies conjugated with different fluorescent dyes and matched isotypes were obtained from eBioscience: including CD4 (555346); CD8 (12-0088-42); CD11b (85-25-0118-42); CD33 (85-45-0338-42), HLA-DR (85-12-9952-42) and IFN-γ (17-55-7319-82). In brief, cells were harvested, washed and stained with surface phenotypic markers for 20 min on ice. After permeabilization and fixation, cells were intracellularly stained with IFNγ-APC antibodies. Positively stained cells were detected using a Beckman Coulter Gallios Flow Cytometer and analyzed using the Flowjo V10 software.

Immunoblot and Immunoprecipitation (IP) assays

For immunoblot assays, NPC or HEK293T cells were subjected to lysis in ice-cold low-salt lysis buffer (LSB, 150 mM NaCl, 50 mM Hepes pH 7.5, 1.5 mM $MgCl_2$,1 mM EDTA, 10% glycerol, 1% Triton X-100) supplemented with 5 mg/mL protease inhibitor cocktail (Roche, Basel, Switzerland). Aliquots of 20–25 μL extracts were subjected to SDS-PAGE. For IP assays, NPC or HEK293T cells were transfected with corresponding expression vectors for indicated times, then Flag- or Myc-tagged proteins were pulled down using Flag-beads (Sigma -Aldrich, St. Louis, MO, USA) or Myc-beads (Immuoway, Newark, DE, USA). The following antibodies were used which were directed to: FLAG (Sigma, A8592), β-actin (Sigma, A2228), HA (Roche Applied Science, clone 3F10), Myc (Roche Applied Science, 11814150001), STING (Proteintech, IL, USA, 19851-1-AP), TRIM29 (Proteintech, 17542-1-AP).

Statistical analysis

All analyses were performed using GraphPad Prism 5 software (La Jolla, CA, USA) and SPSS 18.0 software (Chicago, IL, USA). Numbered results were expressed as mean ± standard error of the mean (SEM). Two-tailed Student's t test was used for comparison of the numerical data. The Kaplan–Meier and log-rank test were used for survival analysis, and a χ^2 test was also used in some experiments as indicated. For IHC scores, cutoff values were the median of each group. In this study, $^{*}p < 0.05$, $^{**}p < 0.01$, $^{***}p < 0.001$, and $p < 0.05$ was considered

significant. The authenticity of this article has been validated by uploading the key raw data onto the Research Data Deposit (RDD) public platform (www.researchdata.org.cn), with the RDD approval number RDDB2019000748.

Acknowledgements
This work was supported by the National Natural Science Foundation of China (8197110786, 81773256, 81572982, 81372442 and 81172164); the National Key R&D Program (2018YFC1313400); the Sci-Tech Key Program of the Guangzhou City Science Foundation (201802020001); the Sci-Tech Key Program of the Guangdong Province Science Foundation (2014A020212066); the Natural Science Foundation of Guangdong Province (2018A030310159); Guangdong Basic and Applied Basic Research Foundation (2019A1515110147); Shenzhen Institute for Innovation and Translational Medicine Shenzhen Peacock Plan (KQTD20130416114522736); Shenzhen Basic Research Program (JCYJ20170412102821202 and JCYJ20180507182902330).

Author details
[1]Department of Biotherapy, State Key Laboratory of Oncology in South China, Collaborative Innovation Center for Cancer Medicine, Guangdong Key Laboratory of Nasopharyngeal Carcinoma Diagnosis and Therapy, Sun Yat-sen University Cancer Center, and School of Life Sciences, Sun Yat-sen University, 510060 Guangzhou, P. R. China. [2]MOE Key Laboratory of Gene Function and Regulation, State Key Laboratory of Biocontrol, Sun Yat-sen University, 510275 Guangzhou, China. [3]Department of Nasopharyngeal Carcinoma, Sun Yat-sen University Cancer Center, 510060 Guangzhou, China. [4]CNRS, UMR 9018, Gustave Roussy and Université Paris-Saclay 39 rue Camille Desmoulins, F-94805 Villejuif, France. [5]Department of Neurosurgery, The First People's Hospital of Changzhou, Changzhou 213000 Jiangsu, China. [6]Department of Research and Development, Shenzhen Institute for Innovation and Translational Medicine, Shenzhen International Biological Valley-Life Science Industrial Park, Dapeng New District, Shenzhen, China

Conflict of interest
The authors declare that they have no conflict of interest.

Supplementary Information accompanies this paper at (https://doi.org/10.1038/s41389-020-00248-0).

Received: 19 February 2020 Revised: 11 June 2020 Accepted: 16 June 2020
Published online: 06 July 2020

References

1. John, S. & Mishra, R. Galectin-9: from cell biology to complex disease dynamics. *J. Biosci.* **41**, 507–534 (2016).
2. Matsumoto, R. et al. Human ecalectin, a variant of human galectin-9, is a novel eosinophil chemoattractant produced by T lymphocytes. *J. Biol. Chem.* **273**, 16976–16984 (1998).
3. Gleason, M. K. et al. Tim-3 is an inducible human natural killer cell receptor that enhances interferon gamma production in response to galectin-9. *Blood* **119**, 3064–3072 (2012).
4. Jia, J. et al. Galectins control MTOR and AMPK in response to lysosomal damage to induce autophagy. *Autophagy* **15**, 169–171 (2019).
5. Bitra, A. et al. Crystal structure of murine 4-1BB and its interaction with 4-1BBL support a role for galectin-9 in 4-1BB signaling. *J. Biol. Chem.* **293**, 1317–1329 (2018).
6. Zhu, C. et al. The Tim-3 ligand galectin-9 negatively regulates T helper type 1 immunity. *Nat. Immunol.* **6**, 1245–1252 (2005).
7. Melief, S. M. et al. Long-term survival and clinical benefit from adoptive T-cell transfer in stage IV melanoma patients is determined by a four-parameter tumor immune signature. *Cancer Immunol. Res.* **5**, 170–179 (2017).
8. Zhou, X. et al. Galectin-9 expression predicts favorable clinical outcome in solid tumors: a systematic review and meta-analysis. *Front. Physiol.* **9**, 452 (2018).
9. Dardalhon, V. et al. Tim-3/galectin-9 pathway: regulation of Th1 immunity through promotion of CD11b+Ly-6G+ myeloid cells. *J. Immunol. (Baltim., Md: 1950)* **185**, 1383–1392 (2010).
10. Cai, T. T. et al. LMP1-mediated glycolysis induces myeloid-derived suppressor cell expansion in nasopharyngeal carcinoma. *PLoS Pathog.* **13**, e1006503 (2017).
11. Li, Z. L. et al. COX-2 promotes metastasis in nasopharyngeal carcinoma by mediating interactions between cancer cells and myeloid-derived suppressor cells. *Oncoimmunology* **4**, e1044712 (2015).
12. Chen, T. C. et al. The immunologic advantage of recurrent nasopharyngeal carcinoma from the viewpoint of Galectin-9/Tim-3-related changes in the tumour microenvironment. *Sci. Rep.* **7**, 10349 (2017).
13. Klibi, J. et al. Blood diffusion and Th1-suppressive effects of galectin-9-containing exosomes released by Epstein-Barr virus-infected nasopharyngeal carcinoma cells. *Blood* **113**, 1957–1966 (2009).
14. Pioche-Durieu, C. et al. In nasopharyngeal carcinoma cells, Epstein-Barr virus LMP1 interacts with galectin 9 in membrane raft elements resistant to simvastatin. *J. Virol.* **79**, 13326–13337 (2005).
15. Gourzones, C., Barjon, C. & Busson, P. Host-tumor interactions in nasopharyngeal carcinomas. *Semin. Cancer Biol.* **22**, 127–136 (2012).
16. Daley-Bauer, L. P., Wynn, G. M. & Mocarski, E. S. Cytomegalovirus impairs antiviral CD8+ T cell immunity by recruiting inflammatory monocytes. *Immunity* **37**, 122–133 (2012).
17. Woller, N. et al. Virus-induced tumor inflammation facilitates effective DC cancer immunotherapy in a Treg-dependent manner in mice. *J. Clin. Investig.* **121**, 2570–2582 (2011).
18. Tu, S. et al. Overexpression of interleukin-1beta induces gastric inflammation and cancer and mobilizes myeloid-derived suppressor cells in mice. *Cancer Cell* **14**, 408–419 (2008).
19. Engblom, C., Pfirschke, C. & Pittet, M. J. The role of myeloid cells in cancer therapies. *Nat. Rev. Cancer* **16**, 447–462 (2016).
20. Hartwig, T. et al. The TRAIL-induced cancer secretome promotes a tumor-supportive immune microenvironment via CCR2. *Mol. Cell* **65**, 730–42 e5 (2017).
21. Liang, H. et al. Host STING-dependent MDSC mobilization drives extrinsic radiation resistance. *Nat. Commun.* **8**, 1736 (2017).
22. Zhang, C. X. et al. STING signaling remodels the tumor microenvironment by antagonizing myeloid-derived suppressor cell expansion. *Cell Death Differ.* **26**, 2314–2328 (2019).
23. Xing, J. et al. TRIM29 promotes DNA virus infections by inhibiting innate immune response. *Nat. Commun.* **8**, 945 (2017).
24. Yamauchi, A. et al. Galectin-9, a novel prognostic factor with antimetastatic potential in breast cancer. *Breast J.* **12**, S196–S200 (2006).
25. Heery, C. R. et al. Avelumab for metastatic or locally advanced previously treated solid tumours (JAVELIN Solid Tumor): a phase 1a, multicohort, dose-escalation trial. *Lancet Oncol.* **18**, 587–598 (2017).
26. Kudo, T. et al. Nivolumab treatment for oesophageal squamous-cell carcinoma: an open-label, multicentre, phase 2 trial. *Lancet Oncol.* **18**, 631–639 (2017).
27. Barlesi, F. et al. Avelumab versus docetaxel in patients with platinum-treated advanced non-small-cell lung cancer (JAVELIN Lung 200): an open-label, randomised, phase 3 study. *Lancet Oncol.* **19**, 1468–1479 (2018).
28. Weber, J. S. et al. Nivolumab versus chemotherapy in patients with advanced melanoma who progressed after anti-CTLA-4 treatment (CheckMate 037): a randomised, controlled, open-label, phase 3 trial. *Lancet Oncol.* **16**, 375–384 (2015).
29. Madireddi, S. et al. Regulatory T Cell-mediated suppression of inflammation induced by DR3 signaling is dependent on Galectin-9. *J. Immunol.* **199**, 2721–2728 (2017).
30. Kikushige, Y. et al. A TIM-3/Gal-9 autocrine stimulatory loop drives self-renewal of human myeloid leukemia stem cells and leukemic progression. *Cell Stem Cell* **17**, 341–352 (2015).
31. Tureci, O., Schmitt, H., Fadle, N., Pfreundschuh, M. & Sahin, U. Molecular definition of a novel human galectin which is immunogenic in patients with Hodgkin's disease. *J. Biol. Chem.* **272**, 6416–6422 (1997).
32. Irie, A. et al. Galectin-9 as a prognostic factor with antimetastatic potential in breast cancer. *Clin. Cancer Res.* **11**, 2962–2968 (2005).
33. Umansky, V., Blattner, C., Gebhardt, C. & Utikal, J. The Role of Myeloid-Derived Suppressor Cells (MDSC) in Cancer Progression. *Vaccines* **4**, 36 (2016).

34. Chen, H. W. et al. Mesenchymal stem cells tune the development of monocyte-derived dendritic cells toward a myeloid-derived suppressive phenotype through growth-regulated oncogene chemokines. *J. Immunol.* **190**, 5065–5077 (2013).
35. Kumar, S. et al. DeltaNp63-driven recruitment of myeloid-derived suppressor cells promotes metastasis in triple-negative breast cancer. *J. Clin. Investig.* **128**, 5095–5109 (2018).
36. Rodriguez-Ubreva, J. et al. Prostaglandin E2 leads to the acquisition of DNMT3A-dependent tolerogenic functions in human myeloid-derived suppressor cells. *Cell Rep.* **21**, 154–167 (2017).
37. Dai, S. Y. et al. Galectin-9 induces maturation of human monocyte-derived dendritic cells. *J. Immunol.* **175**, 2974–2981 (2005).
38. Golden-Mason, L. & Rosen, H. R. Galectin-9: diverse roles in hepatic immune homeostasis and inflammation. *Hepatology* **66**, 271–279 (2017).
39. Nagahara, K. et al. Galectin-9 increases Tim-3+ dendritic cells and CD8+ T cells and enhances antitumor immunity via galectin-9-Tim-3 interactions. *J. Immunol.* **181**, 7660–7669 (2008).
40. Golden-Mason, L. et al. Galectin-9 functionally impairs natural killer cells in humans and mice. *J. Virol.* **87**, 4835–4845 (2013).
41. Zhang, Y. et al. Expansion of CD11b(+)Ly-6C(+) myeloid-derived suppressor cells (MDSCs) driven by galectin-9 attenuates CVB3-induced myocarditis. *Mol. Immunol.* **83**, 62–71 (2017).
42. Lechner, M. G., Liebertz, D. J. & Epstein, A. L. Characterization of cytokine-induced myeloid-derived suppressor cells from normal human peripheral blood mononuclear cells. *J. Immunol.* **185**, 2273–2284 (2010).
43. Ishikawa, H. & Barber, G. N. STING is an endoplasmic reticulum adaptor that facilitates innate immune signalling. *Nature* **455**, 674–678 (2008).
44. Corrales, L., McWhirter, S. M., Dubensky, T. W. Jr. & Gajewski, T. F. The host STING pathway at the interface of cancer and immunity. *J. Clin. Investig.* **126**, 2404–2411 (2016).
45. van den Hoogen, L. L. et al. Galectin-9 is an easy to measure biomarker for the interferon signature in systemic lupus erythematosus and antiphospholipid syndrome. *Ann. Rheum. Dis.* **77**, 1810–1814 (2018).
46. Panda, S. K. et al. Galectin-9 inhibits TLR7-mediated autoimmunity in murine lupus models. *J. Clin. Investig.* **128**, 1873–1887 (2018).
47. Zeggar, S. et al. Role of Lgals9 deficiency in attenuating nephritis and arthritis in BALB/c Mice in a Pristane-Induced Lupus model. *Arthritis Rheumatol.* **70**, 1089–1101 (2018).

BIBLIOGRAPHIE

1. Nagae M, Nishi N, Nakamura-Tsuruta S, Hirabayashi J, Wakatsuki S, Kato R. Structural Analysis of the Human Galectin-9 N-terminal Carbohydrate Recognition Domain Reveals Unexpected Properties that Differ from the Mouse Orthologue. J Mol Biol. 2008 Jan;375(1):119–35.

2. Rabinovich GA, Toscano MA. Turning 'sweet' on immunity: galectin–glycan interactions in immune tolerance and inflammation. Nat Rev Immunol. 2009 May;9(5):338–52.

3. Nio-Kobayashi J. Tissue- and cell-specific localization of galectins, β-galactose-binding animal lectins, and their potential functions in health and disease. Anat Sci Int. 2017 Jan;92(1):25–36.

4. Vasta GR, Ahmed H, Nita-Lazar M, Banerjee A, Pasek M, Shridhar S, et al. Galectins as self/non-self recognition receptors in innate and adaptive immunity: an unresolved paradox. Front Immunol [Internet]. 2012 [cited 2019 Dec 16];3. Available from: http://journal.frontiersin.org/article/10.3389/fimmu.2012.00199/abstract

5. Popa SJ, Stewart SE, Moreau K. Unconventional secretion of annexins and galectins. Semin Cell Dev Biol. 2018 Nov;83:42–50.

6. Johannes L, Billet A. Glycosylation and raft endocytosis in cancer. Cancer Metastasis Rev [Internet]. 2020 May 9 [cited 2020 May 17]; Available from: http://link.springer.com/10.1007/s10555-020-09880-z

7. Lakshminarayan R, Wunder C, Becken U, Howes MT, Benzing C, Arumugam S, et al. Galectin-3 drives glycosphingolipid-dependent biogenesis of clathrin-independent carriers. Nat Cell Biol. 2014 Jun;16(6):592–603.

8. Enninga EAL, Harrington SM, Creedon DJ, Ruano R, Markovic SN, Dong H, et al. Immune checkpoint molecules soluble program death ligand 1 and galectin-9 are increased in pregnancy. Am J Reprod Immunol. 2018 Feb;79(2):e12795.

9. Saqib U, Sarkar S, Suk K, Mohammad O, Baig MS, Savai R. Phytochemicals as modulators of M1-M2 macrophages in inflammation. Oncotarget [Internet]. 2018 Apr 2 [cited 2019 Dec 16];9(25). Available from: http://www.oncotarget.com/fulltext/24788

10. Pardoll DM. The blockade of immune checkpoints in cancer immunotherapy. Nat Rev Cancer. 2012 Apr;12(4):252–64.

11. Lhuillier C. Impact de la galectine-9 exogène sur les lymphocytes T humaines et caractérisation de nouveaux anticorps monoclonaux à visée thérapeutique. Université Paris-Saclay; 2016.

12. Hanahan D, Weinberg RA. Hallmarks of Cancer: The Next Generation. Cell. 2011 Mar;144(5):646–74.

13. Trédan O, Barthelemy P, Villanueva C, Teixeira L. Le cycle cellulaire : données biologiques et thérapies ciblant les cyclines/CDK. Correspondances en Onco-Théranostic; 2017.

14. Swann JB, Smyth MJ. Immune surveillance of tumors. J Clin Invest. 2007 May 1;117(5):1137–46.

15. Stuelten CH, Parent CA, Montell DJ. Cell motility in cancer invasion and metastasis: insights from simple model organisms. Nat Rev Cancer. 2018 May;18(5):296–312.

16. Jiang W, Marraffini LA. CRISPR-Cas: New Tools for Genetic Manipulations from Bacterial Immunity Systems. Annu Rev Microbiol. 2015 Oct 15;69(1):209–28.

17. Southan C, Aitken A, Childs RA, Abbott WM, Feizi T. Amino acid sequence of β-galactoside-binding bovine heart lectin: Member of a novel class of vertebrate proteins. FEBS Lett. 1987 Apr 20;214(2):301–4.

18. Houzelstein D, Gonçalves IR, Fadden AJ, Sidhu SS, Cooper DNW, Drickamer K, et al. Phylogenetic Analysis of the Vertebrate Galectin Family. Mol Biol Evol. 2004 Jul;21(7):1177–87.

19. Meynier C, Feracci M, Espeli M, Chaspoul F, Gallice P, Schiff C, et al. NMR and MD Investigations of Human Galectin-1/Oligosaccharide Complexes. Biophys J. 2009 Dec;97(12):3168–77.

20. Mark Abbott W, Feizi T. Soluble 14-kDa β-Galactoside-specific Bovine Lectin. J Biol Chem. 1991 Mar 25;266(9):5552–7.

21. Hirabayashi J. Oligosaccharide specificity of galectins: a search by frontal affinity chromatography. Biochim Biophys Acta BBA - Gen Subj. 2002 Sep 19;1572(2–3):232–54.

22. Kim B-W, Beom Hong S, Hoe Kim J, Hoon Kwon D, Kyu Song H. Structural basis for recognition of autophagic receptor NDP52 by the sugar receptor galectin-8. Nat Commun. 2013 Jun;4(1):1613.

23. Elantak L, Espeli M, Boned A, Bornet O, Bonzi J, Gauthier L, et al. Structural Basis for Galectin-1-dependent Pre-B Cell Receptor (Pre-BCR) Activation. J Biol Chem. 2012 Dec 28;287(53):44703–13.

24. Daley D, Mani VR, Mohan N, Akkad N, Ochi A, Heindel DW, et al. Dectin 1 activation on macrophages by galectin 9 promotes pancreatic carcinoma and peritumoral immune tolerance. Nat Med. 2017 May;23(5):556–67.

25. Teichberg VI, Silman I, Beitsch DD, RESHEFFt G. A f3-D-Galactoside Binding Protein from Electric Organ Tissue of Electrophorus electricus. Proc Nat Acad Sci USA. 1975;5.

26. Barondes SH, Castronovo V, Cooper DNW, Cummings RD, Drickamer K, Felzi T, et al. Galectins: A family of animal β-galactoside-binding lectins. Cell. 1994 Feb;76(4):597–8.

27. Arthur CM, Baruffi MD, Cummings RD, Stowell SR. Evolving Mechanistic Insights into Galectin Functions. In: Stowell SR, Cummings RD, editors. Galectins [Internet]. New York, NY: Springer New York; 2015 [cited 2019 Aug 22]. p. 1–35. Available from: http://link.springer.com/10.1007/978-1-4939-1396-1_1

28. Hirabayashi J, Kasai K. The family of metazoan metal-independent β-galactoside-binding lectins: structure, function and molecular evolution. Glycobiology. 1993;3(4):297–304.

29. Earl LA, Bi S, Baum LG. Galectin multimerization and lattice formation are regulated by linker region structure. Glycobiology. 2011 Jan 1;21(1):6–12.

30. Poirier F, Timmons PM, Rigby J. Expression of the L14 lectin during mouse embryogenesis suggests multiple roles during pre- and post-implantation development. Development. 1992 May;115(1):143–55.

31. Hsu DK, Liu F-T. Regulation of cellular homeostasis by galectins. Glycoconj J. 2002;19(7–9):507–15.

32. Than NG, Romero R, Balogh A, Karpati E, Mastrolia SA, Staretz-Chacham O, et al. Galectins: Double-edged Swords in the Cross-roads of Pregnancy Complications and Female Reproductive Tract Inflammation and Neoplasia. J Pathol Transl Med. 2015 May 15;49(3):181–208.

33. Sahraravand M, Järvelä IY, Laitinen P, Tekay AH, Ryynänen M. The secretion of PAPP-A, ADAM12, and PP13 correlates with the size of the placenta for the first month of pregnancy. Placenta. 2011 Dec;32(12):999–1003.

34. Niki T, Fujita K, Rosen H, Hirashima M, Masaki T, Hattori T, et al. Plasma Galectin-9 Concentrations in Normal and Diseased Condition. Cell Physiol Biochem. 2018;50(5):1856–68.

35. Barrow H, Guo X, Wandall HH, Pedersen JW, Fu B, Zhao Q, et al. Serum Galectin-2, -4, and -8 Are Greatly Increased in Colon and Breast Cancer Patients and Promote Cancer Cell Adhesion to Blood Vascular Endothelium. Clin Cancer Res. 2011 Nov 15;17(22):7035–46.

36. Vinnai JR, Cumming RC, Thompson GJ, Timoshenko AV. The association between oxidative stress-induced galectins and differentiation of human promyelocytic HL-60 cells. Exp Cell Res. 2017 Jun;355(2):113–23.

37. Rhodes DH, Pini M, Castellanos KJ, Montero-Melendez T, Cooper D, Perretti M, et al. Adipose tissue-specific modulation of galectin expression in lean and obese mice: Evidence for regulatory function. Obesity. 2013 Feb;21(2):310–9.

38. Imaizumi T, Kumagai M, Sasaki N, Kurotaki H, Mori F, Seki M, et al. Interferon-gamma stimulates the expression of galectin-9 in cultured human endothelial cells. J Leukoc Biol. 2002 Sep;72(3):486–91.

39. Gauthier S, Pelletier I, Ouellet M, Vargas A, Tremblay MJ, Sato S, et al. Induction of galectin-1 expression by HTLV-I Tax and its impact on HTLV-I infectivity. Retrovirology. 2008;5(1):105.

40. Georgiadis V, Stewart HJS, Pollard HJ, Tavsanoglu Y, Prasad R, Horwood J, et al. Lack of galectin-1 results in defects in myoblast fusion and muscle regeneration. Dev Dyn. 2007 Apr;236(4):1014–24.

41. Gendronneau G, Sidhu SS, Delacour D, Dang T, Calonne C, Houzelstein D, et al. Galectin-7 in the Control of Epidermal Homeostasis after Injury. Margolis B, editor. Mol Biol Cell. 2008 Dec;19(12):5541–9.

42. Delacour D, Koch A, Ackermann W, Parco IE-L, Elsässer H-P, Poirier F, et al. Loss of galectin-3 impairs membrane polarisation of mouse enterocytes in vivo. J Cell Sci. 2008 Feb 15;121(4):458–65.

43. Shalom-Feuerstein R, Plowman SJ, Rotblat B, Ariotti N, Tian T, Hancock JF, et al. K-Ras Nanoclustering Is Subverted by Overexpression of the Scaffold Protein Galectin-3. Cancer Res. 2008 Aug 15;68(16):6608–16.

44. Elad-Sfadia G, Haklai R, Balan E, Kloog Y. Galectin-3 Augments K-Ras Activation and Triggers a Ras Signal That Attenuates ERK but Not Phosphoinositide 3-Kinase Activity. J Biol Chem. 2004 Aug 13;279(33):34922–30.

45. Paz I, Sachse M, Dupont N, Mounier J, Cederfur C, Enninga J, et al. Galectin-3, a marker for vacuole lysis by invasive pathogens. Cell Microbiol. 2010 Apr;12(4):530–44.

46. Cheng Y-L, Wu Y-W, Kuo C-F, Lu S-L, Liu F-T, Anderson R, et al. Galectin-3 Inhibits Galectin-8/Parkin-Mediated Ubiquitination of Group A Streptococcus. Patton JT, editor. mBio. 2017 Sep 6;8(4):e00899-17, /mbio/8/4/e00899-17.atom.

47. Nakahara S, Hogan V, Inohara H, Raz A. Importin-mediated Nuclear Translocation of Galectin-3. J Biol Chem. 2006 Dec 22;281(51):39649–59.

48. Dagher SF, Wang JL, Patterson RJ. Identification of galectin-3 as a factor in pre-mRNA splicing. Proc Natl Acad Sci. 1995 Feb 14;92(4):1213–7.

49. Thurston TLM, Wandel MP, von Muhlinen N, Foeglein A, Randow F. Galectin 8 targets damaged vesicles for autophagy to defend cells against bacterial invasion. Nature. 2012 Jan 15;482(7385):414–8.

50. Flavin WP, Bousset L, Green ZC, Chu Y, Skarpathiotis S, Chaney MJ, et al. Endocytic vesicle rupture is a conserved mechanism of cellular invasion by amyloid proteins. Acta Neuropathol (Berl). 2017 Oct;134(4):629–53.

51. Johannes L, Jacob R, Leffler H. Galectins at a glance. J Cell Sci. 2018 01;131(9).

52. Johannes L, Wunder C, Shafaq-Zadah M. Glycolipids and Lectins in Endocytic Uptake Processes. J Mol Biol. 2016 Oct 27;

53. Lukyanov P, Furtak V, Ochieng J. Galectin-3 interacts with membrane lipids and penetrates the lipid bilayer. Biochem Biophys Res Commun. 2005 Dec;338(2):1031–6.

54. Cho M, Cummings RD. Galectin-1, a β-Galactoside-binding Lectin in Chinese Hamster Ovary Cells: I. PHYSICAL AND CHEMICAL CHARACTERIZATION. J Biol Chem. 1995 Mar 10;270(10):5198–206.

55. Stewart SE, Menzies SA, Popa SJ, Savinykh N, Petrunkina Harrison A, Lehner PJ, et al. A genome-wide CRISPR screen reconciles the role of N-linked glycosylation in galectin-3 transport to the cell surface. J Cell Sci. 2017 Oct 1;130(19):3234–47.

56. Cooper DN. Evidence for export of a muscle lectin from cytosol to extracellular matrix and for a novel secretory mechanism. J Cell Biol. 1990 May 1;110(5):1681–91.

57. Aits S, Kricker J, Liu B, Ellegaard A-M, Hämälistö S, Tvingsholm S, et al. Sensitive detection of lysosomal membrane permeabilization by lysosomal galectin puncta assay. Autophagy. 2015 Aug 3;11(8):1408–24.

58. Keryer-Bibens C, Pioche-Durieu C, Villemant C, Souquère S, Nishi N, Hirashima M, et al. Exosomes released by EBV-infected nasopharyngeal carcinoma cells convey the viral Latent Membrane Protein 1 and the immunomodulatory protein galectin 9. BMC Cancer. 2006 Dec;6(1):283.

59. Klibi J, Niki T, Riedel A, Pioche-Durieu C, Souquere S, Rubinstein E, et al. Blood diffusion and Th1-suppressive effects of galectin-9–containing exosomes released by Epstein-Barr virus–infected nasopharyngeal carcinoma cells. Blood. 2009 Feb 26;113(9):1957–66.

60. Bänfer S, Schneider D, Dewes J, Strauss MT, Freibert S-A, Heimerl T, et al. Molecular mechanism to recruit galectin-3 into multivesicular bodies for polarized exosomal secretion. Proc Natl Acad Sci. 2018 May 8;115(19):E4396–405.

61. Elola MT, Blidner AG, Ferragut F, Bracalente C, Rabinovich GA. Assembly, organization and regulation of cell-surface receptors by lectin–glycan complexes. Biochem J. 2015 Jul 1;469(1):1–16.

62. Mishra R, Grzybek M, Niki T, Hirashima M, Simons K. Galectin-9 trafficking regulates apical-basal polarity in Madin–Darby canine kidney epithelial cells. Proc Natl Acad Sci. 2010 Oct 12;107(41):17633–8.

63. Jia J, Abudu YP, Claude-Taupin A, Gu Y, Kumar S, Choi SW, et al. Galectins Control mTOR in Response to Endomembrane Damage. Mol Cell. 2018 Apr;70(1):120-135.e8.

64. Wiersma VR, de Bruyn M, Wei Y, van Ginkel RJ, Hirashima M, Niki T, et al. The epithelial polarity regulator LGALS9/galectin-9 induces fatal frustrated autophagy in KRAS mutant colon carcinoma that depends on elevated basal autophagic flux. Autophagy. 2015 Aug 3;11(8):1373–88.

65. Querol Cano L, Tagit O, Dolen Y, van Duffelen A, Dieltjes S, Buschow SI, et al. Intracellular Galectin-9 Controls Dendritic Cell Function by Maintaining Plasma Membrane Rigidity. iScience. 2019 Dec;22:240–55.

66. Chen H-Y, Wu Y-F, Chou F-C, Wu Y-H, Yeh L-T, Lin K-I, et al. Intracellular Galectin-9 Enhances Proximal TCR Signaling and Potentiates Autoimmune Diseases. J Immunol. 2020 Mar 1;204(5):1158–72.

67. Matsumoto R, Hirashima M, Kita H, Gleich GJ. Biological Activities of Ecalectin: A Novel Eosinophil-Activating Factor. J Immunol. 2002 Feb 15;168(4):1961–7.

68. Zhu C, Anderson AC, Schubart A, Xiong H, Imitola J, Khoury SJ, et al. The Tim-3 ligand galectin-9 negatively regulates T helper type 1 immunity. Nat Immunol. 2005 Dec;6(12):1245–52.

69. Matsumoto R, Matsumoto H, Seki M, Hata M, Asano Y, Kanegasaki S, et al. Human Ecalectin, a Variant of Human Galectin-9, Is a Novel Eosinophil Chemoattractant Produced by T Lymphocytes. J Biol Chem. 1998 Jul 3;273(27):16976–84.

70. Wang Y, Sun J, Ma C, Gao W, Song B, Xue H, et al. Reduced Expression of Galectin-9 Contributes to a Poor Outcome in Colon Cancer by Inhibiting NK Cell Chemotaxis Partially through the Rho/ROCK1 Signaling Pathway. St-Pierre Y, editor. PLOS ONE. 2016 Mar 30;11(3):e0152599.

71. Ishikawa A, Imaizumi T, Yoshida H, Nishi N, Nakamura T, Hirashima M, et al. Double-stranded RNA enhances the expression of galectin-9 in vascular endothelial cells. Immunol Cell Biol. 2004 Aug;82(4):410–4.

72. Zhang DL, Lv CH, Yu D hui, Wang ZY. Characterization and functional analysis of a tandem-repeat galectin-9 in large yellow croaker Larimichthys crocea. Fish Shellfish Immunol. 2016 May;52:167–78.

73. Vega-Carrascal I, Bergin DA, McElvaney OJ, McCarthy C, Banville N, Pohl K, et al. Galectin-9 Signaling through TIM-3 Is Involved in Neutrophil-Mediated Gram-Negative Bacterial Killing: An Effect Abrogated within the Cystic Fibrosis Lung. J Immunol. 2014 Mar 1;192(5):2418–31.

74. Shan M, Carrillo J, Yeste A, Gutzeit C, Segura-Garzón D, Walland AC, et al. Secreted IgD Amplifies Humoral T Helper 2 Cell Responses by Binding Basophils via Galectin-9 and CD44. Immunity. 2018 Oct;49(4):709-724.e8.

75. Li Y, Zhang J, Zhang D, Hong X, Tao Y, Wang S, et al. Tim-3 signaling in peripheral NK cells promotes maternal-fetal immune tolerance and alleviates pregnancy loss. Sci Signal. 2017 Sep 26;10(498):eaah4323.

76. Sun J, Yang M, Ban Y, Gao W, Song B, Wang Y, et al. Tim-3 Is Upregulated in NK Cells during Early Pregnancy and Inhibits NK Cytotoxicity toward Trophoblast in Galectin-9 Dependent Pathway. Kanellopoulos-Langevin C, editor. PLOS ONE. 2016 Jan 20;11(1):e0147186.

77. Meggyes M, Miko E, Polgar B, Bogar B, Farkas B, Illes Z, et al. Peripheral Blood TIM-3 Positive NK and CD8+ T Cells throughout Pregnancy: TIM-3/Galectin-9 Interaction and Its Possible Role during Pregnancy. Bobé P, editor. PLoS ONE. 2014 Mar 20;9(3):e92371.

78. Li Y-H, Zhou W-H, Tao Y, Wang S-C, Jiang Y-L, Zhang D, et al. The Galectin-9/Tim-3 pathway is involved in the regulation of NK cell function at the maternal–fetal interface in early pregnancy. Cell Mol Immunol. 2016 Jan;13(1):73–81.

79. Meggyes M, Miko E, Szigeti B, Farkas N, Szereday L. The importance of the PD-1/PD-L1 pathway at the maternal-fetal interface. BMC Pregnancy Childbirth. 2019 Dec;19(1):74.

80. Enninga EAL, Nevala WK, Holtan SG, Leontovich AA, Markovic SN. Galectin-9 modulates immunity by promoting Th2/M2 differentiation and impacts survival in patients with metastatic melanoma: Melanoma Res. 2016 Oct;26(5):429–41.

81. Bertino P, Premeaux TA, Fujita T, Haun BK, Marciel MP, Hoffmann FW, et al. Targeting the C-terminus of galectin-9 induces mesothelioma apoptosis and M2 macrophage depletion. OncoImmunology. 2019 Aug 3;8(8):1601482.

82. Zhang W, Zhang Y, He Y, Wang X, Fang Q. Lipopolysaccharide mediates time-dependent macrophage M1/M2 polarization through the Tim-3/Galectin-9 signalling pathway. Exp Cell Res. 2019 Mar;376(2):124–32.

83. Enninga EAL, Chatzopoulos K, Butterfield JT, Sutor SL, Leontovich AA, Nevala WK, et al. CD206-positive myeloid cells bind galectin-9 and promote a tumor-supportive microenvironment: Galectin-9/CD206 binding. J Pathol. 2018 Aug;245(4):468–77.

84. de Kivit S, Kostadinova AI, Kerperien J, Morgan ME, Muruzabal VA, Hofman GA, et al. Dietary, nondigestible oligosaccharides and *Bifidobacterium breve* M-16V suppress allergic inflammation in intestine via targeting dendritic cell maturation. J Leukoc Biol. 2017 Jul;102(1):105–15.

85. de Kivit S, Kostadinova AI, Kerperien J, Ayechu Muruzabal V, Morgan ME, Knippels LMJ, et al. Galectin-9 Produced by Intestinal Epithelial Cells Enhances Aldehyde Dehydrogenase Activity in Dendritic Cells in a PI3K- and p38-Dependent Manner. J Innate Immun. 2017;9(6):609–20.

86. Dai S-Y, Nakagawa R, Itoh A, Murakami H, Kashio Y, Abe H, et al. Galectin-9 Induces Maturation of Human Monocyte-Derived Dendritic Cells. J Immunol. 2005 Sep 1;175(5):2974–81.

87. Dardalhon V, Anderson AC, Karman J, Apetoh L, Chandwaskar R, Lee DH, et al. Tim-3/Galectin-9 Pathway: Regulation of Th1 Immunity through Promotion of CD11b $^{+}$ Ly-6G $^{+}$ Myeloid Cells. J Immunol. 2010 Aug 1;185(3):1383–92.

88. Limagne E, Richard C, Thibaudin M, Fumet J-D, Truntzer C, Lagrange A, et al. Tim-3/galectin-9 pathway and mMDSC control primary and secondary resistances to PD-1 blockade in lung cancer patients. OncoImmunology. 2019 Apr 3;8(4):e1564505.

89. Lhuillier C, Barjon C, Niki T, Gelin A, Praz F, Morales O, et al. Impact of Exogenous Galectin-9 on Human T Cells: CONTRIBUTION OF THE T CELL RECEPTOR COMPLEX TO ANTIGEN-INDEPENDENT ACTIVATION BUT NOT TO APOPTOSIS INDUCTION. J Biol Chem. 2015 Jul 3;290(27):16797–811.

90. Vahl JC, Drees C, Heger K, Heink S, Fischer JC, Nedjic J, et al. Continuous T Cell Receptor Signals Maintain a Functional Regulatory T Cell Pool. Immunity. 2014 Nov;41(5):722–36.

91. Gooden MJM, Wiersma VR, Samplonius DF, Gerssen J, van Ginkel RJ, Nijman HW, et al. Galectin-9 Activates and Expands Human T-Helper 1 Cells. Tasken K, editor. PLoS ONE. 2013 May 31;8(5):e65616.

92. Wang F, He W, Zhou H, Yuan J, Wu K, Xu L, et al. The Tim-3 ligand galectin-9 negatively regulates CD8+ alloreactive T cell and prolongs survival of skin graft. Cell Immunol. 2007 Nov;250(1–2):68–74.

93. Reddy PBJ, Sehrawat S, Suryawanshi A, Rajasagi NK, Mulik S, Hirashima M, et al. Influence of Galectin-9/Tim-3 Interaction on Herpes Simplex Virus-1 Latency. J Immunol. 2011 Dec 1;187(11):5745–55.

94. Mengshol JA, Golden-Mason L, Arikawa T, Smith M, Niki T, McWilliams R, et al. A Crucial Role for Kupffer Cell-Derived Galectin-9 in Regulation of T Cell Immunity in Hepatitis C Infection. Unutmaz D, editor. PLoS ONE. 2010 Mar 4;5(3):e9504.

95. Nebbia G, Peppa D, Schurich A, Khanna P, Singh HD, Cheng Y, et al. Upregulation of the Tim-3/Galectin-9 Pathway of T Cell Exhaustion in Chronic Hepatitis B Virus Infection. Shoukry NH, editor. PLoS ONE. 2012 Oct 24;7(10):e47648.

96. Seki M, Oomizu S, Sakata K, Sakata A, Arikawa T, Watanabe K, et al. Galectin-9 suppresses the generation of Th17, promotes the induction of regulatory T cells, and regulates experimental autoimmune arthritis. Clin Immunol. 2008 Apr;127(1):78–88.

97. Oomizu S, Arikawa T, Niki T, Kadowaki T, Ueno M, Nishi N, et al. Cell Surface Galectin-9 Expressing Th Cells Regulate Th17 and Foxp3+ Treg Development by Galectin-9 Secretion. Basso AS, editor. PLoS ONE. 2012 Nov 7;7(11):e48574.

98. Wu C, Thalhamer T, Franca RF, Xiao S, Wang C, Hotta C, et al. Galectin-9-CD44 Interaction Enhances Stability and Function of Adaptive Regulatory T Cells. Immunity. 2014 Aug;41(2):270–82.

99. Cao A, Alluqmani N, Buhari FHM, Wasim L, Smith LK, Quaile AT, et al. Galectin-9 binds IgM-BCR to regulate B cell signaling. Nat Commun. 2018 Dec;9(1):3288.

100. Giovannone N, Liang J, Antonopoulos A, Geddes Sweeney J, King SL, Pochebit SM, et al. Galectin-9 suppresses B cell receptor signaling and is regulated by I-branching of N-glycans. Nat Commun. 2018 Dec;9(1):3287.

101. Orr SL, Le D, Long JM, Sobieszczuk P, Ma B, Tian H, et al. A phenotype survey of 36 mutant mouse strains with gene-targeted defects in glycosyltransferases or glycan-binding proteins. Glycobiology. 2013 Mar 1;23(3):363–80.

102. Heusschen R, Schulkens IA, van Beijnum J, Griffioen AW, Thijssen VL. Endothelial LGALS9 splice variant expression in endothelial cell biology and angiogenesis. Biochim Biophys Acta BBA - Mol Basis Dis. 2014 Feb;1842(2):284–92.

103. O'Brien MJ, Shu Q, Stinson WA, Tsou P-S, Ruth JH, Isozaki T, et al. A unique role for galectin-9 in angiogenesis and inflammatory arthritis. Arthritis Res Ther. 2018 Dec;20(1):31.

104. Aanhane E, Schulkens IA, Heusschen R, Castricum K, Leffler H, Griffioen AW, et al. Different angioregulatory activity of monovalent galectin-9 isoforms. Angiogenesis. 2018 Aug;21(3):545–55.

105. Seki M, Sakata K-M, Oomizu S, Arikawa T, Sakata A, Ueno M, et al. Beneficial effect of galectin 9 on rheumatoid arthritis by induction of apoptosis of synovial fibroblasts. Arthritis Rheum. 2007 Dec;56(12):3968–76.

106. Arikawa T, Watanabe K, Seki M, Matsukawa A, Oomizu S, Sakata K, et al. Galectin-9 ameliorates immune complex-induced arthritis by regulating FcγR expression on macrophages. Clin Immunol. 2009 Dec;133(3):382–92.

107. Moritoki M, Kadowaki T, Niki T, Nakano D, Soma G, Mori H, et al. Galectin-9 Ameliorates Clinical Severity of MRL/lpr Lupus-Prone Mice by Inducing Plasma Cell Apoptosis Independently of Tim-3. Bobé P, editor. PLoS ONE. 2013 Apr 9;8(4):e60807.

108. Katoh S, Ishii N, Nobumoto A, Takeshita K, Dai S-Y, Shinonaga R, et al. Galectin-9 Inhibits CD44–Hyaluronan Interaction and Suppresses a Murine Model of Allergic Asthma. Am J Respir Crit Care Med. 2007 Jul;176(1):27–35.

109. Katoh S, Shimizu H, Obase Y, Oomizu S, Niki T, Ikeda M, et al. Preventive effect of galectin-9 on double-stranded RNA-induced airway hyperresponsiveness in an exacerbation model of mite antigen-induced asthma in mice. Exp Lung Res. 2013 Dec;39(10):453–62.

110. Ikeda M, Katoh S, Shimizu H, Hasegawa A, Ohashi-Doi K, Oka M. Beneficial effects of Galectin-9 on allergen-specific sublingual immunotherapy in a Dermatophagoides farinae -induced mouse model of chronic asthma. Allergol Int. 2017 Jul;66(3):432–9.

111. Sziksz E, Kozma GT, Pállinger É, Komlósi ZI, Ádori C, Kovács L, et al. Galectin-9 in Allergic Airway Inflammation and Hyper-Responsiveness in Mice. Int Arch Allergy Immunol. 2010;151(4):308–17.

112. Yamamoto H, Kashio Y, Shoji H, Shinonaga R, Yoshimura T, Nishi N, et al. Involvement of Galectin-9 in Guinea Pig Allergic Airway Inflammation. Int Arch Allergy Immunol. 2007;143(1):95–105.

113. Wang Y, Meng J, Wang X, Liu S, Shu Q, Gao L, et al. Expression of Human TIM-1 and TIM-3 on Lymphocytes from Systemic Lupus Erythematosus Patients: Human TIM-1 and TIM-3 in SLE. Scand J Immunol. 2007 Dec 4;67(1):63–70.

114. Jiao Q, Qian Q, Zhao Z, Fang F, Hu X, An J, et al. Expression of human T cell immunoglobulin domain and mucin-3 (TIM-3) and TIM-3 ligands in peripheral blood from patients with systemic lupus erythematosus. Arch Dermatol Res. 2016 Oct;308(8):553–61.

115. Nakajima R, Miyagaki T, Oka T, Nakao M, Kawaguchi M, Suga H, et al. Elevated serum galectin-9 levels in patients with atopic dermatitis. J Dermatol. 2015 Jul;42(7):723–6.

116. Nofal E, Eldesoky F, Nofal A, Abdelshafy A, Zedan A. Serum galectin-9 levels in atopic dermatitis, psoriasis and allergic contact dermatitis: A cross-sectional study. Indian J Dermatol Venereol Leprol. 2019;85(2):195.

117. Stone KD, Prussin C, Metcalfe DD. IgE, mast cells, basophils, and eosinophils. J Allergy Clin Immunol. 2010 Feb;125(2):S73–80.

118. Wiersma VR, Clarke A, Pouwels SD, Perry E, Abdullah TM, Kelly C, et al. Galectin-9 Is a Possible Promoter of Immunopathology in Rheumatoid Arthritis by Activation of Peptidyl Arginine Deiminase 4 (PAD-4) in Granulocytes. Int J Mol Sci. 2019 Aug 19;20(16):4046.

119. Barjon C, Niki T, Vérillaud B, Opolon P, Bedossa P, Hirashima M, et al. A novel monoclonal antibody for detection of galectin-9 in tissue sections: application to human tissues infected by oncogenic viruses. Infect Agent Cancer. 2012;7(1):16.

120. Harwood NMK, Golden-Mason L, Cheng L, Rosen HR, Mengshol JA. HCV-infected cells and differentiation increase monocyte immunoregulatory galectin-9 production. J Leukoc Biol. 2016 Mar 1;99(3):495–503.

121. Zhuo Y, Zhang Y-F, Wu H-J, Qin L, Wang Y-P, Liu A-M, et al. Interaction between Galectin-9/TIM-3 pathway and follicular helper CD4+ T cells contributes to viral persistence in chronic hepatitis C. Biomed Pharmacother. 2017 Oct;94:386–93.

122. Kared H, Fabre T, Bédard N, Bruneau J, Shoukry NH. Galectin-9 and IL-21 Mediate Cross-regulation between Th17 and Treg Cells during Acute Hepatitis C. Bevan M, editor. PLoS Pathog. 2013 Jun 20;9(6):e1003422.

123. Mrizak D, Martin N, Barjon C, Jimenez-Pailhes A-S, Mustapha R, Niki T, et al. Effect of Nasopharyngeal Carcinoma-Derived Exosomes on Human Regulatory T Cells. JNCI J Natl Cancer Inst [Internet]. 2015 Jan [cited 2019 Dec 6];107(1). Available from: https://academic.oup.com/jnci/article-lookup/doi/10.1093/jnci/dju363

124. Sehrawat S, Suryawanshi A, Hirashima M, Rouse BT. Role of Tim-3/Galectin-9 Inhibitory Interaction in Viral-Induced Immunopathology: Shifting the Balance toward Regulators. J Immunol. 2009 Mar 1;182(5):3191–201.

125. Liu T, Khanna KM, Chen X, Fink DJ, Hendricks RL. Cd8 $^{+}$ T Cells Can Block Herpes Simplex Virus Type 1 (HSV-1) Reactivation from Latency in Sensory Neurons. J Exp Med. 2000 May 1;191(9):1459–66.

126. Tandon R, Chew GM, Byron MM, Borrow P, Niki T, Hirashima M, et al. Galectin-9 Is Rapidly Released During Acute HIV-1 Infection and Remains Sustained at High Levels Despite Viral Suppression Even in Elite Controllers. AIDS Res Hum Retroviruses. 2014 Jul;30(7):654–64.

127. Abdel-Mohsen M, Chavez L, Tandon R, Chew GM, Deng X, Danesh A, et al. Human Galectin-9 Is a Potent Mediator of HIV Transcription and Reactivation. Silvestri G, editor. PLOS Pathog. 2016 Jun 2;12(6):e1005677.

128. Colomb F, Giron LB, Premeaux TA, Mitchell BI, Niki T, Papasavvas E, et al. Galectin-9 Mediates HIV Transcription by Inducing TCR-Dependent ERK Signaling. Front Immunol. 2019 Feb 20;10:267.

129. Yu Q, König R, Pillai S, Chiles K, Kearney M, Palmer S, et al. Single-strand specificity of APOBEC3G accounts for minus-strand deamination of the HIV genome. Nat Struct Mol Biol. 2004 May;11(5):435–42.

130. Bi S, Hong PW, Lee B, Baum LG. Galectin-9 binding to cell surface protein disulfide isomerase regulates the redox environment to enhance T-cell migration and HIV entry. Proc Natl Acad Sci. 2011 Jun 28;108(26):10650–5.

131. Sharma S, Sundararajan A, Suryawanshi A, Kumar N, Veiga-Parga T, Kuchroo VK, et al. T cell immunoglobulin and mucin protein-3 (Tim-3)/Galectin-9 interaction regulates influenza A virus-specific humoral and CD8 T-cell responses. Proc Natl Acad Sci. 2011 Nov 22;108(47):19001–6.

132. Murphree A, Benedict W. Retinoblastoma: clues to human oncogenesis. Science. 1984 Mar 9;223(4640):1028–33.

133. Zakut-Houri R, Oren M, Bienz B, Lavie V, Hazum S, Givol D. A single gene and a pseudogene for the cellular tumour antigen p53. Nature. 1983 Dec;306(5943):594–7.

134. Roake CM, Artandi SE. Regulation of human telomerase in homeostasis and disease. Nat Rev Mol Cell Biol [Internet]. 2020 Apr 2 [cited 2020 Apr 9]; Available from: http://www.nature.com/articles/s41580-020-0234-z

135. Barbacid M. ras genes. Annu Rev Biochem. 1987;56:779–827.

136. Bender W, Peifer M. Oncogenes take wing. Cell. 1987 Aug 14;50(4):519–20.

137. Hayward WS, Neel BG, Astrin SM. Activation of a cellular onc gene by promoter insertion in ALV-induced lymphoid leukosis. Nature. 1981 Apr 9;290(5806):475–80.

138. Bartek J, Lukas J, Bartkova J. DNA Damage Response as an Anti-Cancer Barrier: Damage Threshold and the Concept of 'Conditional Haploinsufficiency'. Cell Cycle. 2007 Oct;6(19):2344–7.

139. Gajecka M. Unrevealed mosaicism in the next-generation sequencing era. Mol Genet Genomics. 2016 Apr;291(2):513–30.

140. Pagès V, Fuchs RP. How DNA lesions are turned into mutations within cells? Oncogene. 2002 Dec;21(58):8957–66.

141. De Bont R. Endogenous DNA damage in humans: a review of quantitative data. Mutagenesis. 2004 May 1;19(3):169–85.

142. Youssoufian H, Pyeritz RE. Mechanisms and consequences of somatic mosaicism in humans. Nat Rev Genet. 2002 Oct;3(10):748–58.

143. Warburg O. On the Origin of Cancer Cells. Science. 1956 Feb 24;123(3191):309–14.

144. Moreno-Sánchez R, Rodríguez-Enríquez S, Marín-Hernández A, Saavedra E. Energy metabolism in tumor cells: Glycolytic and mitochondrial metabolism of tumor cells. FEBS J. 2007 Mar;274(6):1393–418.

145. Goldberg MA, Dunning SP, Bunn HF. Regulation of the erythropoietin gene: evidence that the oxygen sensor is a heme protein. Science. 1988 Dec 9;242(4884):1412–5.

146. Synnestvedt K, Furuta GT, Comerford KM, Louis N, Karhausen J, Eltzschig HK, et al. Ecto-5'-nucleotidase (CD73) regulation by hypoxia-inducible factor-1 mediates permeability changes in intestinal epithelia. J Clin Invest. 2002 Oct;110(7):993–1002.

147. Shweiki D, Itin A, Soffer D, Keshet E. Vascular endothelial growth factor induced by hypoxia may mediate hypoxia-initiated angiogenesis. Nature. 1992 Oct 29;359(6398):843–5.

148. Gilkes DM, Chaturvedi P, Bajpai S, Wong CC, Wei H, Pitcairn S, et al. Collagen prolyl hydroxylases are essential for breast cancer metastasis. Cancer Res. 2013 Jun 1;73(11):3285–96.

149. Zhang H, Gao P, Fukuda R, Kumar G, Krishnamachary B, Zeller KI, et al. HIF-1 inhibits mitochondrial biogenesis and cellular respiration in VHL-deficient renal cell carcinoma by repression of C-MYC activity. Cancer Cell. 2007 May;11(5):407–20.

150. Medzhitov R. Origin and physiological roles of inflammation. Nature. 2008 Jul;454(7203):428–35.

151. Flier JS, Underhill LH, Dvorak HF. Tumors: Wounds That Do Not Heal. N Engl J Med. 1986 Dec 25;315(26):1650–9.

152. Mantovani A, Allavena P, Sica A, Balkwill F. Cancer-related inflammation. Nature. 2008 Jul 24;454(7203):436–44.

153. Mantovani A. Cancer: Inflaming metastasis. Nature. 2009 Jan 1;457(7225):36–7.

154. Olumi AF, Grossfeld GD, Hayward SW, Carroll PR, Tlsty TD, Cunha GR. Carcinoma-associated fibroblasts direct tumor progression of initiated human prostatic epithelium. Cancer Res. 1999 Oct 1;59(19):5002–11.

155. Orimo A, Gupta PB, Sgroi DC, Arenzana-Seisdedos F, Delaunay T, Naeem R, et al. Stromal fibroblasts present in invasive human breast carcinomas promote tumor growth and angiogenesis through elevated SDF-1/CXCL12 secretion. Cell. 2005 May 6;121(3):335–48.

156. Kalluri R, Zeisberg M. Fibroblasts in cancer. Nat Rev Cancer. 2006 May;6(5):392–401.

157. Jung E-J, Moon H-G, Cho BI, Jeong C-Y, Joo Y-T, Lee Y-J, et al. Galectin-1 expression in cancer-associated stromal cells correlates tumor invasiveness and tumor progression in breast cancer. Int J Cancer. 2007 Jun 1;120(11):2331–8.

158. He X-J, Tao H-Q, Hu Z-M, Ma Y-Y, Xu J, Wang H-J, et al. Expression of galectin-1 in carcinoma-associated fibroblasts promotes gastric cancer cell invasion through upregulation of integrin β1. Cancer Sci. 2014 Nov;105(11):1402–10.

159. Kugeratski FG, Atkinson SJ, Neilson LJ, Lilla S, Knight JRP, Serneels J, et al. Hypoxic cancer–associated fibroblasts increase NCBP2-AS2/HIAR to promote endothelial sprouting through enhanced VEGF signaling. Sci Signal. 2019 Feb 5;12(567):eaan8247.

160. Schreiber RD, Old LJ, Smyth MJ. Cancer immunoediting: integrating immunity's roles in cancer suppression and promotion. Science. 2011 Mar 25;331(6024):1565–70.

161. Coulie PG, Van den Eynde BJ, van der Bruggen P, Boon T. Tumour antigens recognized by T lymphocytes: at the core of cancer immunotherapy. Nat Rev Cancer. 2014 Feb;14(2):135–46.

162. Topalian SL, Hodi FS, Brahmer JR, Gettinger SN, Smith DC, McDermott DF, et al. Safety, activity, and immune correlates of anti-PD-1 antibody in cancer. N Engl J Med. 2012 Jun 28;366(26):2443–54.

163. Campoli M, Ferrone S. HLA antigen changes in malignant cells: epigenetic mechanisms and biologic significance. Oncogene. 2008 Oct;27(45):5869–85.

164. Mosser DM, Edwards JP. Exploring the full spectrum of macrophage activation. Nat Rev Immunol. 2008 Dec;8(12):958–69.

165. Bercovici N, Guérin MV, Trautmann A, Donnadieu E. The Remarkable Plasticity of Macrophages: A Chance to Fight Cancer. Front Immunol. 2019 Jul 12;10:1563.

166. Ostrand-Rosenberg S. Myeloid-derived suppressor cells: more mechanisms for inhibiting antitumor immunity. Cancer Immunol Immunother. 2010 Oct;59(10):1593–600.

167. Marvel D, Gabrilovich DI. Myeloid-derived suppressor cells in the tumor microenvironment: expect the unexpected. J Clin Invest. 2015 Sep 1;125(9):3356–64.

168. Vignali DAA, Collison LW, Workman CJ. How regulatory T cells work. Nat Rev Immunol. 2008 Jul;8(7):523–32.

169. Beyer I, van Rensburg R, Lieber A. Overcoming physical barriers in cancer therapy. Tissue Barriers. 2013 Jan;1(1):e23647.

170. Talmadge JE, Fidler IJ. AACR Centennial Series: The Biology of Cancer Metastasis: Historical Perspective. Cancer Res. 2010 Jul 15;70(14):5649–69.

171. Berx G, van Roy F. Involvement of Members of the Cadherin Superfamily in Cancer. Cold Spring Harb Perspect Biol. 2009 Dec 1;1(6):a003129–a003129.

172. Kim D, Xing T, Yang Z, Dudek R, Lu Q, Chen Y-H. Epithelial Mesenchymal Transition in Embryonic Development, Tissue Repair and Cancer: A Comprehensive Overview. J Clin Med. 2017 Dec 22;7(1):1.

173. Yang Y, Zheng H, Zhan Y, Fan S. An emerging tumor invasion mechanism about the collective cell migration. Am J Transl Res. 2019;11(9):5301–12.

174. Cai D, Chen S-C, Prasad M, He L, Wang X, Choesmel-Cadamuro V, et al. Mechanical feedback through E-cadherin promotes direction sensing during collective cell migration. Cell. 2014 May 22;157(5):1146–59.

175. Paget S. THE DISTRIBUTION OF SECONDARY GROWTHS IN CANCER OF THE BREAST. The Lancet. 1889 Mar;133(3421):571–3.

176. Macedo F, Ladeira K, Pinho F, Saraiva N, Bonito N, Pinto L, et al. Bone metastases: an overview. Oncol Rev [Internet]. 2017 May 9 [cited 2020 Apr 10];11(1). Available from: http://www.oncologyreviews.org/index.php/or/article/view/321

177. Saber SH, Ali HEA, Gaballa R, Gaballah M, Ali HI, Zerfaoui M, et al. Exosomes are the Driving Force in Preparing the Soil for the Metastatic Seeds: Lessons from the Prostate Cancer. Cells. 2020 Feb 28;9(3):564.

178. Liu Z, Han H, He X, Li S, Wu C, Yu C, et al. Expression of the galectin-9-Tim-3 pathway in glioma tissues is associated with the clinical manifestations of glioma. Oncol Lett. 2016 Mar;11(3):1829–34.

179. Yuan F, Ming H, Wang Y, Yang Y, Yi L, Li T, et al. Molecular and clinical characterization of Galectin-9 in glioma through 1,027 samples. J Cell Physiol. 2020 May;235(5):4326–34.

180. Liang T, Wang X, Wang F, Feng E, You G. Galectin-9: A Predictive Biomarker Negatively Regulating Immune Response in Glioma Patients. World Neurosurg. 2019 Dec;132:e455–62.

181. Ohue Y, Kurose K, Nozawa R, Isobe M, Nishio Y, Tanaka T, et al. Survival of Lung Adenocarcinoma Patients Predicted from Expression of PD-L1, Galectin-9, and XAGE1 (GAGED2a) on Tumor Cells and Tumor-Infiltrating T Cells. Cancer Immunol Res. 2016 Dec 1;4(12):1049–60.

182. Kawashima H, Obayashi A, Kawamura M, Masaki S, Tamada S, Iguchi T, et al. Galectin 9 and PINCH, novel immunotherapy targets of renal cell carcinoma: a rationale to find potential tumour antigens and the resulting cytotoxic T lymphocytes induced by the derived peptides: Galectin 9 and PINCH as RCC immunotherapy targets. BJU Int. 2014 Feb;113(2):320–32.

183. Fu H, Liu Y, Xu L, Liu W, Fu Q, Liu H, et al. Galectin-9 predicts postoperative recurrence and survival of patients with clear-cell renal cell carcinoma. Tumor Biol. 2015 Aug;36(8):5791–9.

184. Seifert AM, Reiche C, Heiduk M, Tannert A, Meinecke A-C, Baier S, et al. Detection of pancreatic ductal adenocarcinoma with galectin-9 serum levels. Oncogene. 2020 Apr;39(15):3102–13.

185. Daley D, Zambirinis CP, Seifert L, Akkad N, Mohan N, Werba G, et al. γδ T Cells Support Pancreatic Oncogenesis by Restraining αβ T Cell Activation. Cell. 2016 Sep;166(6):1485-1499.e15.

186. Kikushige Y, Miyamoto T, Yuda J, Jabbarzadeh-Tabrizi S, Shima T, Takayanagi S, et al. A TIM-3/Gal-9 Autocrine Stimulatory Loop Drives Self-Renewal of Human Myeloid Leukemia Stem Cells and Leukemic Progression. Cell Stem Cell. 2015 Sep;17(3):341–52.

187. Zhou X, Sun L, Jing D, Xu G, Zhang J, Lin L, et al. Galectin-9 Expression Predicts Favorable Clinical Outcome in Solid Tumors: A Systematic Review and Meta-Analysis. Front Physiol. 2018;9:452.

188. Liang M, Ueno M, Oomizu S, Arikawa T, Shinonaga R, Zhang S, et al. Galectin-9 expression links to malignant potential of cervical squamous cell carcinoma. J Cancer Res Clin Oncol. 2008 Aug;134(8):899–907.

189. Fík Z, Valach J, Chovanec M, Mazánek J, Kodet R, Kodet O, et al. Loss of adhesion/growth-regulatory galectin-9 from squamous cell epithelium in head and neck carcinomas: **Galectin-9 in head and neck cancer**. J Oral Pathol Med. 2013 Feb;42(2):166–73.

190. Chan SW, Kallarakkal TG, Abraham MT. Changed Expression of E-cadherin and Galectin-9 in Oral Squamous Cell Carcinomas but Lack of Potential as Prognostic Markers. Asian Pac J Cancer Prev. 2014 Mar 1;15(5):2145–52.

191. Irie A. Galectin-9 as a Prognostic Factor with Antimetastatic Potential in Breast Cancer. Clin Cancer Res. 2005 Apr 15;11(8):2962–8.

192. de Mingo Pulido Á, Gardner A, Hiebler S, Soliman H, Rugo HS, Krummel MF, et al. TIM-3 Regulates CD103+ Dendritic Cell Function and Response to Chemotherapy in Breast Cancer. Cancer Cell. 2018 Jan;33(1):60-74.e6.

193. Kageshita T, Kashio Y, Yamauchi A, Seki M, Abedin MJ, Nishi N, et al. Possible role of galectin-9 in cell aggregation and apoptosis of human melanoma cell lines and its clinical significance. Int J Cancer. 2002 Jun 20;99(6):809–16.

194. Wiersma VR, de Bruyn M, van Ginkel RJ, Sigar E, Hirashima M, Niki T, et al. The Glycan-Binding Protein Galectin-9 Has Direct Apoptotic Activity toward Melanoma Cells. J Invest Dermatol. 2012 Sep;132(9):2302–5.

195. Nobumoto A, Nagahara K, Oomizu S, Katoh S, Nishi N, Takeshita K, et al. Galectin-9 suppresses tumor metastasis by blocking adhesion to endothelium and extracellular matrices. Glycobiology. 2008 Jun 25;18(9):735–44.

196. Melief SM, Visconti VV, Visser M, van Diepen M, Kapiteijn EHW, van den Berg JH, et al. Long-term Survival and Clinical Benefit from Adoptive T-cell Transfer in Stage IV Melanoma Patients Is Determined by a Four-Parameter Tumor Immune Signature. Cancer Immunol Res. 2017 Feb;5(2):170–9.

197. He Y, Jia K, Dziadziuszko R, Zhao S, Zhang X, Deng J, et al. Galectin-9 in non-small cell lung cancer. Lung Cancer. 2019 Oct;136:80–5.

198. Vilar K de M, Pereira MC, Tavares Dantas A, de Melo Rêgo MJB, Pitta I da R, Pinto Duarte ÂLB, et al. Galectin-9 gene (LGALS9) polymorphisms are associated with rheumatoid arthritis in Brazilian patients. Beavis PA, editor. PLOS ONE. 2019 Oct 10;14(10):e0223191.

199. Holderried TAW, de Vos L, Bawden EG, Vogt TJ, Dietrich J, Zarbl R, et al. Molecular and immune correlates of TIM-3 (HAVCR2) and galectin 9 (LGALS9) mRNA expression and DNA methylation in melanoma. Clin Epigenetics. 2019 Dec;11(1):161.

200. Sasidharan Nair V, Toor SM, Taha RZ, Shaath H, Elkord E. DNA methylation and repressive histones in the promoters of PD-1, CTLA-4, TIM-3, LAG-3, TIGIT, PD-L1, and galectin-9 genes in human colorectal cancer. Clin Epigenetics. 2018 Dec;10(1):104.

201. Yang Q, Hou C, Huang D, Zhuang C, Jiang W, Geng Z, et al. miR-455-5p functions as a potential oncogene by targeting galectin-9 in colon cancer. Oncol Lett. 2017 Mar;13(3):1958–64.

202. Yang Q, Jiang W, Zhuang C, Geng Z, Hou C, Huang D, et al. microRNA-22 downregulation of galectin-9 influences lymphocyte apoptosis and tumor cell proliferation in liver cancer. Oncol Rep. 2015 Oct;34(4):1771–8.

203. Gupta R, Leon F, Rauth S, Batra SK, Ponnusamy MP. A Systematic Review on the Implications of O-linked Glycan Branching and Truncating Enzymes on Cancer Progression and Metastasis. Cells. 2020 Feb 14;9(2):446.

204. Giguère D, Sato S, St-Pierre C, Sirois S, Roy R. Aryl O- and S-galactosides and lactosides as specific inhibitors of human galectins-1 and -3: Role of electrostatic potential at O-3. Bioorg Med Chem Lett. 2006 Mar;16(6):1668–72.

205. Glinsky GV, Price JE, Glinsky VV, Mossine VV, Kiriakova G, Metcalf JB. Inhibition of human breast cancer metastasis in nude mice by synthetic glycoamines. Cancer Res. 1996 Dec 1;56(23):5319–24.

206. John CM, Leffler H, Kahl-Knutsson B, Svensson I, Jarvis GA. Truncated galectin-3 inhibits tumor growth and metastasis in orthotopic nude mouse model of human breast cancer. Clin Cancer Res Off J Am Assoc Cancer Res. 2003 Jun;9(6):2374–83.

207. Zou J, Glinsky VV, Landon LA, Matthews L, Deutscher SL. Peptides specific to the galectin-3 carbohydrate recognition domain inhibit metastasis-associated cancer cell adhesion. Carcinogenesis. 2005 Feb;26(2):309–18.

208. Lee J-H, Canny MD, De Erkenez A, Krilleke D, Ng Y-S, Shima DT, et al. A therapeutic aptamer inhibits angiogenesis by specifically targeting the heparin binding domain of VEGF165. Proc Natl Acad Sci. 2005 Dec 27;102(52):18902–7.

209. Chang Y-C, Kao W-C, Wang W-Y, Wang W-Y, Yang R-B, Peck K. Identification and characterization of oligonucleotides that inhibit Toll-like receptor 2-associated immune responses. FASEB J. 2009 Sep;23(9):3078–88.

210. Tsai Y-T, Liang C-H, Yu J-H, Huang K-C, Tung C-H, Wu J-E, et al. A DNA Aptamer Targeting Galectin-1 as a Novel Immunotherapeutic Strategy for Lung Cancer. Mol Ther - Nucleic Acids. 2019 Dec;18:991–8.

211. Lhuillier C, Barjon C, Baloche V, Niki T, Gelin A, Mustapha R, et al. Characterization of neutralizing antibodies reacting with the 213-224 amino-acid segment of human galectin-9. Nabi IR, editor. PLOS ONE. 2018 Sep 11;13(9):e0202512.

212. Ishino Y, Shinagawa H, Makino K, Amemura M, Nakata A. Nucleotide sequence of the iap gene, responsible for alkaline phosphatase isozyme conversion in Escherichia coli, and identification of the gene product. J Bacteriol. 1987 Dec;169(12):5429–33.

213. Mojica FJM, Juez G, Rodriguez-Valera F. Transcription at different salinities of Haloferax mediterranei sequences adjacent to partially modified PstI sites. Mol Microbiol. 1993 Aug;9(3):613–21.

214. Jansen R, van Embden JDA, Gaastra W, Schouls LM. Identification of a Novel Family of Sequence Repeats among Prokaryotes. OMICS J Integr Biol. 2002 Jan;6(1):23–33.

215. Jansen Ruud, Embden JanDA van, Gaastra Wim, Schouls LeoM. Identification of genes that are associated with DNA repeats in prokaryotes. Mol Microbiol. 2002 Mar;43(6):1565–75.

216. Mojica FJM, Diez-Villasenor C, Garcia-Martinez J, Soria E. Intervening Sequences of Regularly Spaced Prokaryotic Repeats Derive from Foreign Genetic Elements. J Mol Evol. 2005 Feb;60(2):174–82.

217. Bolotin A, Quinquis B, Sorokin A, Ehrlich SD. Clustered regularly interspaced short palindrome repeats (CRISPRs) have spacers of extrachromosomal origin. Microbiology. 2005 Aug 1;151(8):2551–61.

218. CRISPR elements in Yersinia pestis acquire new repeats by preferential uptake of bacteriophage DNA, and provide additional tools for evolutionary studies. Microbiology. 2005 Mar 1;151(3):653–63.

219. Makarova KS, Grishin NV, Shabalina SA, Wolf YI, Koonin EV. A putative RNA-interference-based immune system in prokaryotes: computational analysis of the predicted enzymatic machinery, functional analogies with eukaryotic RNAi, and hypothetical mechanisms of action. Biol Direct. 2006;1(1):7.

220. Makarova KS, Haft DH, Barrangou R, Brouns SJJ, Charpentier E, Horvath P, et al. Evolution and classification of the CRISPR–Cas systems. Nat Rev Microbiol. 2011 Jun;9(6):467–77.

221. Jinek M, Chylinski K, Fonfara I, Hauer M, Doudna JA, Charpentier E. A Programmable Dual-RNA-Guided DNA Endonuclease in Adaptive Bacterial Immunity. Science. 2012 Aug 17;337(6096):816–21.

222. Qi LS, Larson MH, Gilbert LA, Doudna JA, Weissman JS, Arkin AP, et al. Repurposing CRISPR as an RNA-Guided Platform for Sequence-Specific Control of Gene Expression. Cell. 2013 Feb;152(5):1173–83.

223. Dominguez AA, Lim WA, Qi LS. Beyond editing: repurposing CRISPR–Cas9 for precision genome regulation and interrogation. Nat Rev Mol Cell Biol. 2016 Jan;17(1):5–15.

224. Kearns NA, Pham H, Tabak B, Genga RM, Silverstein NJ, Garber M, et al. Functional annotation of native enhancers with a Cas9–histone demethylase fusion. Nat Methods. 2015 May;12(5):401–3.

225. Chen B, Gilbert LA, Cimini BA, Schnitzbauer J, Zhang W, Li G-W, et al. Dynamic Imaging of Genomic Loci in Living Human Cells by an Optimized CRISPR/Cas System. Cell. 2013 Dec;155(7):1479–91.

226. Ma H, Tu L-C, Naseri A, Huisman M, Zhang S, Grunwald D, et al. Multiplexed labeling of genomic loci with dCas9 and engineered sgRNAs using CRISPRainbow. Nat Biotechnol. 2016 May;34(5):528–30.

227. Fujita T, Yuno M, Fujii H. enChIP systems using different CRISPR orthologues and epitope tags. BMC Res Notes. 2018 Dec;11(1):154.

228. Jung I-Y, Lee J. Unleashing the Therapeutic Potential of CAR-T Cell Therapy Using Gene-Editing Technologies. Mol Cells. 2018 Aug 31;41(8):717–23.

229. Fu Y, Foden JA, Khayter C, Maeder ML, Reyon D, Joung JK, et al. High-frequency off-target mutagenesis induced by CRISPR-Cas nucleases in human cells. Nat Biotechnol. 2013 Sep;31(9):822–6.

230. Duan J, Lu G, Xie Z, Lou M, Luo J, Guo L, et al. Genome-wide identification of CRISPR/Cas9 off-targets in human genome. Cell Res. 2014 Aug;24(8):1009–12.

231. Kuscu C, Arslan S, Singh R, Thorpe J, Adli M. Genome-wide analysis reveals characteristics of off-target sites bound by the Cas9 endonuclease. Nat Biotechnol. 2014 Jul;32(7):677–83.

232. Griswold DP, Corbett TH. A colon tumor model for anticancer agent evaluation. Cancer. 1975 Dec;36(6 Suppl):2441–4.

233. Castle JC, Loewer M, Boegel S, de Graaf J, Bender C, Tadmor AD, et al. Immunomic, genomic and transcriptomic characterization of CT26 colorectal carcinoma. BMC Genomics. 2014;15(1):190.

234. Dalerba P, Kalisky T, Sahoo D, Rajendran PS, Rothenberg ME, Leyrat AA, et al. Single-cell dissection of transcriptional heterogeneity in human colon tumors. Nat Biotechnol. 2011 Dec;29(12):1120–7.

235. De Sousa E Melo F, Wang X, Jansen M, Fessler E, Trinh A, de Rooij LPMH, et al. Poor-prognosis colon cancer is defined by a molecularly distinct subtype and develops from serrated precursor lesions. Nat Med. 2013 May;19(5):614–8.

236. Sadanandam A, Lyssiotis CA, Homicsko K, Collisson EA, Gibb WJ, Wullschleger S, et al. A colorectal cancer classification system that associates cellular phenotype and responses to therapy. Nat Med. 2013 May;19(5):619–25.

237. van Houdt WJ, Hoogwater FJH, de Bruijn MT, Emmink BL, Nijkamp MW, Raats DAE, et al. Oncogenic KRAS Desensitizes Colorectal Tumor Cells to Epidermal Growth Factor Receptor Inhibition and Activation. Neoplasia. 2010 Jun;12(6):443-IN2.

238. Yeh JJ, Routh ED, Rubinas T, Peacock J, Martin TD, Shen XJ, et al. KRAS/BRAF mutation status and ERK1/2 activation as biomarkers for MEK1/2 inhibitor therapy in colorectal cancer. Mol Cancer Ther. 2009 Apr 1;8(4):834–43.

239. Jordan KR, McMahan RH, Kemmler CB, Kappler JW, Slansky JE. Peptide vaccines prevent tumor growth by activating T cells that respond to native tumor antigens. Proc Natl Acad Sci. 2010 Mar 9;107(10):4652–7.

240. McWilliams JA, Sullivan RT, Jordan KR, McMahan RH, Kemmler CB, McDuffie M, et al. Age-dependent tolerance to an endogenous tumor-associated antigen. Vaccine. 2008 Mar 28;26(15):1863–73.

241. Takeda J, Sato Y, Kiyosawa H, Mori T, Yokoya S, Irisawa A, et al. Anti-tumor Immunity against CT26 Colon Tumor in Mice Immunized with Plasmid DNA Encoding β-Galactosidase Fused to an Envelope Protein of Endogenous Retrovirus. Cell Immunol. 2000 Aug;204(1):11–8.

242. Selby MJ, Engelhardt JJ, Johnston RJ, Lu L-S, Han M, Thudium K, et al. Preclinical Development of Ipilimumab and Nivolumab Combination Immunotherapy: Mouse Tumor Models, In Vitro Functional Studies, and Cynomolgus Macaque Toxicology. Ahmad A, editor. PLOS ONE. 2016 Sep 9;11(9):e0161779.

243. Devaud C, Westwood JA, John LB, Flynn JK, Paquet-Fifield S, Duong CP, et al. Tissues in Different Anatomical Sites Can Sculpt and Vary the Tumor Microenvironment to Affect Responses to Therapy. Mol Ther. 2014 Jan;22(1):18–27.

244. Yu JW, Bhattacharya S, Yanamandra N, Kilian D, Shi H, Yadavilli S, et al. Tumor-immune profiling of murine syngeneic tumor models as a framework to guide mechanistic studies and predict therapy response in distinct tumor microenvironments. Mattei F, editor. PLOS ONE. 2018 Nov 2;13(11):e0206223.

245. Wherry EJ, Kurachi M. Molecular and cellular insights into T cell exhaustion. Nat Rev Immunol. 2015 Aug;15(8):486–99.

246. Wherry EJ, Ha S-J, Kaech SM, Haining WN, Sarkar S, Kalia V, et al. Molecular signature of CD8+ T cell exhaustion during chronic viral infection. Immunity. 2007 Oct;27(4):670–84.

247. Summerhayes IC, Franks LM. Effects of donor age on neoplastic transformation of adult mouse bladder epithelium in vitro. J Natl Cancer Inst. 1979 Apr;62(4):1017–23.

248. Chade DC, Andrade PM, Borra RC, Leite KR, Andrade E, Villanova FE, et al. Histopathological characterization of a syngeneic orthotopic murine bladder cancer model. Int Braz J Urol. 2008 Mar;34(2):220–9.

249. Liu Y-R, Yin P-N, Silvers CR, Lee Y-F. Enhanced metastatic potential in the MB49 urothelial carcinoma model. Sci Rep. 2019 Dec;9(1):7425.

250. Douville Y, Pelouze G, Roy R, Charrois R, Kibrité A, Martin M, et al. Recurrent bladder papillomata treated with bacillus Calmette-Guérin: a preliminary report (phase I trial). Cancer Treat Rep. 1978 Apr;62(4):551–2.

251. Böhle A, Gerdes J, Ulmer AJ, Hofstetter AG, Flad H-D. Effects of Local Bacillus Calmette-Guerin Therapy in Patients with Bladder Carcinoma on Immunocompetent Cells of the Bladder Wall. J Urol. 1990 Jul;144(1):53–8.

252. Böhle A, Nowc Ch, Ulmer AJ, Musehold J, Gerdes J, Hofstetter AG, et al. Elevations of Cytokines Interleukin-1, Interleukin-2 and Tumor Necrosis Factor in the Urine of Patients after Intravesical Bacillus Calmette-Guerin Immunotherapy. J Urol. 1990 Jul;144(1):59–64.

253. Lattime EC, Gomella LG, McCue PA. Murine bladder carcinoma cells present antigen to BCG-specific CD4+ T-cells. Cancer Res. 1992 Aug 1;52(15):4286–90.

254. Lodillinsky C, Umerez MS, Jasnis MA, Casabé A, Sandes E, Eiján AM. Bacillus Calmette-Guérin induces the expression of peroxisome proliferator-activated receptor gamma in bladder cancer cells. Int J Mol Med. 2006 Feb;17(2):269–73.

255. Sandes E, Lodillinsky C, Cwirenbaum R, Argüelles C, Casabé A, Eiján AM. Cathepsin B is involved in the apoptosis intrinsic pathway induced by Bacillus Calmette-Guérin in transitional cancer cell lines. Int J Mol Med. 2007 Dec;20(6):823–8.

256. Zhang G, Chen F, Cao Y, Johnson B, See WA. HMGB1 Release by Urothelial Carcinoma Cells is Required for the In Vivo Antitumor Response to Bacillus Calmette-Guérin. J Urol. 2013 Apr;189(4):1541–6.

257. Lodillinsky C, Langle Y, Guionet A, Góngora A, Baldi A, Sandes EO, et al. Bacillus Calmette Guerin Induces Fibroblast Activation Both Directly and through Macrophages in a Mouse Bladder Cancer Model. Tailleux L, editor. PLoS ONE. 2010 Oct 22;5(10):e13571.

258. Sonoda T, Sugimura K, Ikemoto S-I, Kawashima H, Nakatani T. Significance of target cell infection and natural killer cells in the anti-tumor effects of bacillus Calmette-Guerin in murine bladder cancer. Oncol Rep. 2007 Jun;17(6):1469–74.

259. Arnold J, de Boer EC, O'Donnell MA, Böhle A, Brandau S. Immunotherapy of Experimental Bladder Cancer with Recombinant BCG Expressing Interferon-γ: J Immunother. 2004;27(2):116–23.

260. Sun E, Fan X, Wang L, Lei M, Zhou X, Liu C, et al. Recombinant h IFN-α2b-BCG inhibits tumor growth in a mouse model of bladder cancer. Oncol Rep. 2015 Jul;34(1):183–94.

261. Andrade PM, Chade DC, Borra RC, Nascimento IP, Villanova FE, Leite LCC, et al. The therapeutic potential of recombinant BCG expressing the antigen S1PT in the intravesical treatment of bladder cancer. Urol Oncol Semin Orig Investig. 2010 Sep;28(5):520–5.

262. Vandeveer AJ, Fallon JK, Tighe R, Sabzevari H, Schlom J, Greiner JW. Systemic Immunotherapy of Non-Muscle Invasive Mouse Bladder Cancer with Avelumab, an Anti-PD-L1 Immune Checkpoint Inhibitor. Cancer Immunol Res. 2016 May 1;4(5):452–62.

263. van Hooren L, Sandin LC, Moskalev I, Ellmark P, Dimberg A, Black P, et al. Local checkpoint inhibition of CTLA-4 as a monotherapy or in combination with anti-PD1 prevents the growth of murine bladder cancer. Eur J Immunol. 2017 Feb;47(2):385–93.

264. Autenrieth IB, Beer M, Bohn E, Kaufmann SH, Heesemann J. Immune responses to Yersinia enterocolitica in susceptible BALB/c and resistant C57BL/6 mice: an essential role for gamma interferon. Infect Immun. 1994 Jun;62(6):2590–9.

265. Autenrieth IB, Reissbrodt R, Saken E, Berner R, Vogel U, Rabsch W, et al. Desferrioxamine-promoted virulence of Yersinia enterocolitica in mice depends on both desferrioxamine type and mouse strain. J Infect Dis. 1994 Mar;169(3):562–7.

266. Watanabe H, Numata K, Ito T, Takagi K, Matsukawa A. Innate immune response in Th1- and Th2-dominant mouse strains. Shock Augusta Ga. 2004 Nov;22(5):460–6.

267. Loskog A, Ninalga C, Hedlund T, Alimohammadi M, Malmström P-U, Tötterman TH. Optimization of the MB49 mouse bladder cancer model for adenoviral gene therapy. Lab Anim. 2005 Oct;39(4):384–93.

268. Millrain M, Chandler P, Dazzi F, Scott D, Simpson E, Dyson PJ. Examination of HY Response: T Cell Expansion, Immunodominance, and Cross-Priming Revealed by HY Tetramer Analysis. J Immunol. 2001 Oct 1;167(7):3756–64.

269. El Behi M, Krumeich S, Lodillinsky C, Kamoun A, Tibaldi L, Sugano G, et al. An essential role for decorin in bladder cancer invasiveness. EMBO Mol Med. 2013 Dec;5(12):1835–51.

270. Fabris VT, Lodillinsky C, Pampena MB, Belgorosky D, Lanari C, Eiján AM. Cytogenetic characterization of the murine bladder cancer model MB49 and the derived invasive line MB49-I. Cancer Genet. 2012 Apr;205(4):168–76.

271. International Lung Cancer Consortium (INTEGRAL-ILCCO), The Breast Cancer Association Consortium, Consortium of Investigators of Modifiers of BRCA1/2, The Endometrial Cancer Association Consortium, The Ovarian Cancer Association Consortium, The Prostate Cancer Association Group to Investigate Cancer Associated Alterations in the Genome (PRACTICAL) Consortium, et al. Genetic predisposition to mosaic Y chromosome loss in blood. Nature. 2019 Nov;575(7784):652–7.

272. Minner S, Kilgué A, Stahl P, Weikert S, Rink M, Dahlem R, et al. Y chromosome loss is a frequent early event in urothelial bladder cancer. Pathology (Phila). 2010 Jun;42(4):356–9.

273. Liu Y, Liu Z, Fu Q, Wang Z, Fu H, Liu W, et al. Galectin-9 as a prognostic and predictive biomarker in bladder urothelial carcinoma. Urol Oncol Semin Orig Investig. 2017 Jun;35(6):349–55.

274. Alifrangis C, McGovern U, Freeman A, Powles T, Linch M. Molecular and histopathology directed therapy for advanced bladder cancer. Nat Rev Urol. 2019;16(8):465–83.

275. Borcoman E, De La Rochere P, Richer W, Vacher S, Chemlali W, Krucker C, et al. Inhibition of PI3K pathway increases immune infiltrate in muscle-invasive bladder cancer. Oncoimmunology. 2019;8(5):e1581556.

276. Kamoun A, de Reyniès A, Allory Y, Sjödahl G, Robertson AG, Seiler R, et al. A Consensus Molecular Classification of Muscle-invasive Bladder Cancer. Eur Urol. 2020 Apr;77(4):420–33.

277. Babjuk M, Burger M, Compérat EM, Gontero P, Mostafid AH, Palou J, et al. European Association of Urology Guidelines on Non-muscle-invasive Bladder Cancer (TaT1 and Carcinoma In Situ) - 2019 Update. Eur Urol. 2019 Nov;76(5):639–57.

278. Lavoie J-M, Black PC, Eigl BJ. Predictive Biomarkers for Checkpoint Blockade in Urothelial Cancer: A Systematic Review. J Urol. 2019;202(1):49–56.

279. Pan S, Zhan Y, Chen X, Wu B, Liu B. Bladder Cancer Exhibiting High Immune Infiltration Shows the Lowest Response Rate to Immune Checkpoint Inhibitors. Front Oncol. 2019;9:1101.

280. Hou W, Xue M, Shi J, Yang M, Zhong W, Fan X, et al. PD-1 topographically defines distinct T cell subpopulations in urothelial cell carcinoma of the bladder and predicts patient survival. Urol Oncol. 2020 May 11;

281. Chevalier MF, Bohner P, Pieraerts C, Lhermitte B, Gourmaud J, Nobile A, et al. Immunoregulation of Dendritic Cell Subsets by Inhibitory Receptors in Urothelial Cancer. Eur Urol. 2017;71(6):854–7.

282. John S, Mishra R. Galectin-9: From cell biology to complex disease dynamics. J Biosci. 2016 Sep;41(3):507–34.

283. Gonçalves Silva I, Yasinska IM, Sakhnevych SS, Fiedler W, Wellbrock J, Bardelli M, et al. The Tim-3-galectin-9 Secretory Pathway is Involved in the Immune Escape of Human Acute Myeloid Leukemia Cells. EBioMedicine. 2017 Aug;22:44–57.

284. Golden-Mason L, McMahan RH, Strong M, Reisdorph R, Mahaffey S, Palmer BE, et al. Galectin-9 Functionally Impairs Natural Killer Cells in Humans and Mice. J Virol. 2013 May 1;87(9):4835–45.

285. Zhou Q, Munger ME, Veenstra RG, Weigel BJ, Hirashima M, Munn DH, et al. Coexpression of Tim-3 and PD-1 identifies a CD8+ T-cell exhaustion phenotype in mice with disseminated acute myelogenous leukemia. Blood. 2011 Apr 28;117(17):4501–10.

286. Oomizu S, Arikawa T, Niki T, Kadowaki T, Ueno M, Nishi N, et al. Galectin-9 suppresses Th17 cell development in an IL-2-dependent but Tim-3-independent manner. Clin Immunol Orlando Fla. 2012 Apr;143(1):51–8.

287. Tavares LB, Silva-Filho AF, Martins MR, Vilar KM, Pitta MGR, Rêgo MJBM. Patients With Pancreatic Ductal Adenocarcinoma Have High Serum Galectin-9 Levels: A Sweet Molecule to Keep an Eye On. Pancreas. 2018;47(9):e59–60.

288. Melchionda F, Fry TJ, Milliron MJ, McKirdy MA, Tagaya Y, Mackall CL. Adjuvant IL-7 or IL-15 overcomes immunodominance and improves survival of the CD8+ memory cell pool. J Clin Invest. 2005 May;115(5):1177–87.

289. Perez-Diez A, Joncker NT, Choi K, Chan WFN, Anderson CC, Lantz O, et al. CD4 cells can be more efficient at tumor rejection than CD8 cells. Blood. 2007 Jun 15;109(12):5346–54.

290. Whiting D, Hsieh G, Yun JJ, Banerji A, Yao W, Fishbein MC, et al. Chemokine Monokine Induced by IFN-γ/CXC Chemokine Ligand 9 Stimulates T Lymphocyte Proliferation and Effector Cytokine Production. J Immunol. 2004 Jun 15;172(12):7417–24.

université PARIS-SACLAY

Ecole doctorale n°582

Cancérologie : biologie - médecine – santé (CBMS)

Titre : Contributions négatives et positives de la galectine-9 au développement tumoral : étude dans des modèles tumoraux murins syngéniques.

Mots clés : galectine-9, immunologie des tumeurs, modèles tumoraux murins, anticorps thérapeutiques

Résumé : Comme les autres galectines, la galectine-9 (gal-9) est une lectine animale qui interagit avec un sous-groupe défini de polysaccharides portés par des glycoprotéines ou des glycolipides. La gal-9 associée aux cellules exerce de multiples fonctions dans le cytoplasme, dans le noyau et à la surface de la membrane plasmique. Quelques publications suggèrent que la gal-9 intra-cellulaire inhibe la mobilité des cellules malignes et exerce un effet anti-métastatique. En outre la gal-9 peut être sécrétée dans le milieu extra-cellulaire où elle se comporte comme une cytokine avec des effets principalement immunosuppresseurs. Ces effets ont été mis en évidence dans un contexte tumoral chez l'homme et dans des modèles murins. Cependant, on ne disposait pas jusqu'à présent d'un modèle tumoral murin permettant d'évaluer les effets pro-tumoraux ou anti-tumoraux de la gal-9 indépendamment de la gal-9 des cellules infiltrantes. Pour résoudre ce problème, nous avons dérivé, en employant la technologie CRISPR/Cas9, des clones isogéniques invalidés ou non pour la gal-9 à partir de 2 lignées tumorales murines : CT26 (fond génétique BALB/c) et MB49 (fond génétique C57BL/6). Dans le cas de la lignée MB49, nous avons pu mettre en évidence un phénotype remarquable *in vivo*. Lors de transplantations itératives, on assiste pour les tumeurs dérivées des clones invalidées à une réduction drastique de la croissance tumorale au bout de 3 ou 4 passages sur les souris syngéniques mais pas sur les souris immunodéficientes. L'émergence de la réponse immunitaire responsable de cet arrêt de la croissance tumorale a été étudiée par immunohistochimie, dosage de cytokines en multiplex dans les extraits tumoraux et analyse du transcriptome par RNAseq. L'augmentation de la production intra-tumorale d'interféron-γ, de CXCL9 et d'Il-6 semble jouer un rôle important dans le renforcement de la réponse immunitaire contre les tumeurs KO-gal-9.

Title: Negative and positive contributions of galectin-9 to tumor development: study in syngenic murin tumor models.

Keywords: galectin-9, tumor immunology, murine tumor model, therapeutic antibodies

Abstract: Like other galectins, galectin-9 (gal-9) is an animal lectin which interacts with a defined subgroup of glycans carried by glycoproteins or glycolipids. Gal-9 associated with cells performs multiple functions in the cytoplasm, in the nucleus and at the surface of the plasma membrane. Some publications suggest that intracellular gal-9 inhibits the mobility of malignant cells and exerts an anti-metastatic effect. In addition, gal-9 can be secreted into the extracellular medium where it behaves like a cytokine with mainly immunosuppressive effects. These effects have been demonstrated in the context of human tumors and in mouse tumor models. However, so far there was no murine tumor model available to assess the pro-tumor or anti-tumor effet of gal-9 independently of gal-9 produced by infiltrating cells. To address this issue, we derived isogenic clones invalidated or not for gal-9 from 2 murine tumoral lines : CT26 (BABL/c genetic background) and MB49 (C57BL/6 genetic background), using CRISPR/Cas9 technology. In the case of the MB49 line, we were able to demonstrate a remarkable phenotype *in vivo*. During serial transplantations, we saw, for tumors derived from invalidated clones, a dramatic reduction in tumor growth after 3 or 4 passages in syngenic mice but not in immunodeficient mice. The emergence of the immune response responsible for this arrest of tumor growth was investigated by immunohistochemistry, multiplex cytokine assay in tumor extracts and transcriptome analysis by RNAseq. Increased intra-tumor production of interferon-γ, CXCL9 and Il-6 appears to play an important role in enhancing the immune response against KO-gal-9 tumors.

Université Paris-Saclay
Espace Technologique / Immeuble Discovery
Route de l'Orme aux Merisiers RD 128 / 91190 Saint-Aubin, France